

SEASONAL AND SPATIAL VARIABILITY OF BEACH MORPHODYNAMICS AT AN
AUTONOMOUS TIDAL INLET: MATANZAS INLET, FLORIDA ATLANTIC COAST

By

KATHERINE KELLY MALONE

A THESIS PRESENTED TO THE GRADUATE SCHOOL
OF THE UNIVERSITY OF FLORIDA IN PARTIAL FULFILLMENT
OF THE REQUIREMENTS FOR THE DEGREE OF
MASTER OF SCIENCE

UNIVERSITY OF FLORIDA

2011

© 2011 Katherine K. Malone

To my Dad

ACKNOWLEDGMENTS

I am in great debt to a number of friends and colleagues. First and foremost, I'd like to thank Peter Adams for his guidance and intellectual support throughout my research. I'd also like to thank John Jaeger and Joann Mossa for their assistance as committee members.

I suffered a great loss with the death of my father in March 2008 just prior to beginning my degree program. He was a great inspiration to me as we shared a mutual love for nature and for science. At first, I thought I had lost my momentum – but I gained it back and I felt close to my father in the process of scientific discovery. I'd like to thank him for teaching me to appreciate things we cannot understand. Without continual encouragement from my mother to push through this difficult time, I could have never finished.

Jessica Lovering and Shaun Kline encouraged me to think analytically and made me love coming to work every day. Rich Mackenzie taught me how to use the equipment and his door was always open if I had any problems. I'd like to thank my friends, especially Sean Keough. I could not have completed this research without the field support of Earl Soeder, Tim Kirchner, and Derrick Newkirk; I am in great debt to them. In addition, I'd like to thank the staff of Fort Matanzas State Park who allowed me the freedom to explore such a beautiful place.

TABLE OF CONTENTS

	<u>page</u>
ACKNOWLEDGMENTS.....	4
LIST OF TABLES.....	7
LIST OF FIGURES.....	8
LIST OF ABBREVIATIONS.....	10
ABSTRACT.....	11
CHAPTER	
1 INTRODUCTION.....	12
1.1 Previous Work.....	12
1.2 Problem Statement and Objectives.....	18
2 METHODS.....	21
2.1 Study Site.....	21
2.1.1 Historical Landform Changes.....	21
2.1.2 Site Description.....	21
2.2 GPS Surveys.....	22
2.3 Data Processing.....	23
2.3.1 Digital Elevation Model Grid Generation.....	23
2.3.2 Cross Shore Transect Generation.....	24
2.3.3 Cross-shore Profile Interpolation.....	24
2.3.4 Shoreline Interpolation and Beach Width Calculation.....	25
2.3.5 Beach Slope Calculation.....	25
2.3.6 Wave Conditions Data Processing.....	26
3 RESULTS AND ANALYSIS.....	33
3.1 Shoreline Position / Beach Width.....	33
3.1.1 Spatial Variation of Shoreline Position (Beach Width).....	33
3.1.2 Temporal Variation of Shoreline Position (Beach Width).....	34
3.2 Beach Morphology / Profile Shape.....	35
3.2.1 Spatial and Temporal Variation of Cross–Shore Profiles.....	35
3.2.2 Analysis of Variation of Cross–Shore Profiles.....	36
3.2.3 Beach Slope Analysis.....	37
3.3 Beach Response to Wave Forcing.....	38
3.3.1 Offshore Wave Climate During Observation Period.....	38
3.3.2 Shoreline Variation and Wave Height.....	39

4	DISCUSSION AND CONCLUSIONS.....	62
4.1	Shoreline Position Variation With Distance From Inlet.....	62
4.2	Seasonal Variability in Shoreline Position.....	62
4.3	Beach Morphology Variation – Spatial and Temporal.....	63
4.4	Relationship of Beach Response to Forcing.....	64
4.5	Summary.....	64
APPENDIX		
	APPENDIX: SUPPLEMENTARY FIGURES.....	66
	LIST OF REFERENCES.....	287
	BIOGRAPHICAL SKETCH.....	291

LIST OF TABLES

<u>Table</u>	<u>page</u>
2-1 Table highlighting mean high water and mean range for the area.....	27

LIST OF FIGURES

<u>Figure</u>	<u>page</u>
1-1	Location map of Matanzas Inlet, North Florida Atlantic coast. 20
2-1	Time series of air photos illustrating ~4m/yr southward migration (net narrowing ~3m/yr) of the inlet during February 1995 – January 2008. 28
2-2	Example of survey pattern deemed most efficient at collecting a large aerial extent of data. 29
2-3	Example of scatter diagram. 30
2-4	Example of DEM grid (1m resolution) interpolated from scatter diagram and polygon. 31
2-5	Figure illustrating 30 shore normal transects within the 1.5 km reach of coast directly north of Matanzas Inlet. 32
3-1	Complete record of surveyed, monthly MHW shoreline positions throughout the study reach. 41
3-2a	Temporal beach width of transect 15. 42
3-2b	Temporal beach width of transect 27. 43
3-3	Spatial summary of shoreline change rates over the observation interval. 44
3-4	Histogram showing time at which beach width maximum is reached. 45
3-5a	Cross-shore topographic profile variation at transect 15. 46
3-5b	Cross-shore topographic profile variation at transect 27. 47
3-6a	Time series of survey profiles for transect 15. 48
3-6b	Time series of survey profiles for transect 27. 49
3-7	Colormap illustrating cross-shore and alongshore distributions of temporal topographic variation plotted as standard deviation. 50
3-8a	Figure illustrating MHW shoreline slope for transect 15. 51
3-8b	Figure illustrating MHW shoreline slope for transect 27. 52
3-9	Alongshore compilation of MHW shoreline slopes for each survey plotted as connected lines. 53

3-10	Temporal analysis of beach slopes broken up into two groups according to location.	54
3-11	Combined spatial and temporal analysis of the MHW shoreline beach slope illustrated as a colormap.....	55
3-12	NDBC wave buoy 41012 data illustrating significant wave height (m), wave period (s), and wave direction (degT) during the survey interval.	56
3-13a	Temporal analysis of MHW shoreline position change rate plotted against average significant wave height for each survey interval at transect 15.	57
3-13b	Temporal analysis of MHW shoreline position change rate plotted against average significant wave height for each survey interval at transect 27.	58
3-14a	Cross plot illustrating the relationship between average significant wave height and MHW shoreline position migration rate at transect 3.....	59
3-14b	Cross plot illustrating the relationship between average significant wave height and MHW shoreline position migration rate at transect 26.....	60
3-15	Summary of analyses of potential correlation between shoreline change rate and offshore wave height (H_s).	61

LIST OF ABBREVIATIONS

dGPS	Differential Global Positioning System
DEM	Digital Elevation Model
MHW	Mean High Water, 0.45 m
NGS	National Geodetic Survey
PDBL	Proto-dune Base Line
UTM	Universal Transverse Mercator

Abstract of Thesis Presented to the Graduate School
of the University of Florida in Partial Fulfillment of the
Requirements for the Degree of Master of Science

SEASONAL AND SPATIAL VARIABILITY OF BEACH MORPHODYNAMICS AT AN
AUTONOMOUS TIDAL INLET: MATANZAS INLET, FLORIDA ATLANTIC COAST

By

Katherine Kelly Malone

May 2011

Chair: Peter Adams

Major: Geology

A study of beach topography was conducted along a 1.6 km coastal reach adjacent to the Matanzas Inlet, Florida, an inlet that has not experienced any anthropogenic modification. This thesis describes the seasonal and spatial variability of the mean high water (MHW) shoreline position and cross-shore beach morphology, from January 2009 through February 2010. Results indicate that there is an alongshore variability in the behavior of shoreline position and beach morphology that may be related to the inlet mouth. Beach width and width variability are comparatively large in the southern region (within 500 meters immediately adjacent to the inlet), whereas seasonal signals in beach width are discernable only in the northern region (600 - 1600 meters from the inlet). The northern region displays high topographic variability on the upper beach, near to the proto-dune base line (PDBL); the southern region displays high topographic variability on the lower beach near the MHW shoreline. During summer, the northern portion steepens at the MHW shoreline; the southern portion becomes more gently sloped. Correlation analyses imply that there is some, albeit weak, association between changes beach morphology and offshore wave conditions.

CHAPTER 1 INTRODUCTION

On naturally occurring sandy beaches, beach morphology is influenced by waves and tides. While the influence of waves and tides are well documented on continuous, straight, and planar beaches [*Masselink and Short, 1993; Wright and Short, 1984; Wright et al., 1985; Wright et al., 1987*], these effects are less well understood on beaches adjacent to tidal inlets. At tidal inlets, significant quantities of water and sediment are exchanged between the open ocean and the protected back barrier bay, resulting in hydrodynamic discontinuities (two way jets), and bathymetric discontinuities (ebb shoals and ebb tidal deltas) alongshore. The presence of these discontinuities disturbs the simple, predictable pattern of wave-driven longshore sediment transport, which is critical to coastal morphologic evolution [*FitzGerald, 1996*].

The development of numerical models to simulate coastal geomorphic response to changes in wave climate, sea level rise, and terrestrial sedimentary inputs are currently being developed [*Ashton et al., 2001; Ruggiero et al., in press*] and their improvement will be supplemented by data sets documenting oceanic forcing and beach morphologic change at inlets. Quantifying shoreline variability is only one method of examining the behavior of the coastal system; scientific understanding and engineering solutions require quantitative information regarding the behavior of multiple relevant morphologic characteristics (e.g., beach width, slope, and volume change) to facilitate effective coastal planning [*Stive et al., 2002*].

1.1 Previous Work

Much of the scientific literature regarding beach volumetric change (erosion or accretion), has focused on seasonal variability, which has helped to advance our limited

understanding of intermediate term (annual to decadal) advances and retreats of the shoreline [*Komar and Inman, 1970; Winant et al., 1975; Dolan et al., 1977; Aubrey, 1979; Hayes, 1980; Eliot and Clarke, 1982; Wright et al., 1985; Larson and Kraus, 1995; Stive et al., 2002; Ruggiero et al., 2003; List et al., 2006*].

Through a series of case studies, *Stive et al, [2002]* illustrate potential causes for variability in shoreline evolution through a range of different time and space scales (hours to years/~10 m – 1 km). Although some qualitative observations and correlations between forcing and response attempt to describe the reasons behind shoreline variability (i.e., wave, tide and surge conditions, and climate variations), the authors found it difficult to derive generic quantitative relationships that attempt to describe certain behavior [*Stive et al, 2002*].

Wright and Short [1984] predicted modal beach state and beach surf zone variability in terms of environmental conditions from 1979 – 1982 on shore environments exhibiting the full natural range of beach and surf zone morphodynamics. Although their study was limited to sites in Australia, their morphodynamic states model has been shown to be applicable to other coasts with minor modifications. The results of the authors' field studies [*Short, 1979a, b; Wright et al., 1979a, b, 1982a, b, c; Short & Wright, 1981; Wright, 1981, 1982; Wright and Short, 1983*] culminate in six generalizations that describe relationships among environmental conditions, sediment types, and morphodynamic states. Most applicable to this study, is their generalization that states beaches and surf zones may be dissipative, reflective, or in any of at least four intermediate states depending on local environmental conditions, sediments and wave conditions.

Dissipative beaches are generally low in slope, wherein waves break offshore and continue to lose energy as they cross the wide surf zone; dissipative beaches are highly effective in dissipating wave energy of incident waves. Reflective beaches are steep, wherein dominantly incident waves break close to the shore and immediately wash up on the beach face. The authors elaborate upon these two end members with the addition of several intermediate beach morphologies [*Wright et al.*, 1978, 1979]. The occurrences of these intermediate beach states (longshore bar-trough, rhythmic bar and beach, transverse bar and rip, and ridge-runnel or low tide terrace) vary according to a dimensionless ratio of beach steepness to wave steepness known as the Iribarren number (ξ) [*Wright and Short*, 1983]. Dissipative beaches are found to correspond to very low Iribarren numbers ($\xi = 0.2 - 0.3$), and reflective beaches occur at approximately $\xi > 2$. The four intermediate stages are more difficult to assess in terms of Iribarren number because of widely ranging local conditions of bottom slope and wave parameters. It is valuable to be able to predict short-term fluctuations in these beach states, as the beach state is an important indicator of dominant surf zone processes that influence the likelihood of beach erosion or accretion [*Short and Hesp*, 1982; *Wright*, 1981; *Wright et al.*, 1985].

There have been numerous studies that attempted to correlate changes in beach morphology to event-scale and seasonal changes in wave fields [e.g. *Dubois*, 1988; *List et al.*, 2006; *Quartel et al.*, 2008]. Such studies are valuable in establishing the magnitudes of shoreline variability on the event- and seasonal-scales, which can be compared to long-term shoreline retreat resulting from relative sea level rise.

List et al., [2006] noted an intriguing mystery: how could one section of beach exhibit significant erosion during a storm consistent with the classic storm to fair weather transition, while an adjacent similar section of coast a few kilometers away remains unresponsive? Reversing storm hotspots are referred to as such because the erosion typical of coastal erosional hotspots is reversed by accretion of a similar magnitude to storm induced erosion within a few days or weeks of fair weather after a storm. The authors aimed to quantify the spatial and temporal characteristics of the observed pattern of storm induced erosional variability along with its associated post storm accretion of reversing storm hotspots.

List et al., [2006] studied the large-scale (tens of kilometers) variability of two sandy, uninterrupted, shorelines of the US east coast for three years, 45 km on Cape Cod, Massachusetts, and 133 km on North Carolina's Outer Banks. Six wheeled amphibious all terrain vehicles (ATVs) were used as a platform for GPS measurements during low tide. Data gathered included three dimensional shoreline positions of MHW tidal datum's intersections with beach foreshore slopes along a shore parallel transect. Measurements were conducted at three intervals: pre-storm, storm, and post-storm for eight storms on the Outer Banks and seven storms on Cape cod of the Nor'easter type. Shoreline change was then found as the difference between shoreline positions surveyed on two dates. NDBC buoys provided additional wave and tide information for both locations.

Reversing storm hotspot patterns suggest coherent processes acting over large distances. These processes control the degree to which sand is removed from the subaerial beach during storms. *List et al.*, [2006] provide several hypotheses that

attempt to explain the nature of these processes. Areas exhibiting reversing storm hotspot response may lack a nearshore bar prior to storm initiation, thereby allowing more wave energy to act upon the shore. This is in contrast to areas with one or more nearshore bar(s) that dissipate offshore wave energy; however, the responsible processes that act to alter the nearshore bars remain unknown. Additional hypotheses include effective underlying geologic framework and longshore variations in wave characteristics; however, preliminary wave modeling using SWAN [Booij *et al.*, 1999] fail to reveal any longshore variation consistent with the pattern of reversing storm hotspots. The results of the authors' work demonstrate that storm induced hotspots may be the result of a variety of processes, and the response of the shoreline to storms is complicated and requires further understanding and research [List *et al.*, 2006].

Dubois [1988] sought to understand the nature of a cyclic beach along a shore segment of the Delaware coast, and presented evidence that attempted to explain how the wave regime affected beach topography and beach volume. The author conducted a beach survey along the south area of Dewey Beach in Delaware Seashore State Park where the long-term beach erosion was between 0.6-0.9 m/yr [Kraft *et al.*, 1978]. Wave conditions, specifically mean monthly surge variability, were estimated from NOAA tide tables measured in the Indian River Bay near the Indian River Inlet. Six profiles, spaced 40 m apart, extending from a 200 m long baseline were surveyed one to three times a month from May 3, 1982 until June 1983. The author concluded that beach topography and beach volume varied with changes in wave regime in phase with winter and summer seasons. During the winter, when the magnitude and frequency of waves were higher, the beach shape was concave upward. Additionally, the concave upward profile

was consistent with when the beach was at its maximum sediment volume. *Dubois* [1988] also found an inverse relationship between the mean monthly sediment volume and the mean monthly surge variability. High surge levels occurred with large waves, while low surge levels occurred with small waves. During the winter, surge variability was high and sediment volume was low. In the summer, surge variability was low and sediment volume was high.

Quartel et al. [2008] conducted monthly beach surveys over a 1.5 km reach of coast at Noordwijk, in The Netherlands, to investigate the dependence of seasonal variability in shoreline position and beach volume on offshore wave characteristics. Seasonal patterns show a narrow, large volume beach in the summer, and a wide small volume beach at the end of the winter, in general agreement with seasonally-averaged, offshore wave conditions. In spite of general seasonal agreement, the daily- to weekly-averaged wave conditions did not show a clear, correlative relationship with beach response on the same time scale, which the authors attribute to antecedent morphology preceding storms [*Quartel et al.*, 2008].

Fenster and Dolan [1996] used aerial photography to investigate the influence of inlets on beach morphodynamics at two locations along the Atlantic coast: one wave dominated site at the Outer Banks of North Carolina (11 photographs from 1949-1986), and one tide dominated site at the Virginia Barrier Islands (9 photographs from 1949-1989). While their study is limited to snapshots in time and is focused on large-scale (5-15 km) beach morphodynamics, the authors concluded that (1) the barrier zone in which inlet processes dominate shoreline trends can extend to distances of up to 4 - 5 km

from an inlet, and (2) the zone in which inlet related processes influence shoreline trends can extend to distances of up to 6 -13 km [*Fenster and Dolan, 1996*].

In a study aimed largely at understanding the hydrodynamic discontinuities and sediment interaction at modified coastal inlets, *Dean* [1988] implores the necessity to understand the complex behavior of naturally occurring inlets. This is not necessarily for navigational or recreational necessities, but because the associated effects of sand transport on adjacent shorelines depend substantially on longshore sediment transport. Dean believes being able to predict the detailed behavior of inlets must be the subject of considerable future research [*Dean, 1988*].

1.2 Problem Statement and Objectives

This thesis presents the results of a field based monitoring program that was conducted to: (1) quantify spatial and temporal variability of beach size and shape adjacent to a natural inlet, and (2) identify the forcing responsible for the morphologic changes observed. The study examines changes in shoreline position (beach width) for one vertical elevation datum - mean high water (MHW), and beach profile change at 30 cross-shore transects over 14 months (January 2009 – February 2010) at Matanzas Inlet on the North Florida Atlantic coast (Figure 1-1). Correlations between offshore wave conditions and the beach morphologic response are investigated to explore potential links between oceanic forcing and geomorphic response.

A simple hypothesis motivates the research: tidal inlet dynamics exert a spatially-limited influence on the temporal behavior of nearby shoreline position and beach morphology. This hypothesis can be addressed by targeting a series of questions, which are used to guide the analyses in this thesis:

1. How does the shoreline position (beach width) vary as a function of distance from an inlet?
2. Does the spatial variability in shoreline position (beach width) exhibit a seasonal variability?
3. How does beach morphology (profile shape) vary as a function of distance from an inlet?
4. Does the spatial variability in beach morphology (profile shape) exhibit a seasonal variability?
5. How do temporal trends in shoreline position (beach width) and beach morphology (profile shape) correlate with offshore wave conditions, thought to dominate the forcing?



Figure 1-1. Location map of Matanzas Inlet, North Florida Atlantic coast. The study area includes ~1600 m on the northern of the beach north of the inlet mouth.

CHAPTER 2 METHODS

2.1 Study Site

The Matanzas Inlet, located ~7.8 km south of the intersection of Florida routes 206 and A1A, constitutes the southern end of Anastasia Island, a 24 km-long barrier island on the North Florida Atlantic coast. It provides a connection between the Matanzas River and the Atlantic Ocean, and is the only inlet (of 19 on the Florida Atlantic coast) that has not experienced substantial anthropogenic modification [*Mehta and Jones, 1977*].

2.1.1 Historical Landform Changes

This inlet has historical significance, as it is the site of Spanish Colonial Fort Matanzas, which was constructed in 1742 to protect the southern entrance into the Matanzas River and the city of St. Augustine. At the time of construction, the fort was situated at the mouth of the inlet to the Atlantic Ocean. Today, the inlet is located ~1200 m south of the Fort, testifying to its migration. According to historical maps, the northern shoreline of the inlet is migrating southward at ~4 m/yr (761 m/191 yrs), and the southern shoreline of the inlet is migrating southward at ~1 m/yr (229 m/191 yrs), netting a total narrowing of the inlet of ~3 m/yr [*Dunkle, 1964*]. This behavior is evident from the time series of air photos shown in Figure 2-1.

2.1.2 Site Description

This study focused on the 1600-meter alongshore reach of intertidal beach on the north side of the Matanzas Inlet. The beach on the south side of the inlet is armored with riprap, for stabilization purposes and was not investigated in this study. The beach in the study reach varies in width (measured from dune base to 0 m elevation contour,

NAVD 88) between ~40-100 meters. The width of the barrier island itself, at the study site, varies from ~300-500 meters.

Tidal information was gathered from benchmark sheets for station number 8720587 located at Saint Augustine Beach and operated by NOAA. The station's benchmark sheet denotes a MHW of 0.45 m and MLW of -0.91 m resulting in a mean range of 1.35 m ['St. Augustine Beach, FL Station ID: 8720587 Station Information,' 2005; *Weber et al.*, 2005].

2.2 GPS Surveys

A total of 14 monthly surveys were conducted between January 2009 and February 2010, during the lunar new moon phase at low tide. Specific details, including tide level and number of survey points collected, are provided in Table 2.1. The beach and northern inlet mouth were surveyed on foot with backpack-mounted differential Global Positioning System (dGPS) Trimble TSC2 controllers and 5800 mobile backpack antennas connected to a consistently occupied HPB450 radio base station. The base station was set up over a Department of Environmental Protection monument (identification number: DEP J796) located at Easting: 477861.574 m, Northing: 3287070.280 m (UTM Zone 17R), Elevation: 6.312 m (NAVD 88), on the boardwalk of Fort Matanzas National Monument, St. Augustine, Florida.

Several survey patterns were employed throughout the study. The survey pattern deemed most efficient at collecting a large areal extent of data consisted of various oblique transects at which the controllers would collect northing, easting, and elevation values at each meter along the traverse. An example of the data point distribution collected during a typical survey is shown in Figure 2-2, and maps of the beach traverses, from each of the 14 site visits, are compiled in Appendix A-1 (Page 66).

2.3 Data Processing

Following each dGPS survey, elevation data were uploaded from the survey controllers into the Trimble Business software[®]. After being quality checked and, if necessary, corrected for elevation discrepancies, elevation data were organized in a spreadsheet and exported to comma-separated-values (.csv) ascii text files, which were considered to be a general format that could be imported into most data analysis software. Periodically, hourly summary wave data (significant wave height, spectral peak period, and peak direction) were obtained from the NDBC website [‘Station 41012 (LLNR 845.3) - St. Augustine, FL 40NM ENE of St Augustine, FL,’ 2011] for the St. Augustine mid-shelf wave buoy (#41012). These data were used to compare with the shoreline position, and beach morphology characteristics after dGPS data processing. All analyses in this study were conducted using MATLAB software by The Mathworks, Inc.

2.3.1 Digital Elevation Model Grid Generation

For each of the 14 surveys conducted, the quality-controlled dGPS data point clouds were initially plotted in scatter diagrams that use color to denote elevation. An example of this plot is provided in Figure 2-3, and the complete set of 14 plots is provided in Appendix A-2 (Page 86). These scatter plots were produced with the MATLAB script named ‘dgpsMtnzsScatter3.m’.

Also shown in the example Figure 2-3, is the outline of the data polygon used to convert the data point clouds to regularly spaced Digital Elevation Model (DEM) grids described below. For each of the 14 surveys, a unique polygon was drawn to maximize the data coverage for each survey, while minimizing the error arising from interpolating

elevations over a broad region where data may be absent. Each unique polygon is plotted on each of the point cloud scatter diagrams in Appendix A-2 (Page 86).

Regularly-spaced rectangular grids, of 1 m resolution and of size sufficient to cover each survey polygon, were generated for each of the 14 surveys. The data point cloud and polygon for each survey were used to interpolate a topographic surface onto each grid. An example of the resulting DEM grid, showing the unique survey polygon, is provided in Figure 2-4, and the complete set of 14 DEM grids is provided in Appendix A-3 (Page 94). These DEM grid plots were produced with the MATLAB script named 'dgpsMtnzsDEMGrid.m'.

2.3.2 Cross Shore Transect Generation

Thirty (30) shore-normal transects within the 1.5 km reach of coast directly north of Matanzas Inlet were generated, along which MHW shorelines and topographic profiles could be interpolated (Figure 2-5). Transects were anchored on a proto-dune base line (PDBL), identified in the field to be the furthest-seaward cross-shore position where the lower dune is vegetated with pioneer species. For each transect, the PDBL occupies the position of 100 m from the landward transect end. Transects were 330 m-long and spaced 50 m apart along the PDBL, with an along transect point spacing of 1 m. This procedure was executed with the MATLAB script named 'dgpsMtnzsTransectOrienter.m'.

2.3.3 Cross-shore Profile Interpolation

The 30 shore-normal cross-shore transects were overlain onto each of the 14 survey DEM grids to interpolate cross-shore topographic profiles along the transects. The cross shore coverage at each transect varies significantly over the survey series due to the range of low tide elevations during which the surveys were conducted (Table

2-1) and restrictions imposed upon beach access for areas marked off as shorebird nesting habitat during April-September of 2009. The complete set of 14 survey profiles as each of the 30 cross-shore transects is provided in Appendix A-5 (Page 138). These cross-shore profile plots were produced with the MATLAB script named 'dgpsMtnzsProfileBuilder.m'.

2.3.4 Shoreline Interpolation and Beach Width Calculation

MHW shoreline positions along each transect were determined by finding the shoreward-most position of intersection between the interpolated topographic profile and the MHW elevation of 0.45 m NAVD88. Beach width was then determined by subtracting the position of the PDBL (100m) from the shoreline position. This procedure was repeated, for each of the 30 shore-normal transects and for each of the 14 surveys, with a MATLAB function called 'dgpsMtnzsShorelinesBuilder.m', totaling 420 shoreline position calculations. It should be noted that 31 of the 420 (7.5%) shoreline calculations resulted in no value (NaN), because of mistakes in the data collection procedure during some of the surveys.

2.3.5 Beach Slope Calculation

Calculation of beach slope is an elusive task due to the fact that most beaches are not planar, making a simple "rise over run" calculation highly dependent on the portion of the topographic profile being considered. In this thesis, the slope is quantified by calculating a least squares residual fit as a first-order polynomial trend line to the portion of profile beginning 5 meters landward of the MHW shoreline position, and ending 5 meters seaward of the MHW shoreline position. This allows for consistency of slope calculation by linking to a datum-derived portion of the beach - i.e. the portion on either side of the MHW shoreline.

2.3.6 Wave Conditions Data Processing

NOAA's NDBC operates a 3 m discus buoy that is anchored at a depth of 37.2 m, and located at [30.041 N 80.533 W need to convert to UTM] off the coast of Saint Augustine, FL. Available online ['Station 41012 (LLNR 845.3) - St. Augustine, FL 40NM ENE of St Augustine, FL,' 2011], standard meteorological data chronicles wave, wind, and solar radiation conditions. Present and historical data are available to download as a text (.txt) file. For the purposes of this project, wave height, dominant wave period, and wave direction were imported and analyzed with the MATLAB script named 'MakeWvFigs.m'.to summarize offshore wave conditions.

Table 2-1. Table highlighting mean high water and mean range for the area. Survey date, tide level and number of data points collected for St. Augustine Beach tidal station 8720587 are listed ['St. Augustine Beach, FL Station ID: 8720587 Station Information,' 2005; *Weber et al.*, 2005].

	Survey Date	Tide Level (m) (NAVD 88)	Number of Data Points Collected
1	1/16/2009	-1.05	8,159
2	2/20/2009	-0.75	12,025
3	3/24/2009	-0.87	9,843
4	4/24/2009	-1.02	10,669
5	5/22/2009	-0.99	5,863
6	6/22/2009	-1.14	12,386
7	7/21/2009	-1.17	16,424
8	8/19/2009	-1.14	11,996
9	9/17/2009	-1.05	15,262
10	10/19/2009	-0.99	11,564
11	11/18/2009	-0.93	15,118
12	12/11/2009	-0.93	12,364
13	1/15/2010	-1.02	15,976
14	2/12/2010	-0.96	12,470

St. Augustine Beach, Atlantic Ocean

Mean Range = 1.35 m

MHW = 0.45 m

MLW = -0.9 m

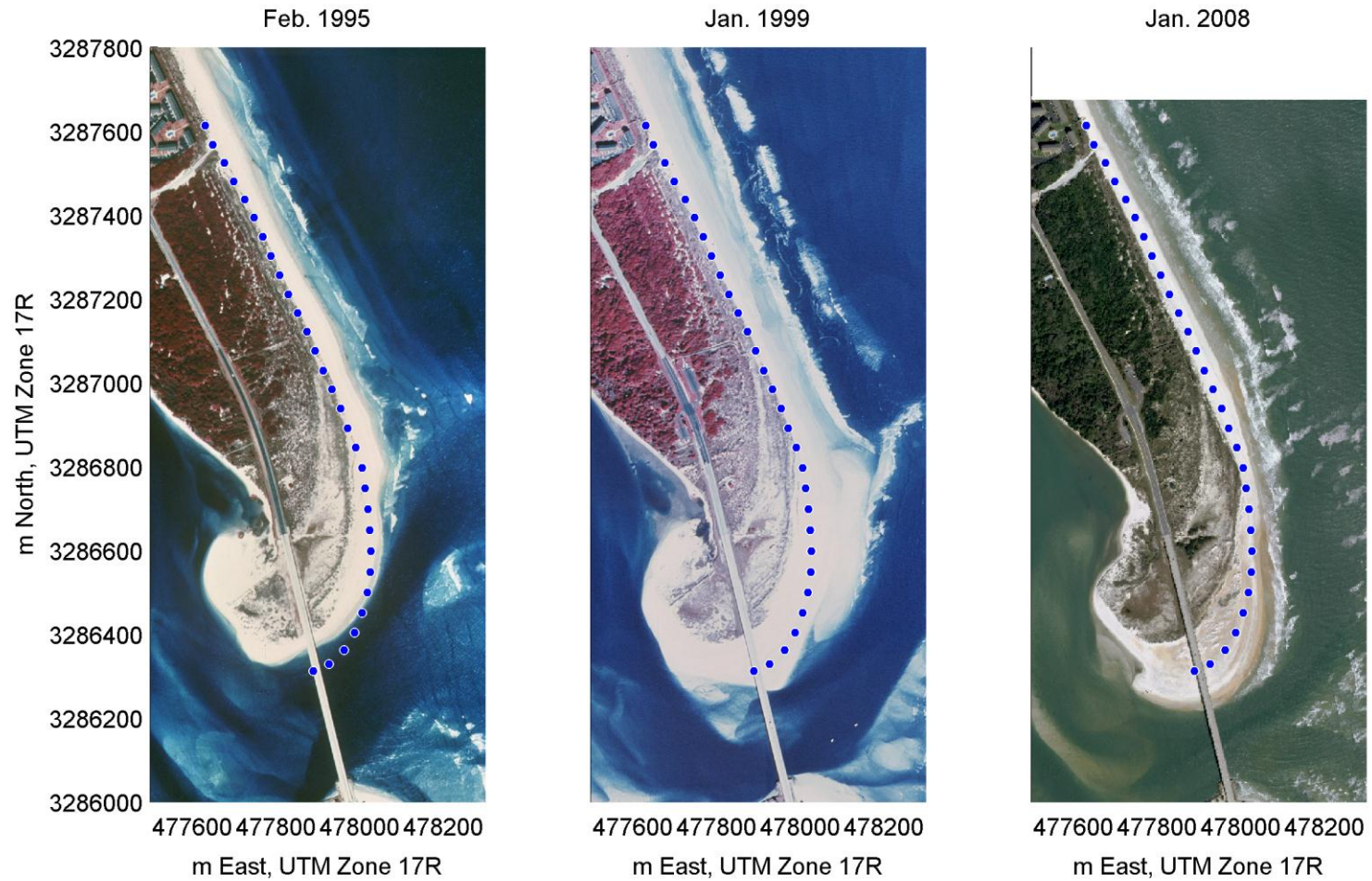


Figure 2-1. Time series of air photos illustrating ~4m/yr southward migration (net narrowing ~3m/yr) of the inlet during February 1995 – January 2008. The blue dots are a consistently occupied line (later termed as the proto-dune base line (PDBL)), occupying the position of 100 m from the landward transect end.

November 18, 2009

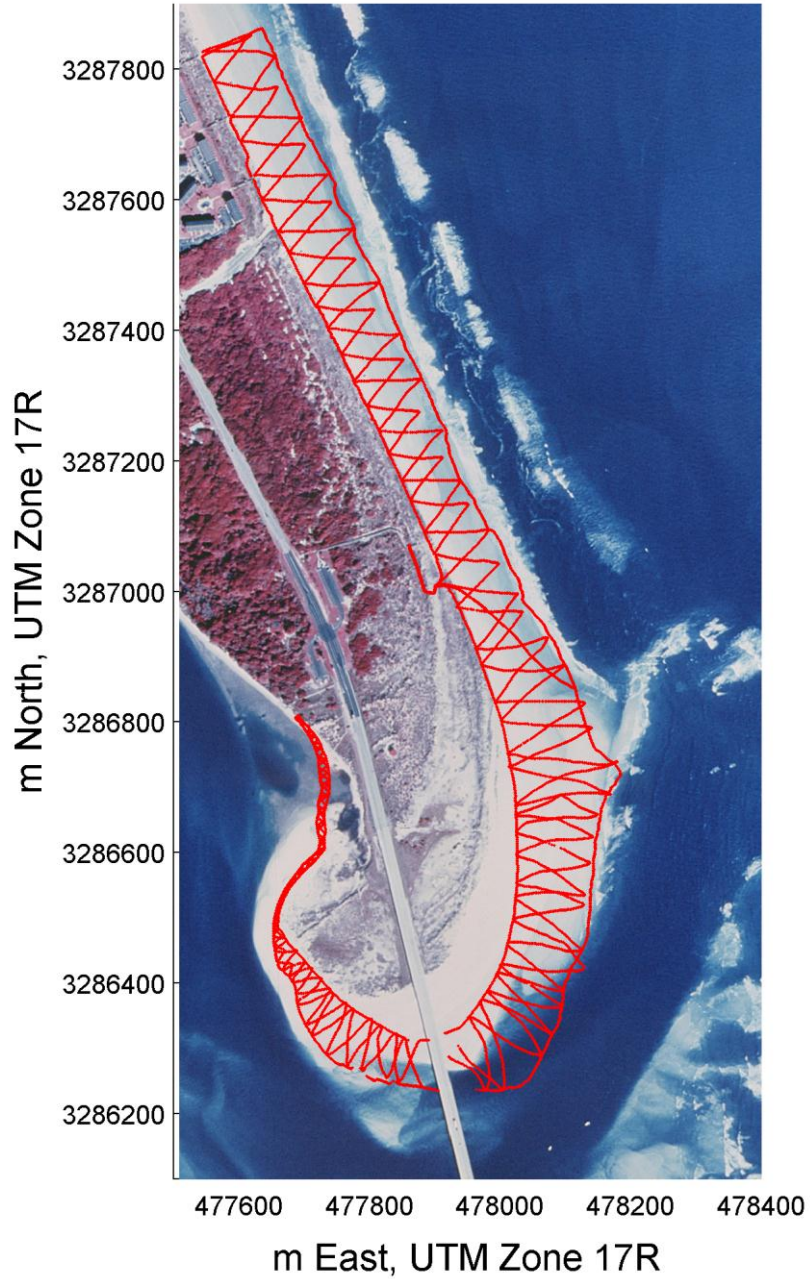


Figure 2-2. Example of survey pattern deemed most efficient at collecting a large aerial extent of data. Various oblique transects collect northing, easting, and elevation values at each meter along the traverse. All survey patterns are found in Appendix A-1 (Page 66).

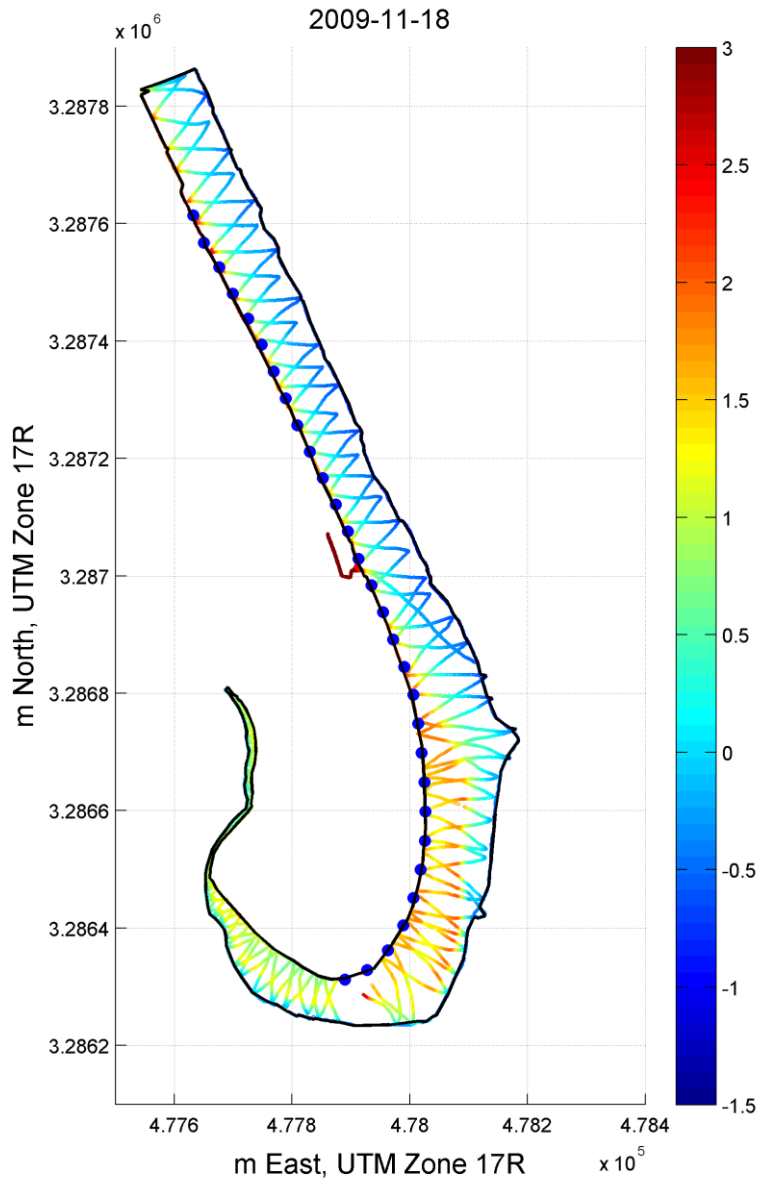


Figure 2-3. Example of scatter diagram. Each data point contains a northing and easting, while color denotes elevation. Also shown is the dark black line that highlights the unique polygon for this survey month. All scatter diagrams are found in Appendix A-2 (Page 86). Colorbar denotes elevation in meters (NAVD88).

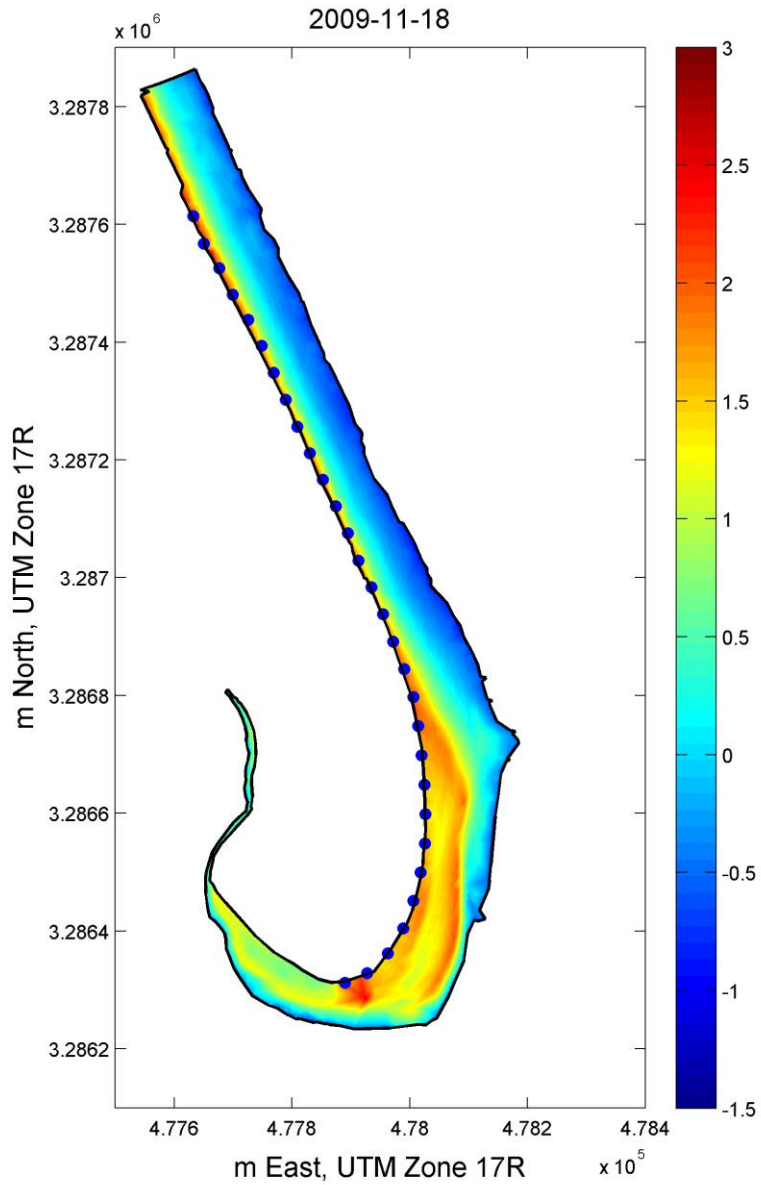


Figure 2-4. Example of DEM grid (1m resolution) interpolated from scatter diagram and polygon. All DEMs are found in Appendix A-3 (Page 94). Colorbar denotes elevation in meters (NAVD88)

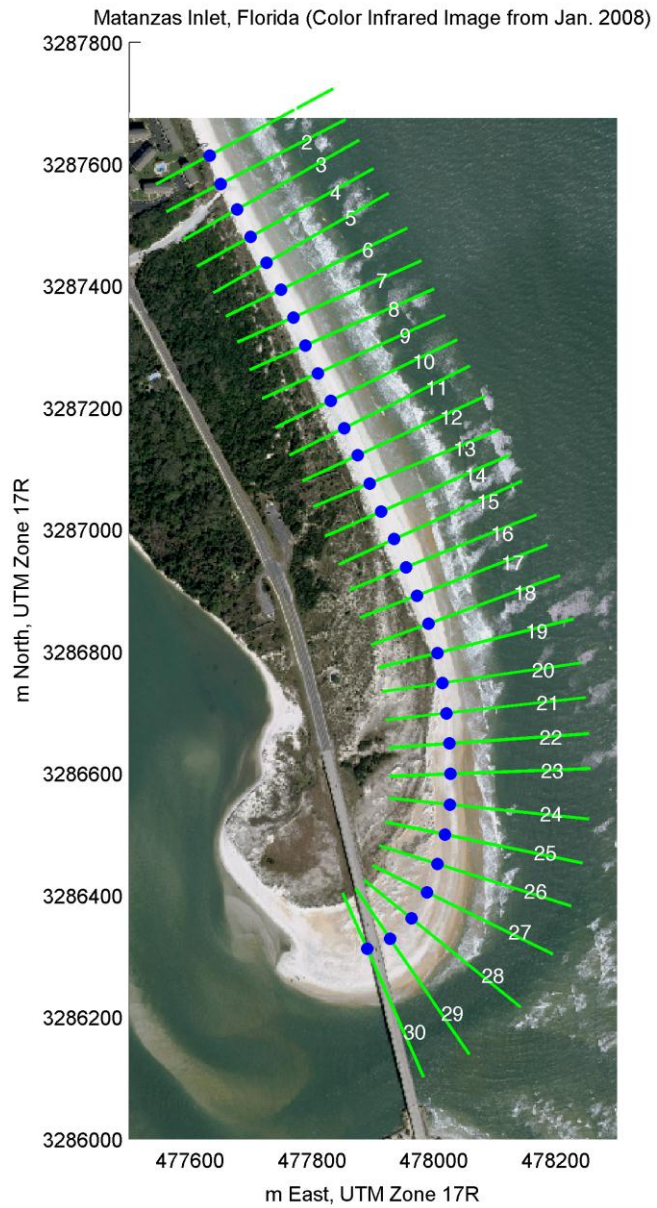


Figure 2-5. Figure illustrating 30 shore normal transects within the 1.5 km reach of coast directly north of Matanzas Inlet. Blue dots denote the proto-dune base line (PDBL). PDBL is 100 m from the landward end of each transect.

CHAPTER 3 RESULTS AND ANALYSIS

In this chapter, the data compilations are presented, organized, and analyzed to address the specific research questions presented in section 1.2; namely, how does beach morphology vary within the vicinity of an inlet? More specifically, how do the shoreline positions (beach widths) and cross-shore profiles vary alongshore with respect to distance from the inlet? To do this, variations in shoreline position (beach width) and cross-shore morphology throughout one year of observation are examined. Then, wave forcing responsible is considered by correlating the changes witnessed on the beach with the offshore wave characteristics.

3.1 Shoreline Position / Beach Width

3.1.1 Spatial Variation of Shoreline Position (Beach Width)

The complete record of surveyed, monthly MHW shoreline positions throughout the study reach, as well as mean shoreline position and standard deviation over the entire observation period, are presented in Figure 3-1. Beach widths are calculated by subtracting 100 m from each transect's shoreline position, to account for the location of the PDBL, the morphologic feature that anchors the cross shore topographic analyses in this study. The most striking feature of Figure 3-1 is the abrupt change in shoreline position (beach width) in the vicinity of Transect 20, where the beach width more than doubles from ~40 m, in the northern portion of the reach, to ~90 m directly next to the inlet. The variability of shoreline position experiences a modest increase from the northern portion to the southern portion, as illustrated by the standard deviation values shown on Figure 3-1.

3.1.2 Temporal Variation of Shoreline Position (Beach Width)

For each transect, a linear fit of shoreline position (beach width) through time rendered a shoreline change rate during the 14-month observation interval. Examples of these analyses, for the northern and southern portions of the study area, are provided in Figures 3-2A and 3-2B, respectively. Temporal variation plots of MHW shoreline position (beach width) for all transects can be found in Appendix A-4 (Page 108). Negative change rates denote a shoreward migration of the shoreline (beach narrowing), whereas positive change rates reflect a seaward migration of the shoreline (beach widening). The spatial summary of shoreline change rates over the observation interval is provided in Figure 3-3. Transects 1-17 and 23-25 reflect a beach narrowing, while transects 18-22 and 26-30 reflect beach widening over time. Values range from -11.9 cm/day (transect 13) to 14.7 cm/day (transect 28).

For transects 1-17, change rates were negative, ranging from -11.9 cm/day (transect 13) to -2.1 cm/day (transect 1). Transects 18 illustrates a change rate nearing zero (0.5 cm/day), as the shoreline variations transition from negative trends to a period of positive trends. Transects 18-22 display positive change rates, ranging from 0.5 cm/day (transect 18) to 10.6 cm/day (transect 20). A brief aberration occurs at transects 23-25, as this portion of the inlet experiences a return to negative trends ranging from -0.3 cm/day (transect 25) to -3.4 cm/day (transect 24). Transects 26-30 return to positive change rates, ranging from a minimum of 0.8 (transect 30), to including the greatest positive change rate in the data set of 14.7 cm/day (transect 28).

Figure 3-4 is a histogram that shows the time at which each transect experiences maximum beach width over the survey interval. Each bin corresponds to a survey date and contains the number of transects at which beach width was at its maximum for that

interval. Transects 1-9 reach their maximum beach width during the summer months (June and July of 2009). Transects 10-19 reach their maximums during the late winter months (February and March of 2009), with one exception during February 2010. For transects 20-30, the data do not behave consistently, as beach width maxima are reached during February 2009, July 2009, August 2009, October 2009, November 2009, January 2010 and February 2010.

3.2 Beach Morphology / Profile Shape

3.2.1 Spatial and Temporal Variation of Cross–Shore Profiles

Examples of cross-shore profiles for the 14 surveys are given in Figure 3-5A (Transect 15) and Figure 3-5B (Transect 27). Also shown in Figures 3-5A and 3-5B, the cross-shore distributions of temporal data coverage along each transect, and the cross-shore distribution of the standard deviation of elevation along each transect. Simple observations of the cross-shore profiles reveal that the northern portion of the study reach contains, generally, planar beach profiles (Transects 1-20), whereas profiles within the southern portion (Transects 21-30), adjacent to the inlet mouth, exhibit a fair greater vertical relief.

Another way of examining the time series of cross-shore profile evolution is provided in Figures 3-6A and 3-6B, which display complete time series sets of 14 surveyed profiles at two specific transects. The cross-shore topography is shown in color, and the migration of the shoreline is given as black dots. Locations of the PDBL are also provided (position 100 on all profiles), allowing for an uncomplicated display of beach width through time. The compilation of these diagrams for each of the transects is provided in Appendix A-5 (Page 138).

3.2.2 Analysis of Variation of Cross–Shore Profiles

To better understand cross-shore topographic profile variation at this site, standard deviation analyses were conducted. To account for the fact that not all profiles had equal coverage during all surveys, we establish a minimum number of observations, 10 out of 14 total surveys (71%), required to compute a meaningful standard deviation. These portions of the profiles are shown in red on the middle and lower panels of Figures 3-5A and 3-5B. The compilation of these diagrams is located in Appendix A-6 (Page 167).

Low standard deviation values (0.01 - 0.44 m) reflect low variability, or a more stable profile; profiles with low standard deviation are typical of profiles farther from the inlet. High standard deviations (0.45 - 0.7 m) are characteristic of cross-shore profiles where the variability about the mean is relatively high, and is typical of the profiles closer to the inlet.

Of particular interest are two characteristics of the standard deviation analyses: (1) Where are the greatest variations in elevation with respect to alongshore position within the study reach?, and (2) Where are the greatest variations in elevation with respect to cross-shore position within the study reach, and how are the cross-shore maxima in standard deviation distributed alongshore? These questions can be addressed by examination of Figure 3-7, in which both cross-shore and alongshore distributions of temporal topographic variation are displayed as a colormap.

The analysis of Figure 3-7 illustrates a seaward shift in the peak (maximum) standard deviation values as one moves from north to south, from lower to higher number transects, toward the inlet. The highest standard deviation values, in the entire data set, are at the most seaward positions immediately adjacent to the inlet. At transects 1-18,

the highest topographic variability occurs within 20-60 meters of the PDBL, whereas at transects 20-30, the highest topographic variability is 60-120 meters seaward of the PDBL. An isolated cloud of high variability, comparable in magnitude to the highest standard deviation values observed within the entire data set (> 0.5 m), occupies the upper beach from transects 11-15.

3.2.3 Beach Slope Analysis

Graphical examples of the MHW shoreline slope calculations, described in Section 2.3.5, are provided in Figure 3-8A and 3-8B, for transects 15 and 27, respectively. The compilation of all slope calculations for each of the 389 MHW shorelines identified is provided in Appendix A-7 (Page 197). The high vertical exaggeration (75x) distorts the slope calculation, but also permits some general evaluation of beach slope change by simple inspection. Figure 3-9 shows alongshore compilations of slopes for each survey (plotted as connected lines). In general, beach slopes are lower in the northern portion of the study reach (Transects 1-20), than in the southern portion (Transects 21-30) adjacent to the inlet. Figure 3-10 presents a simple temporal analysis of the beach slopes broken up into two groups according to location: the northern portion of the study reach (Transects 1-20) shown in blue, and the southern portion of the study reach (Transects 21-30) shown in red. Comparisons of the temporal means of the two groups illustrate that during the summer (July 2009, in particular), the two regions behave quite differently – the northern portion steepens at the MHW shoreline, while the southern portion becomes more gently sloped. Also, it is striking that during the end of the observation period (Oct. 2009- Feb. 2010), the southern portion of the study reach witnesses a pronounced increase in MHW shoreline slope that is not found in the

northern portion of the study reach. A combined spatial and temporal analysis of the MHW shoreline beach slope is compiled as a colormap in Figure 3-11.

3.3 Beach Response to Wave Forcing

Wave data was obtained from the St. Augustine wave buoy number 41012, owned and operated by the National Data Buoy Center (NDBC). The buoy is a 3 meter discus buoy in 37.2 m of water located at Easting: 544990 and Northing: 3323463 (UTM Zone 17), off the coast of St. Augustine, Florida [Station 41012 (LLNR 845.3) - St. Augustine, FL 40NM ENE of St Augustine, FL, 2011]. Figure 3-12 highlights the area's significant wave heights, wave periods, and wave directions for the survey period. Also shown in Figure 3-12, are average significant wave height, average wave period, and modal wave direction for the survey interval.

3.3.1 Offshore Wave Climate During Observation Period

Wave heights range from 1-1.6 m during January, February, March, April, May, October, November, and December of 2009. During the quiescent summer period, wave heights range from 0.74 - 0.89 m, except for a storm event in August, which caused an increase in significant wave height average to 1.14 m.

The wave data illustrates three 'events' during the survey period. Event one was a storm that occurring around May 20, 2009. Significant wave heights of 5 m were recorded at the buoy. Additionally, there was a shift in modal wave direction from 57 degrees to 93 degrees (37 degrees and 73 degrees shore normal).

The second event, Hurricane Bill, was a tropical depression that formed off the coast of Africa around August 15, 2009, tracked West-Northwest, became a Category 4 hurricane (according to the Saffir-Simpson Hurricane Scale), and dissipated August 24, 2009; however, effects of the storm were recorded until August 28, 2009 as wave

heights neared 3 m. The storm affected the East coast of the United States, Bermuda, Nova Scotia, and Newfoundland. Unfortunately, the buoy malfunctioned and did not record data from August 15, 2009 until August 25, 2009. Modal wave direction data for this period was recorded as 78 degrees shore normal.

Event three, is characterized not necessarily as an 'event', but as a period of highly oscillatory significant wave heights from the end of October 2009 until February 2010. Average significant wave heights during this period ranged from 1.24 to 1.60 m, while average significant wave heights during January and February of 2009 were noticeably steadier, ranging from 0.99 to 1.17 m.

3.3.2 Shoreline Variation and Wave Height

MHW shoreline position change rates, calculated as the difference of two monthly MHW shoreline positions divided by time between measurements, are plotted against average significant wave height over the interval between surveys. Examples are provided in Figures 3-13a (transect 15) and 3-13b (transect 27). Shoreline variation and wave height time series display for all 30 transects are provided in Appendix A-8 (Page 227).

The most striking feature on Figures 3-13a and 3-13b are the significant wave height peak of ~1.6 m during the October/November 2009 interval. During this period, nearly all transects (except 17-22) experience a narrowing of the beach, ranging from -0.1 to -0.4 m/day. From January through April 2009 survey period, average significant wave height increases from ~1 to 1.3 m. During this period, transects 1-7 demonstrate a similar seeming stepwise decrease in MHW shoreline position migration rate. The transition from the quiescent summer June/July/August 2009 interval to the August/September 2009 interval is interesting, in that significant wave heights jump

from ~0.7 to ~1.1 m. The beach responds by narrowing in transects 1-21 and transects 24-27.

Transect 18 behaves according to the accepted conceptual model of shoreline position change to wave height [Dean, 1991]. When wave heights increase, the beach narrows. During the summer, when wave heights stabilize at relatively low heights, the beach remains near equilibrium, hovering around 0 m/day of MHW shoreline position migration rates. Then, when wave heights increase between August and September 2009, the beach narrows, somewhat drastically, following its seemingly stable summer position. Wave heights calm between September/October 2009 and the beach responds by widening.

Analyses of cross plots (average significant wave height vs. shoreline position migration rate of MHW) render inconsistent, yet intriguing, results. Results for two example transects (Transects 3 and 26) are provided in Figure 3-14, and illustrate the apparent negative correlation between the two variables. Cross plots between these two variables for each of the 30 transects can be found in Appendix A-9 (Page 257).

Correlation coefficients, calculated for the proposed wave height – shoreline change relationship for each of the 30 transects, are compiled in the upper panel of Figure 3-15. Of the 30 transects analyzed, 22 exhibit negative correlations between offshore wave height and shoreline change. Results of the test of statistical significance (Student's t test) are provided in the lower panel of Figure 3-15. Of the 22 transects that exhibit a negative correlation, 7 (32%) transects have a t-statistic which exceeds the critical t value for a statistically significant correlation at the 90% confidence limits.

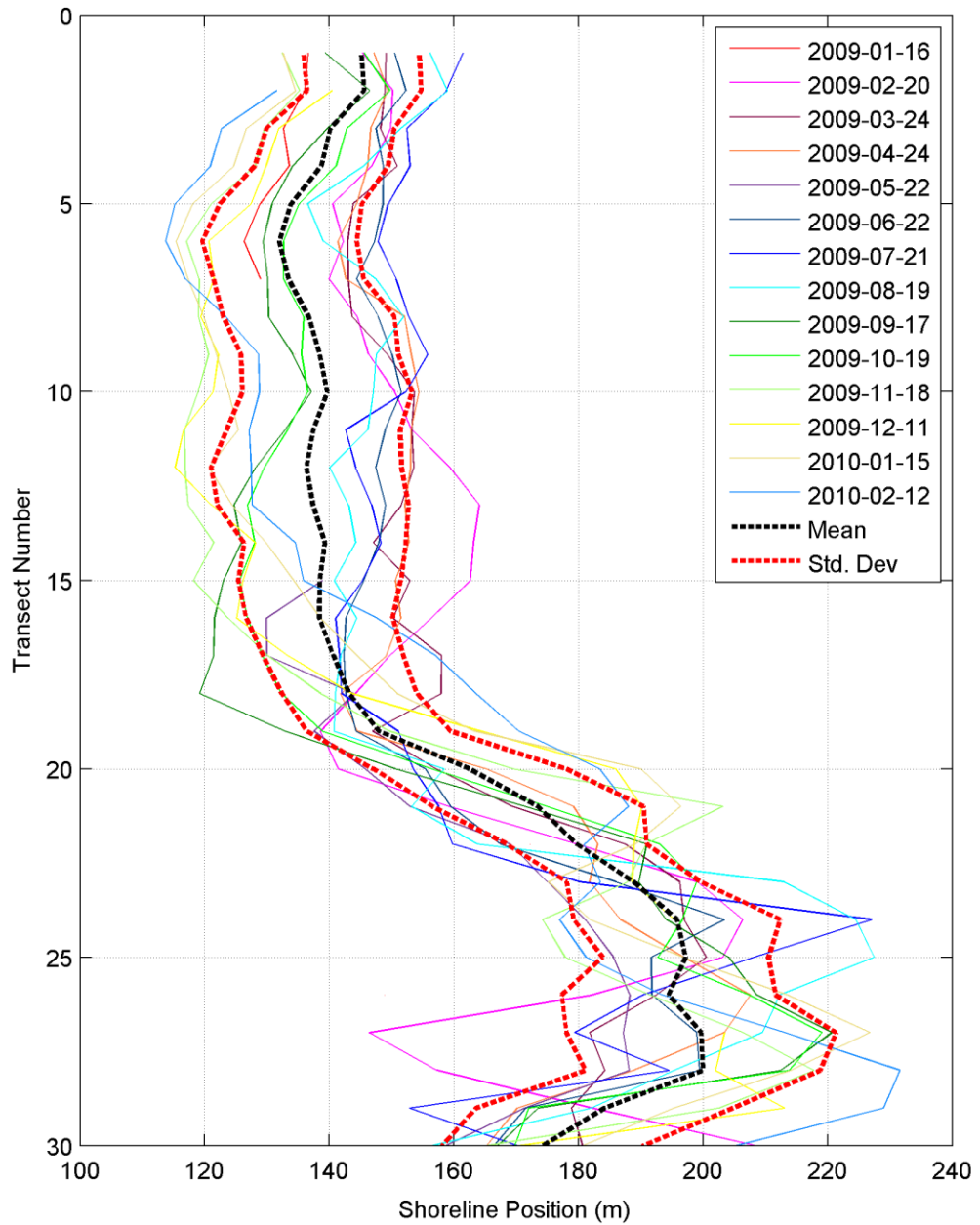


Figure 3-1. Complete record of surveyed, monthly MHW shoreline positions throughout the study reach, including mean shoreline position and standard deviation of entire observation period. The location of transects are listed in Figure 2-5.

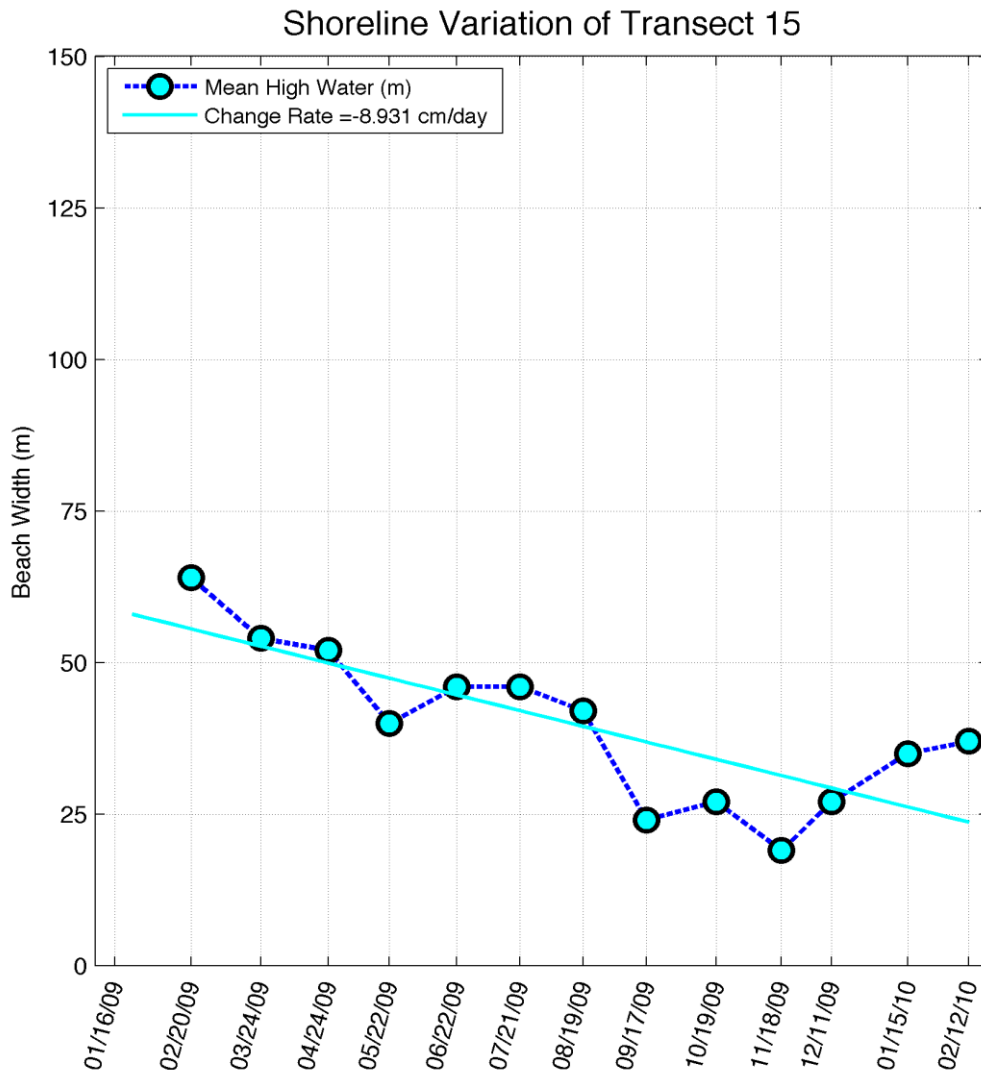


Figure 3-2a. Temporal beach width of transect 15. A linear fit of the data rendered a change rate. Negative change rates denote a landward migration of the shoreline position.

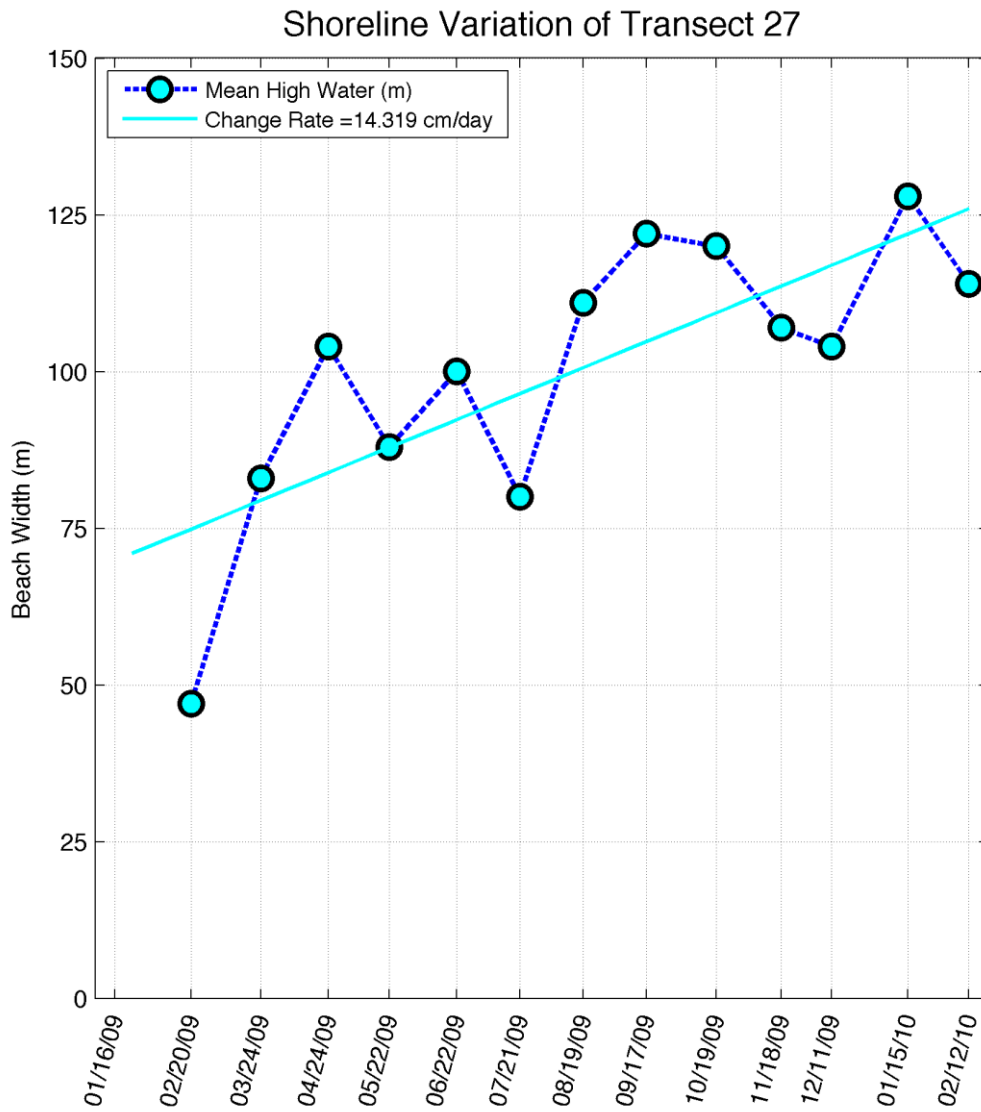


Figure 3-2b. Temporal beach width of transect 27. A linear fit of the data rendered a change rate. Positive rates denote a seaward migration of the shoreline position.

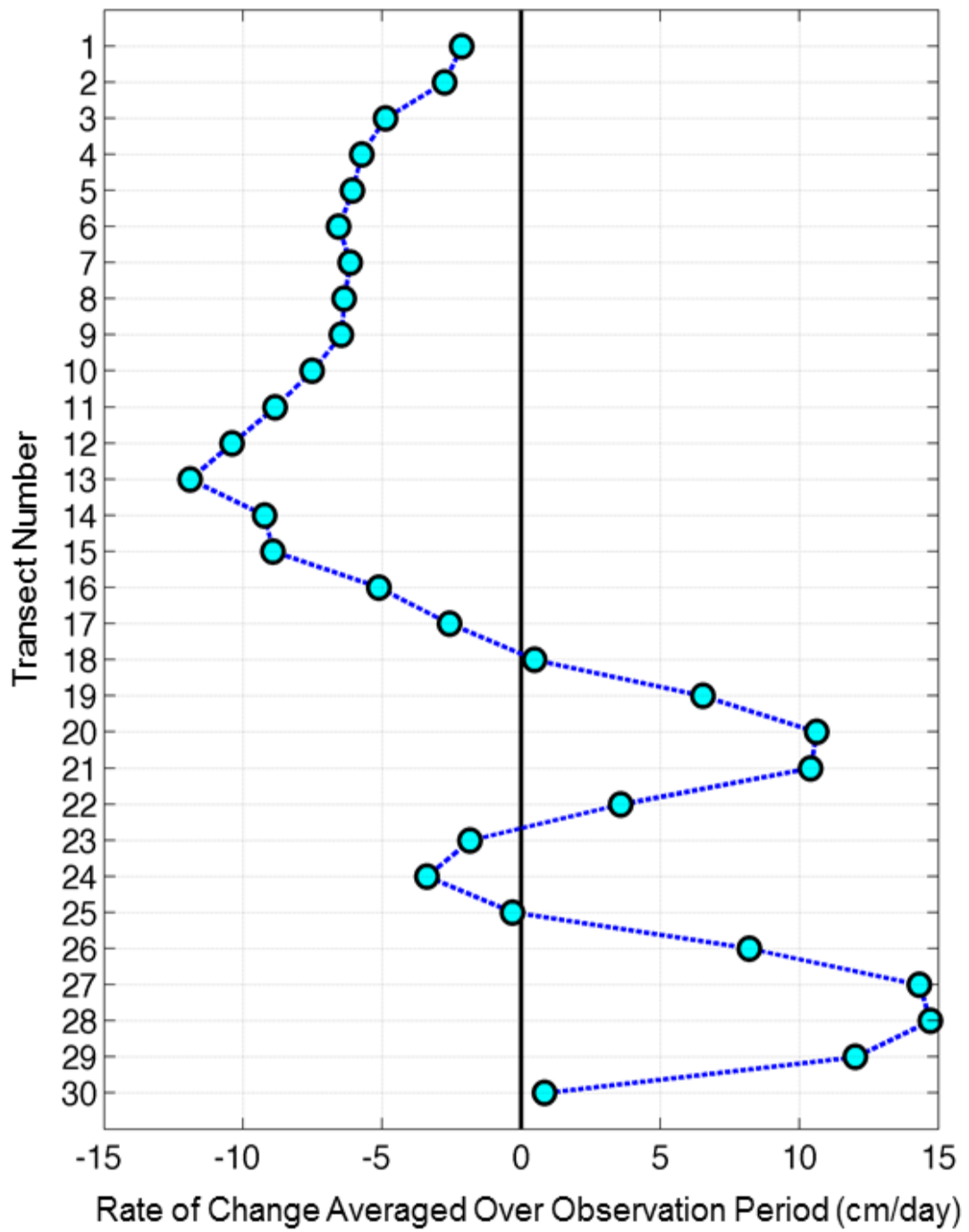


Figure 3-3. Spatial summary of shoreline change rates over the observation interval.

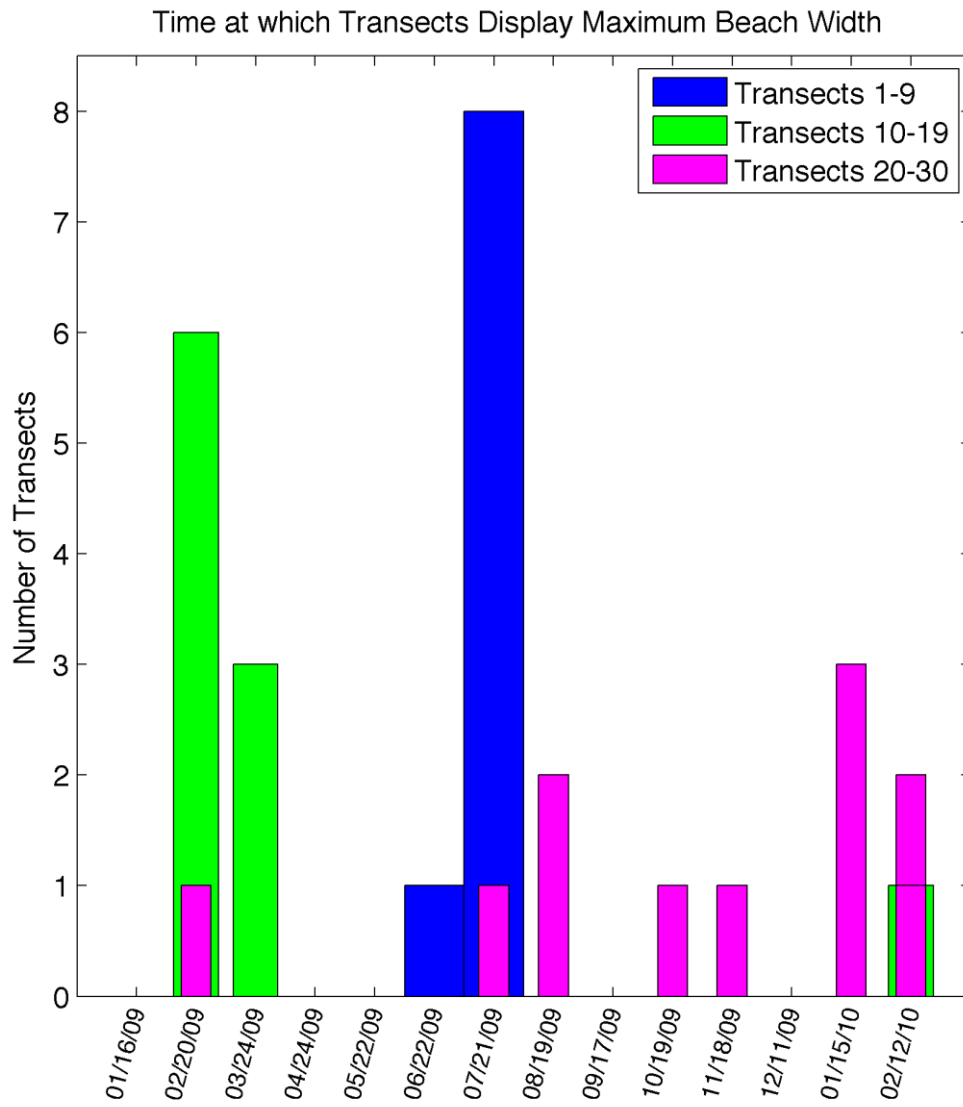


Figure 3-4. Histogram showing time at which beach width maximum is reached.

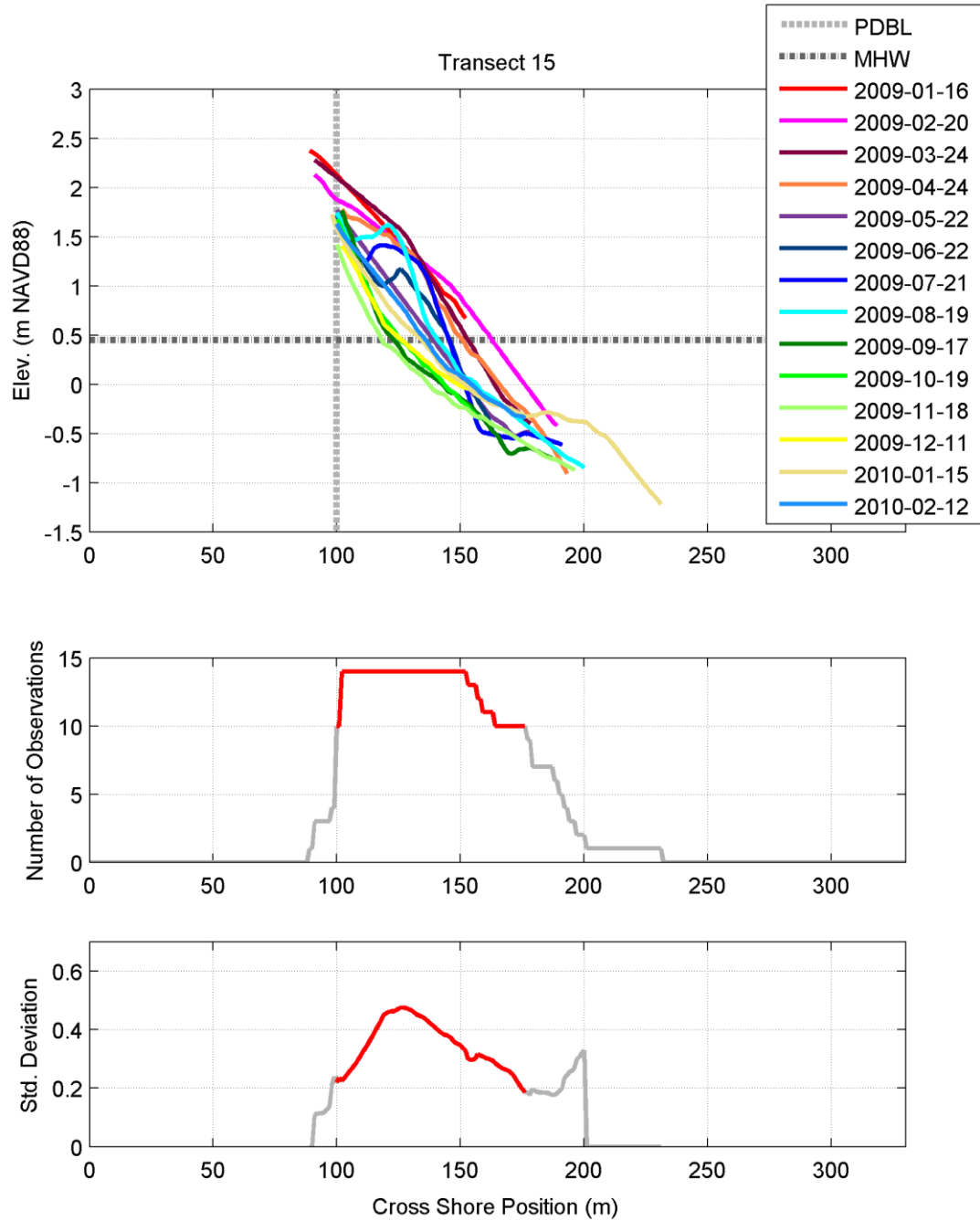


Figure 3-5a. Cross-shore topographic profile variation at transect 15 illustrating the cross-shore distributions of temporal coverage and cross-shore distribution of standard deviation. A minimum number of nine surveys are required to complete a meaningful standard deviation; these are highlighted in orange.

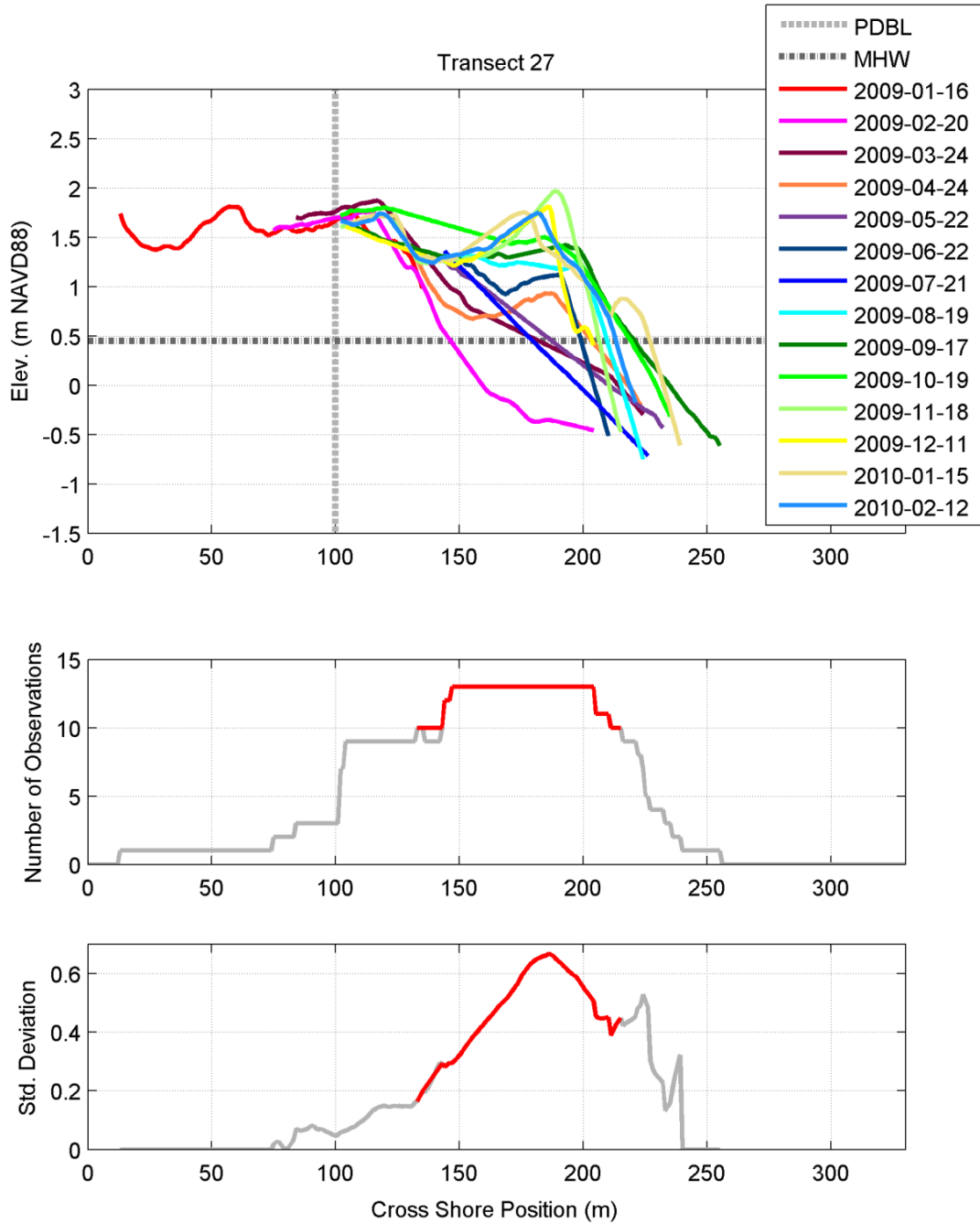


Figure 3-5b. Cross-shore topographic profile variation at transect 27 illustrating the cross-shore distributions of temporal coverage and cross-shore distribution of standard deviation. A minimum number of nine surveys are required to complete a meaningful standard deviation; these are highlighted in orange.

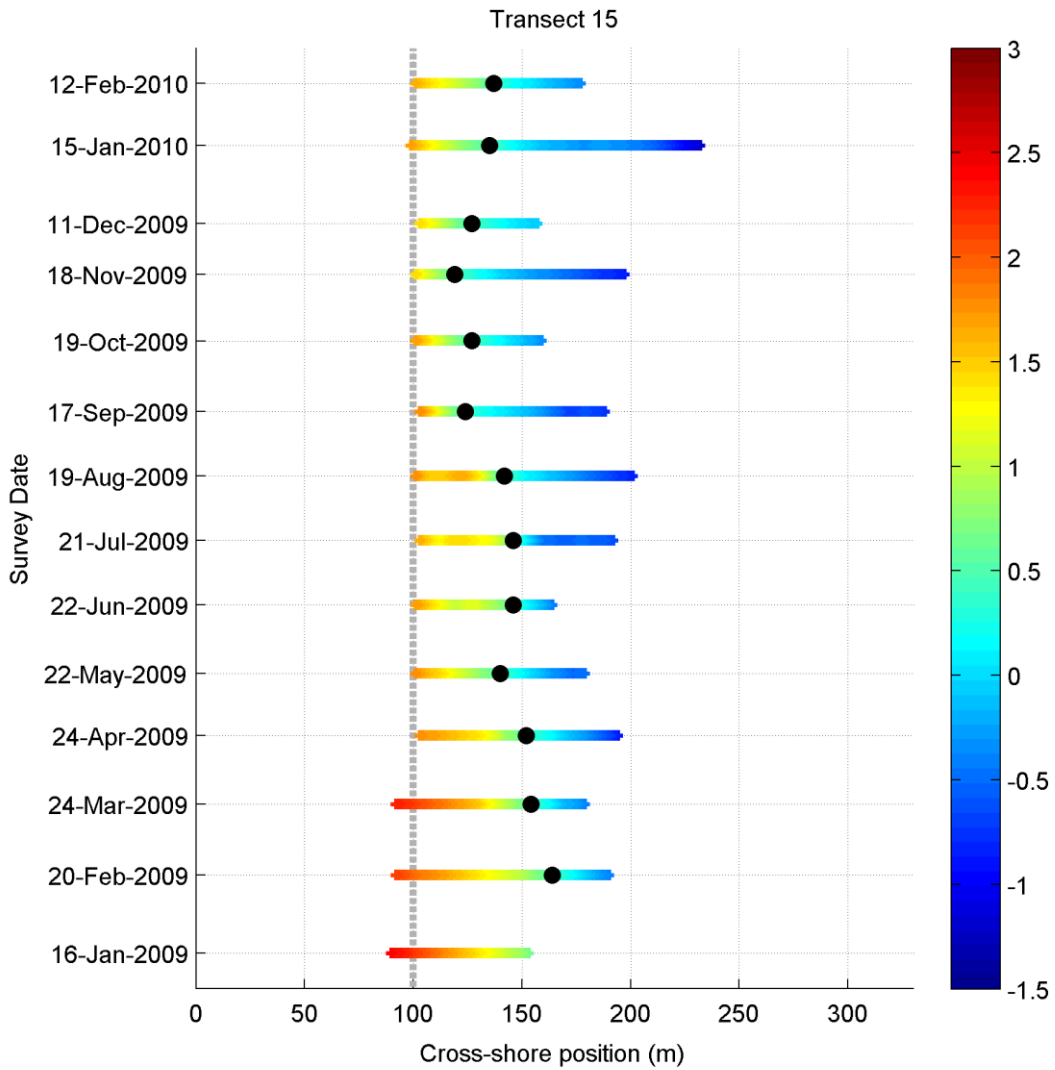


Figure 3-6a. Time series of survey profiles for transect 15. Cross-shore topography is shown in color, and the migration of the shoreline is given in black dots. Colorbar denotes elevation in meters (NAVD88)

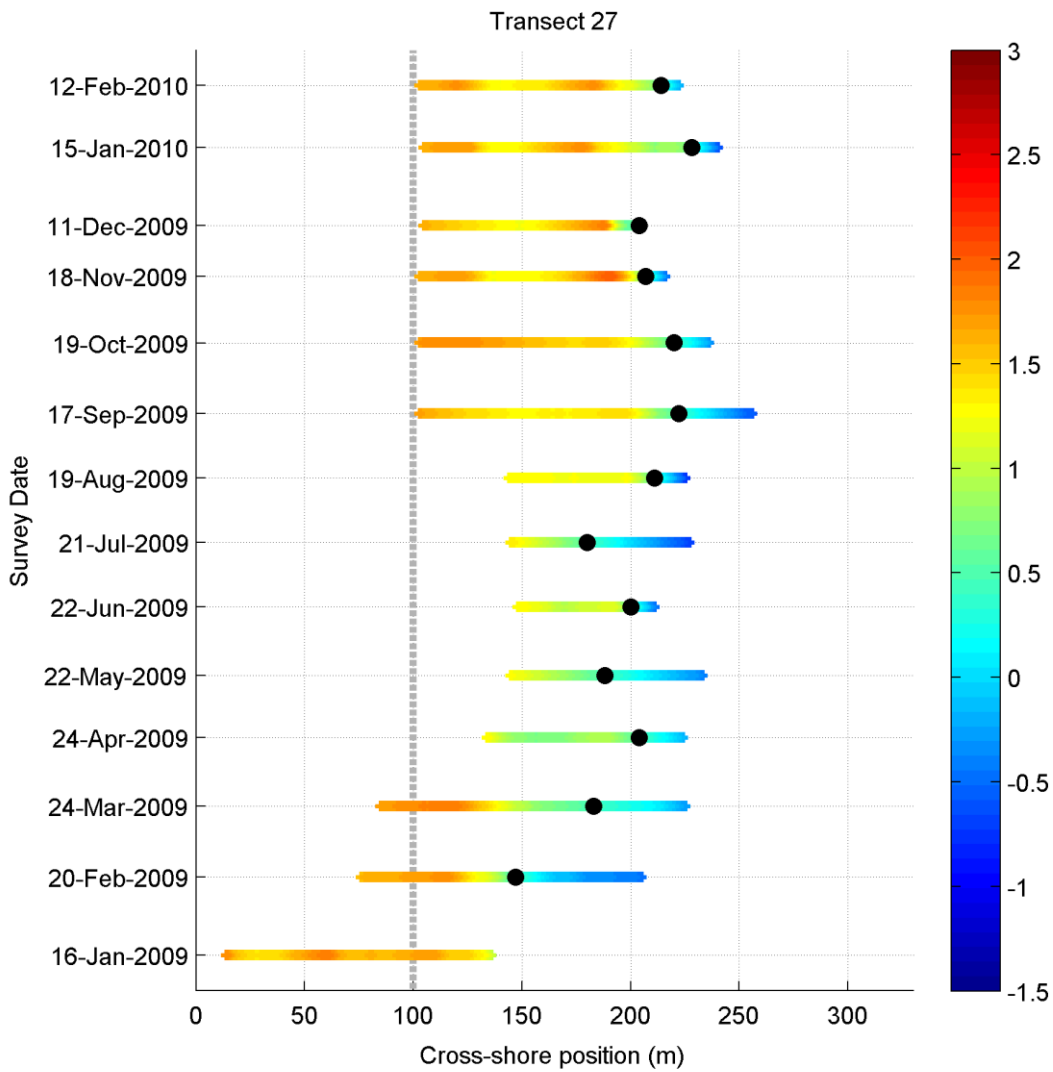


Figure 3-6b. Time series of survey profiles for transect 27. Cross-shore topography is shown in color, and the migration of the shoreline is given in black dots. Colorbar denotes elevation in meters (NAVD88)

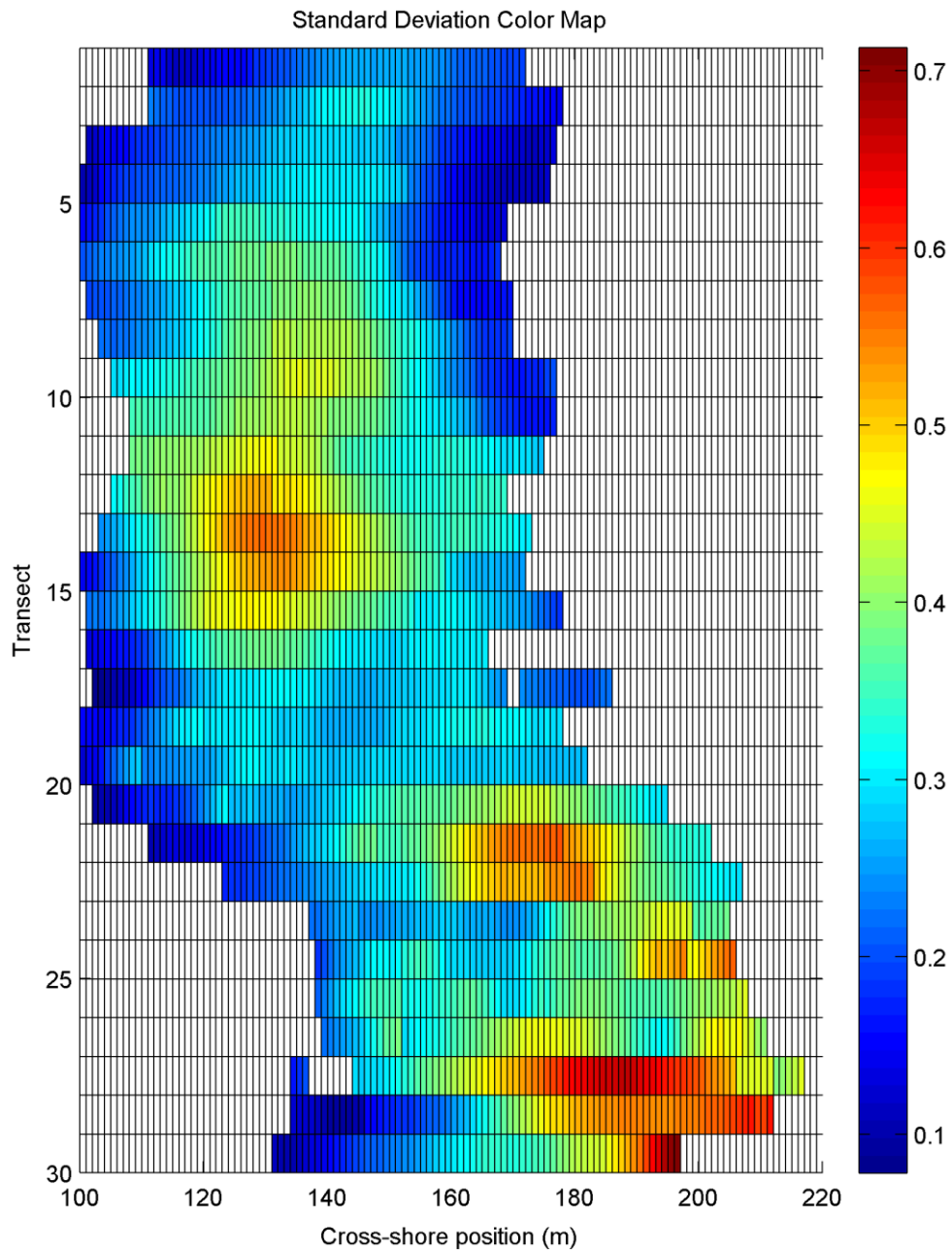


Figure 3-7. Colormap illustrating cross-shore and alongshore distributions of temporal topographic variation plotted as standard deviation. Colorbar denotes standard deviation value.

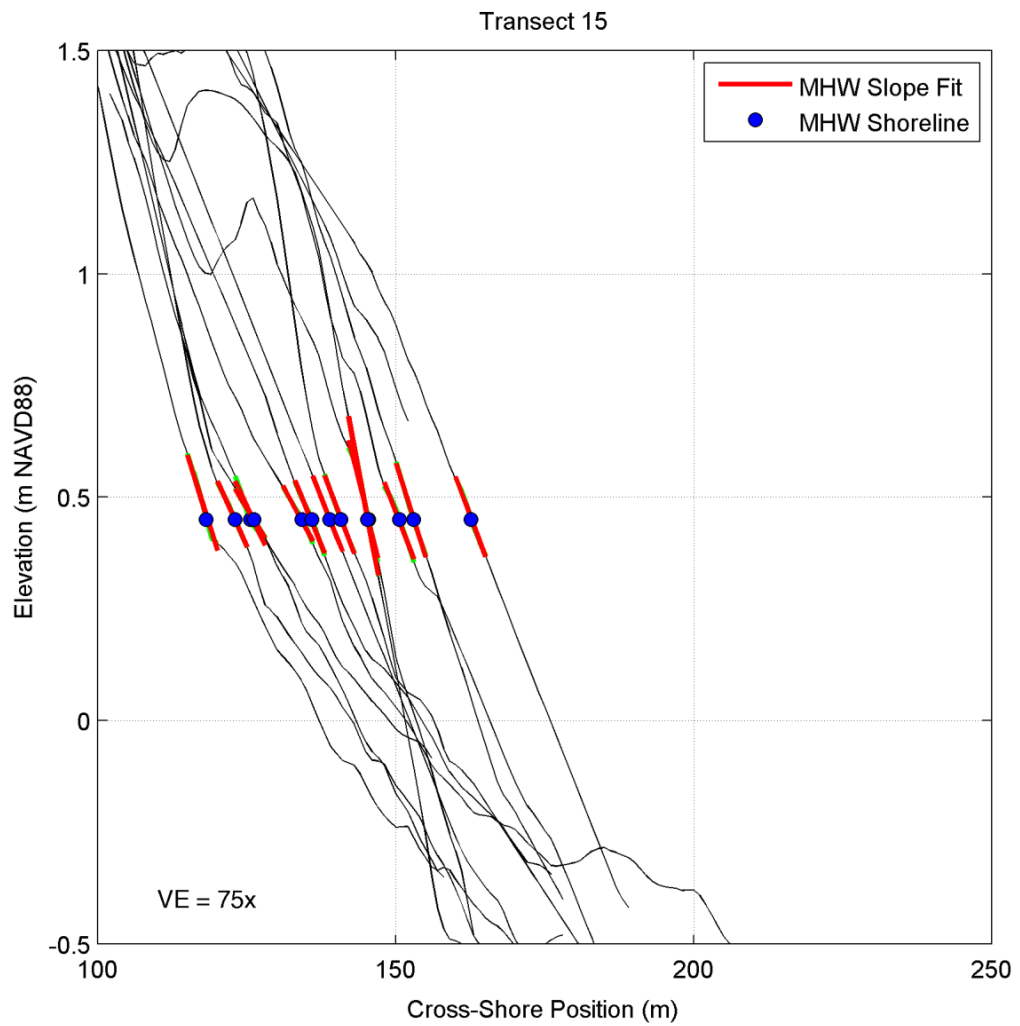


Figure 3-8a. Figure illustrating MHW shoreline slope for transect 15 plotted as a trend line to the portion of the profile beginning five meters landward of MHW and five meters shoreward of MHW.

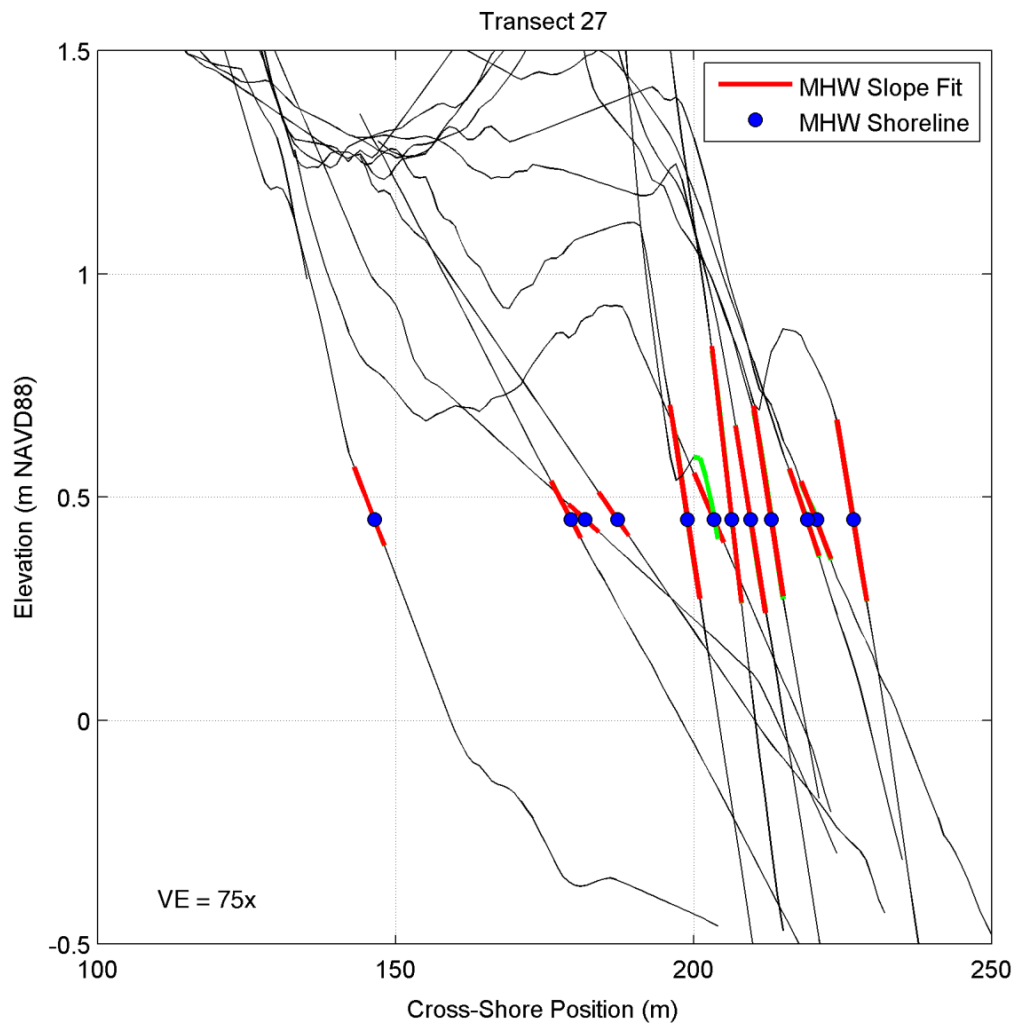


Figure 3-8b. Figure illustrating MHW shoreline slope for transect 27 plotted as a trend line to the portion of the profile beginning five meters landward of MHW and five meters shoreward of MHW.

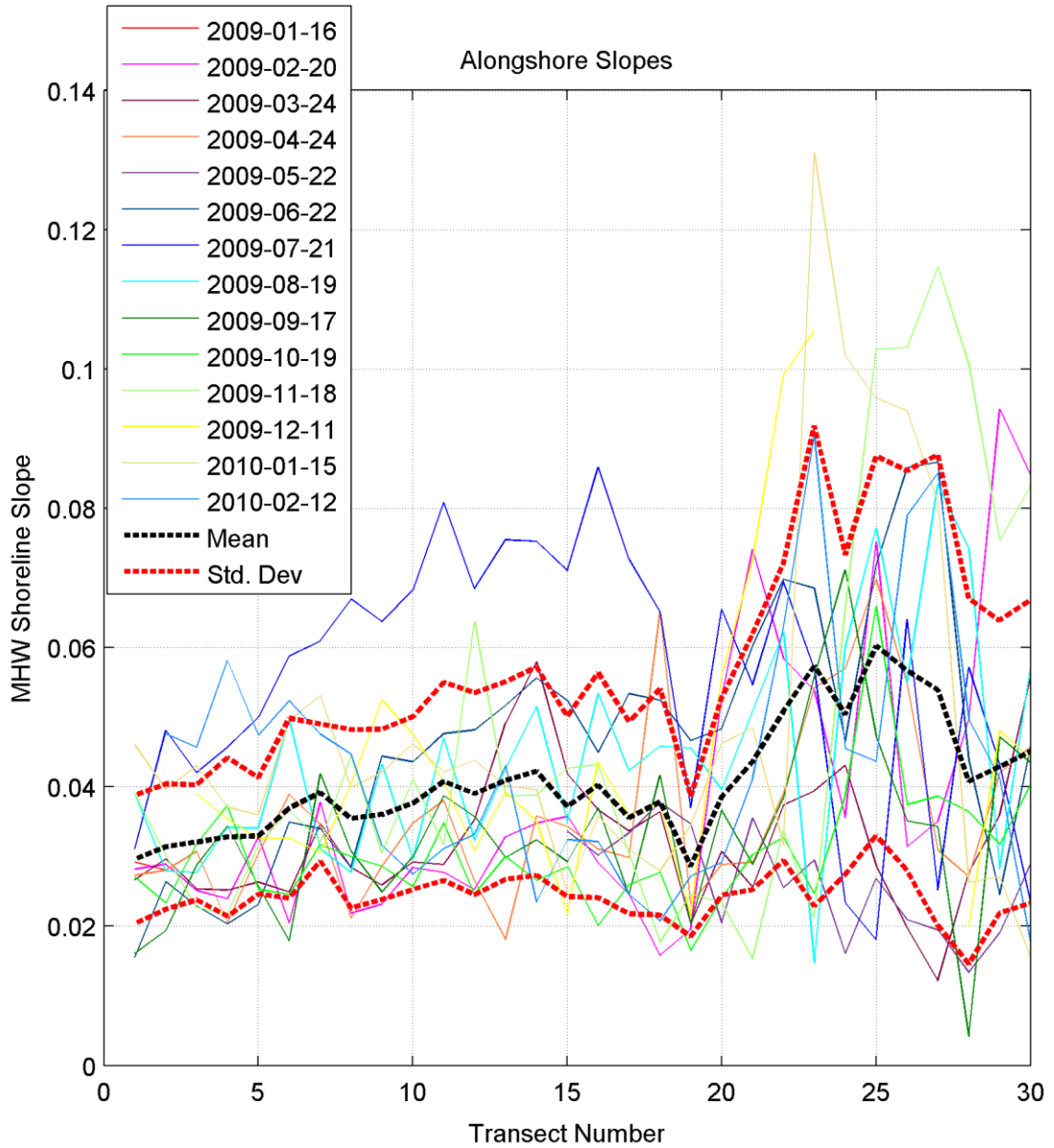


Figure 3-9. Alongshore compilation of MHW shoreline slopes for each survey plotted as connected lines.

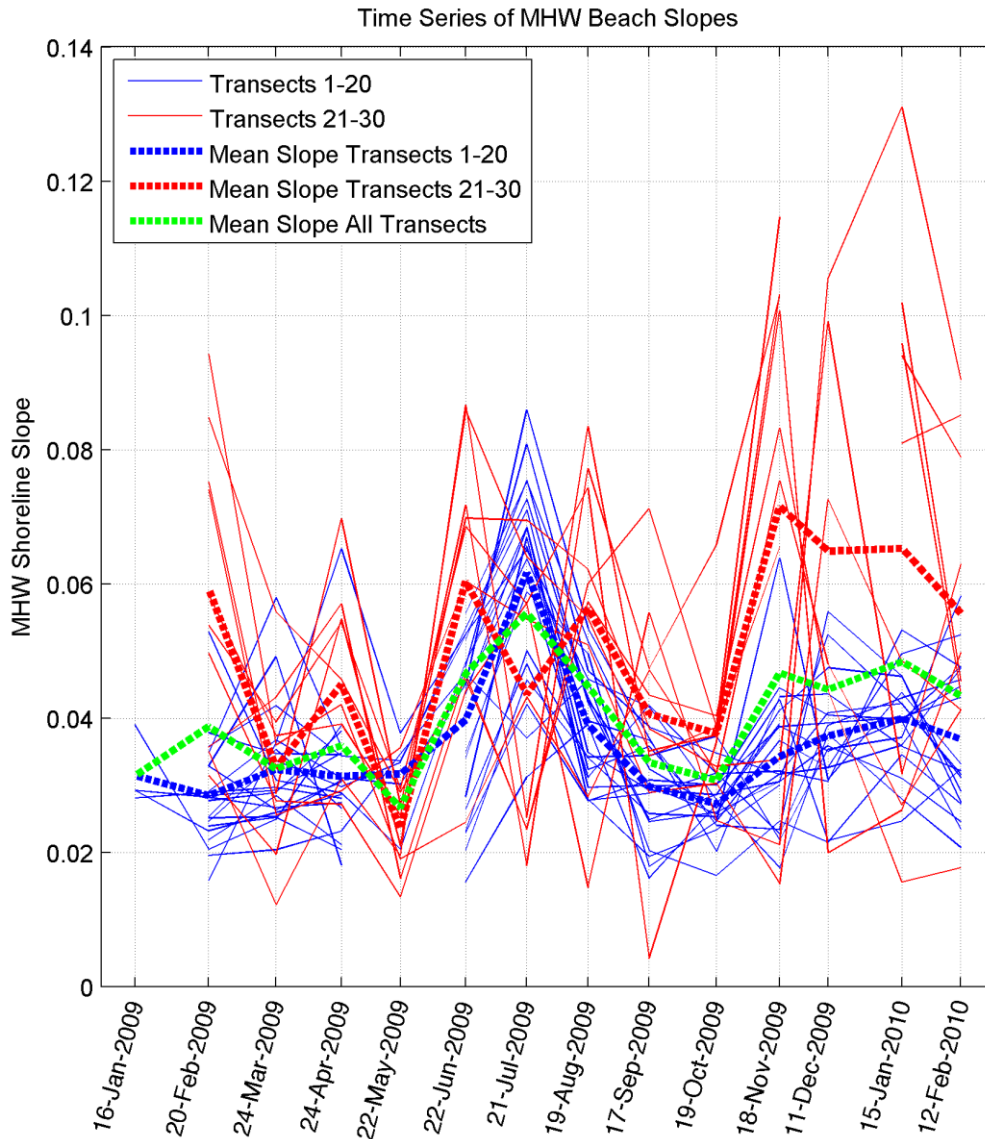


Figure 3-10. Temporal analysis of beach slopes broken up into two groups according to location. Blue denotes the northern portion (transects 1-20) of the study reach, and red denotes the southern portion (transects 21-30) of the study reach. The green dotted line denotes the mean slope for all transects.

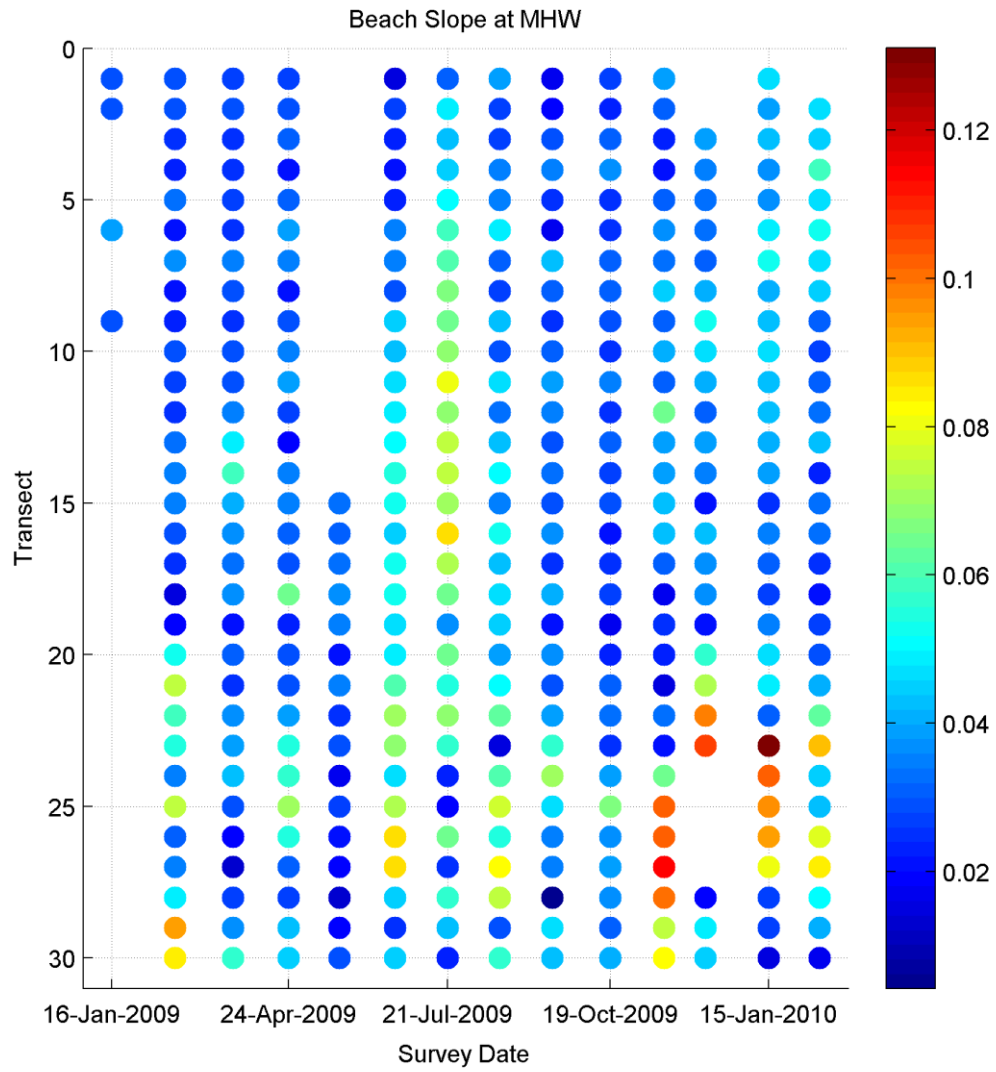


Figure 3-11. Combined spatial and temporal analysis of the MHW shoreline beach slope illustrated as a colormap. Colorbar denotes beach slope.

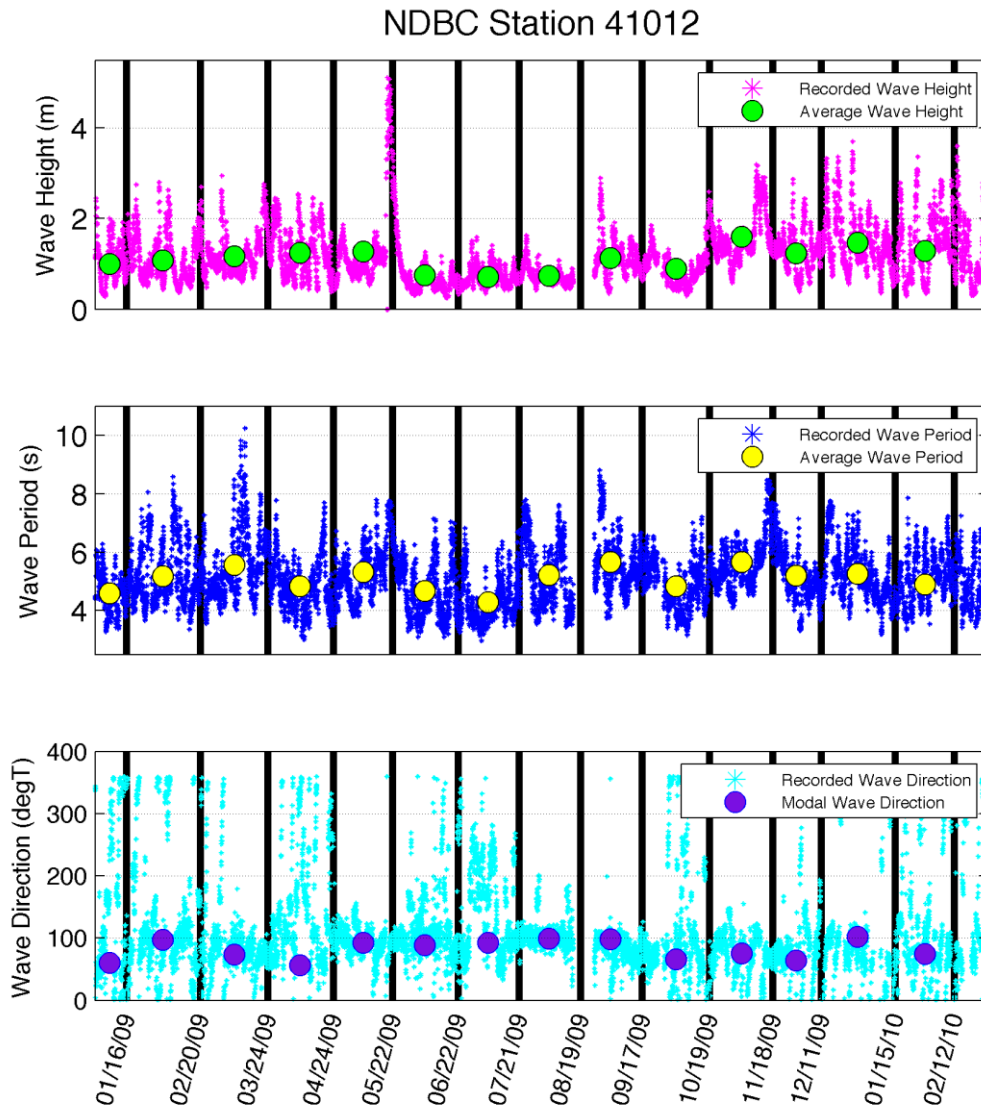


Figure 3-12. NDBC wave buoy 41012 data illustrating significant wave height (m), wave period (s), and wave direction (degT) during the survey interval. Bold black lines denote date at which a survey occurred. Also shown are the average wave height, average wave period, and modal direction for each survey interval [Station 41012 (LLNR 845.3) - St. Augustine, FL 40NM ENE of St Augustine, FL, 2011].

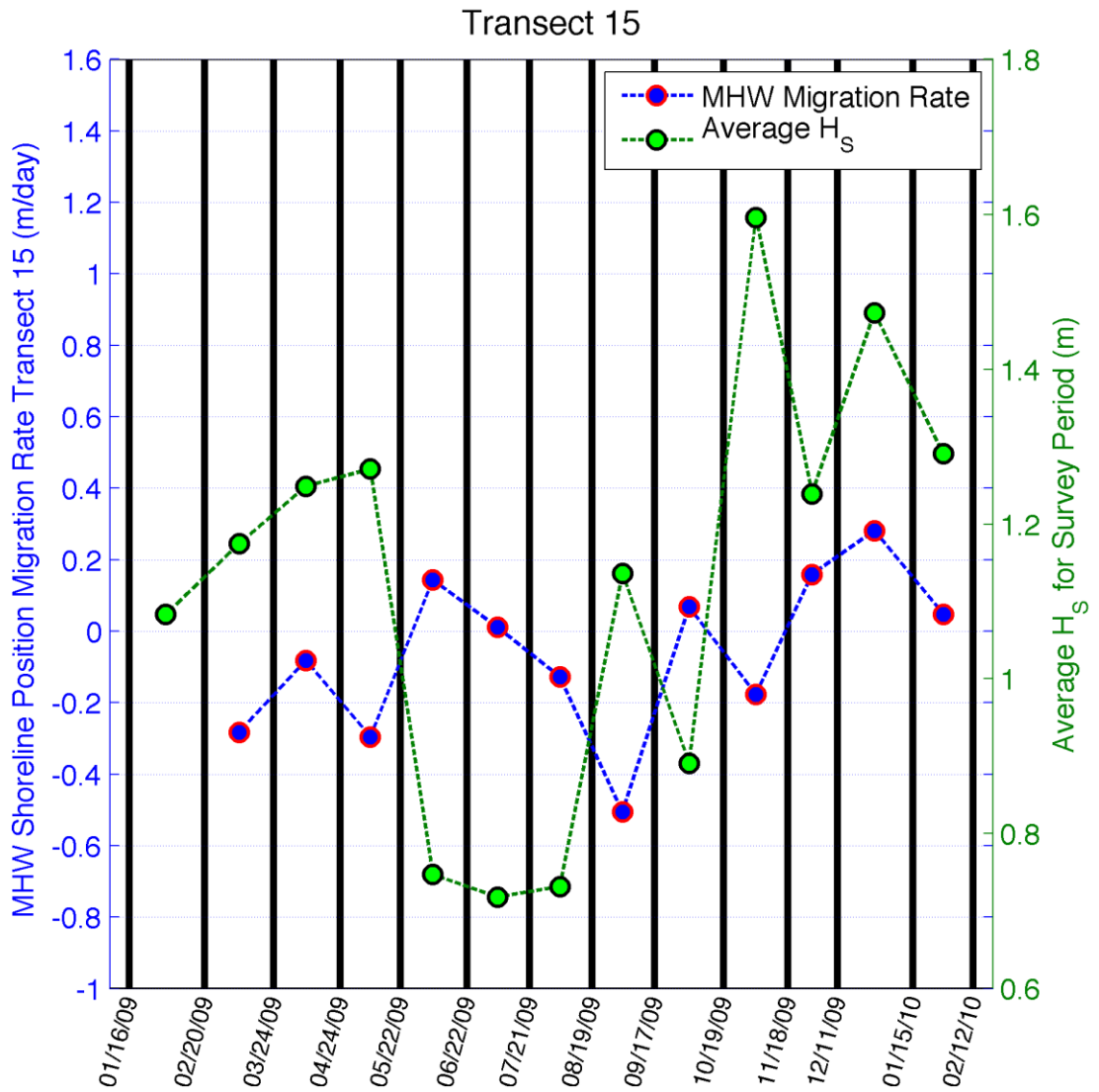


Figure 3-13a. Temporal analysis of MHW shoreline position change rate plotted against average significant wave height for each survey interval at transect 15.

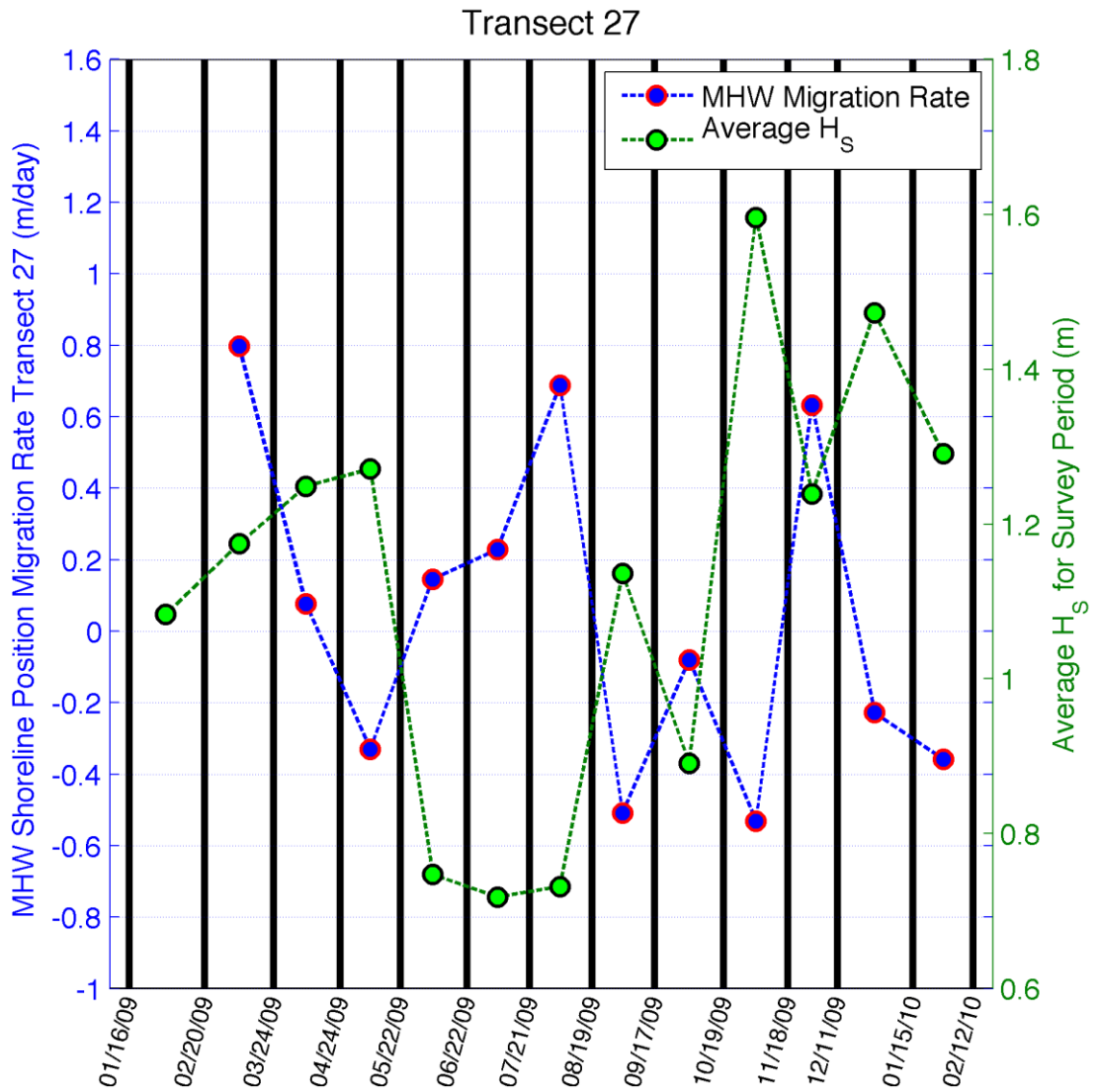


Figure 3-13b. Temporal analysis of MHW shoreline position change rate plotted against average significant wave height for each survey interval at transect 27.

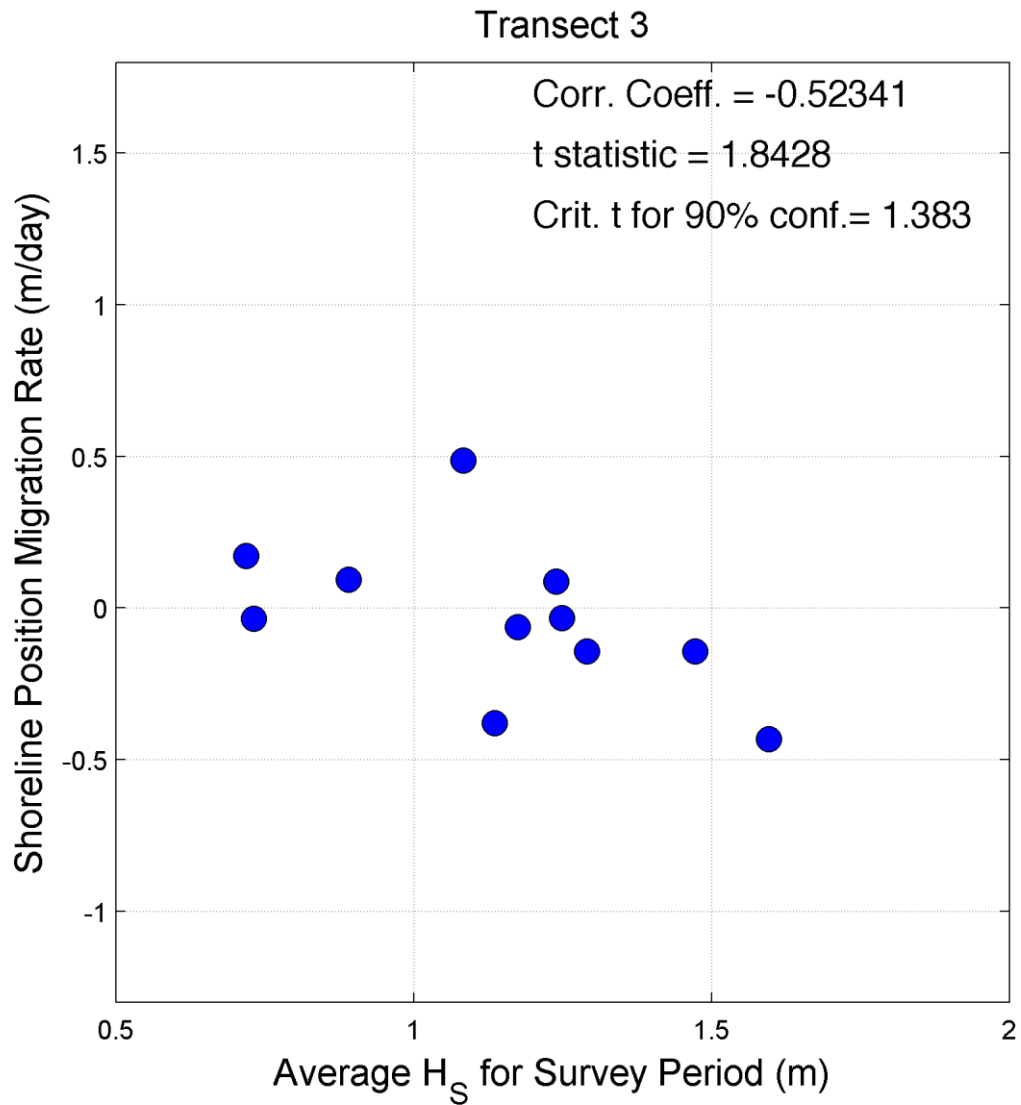


Figure 3-14a. Cross plot illustrating the relationship between average significant wave height and MHW shoreline position migration rate at transect 3. Student's t test indicates that the correlation coefficient is statistically significant at the 90% confidence interval for this transect.

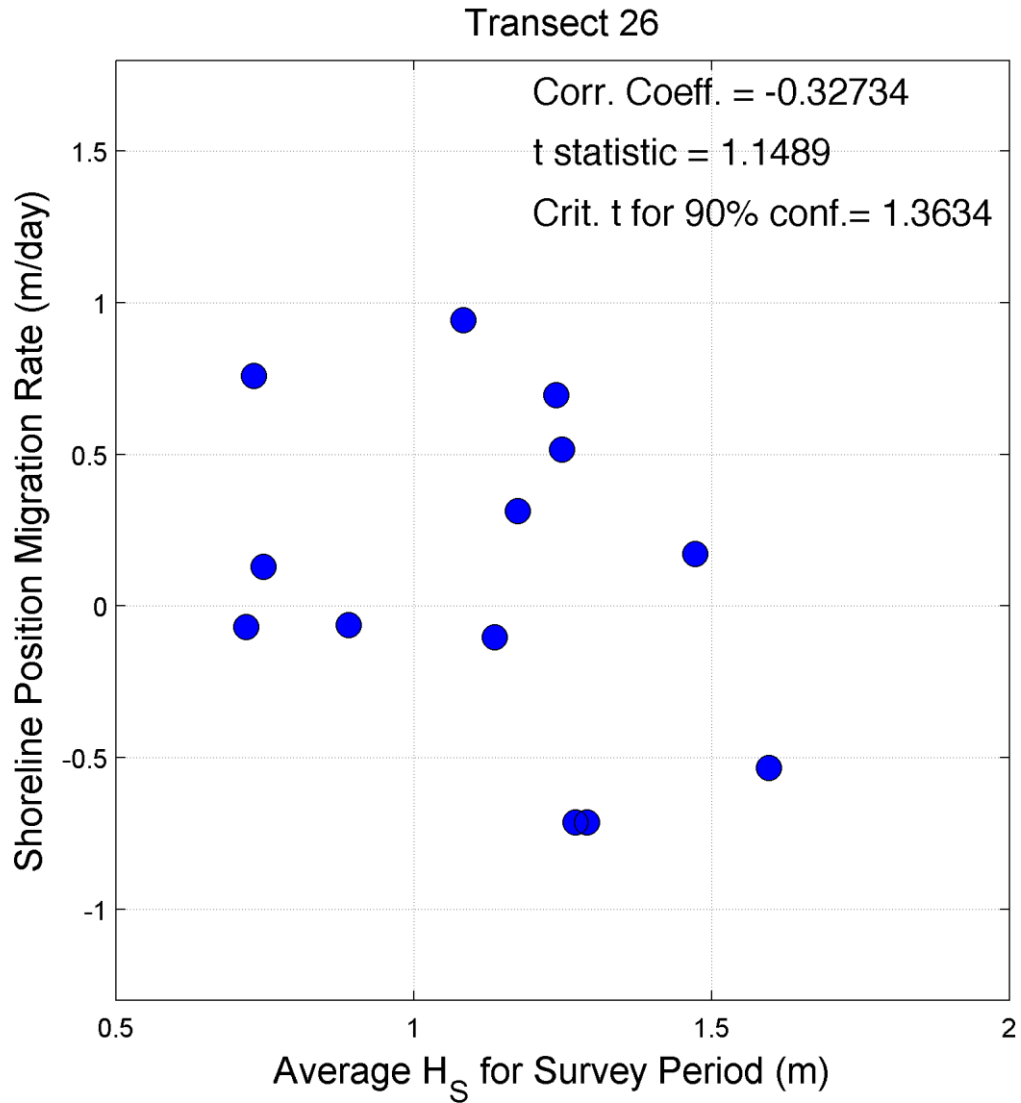


Figure 3-14b. Cross plot illustrating the relationship between average significant wave height and MHW shoreline position migration rate at transect 26. Student's t test indicates that the correlation coefficient is statistically significant at the 90% confidence interval for this transect.

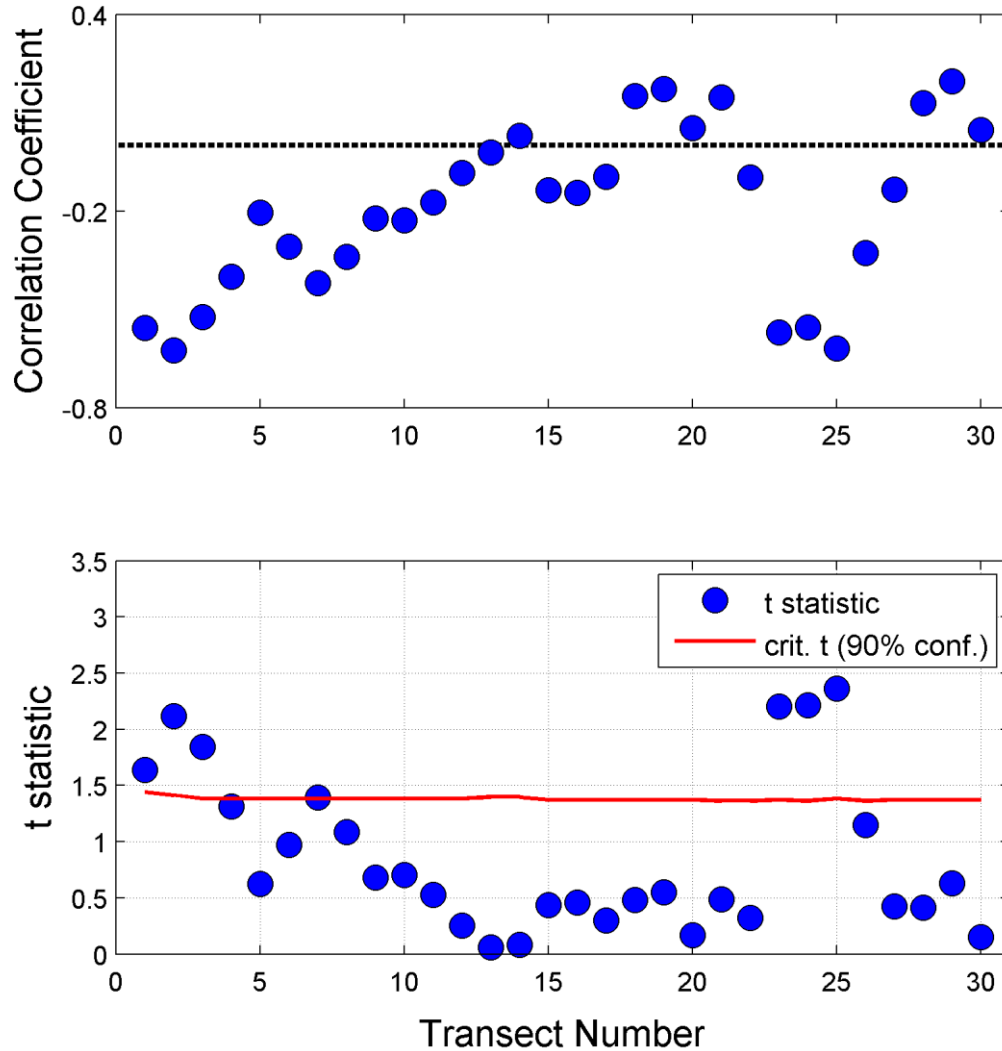


Figure 3-15. Summary of analyses of potential correlation between shoreline change rate and offshore wave height (H_s). Upper panel shows the dominance of negative correlation coefficients over the transect series, implying a negative relationship between wave climate and shoreline change rate. Lower panel displays results of Student's t test on the data set. Transects whose t statistic exceeds the critical t value (as determined by degrees of freedom/number of temporal observations), have a correlation between the variables that is statistically significant at the 90% confidence limit.

CHAPTER 4 DISCUSSION AND CONCLUSIONS

Below is a discussion of the results of this project. Conclusions are drawn that attempt to identify the validity of the hypothesis: tidal inlet dynamics exert a spatially-limited influence on the temporal behavior of nearby shoreline position and beach morphology. To accomplish this, the research questions identified in section 1.2 are explicitly addressed.

4.1 Shoreline Position Variation With Distance From Inlet

How does the shoreline position (beach width) vary as a function of distance from an inlet? Results from this investigation indicate that shoreline position (beach width) varies considerably as a function of distance from the inlet. There is an abrupt change in beach width at a location 500 m north of the inlet. The beach width more than doubles from ~40 m to ~90 m at this location. Also, there is an increase in the variability of the shoreline position, from a standard deviation value of ~10 m in the northern section of the study area to ~ 20 m in the southern portion of the study area (close to the inlet). Therefore, the beach experiences increases in width and width variability in the southern portion of the study area (within 500 m of the inlet), which are likely to be associated with inlet sedimentary and hydraulic processes that control the morphology of the ebb shoal.

4.2 Seasonal Variability in Shoreline Position

Does the spatial variability in shoreline position (beach width) exhibit a seasonal variability? Over the observation interval (Jan. 2009 – Feb. 2010), an overall trend of beach narrowing is evident in the northern portion of the study area (at distances greater than ~650 m from the inlet), whereas a more complex pattern is evident in the

southern portion of the study area adjacent to the inlet. The portion of the beach within ~650 m of the inlet contains two prominent areas of beach widening separated by a ~100 m band of narrowing. There is a seasonal signal between distances ~1450 m - 1050 m from the inlet where beach widths reach their maximum during summer months (June and July 2009), and between distances ~1000 m – 550 m from the inlet where beach widths reach their maximum in late winter (February and March 2009). The spread in maximum beach width is difficult to characterize for the alongshore distance of 0 m – 500 m from the inlet as maximum beach widths occur sporadically throughout the survey duration. Seasonal signals are more discernable for the northern portion of the study area, at distances greater than 600 m from the inlet. Sedimentary and hydraulic processes associated with the inlet may be responsible for the lack of seasonal variability evident of shoreline position within the southern portion of the study area, at locations less than 600 m from the inlet.

4.3 Beach Morphology Variation – Spatial and Temporal

How does beach morphology (profile shape) vary as a function of distance from an inlet? Does the spatial variability in beach morphology (profile shape) exhibit a seasonal variability? Beach morphology (profile shape) varies spatially and temporally according to distance from an inlet. The northern portion of the study reach, at distances greater than ~500 m from the inlet, contains gently-sloped profiles, whereas, the southern portion of the study reach, at distances within ~500 m of the inlet, contains comparatively steeper profiles. The greatest variation in topography occurs near the PBDL for the portion of the study reach greater than ~600 m from the inlet, whereas the southern portion of the study area, within ~500 m of the inlet, exhibits increased temporal variability in topography towards the seaward end of the cross-shore profile,

which can be identified as increased lower beach berm-building behavior. Beach slopes are lower in the southern, portion of the study area, as compared to the northern portion. During the summer months, the northern portion steepens at the MHW shoreline, whereas the southern portion becomes more gently sloped. Sedimentary and hydraulic processes associated with the inlet may influence beach morphology (profile shape) within the southern portion of the study area.

4.4 Relationship of Beach Response to Forcing

How do temporal trends in shoreline position (beach width) and beach morphology (profile shape) correlate with offshore wave conditions, thought to dominate the forcing? It is difficult to discern a clear relationship between temporal trends in shoreline position and beach morphology and offshore wave conditions, from data collected in this study. Some transects (18, for example) appear to follow a proposed conceptual model relating shoreline position change rate to wave height [Dean, 1991], but other transects do not. This may be a result of the influence of the tidal inlet overprinting the influence of the wave forcing. The data indicate some association (negative correlation) of shoreline change with changes in offshore wave conditions; however, only 32% of the transects with negative correlation coefficients exhibited statistical significance of the proposed relationship. Hence, the association is not strong enough to draw definitive conclusions correlating offshore wave conditions to observed shoreline position and beach morphological changes.

4.5 Summary

In summary, this study presents data that illustrate an abrupt change in the behavior of shoreline position and beach morphology at approximately 500-600m from a natural tidal inlet. A possible origin of this behavioral difference may lie in the dynamic

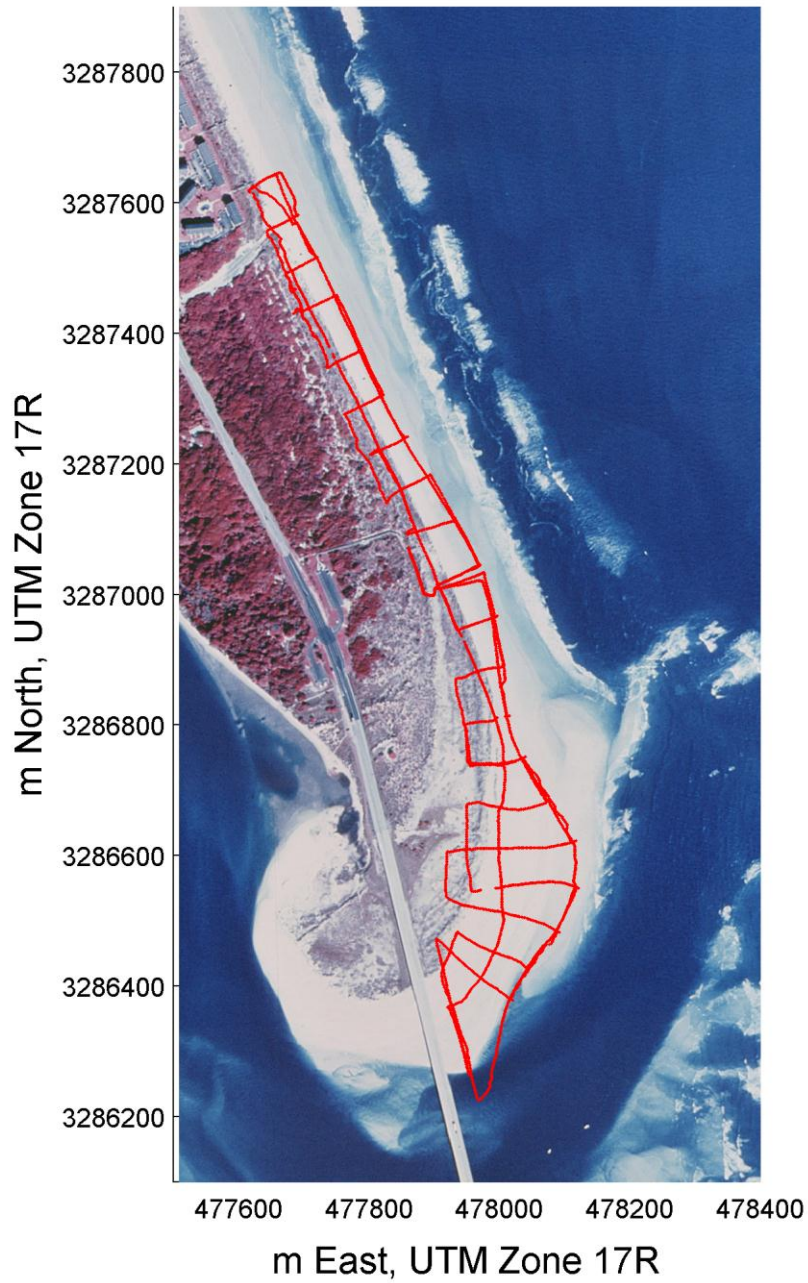
behavior of the sedimentary and hydraulic mechanics of the subaqueous ebb-shoal on the seaward side of the tidal inlet. The presence of this bathymetric discontinuity may disrupt the pattern of longshore sediment transport, which is reflected as an alongshore inconsistency in beach behavior approximately 500 m from the inlet. North of this inconsistency, the beach behavior can be considered to be influenced primarily by oceanic forcing, whereas south of the inconsistency, the beach is overwhelmed by the presence of the tidal inlet processes.

In the future, the following improvements to the project are suggested: (1) increase survey frequency (2) improve consistency of survey coverage, (3) extend observation period, as multiple years of data will provide a better handle on seasonality, and (4) gather nearshore wave data at multiple positions alongshore to obtain a clear signal of wave forcing in the nearshore region.

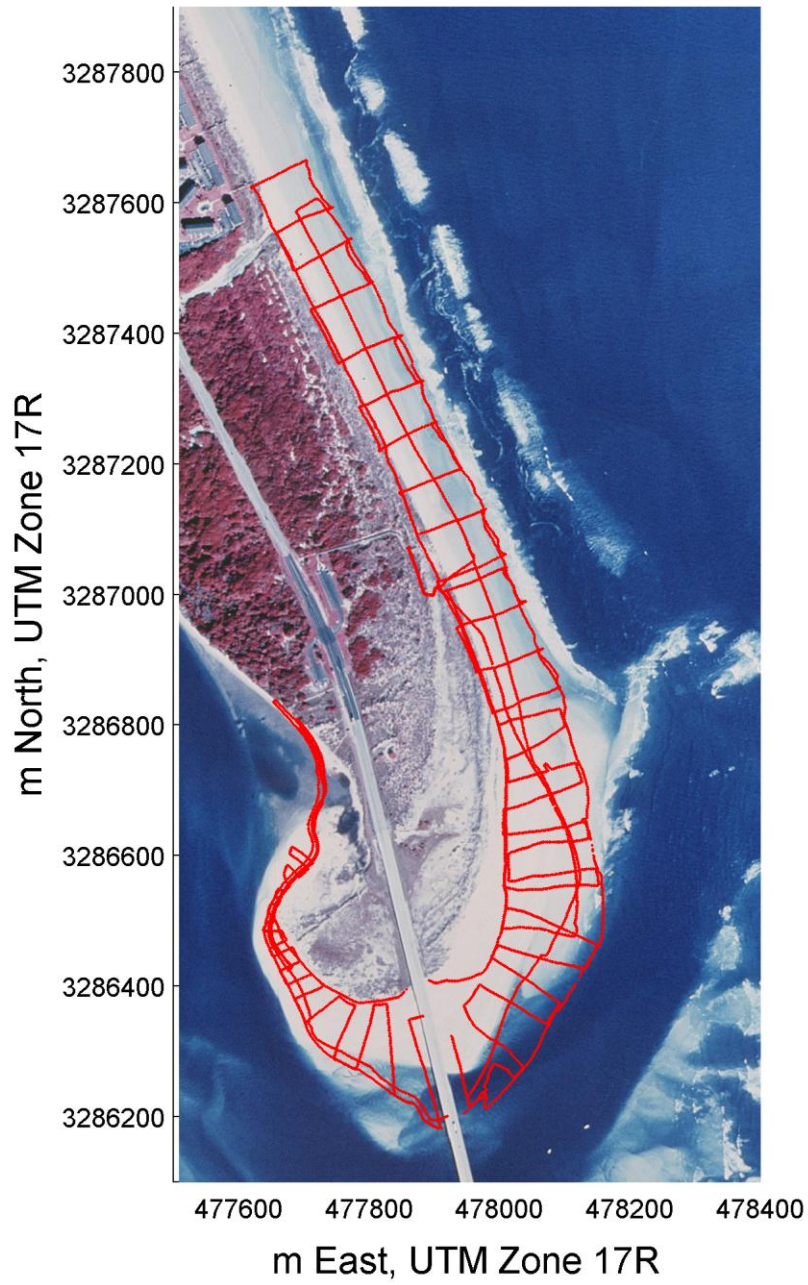
APPENDIX: SUPPLEMENTARY FIGURES

A-1

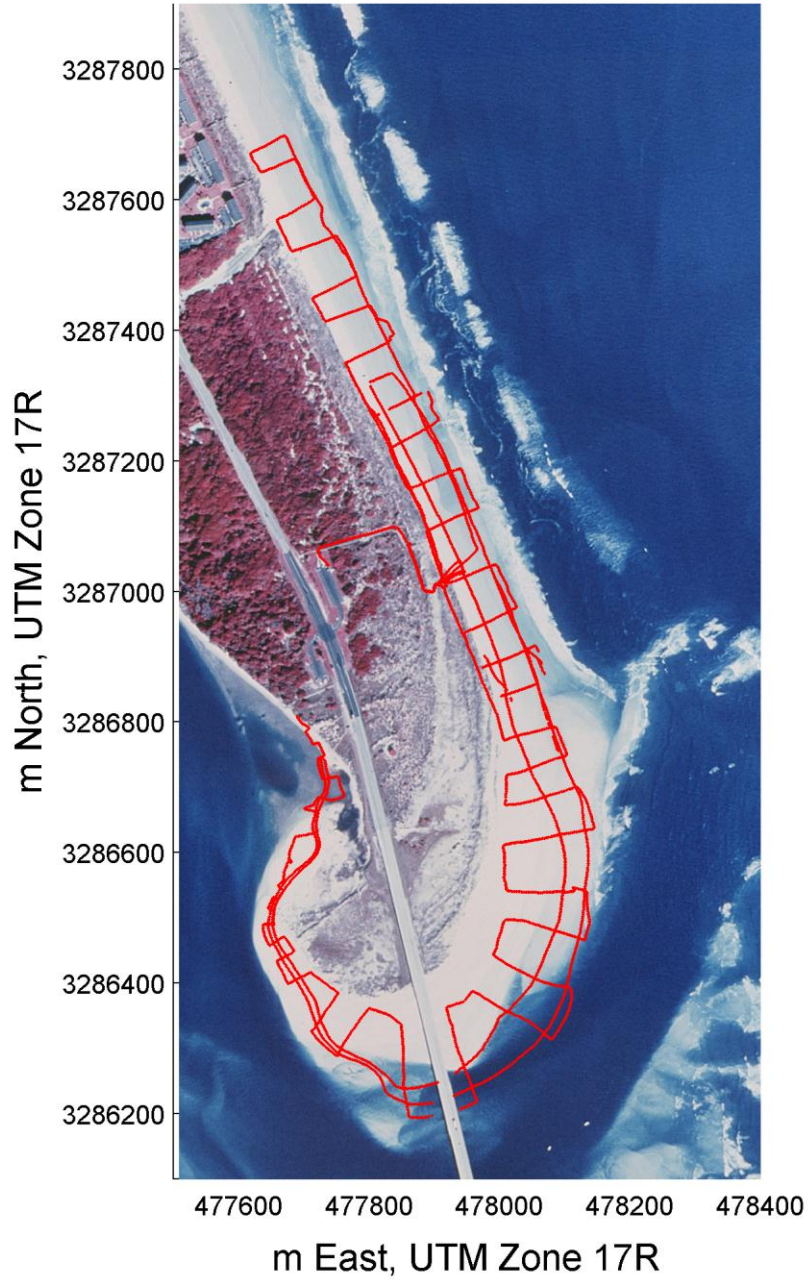
January 16, 2009



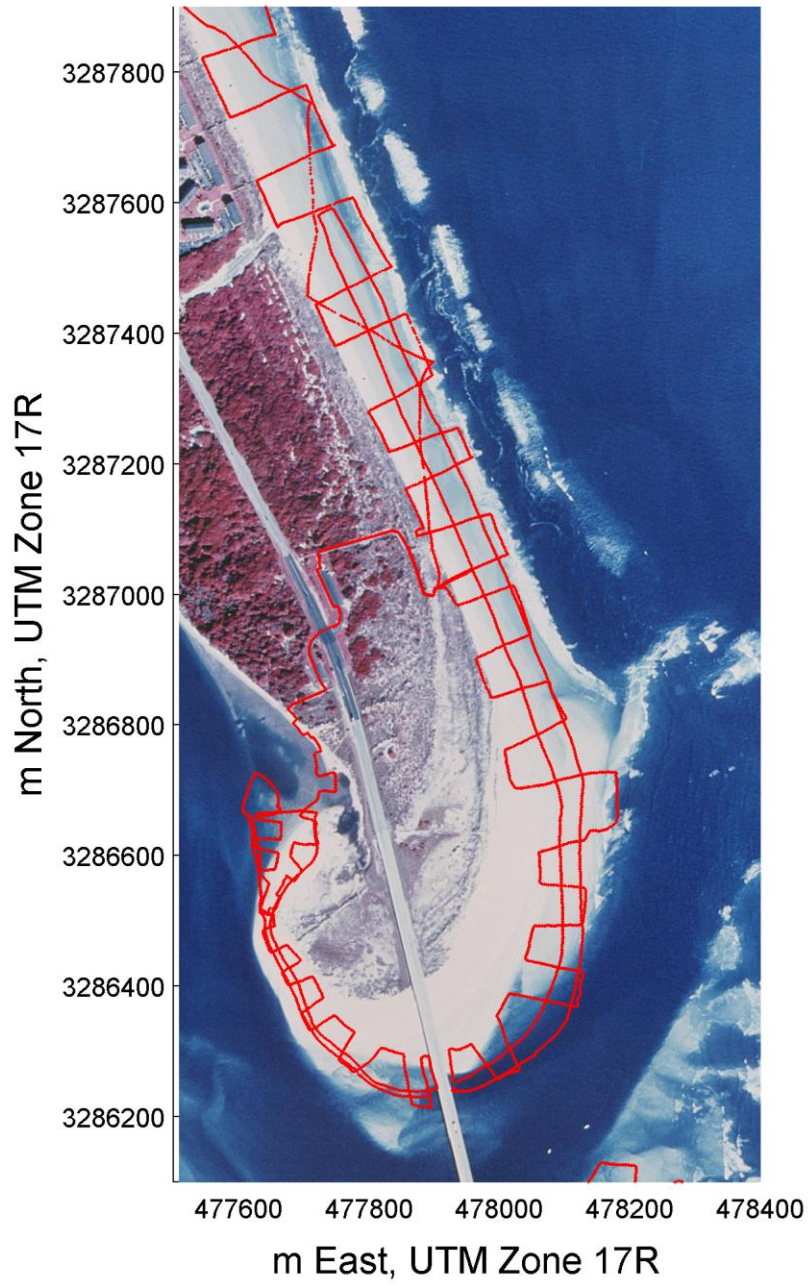
February 20, 2009



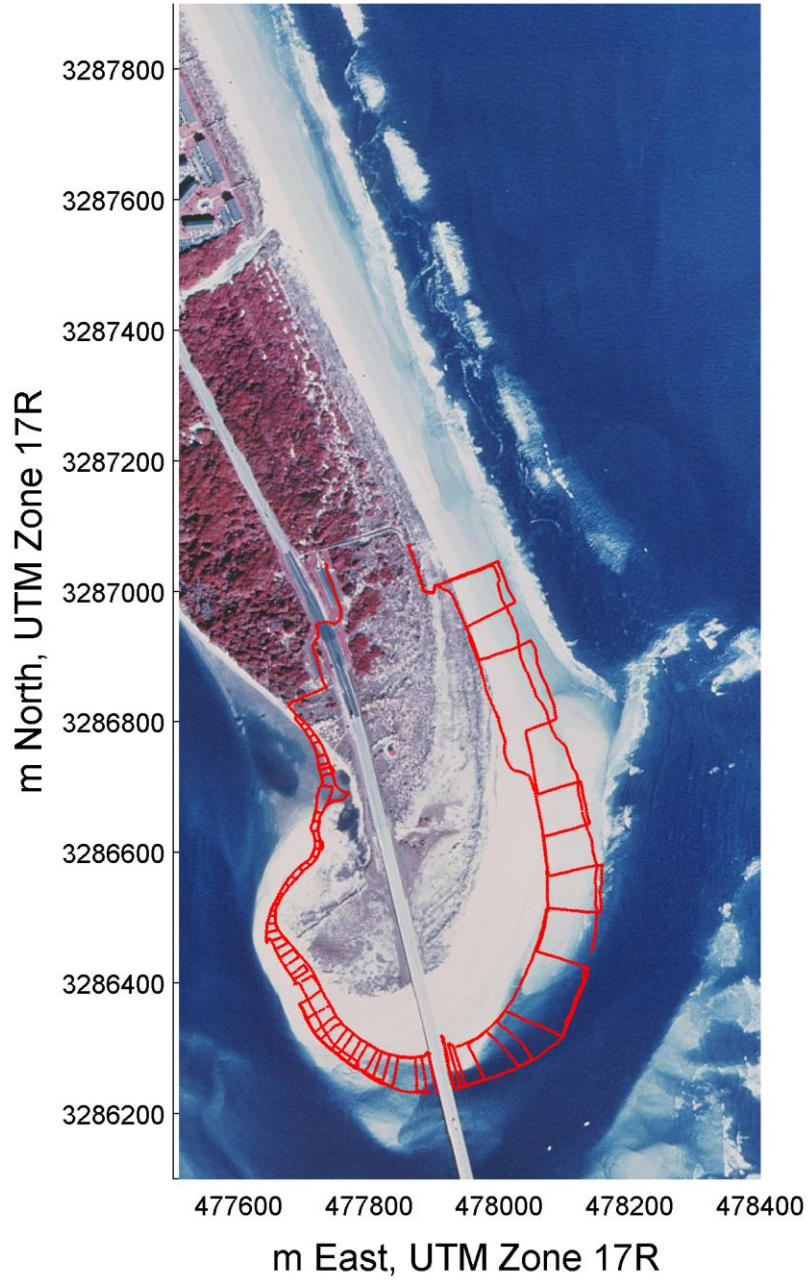
March 24, 2009



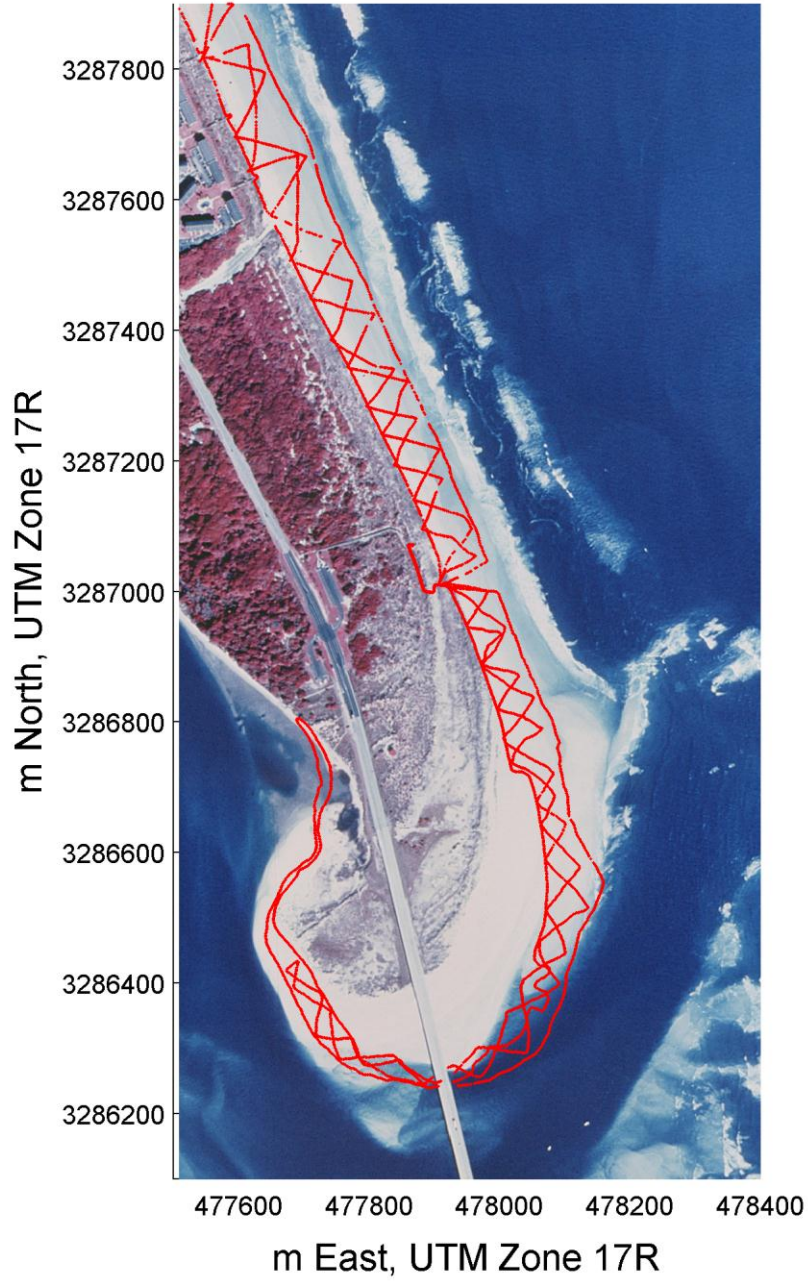
April 24, 2009



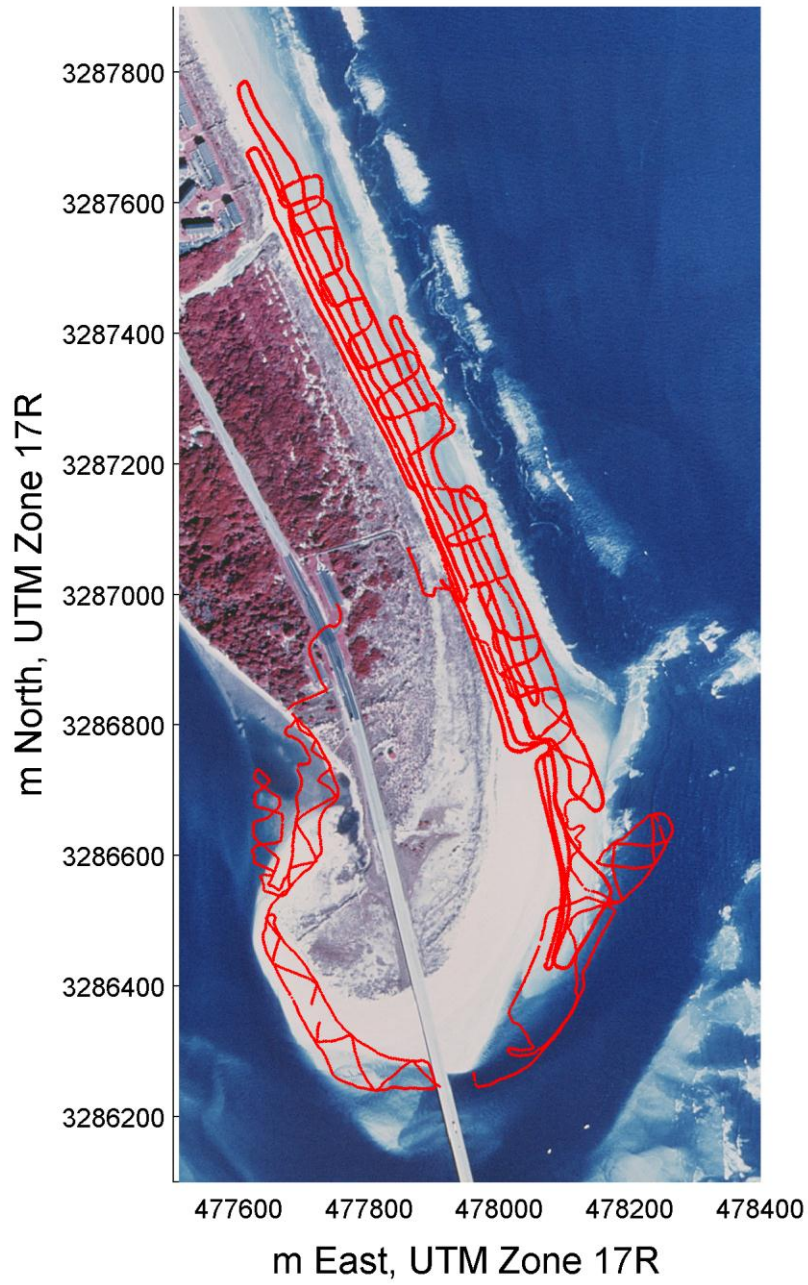
May 22, 2009



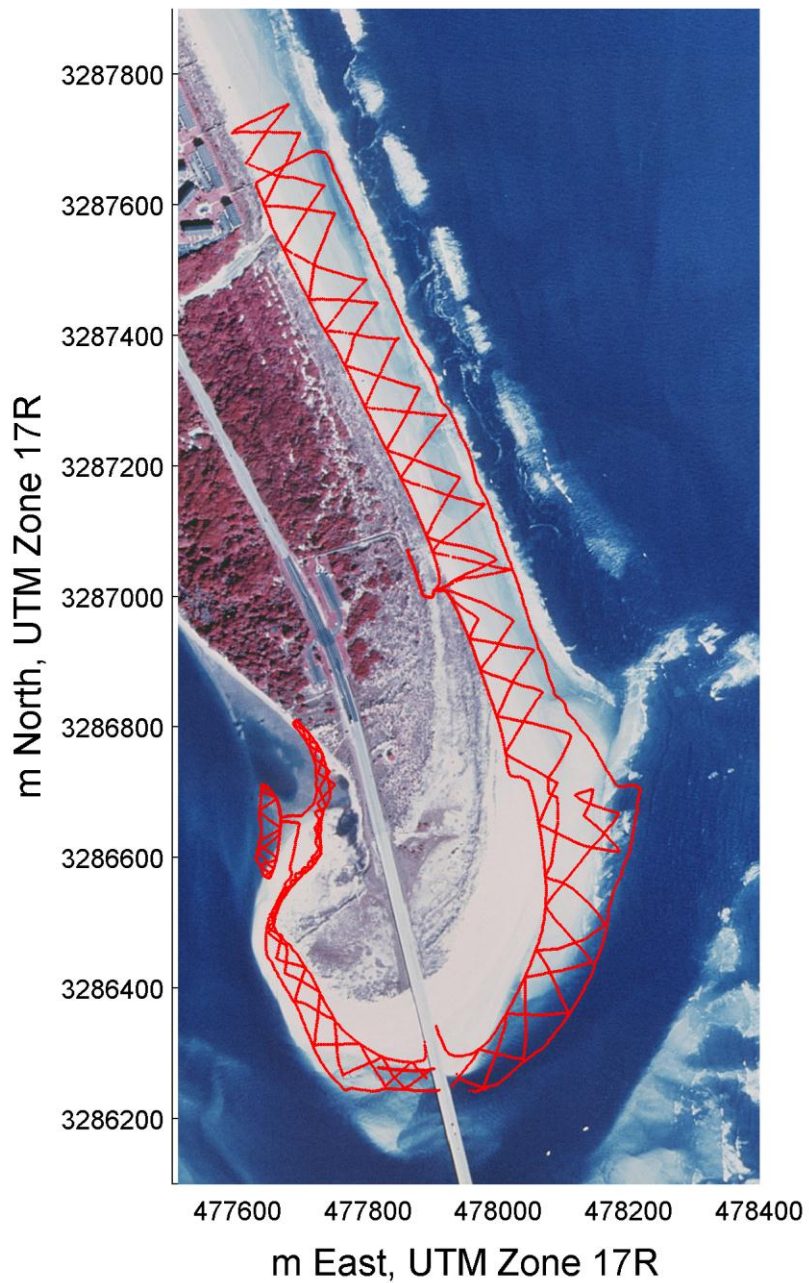
June 22, 2009



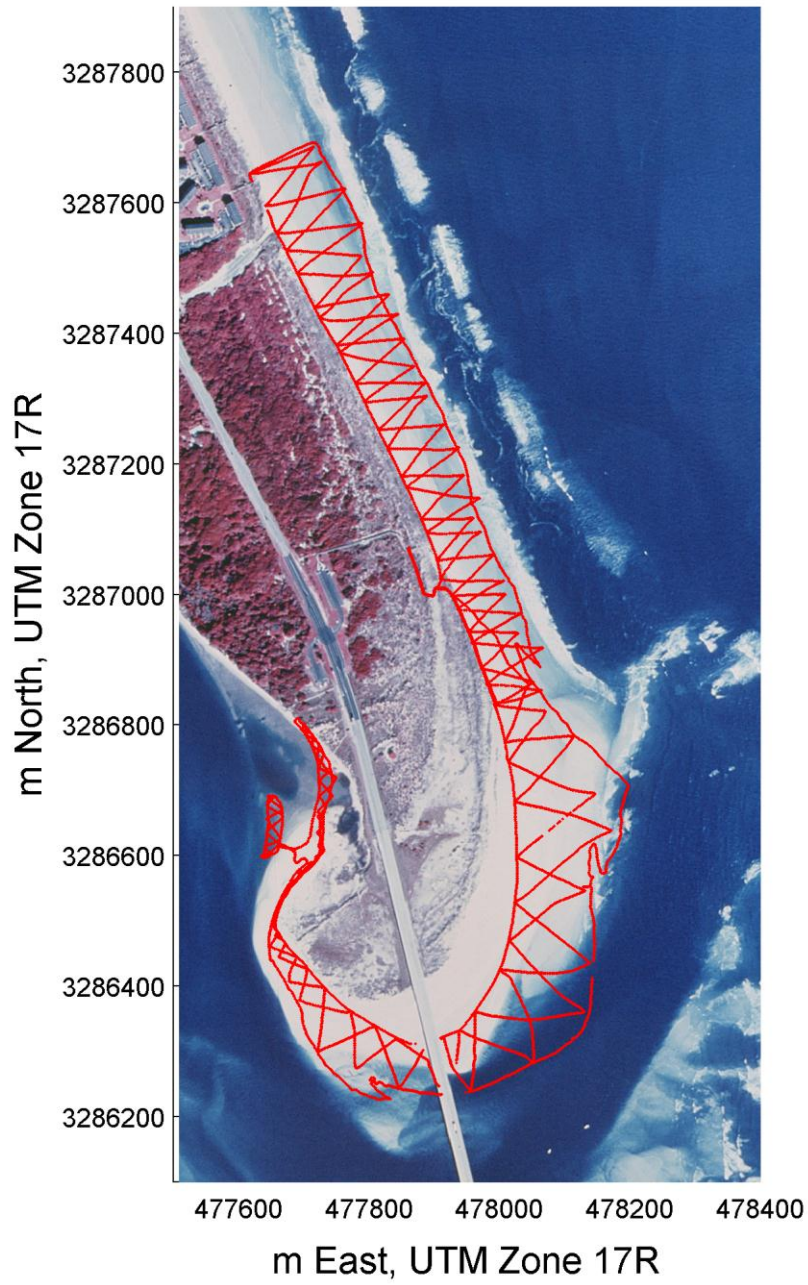
July 21, 2009



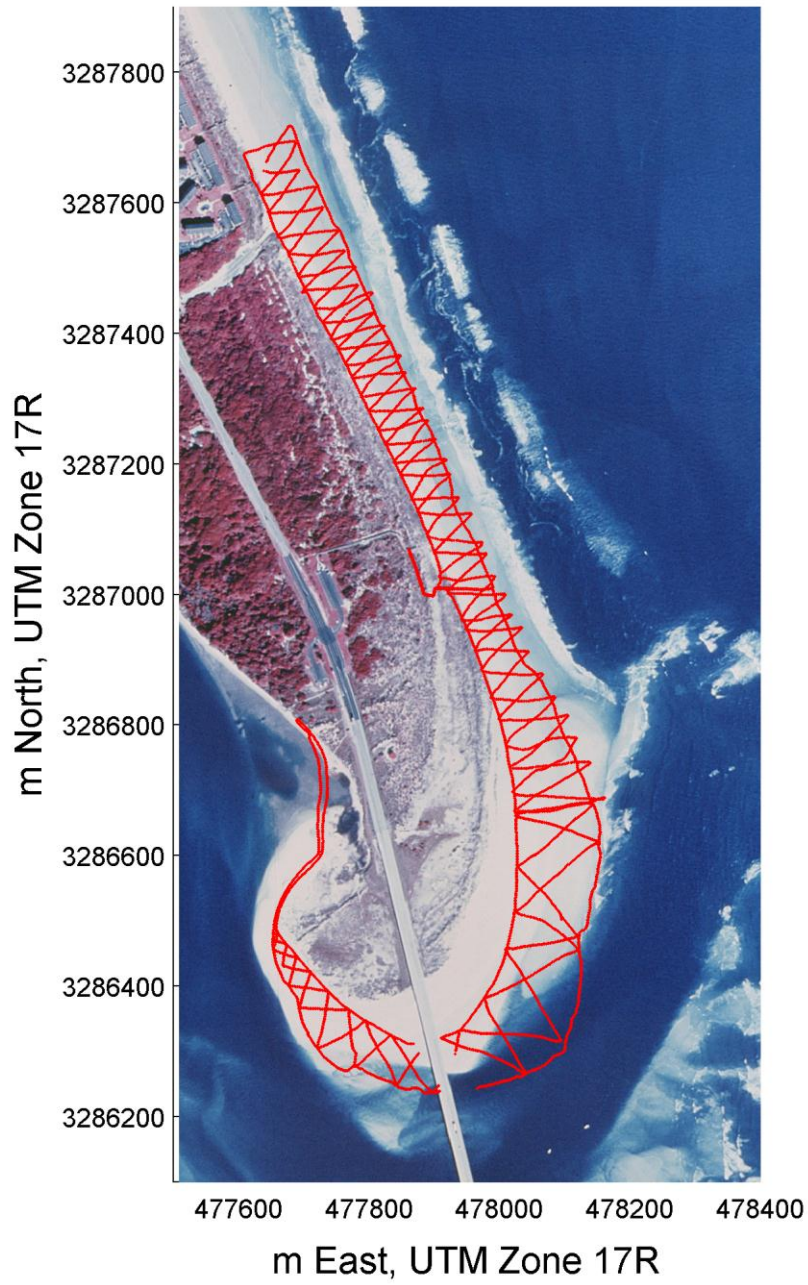
August 19, 2009



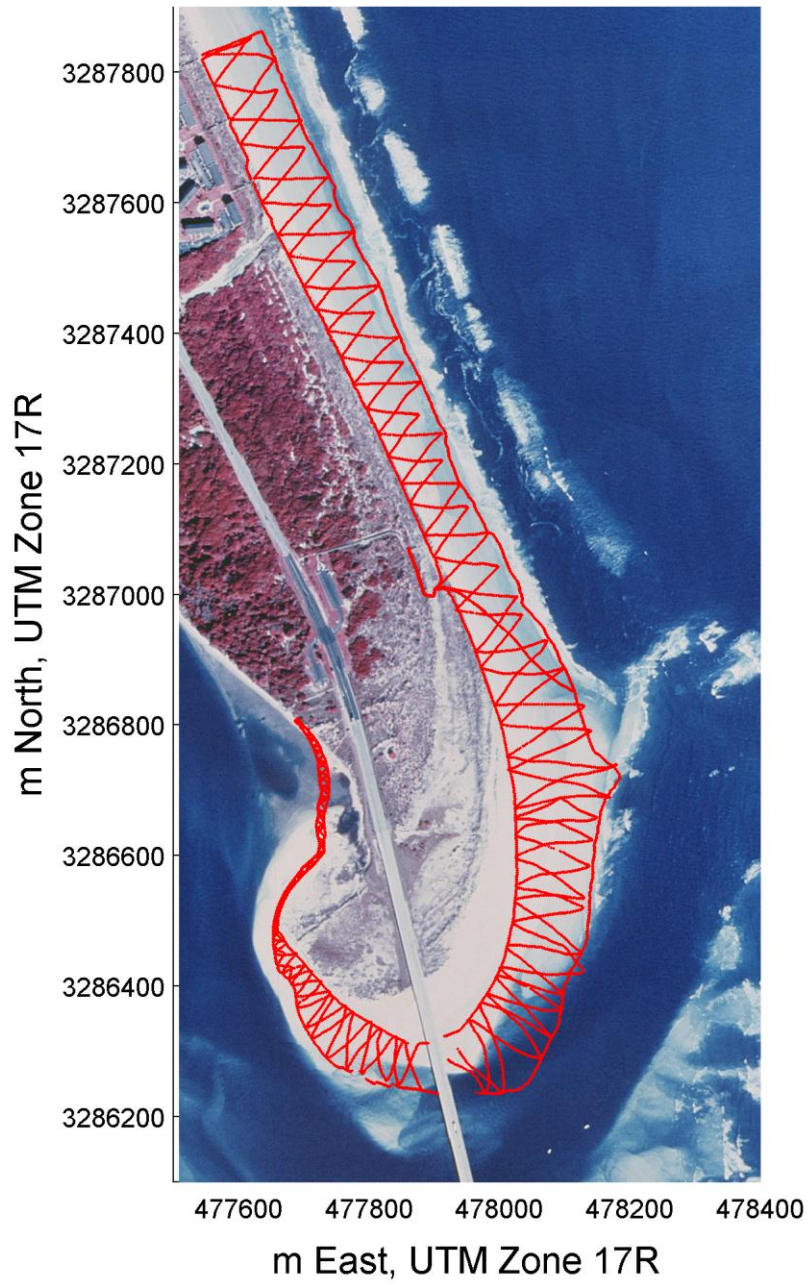
September 17, 2009



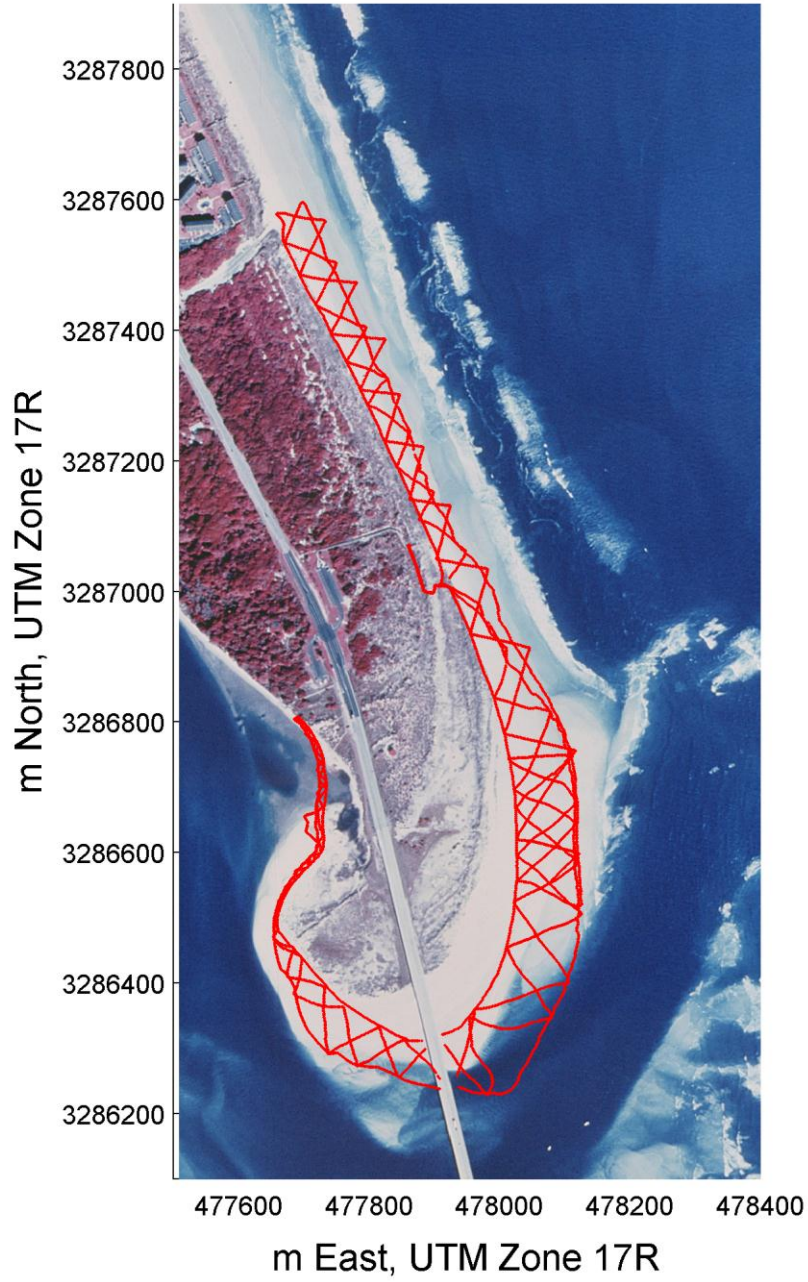
October 19, 2009



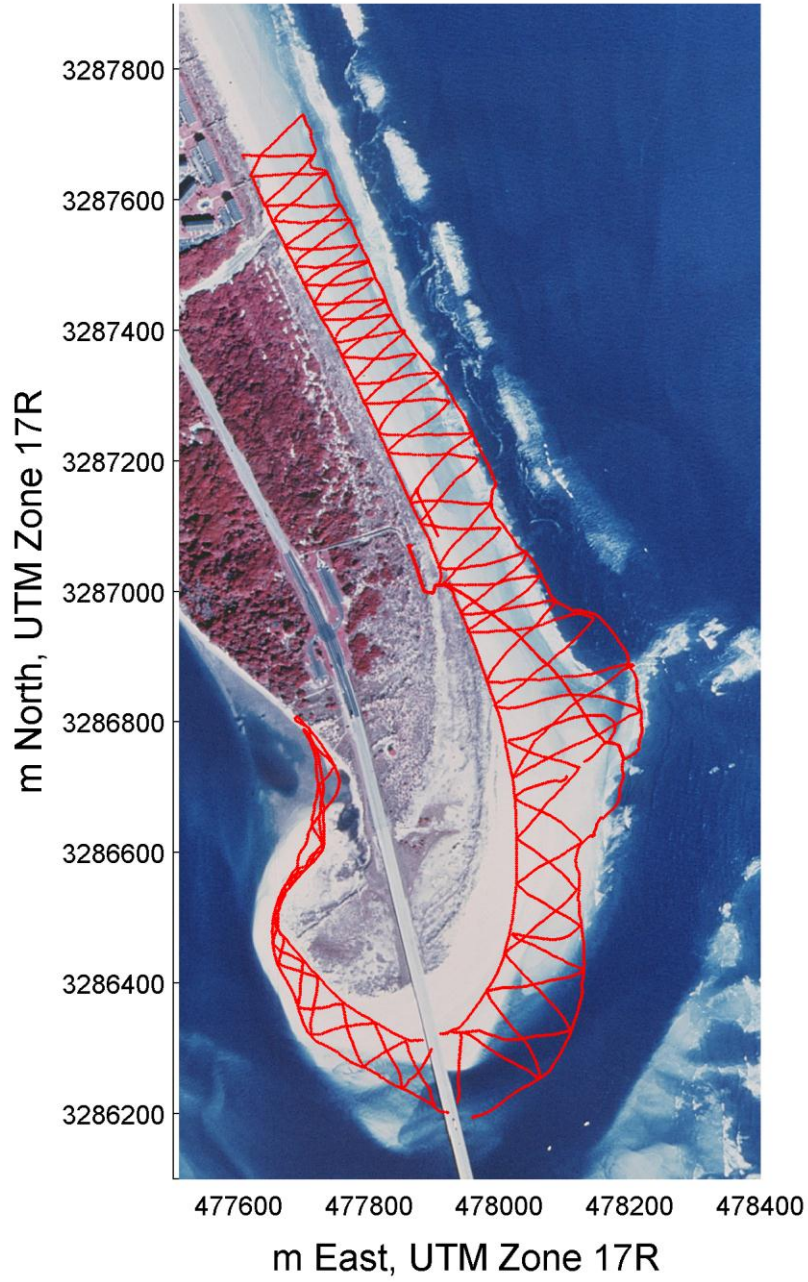
November 18, 2009



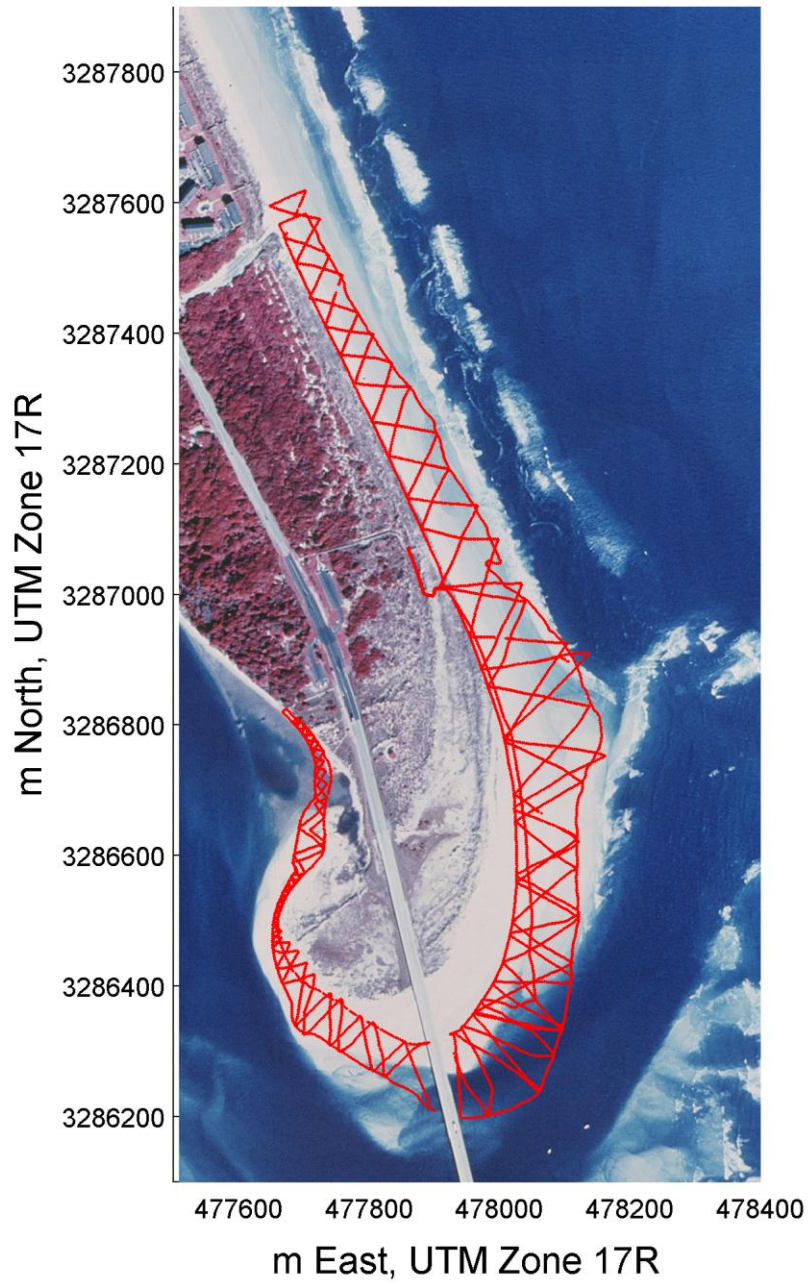
December 11, 2009

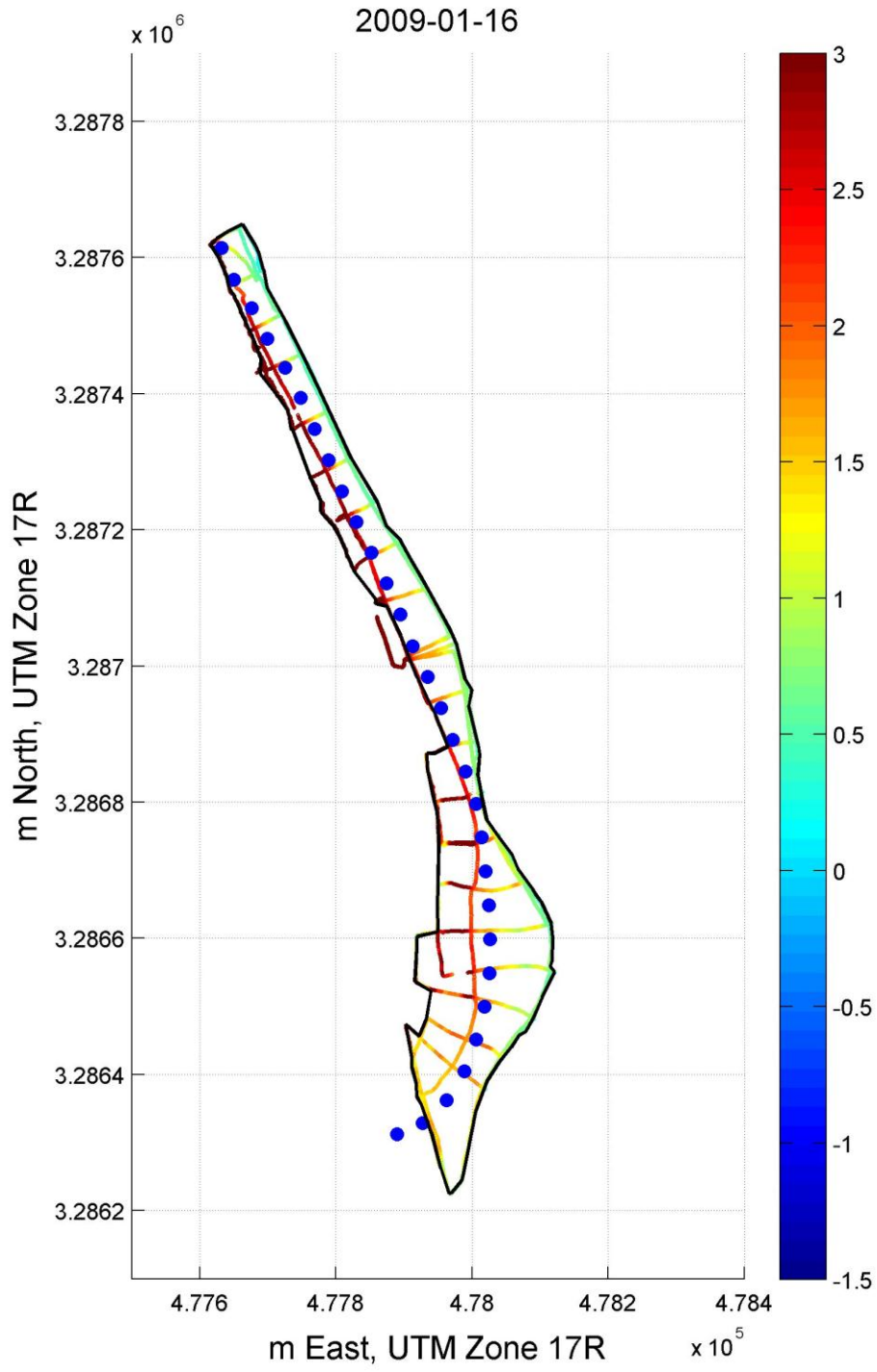


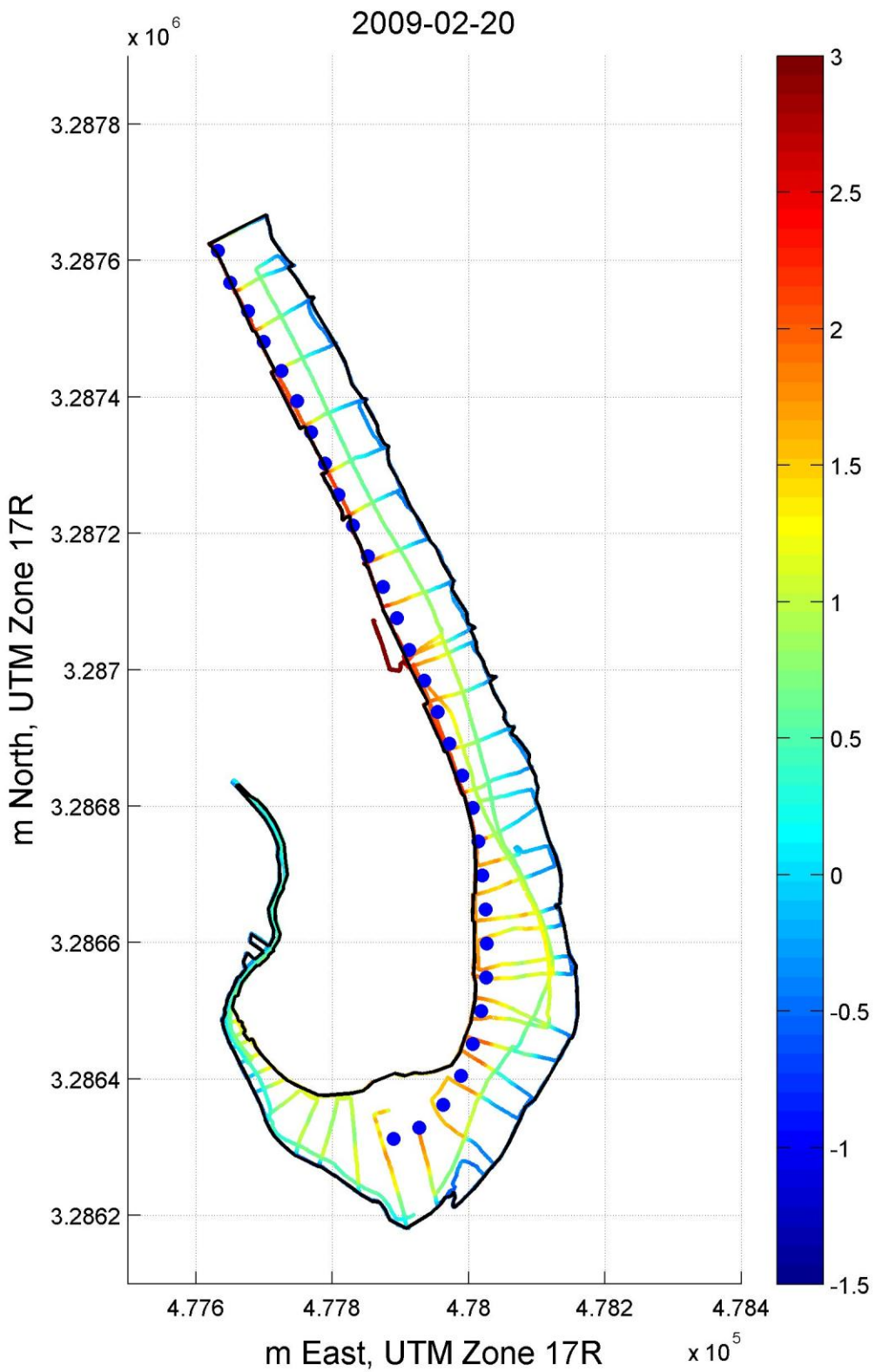
January 15, 2010

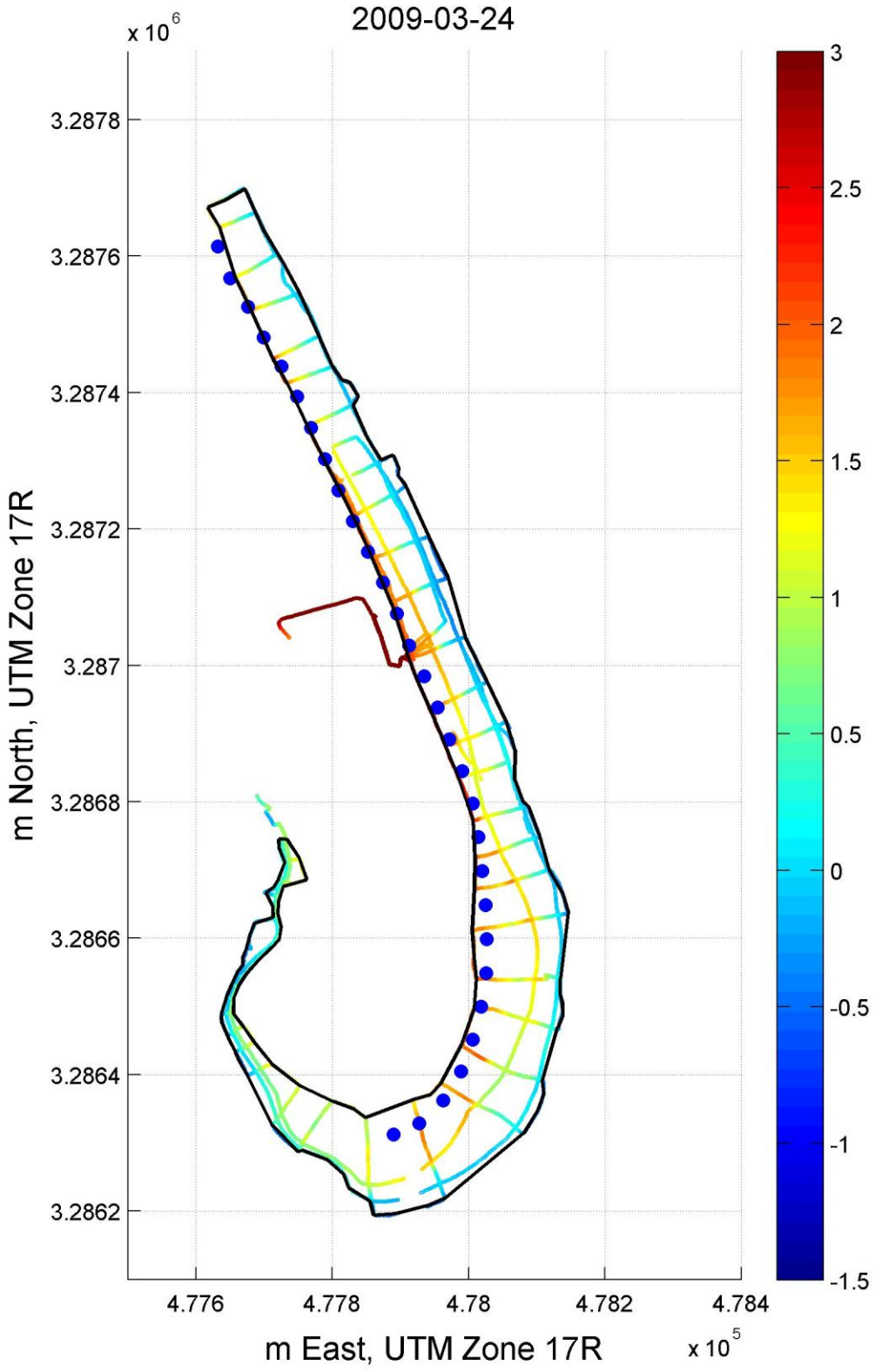


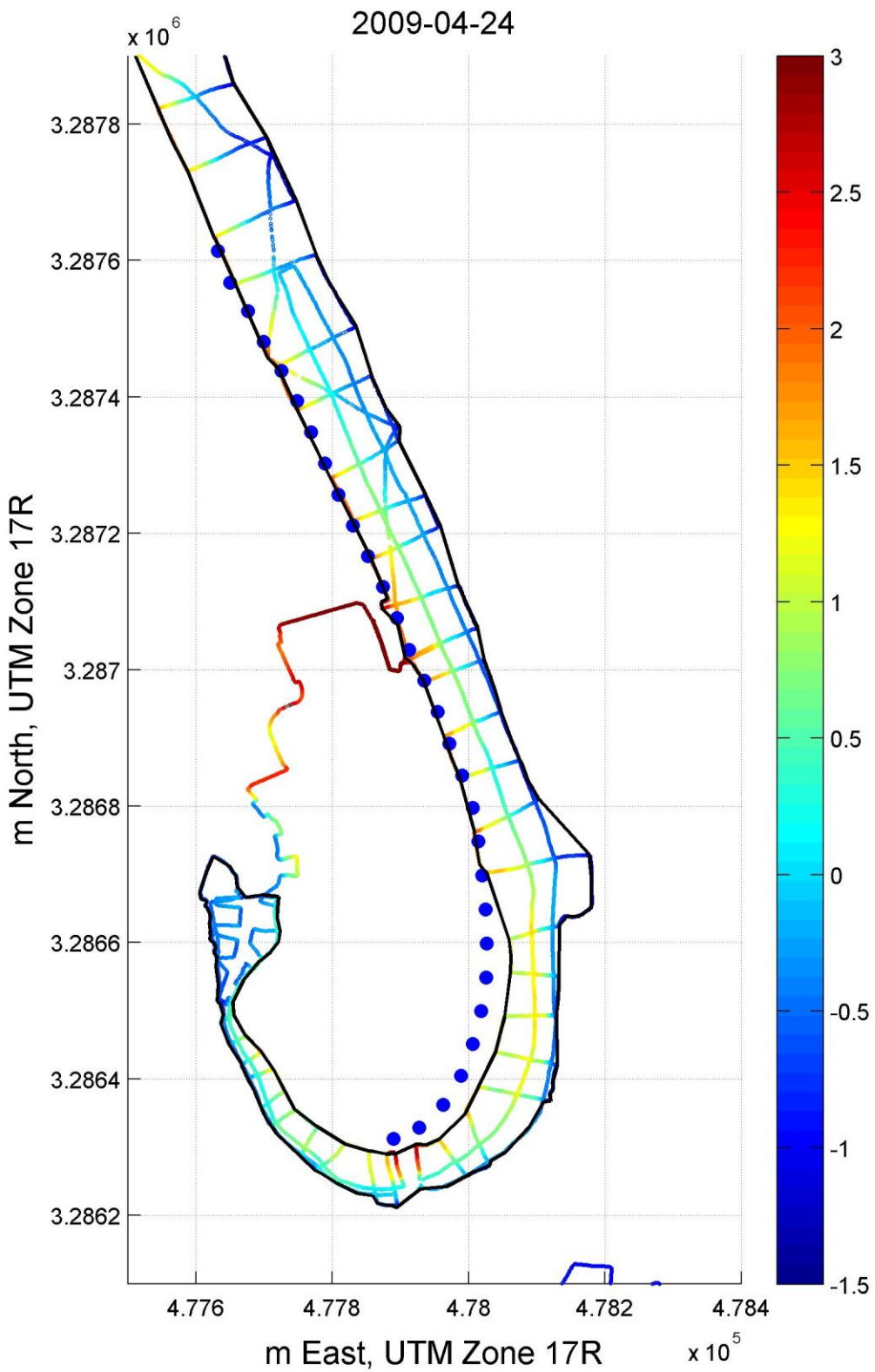
February 12, 2010

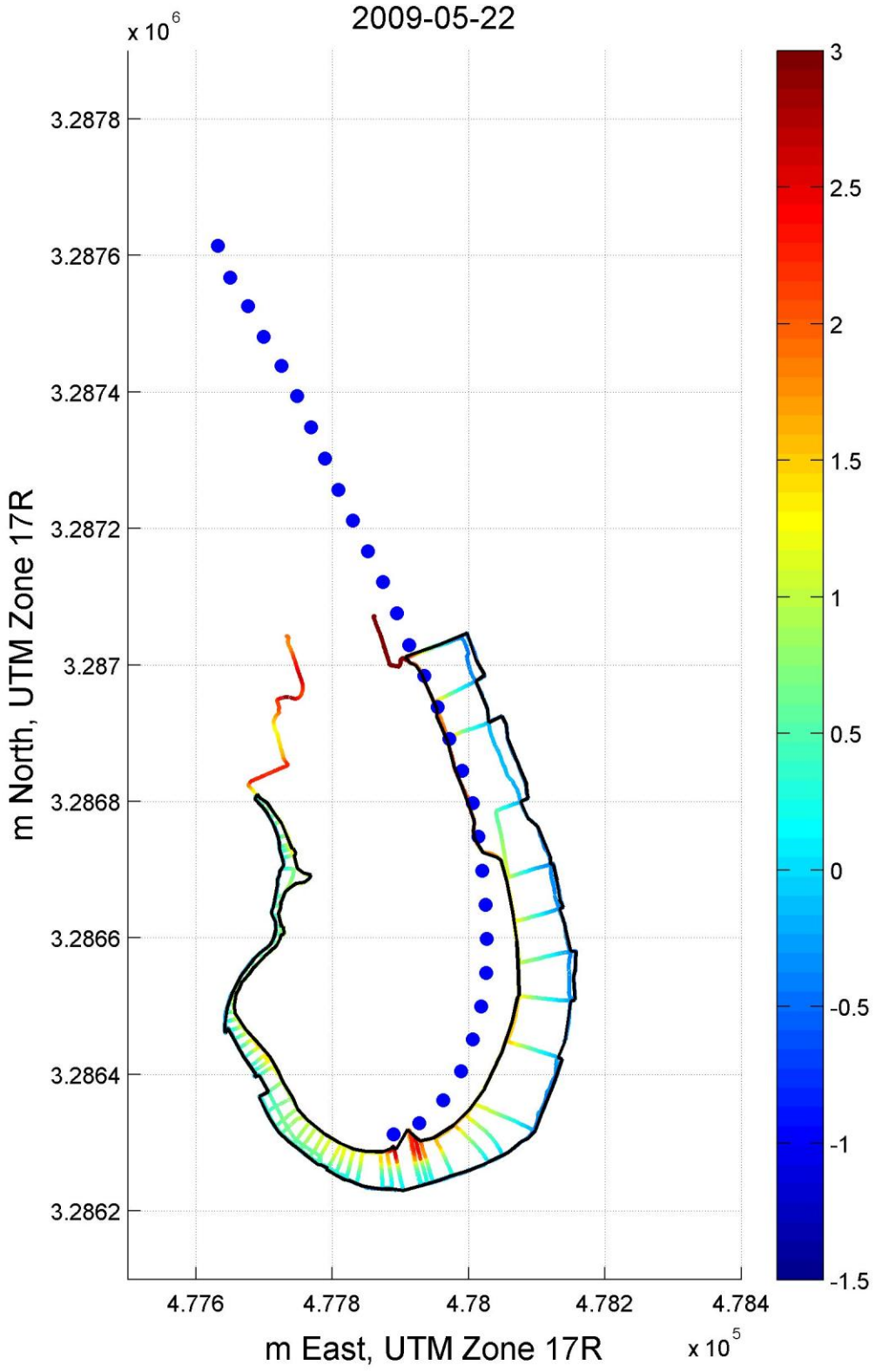


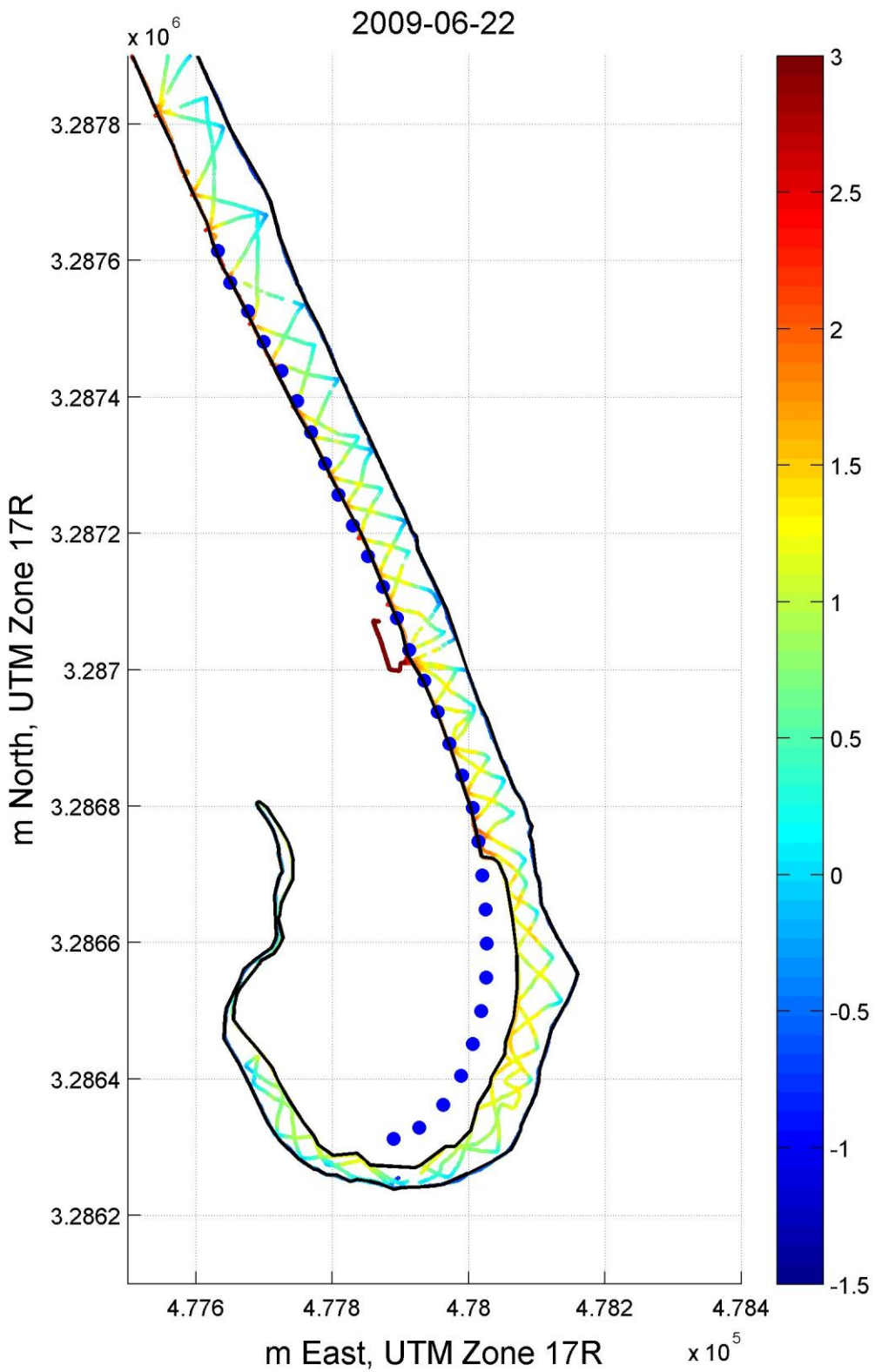


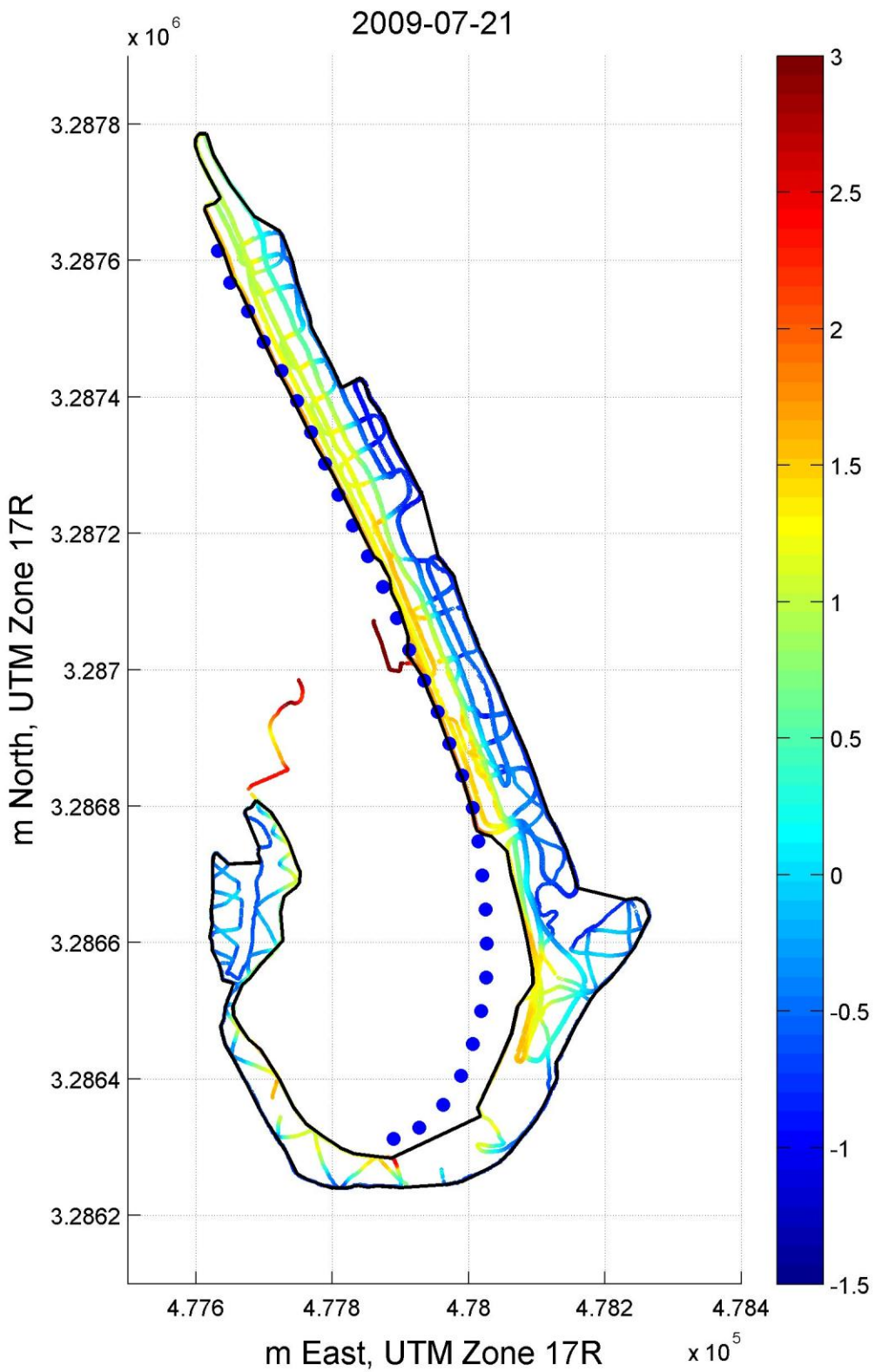


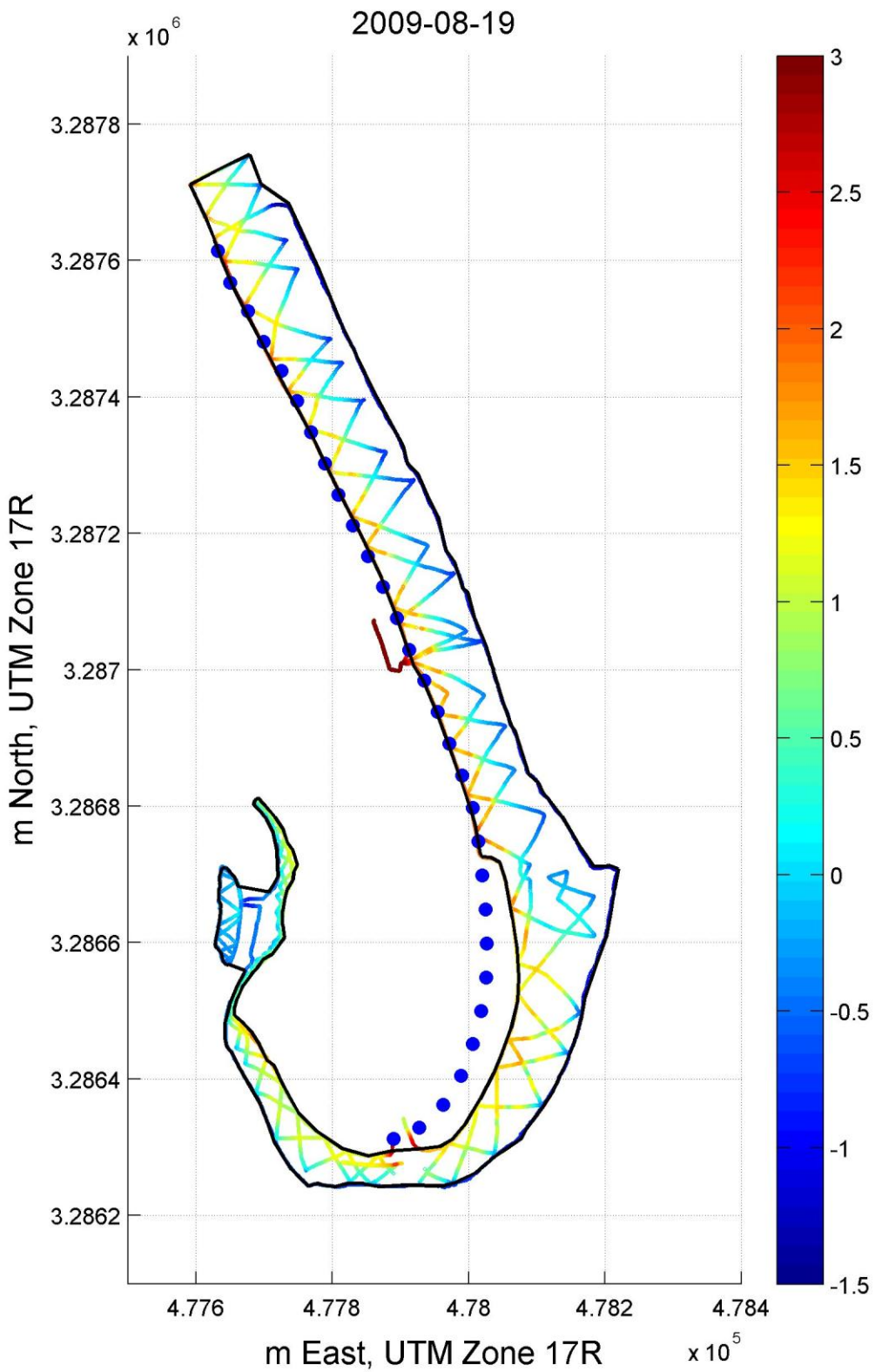


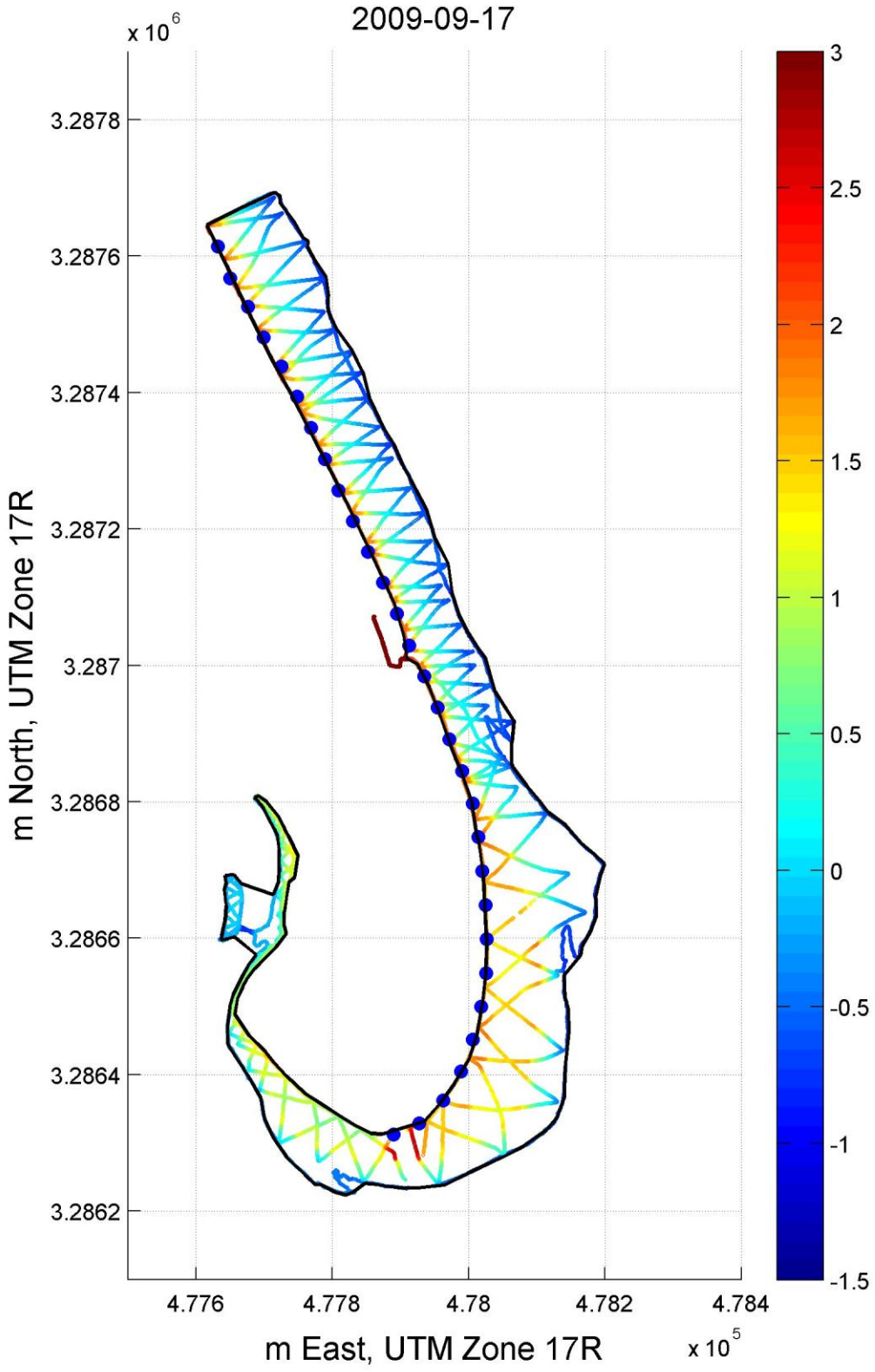


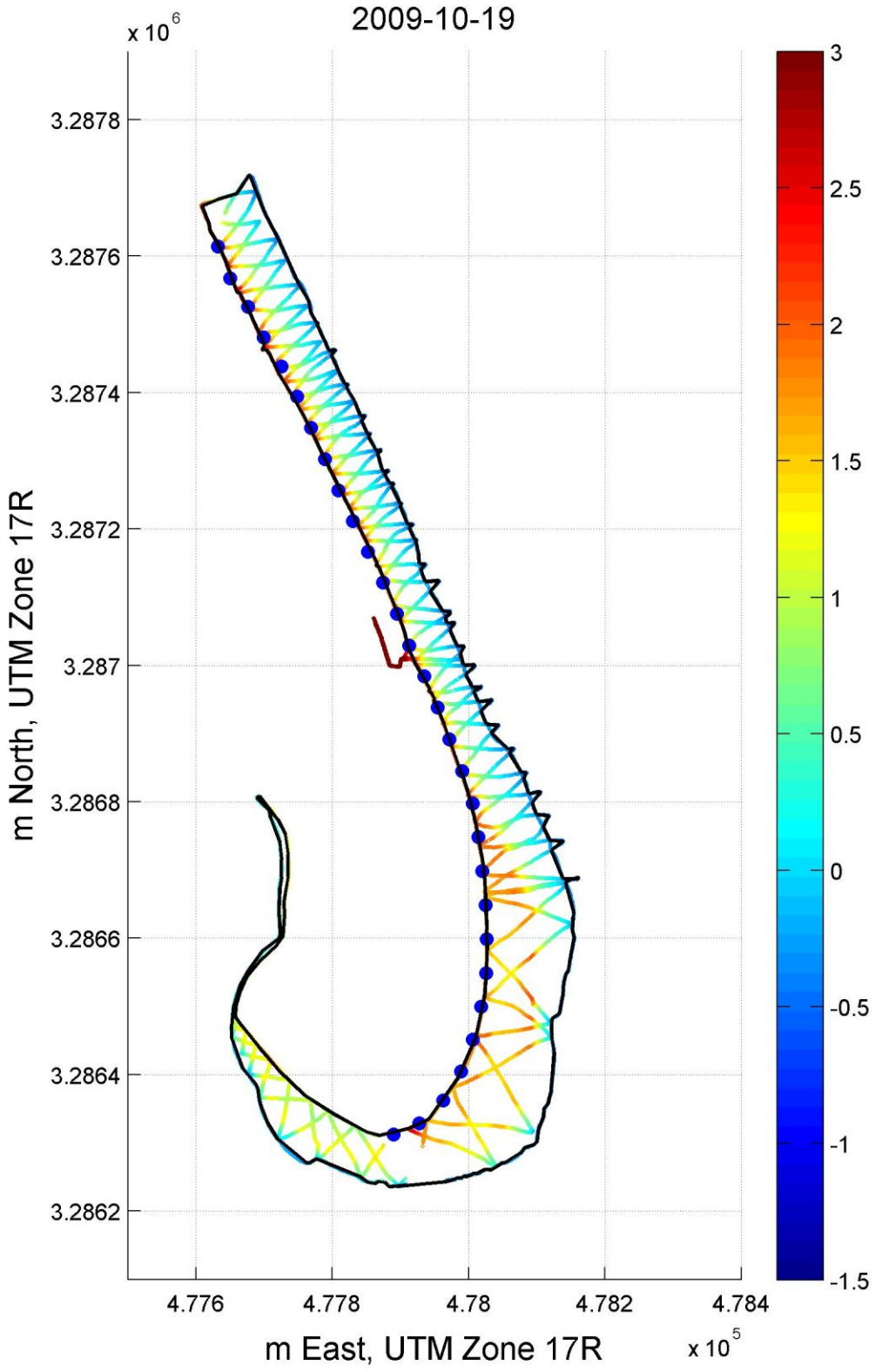


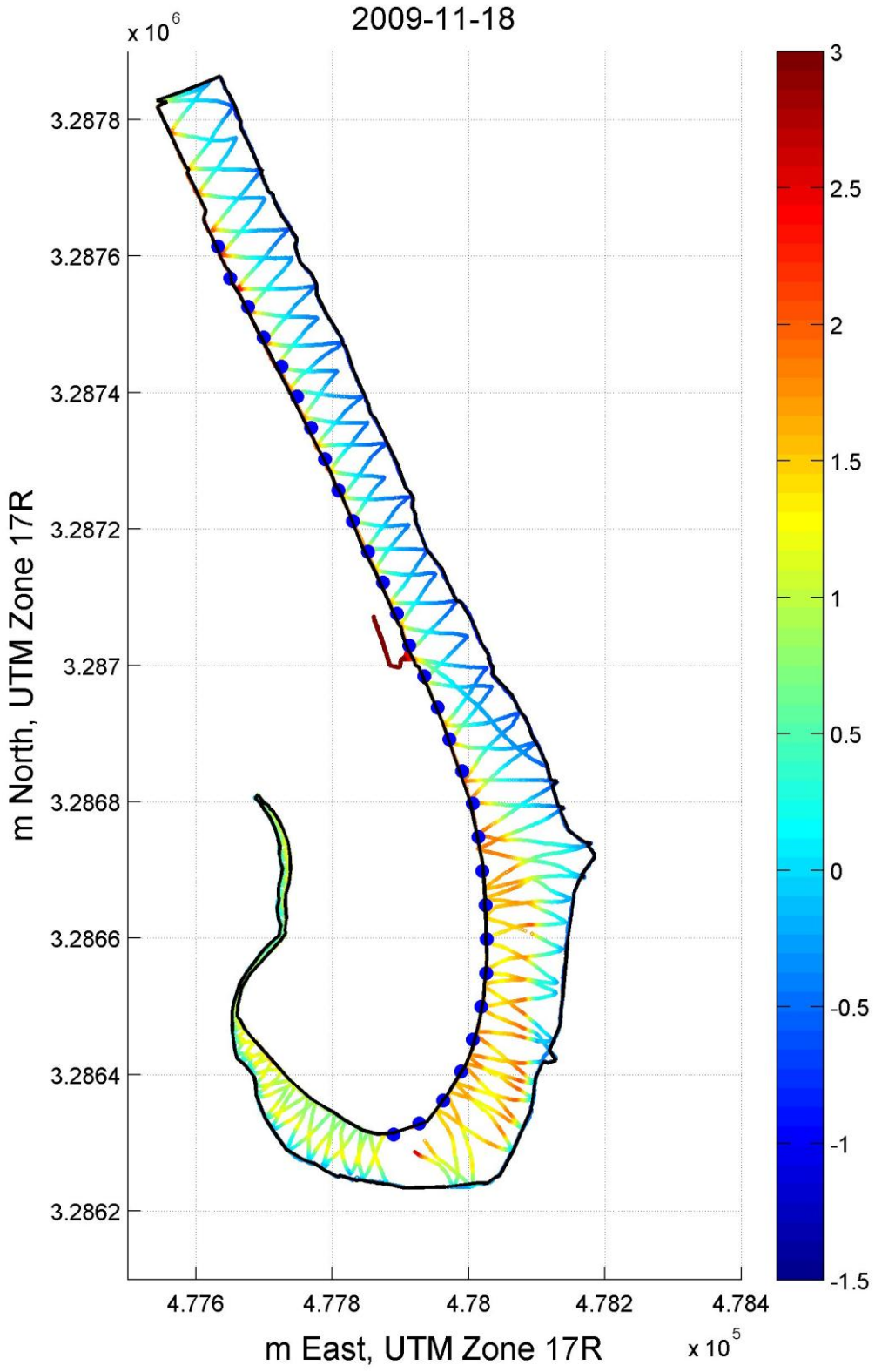


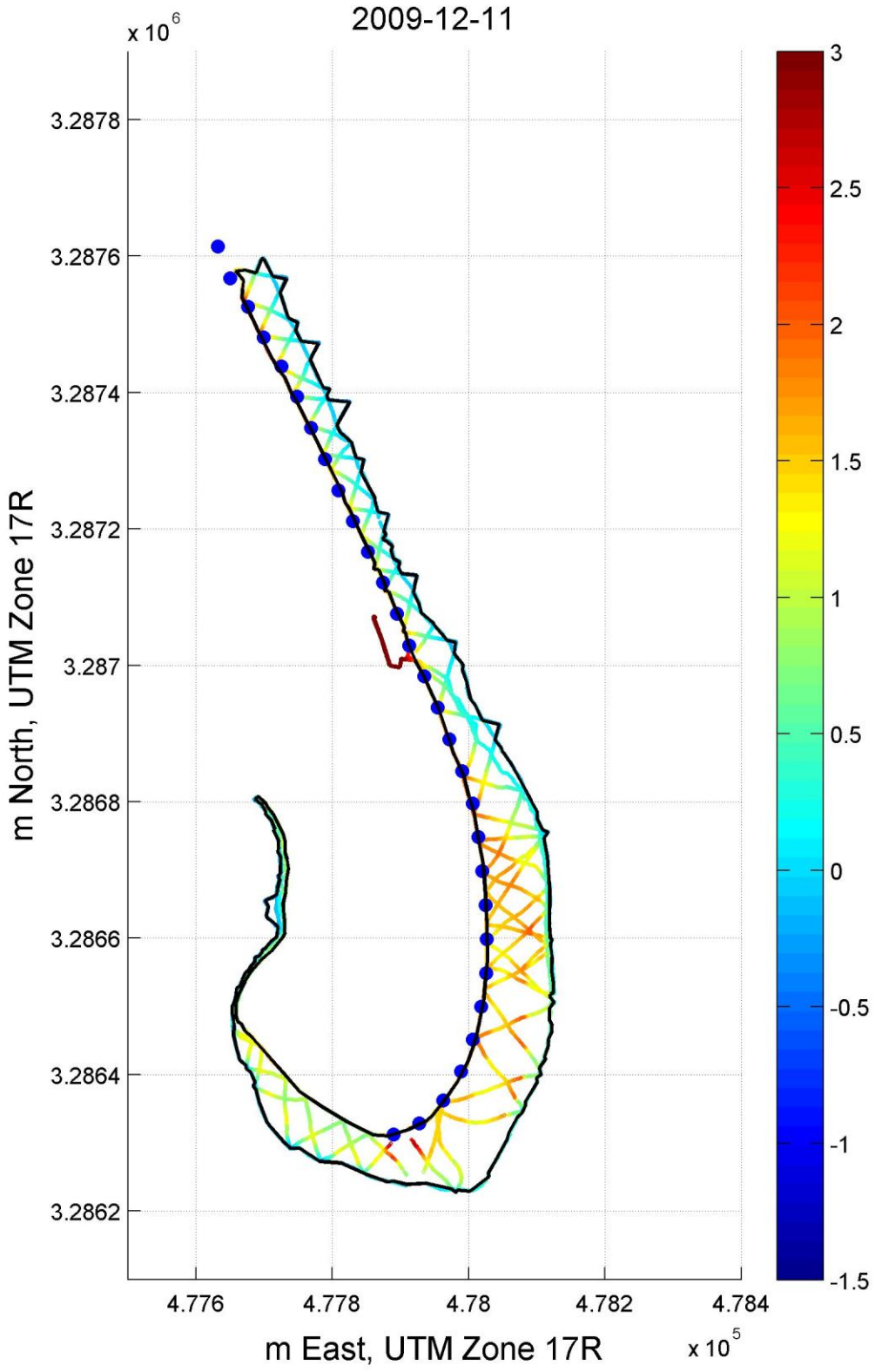


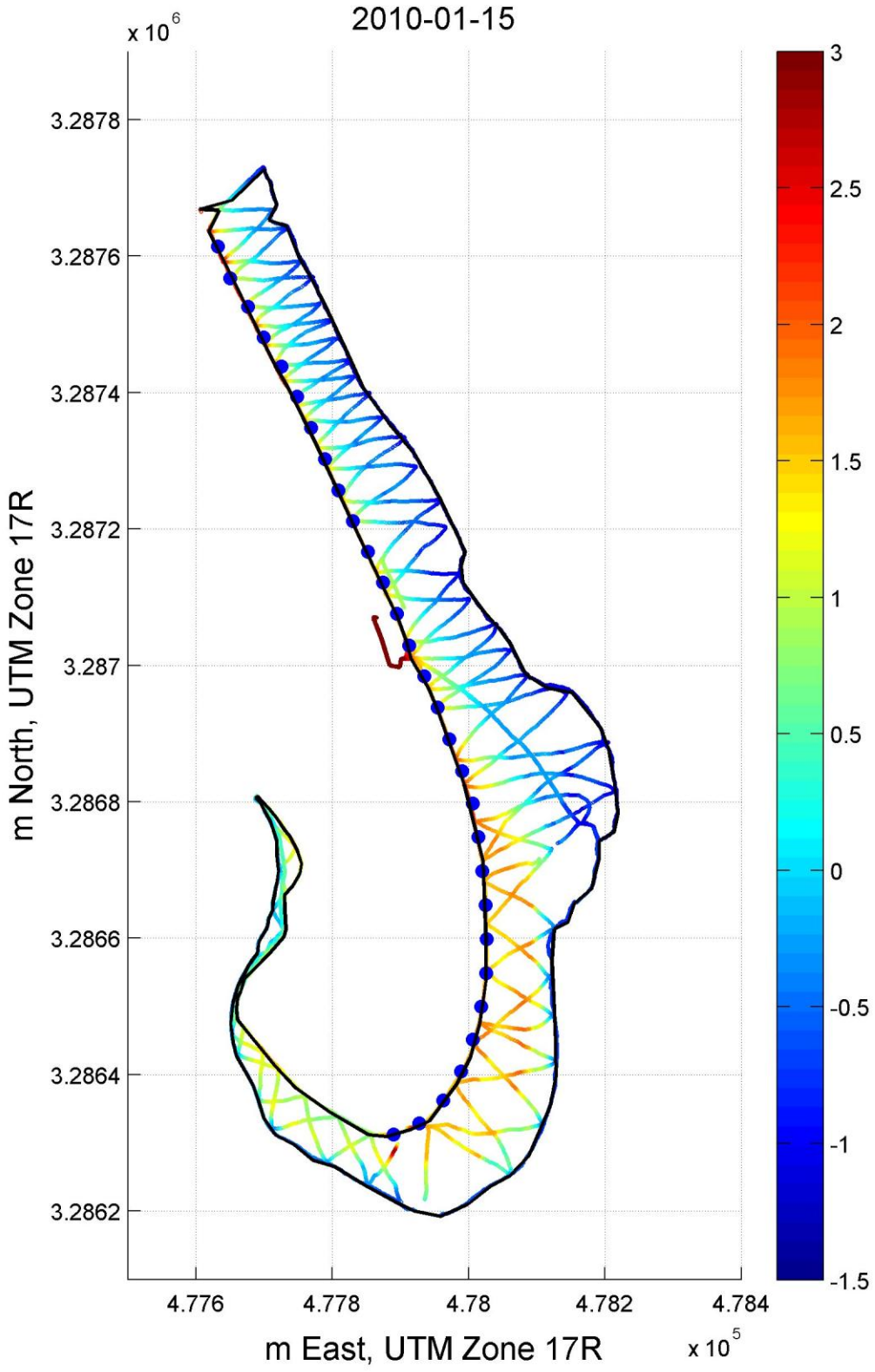


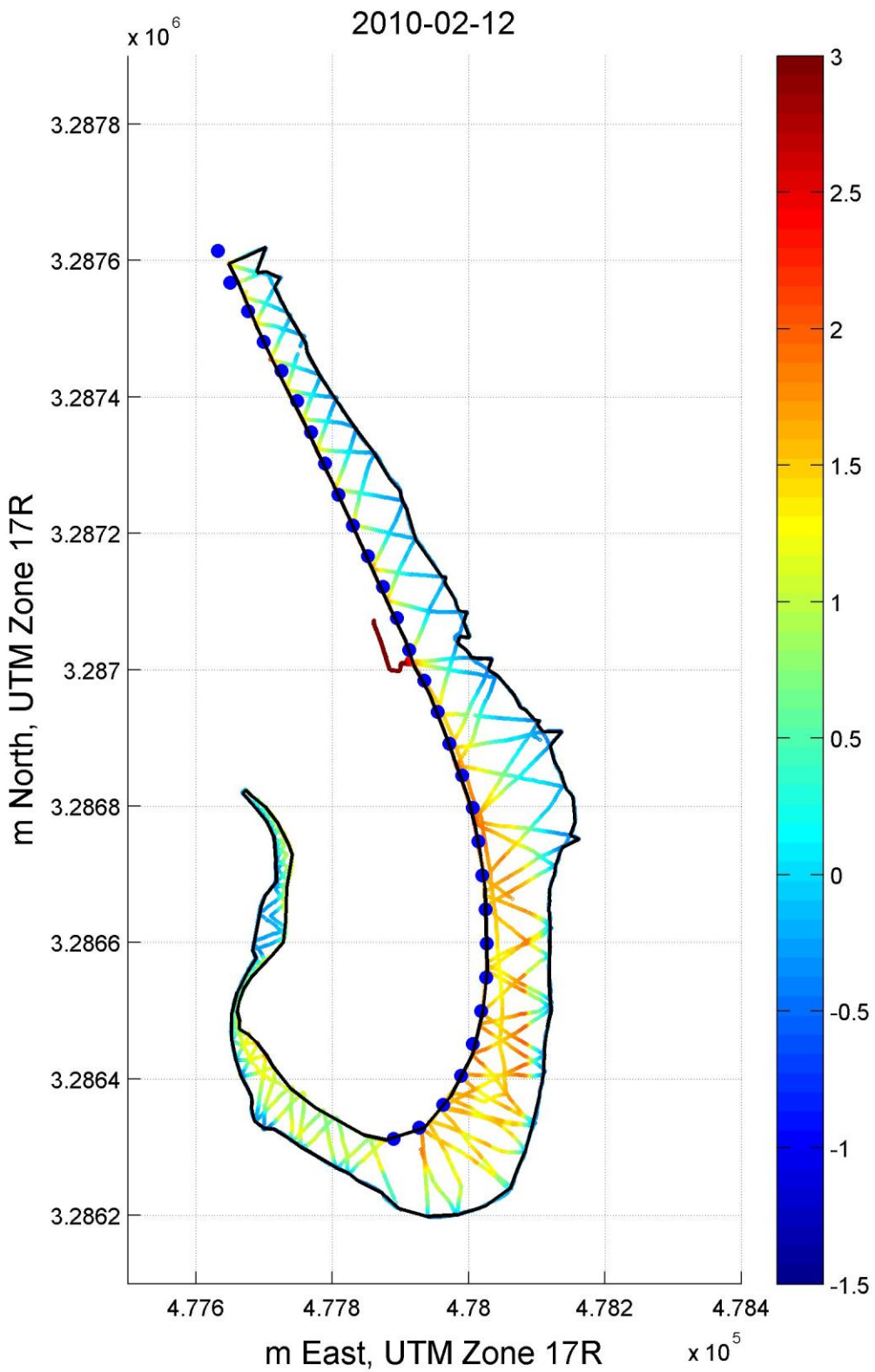


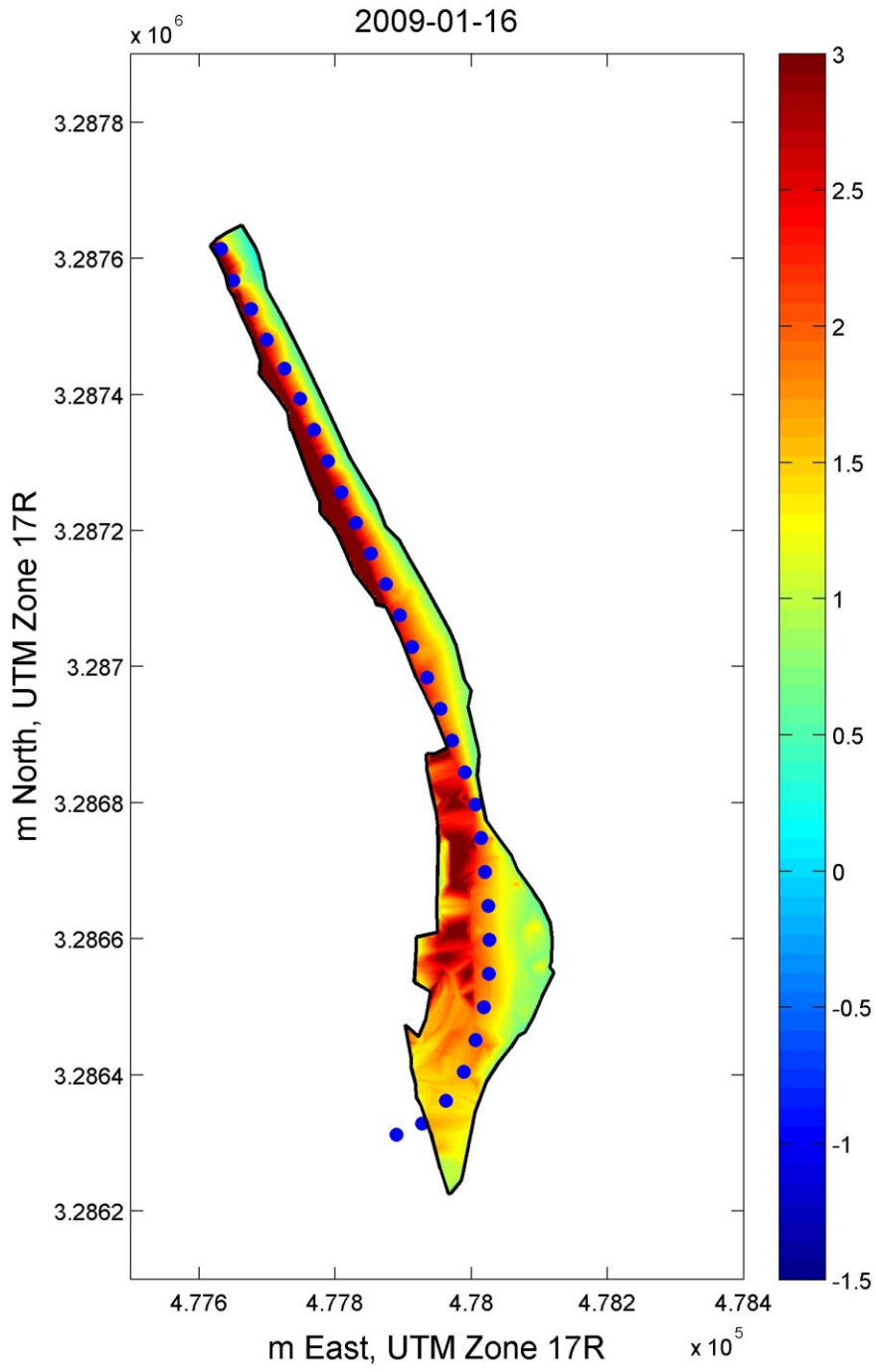


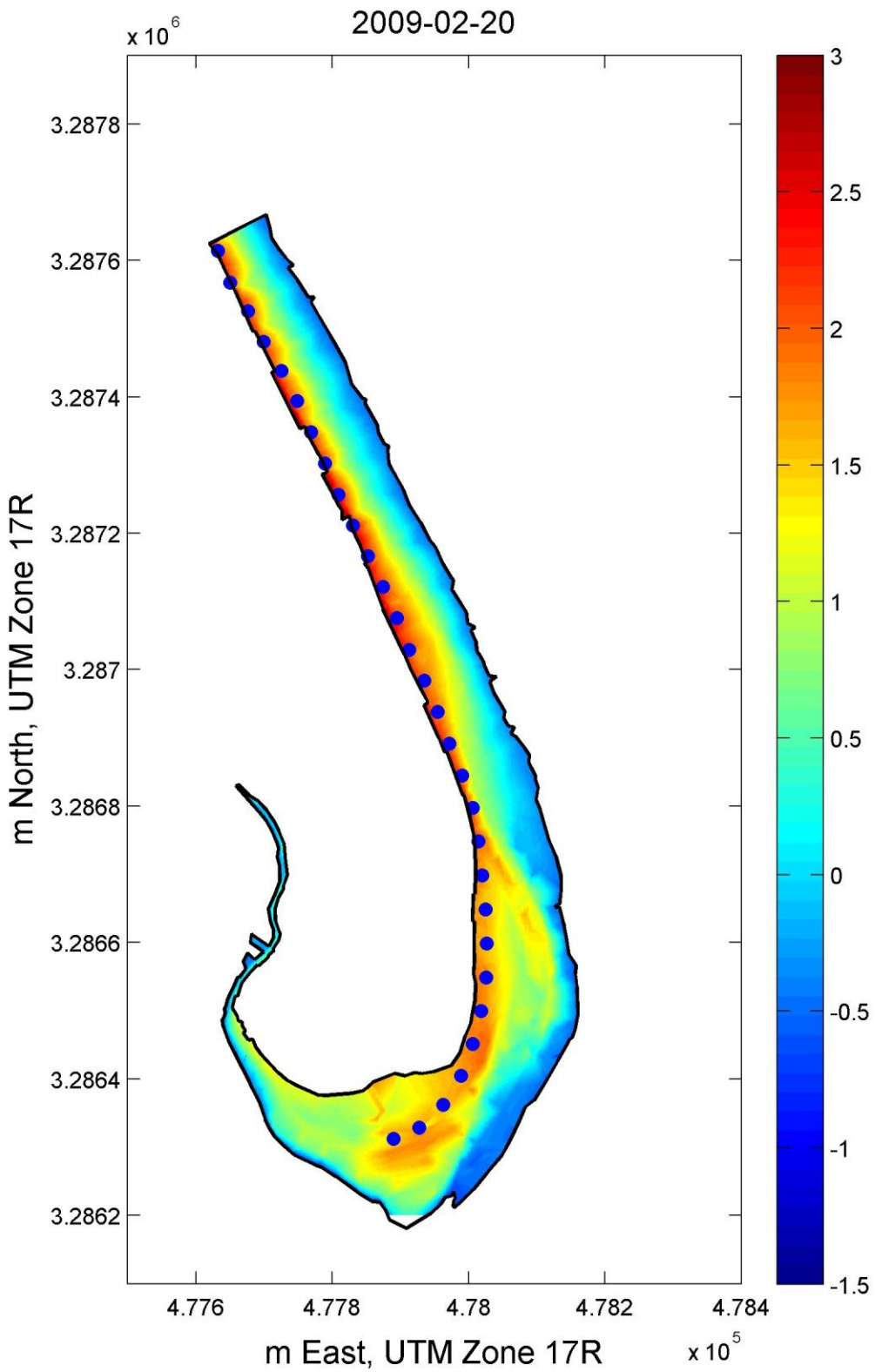


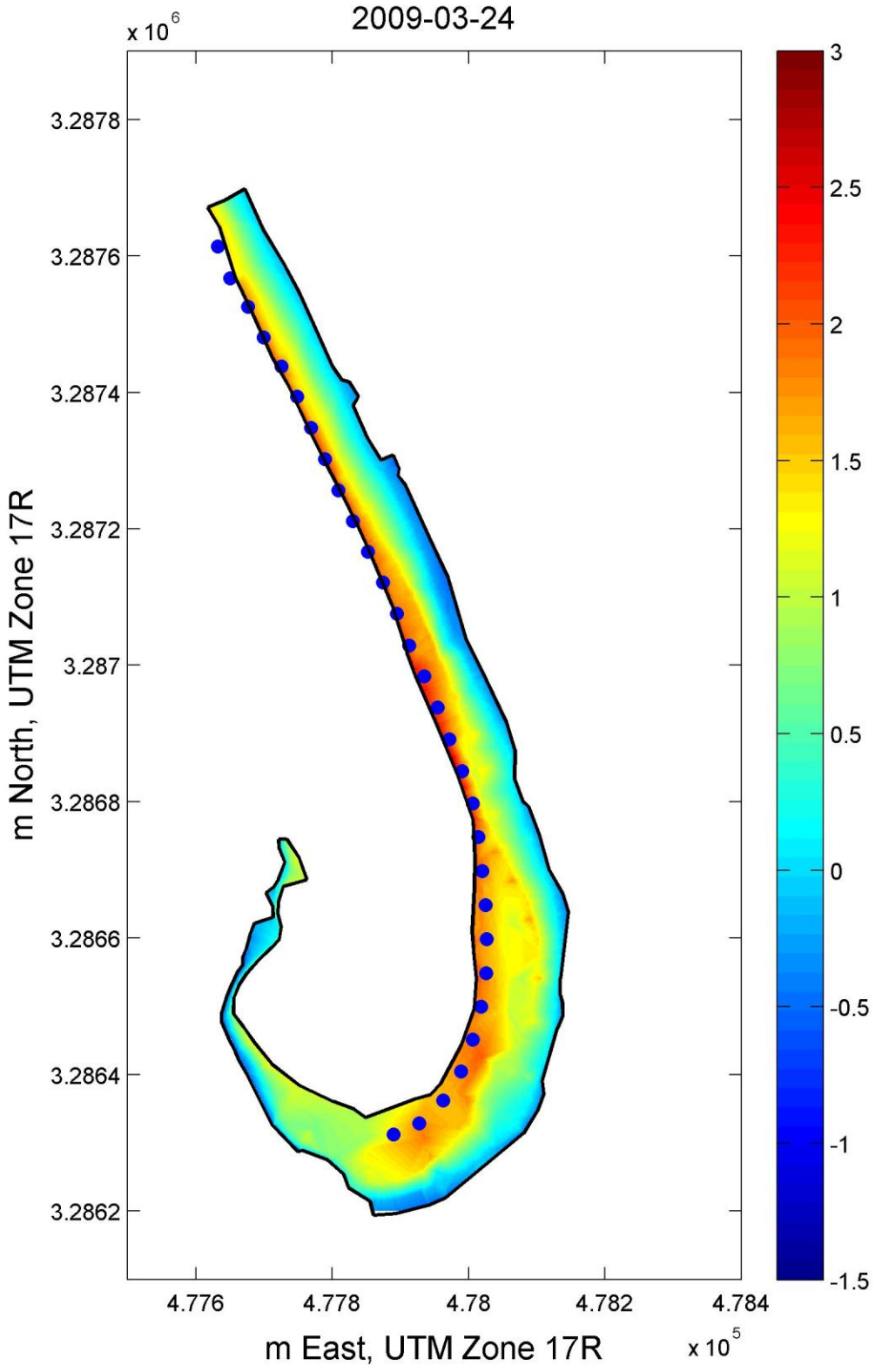


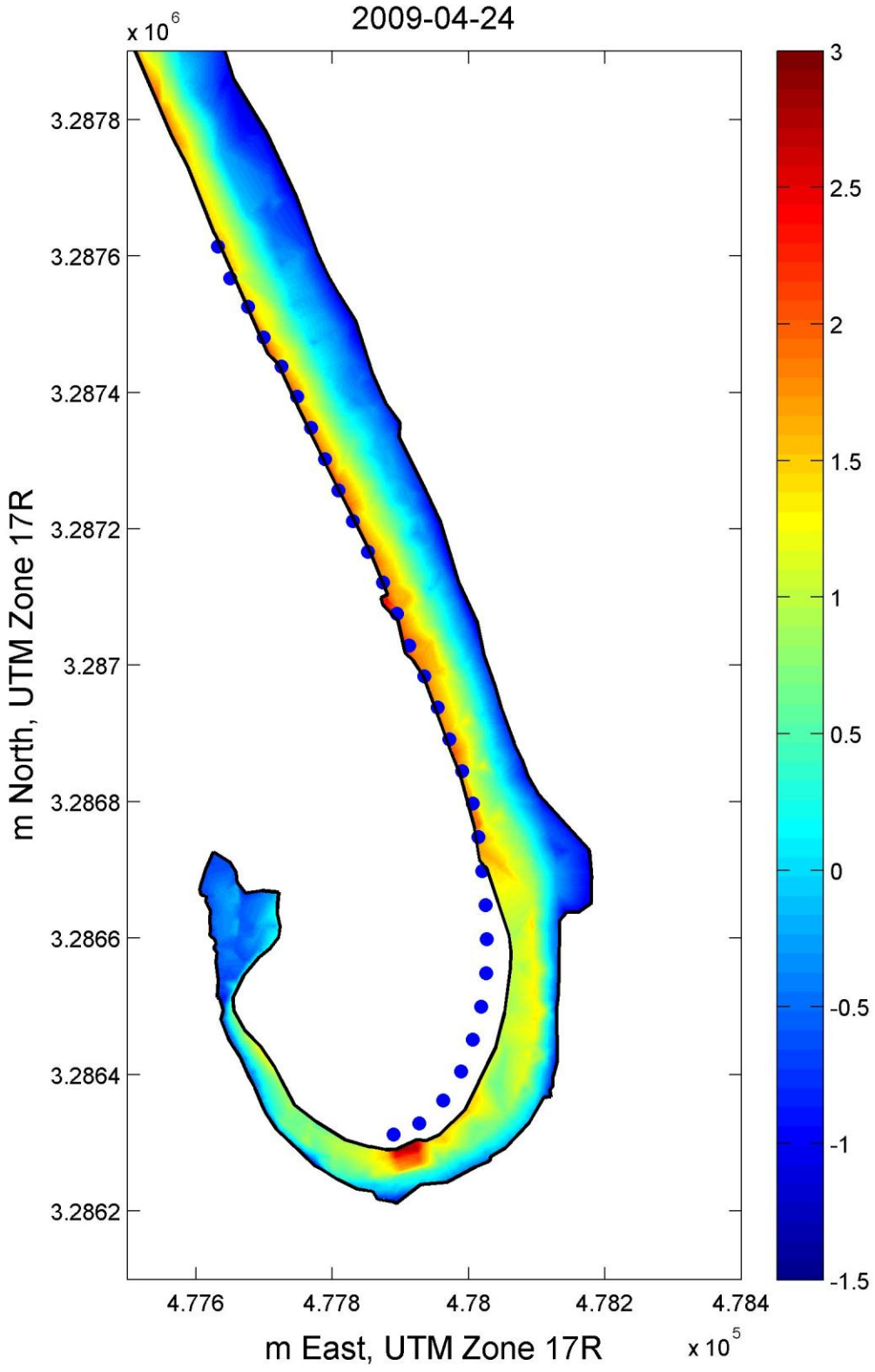


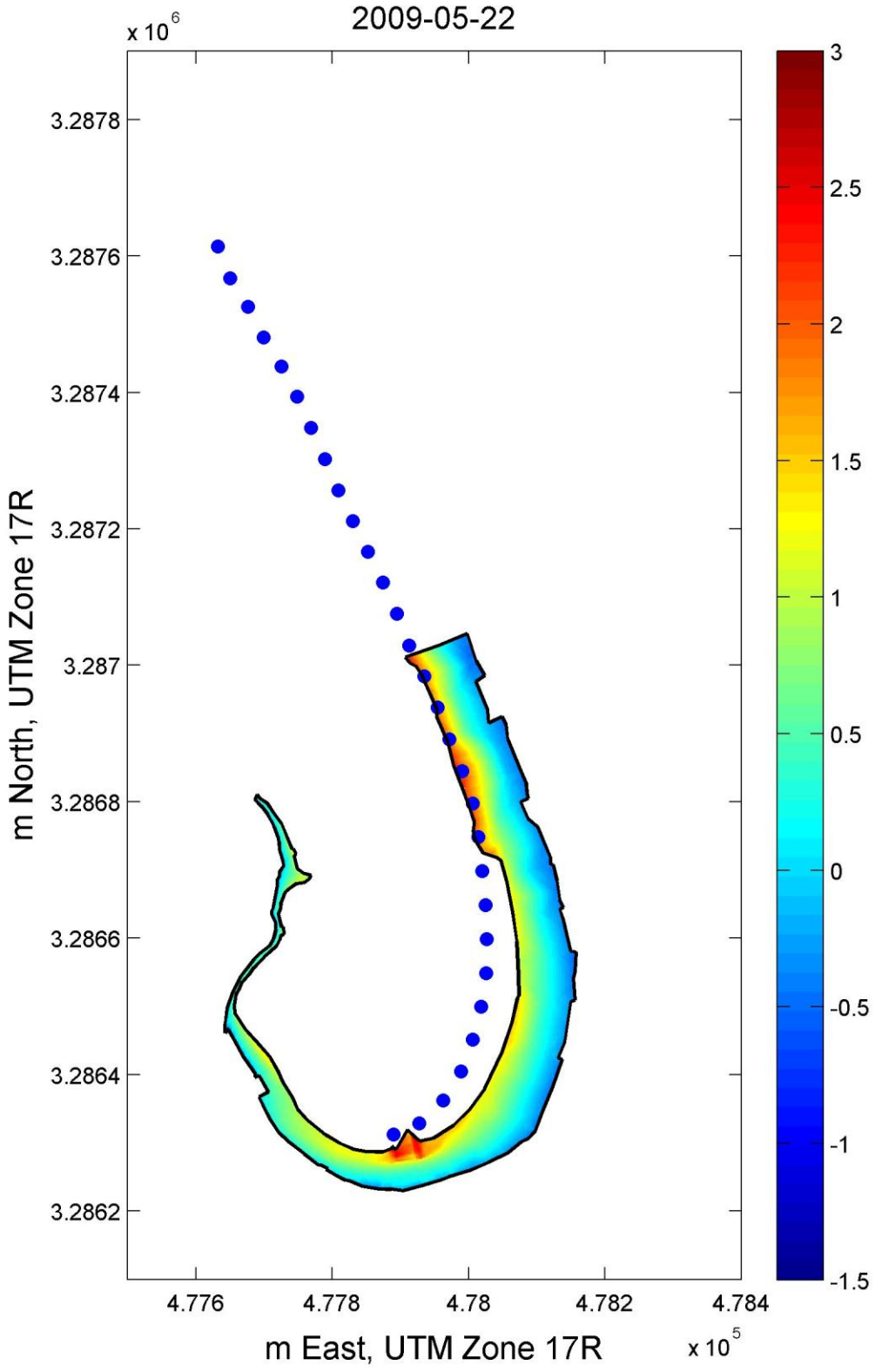


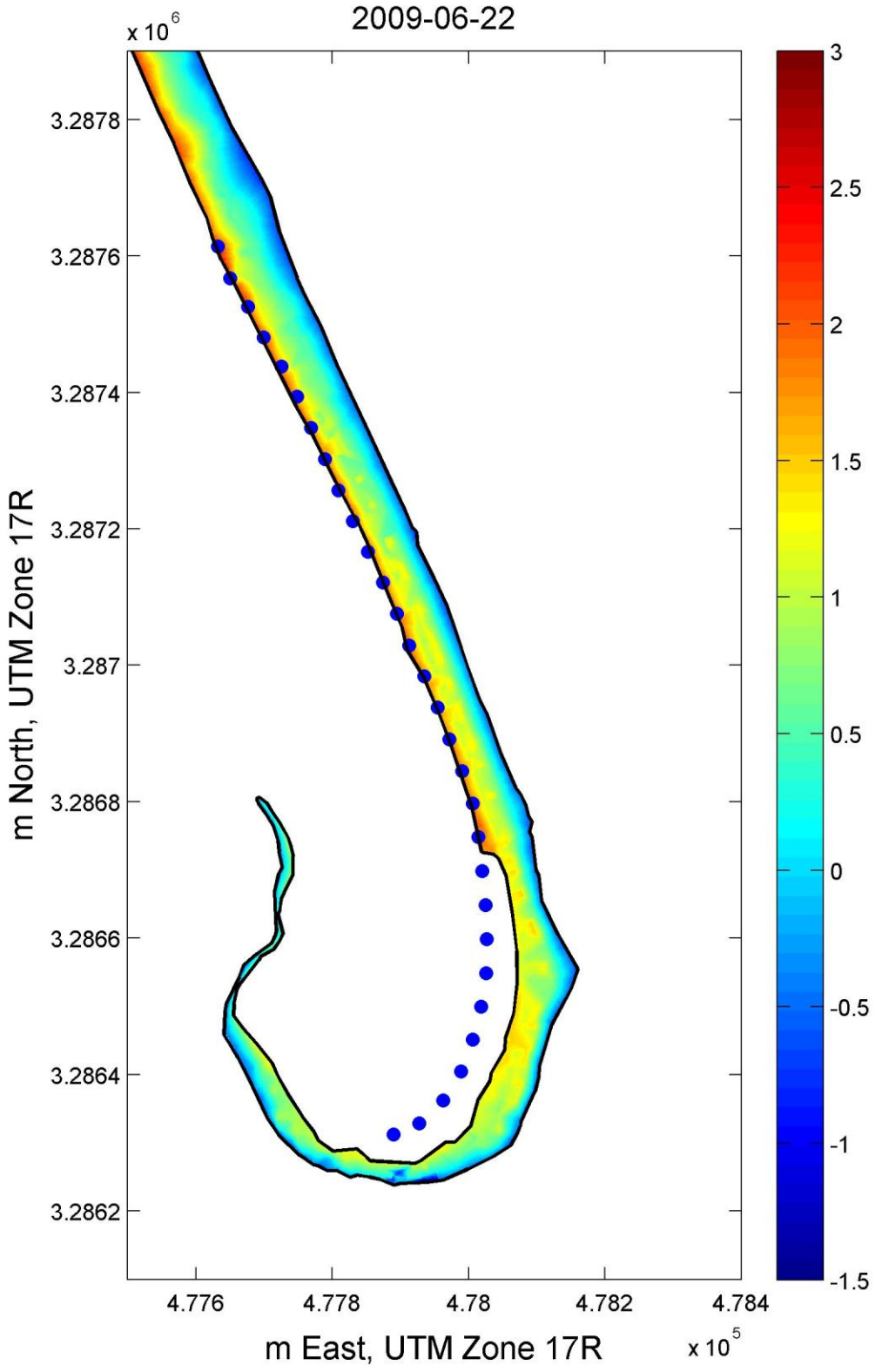


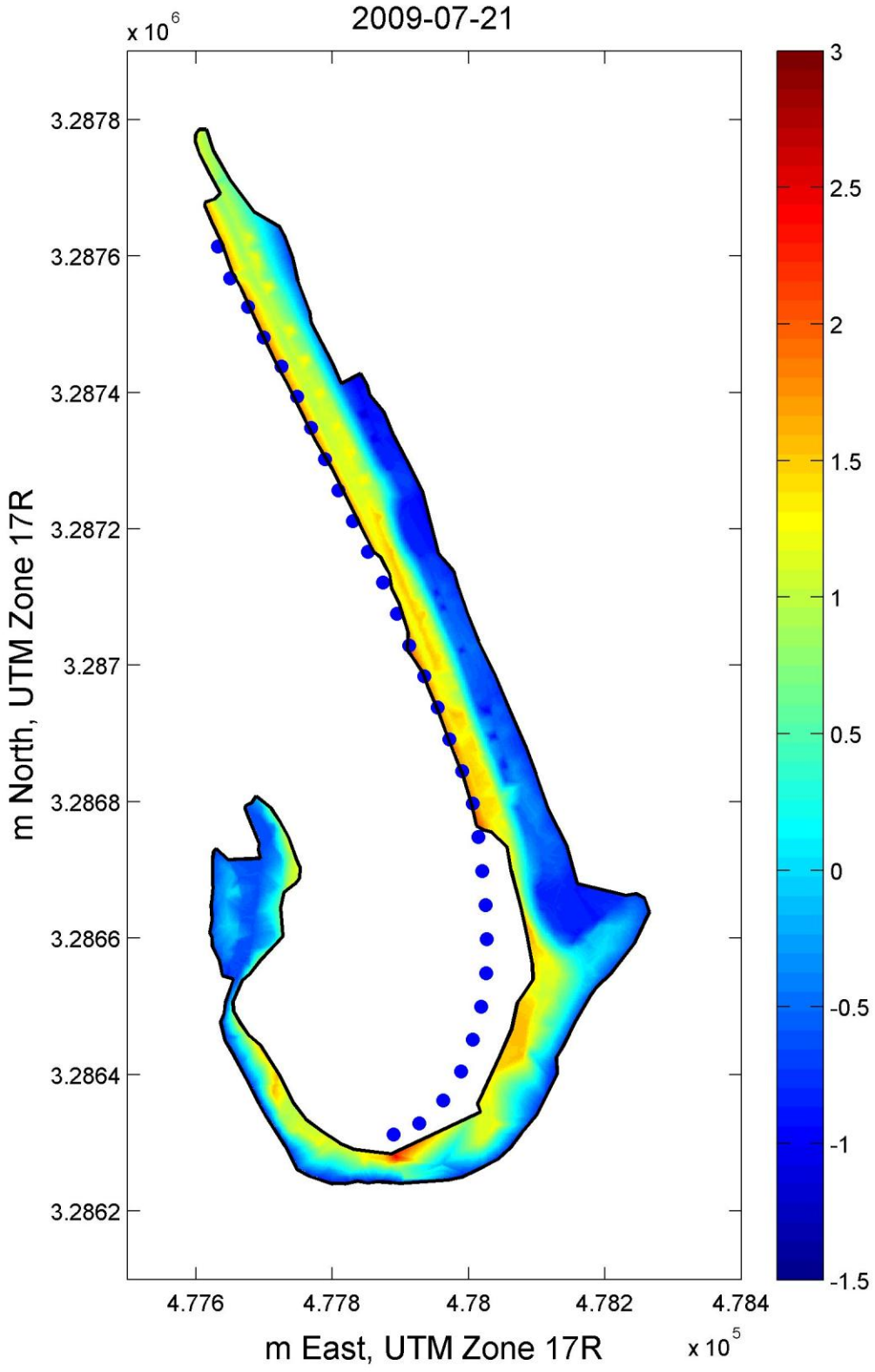


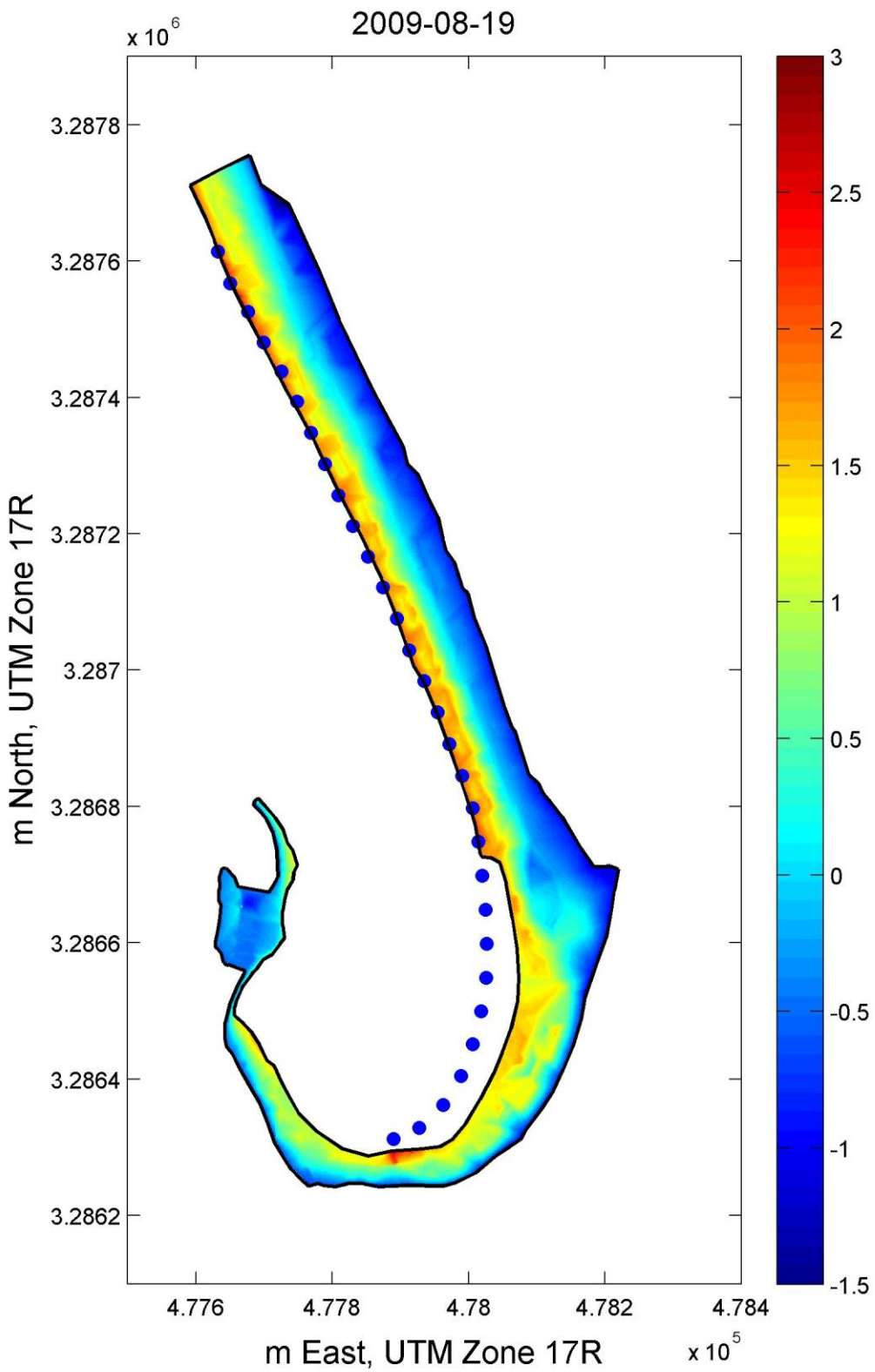


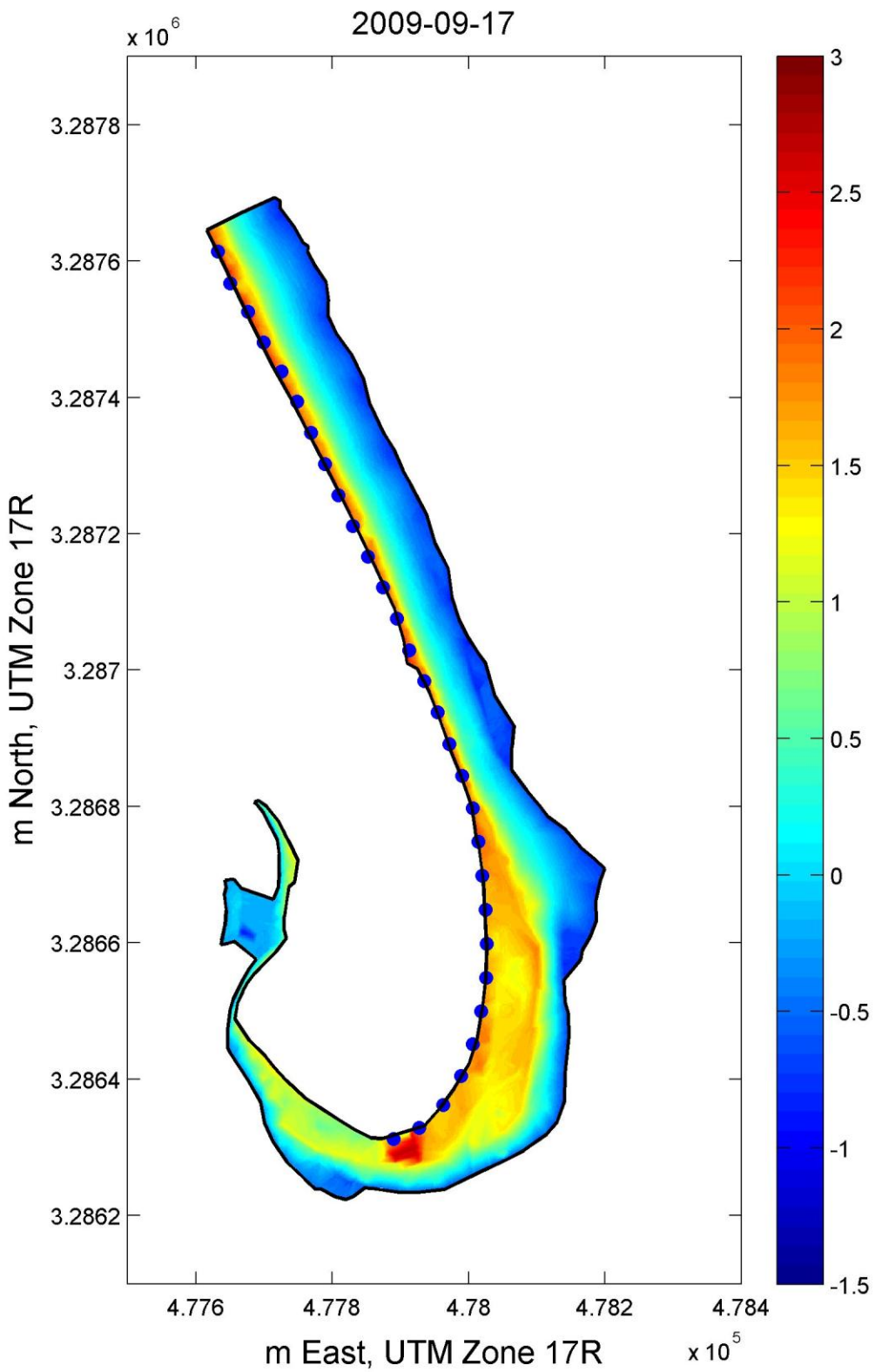


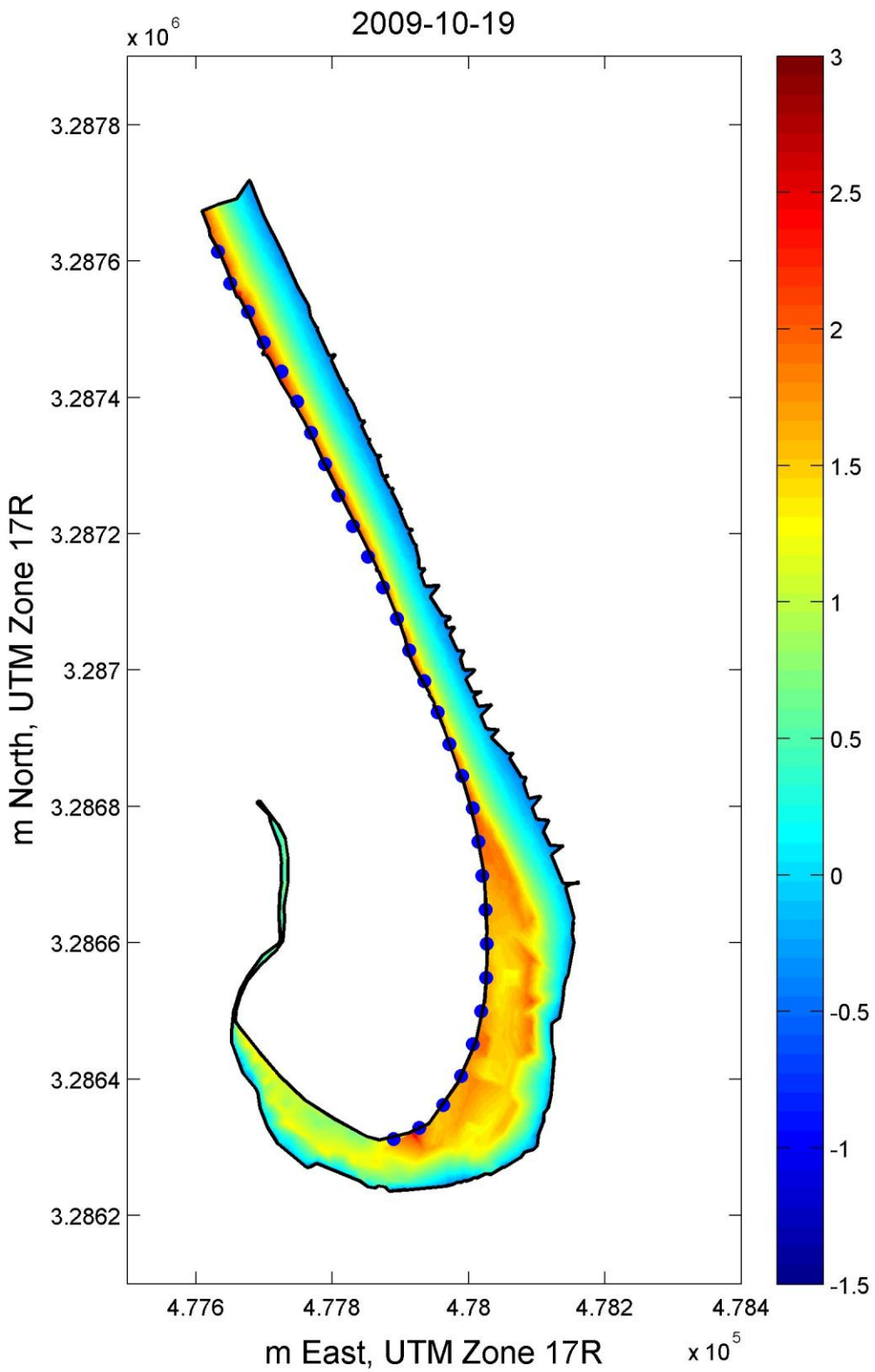


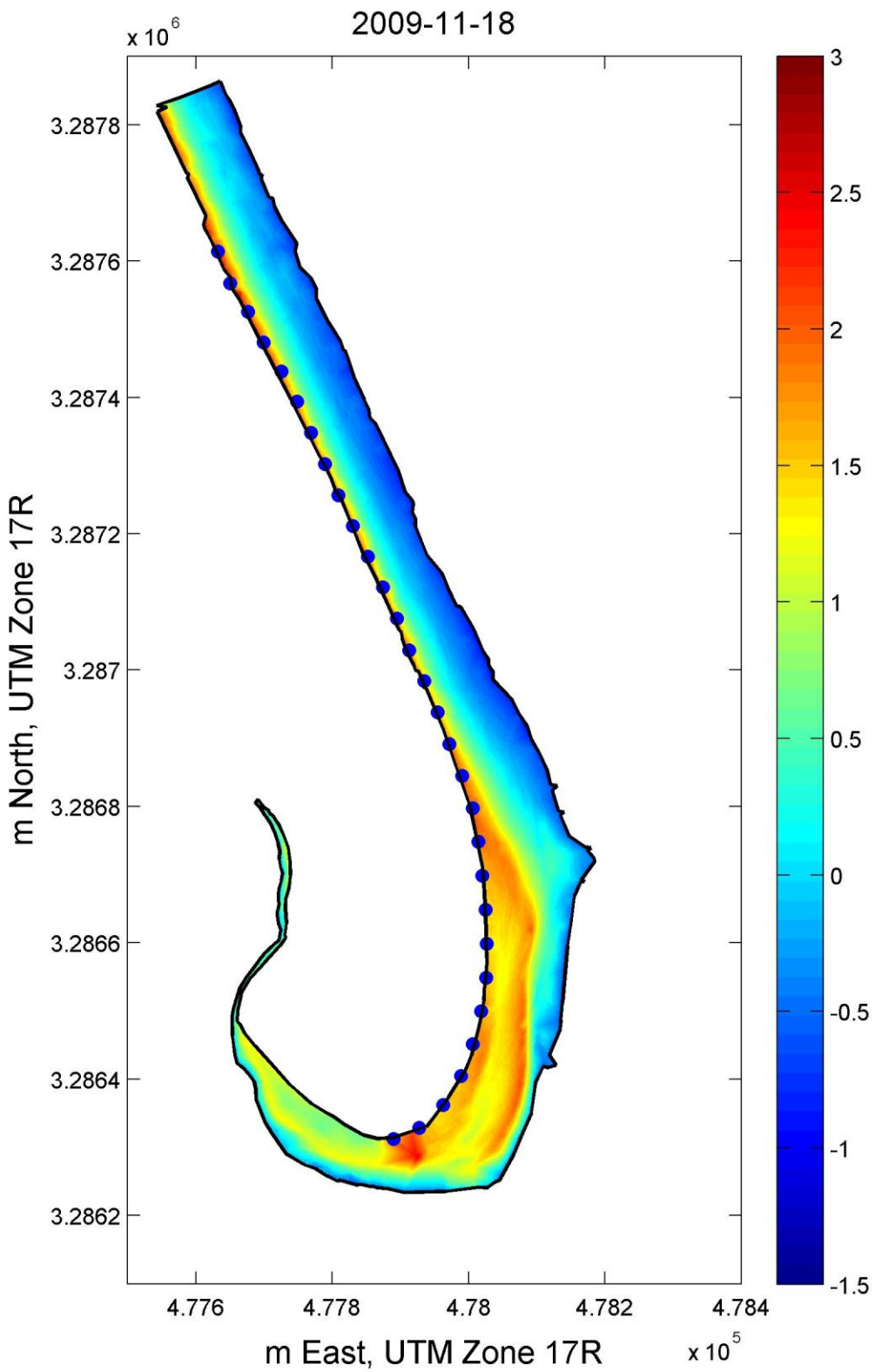


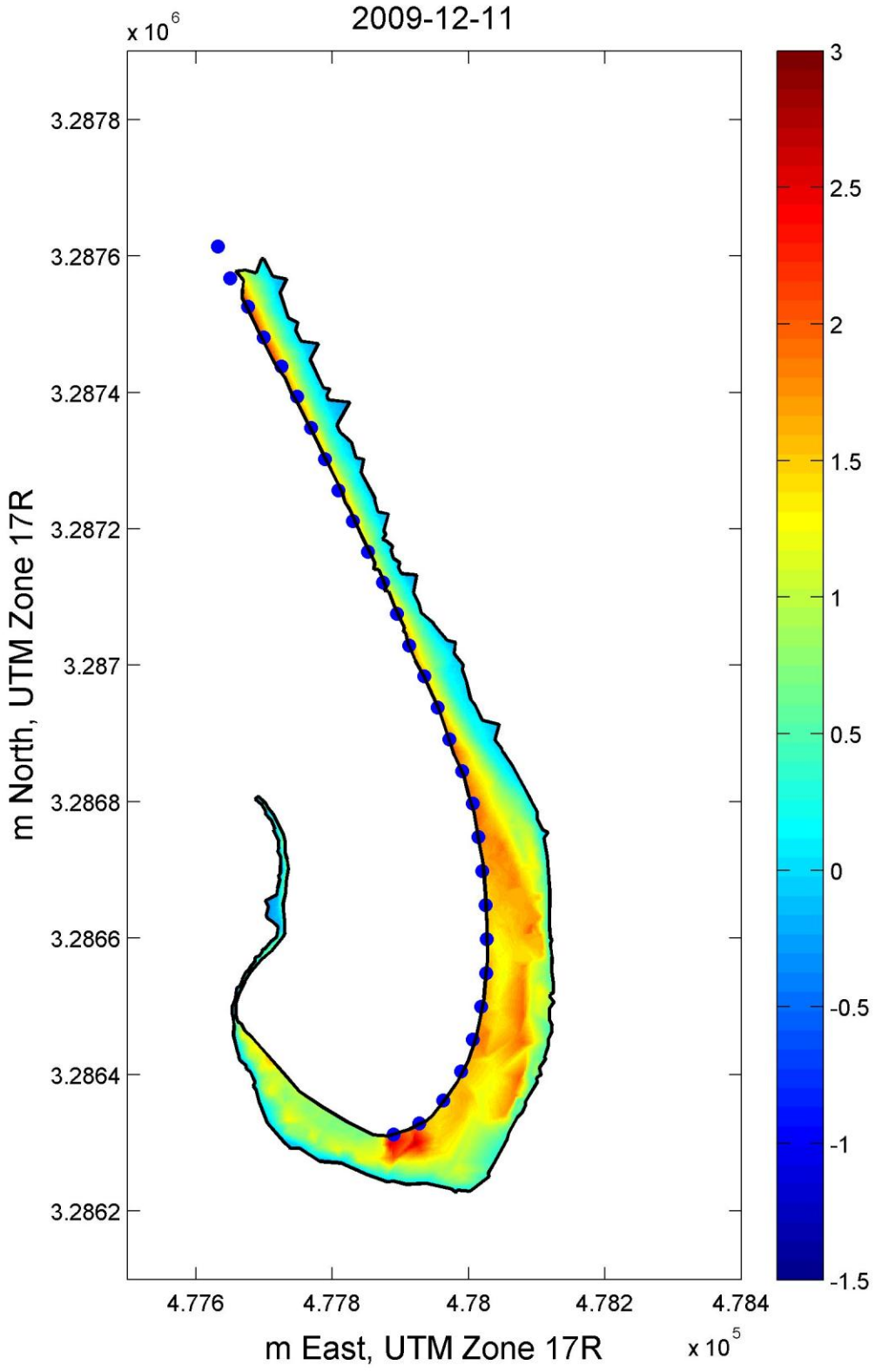


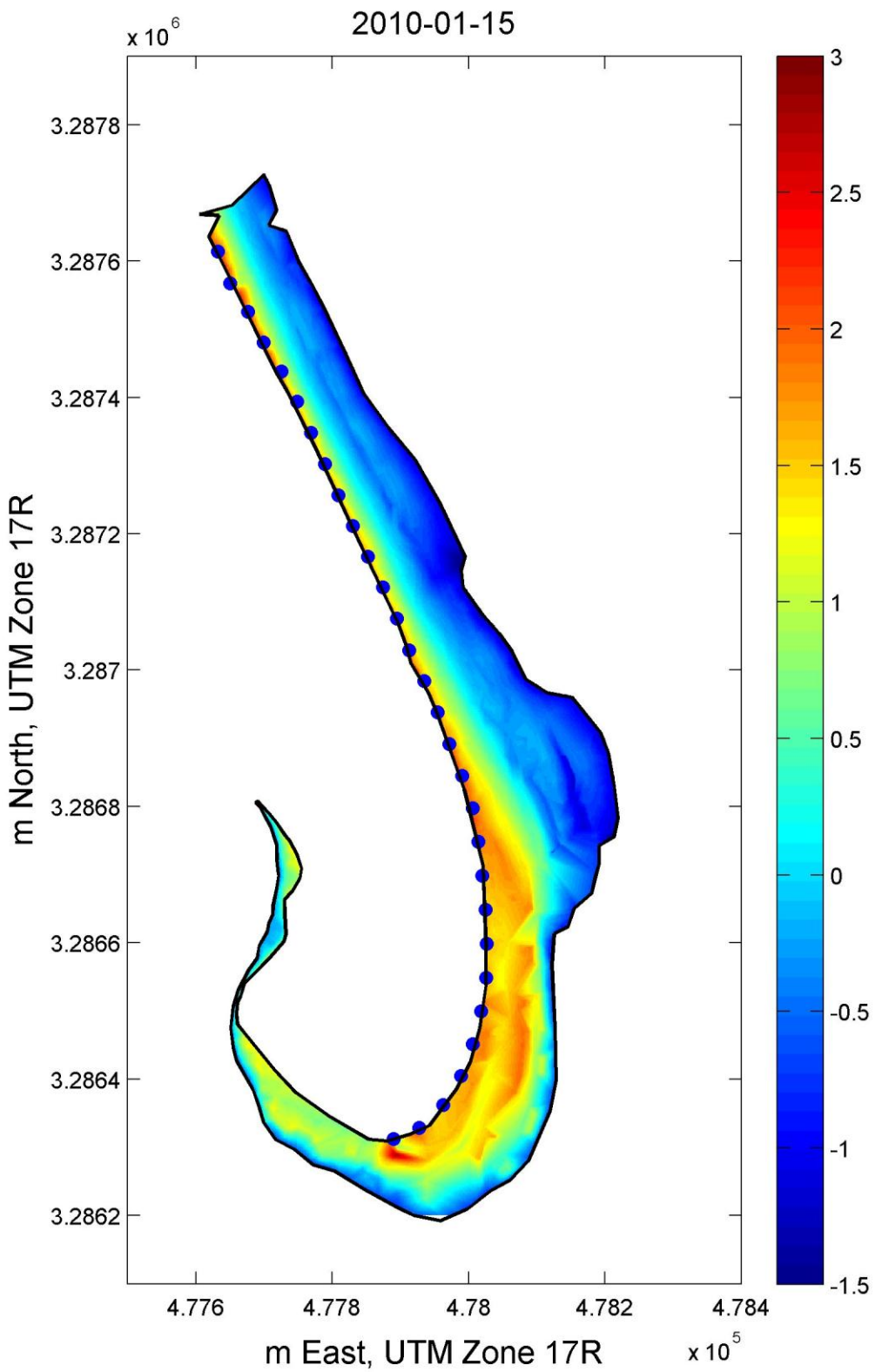


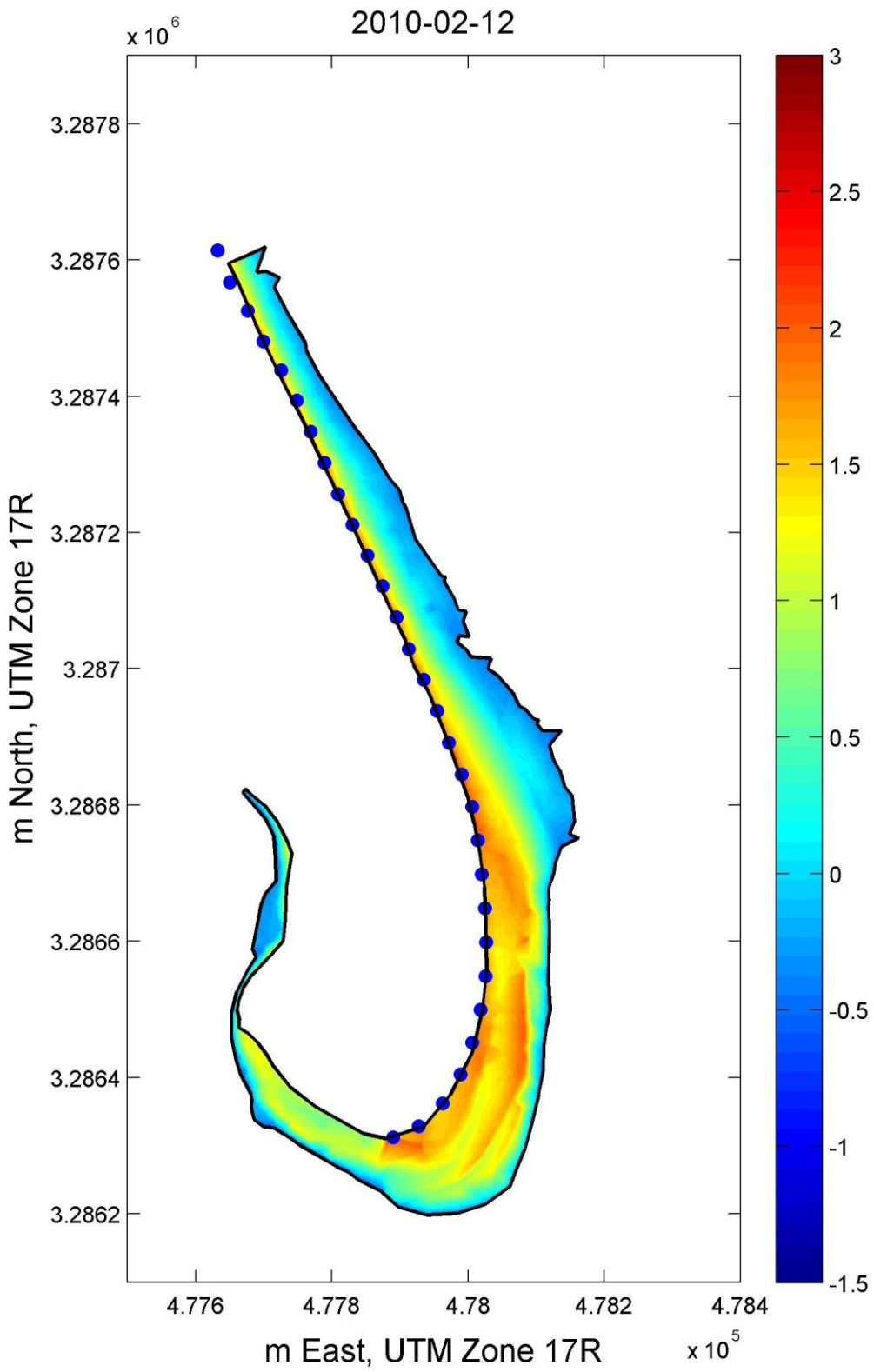




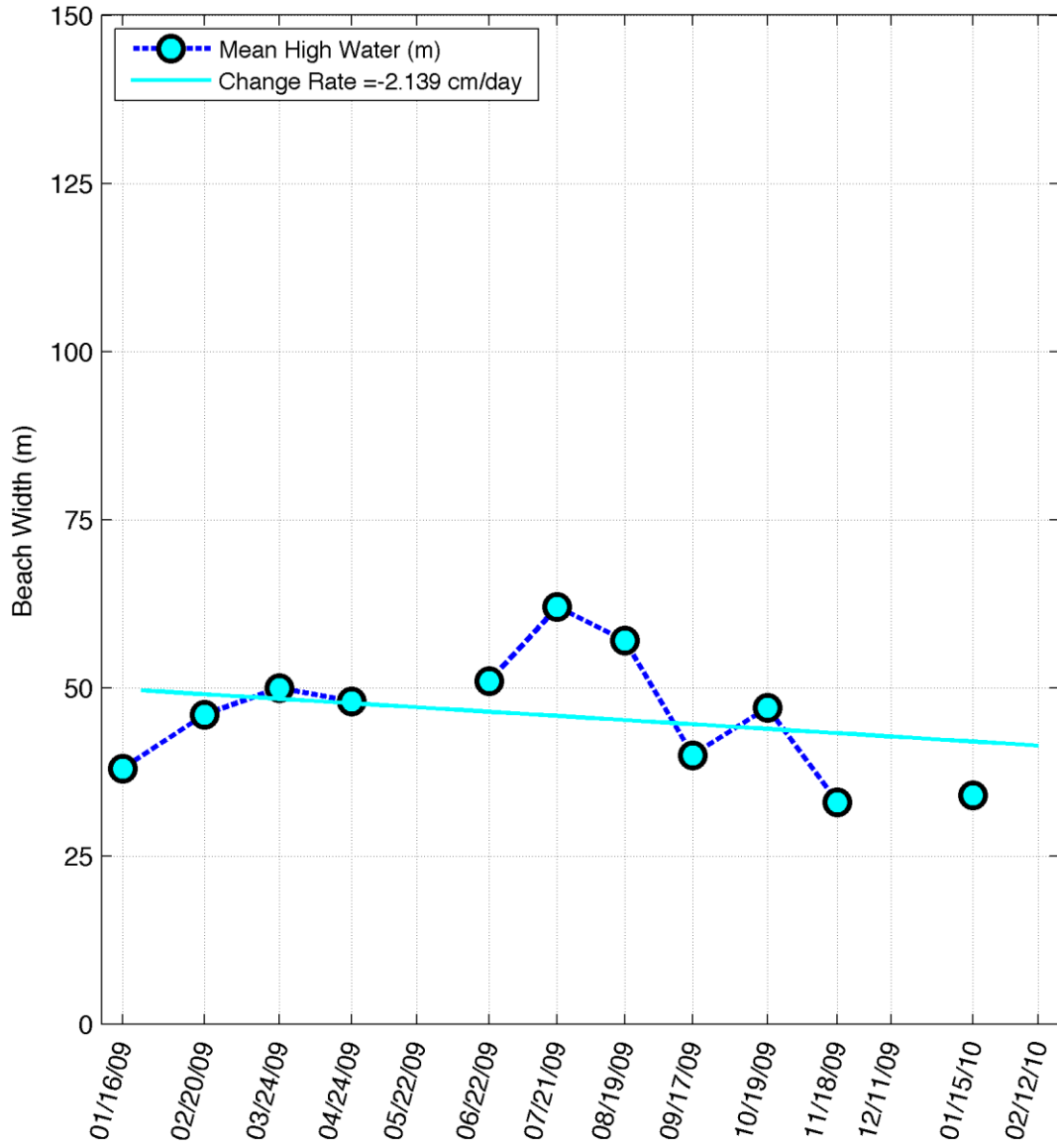




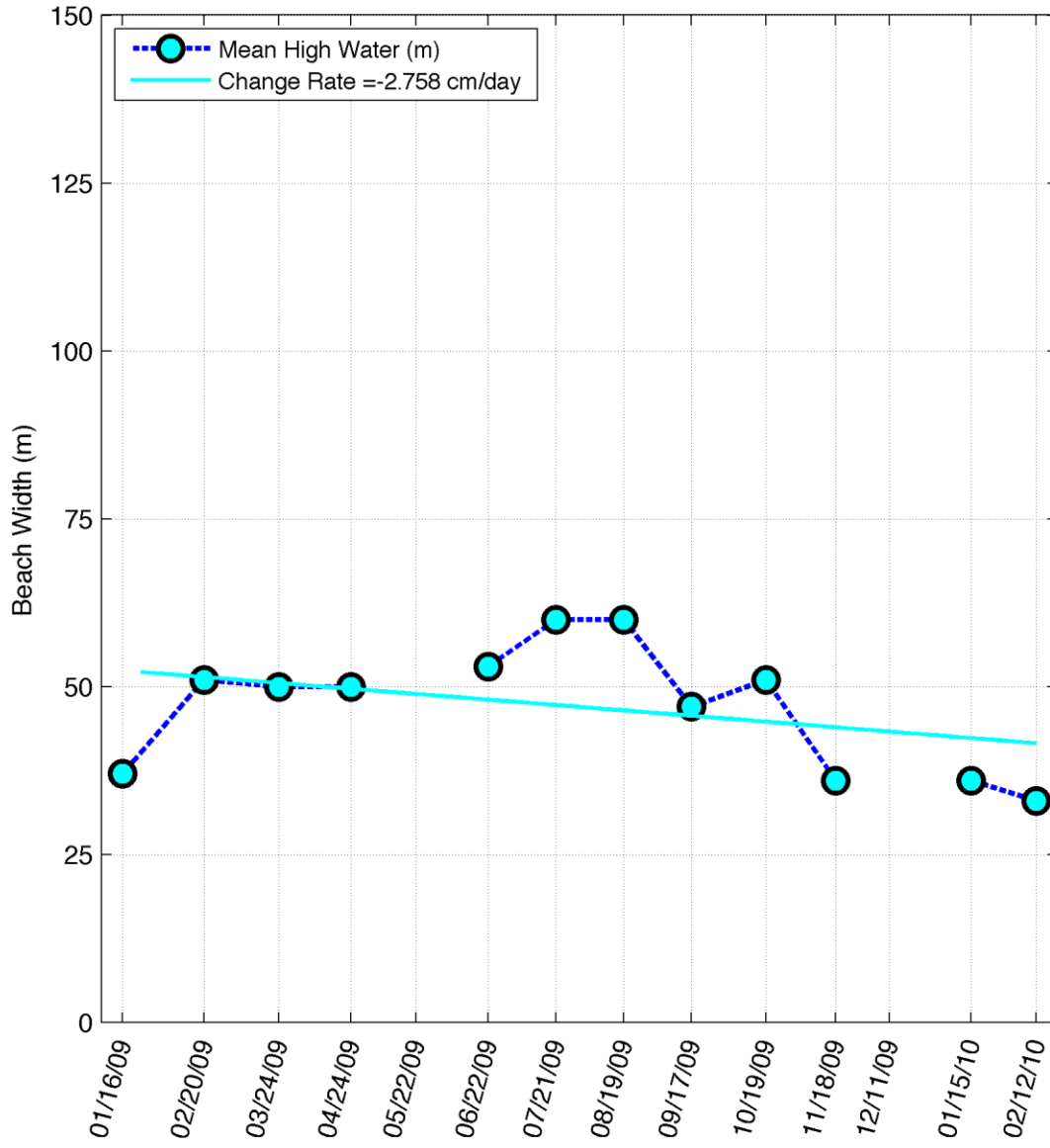




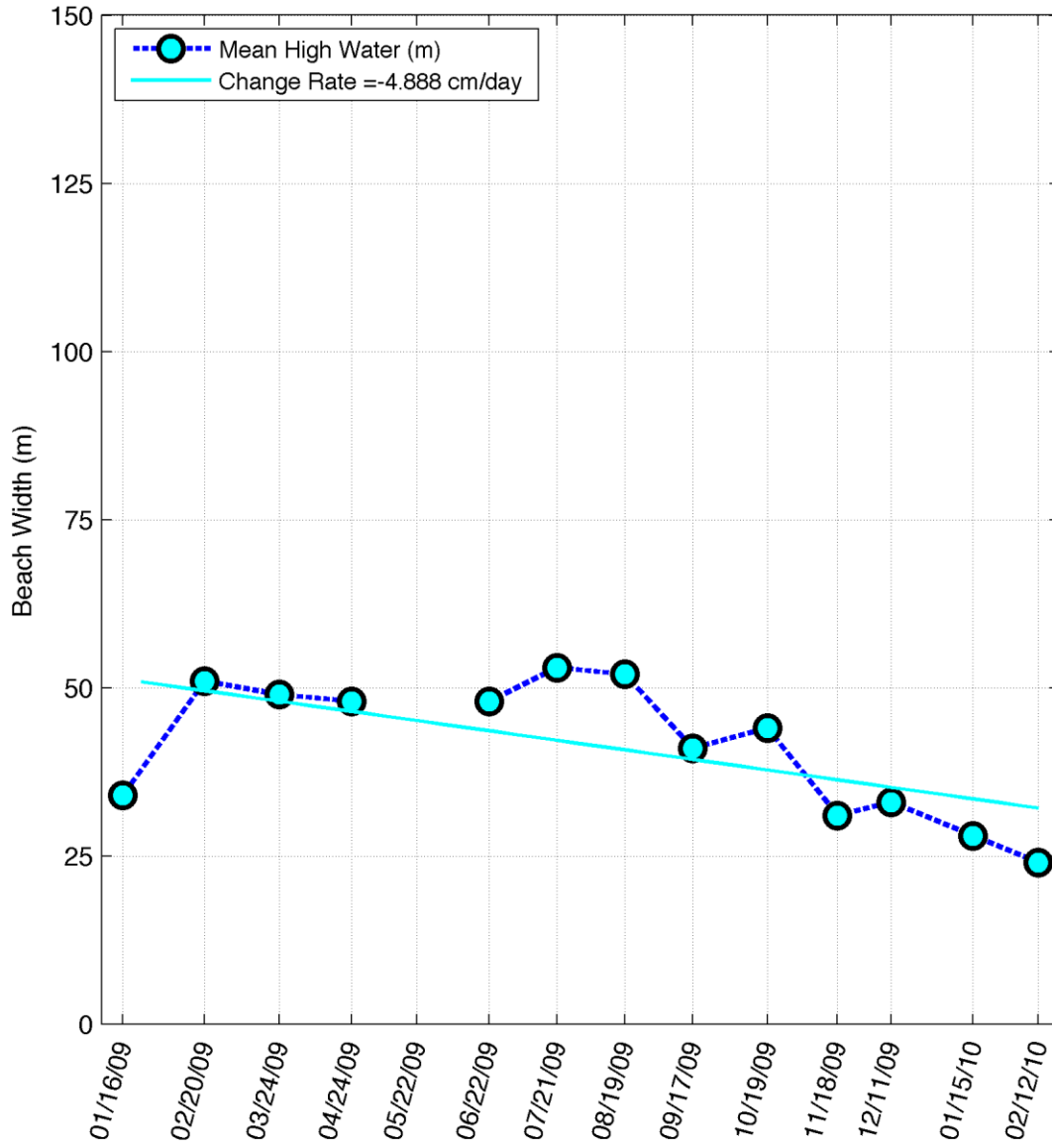
Shoreline Variation of Transect 1



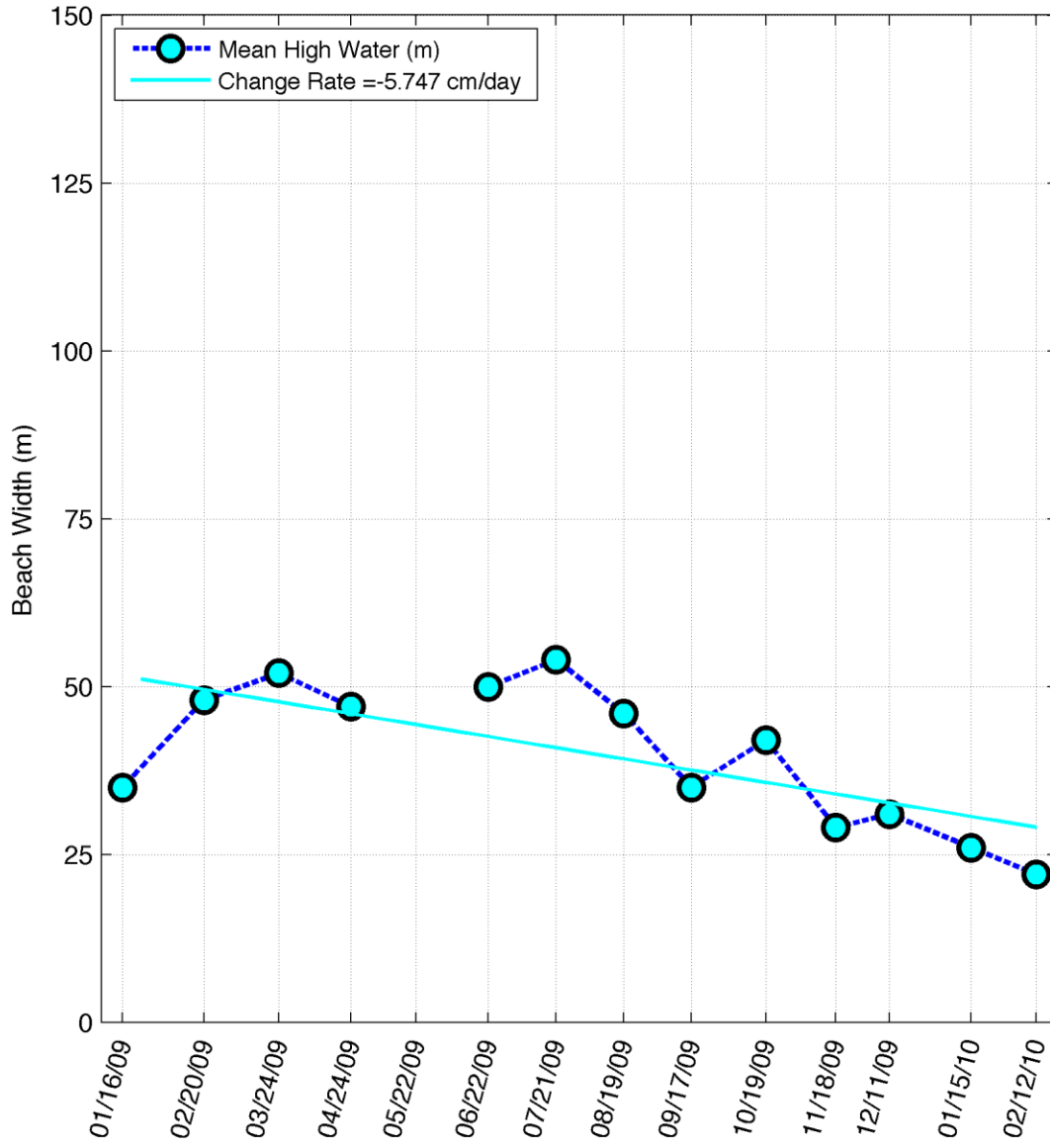
Shoreline Variation of Transect 2



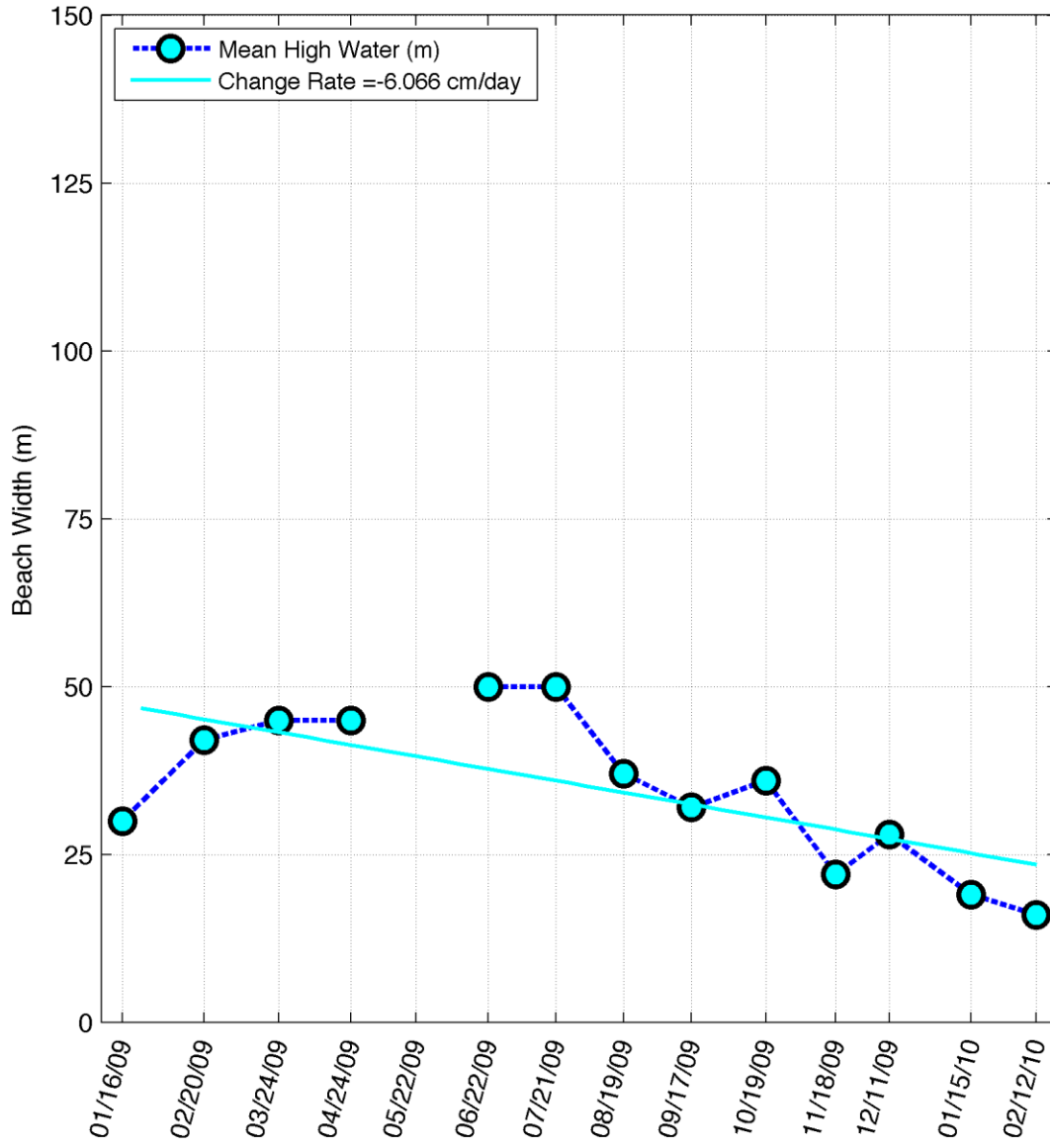
Shoreline Variation of Transect 3



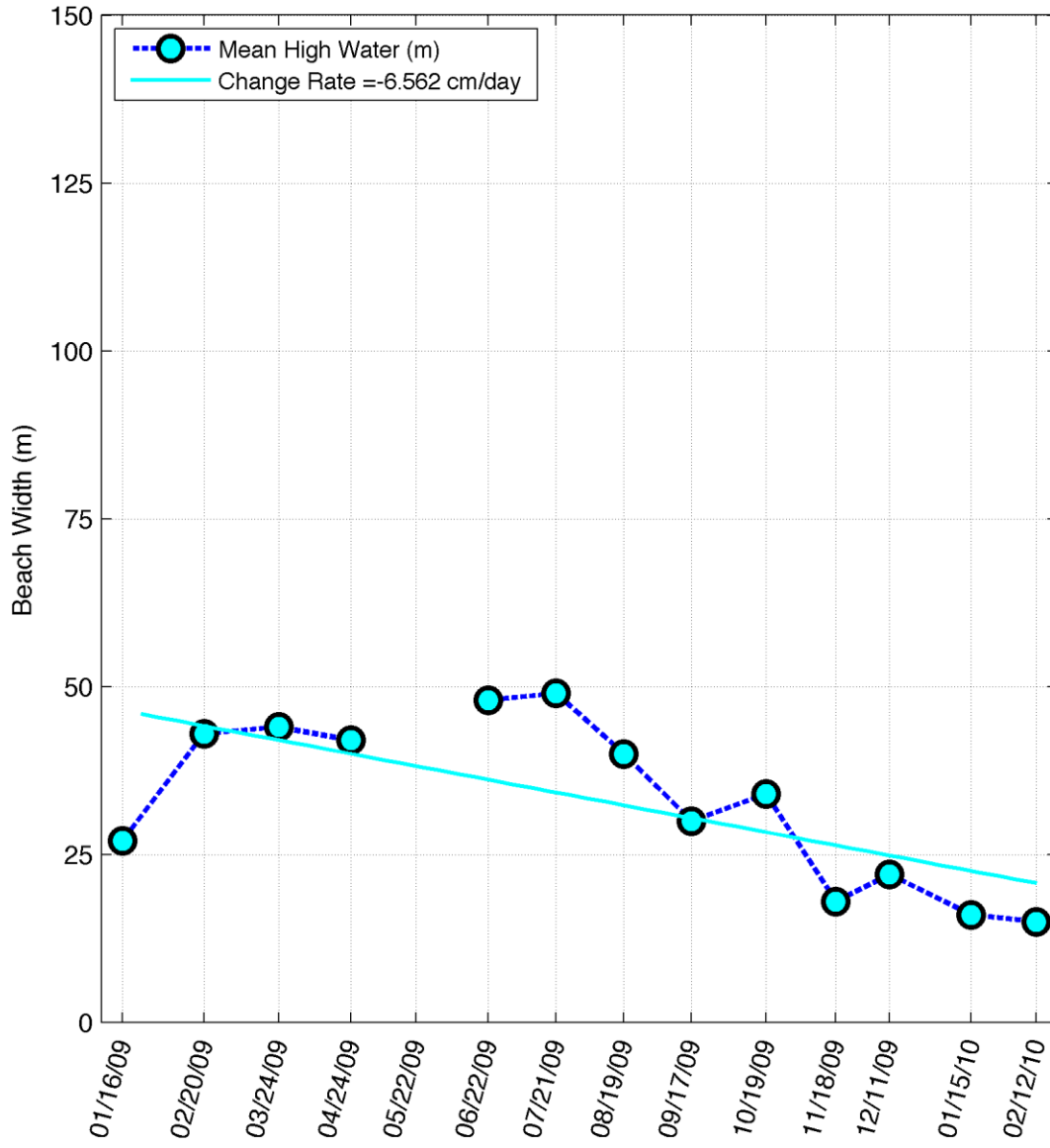
Shoreline Variation of Transect 4



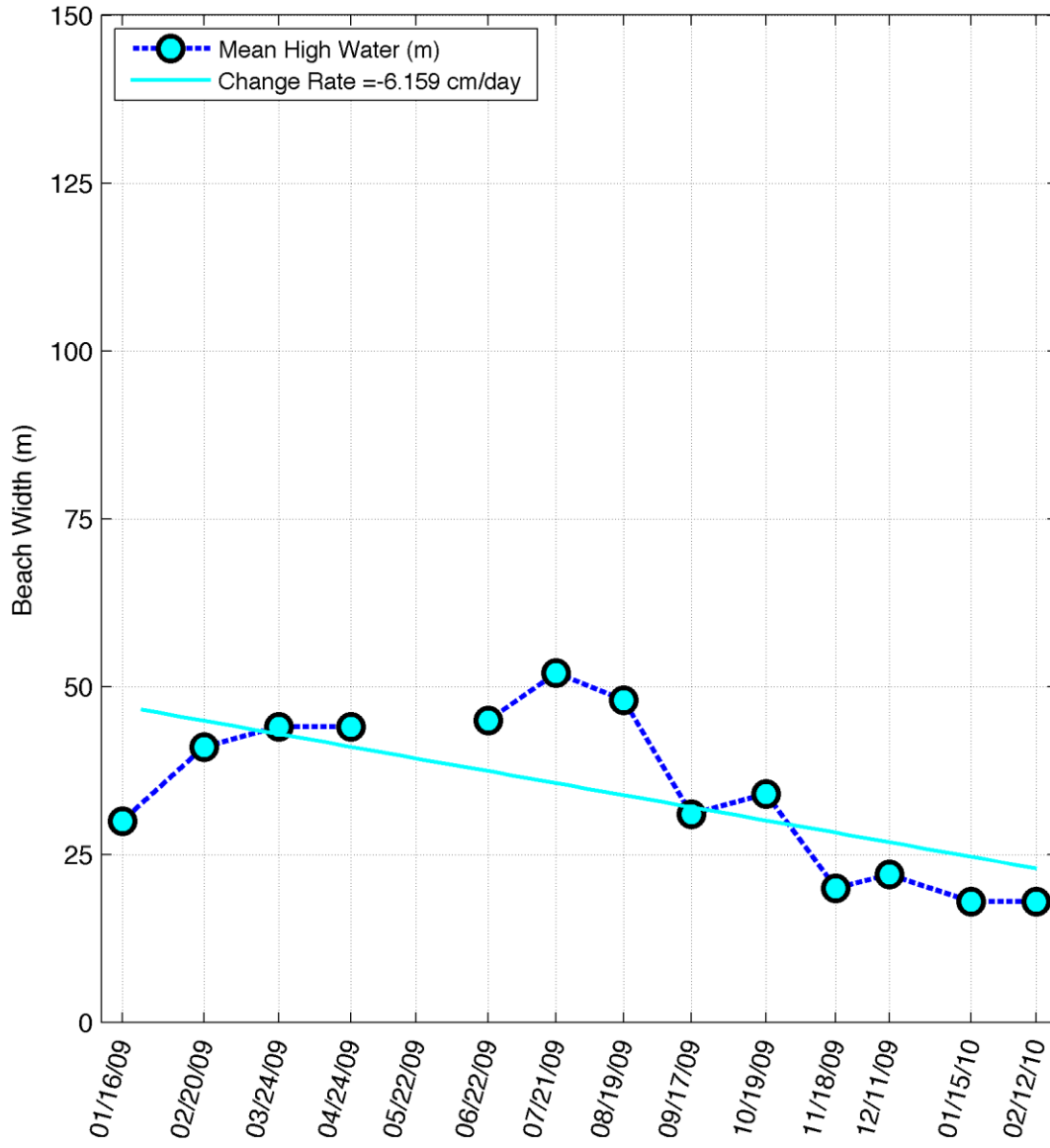
Shoreline Variation of Transect 5



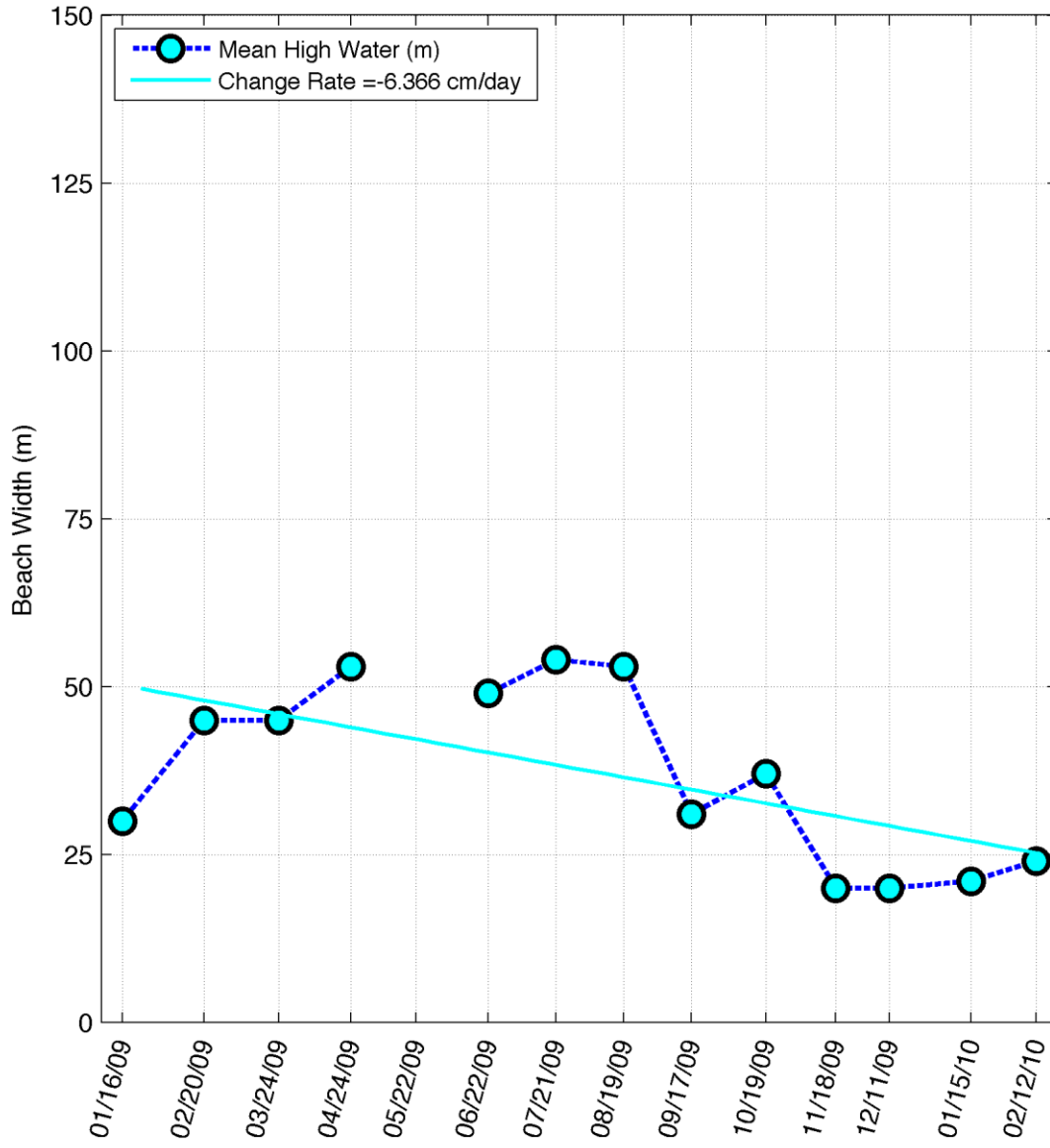
Shoreline Variation of Transect 6



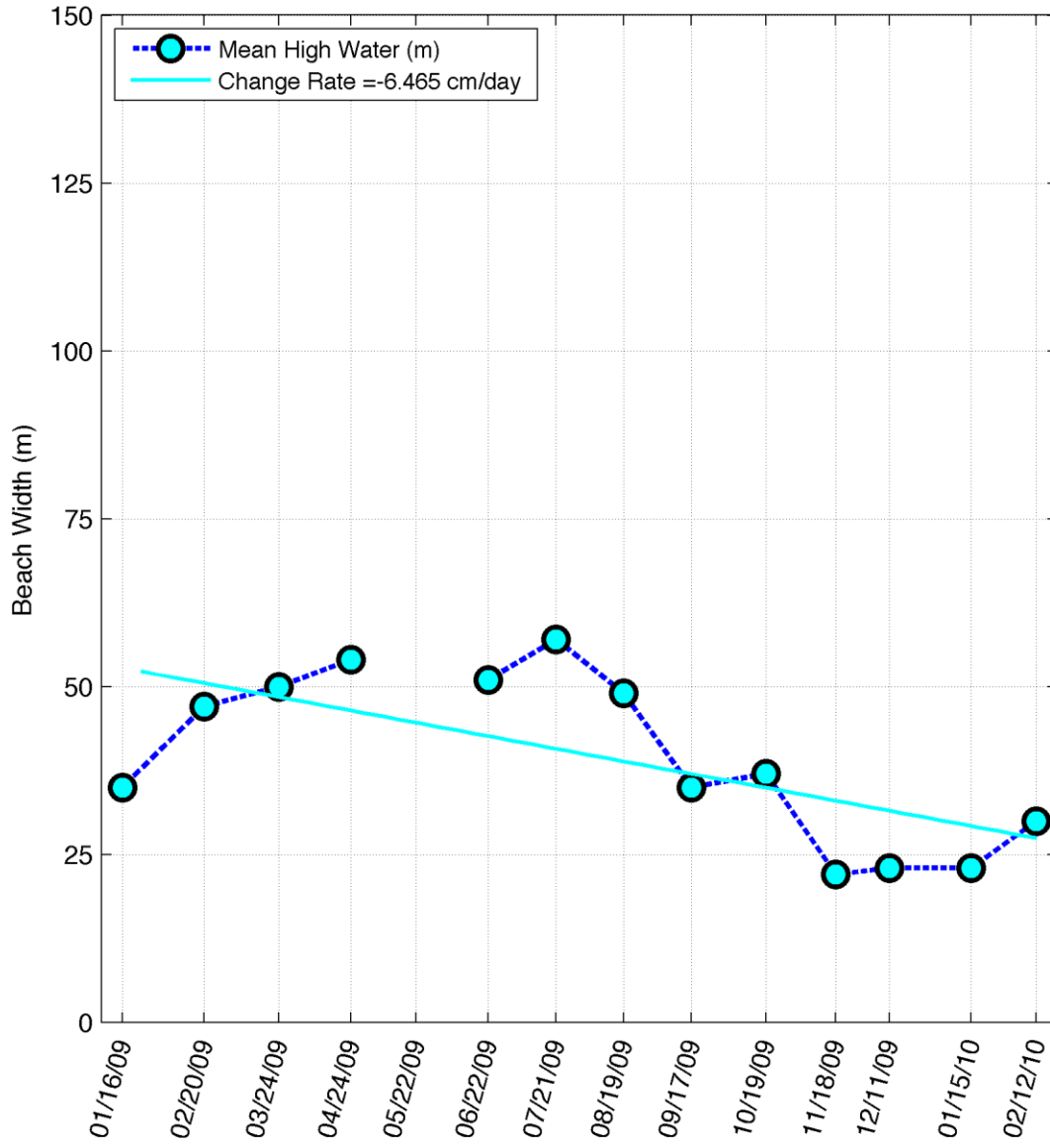
Shoreline Variation of Transect 7



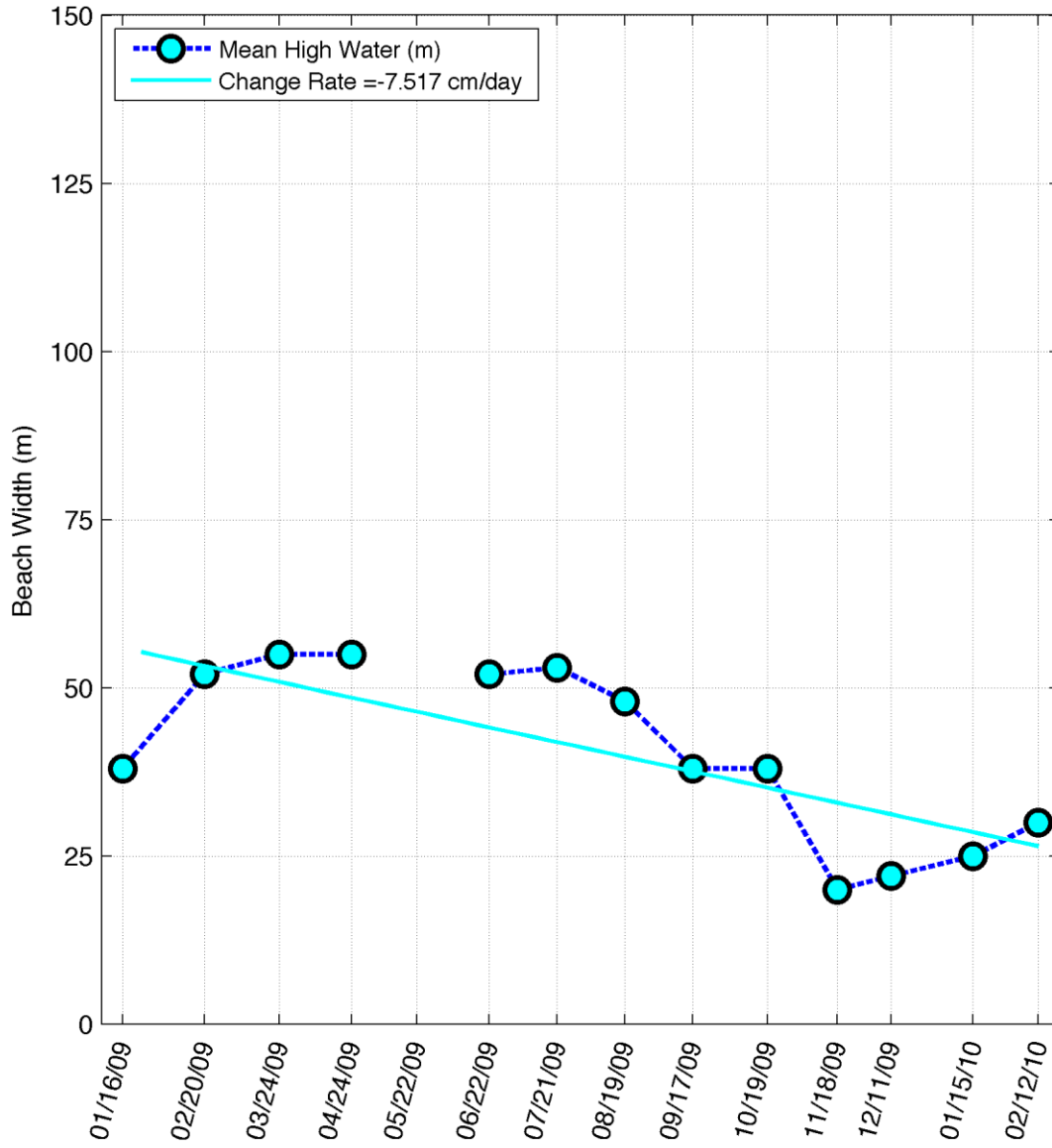
Shoreline Variation of Transect 8



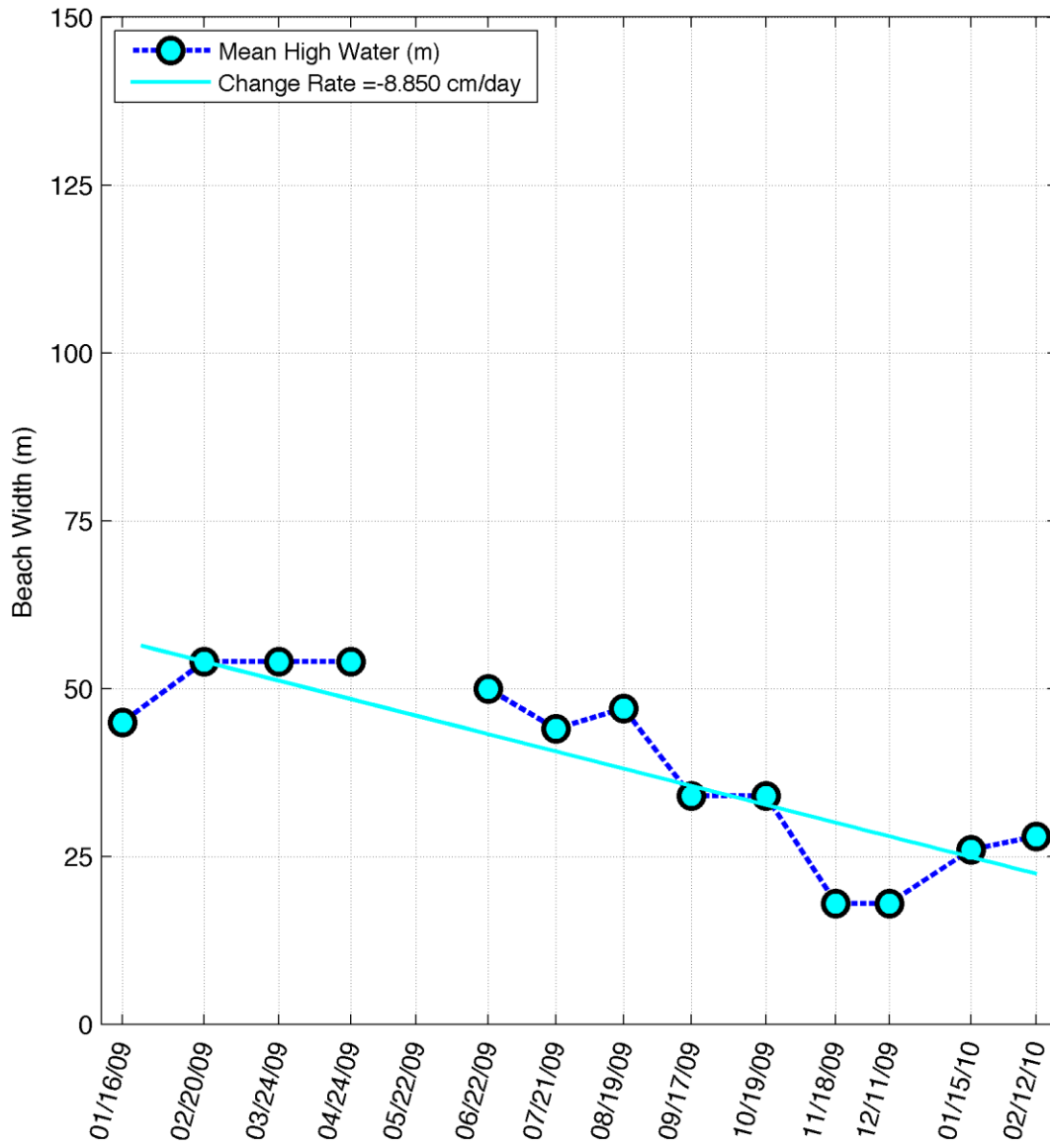
Shoreline Variation of Transect 9



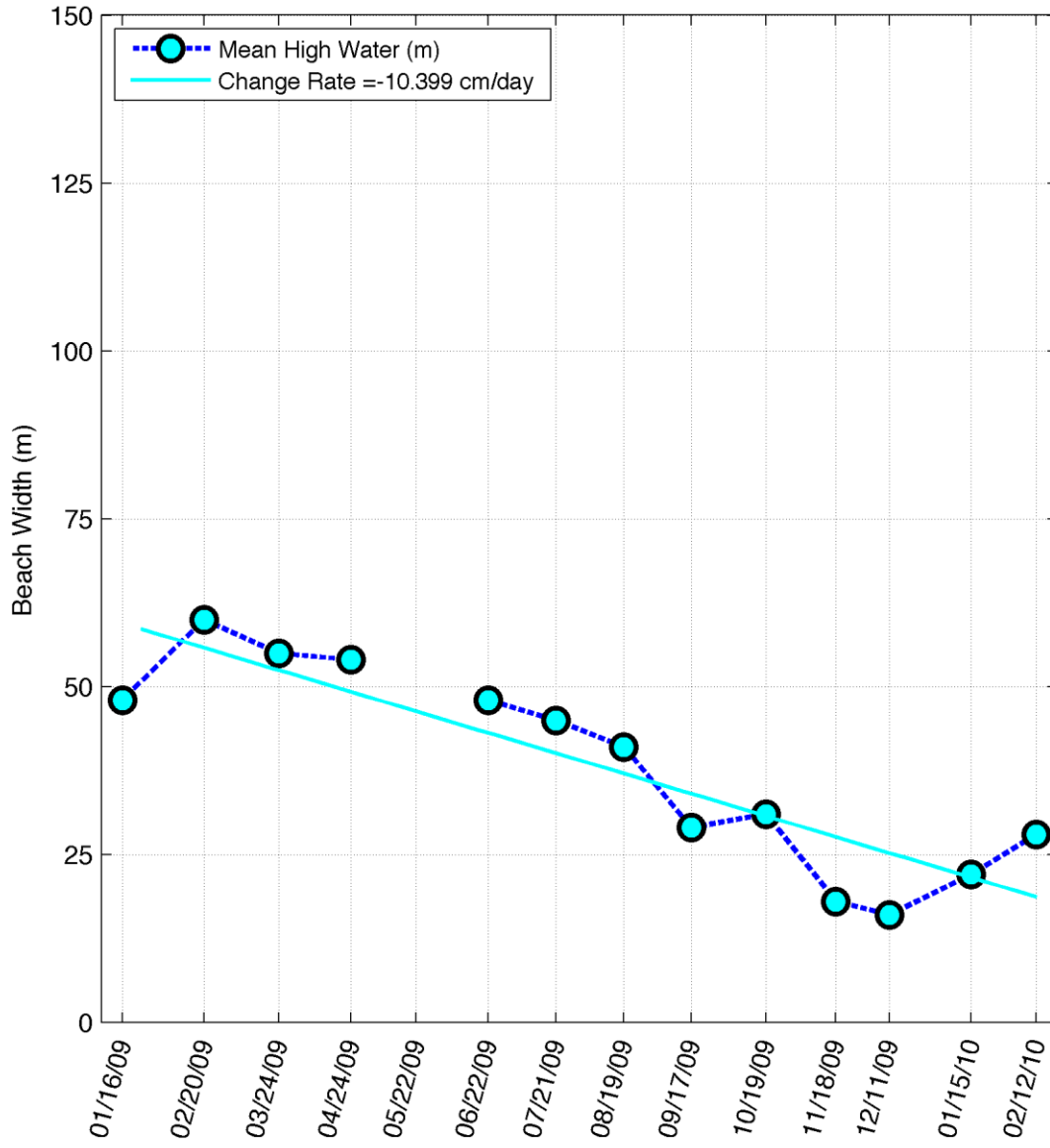
Shoreline Variation of Transect 10



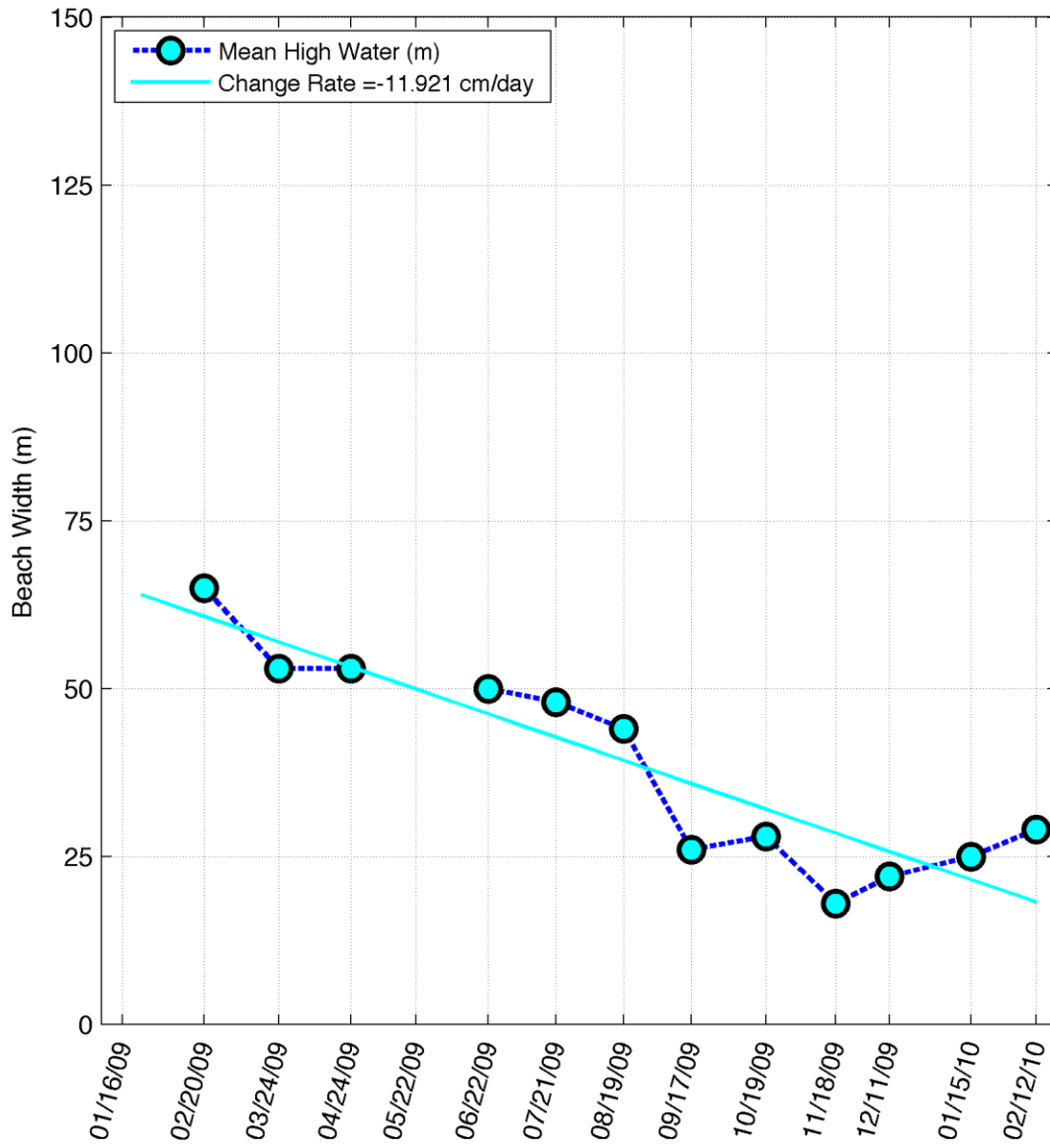
Shoreline Variation of Transect 11



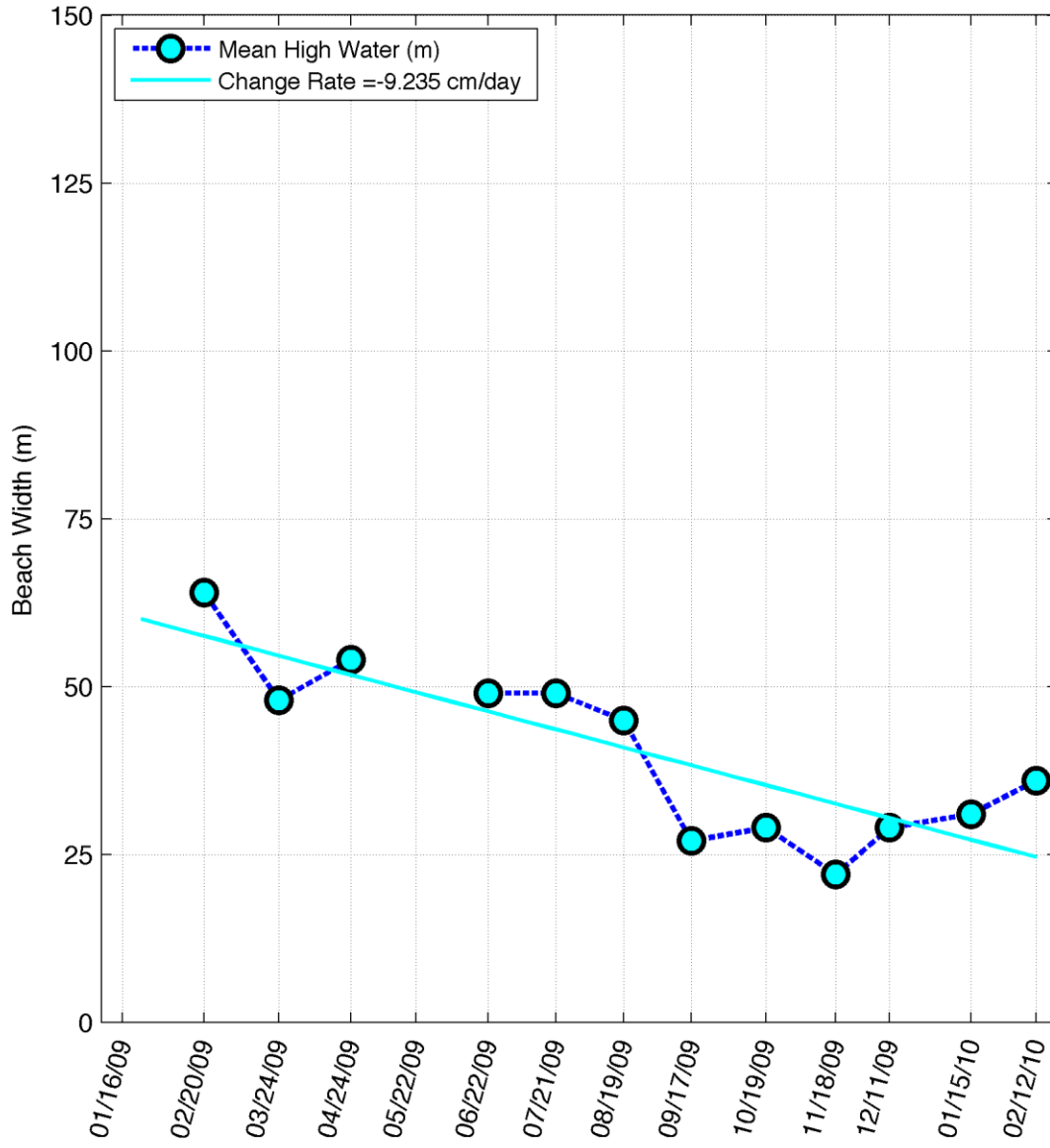
Shoreline Variation of Transect 12



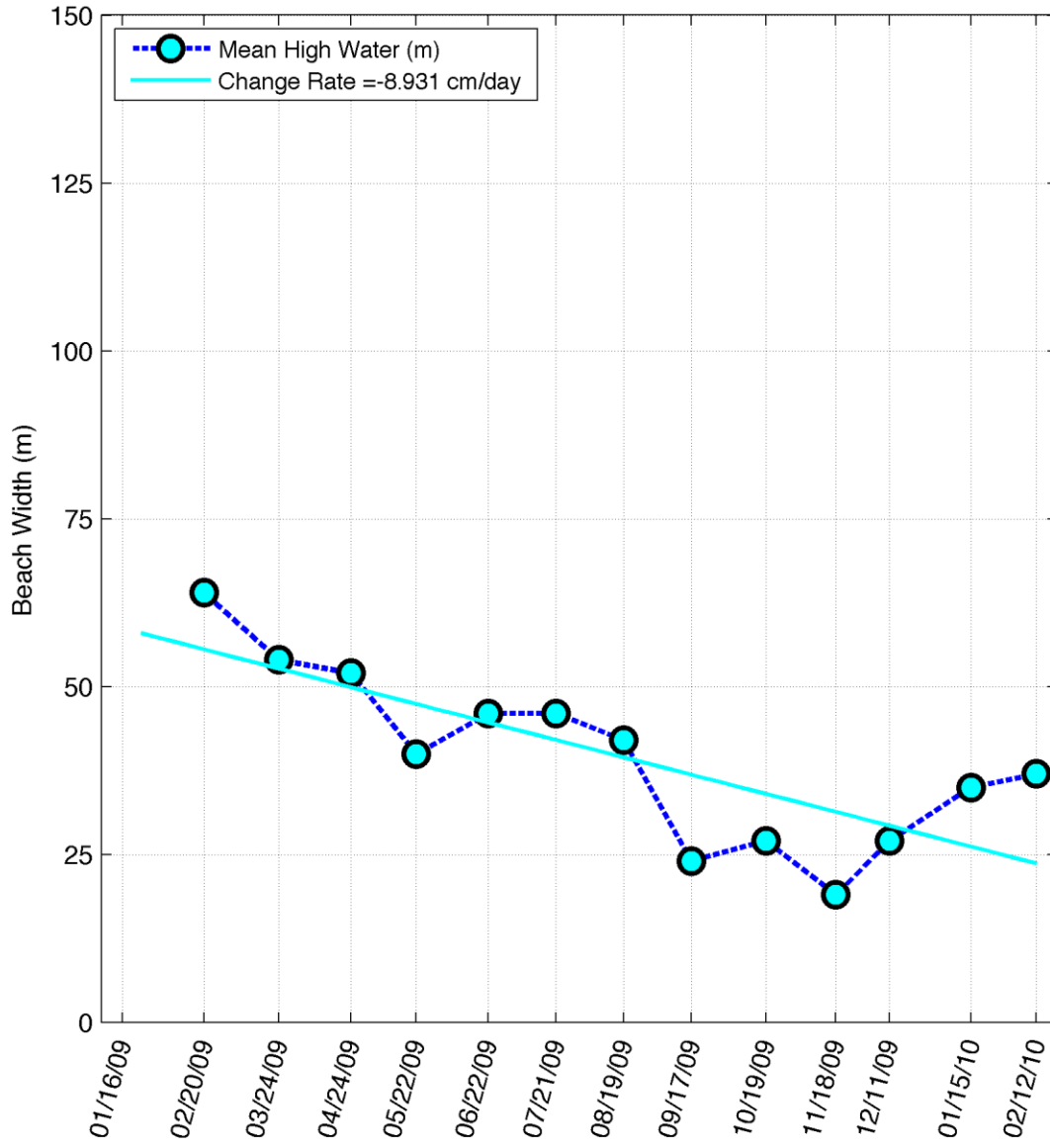
Shoreline Variation of Transect 13



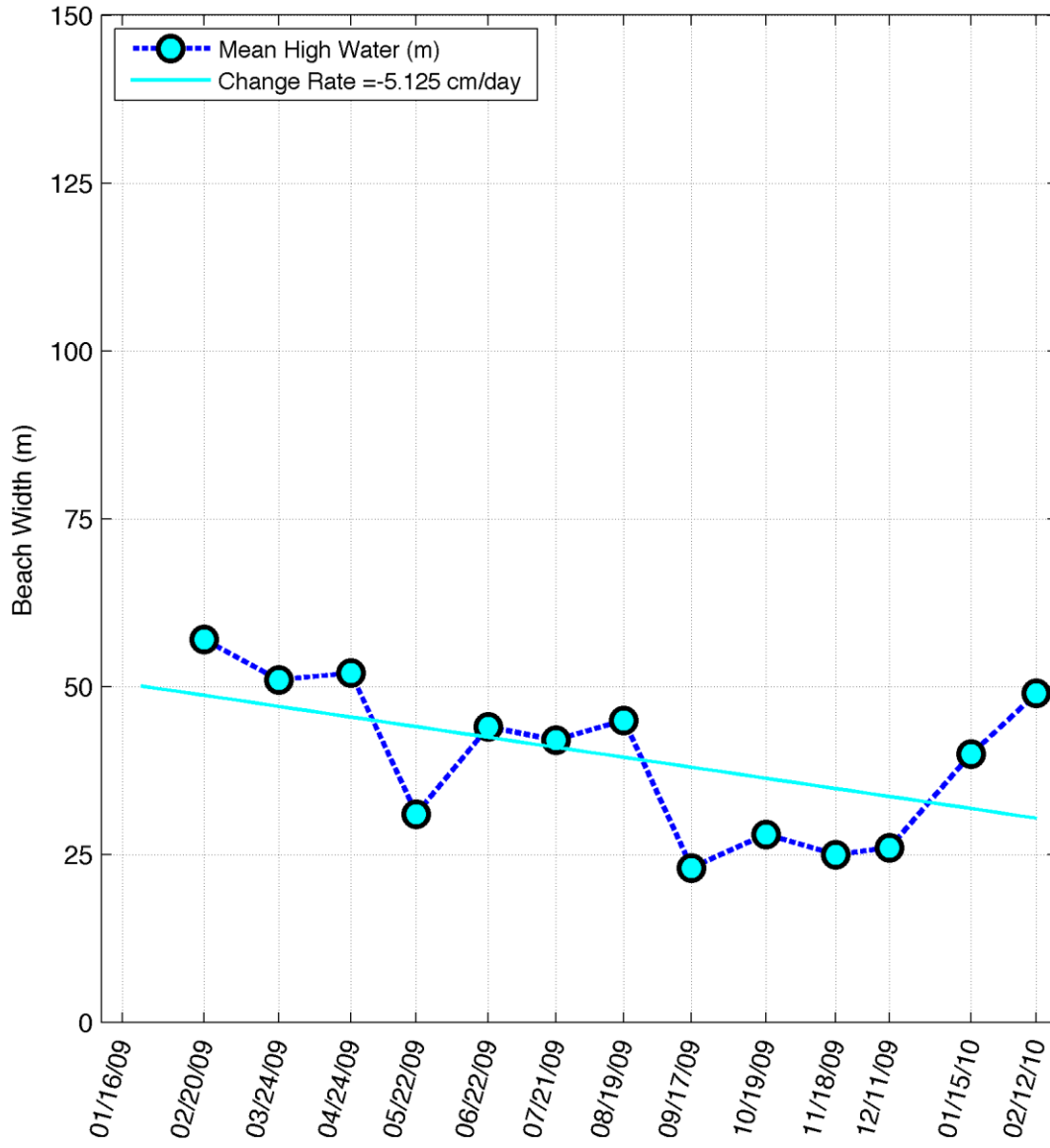
Shoreline Variation of Transect 14



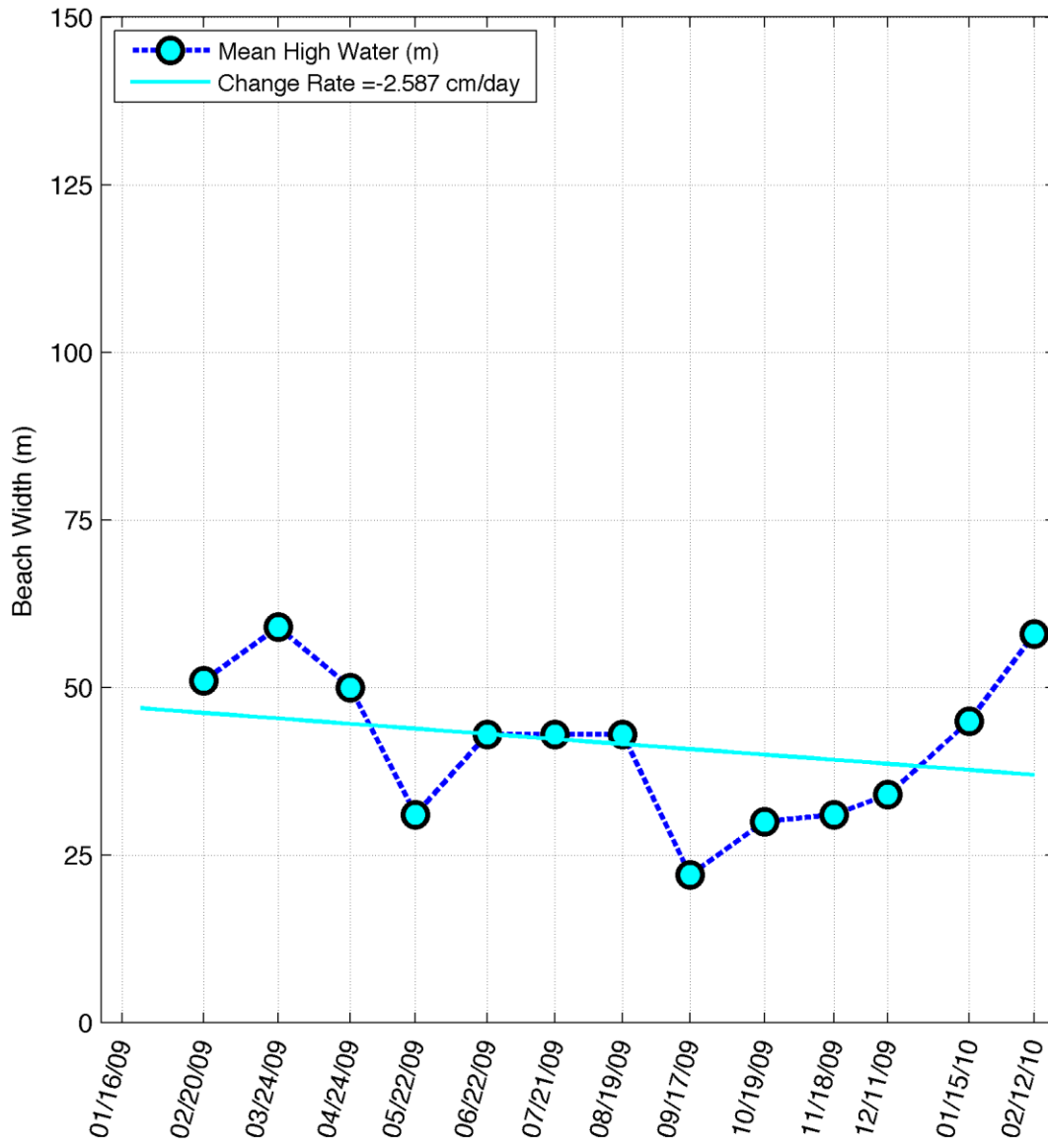
Shoreline Variation of Transect 15



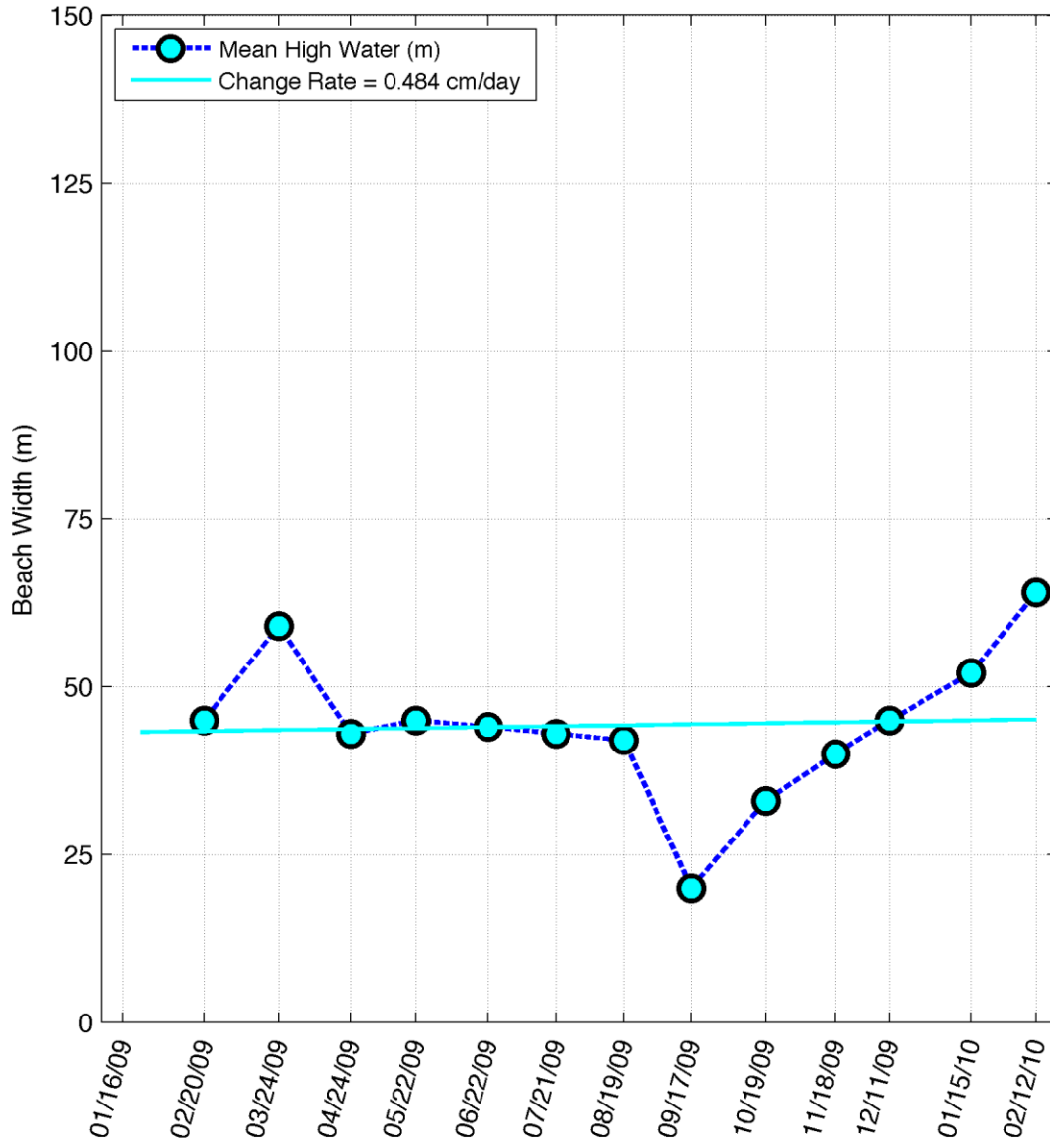
Shoreline Variation of Transect 16



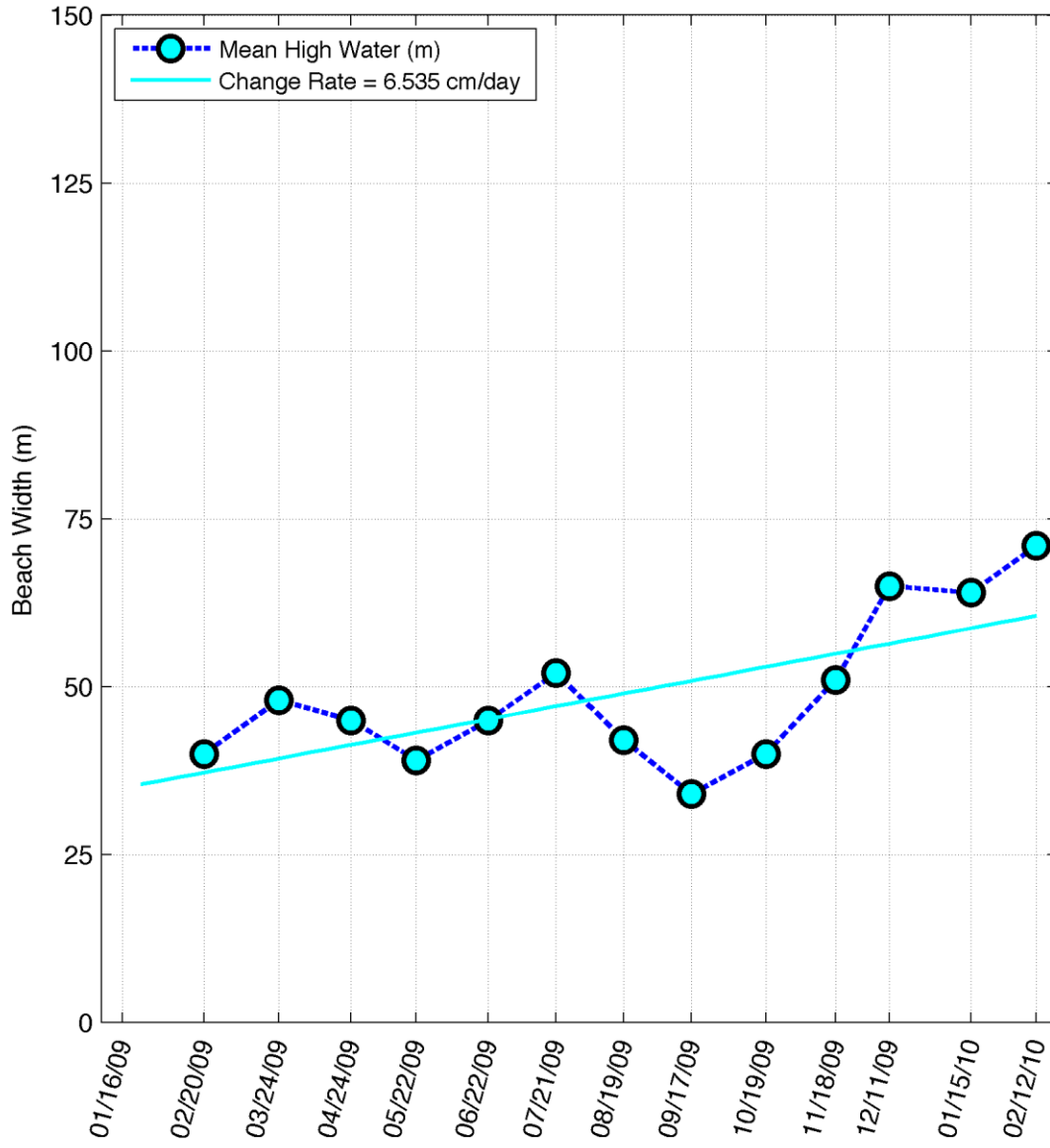
Shoreline Variation of Transect 17



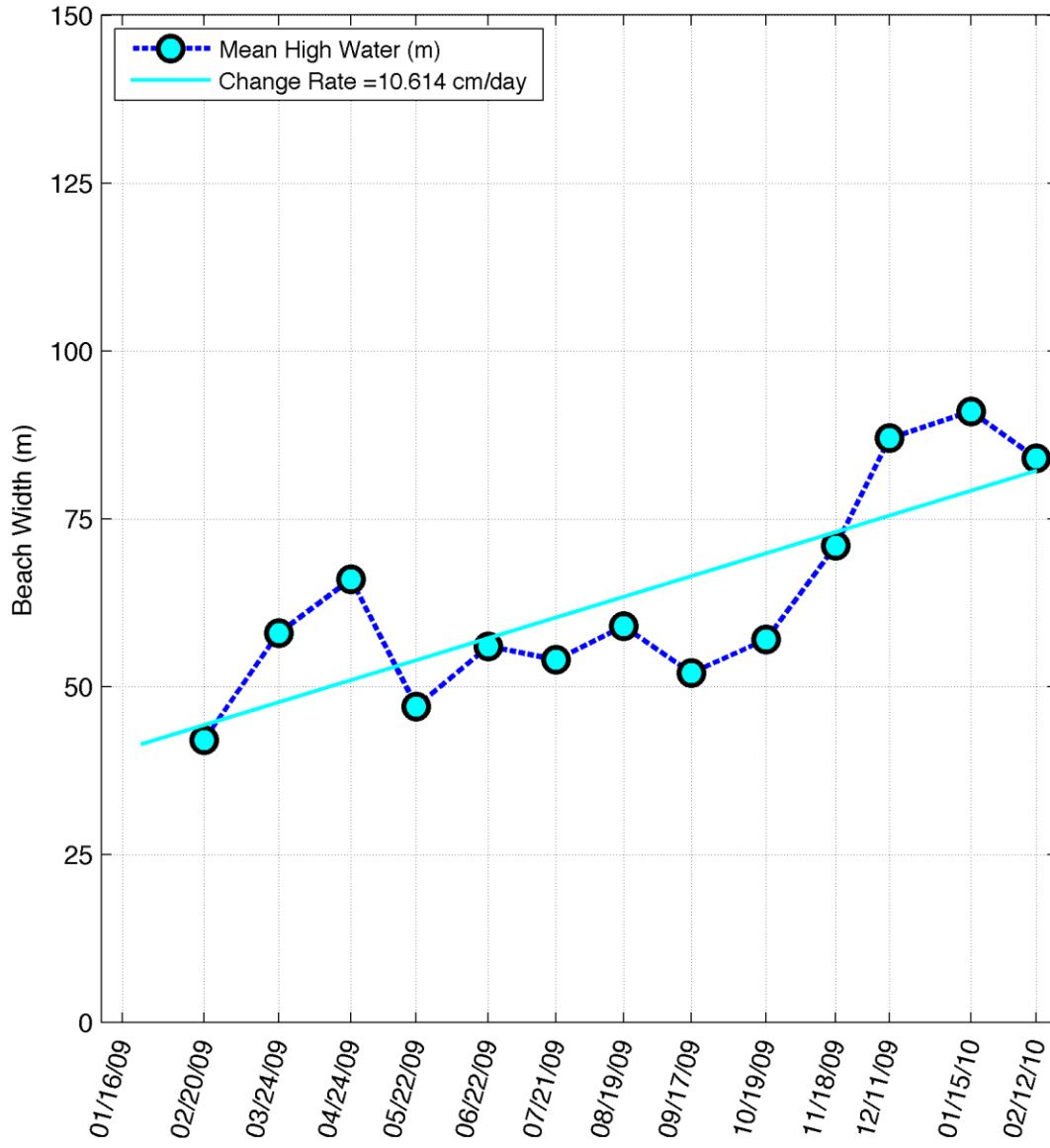
Shoreline Variation of Transect 18



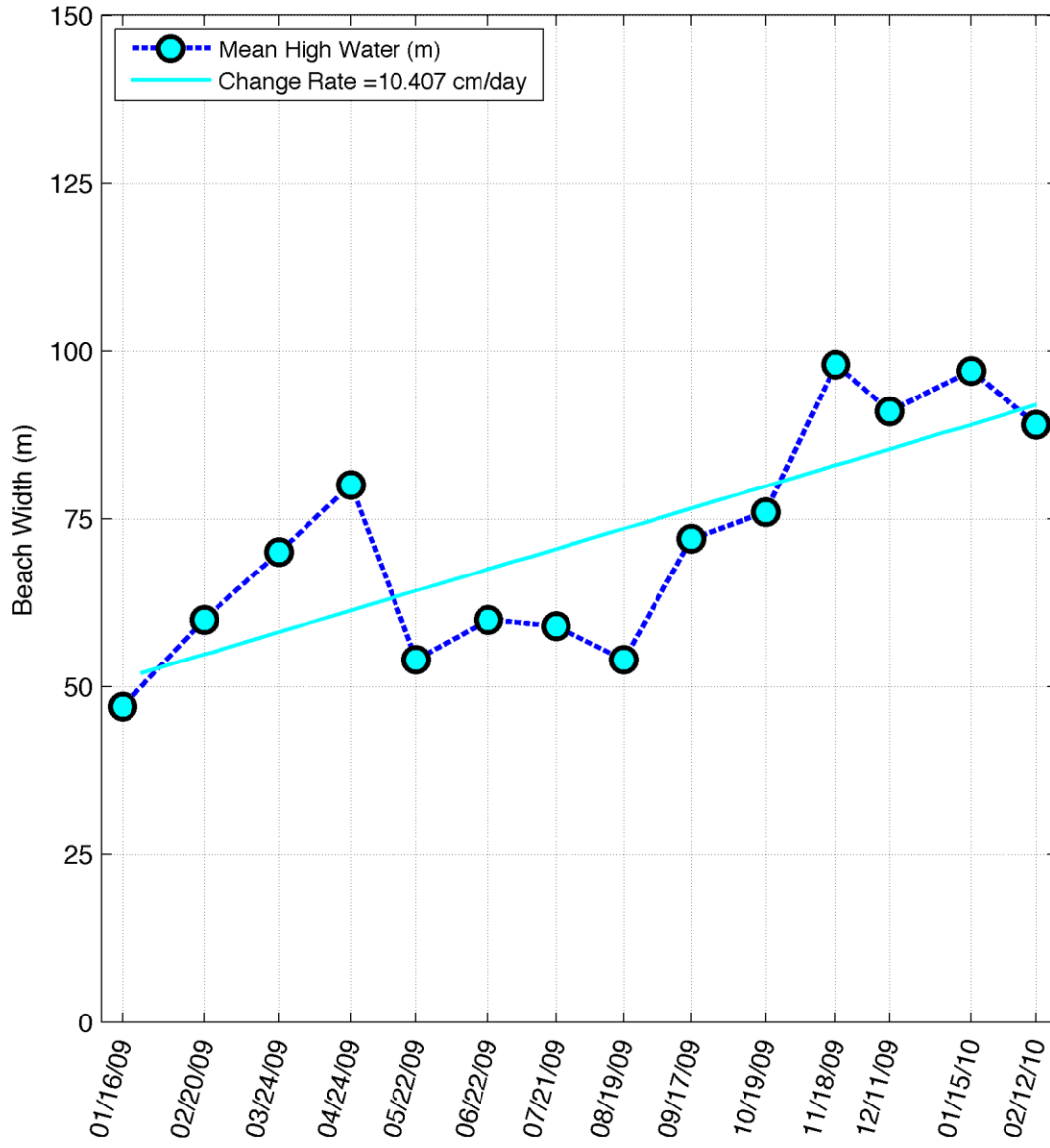
Shoreline Variation of Transect 19



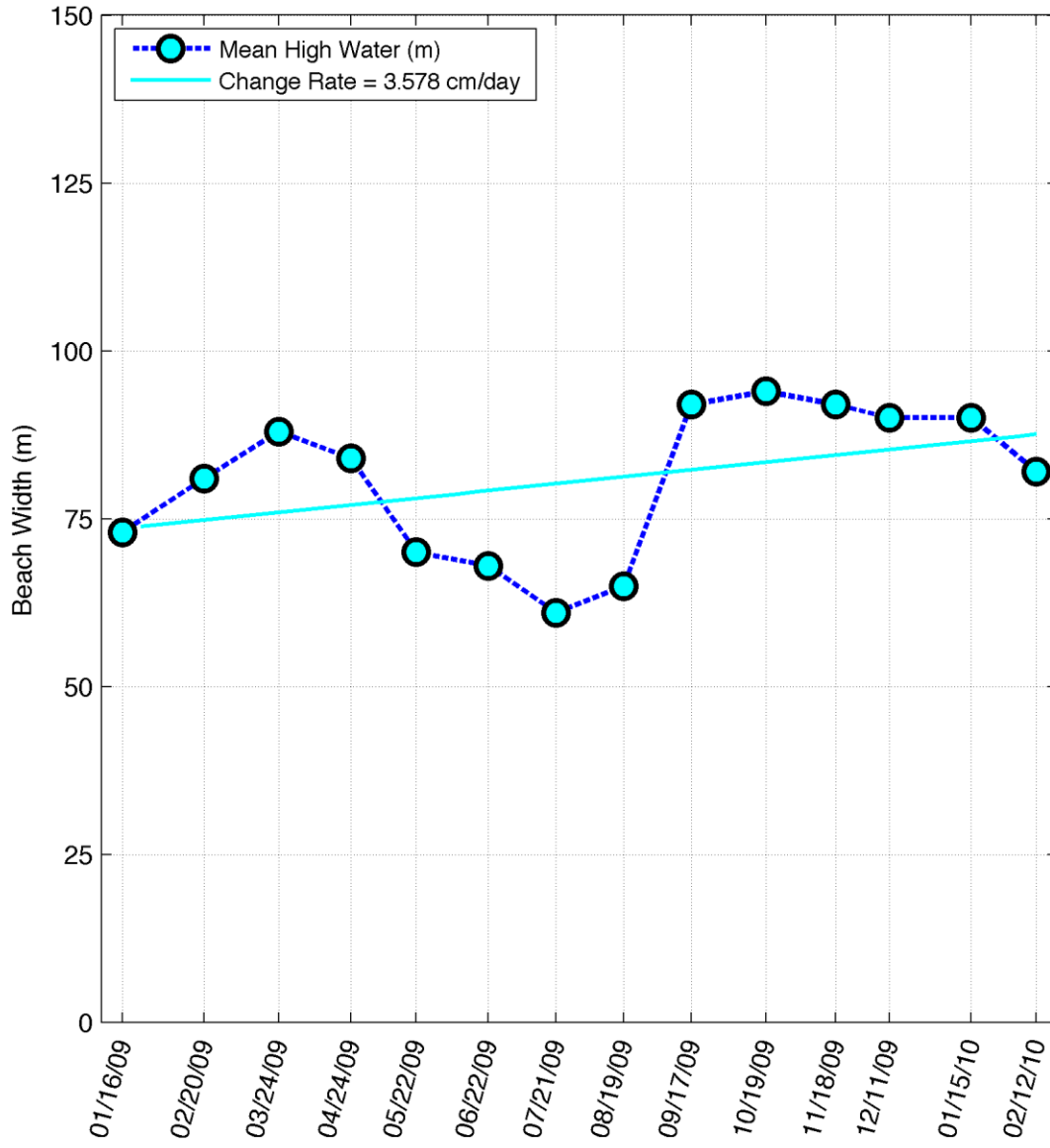
Shoreline Variation of Transect 20



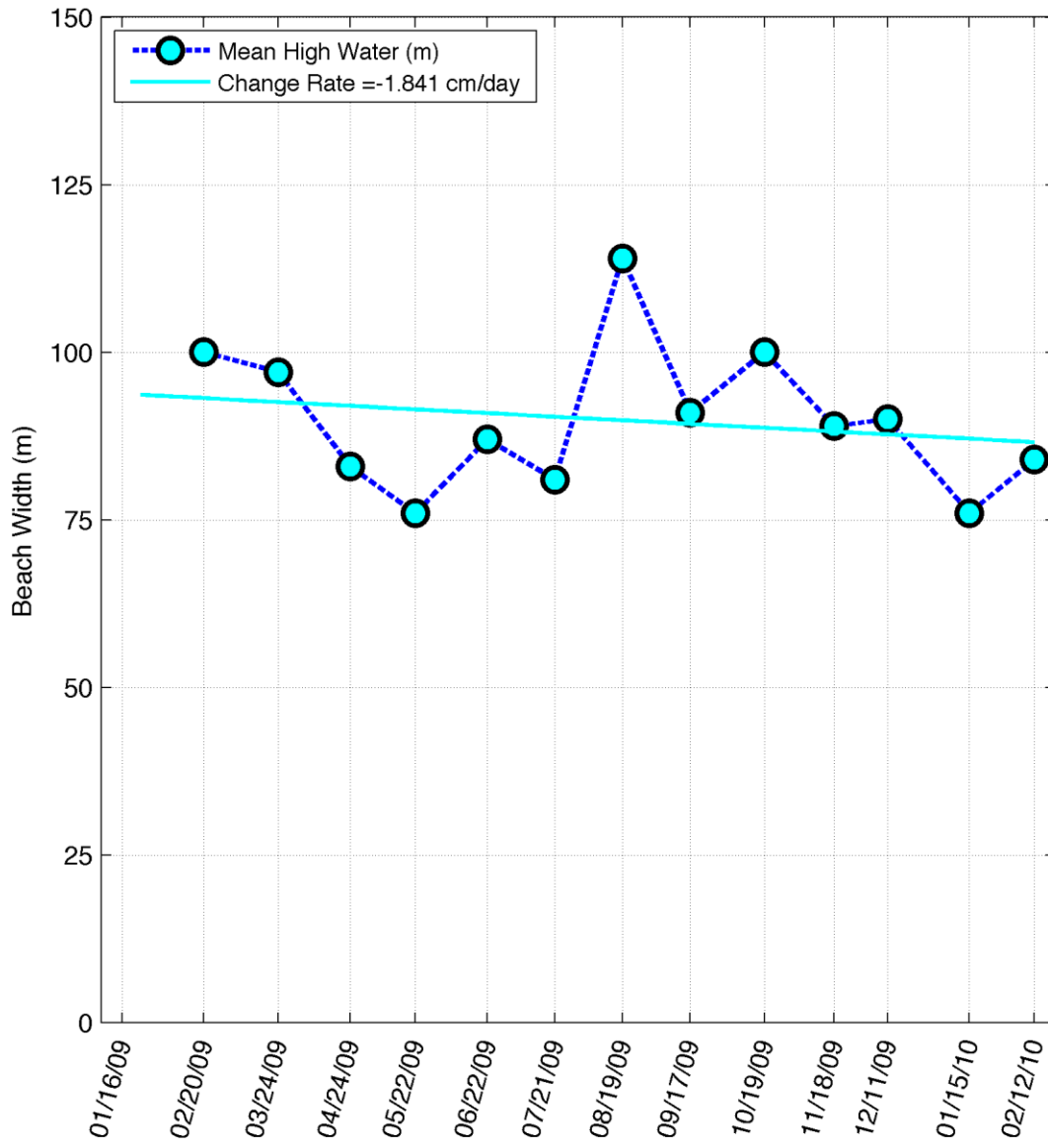
Shoreline Variation of Transect 21



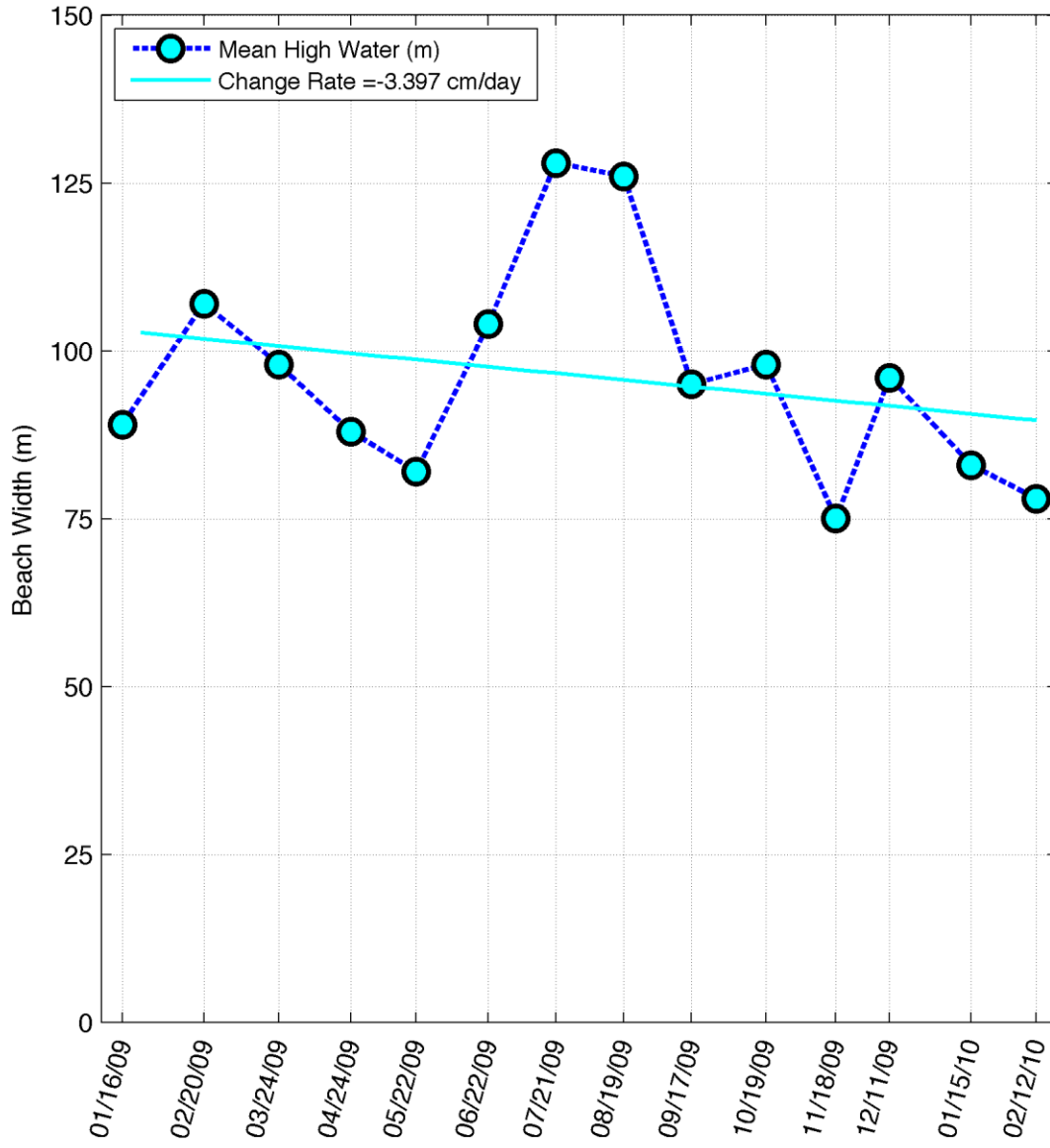
Shoreline Variation of Transect 22



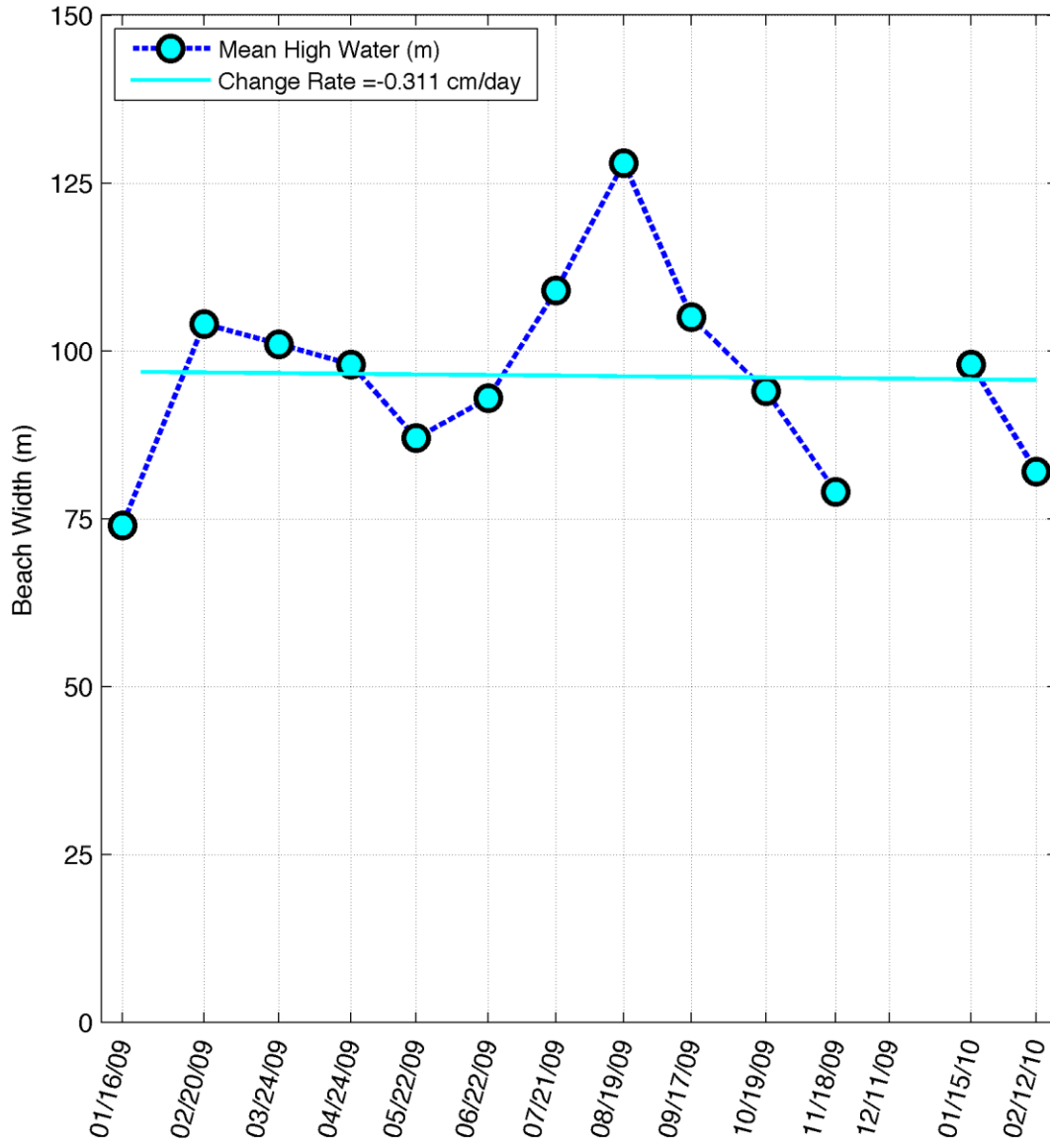
Shoreline Variation of Transect 23



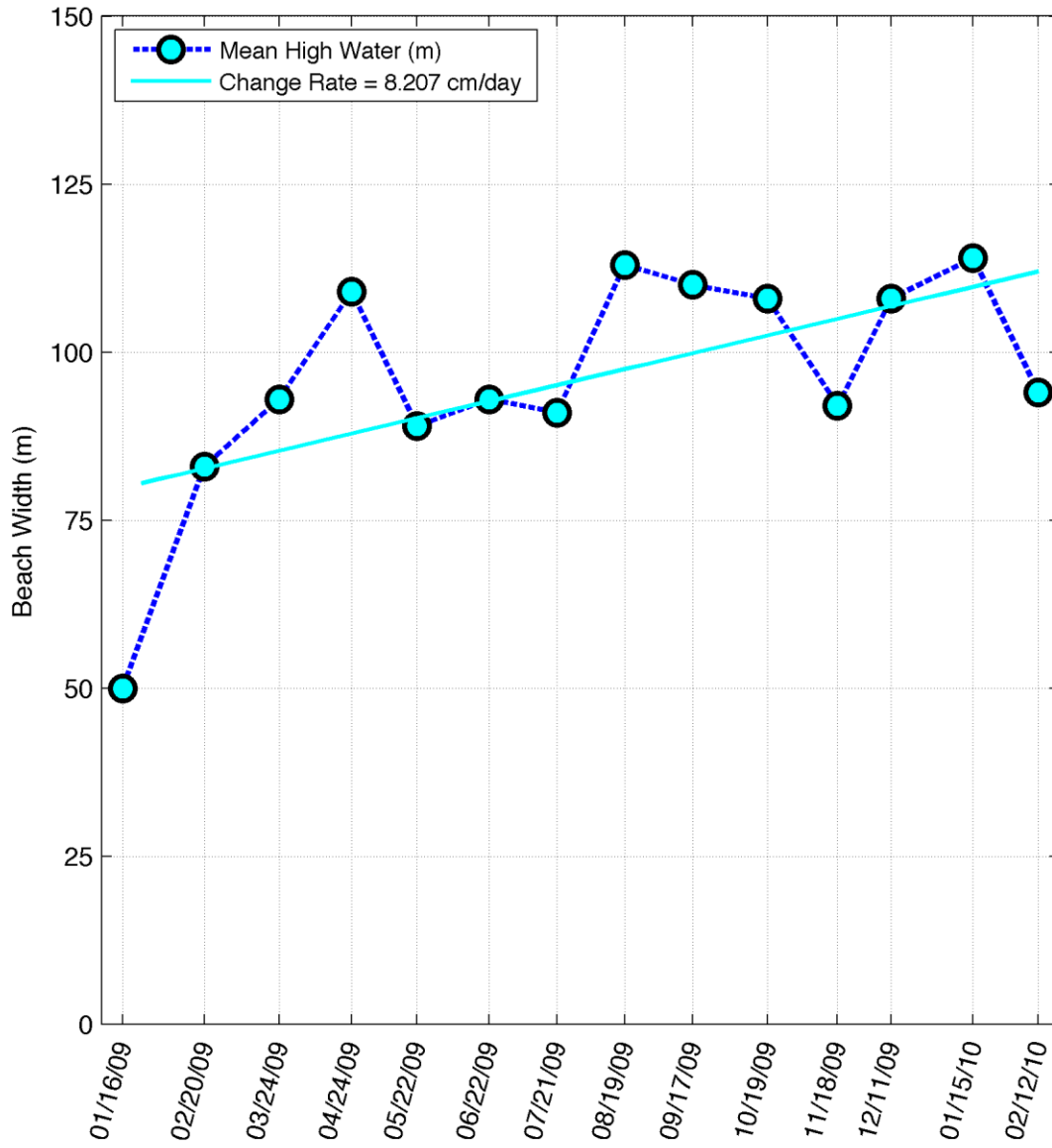
Shoreline Variation of Transect 24



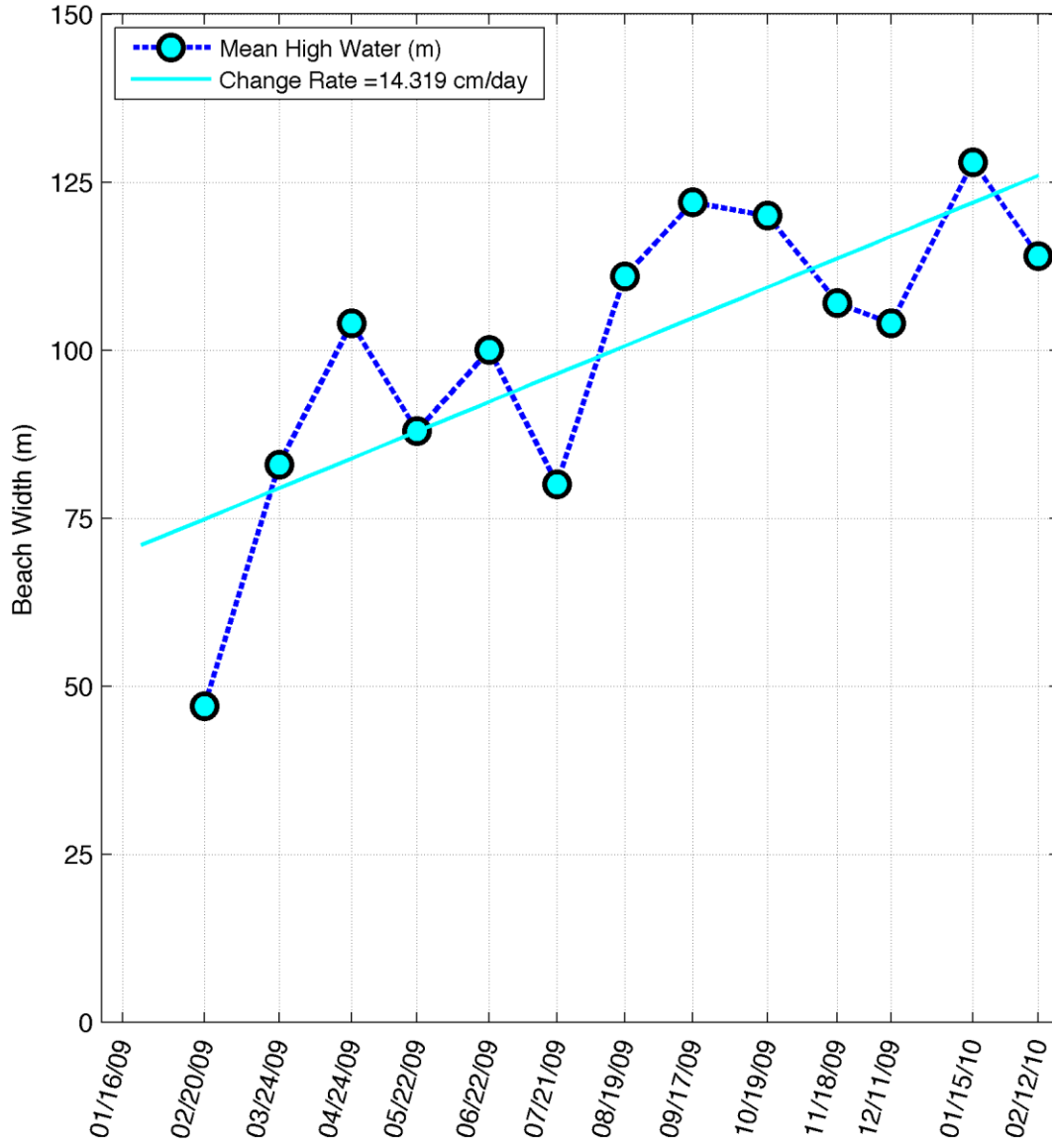
Shoreline Variation of Transect 25



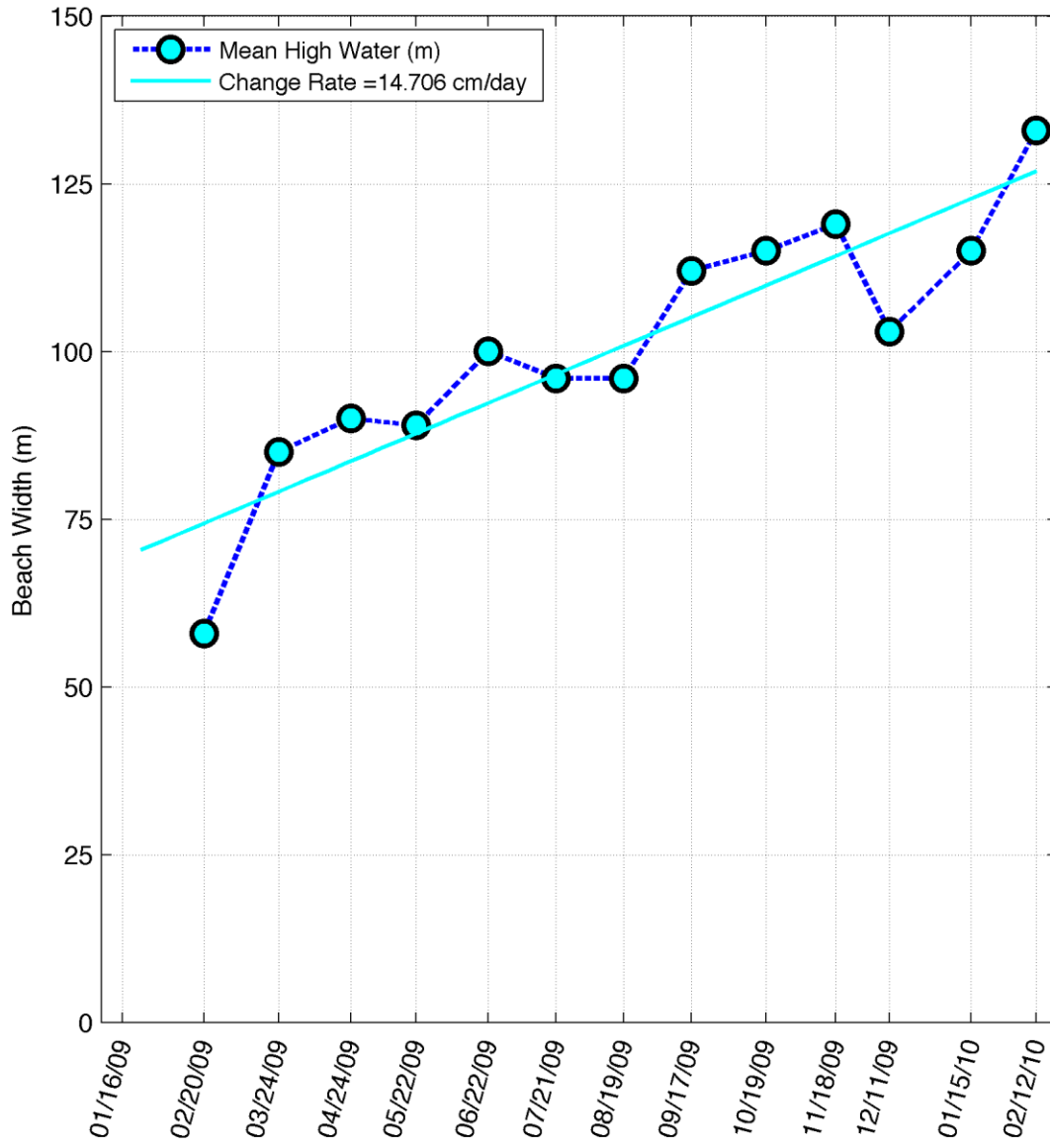
Shoreline Variation of Transect 26



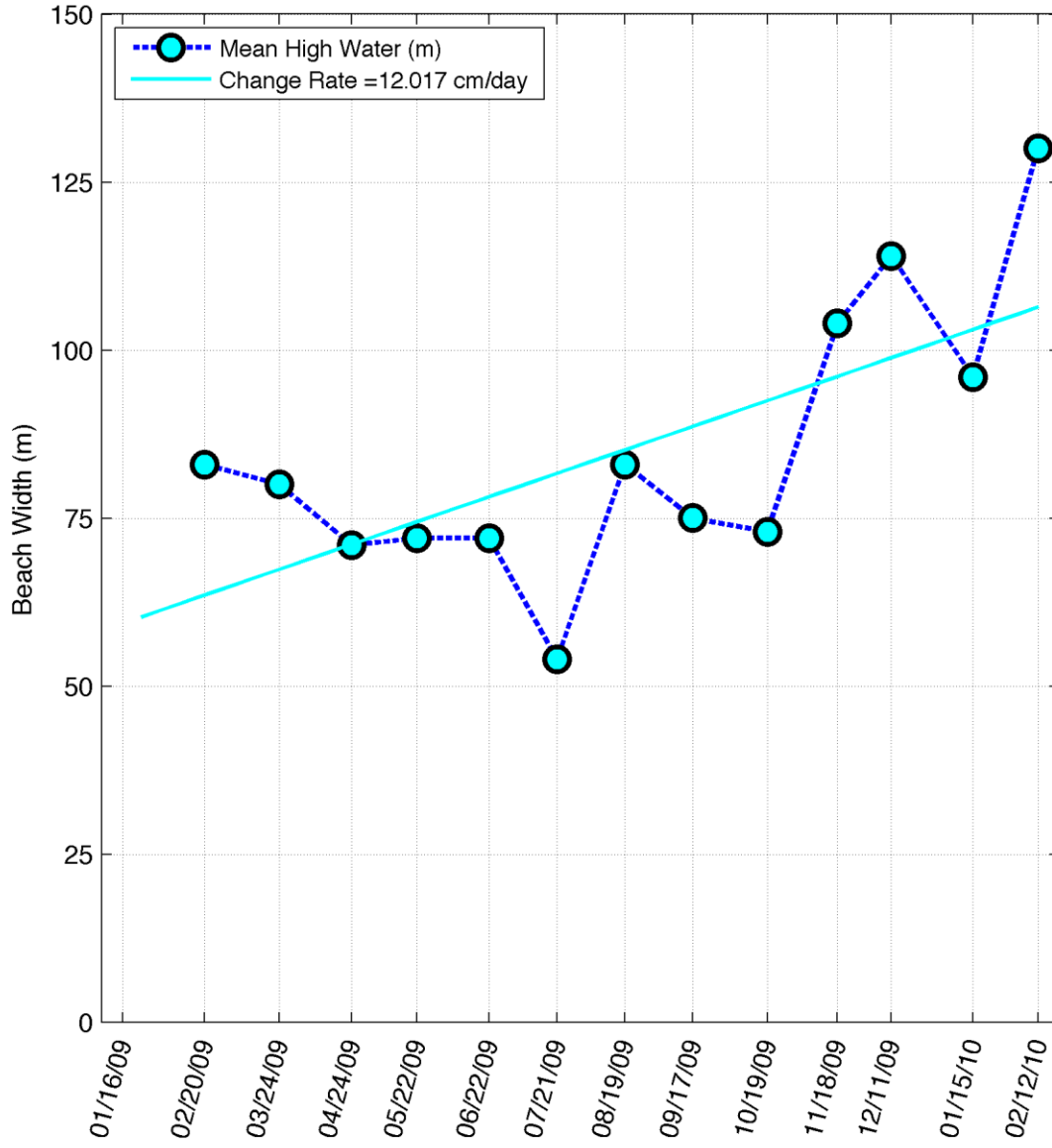
Shoreline Variation of Transect 27



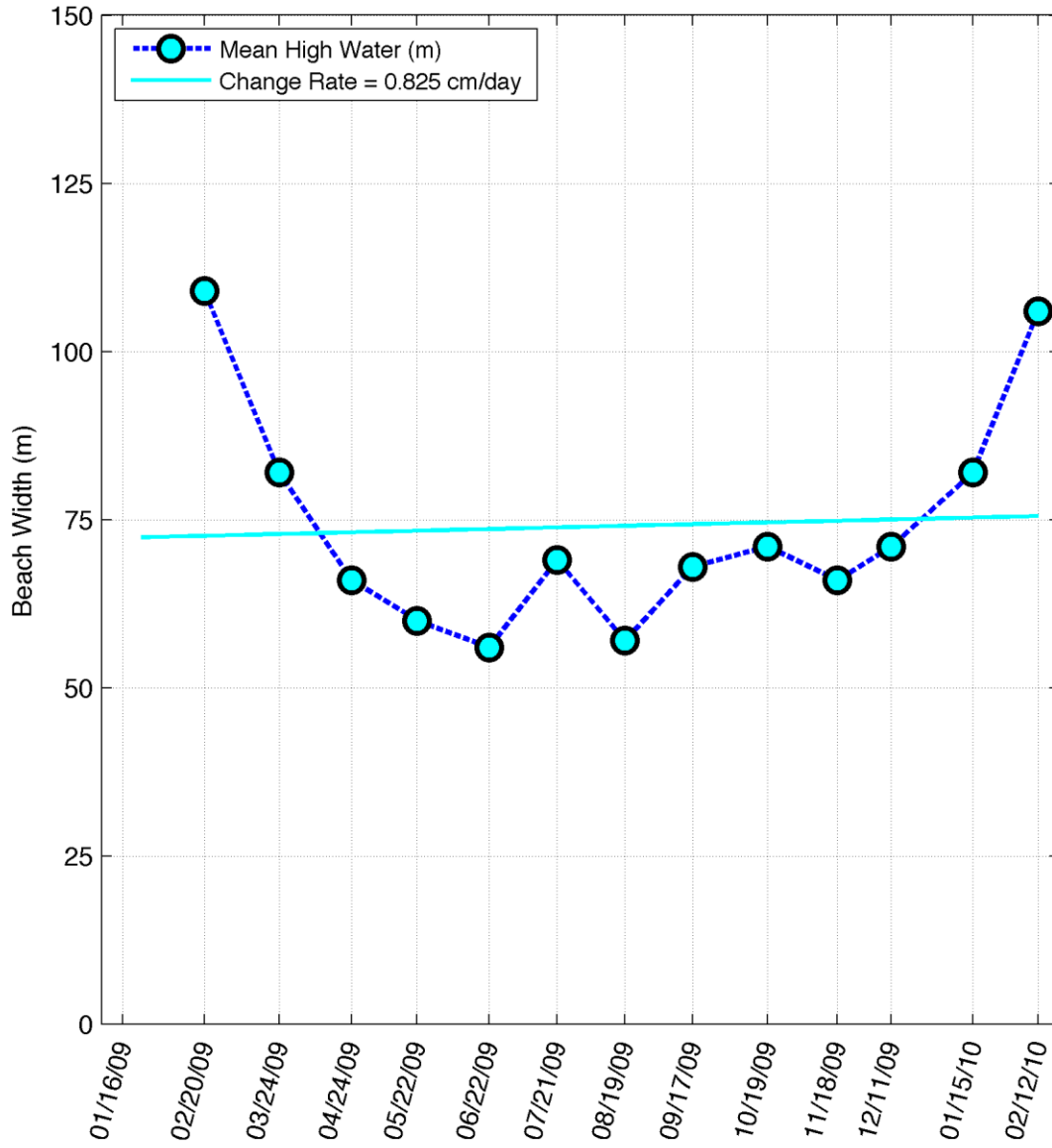
Shoreline Variation of Transect 28



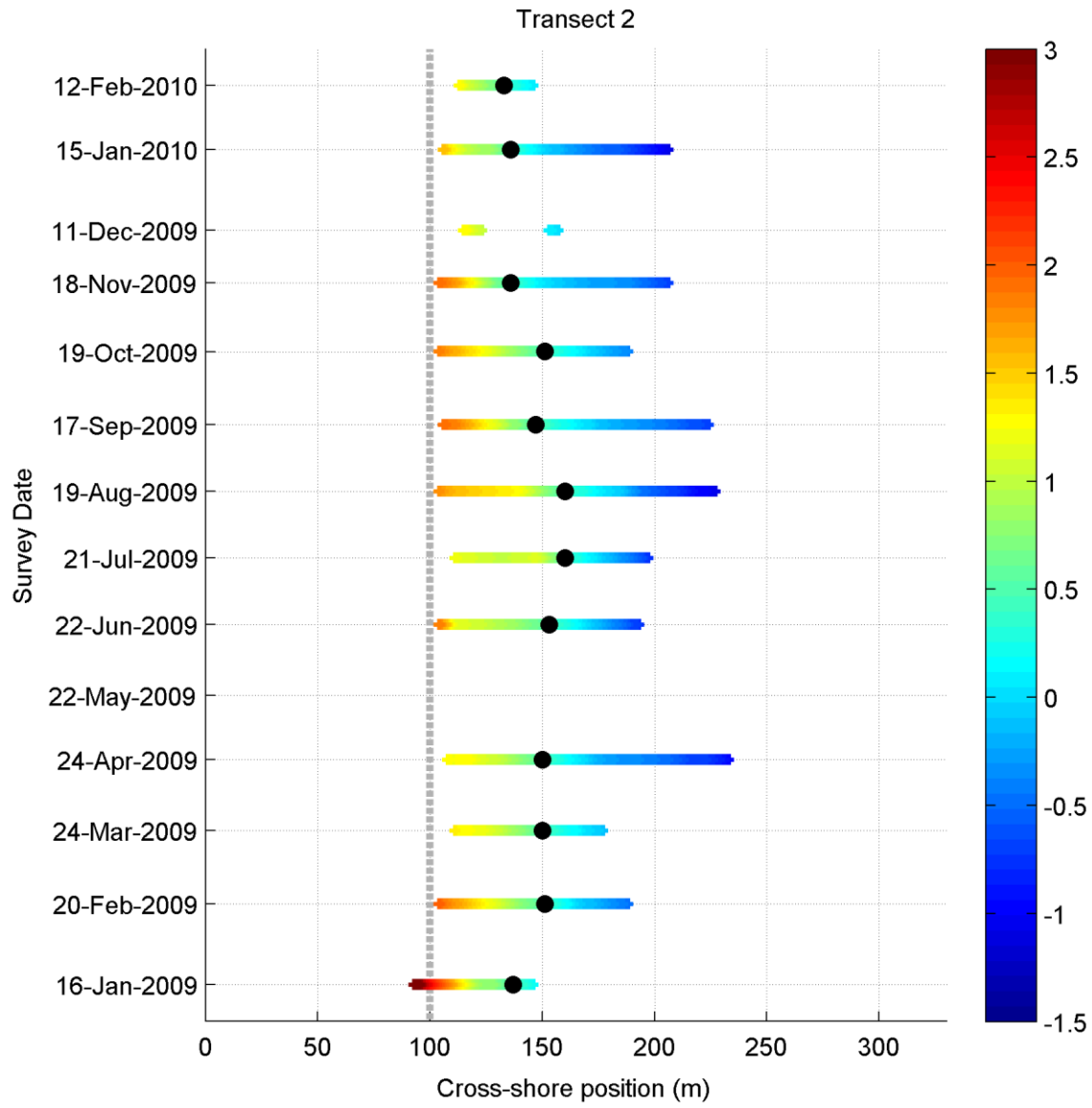
Shoreline Variation of Transect 29

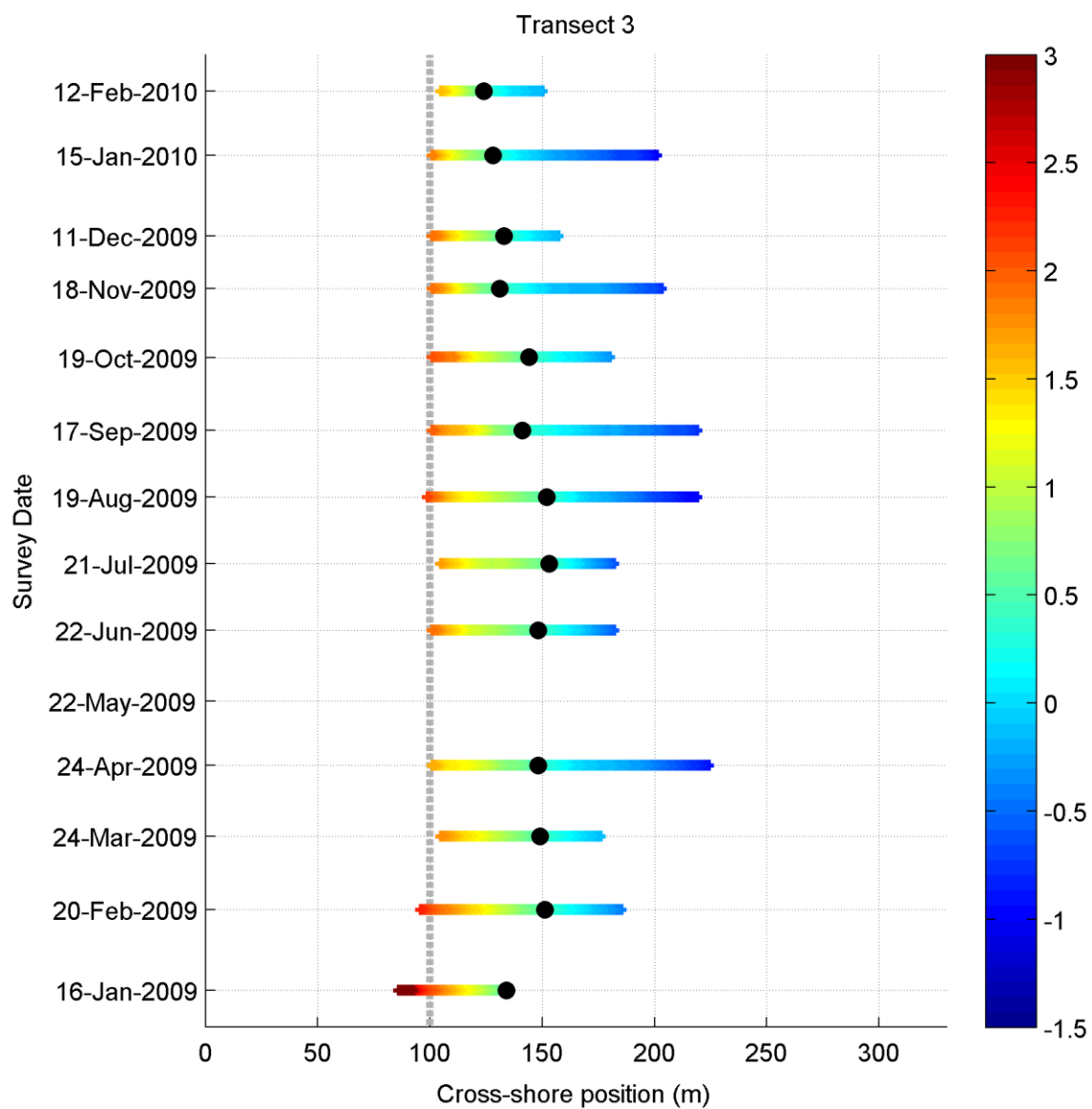


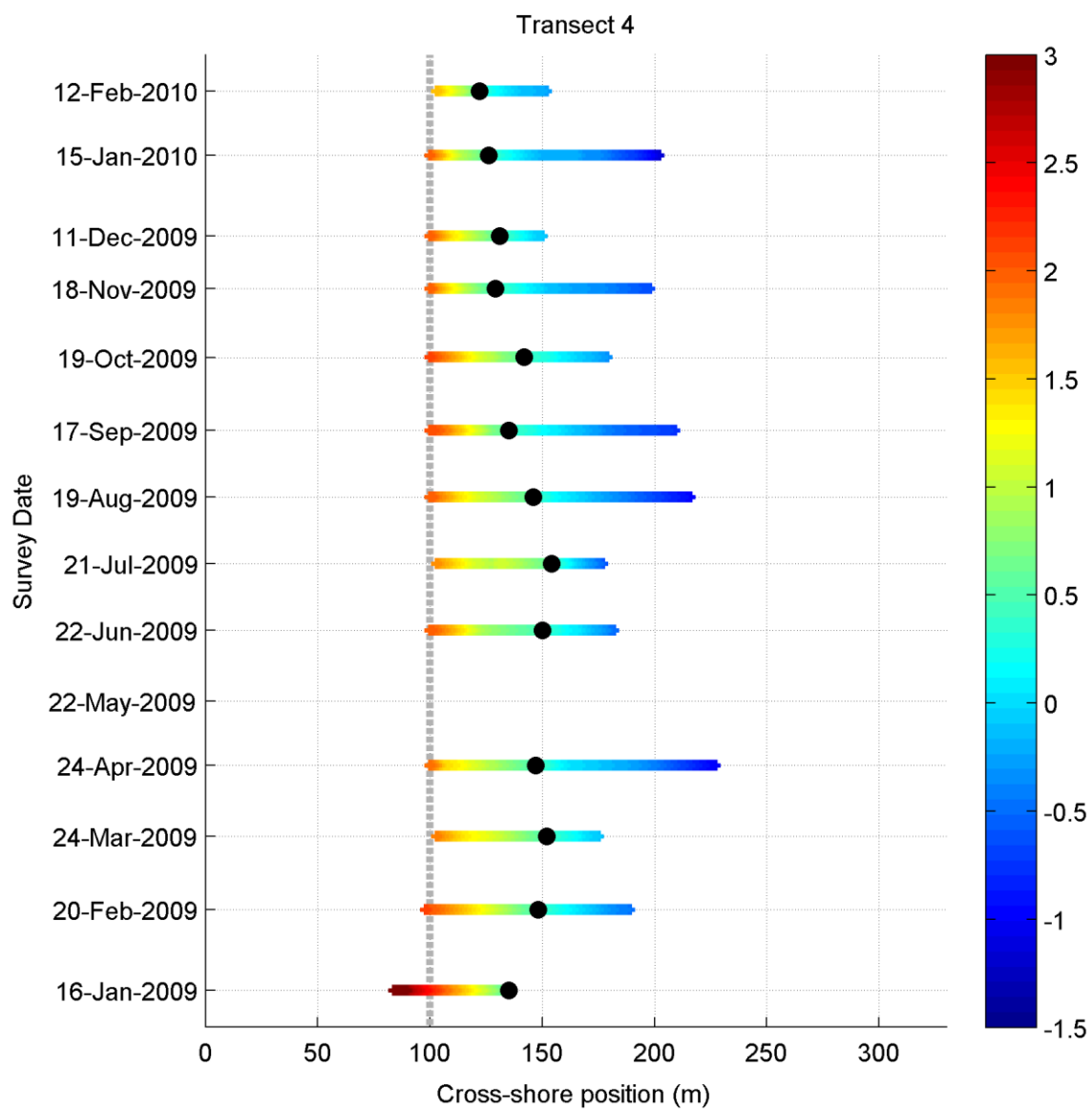
Shoreline Variation of Transect 30

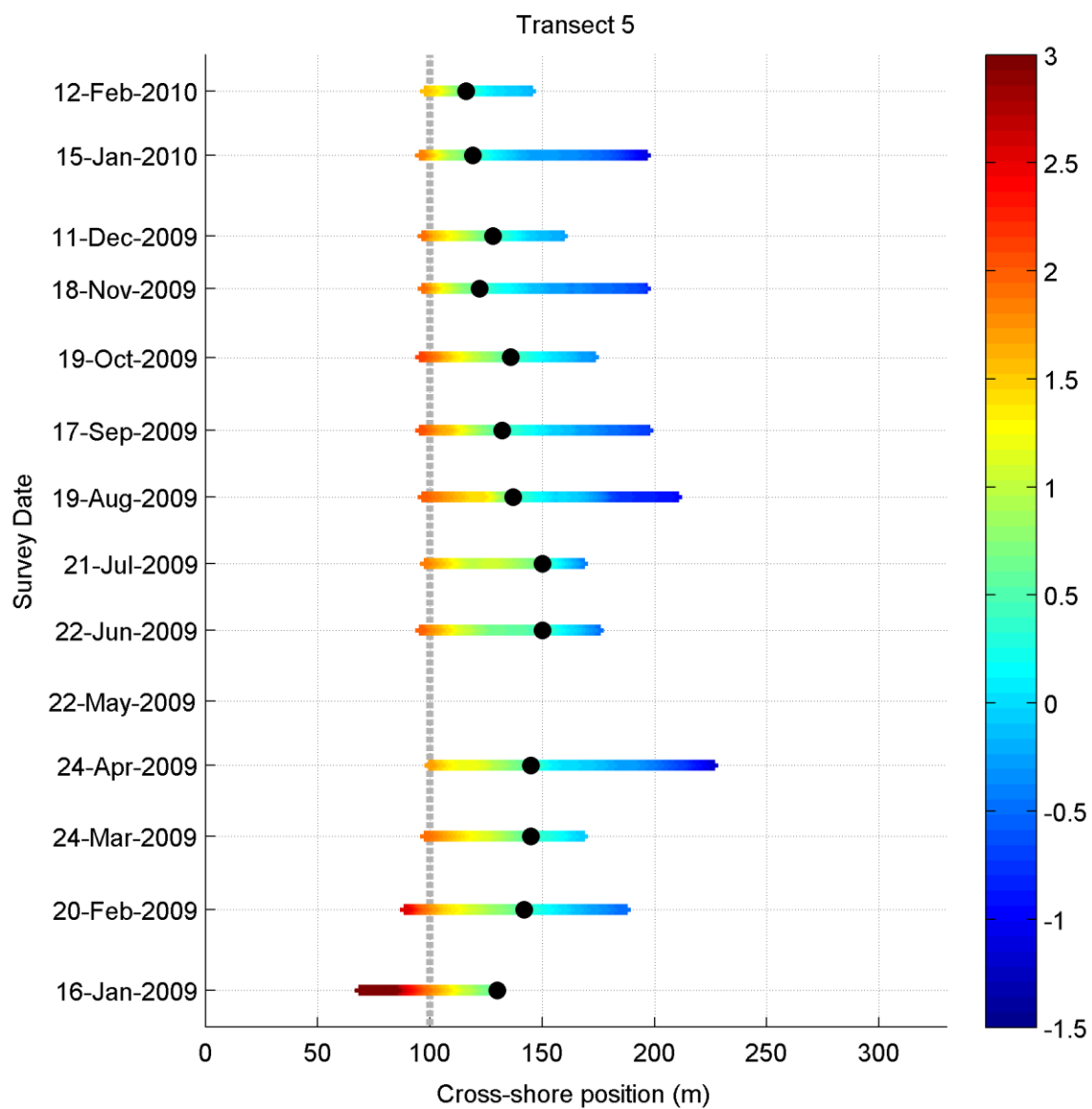


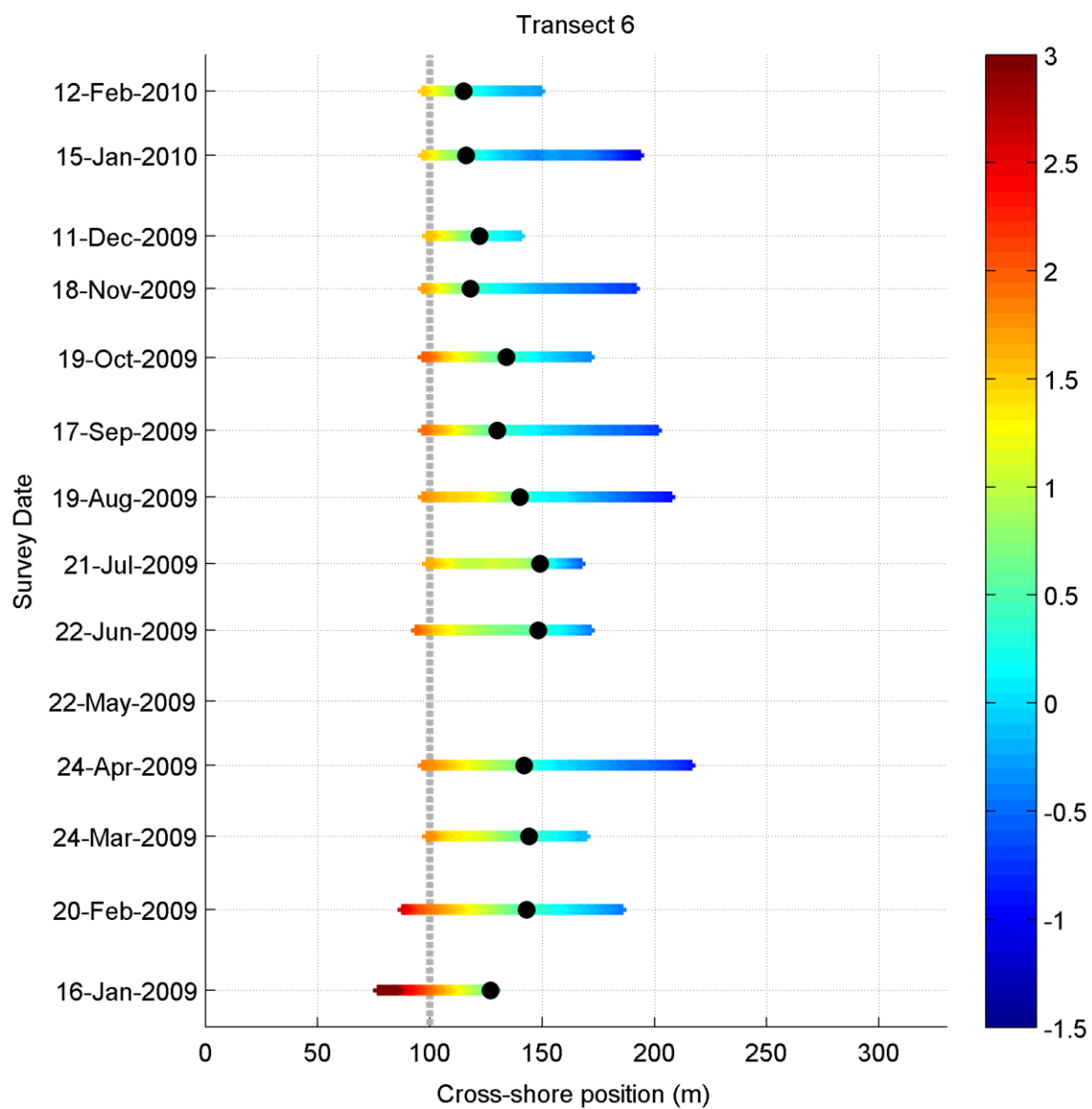
A-5

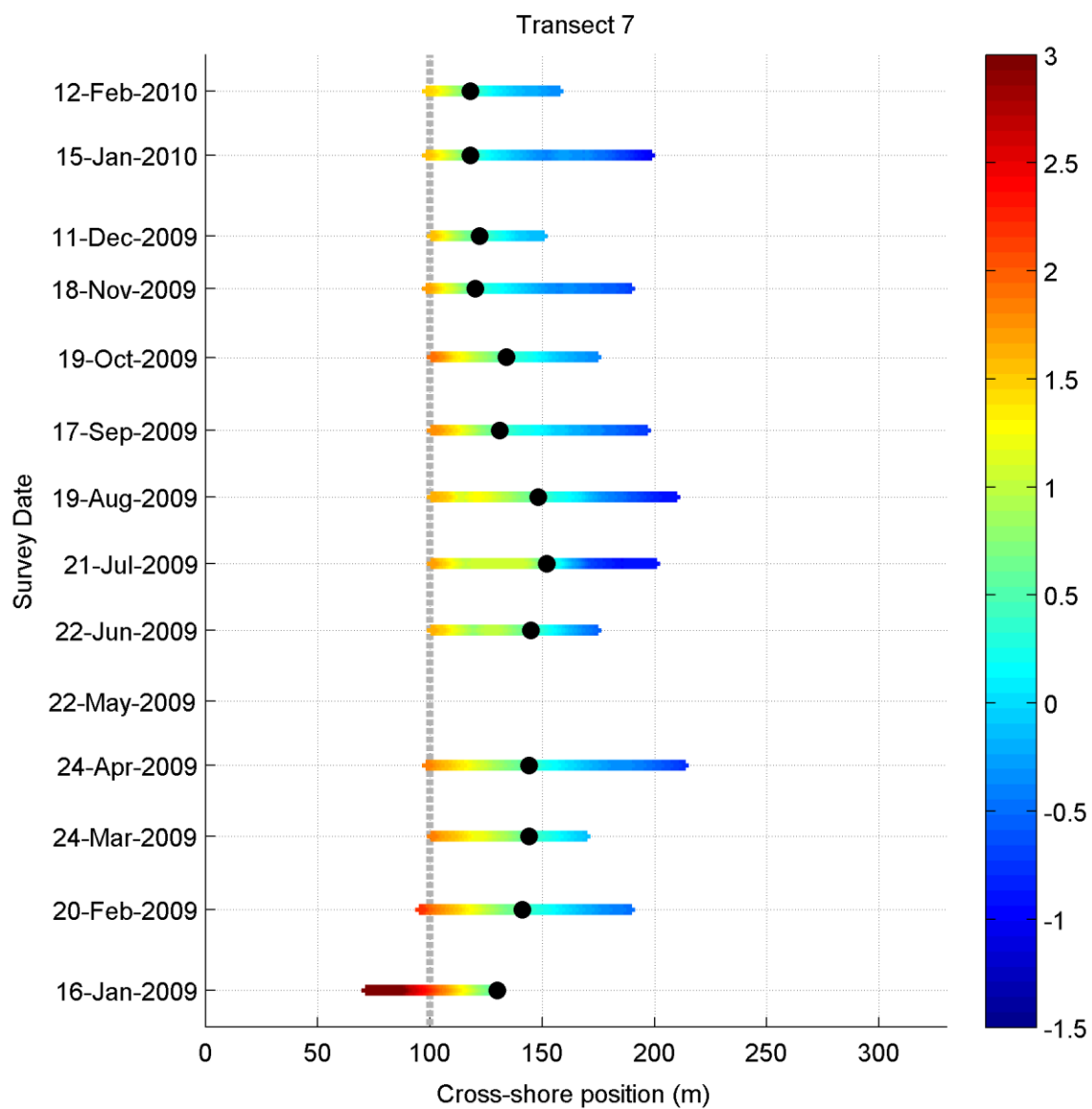


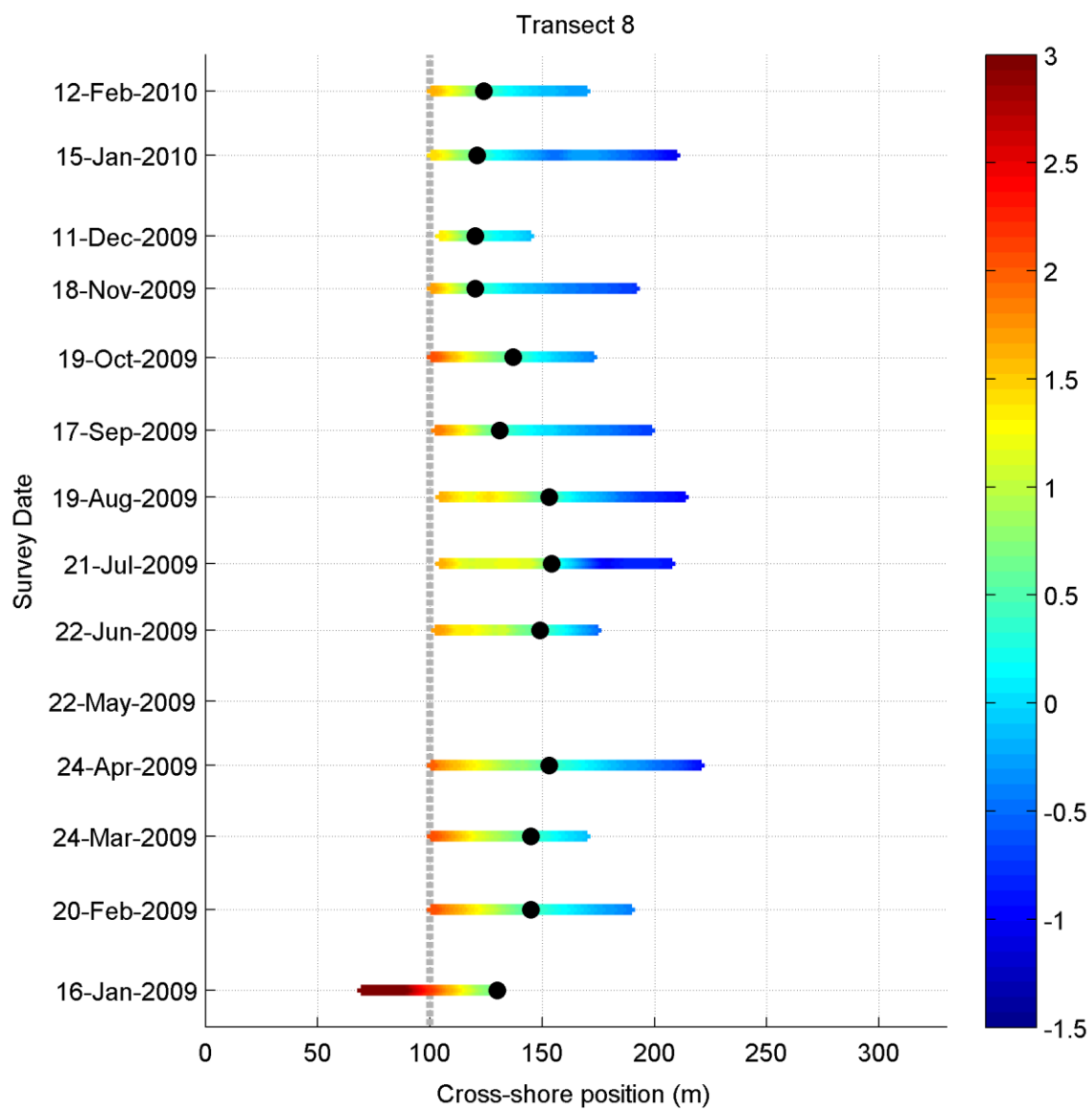


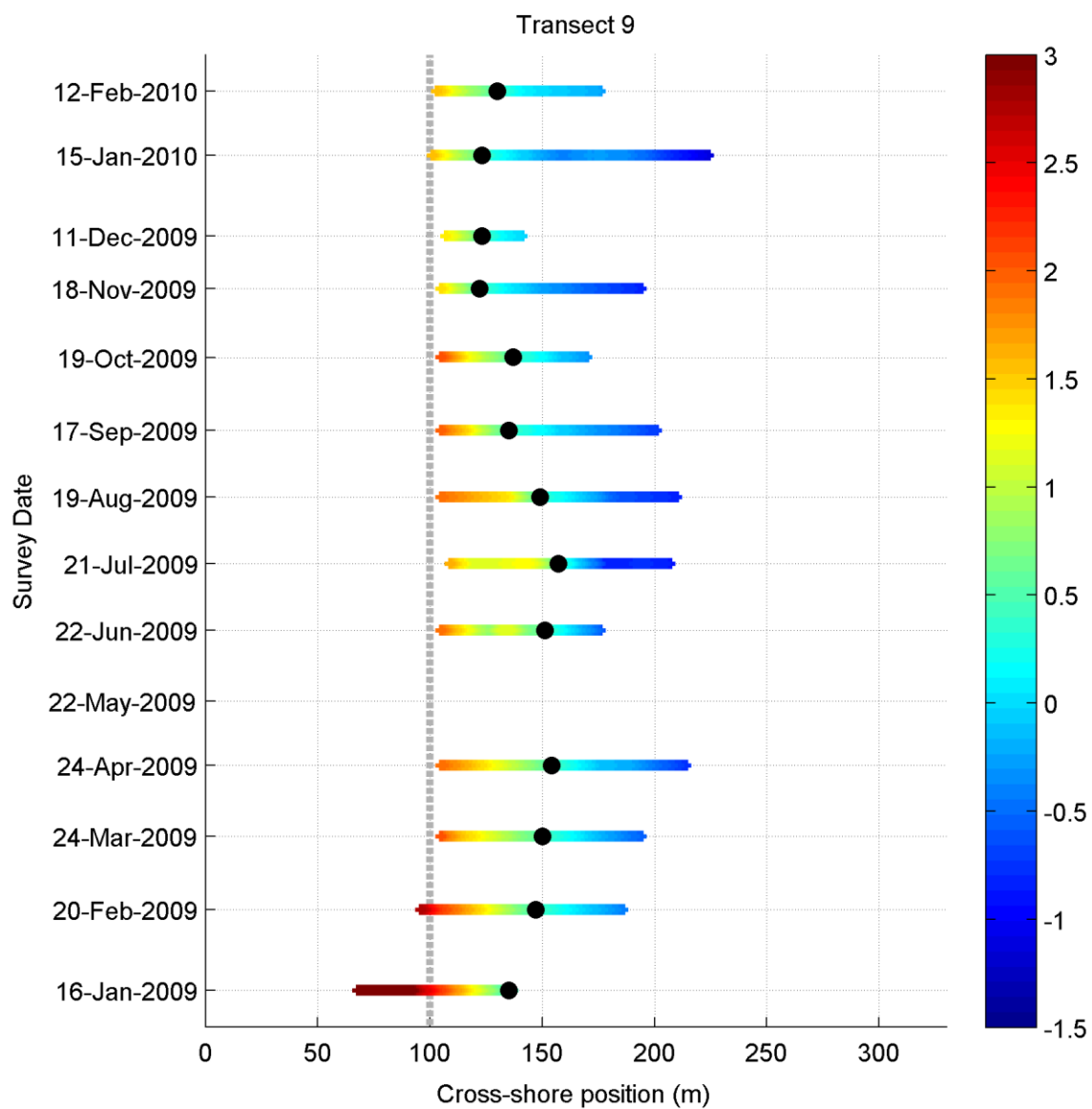


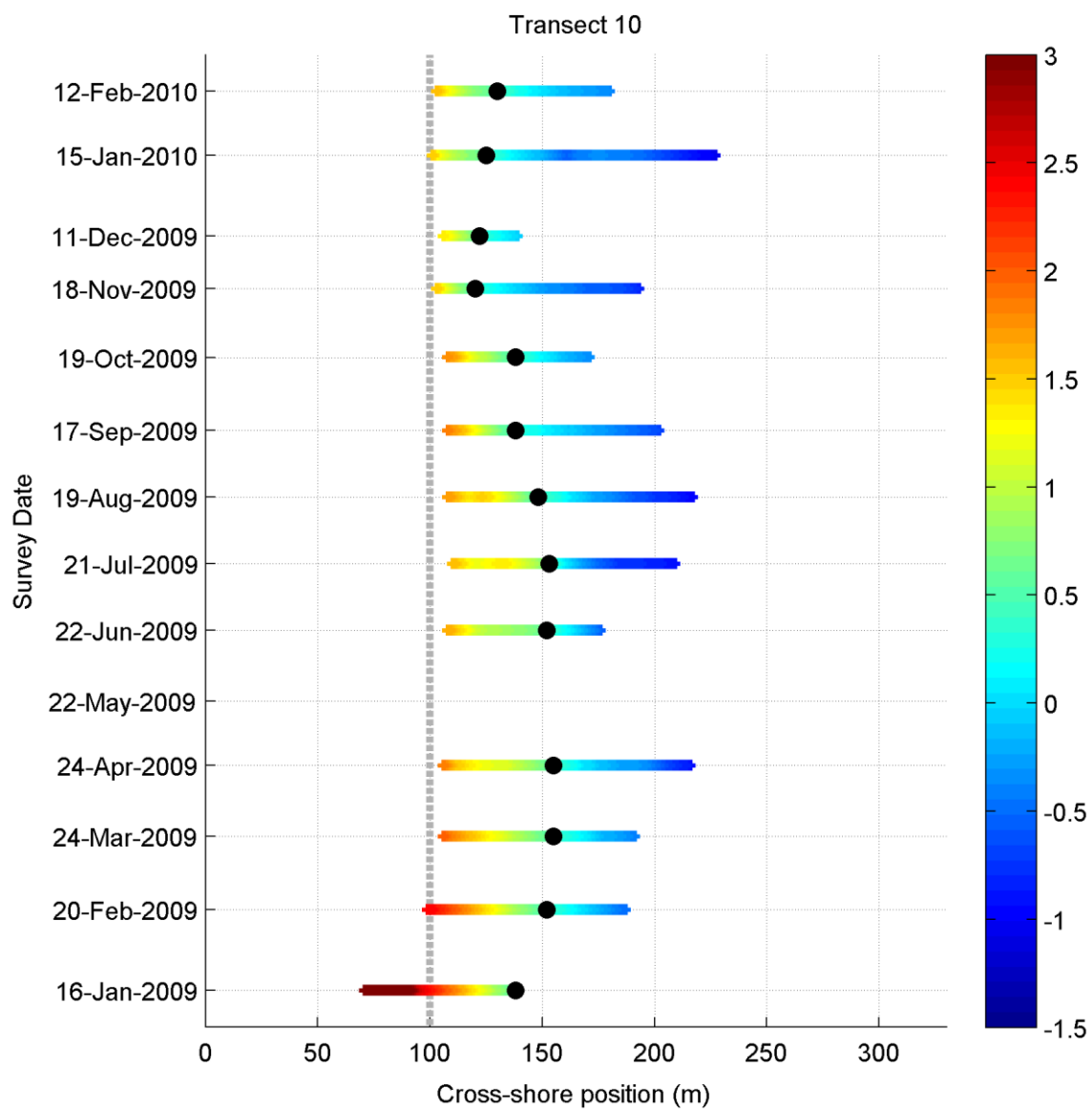


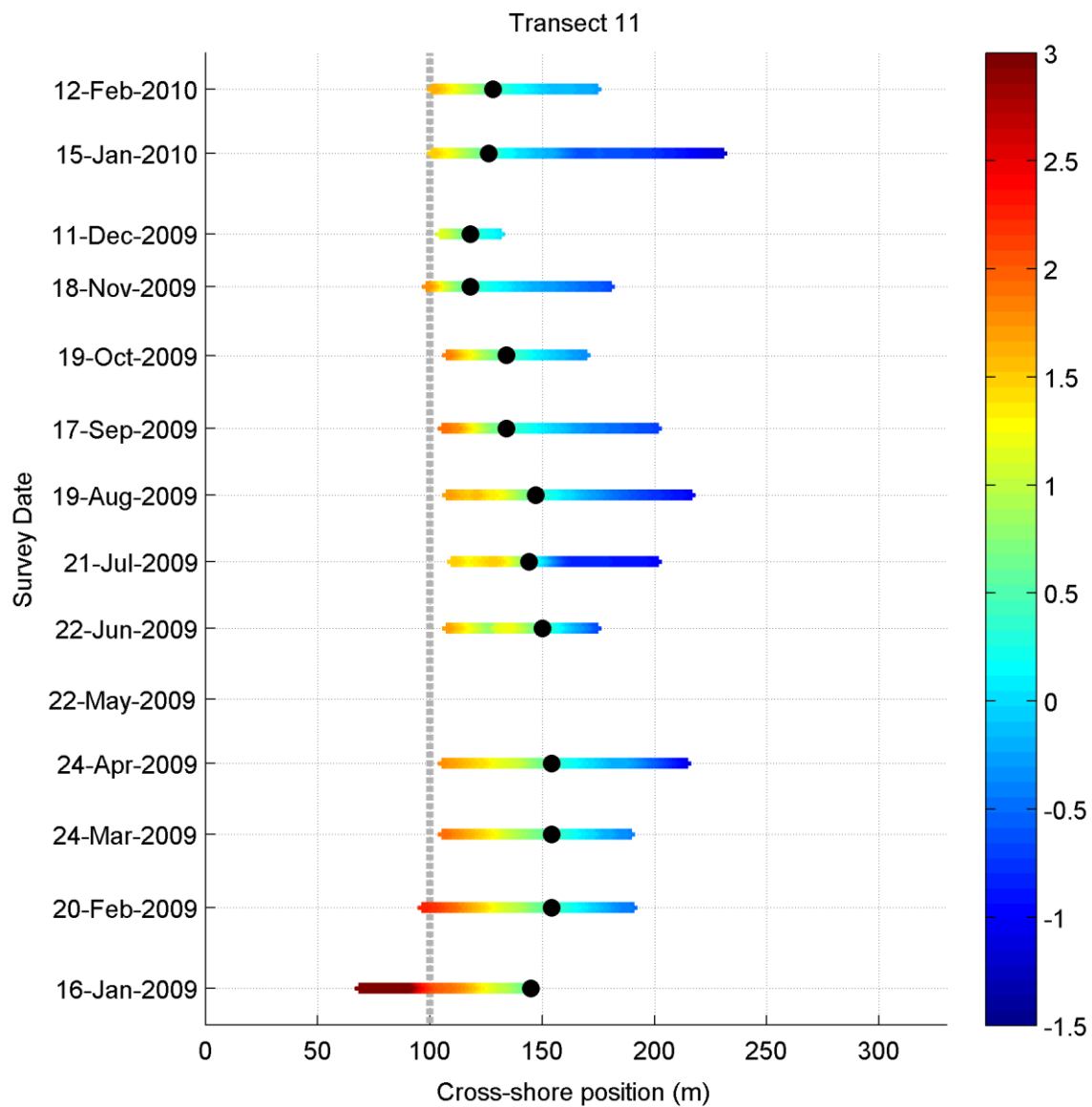


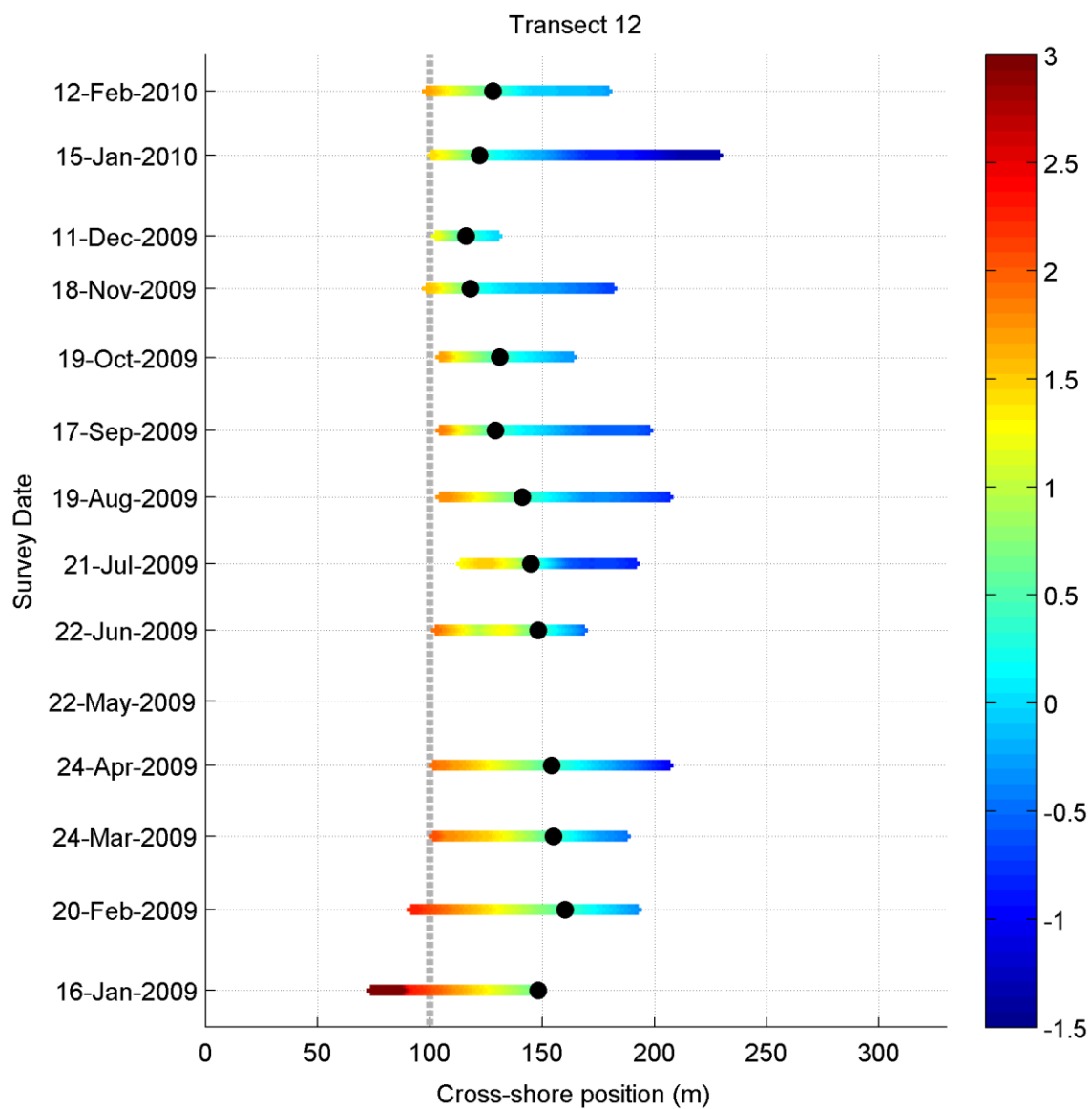


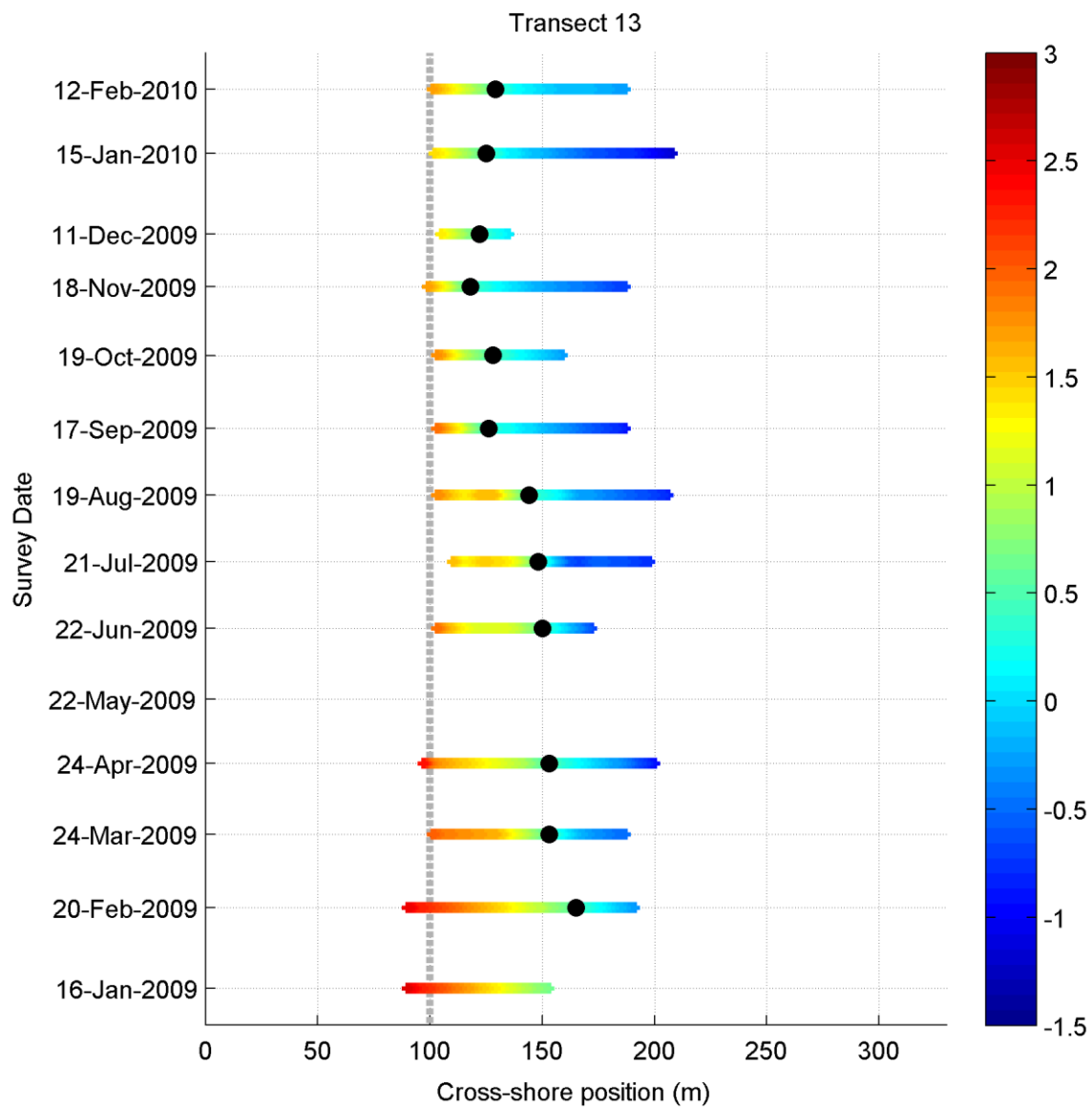


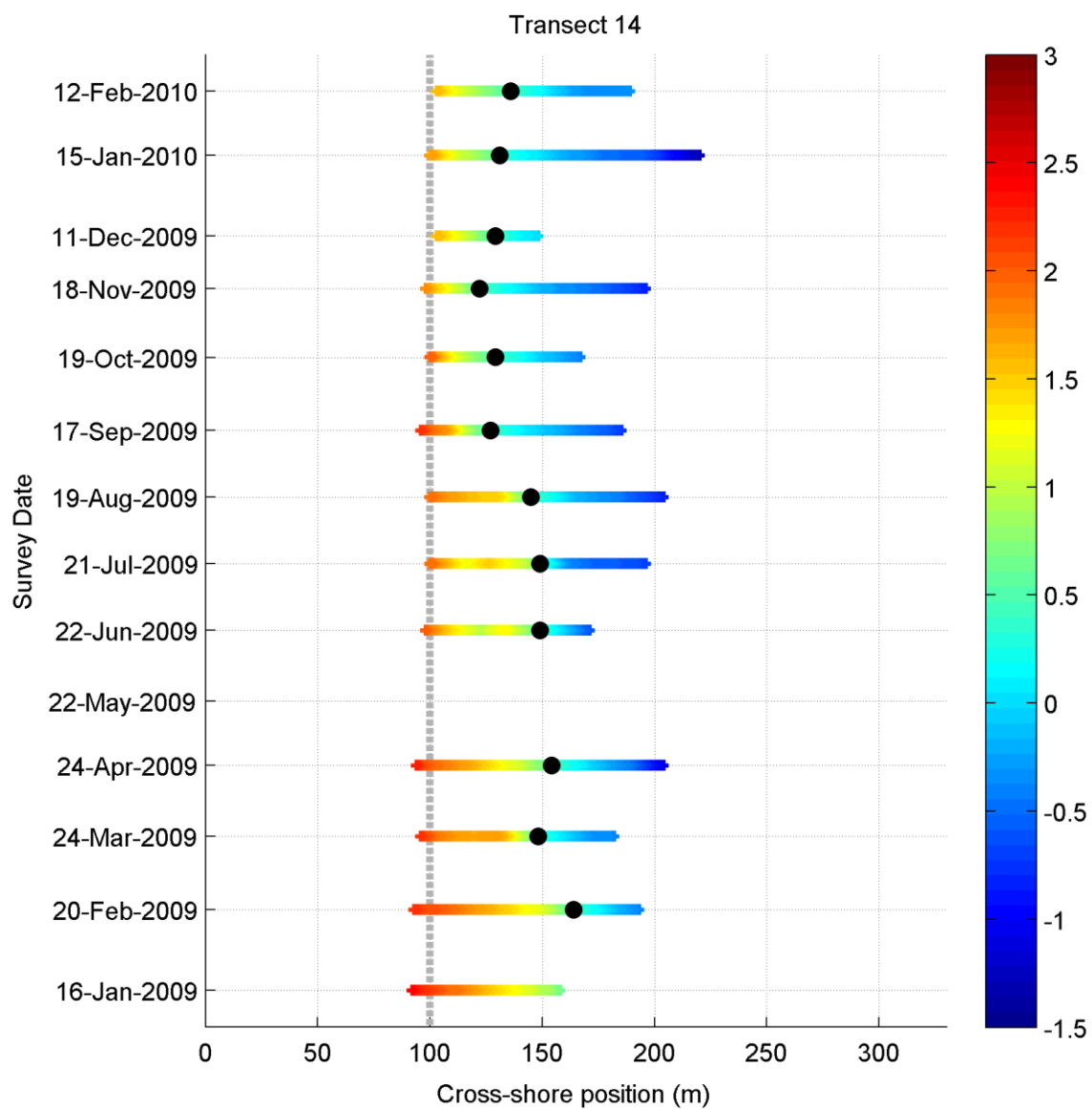


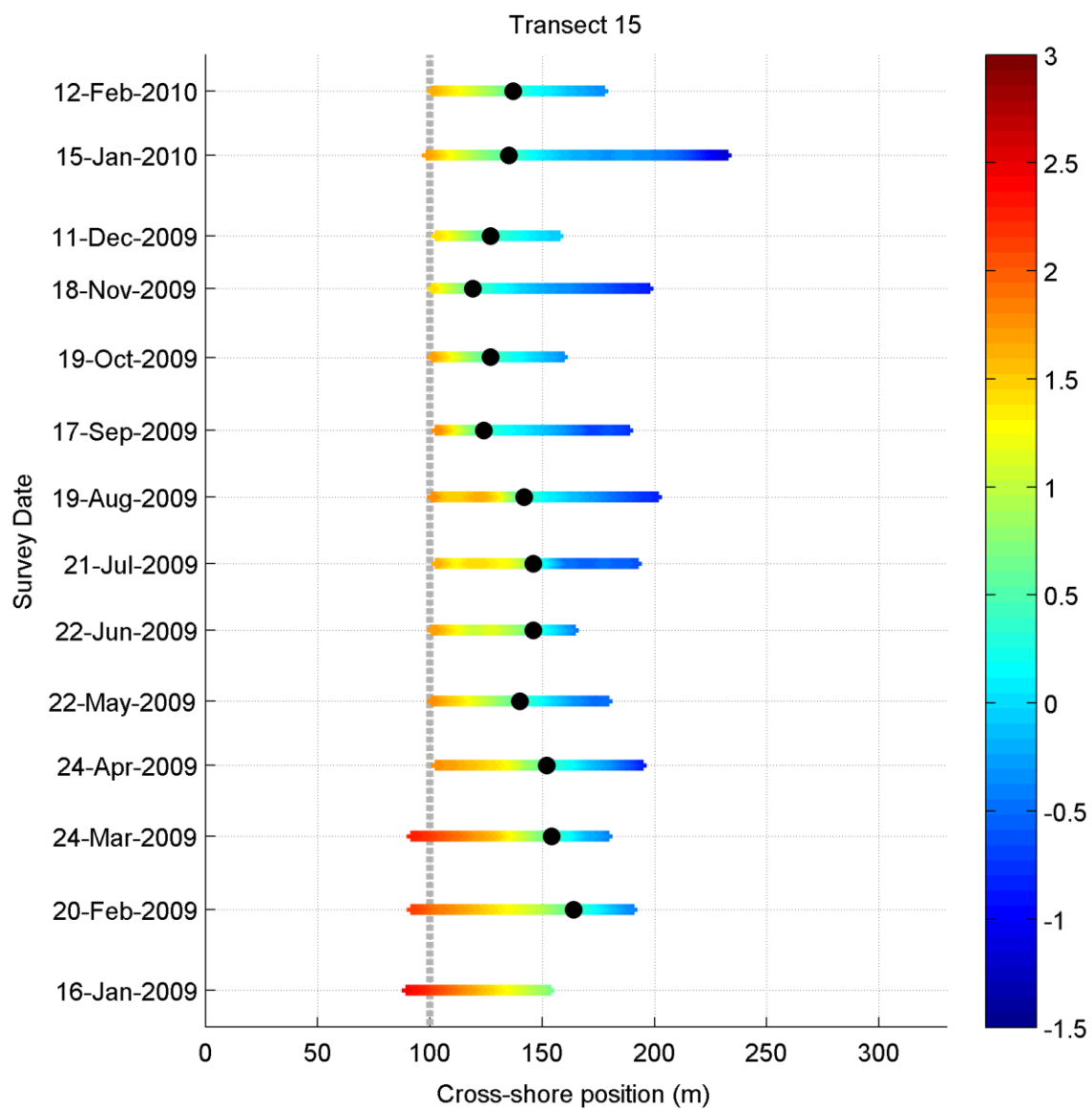


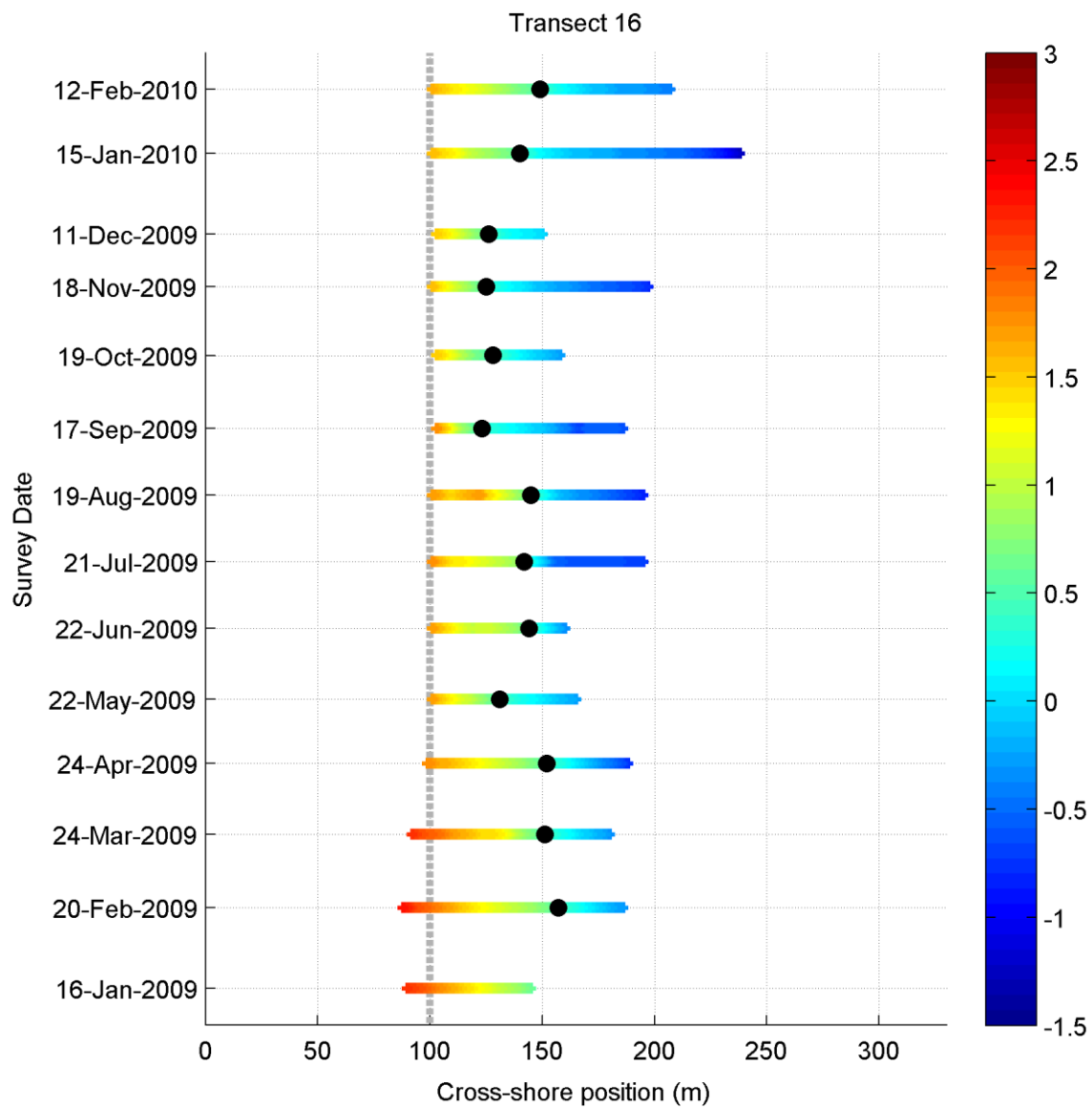


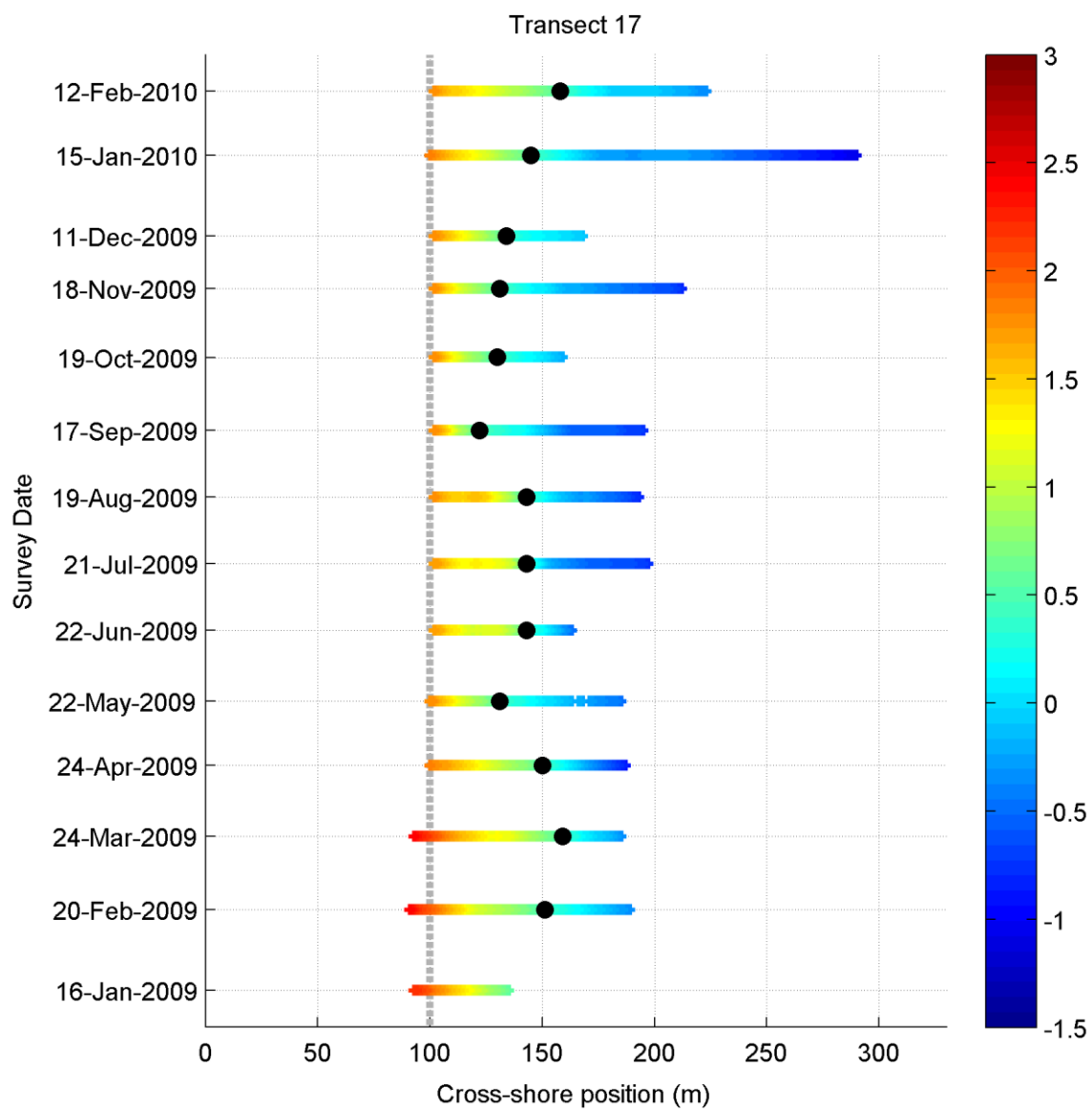


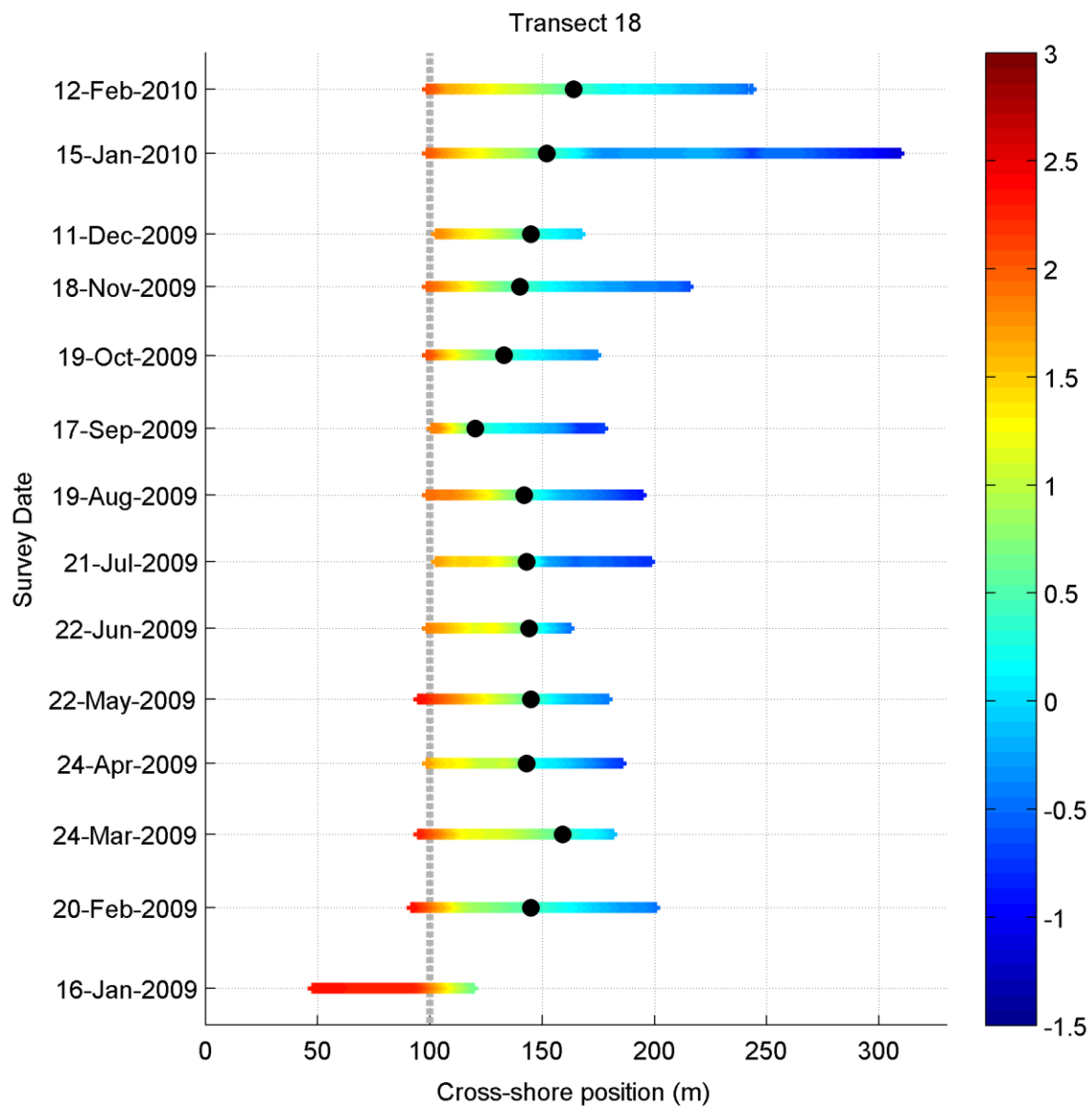


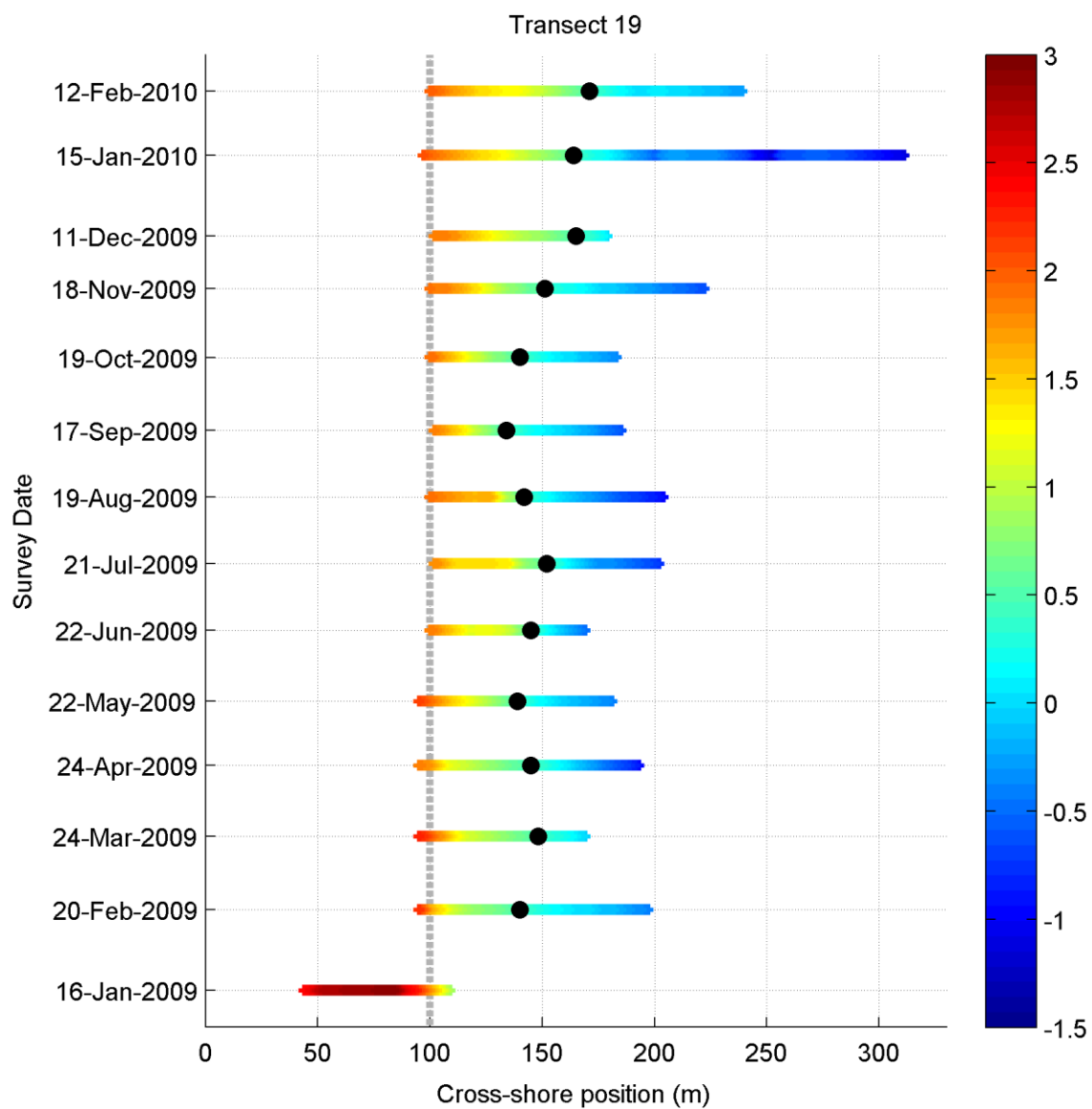


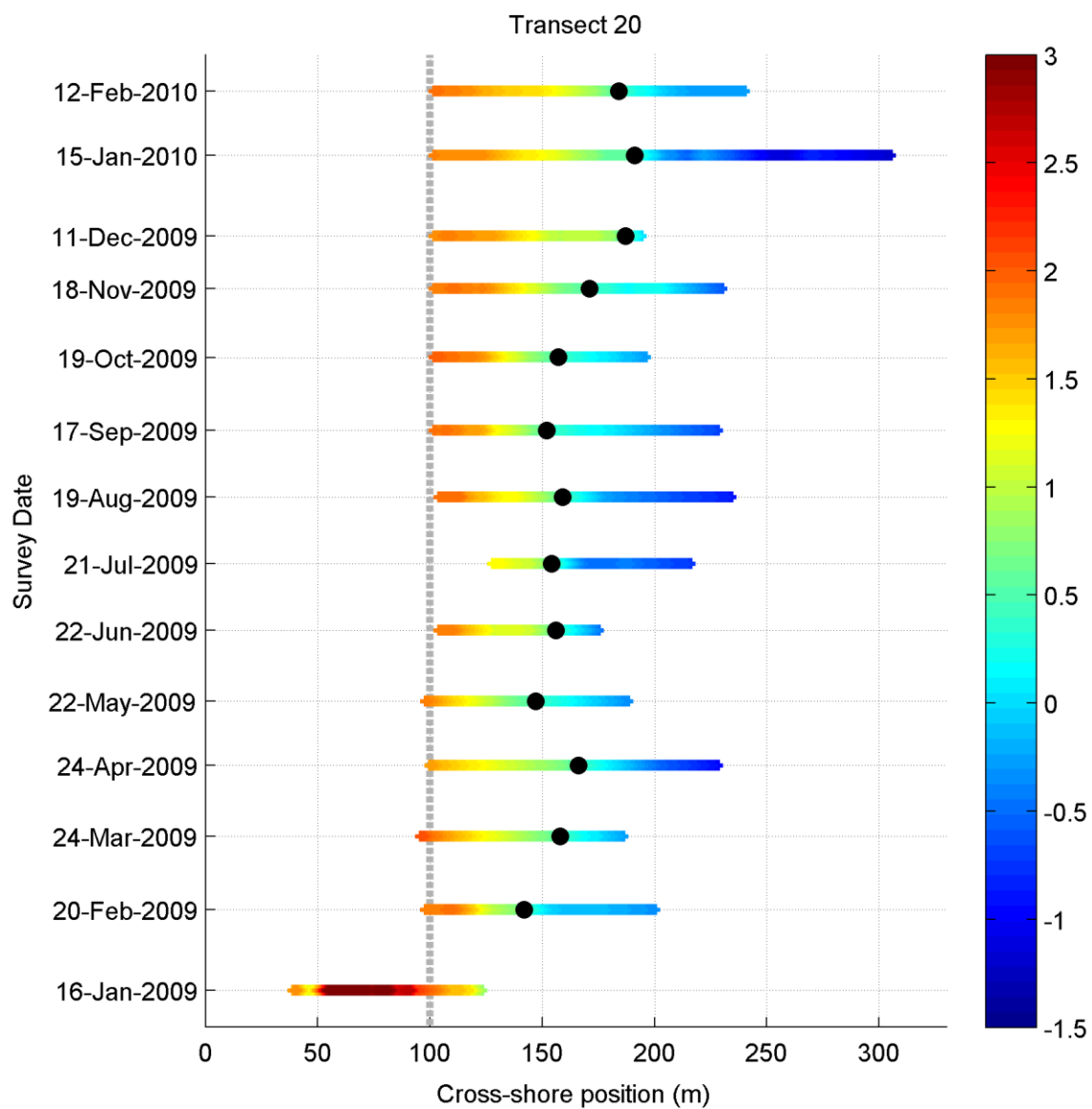


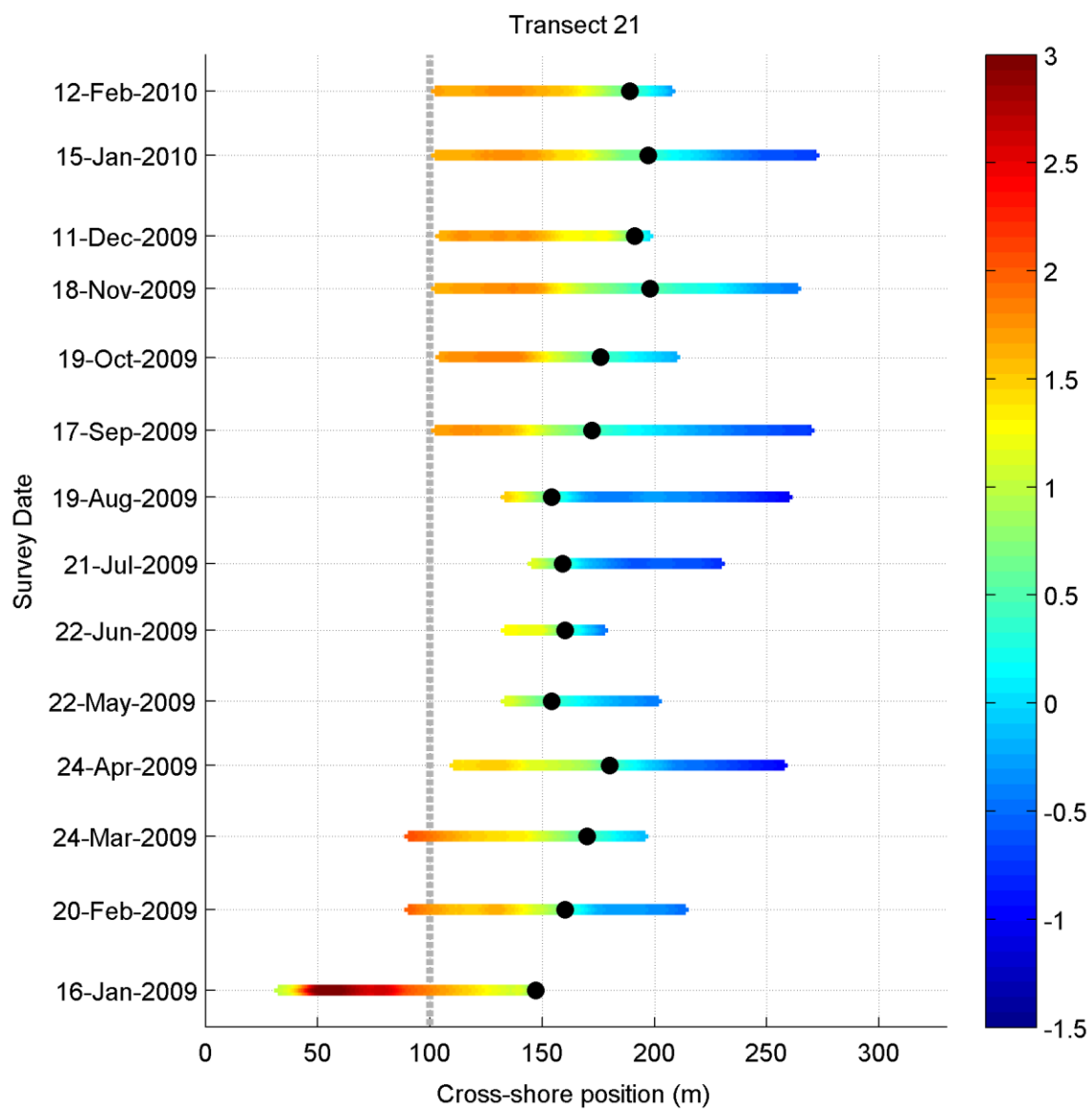


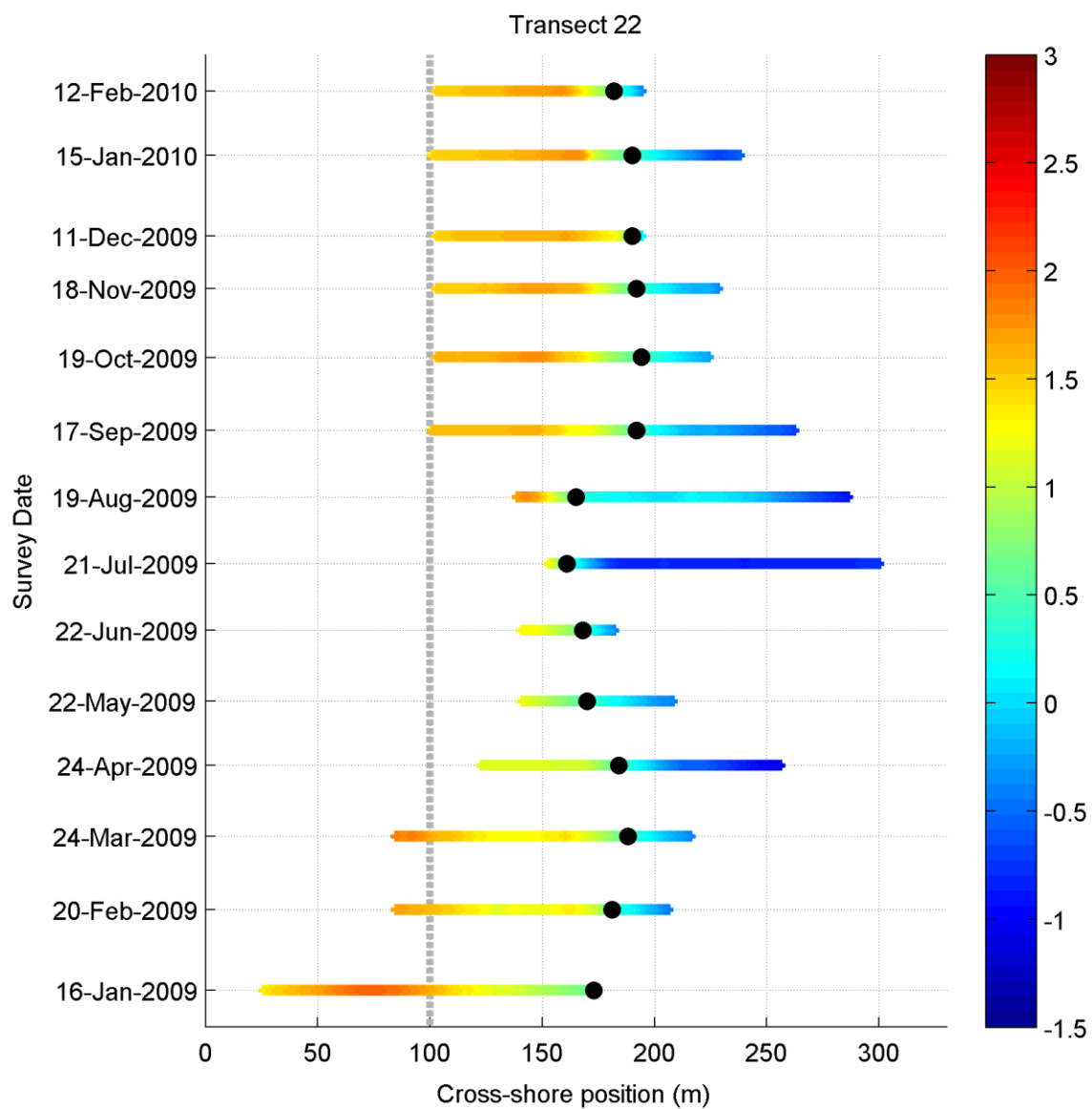


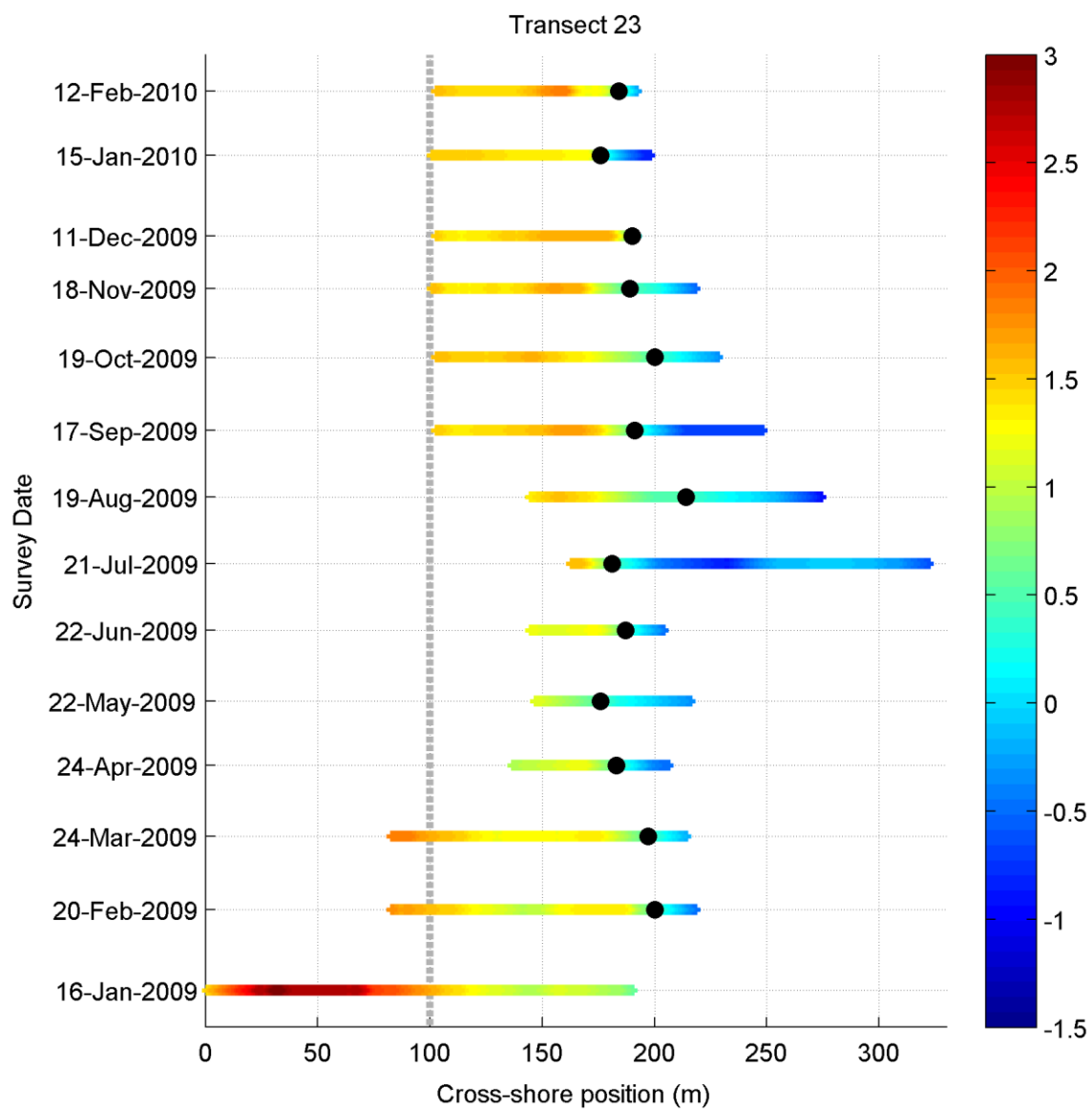


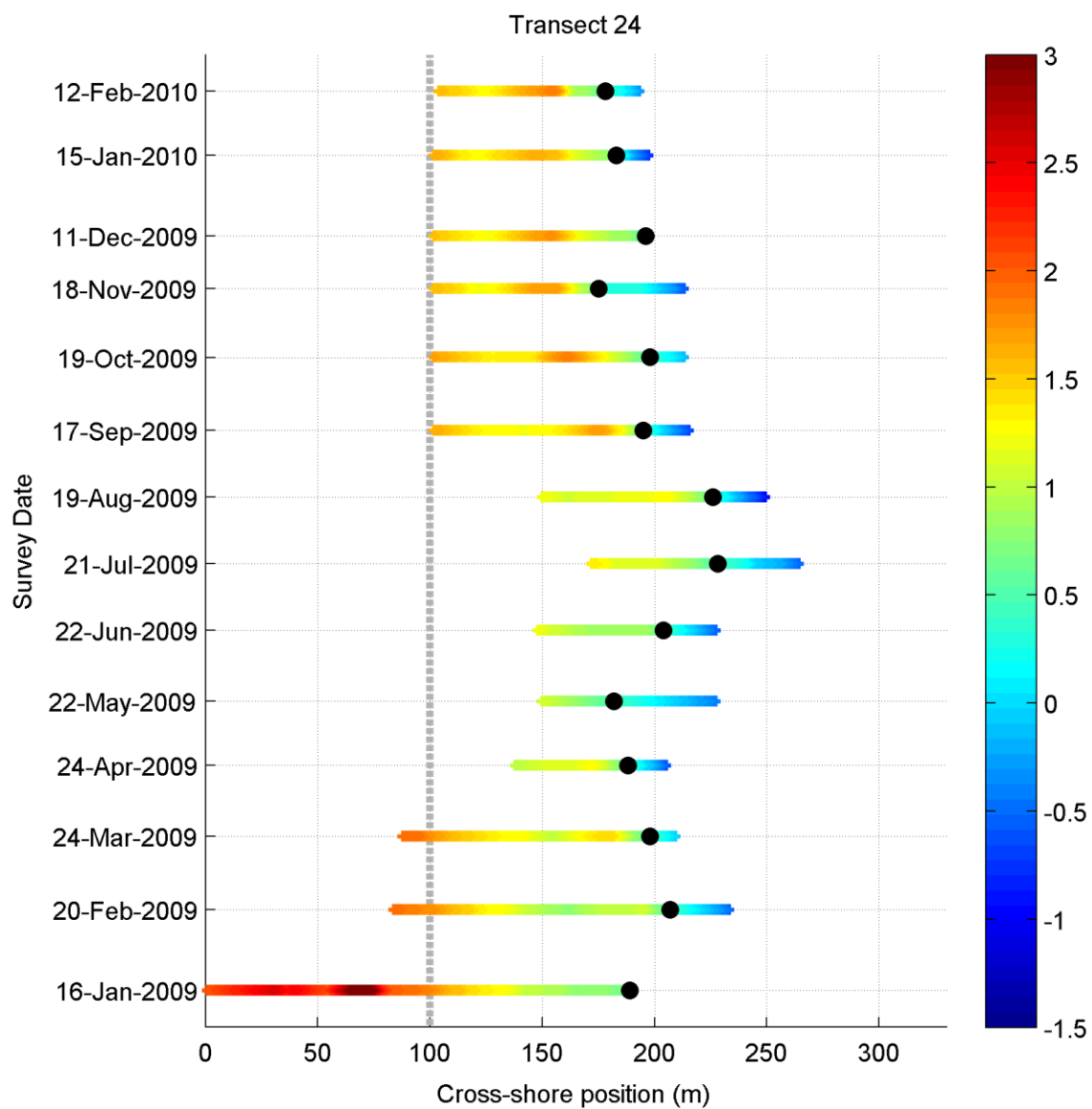


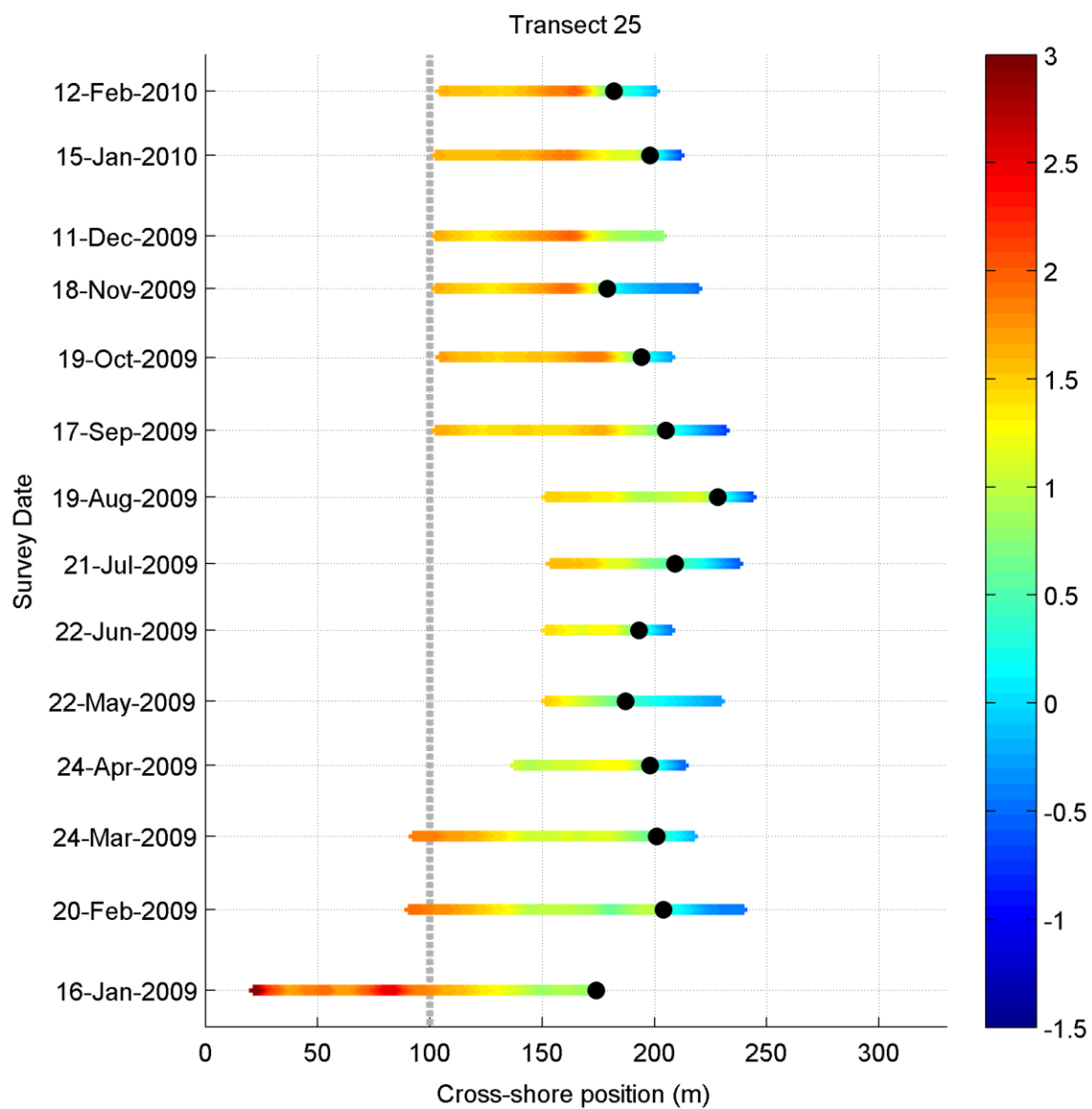


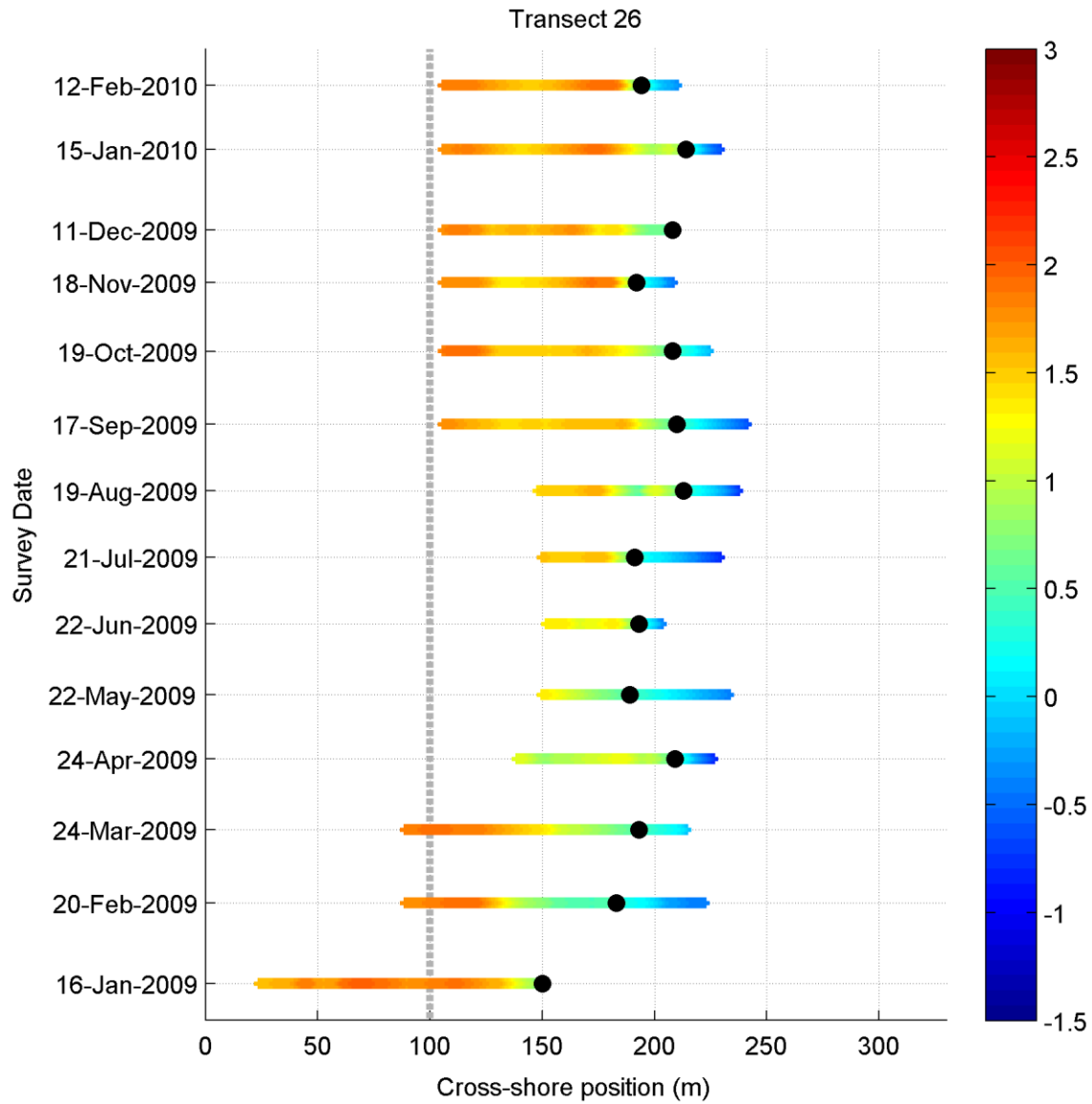


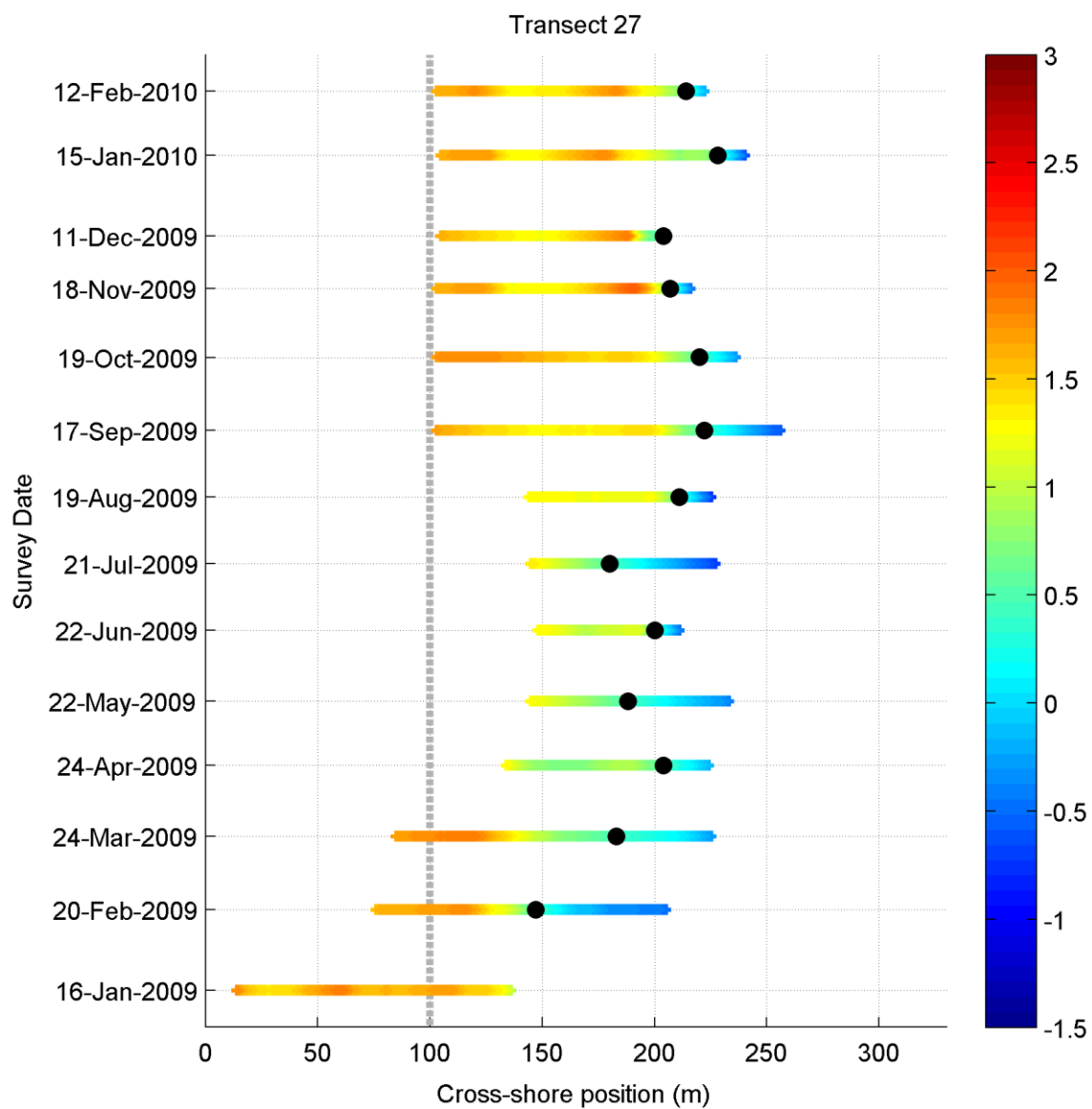


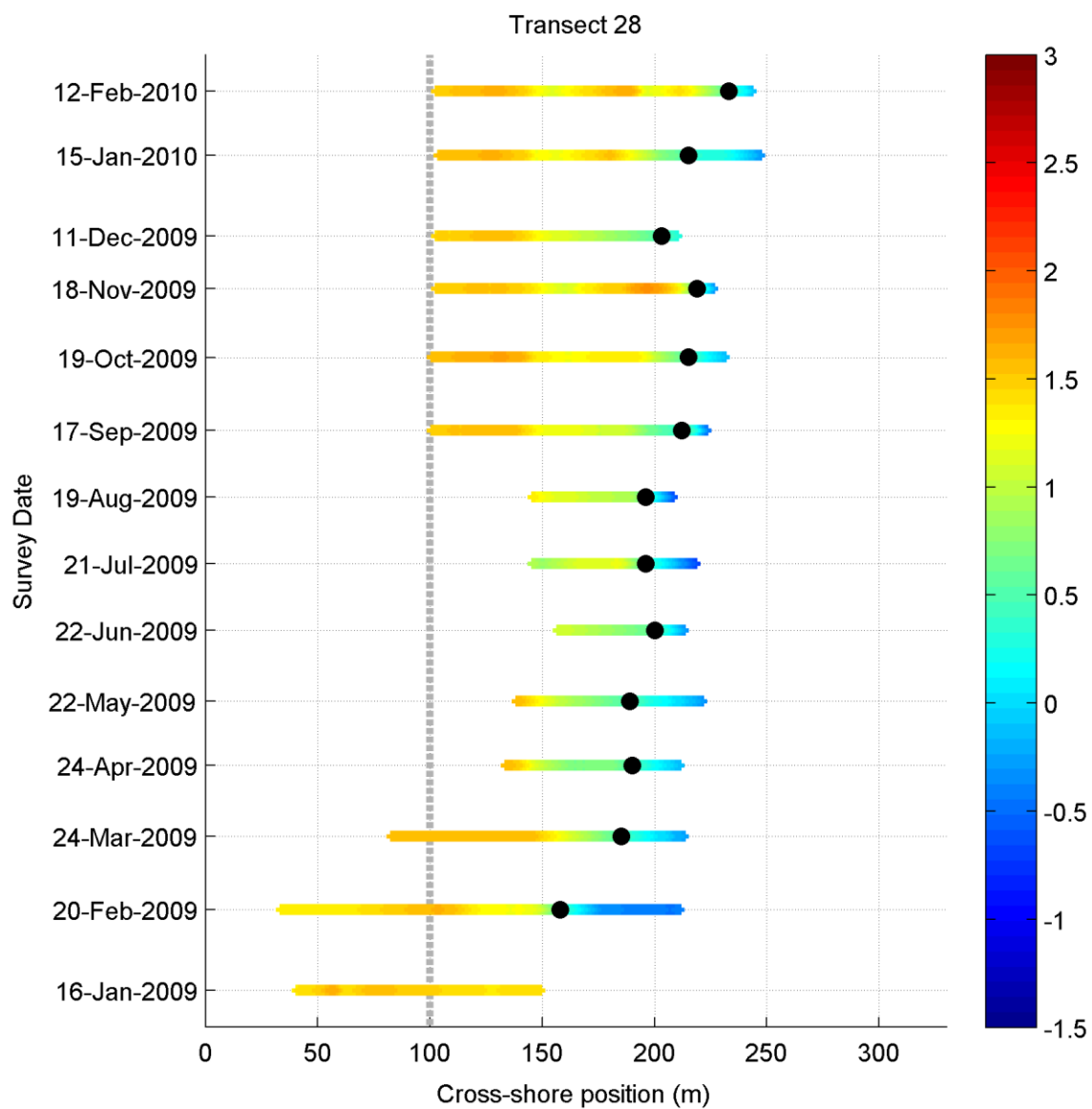


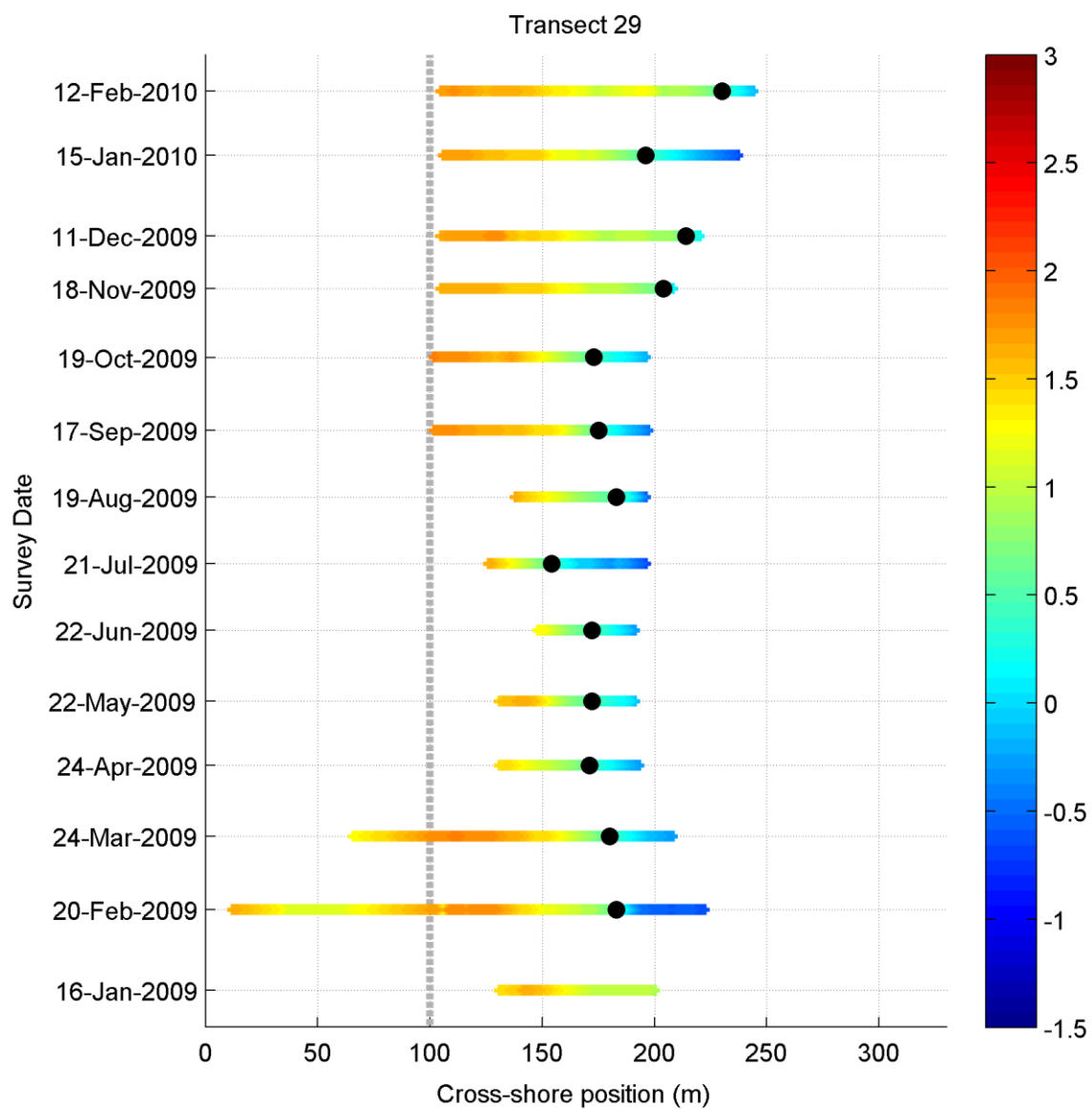


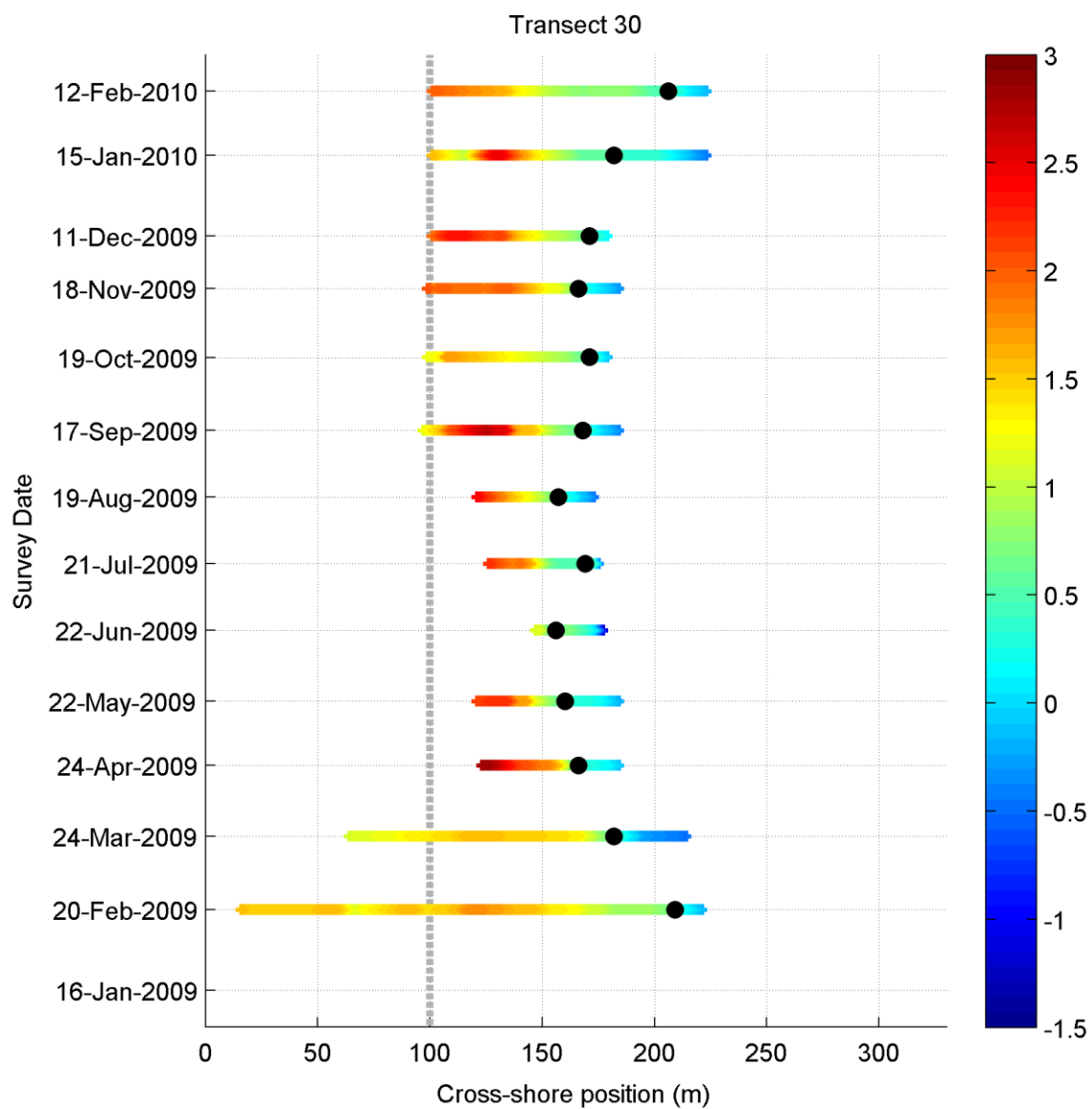




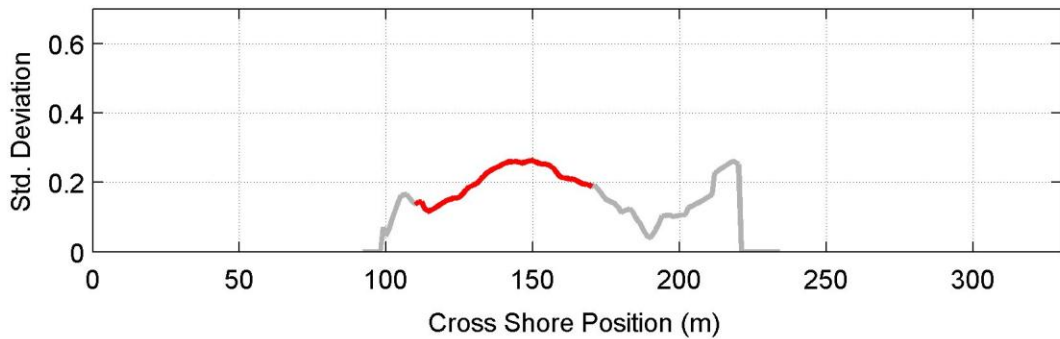
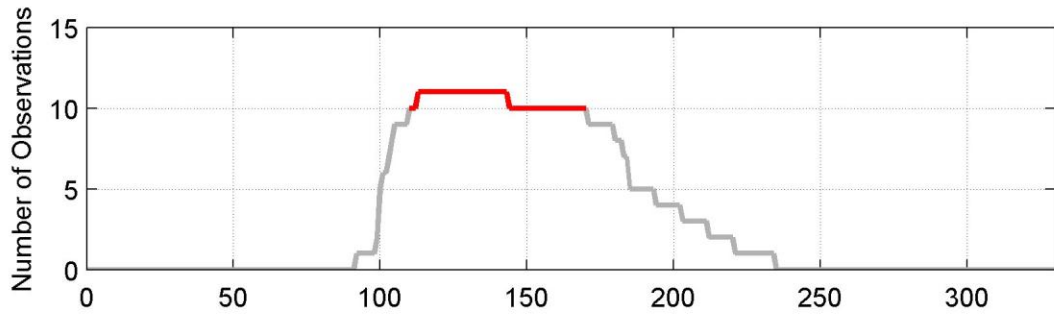
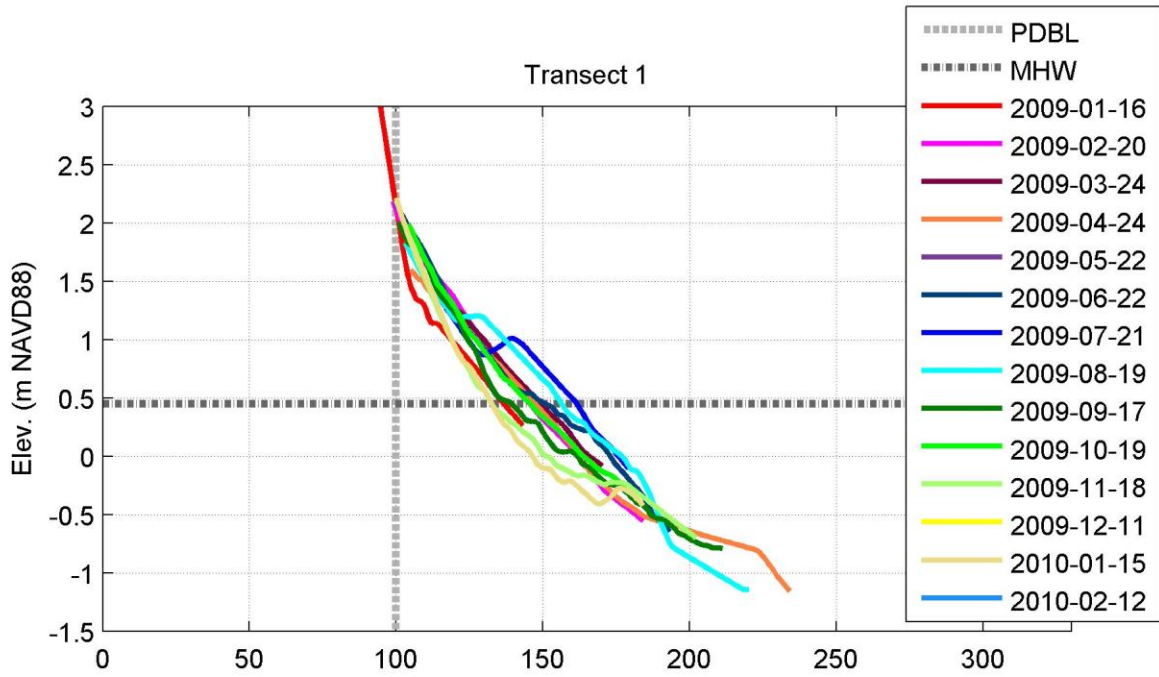


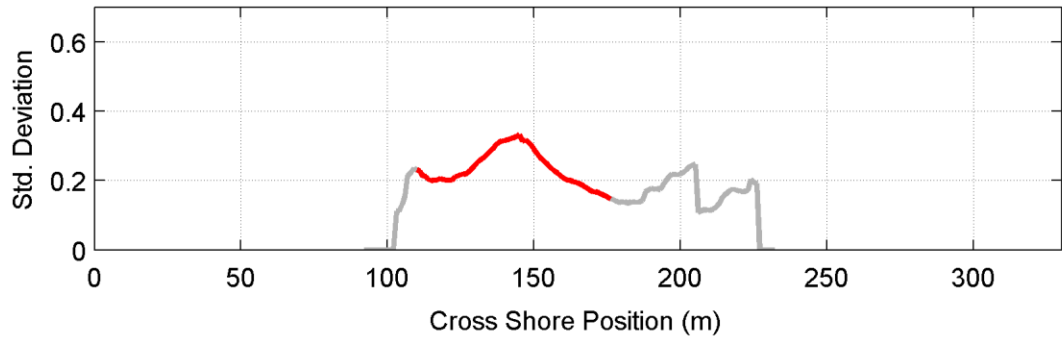
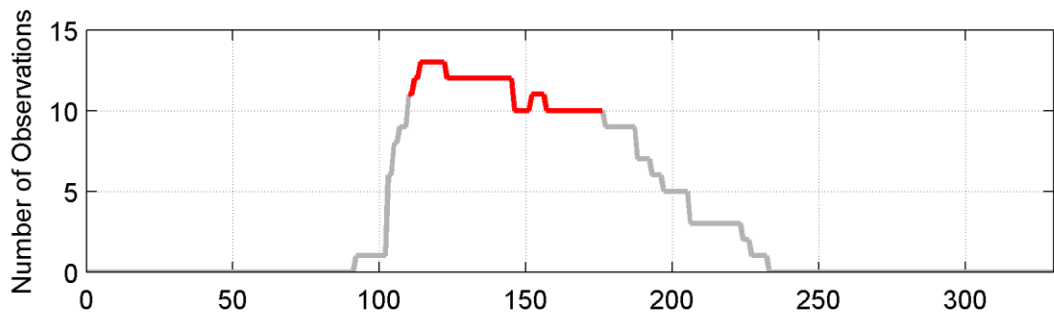
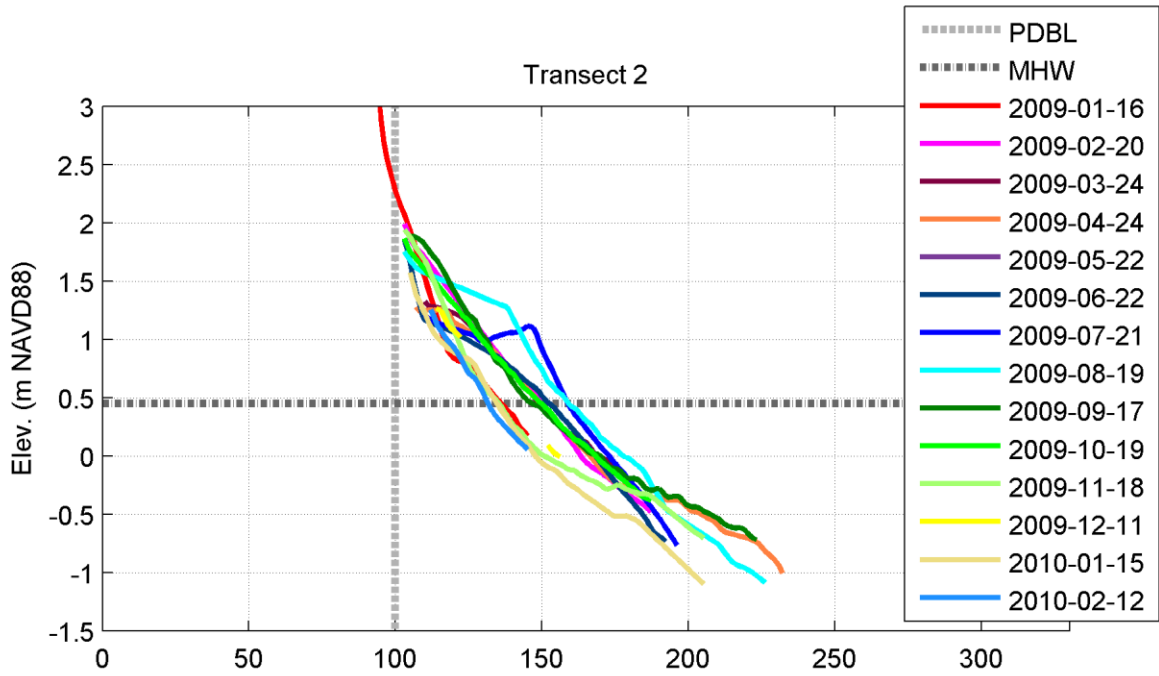


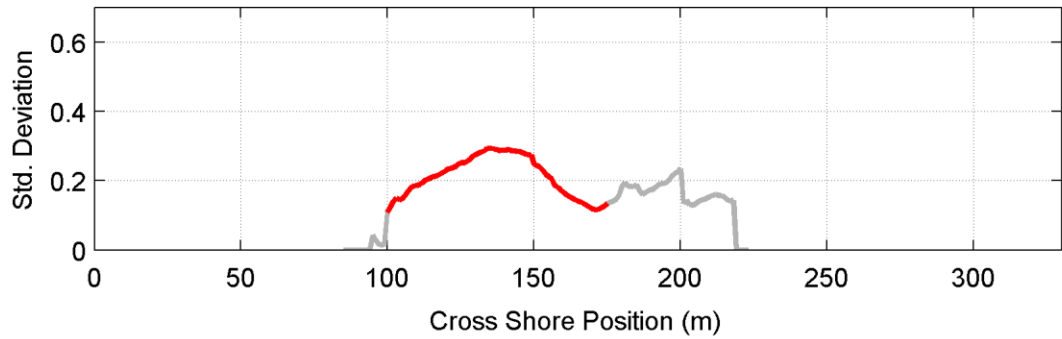
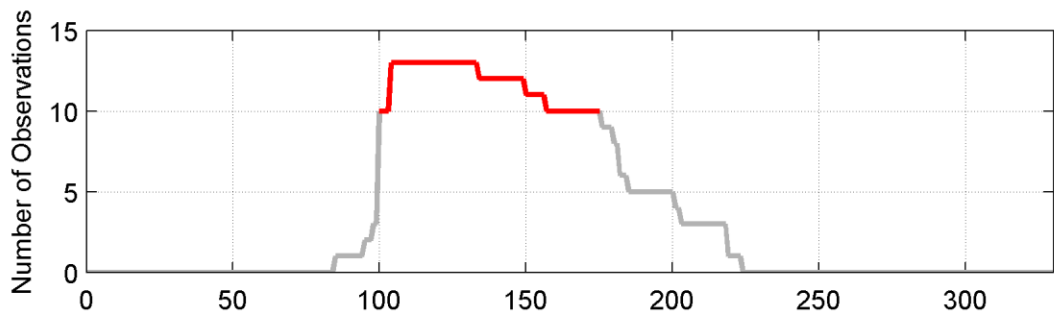
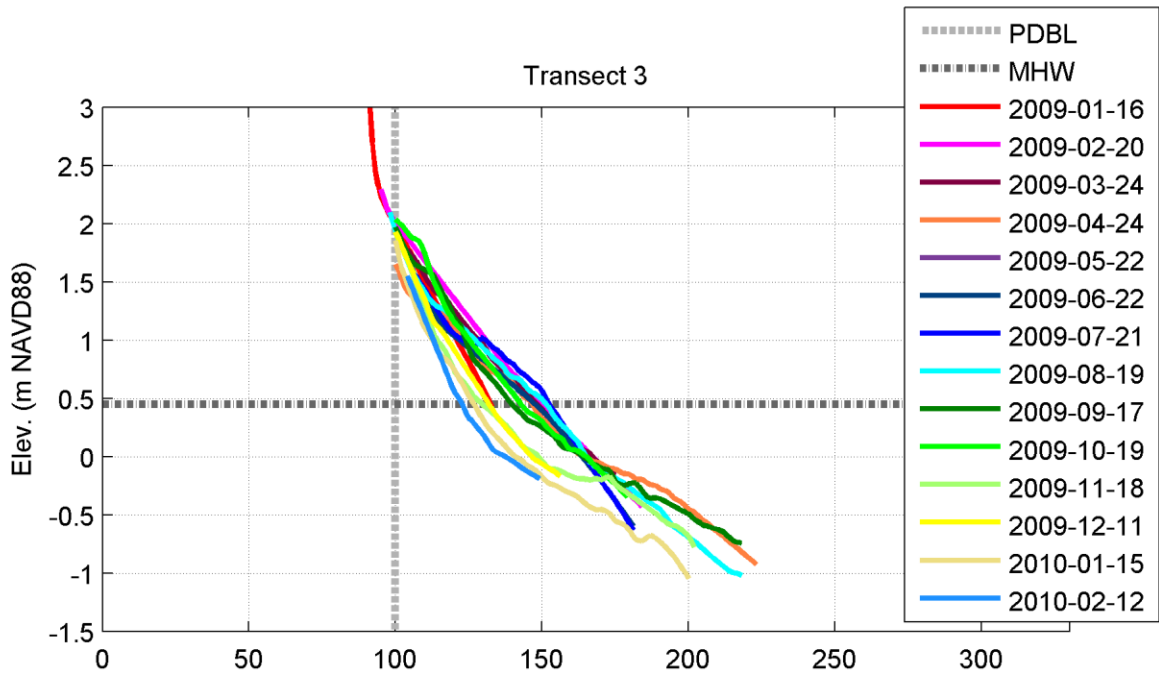


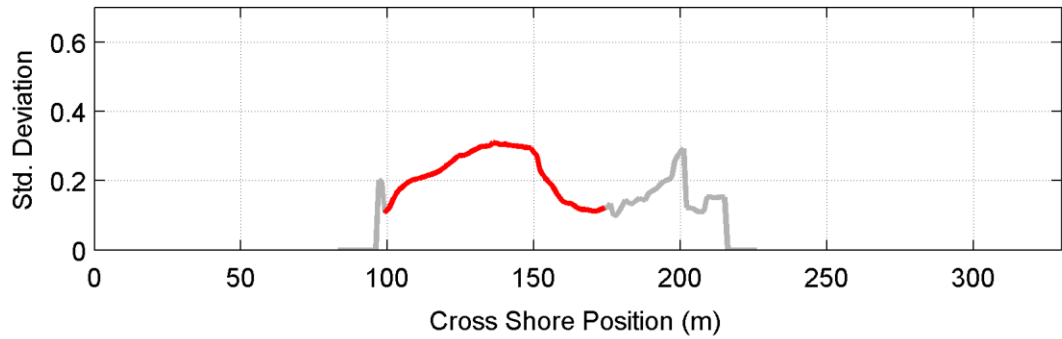
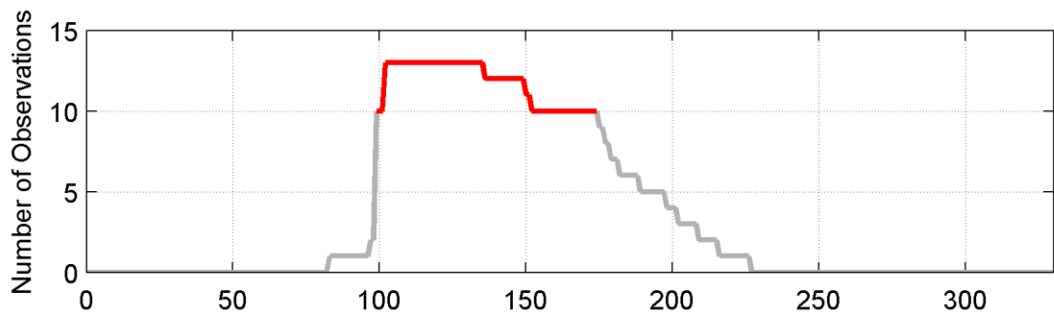
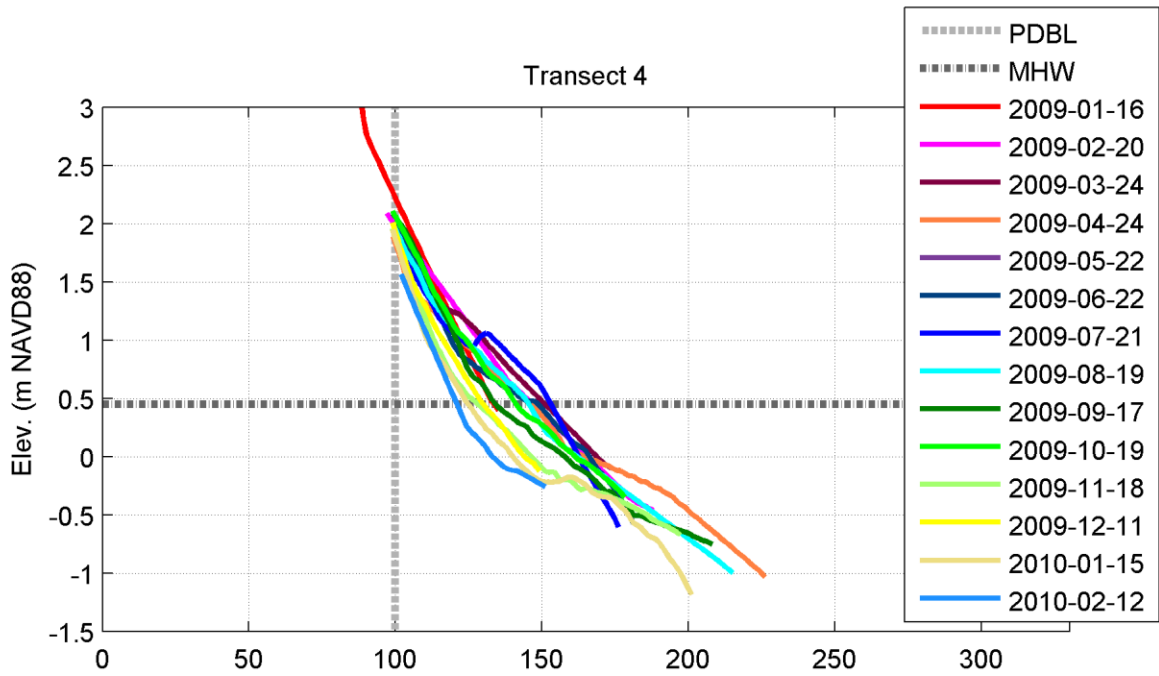


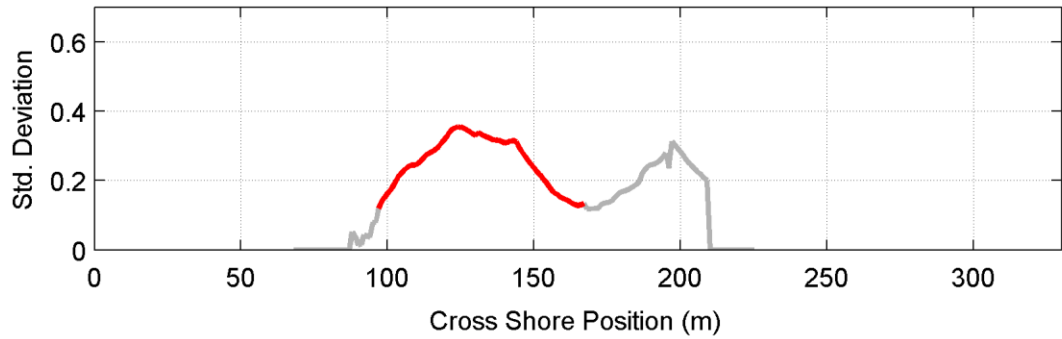
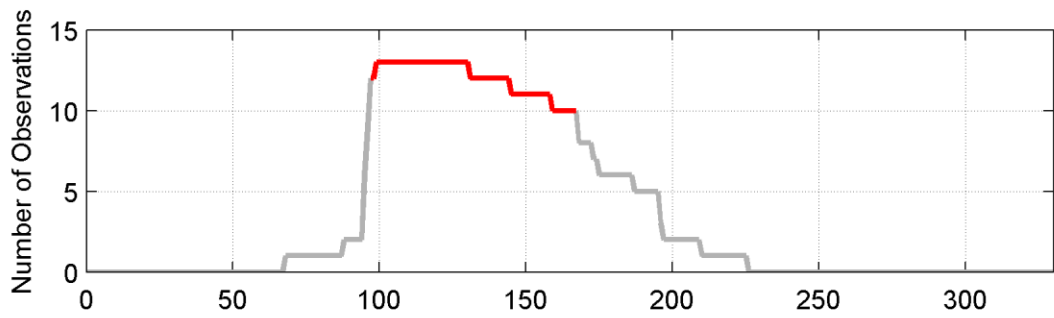
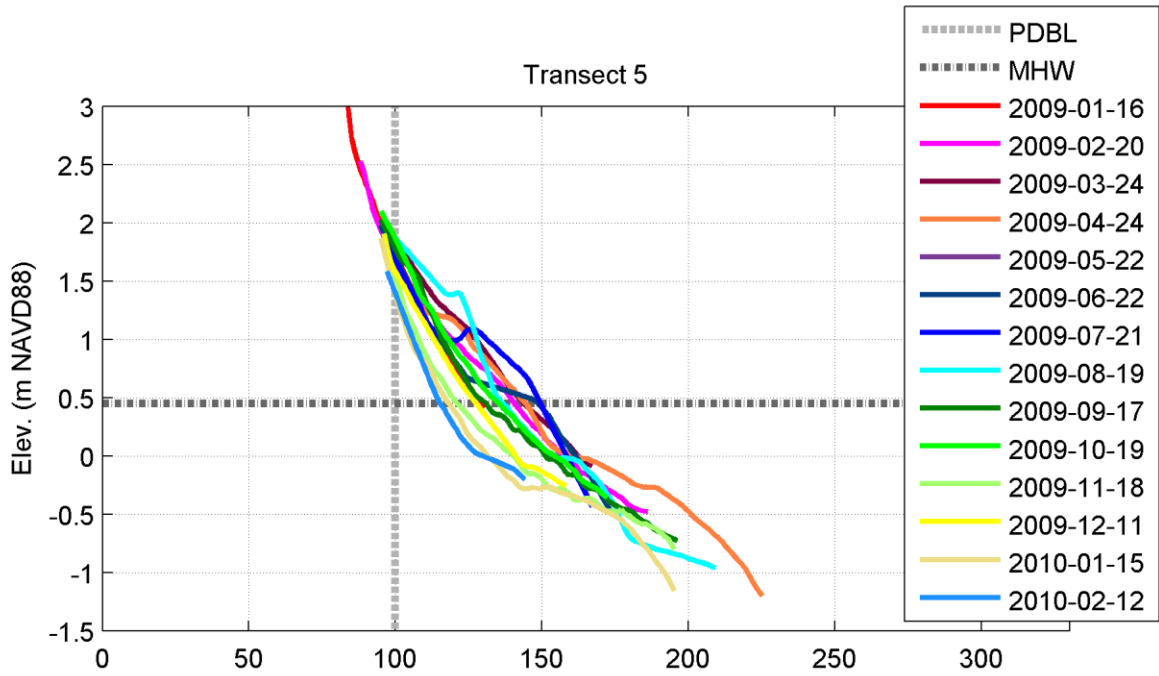
A-6

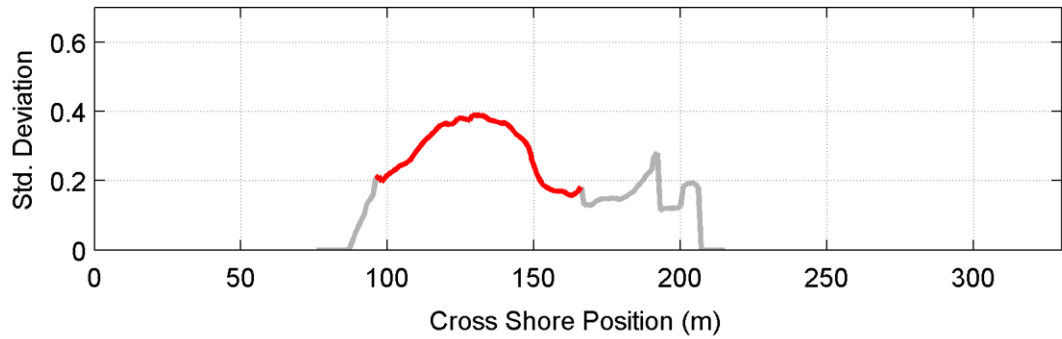
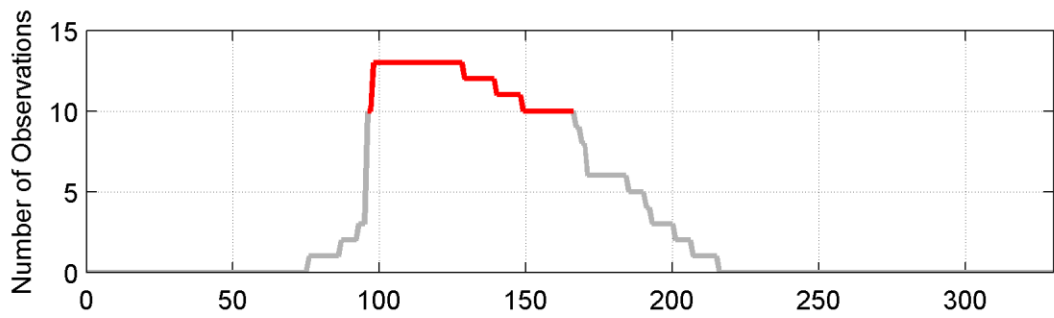
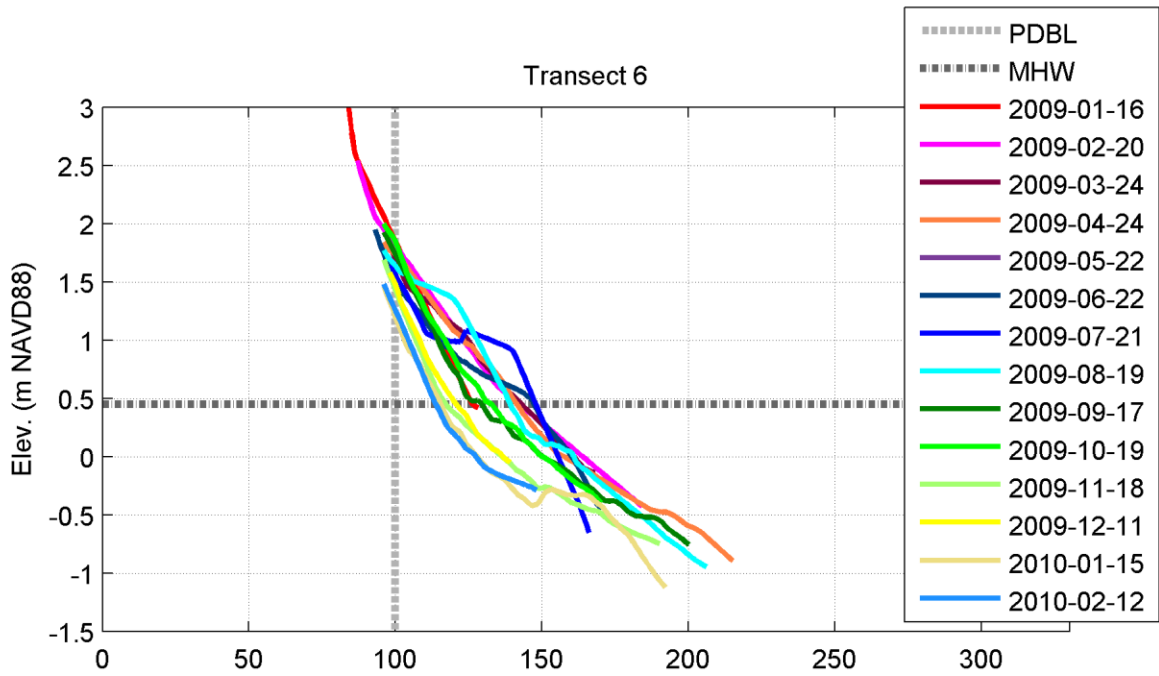


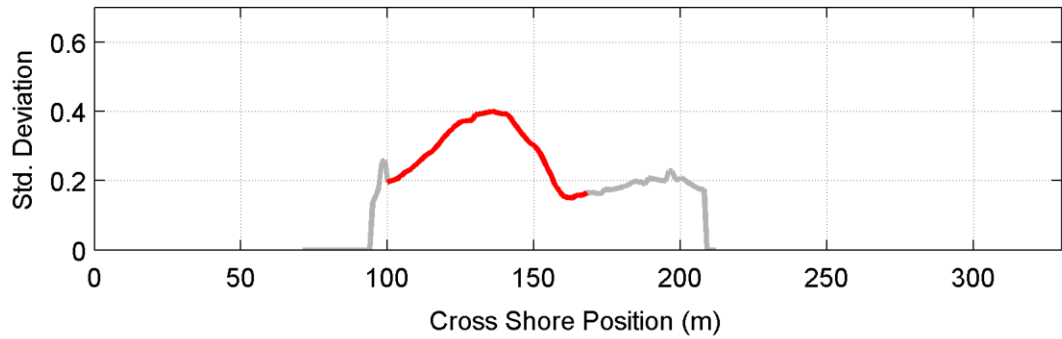
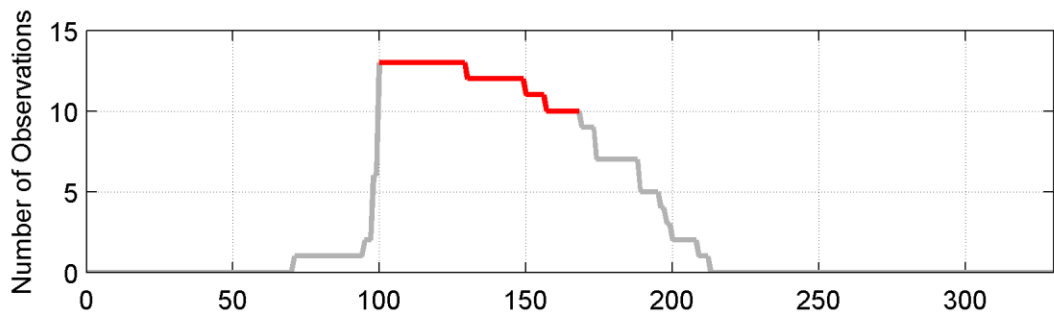
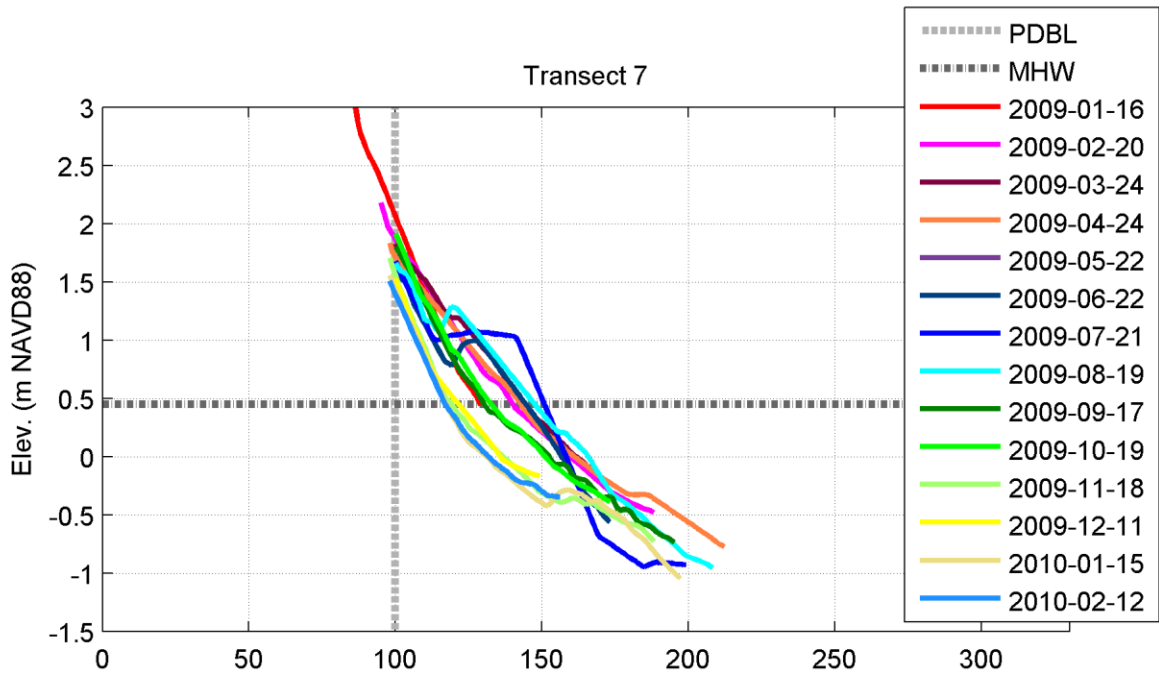


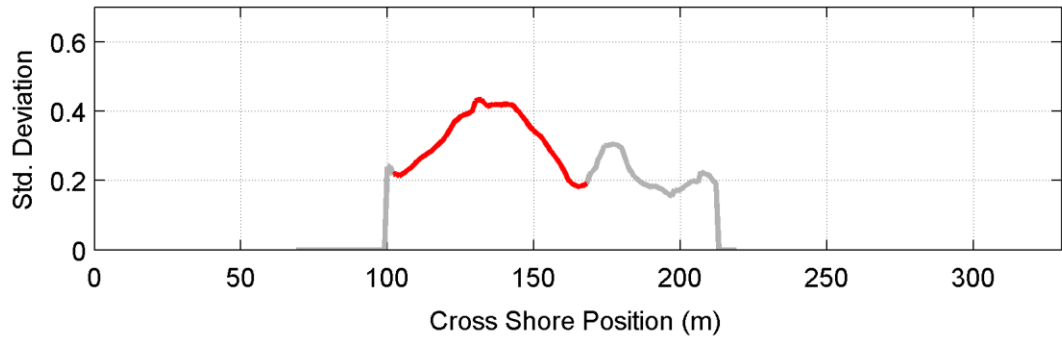
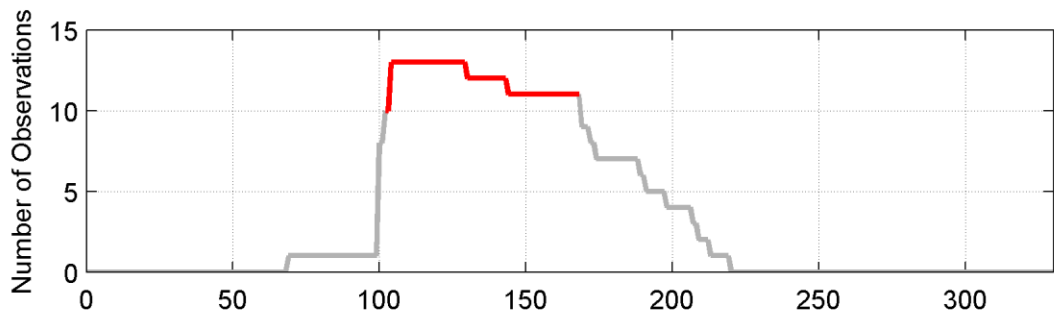
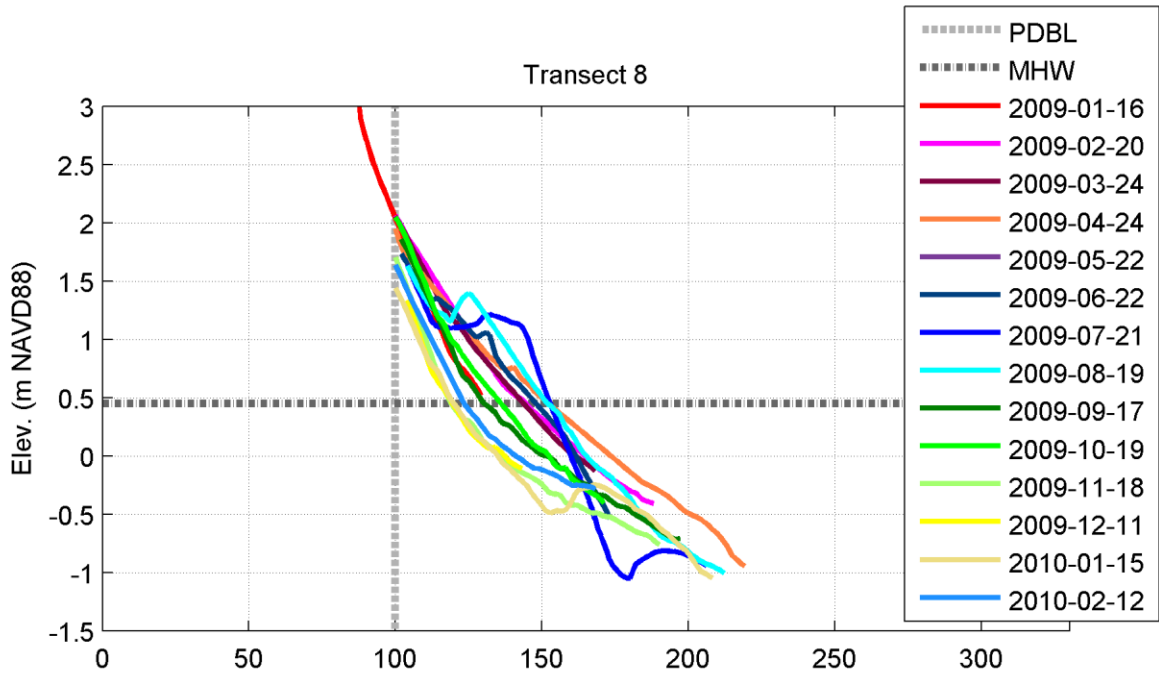


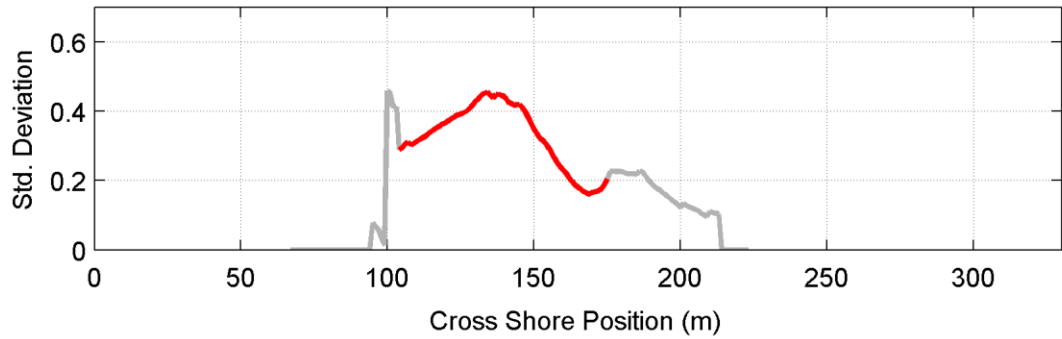
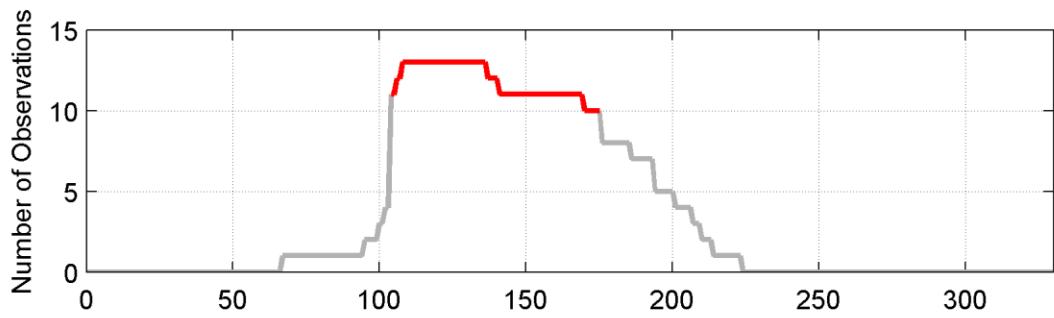
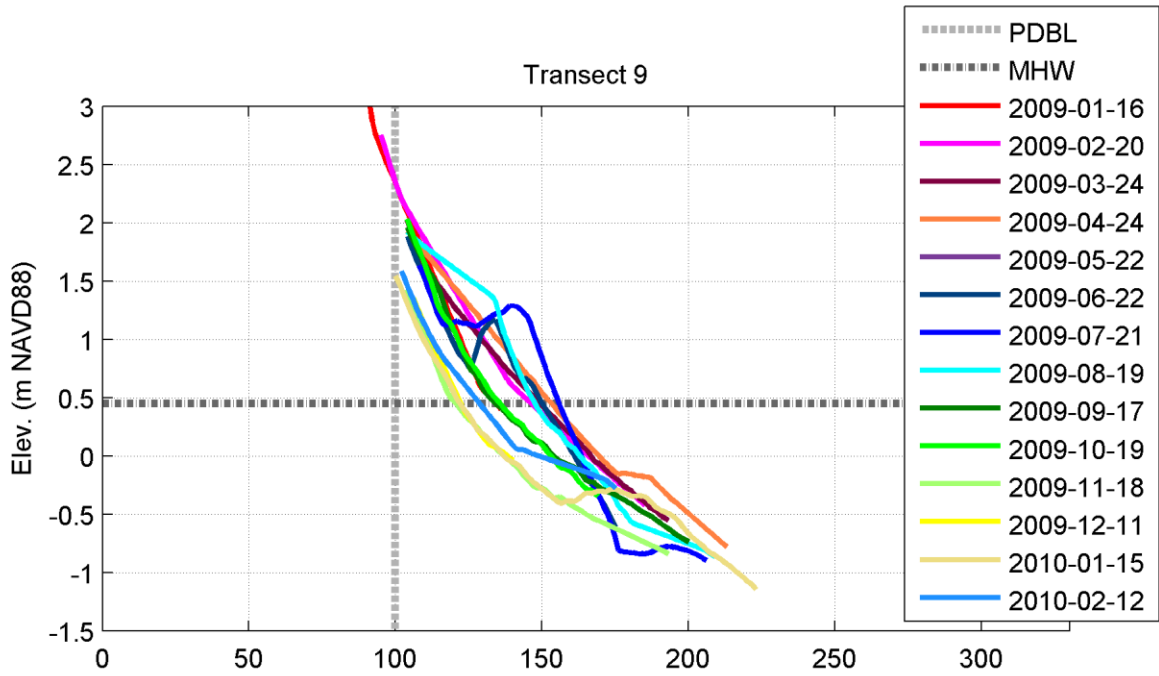


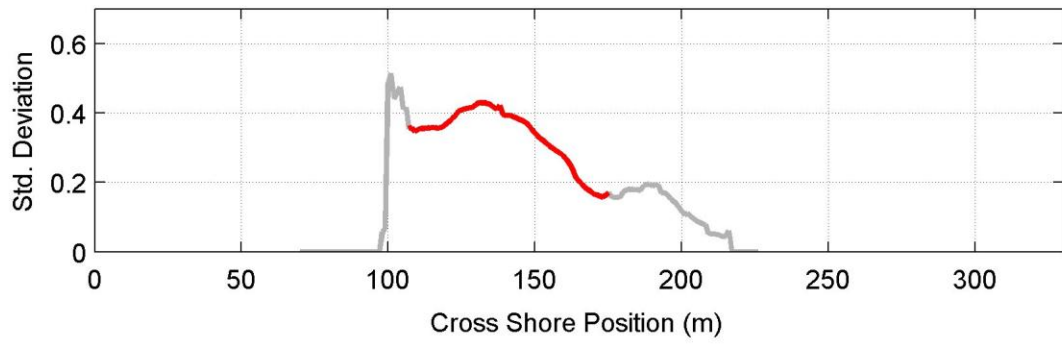
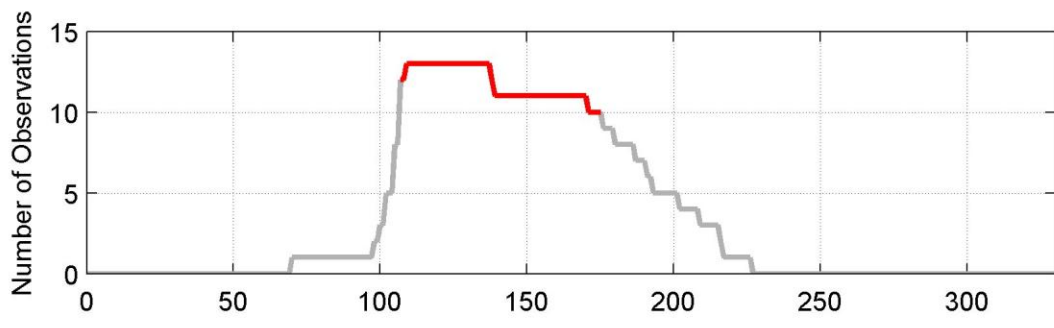
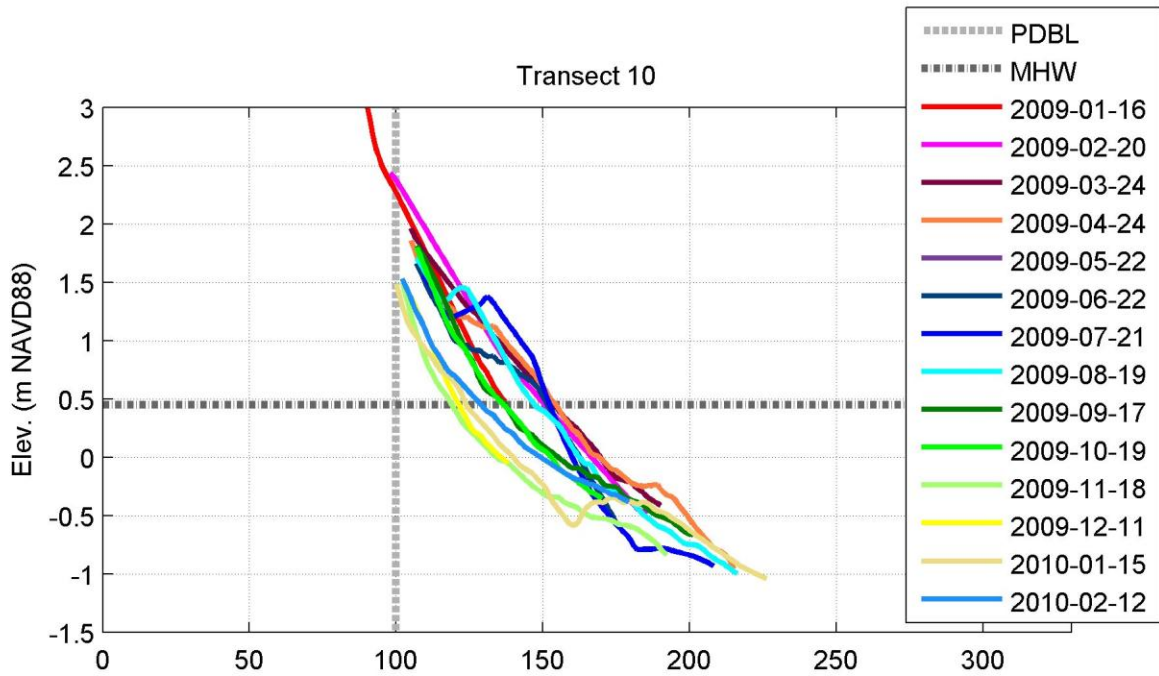


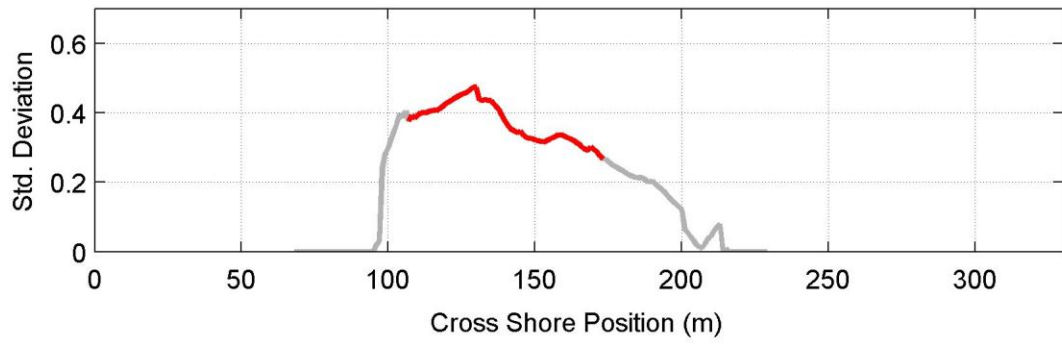
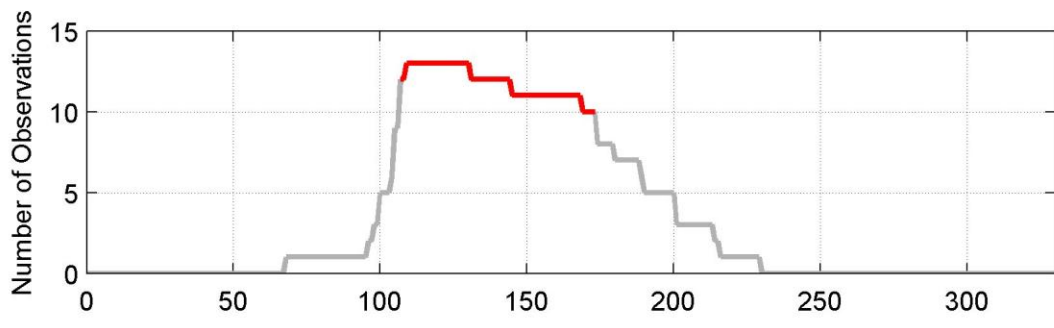
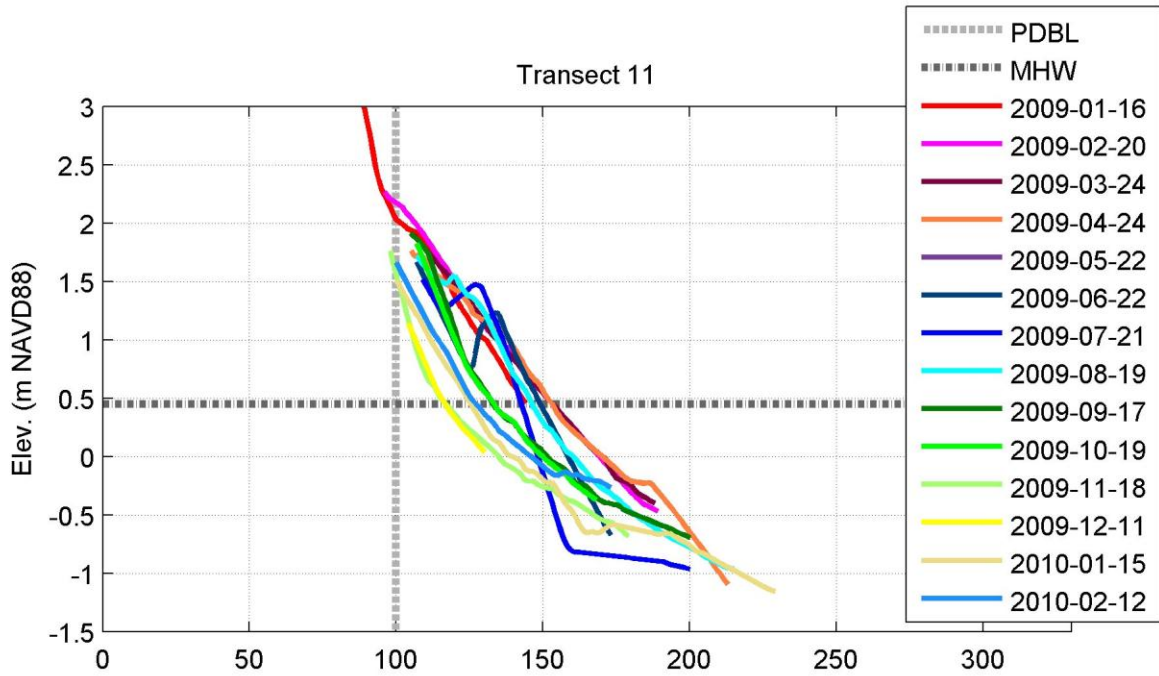


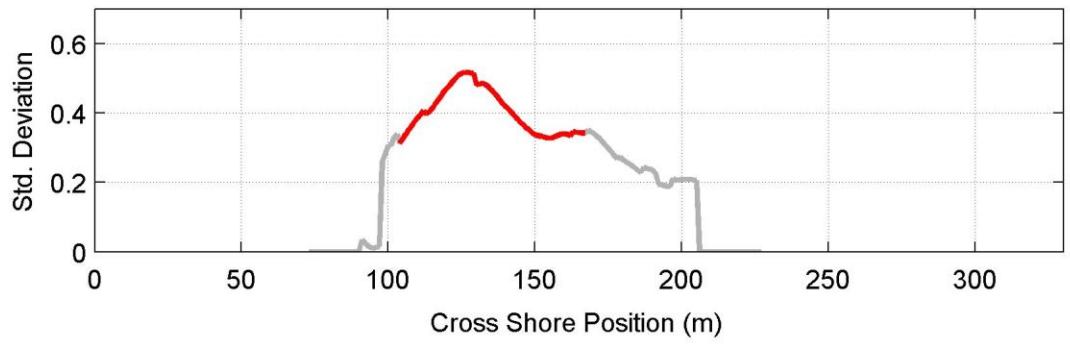
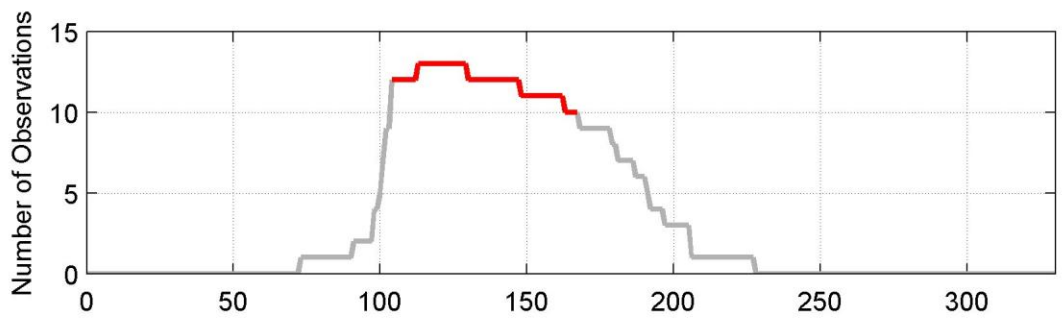
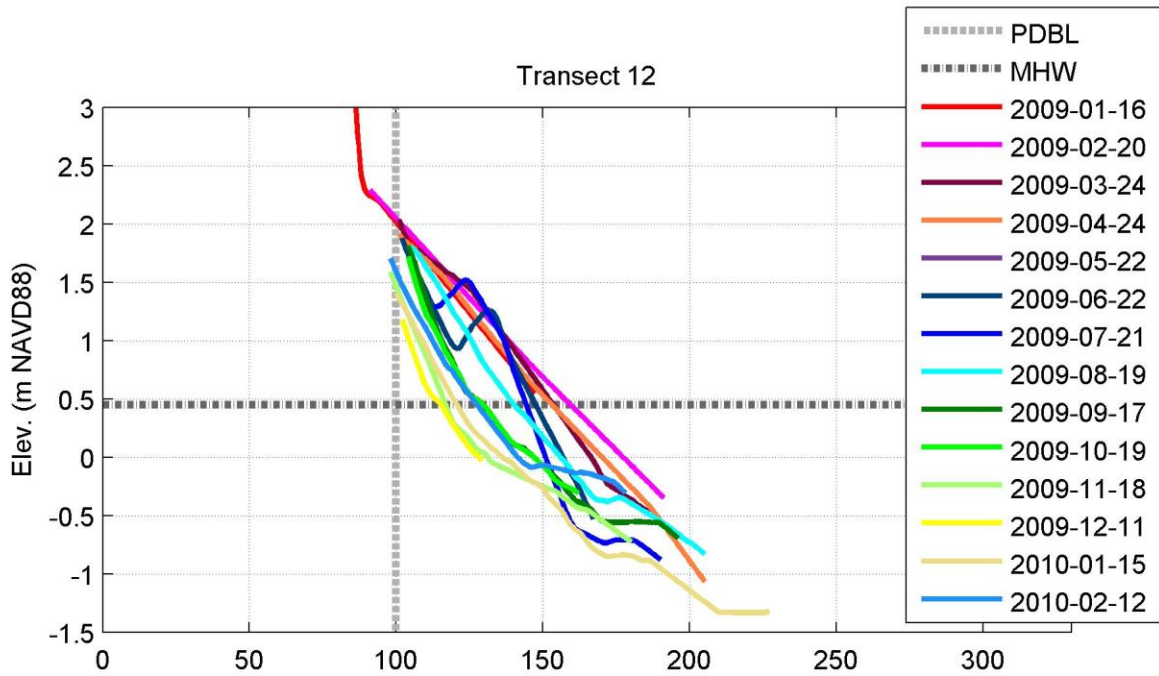


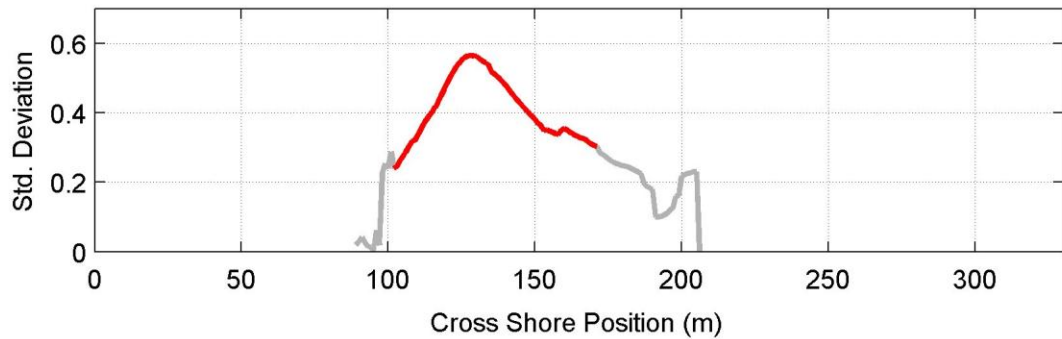
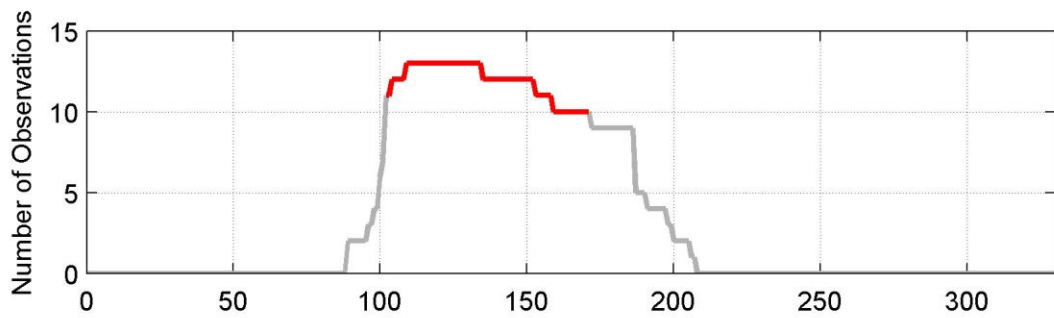
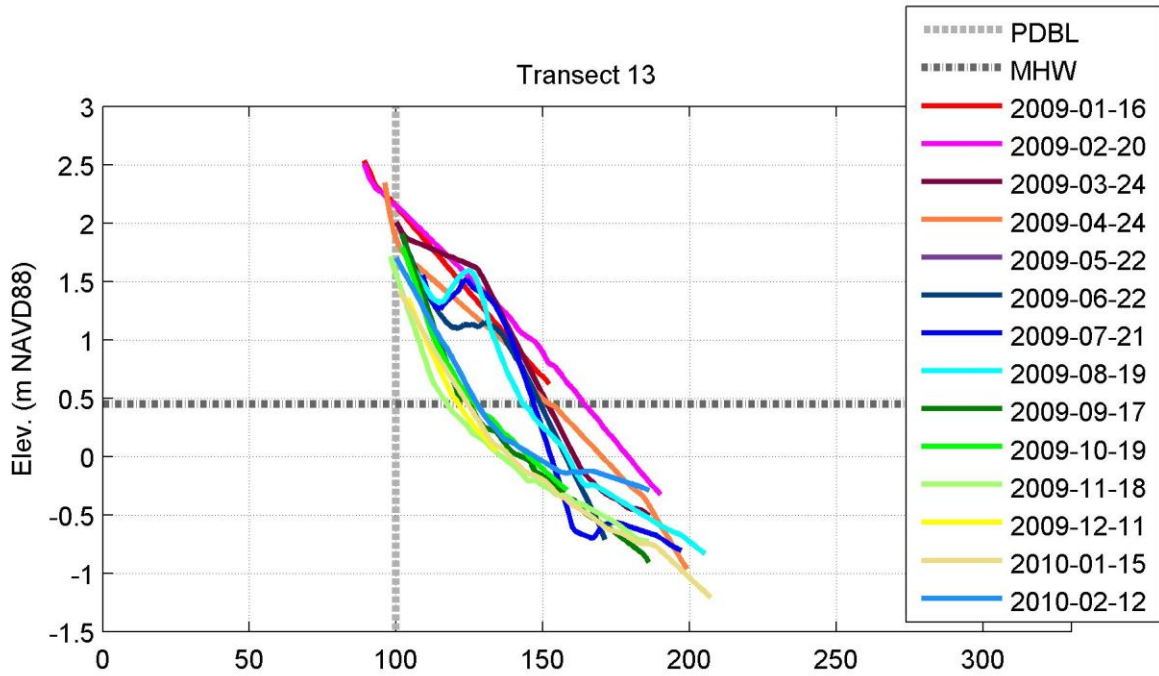


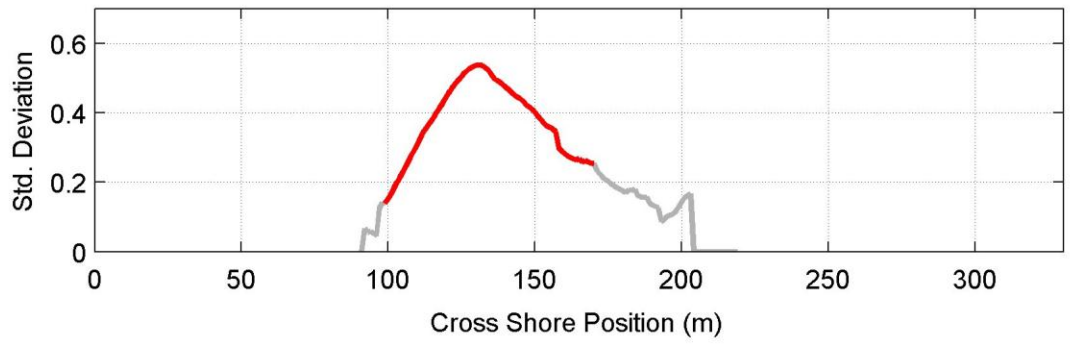
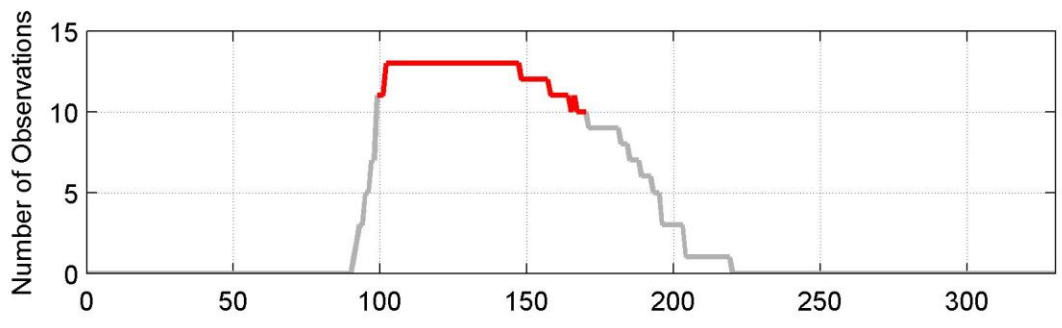
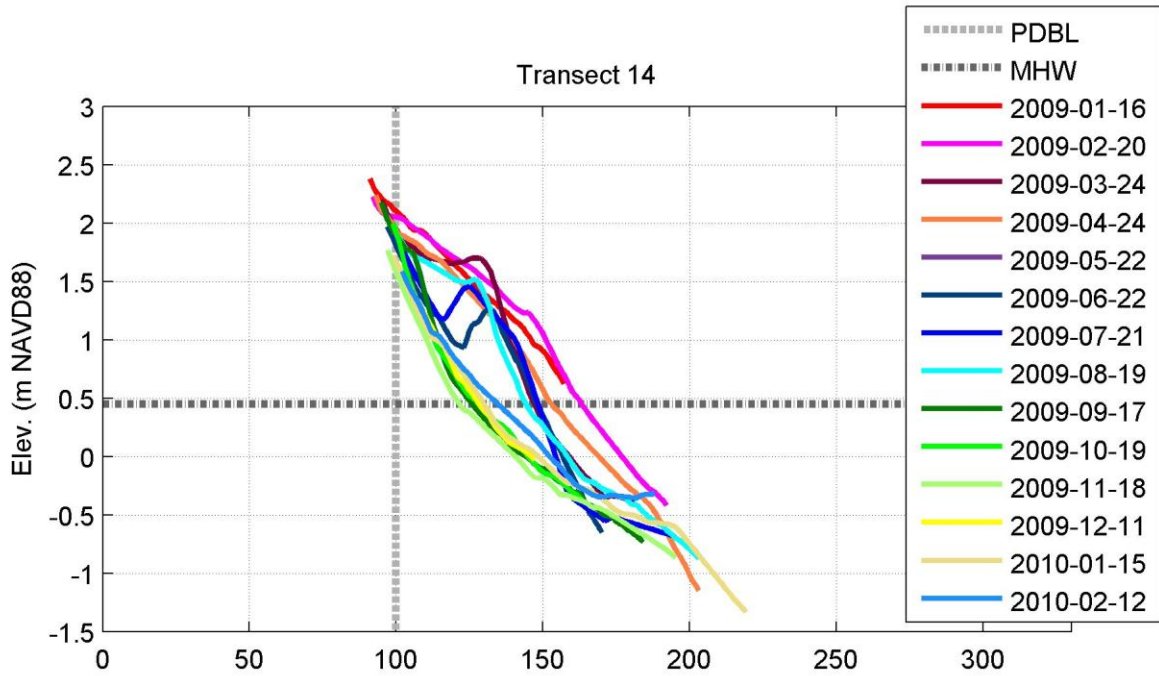


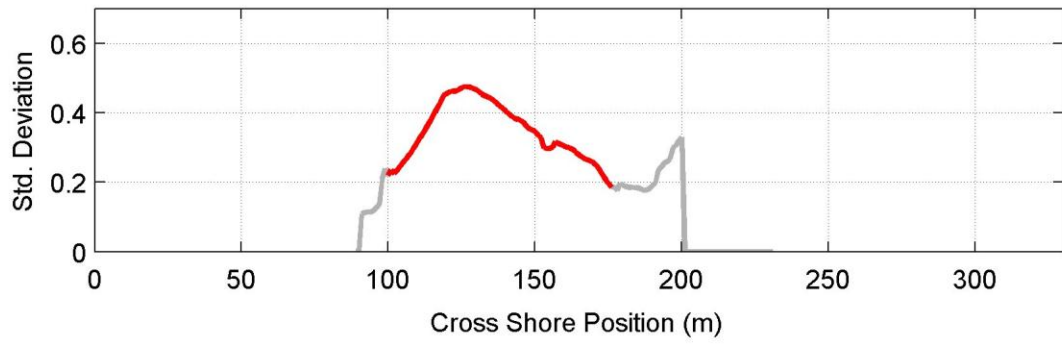
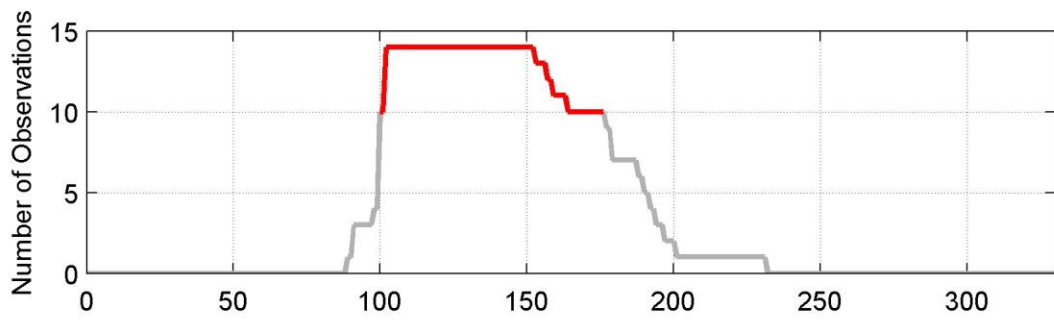
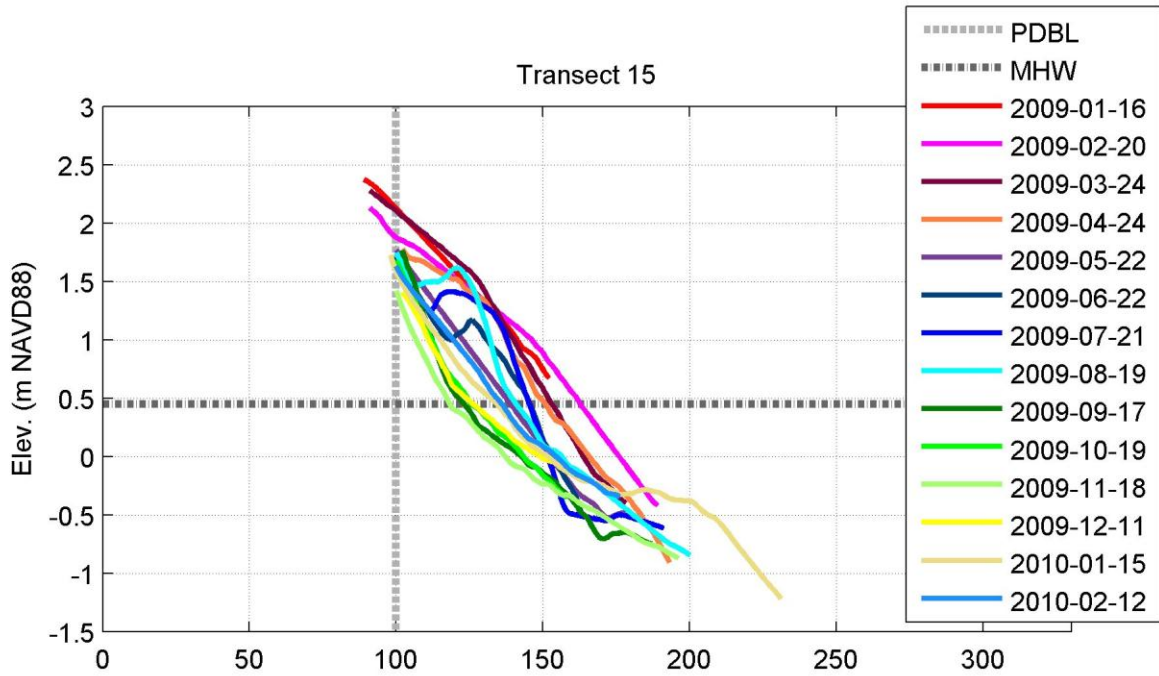


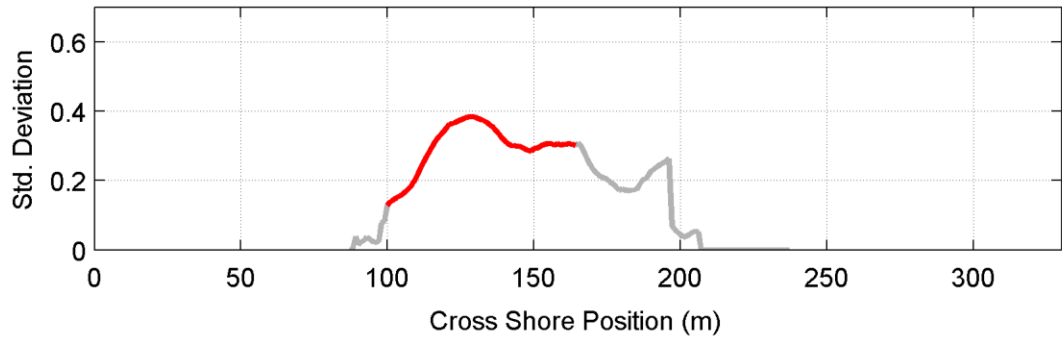
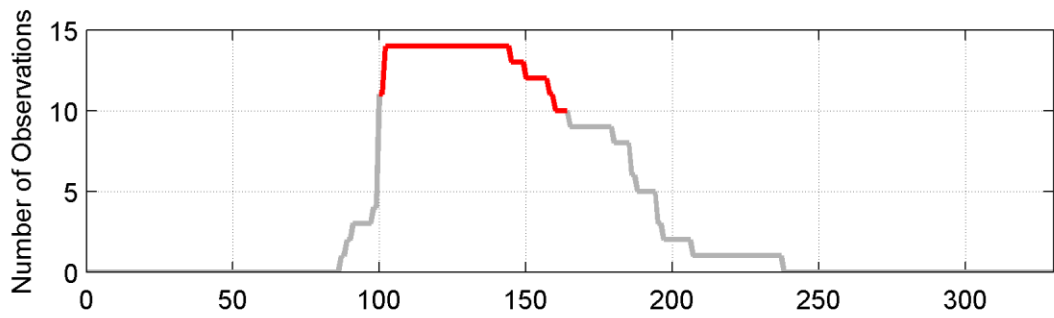
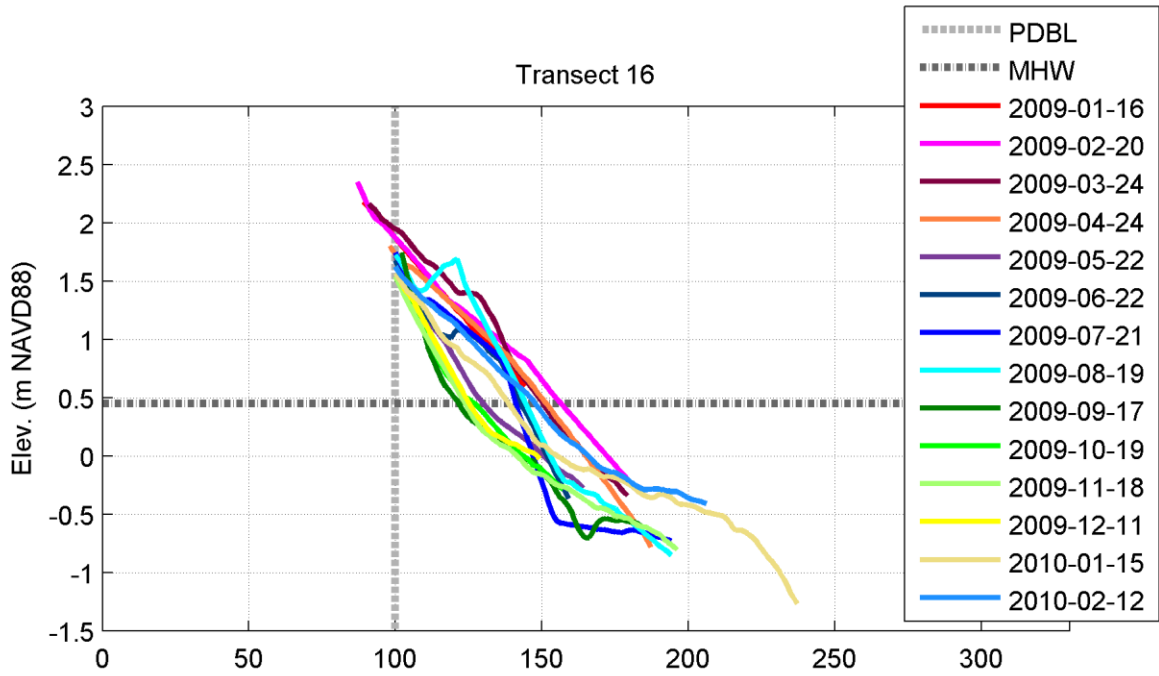


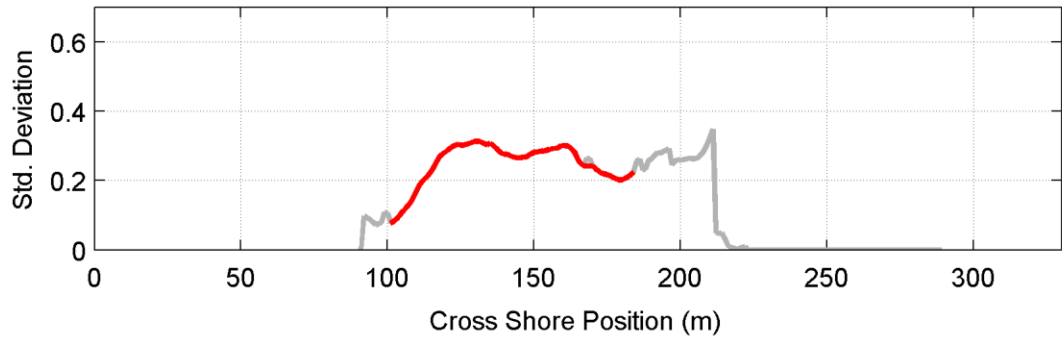
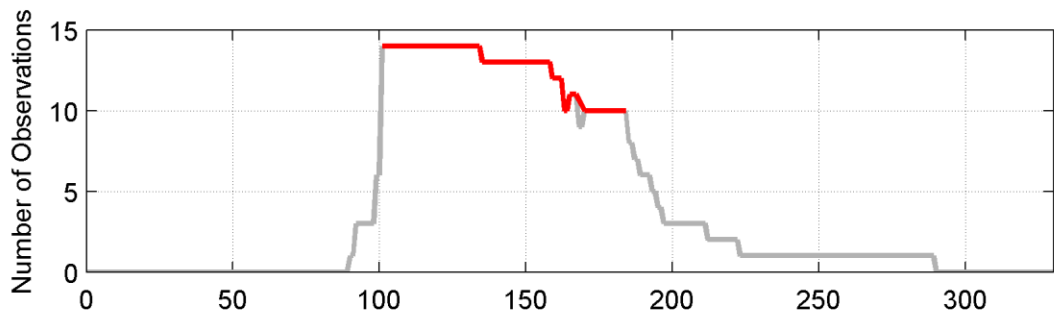
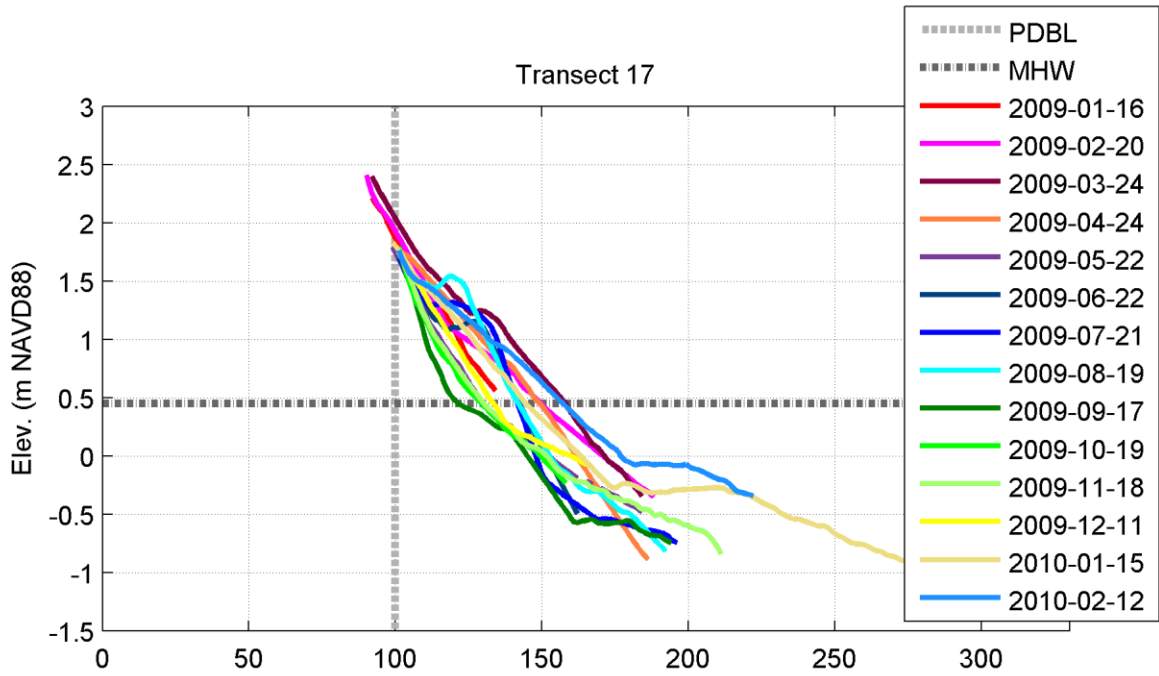


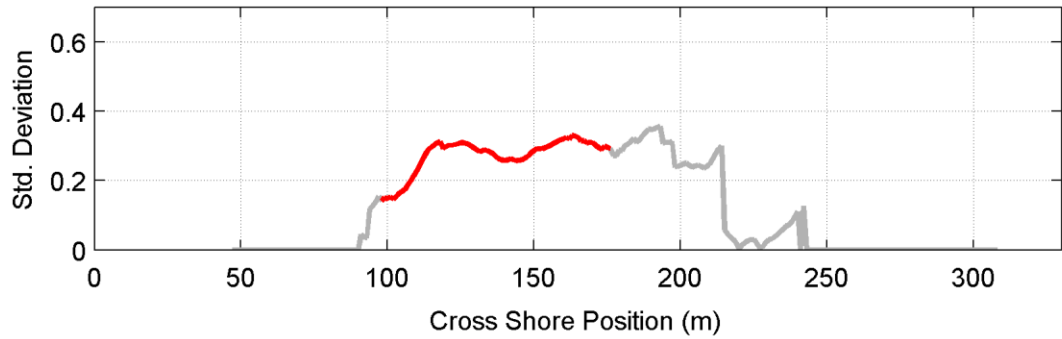
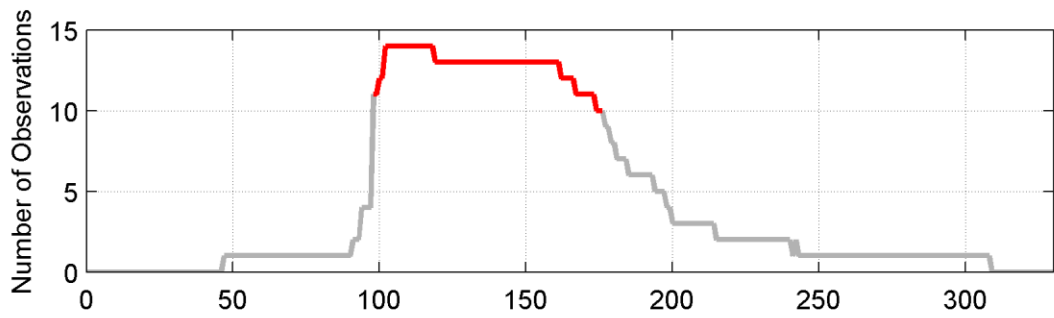
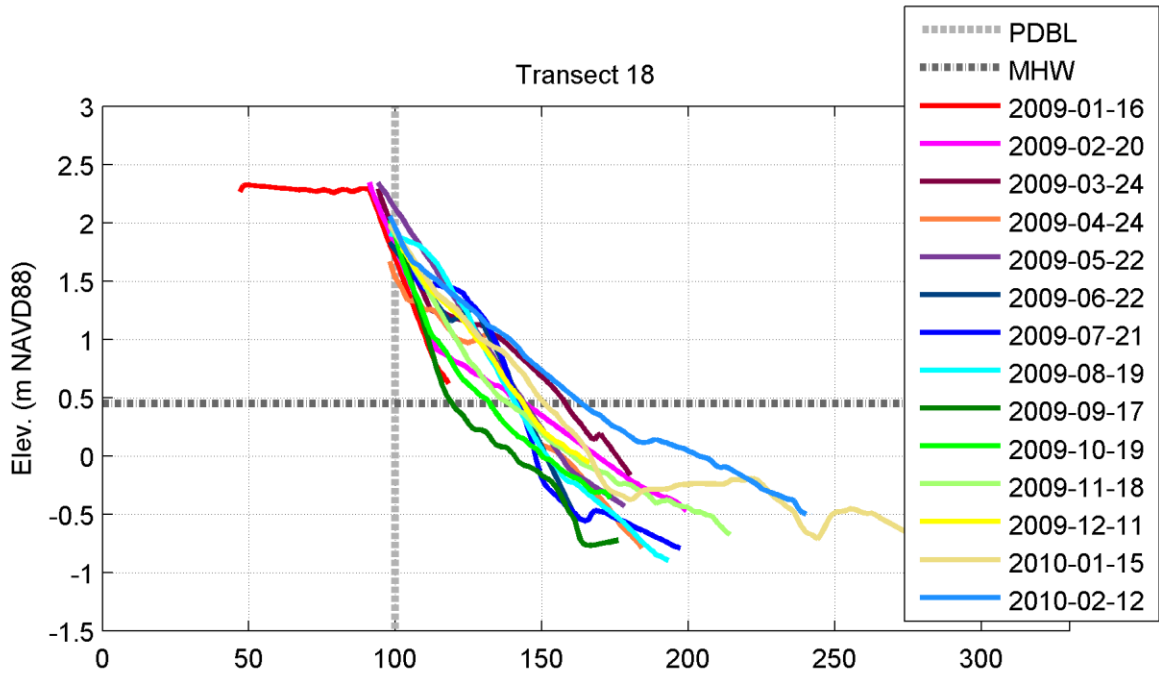


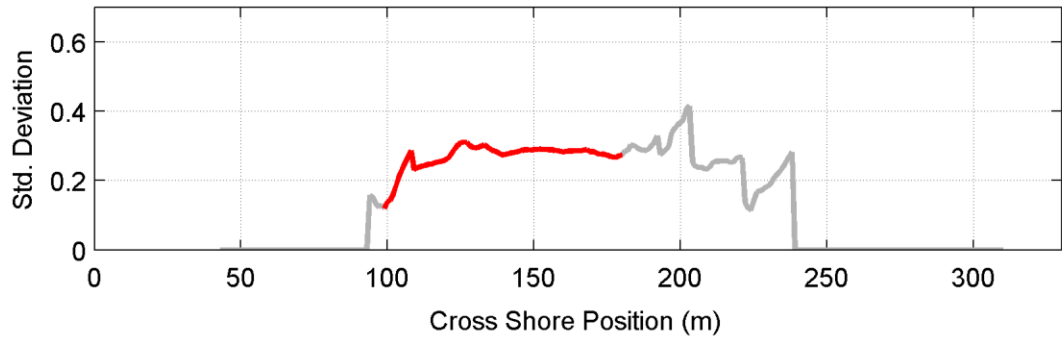
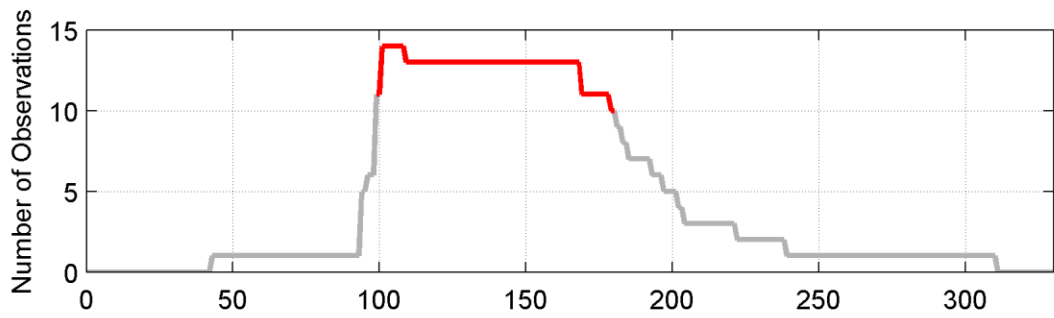
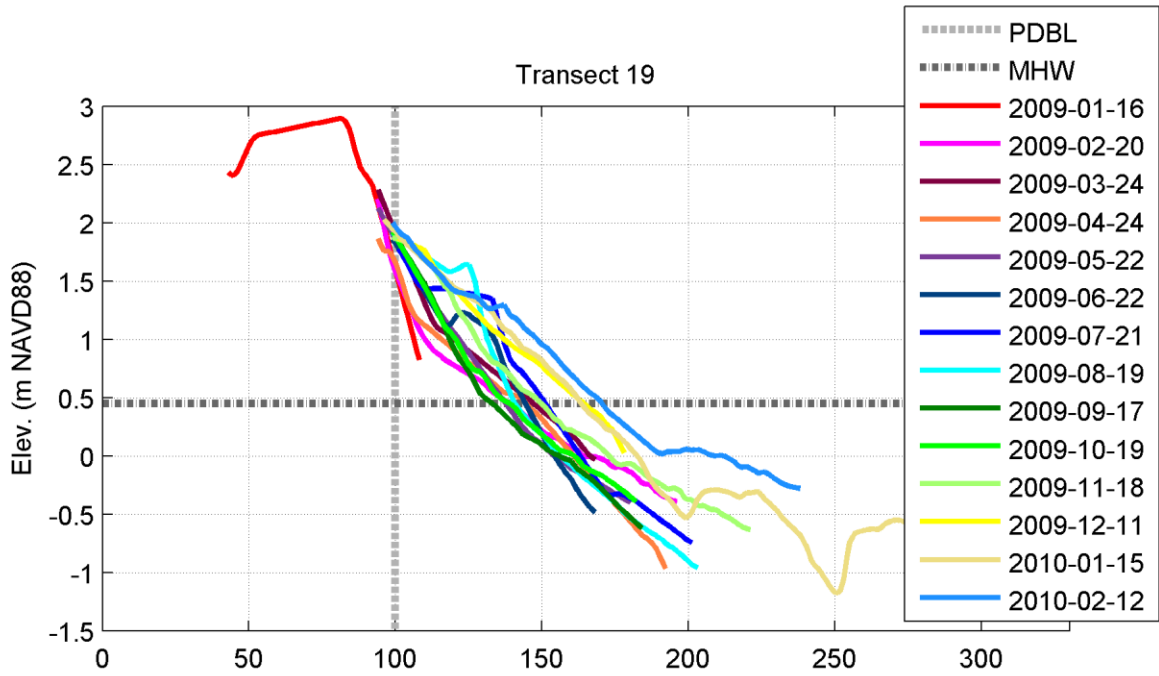


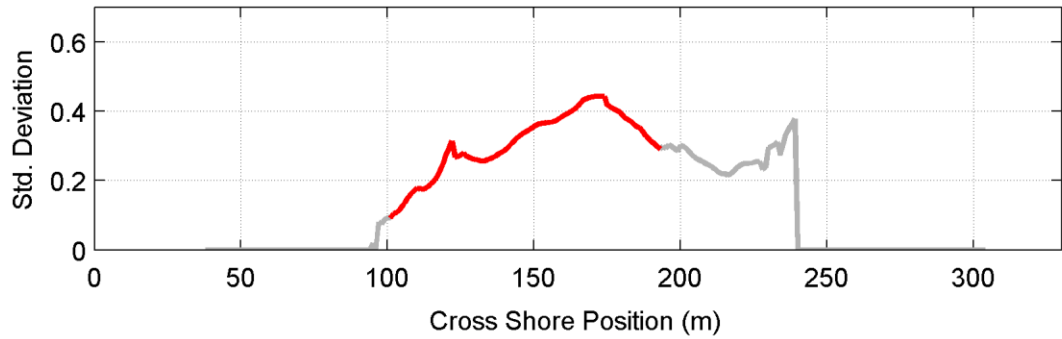
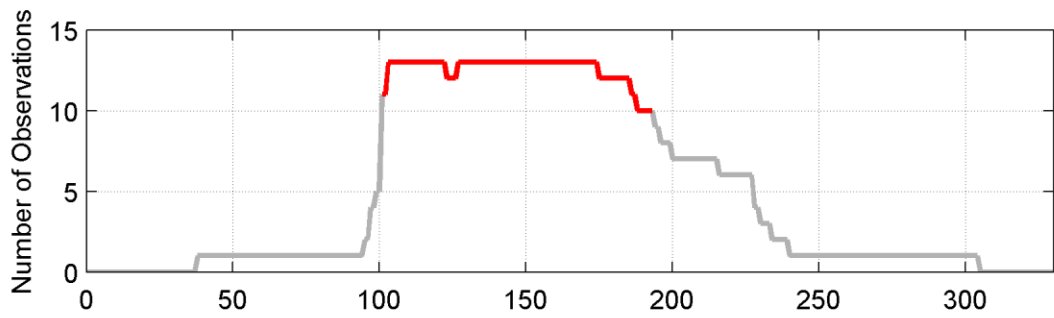
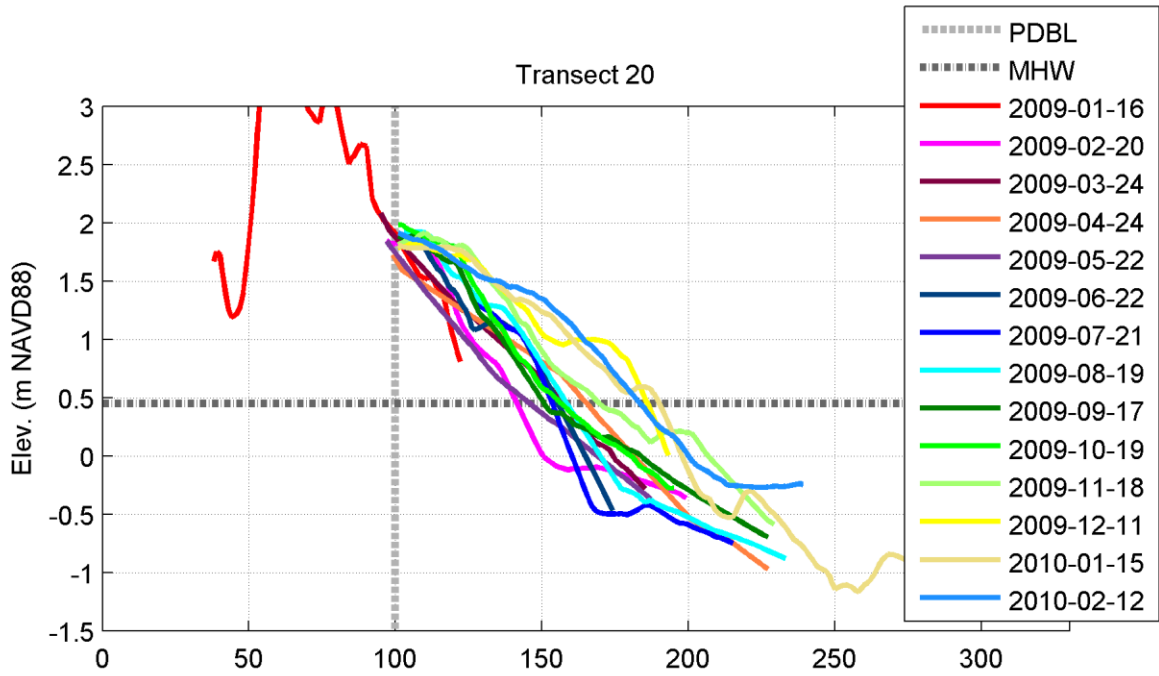


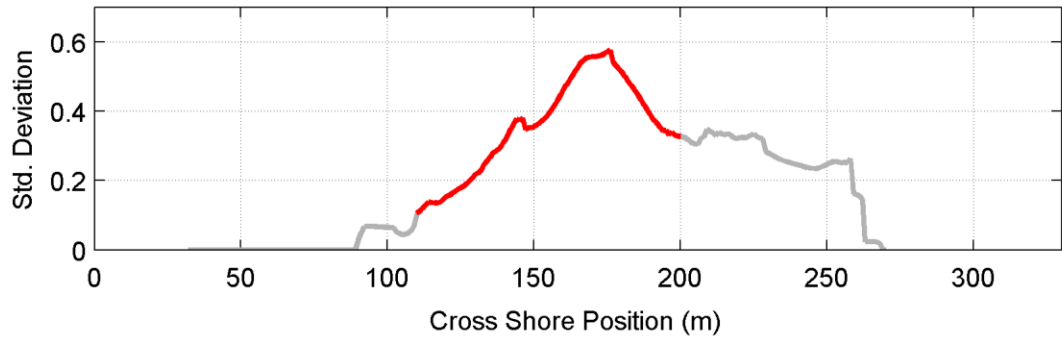
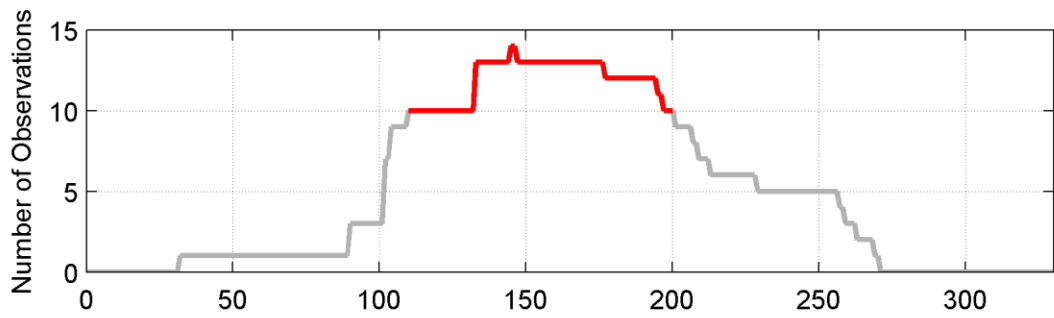
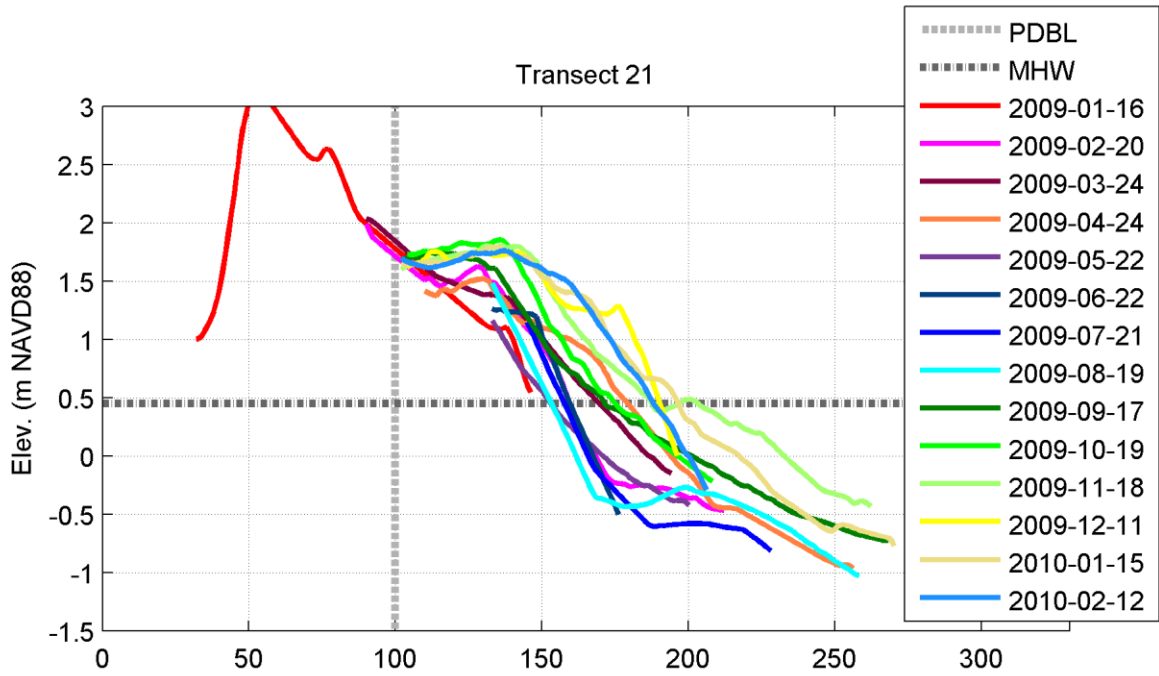


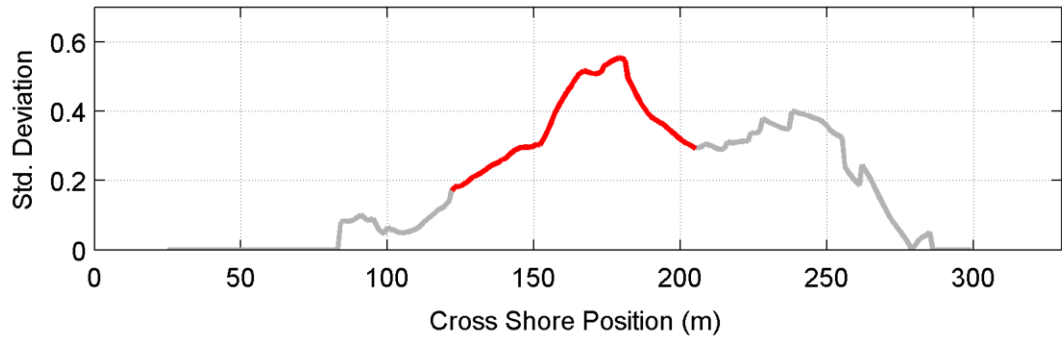
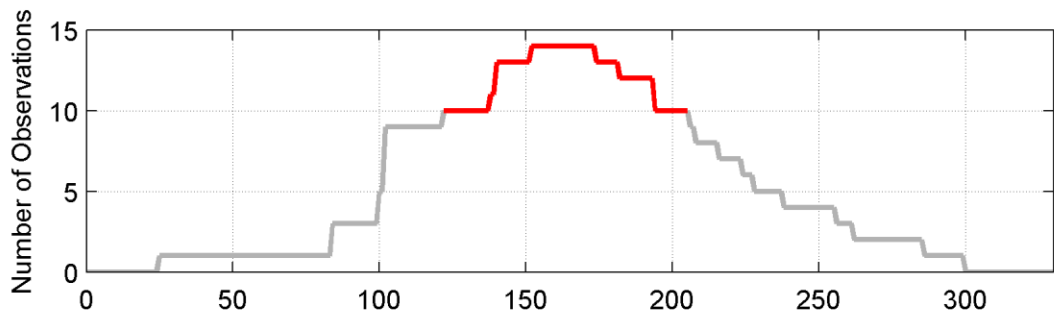
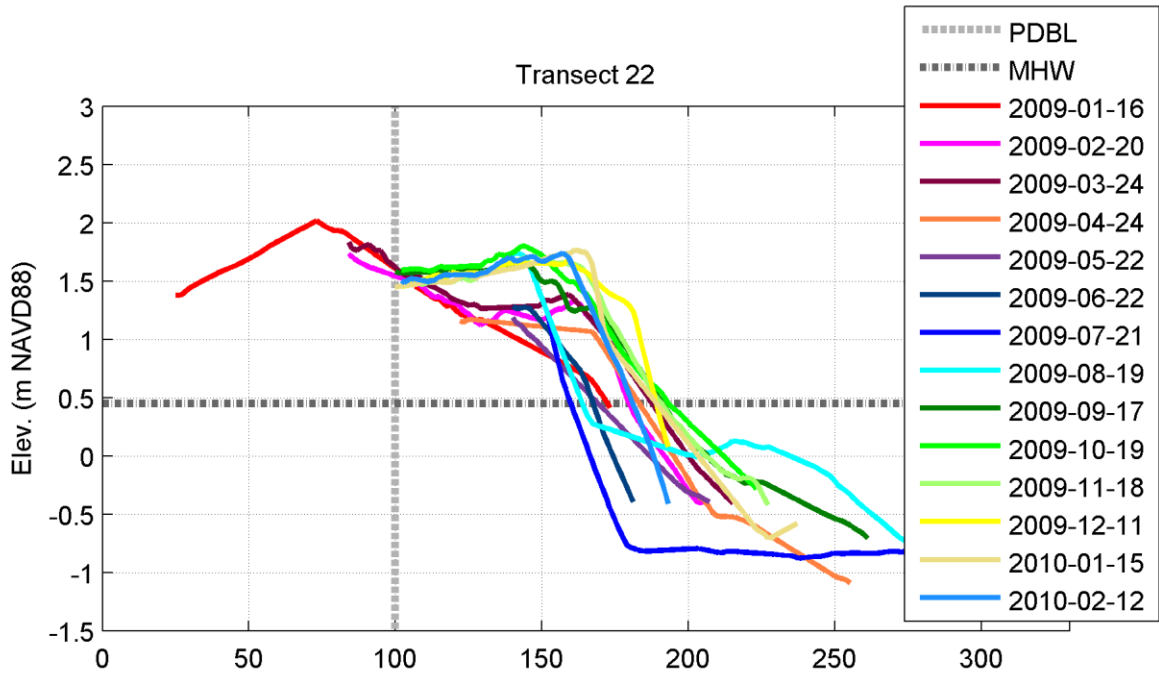


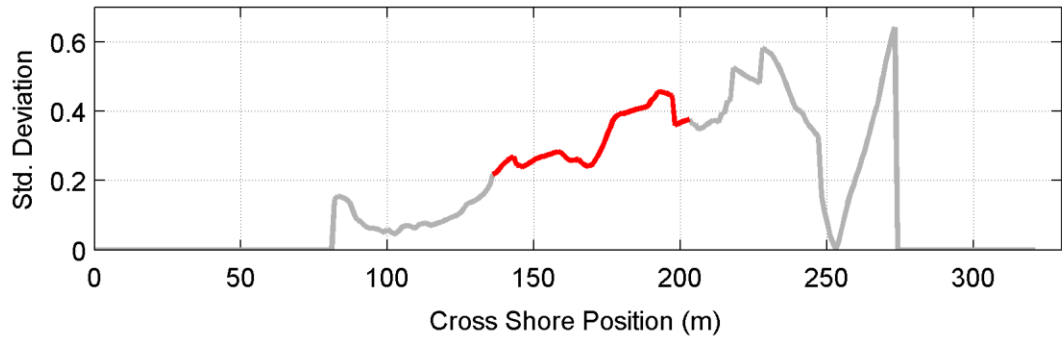
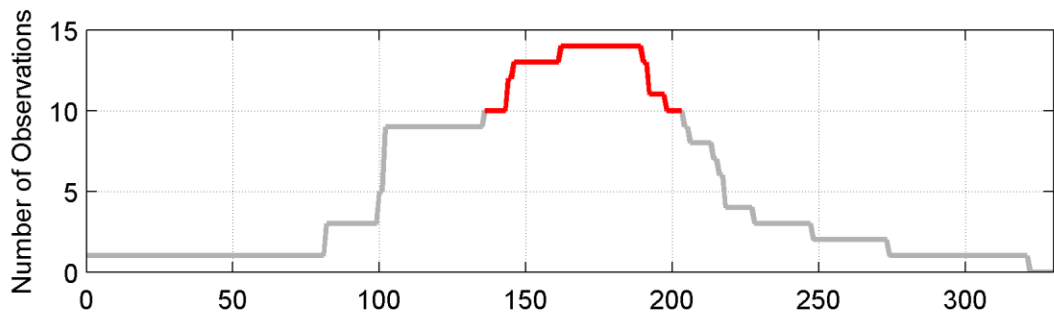
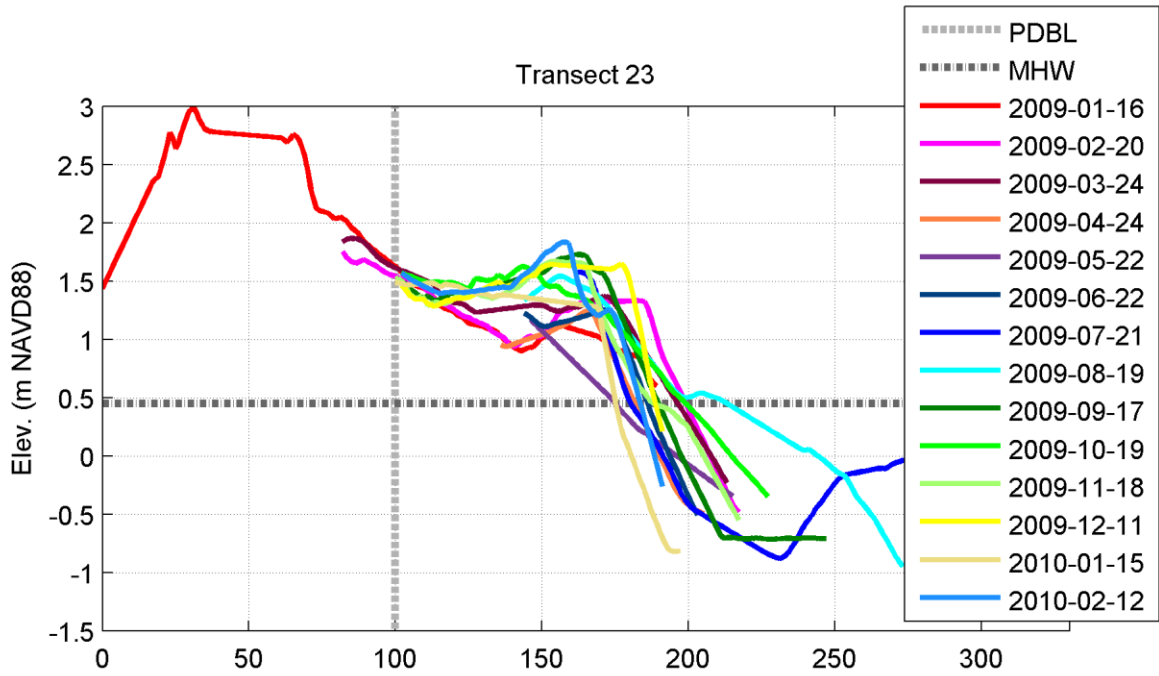


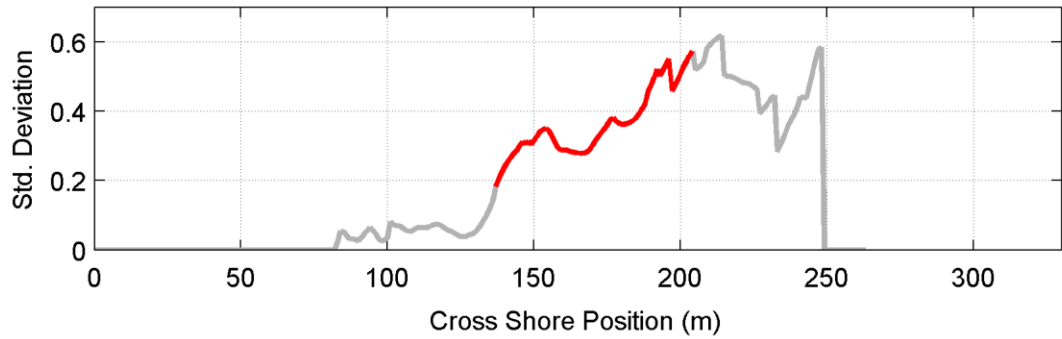
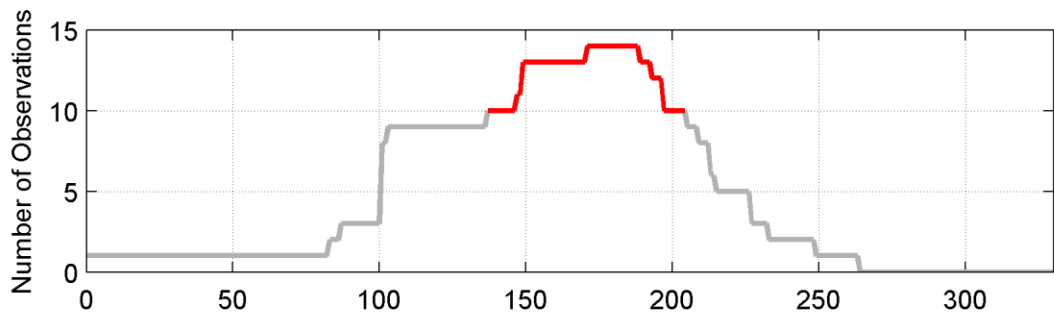
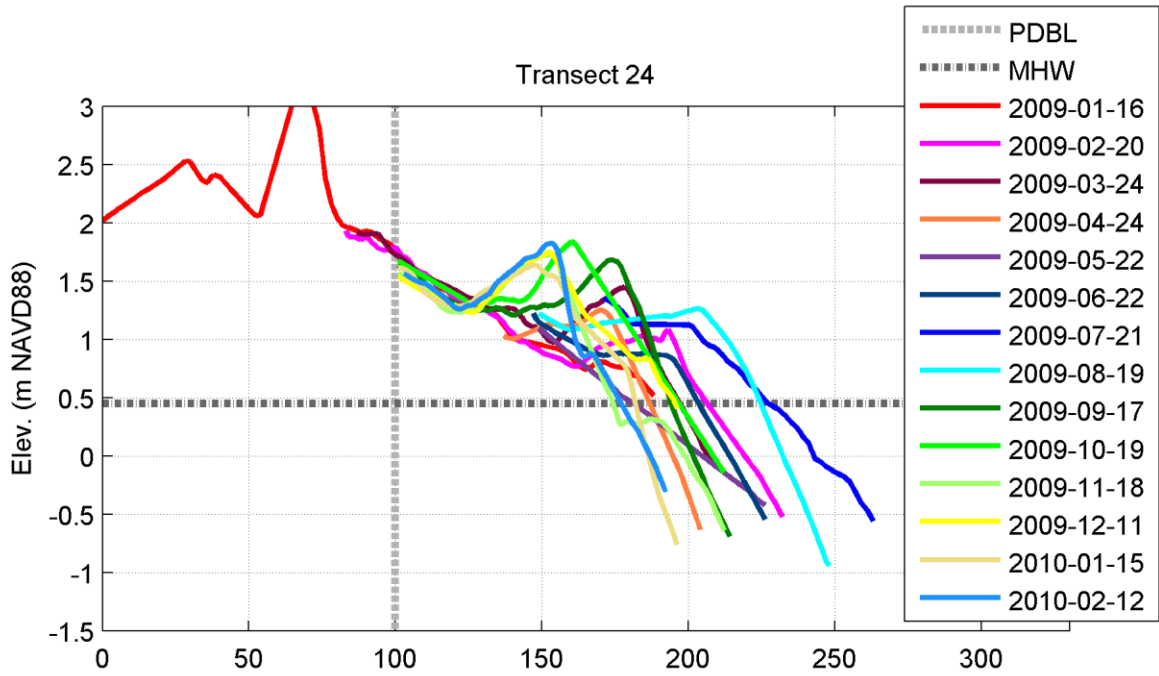


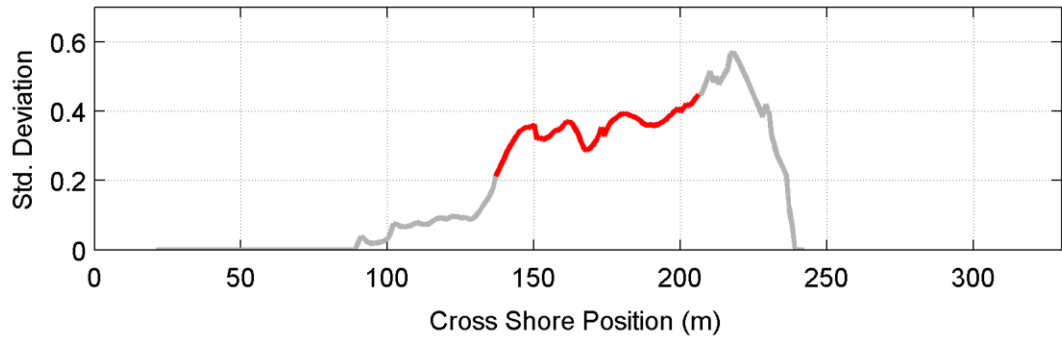
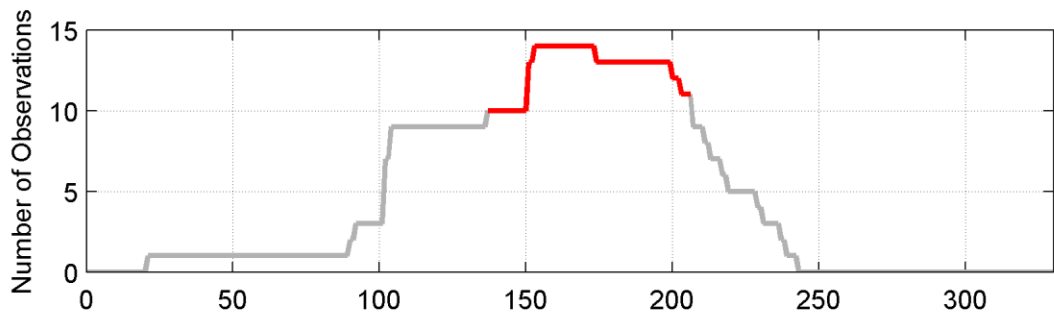
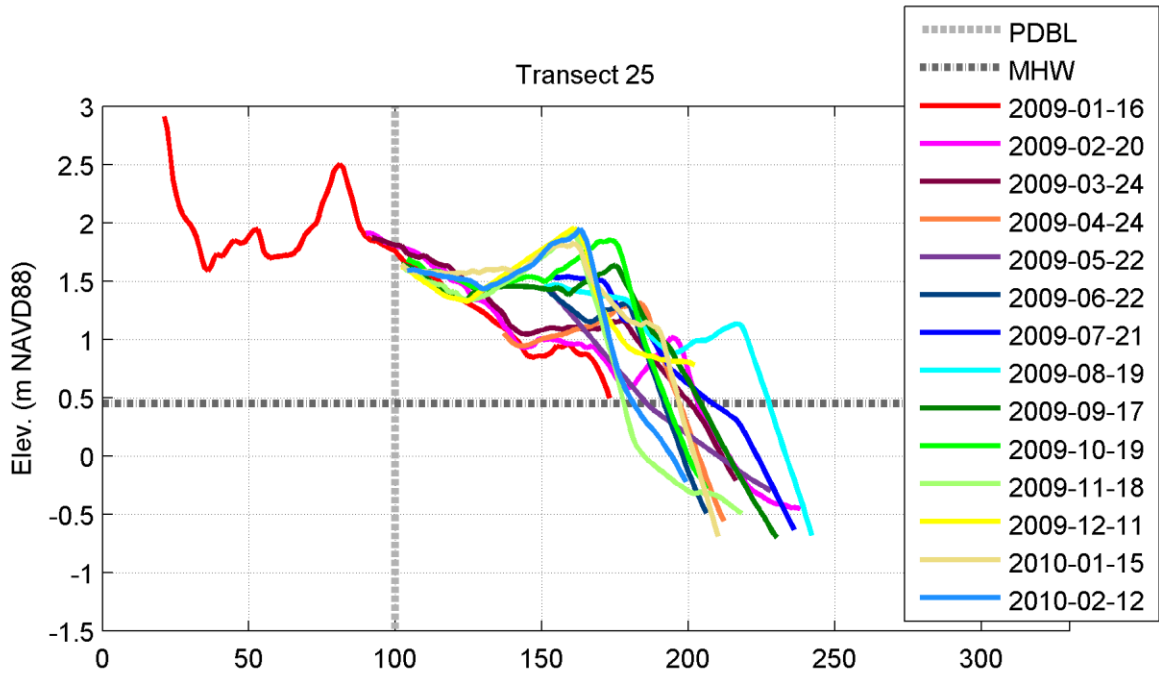


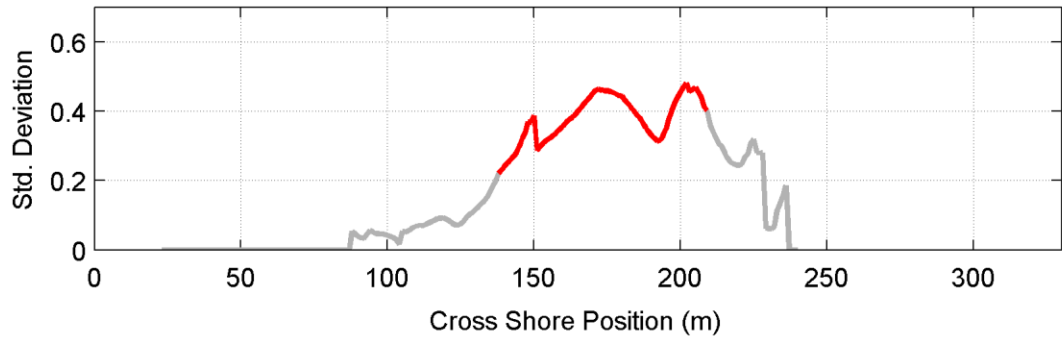
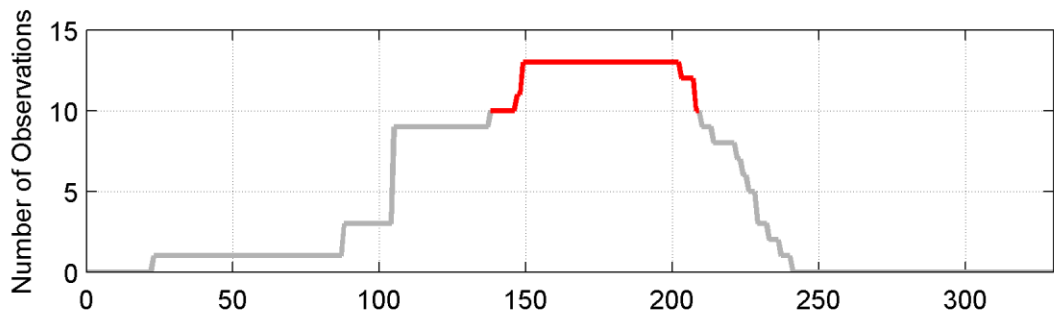
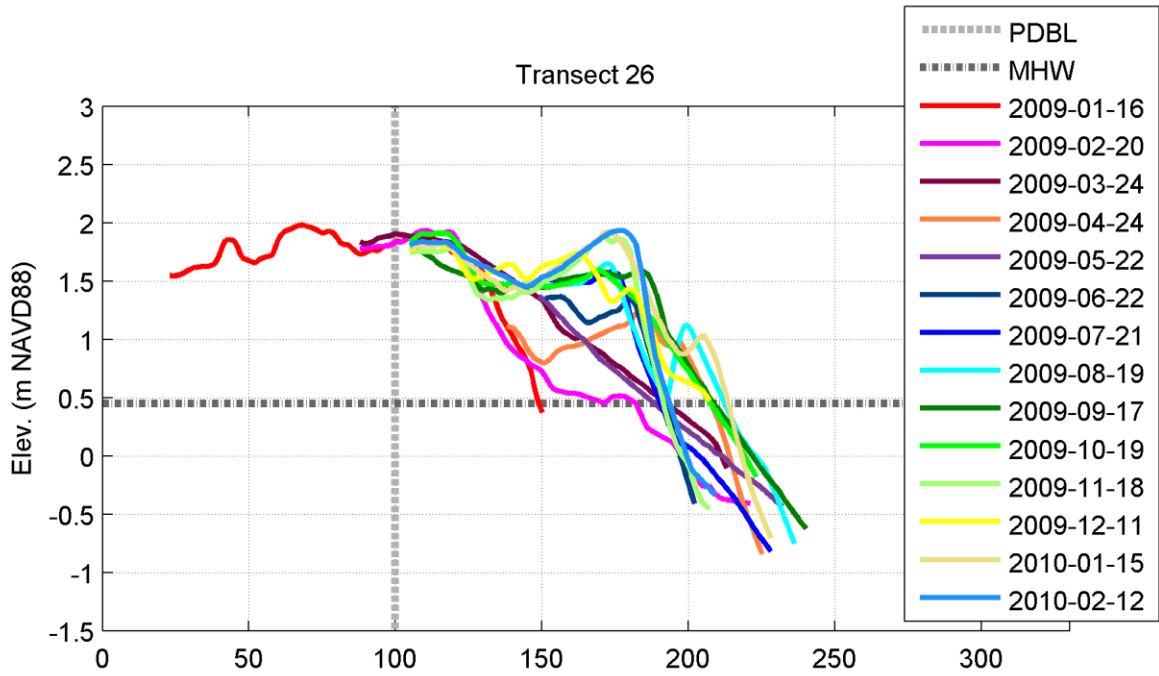


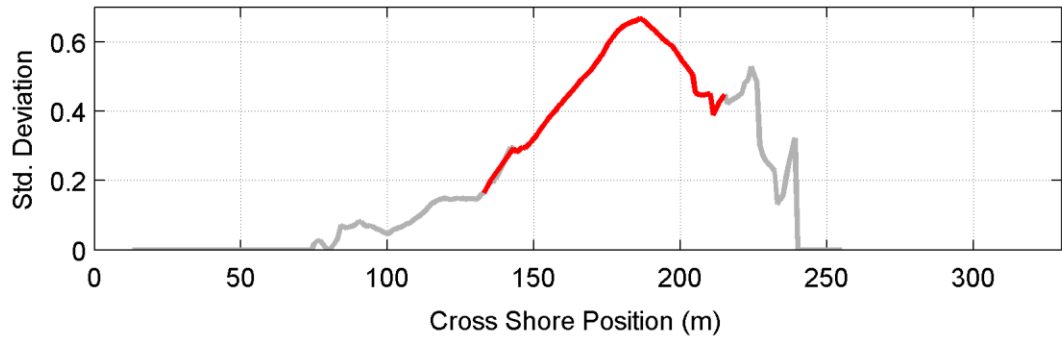
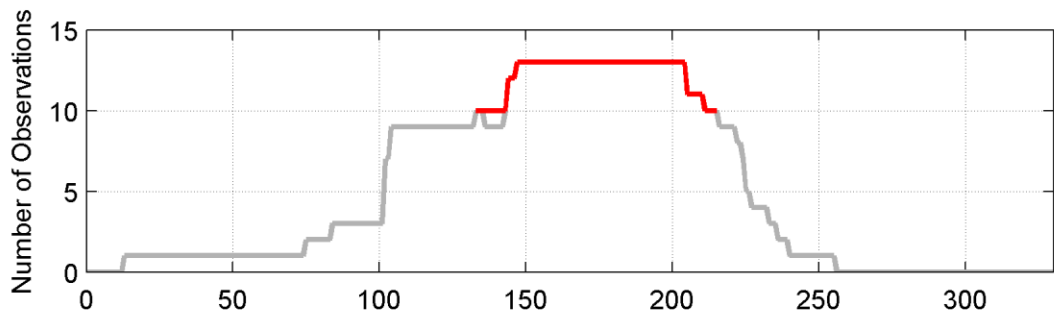
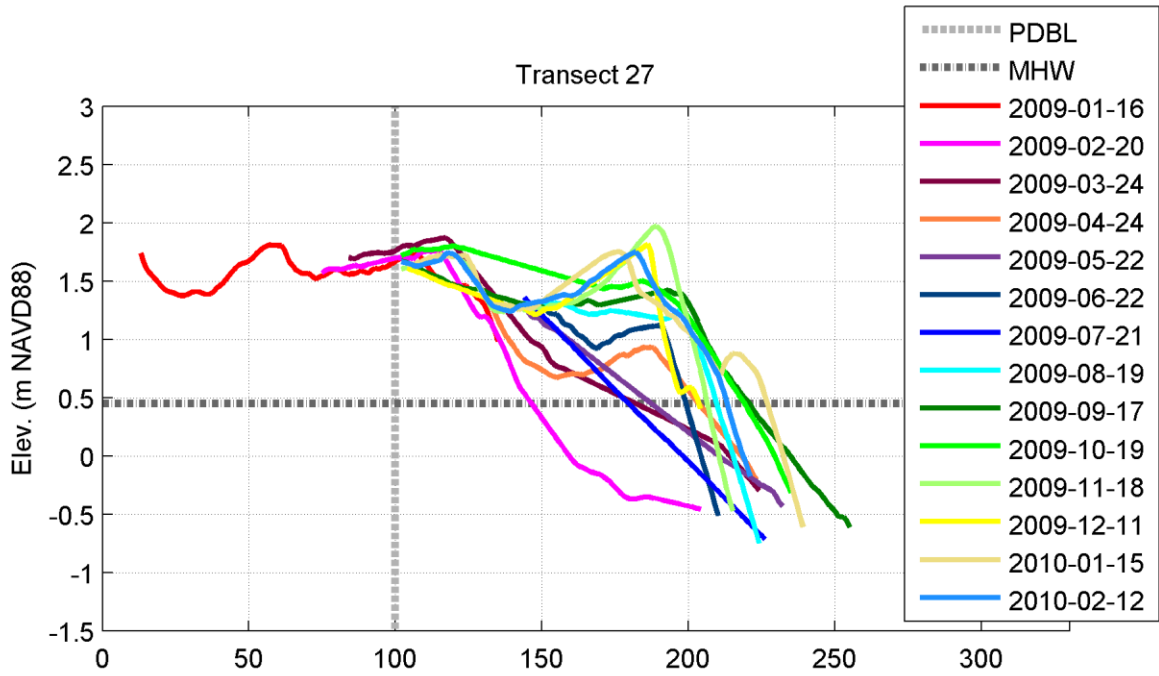


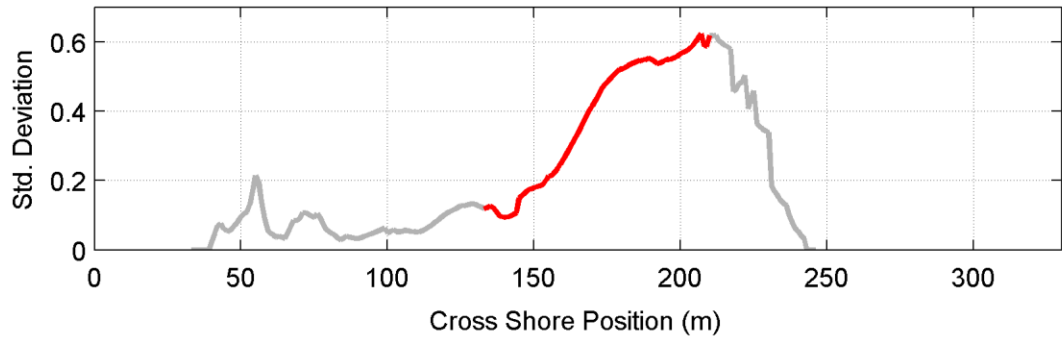
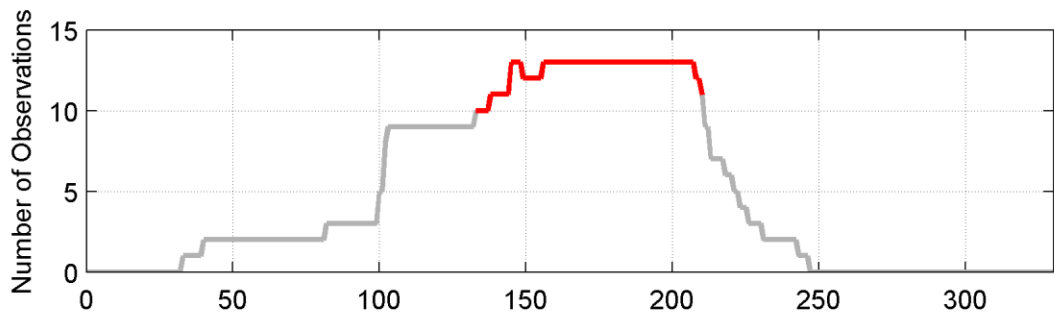
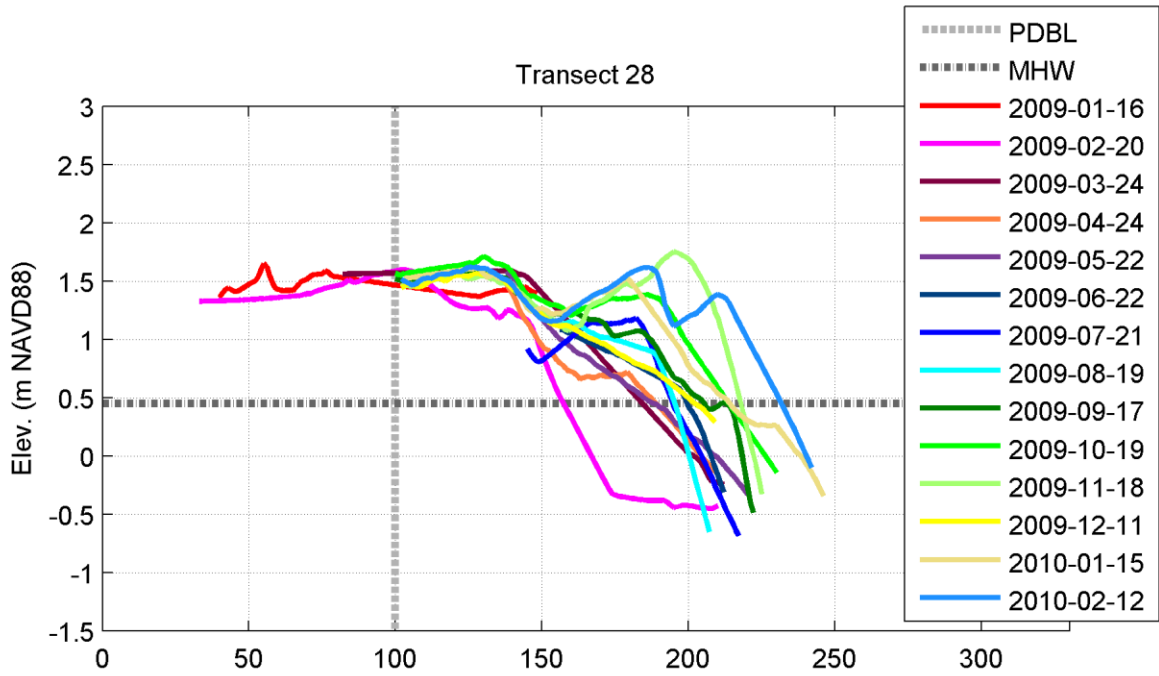


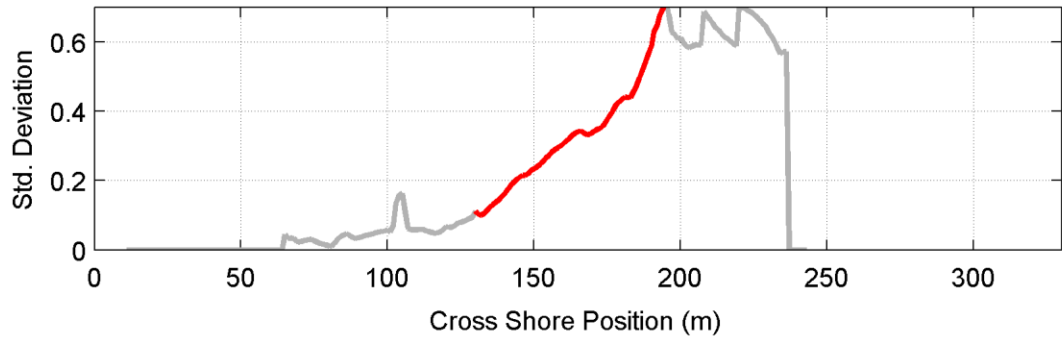
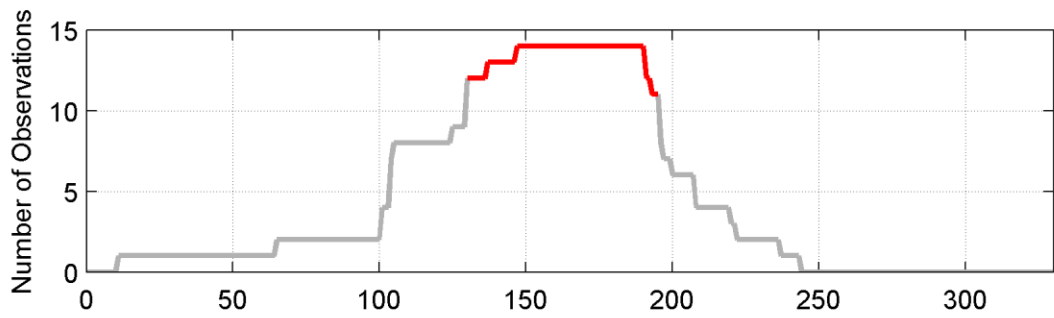
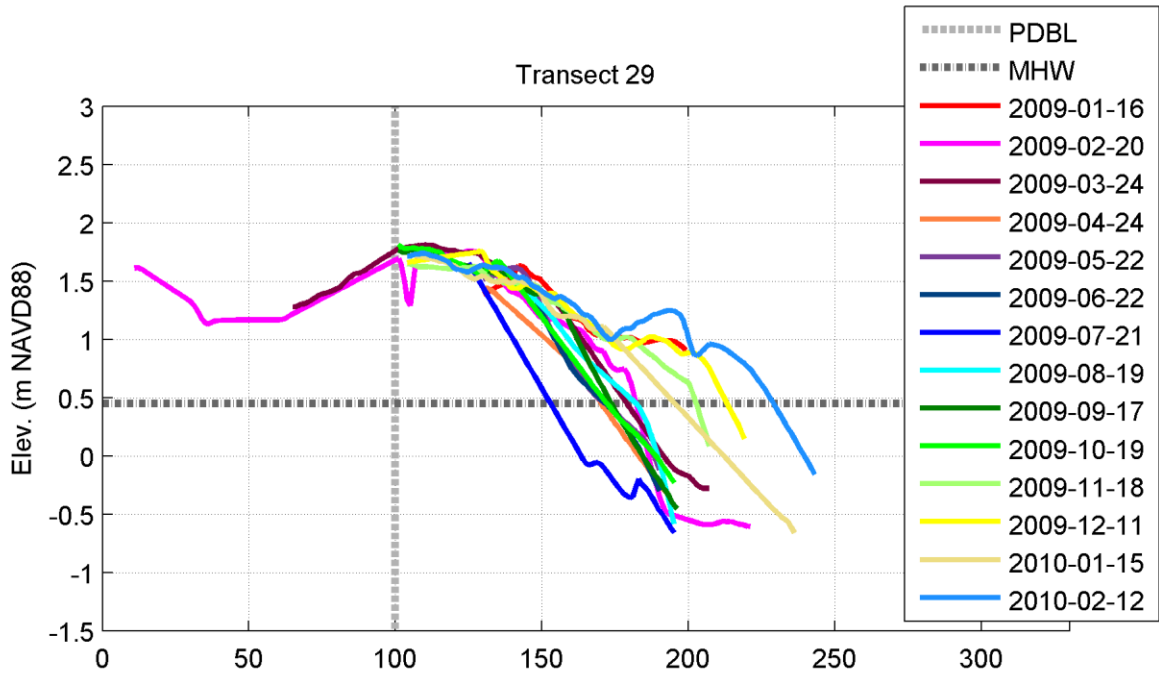


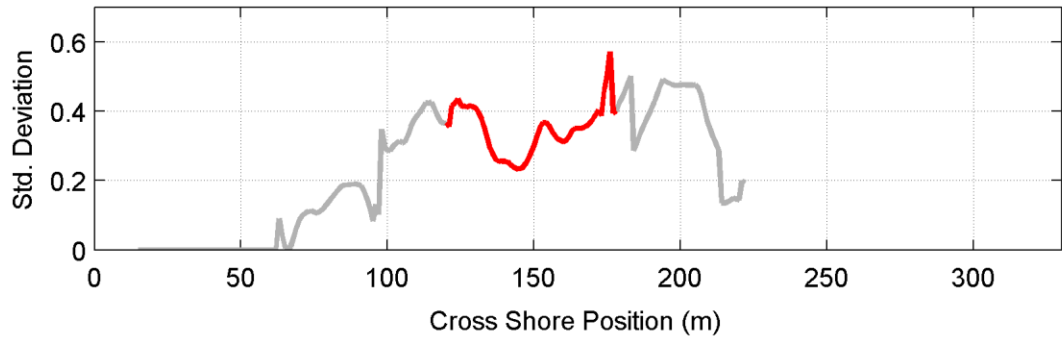
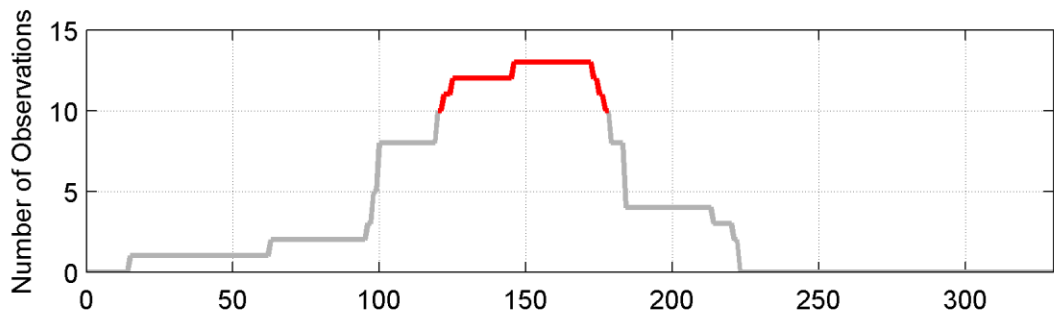
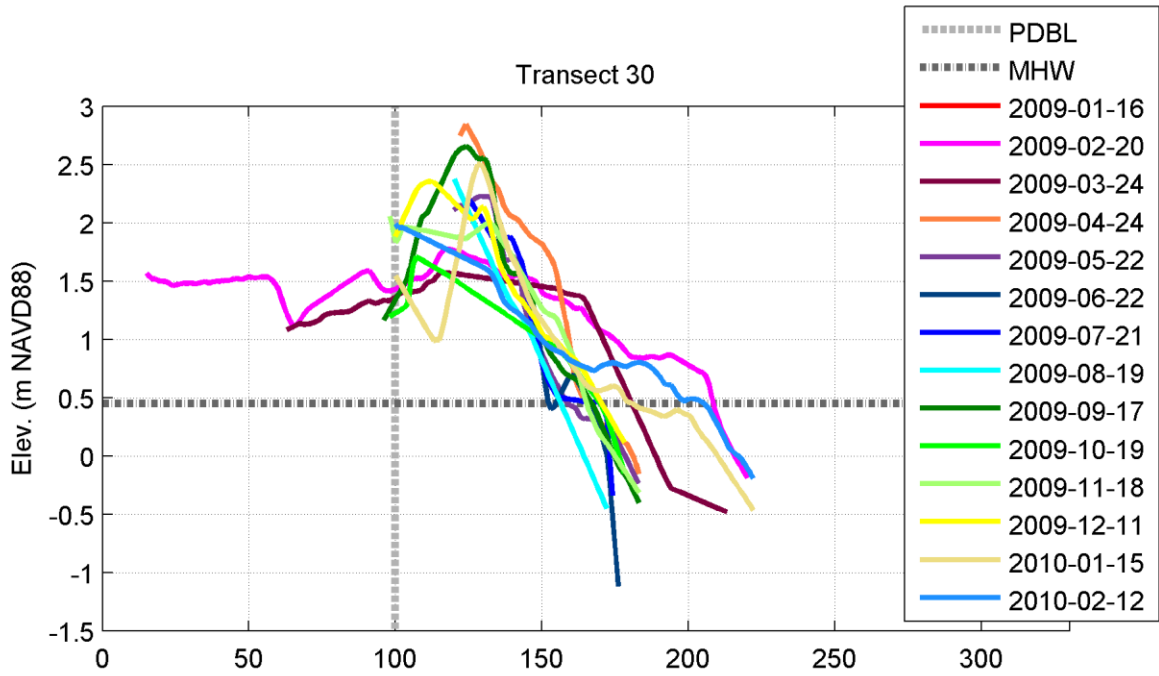




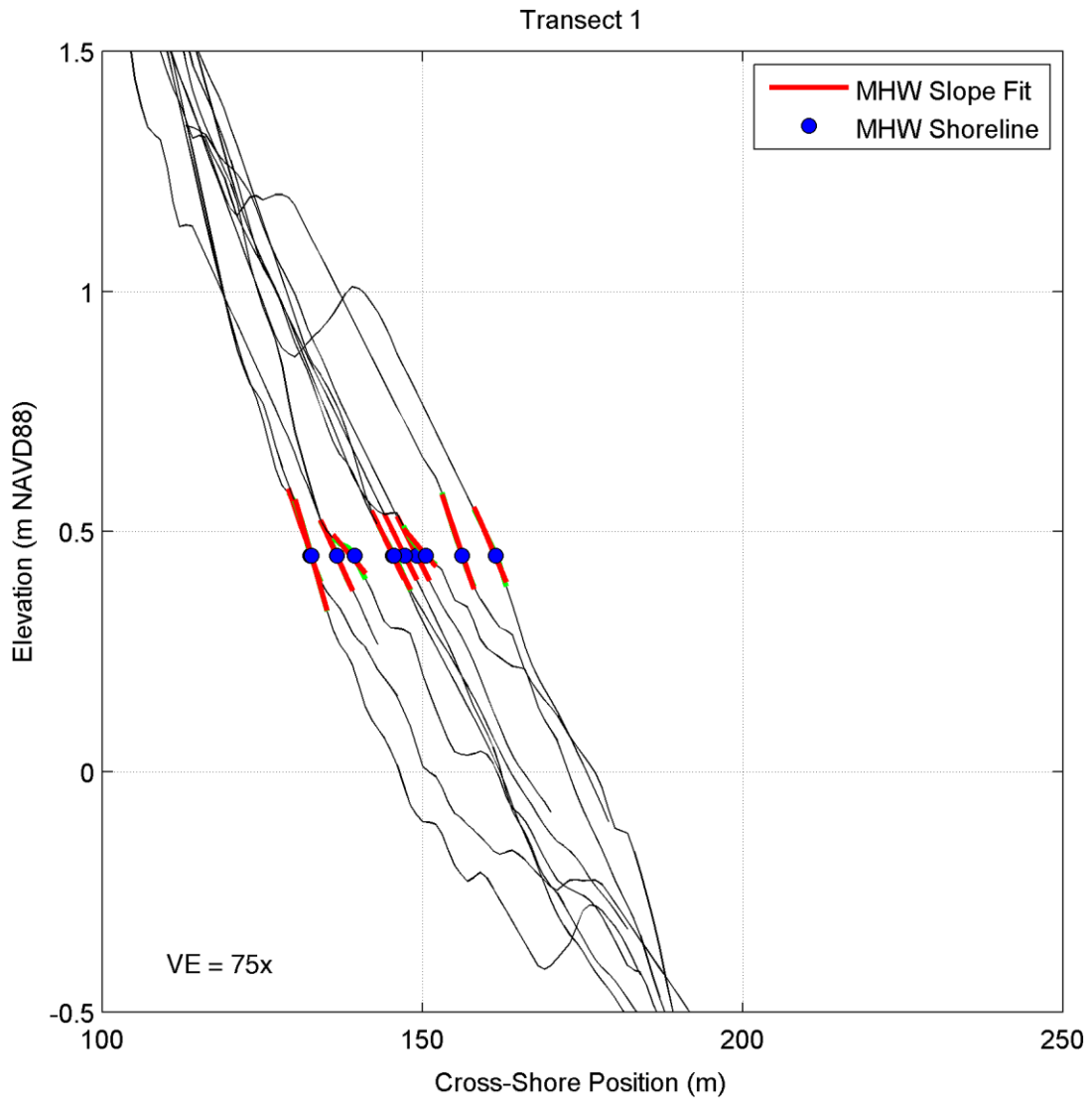


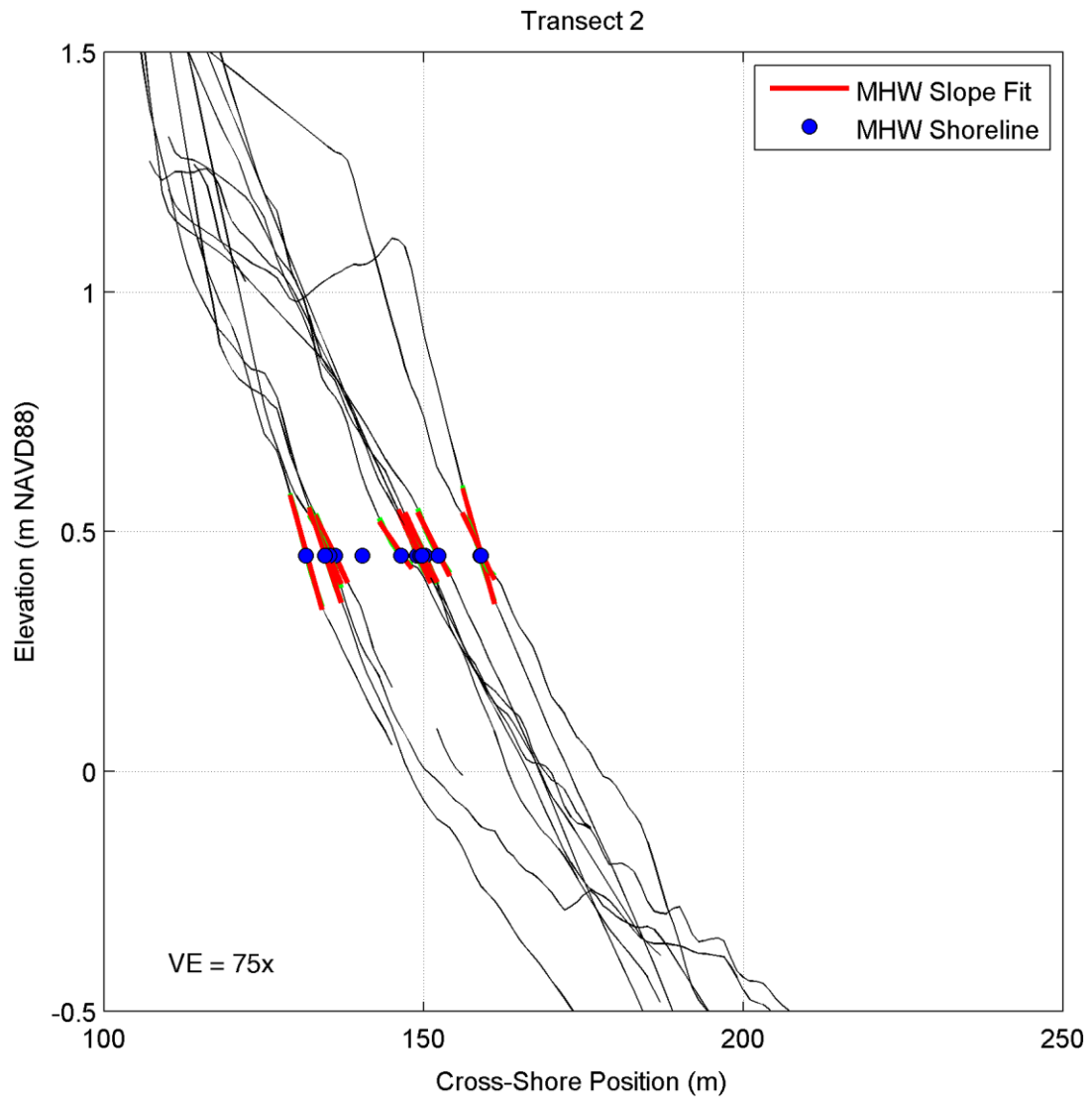


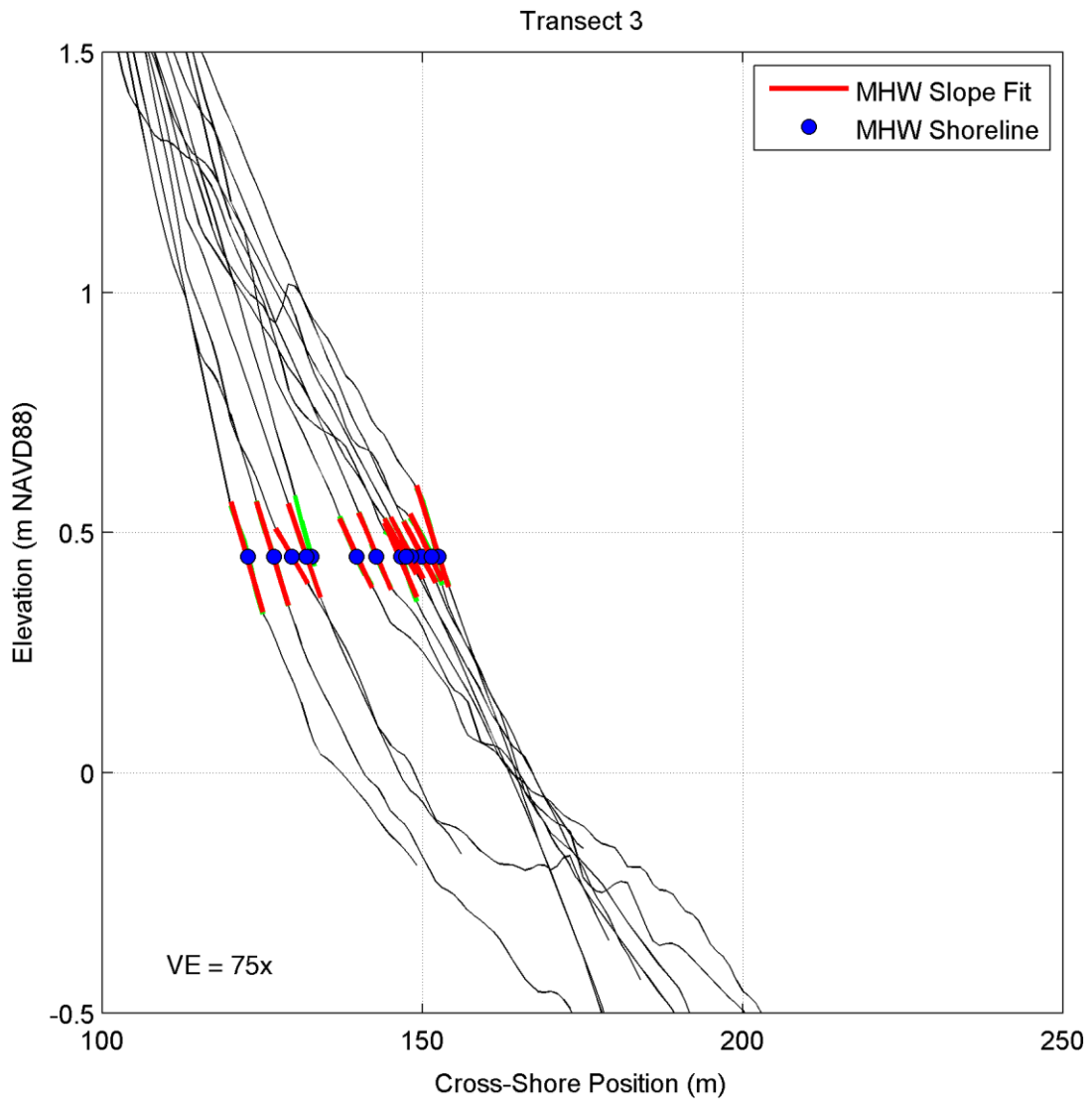


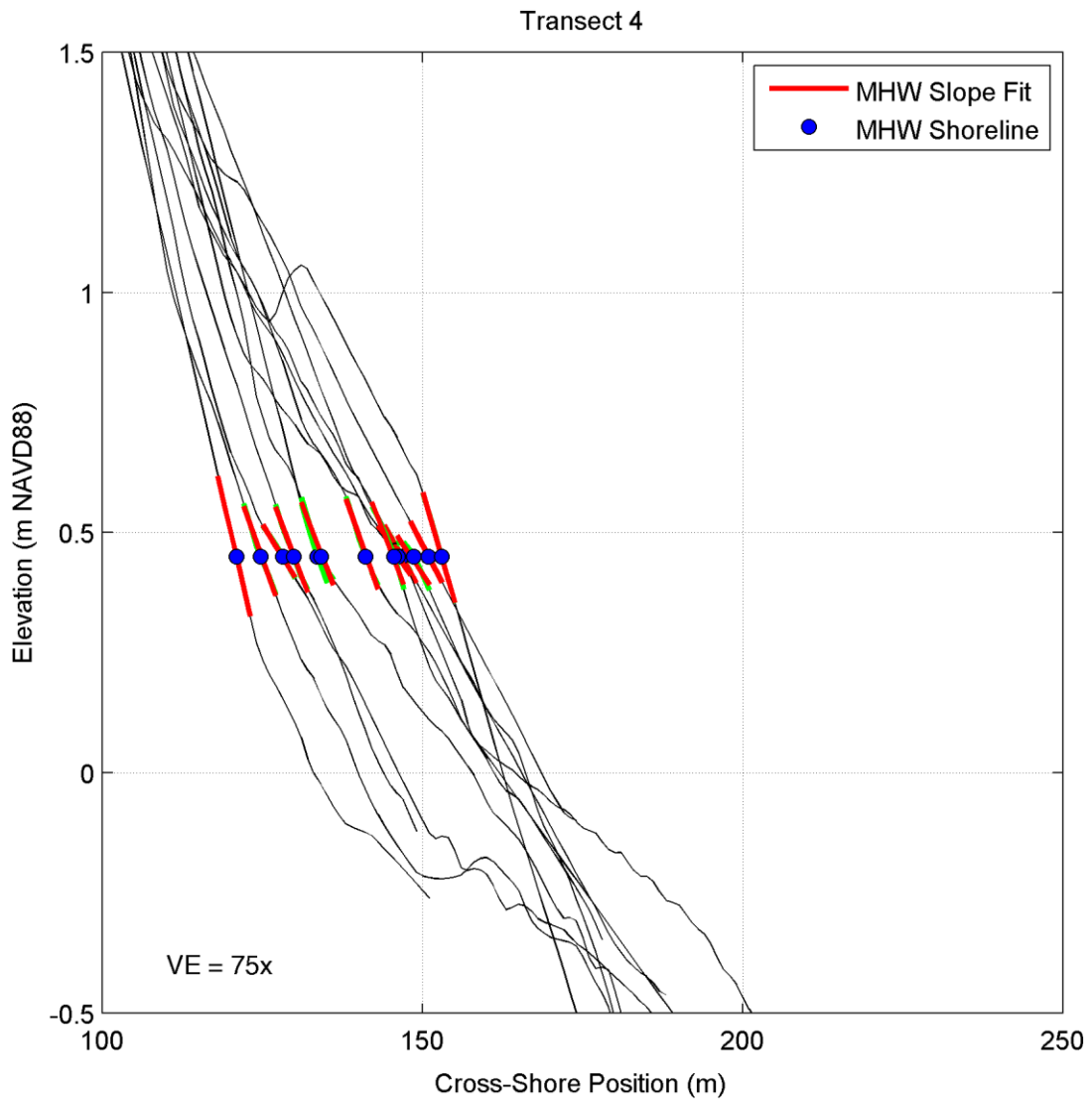


A-7

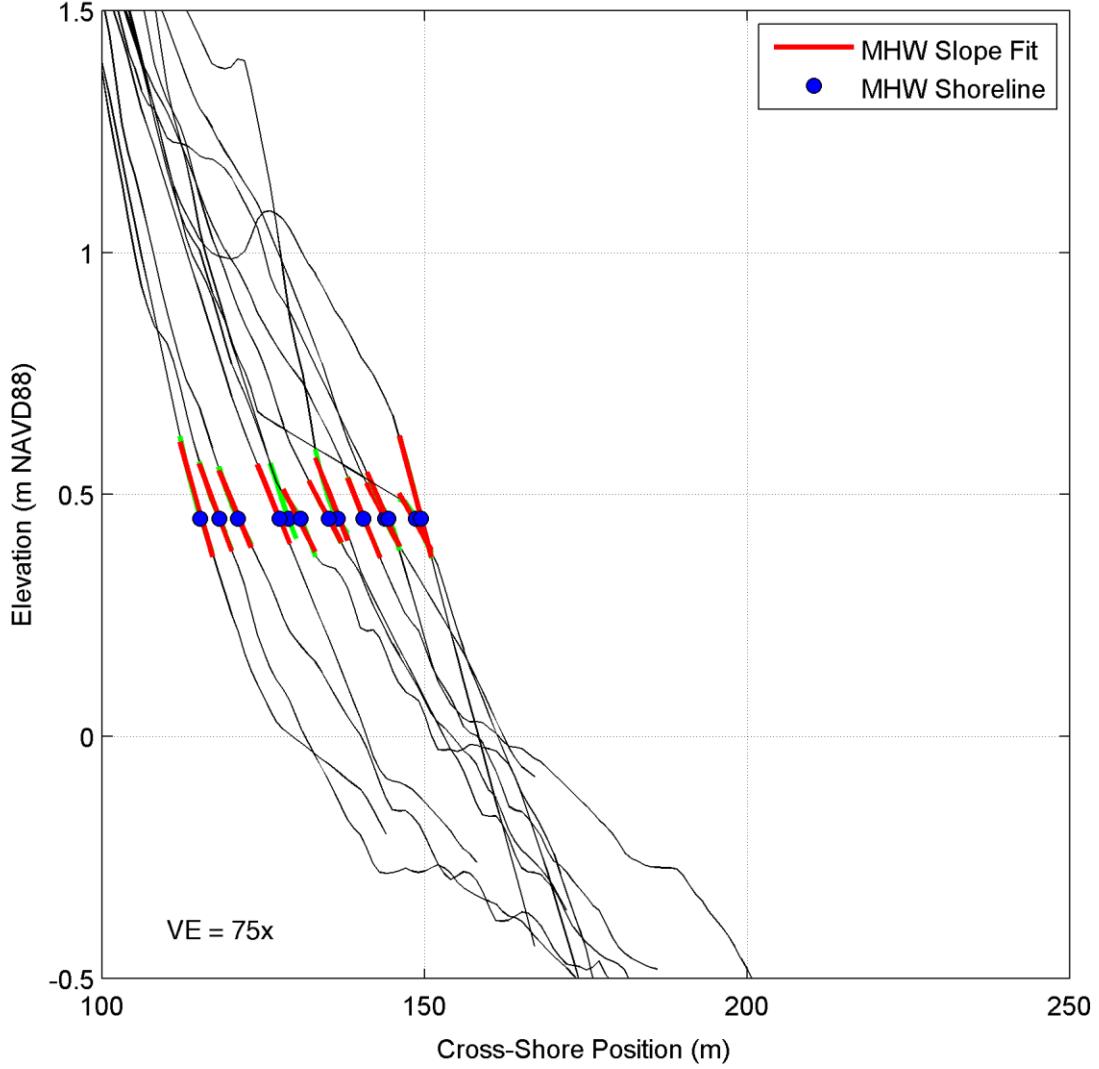




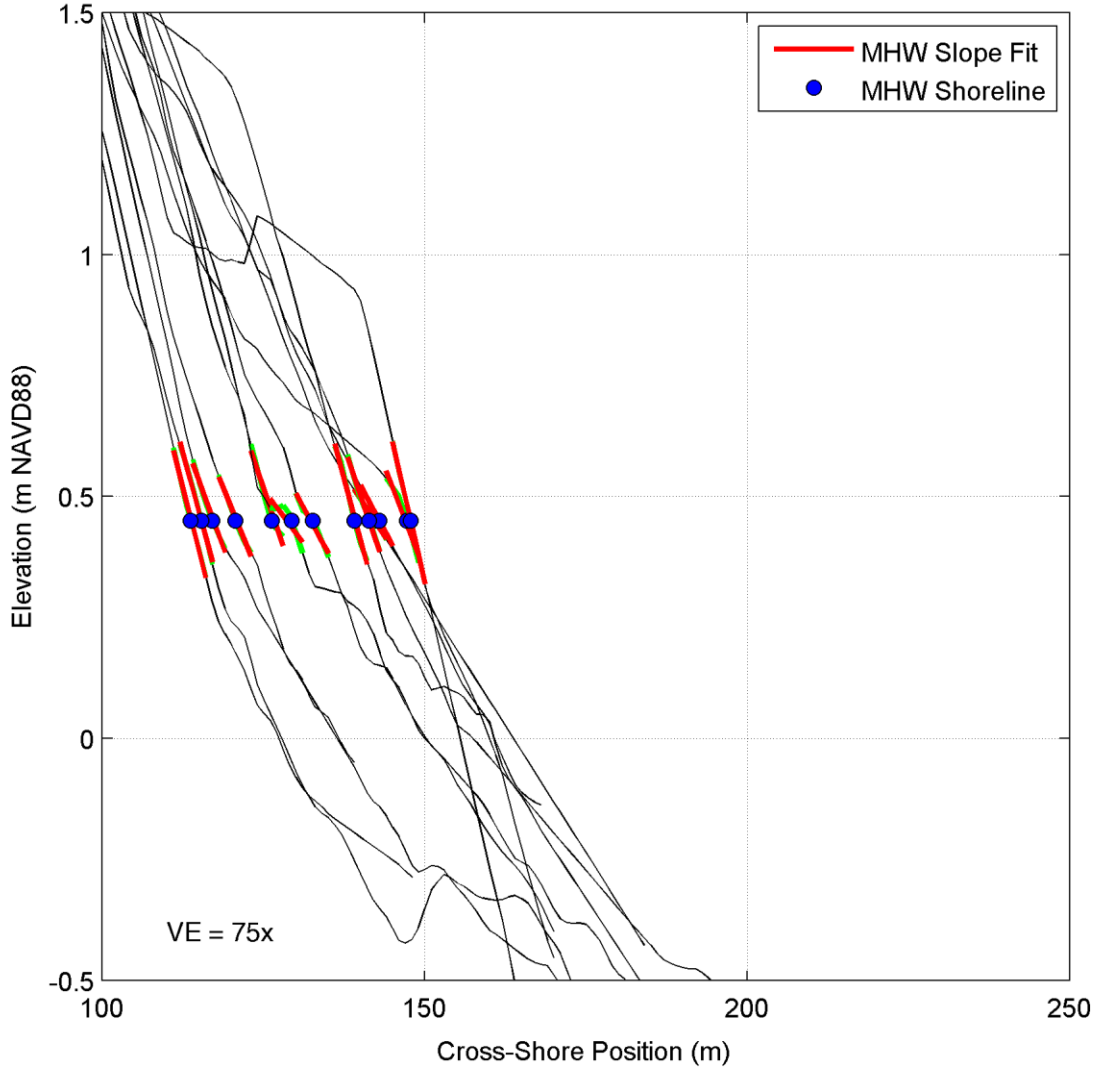




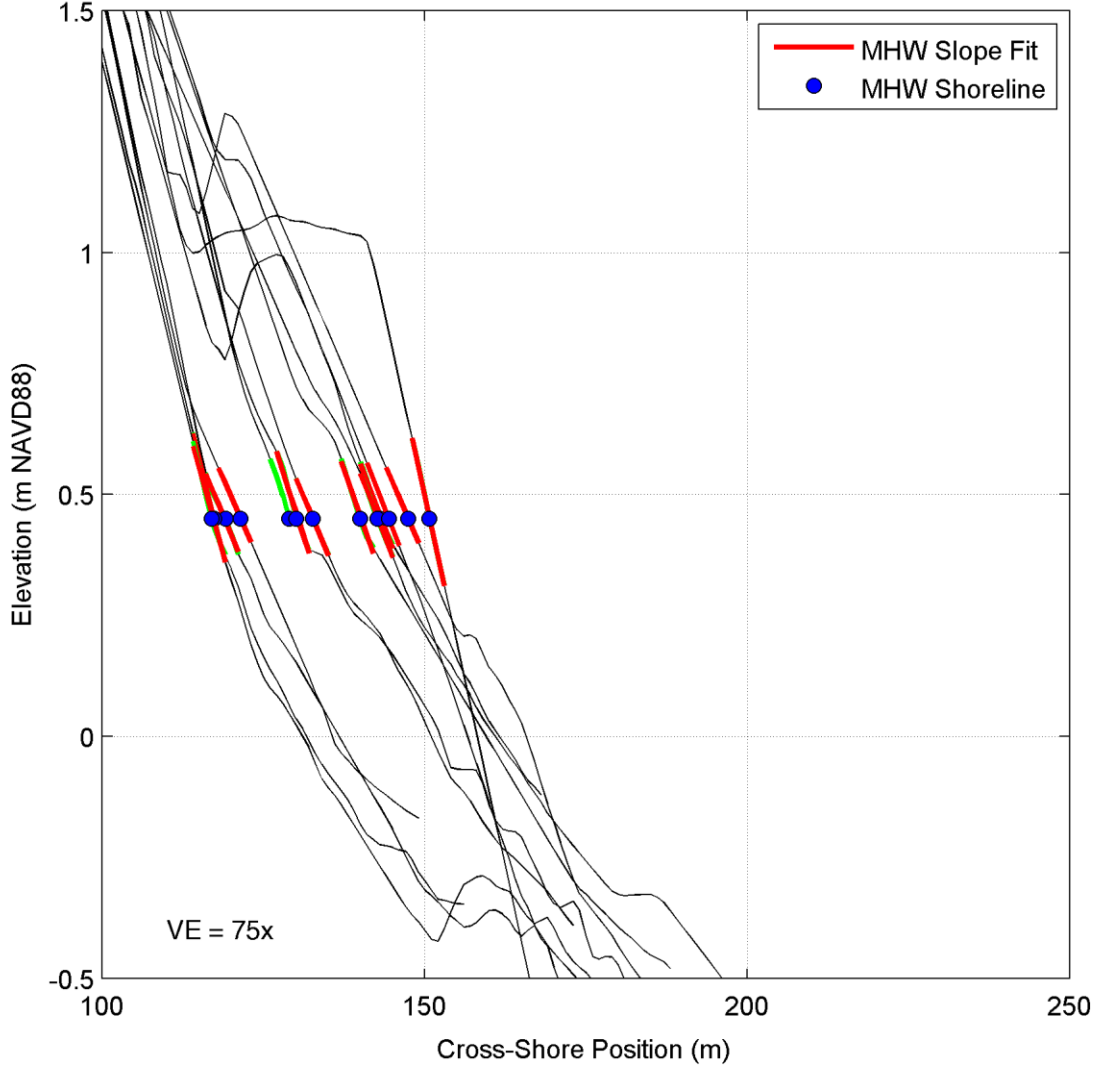
Transect 5



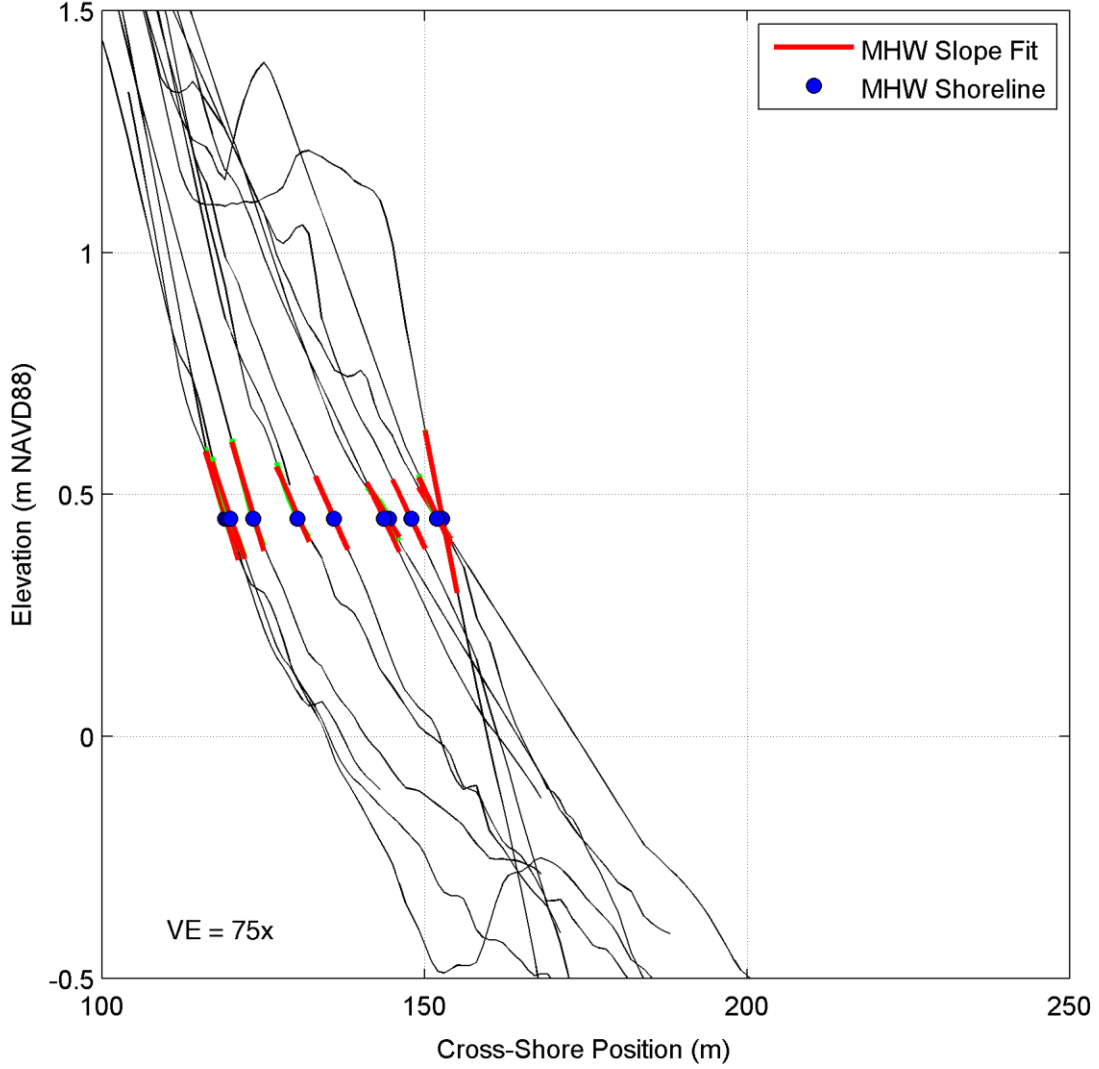
Transect 6



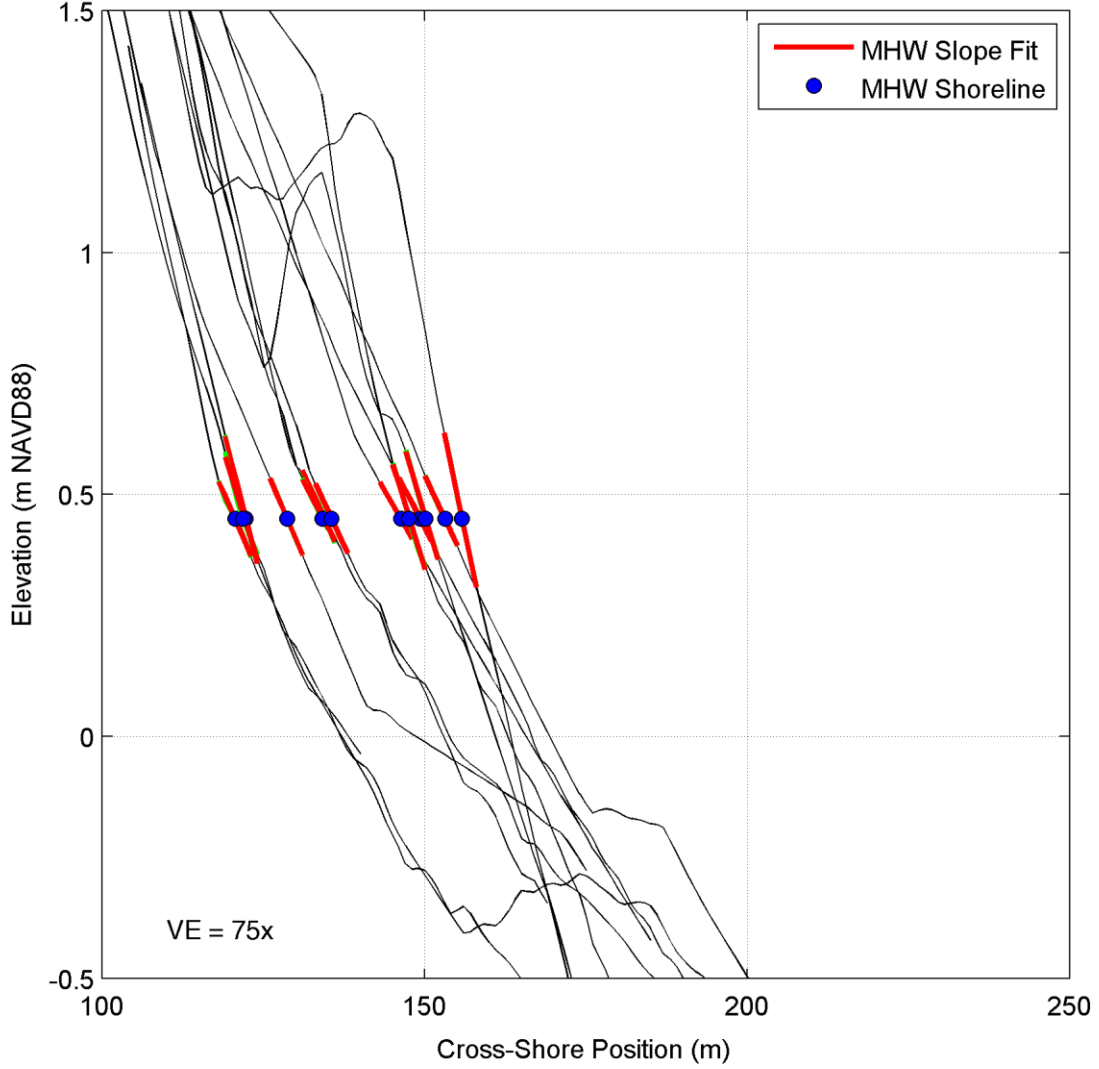
Transect 7



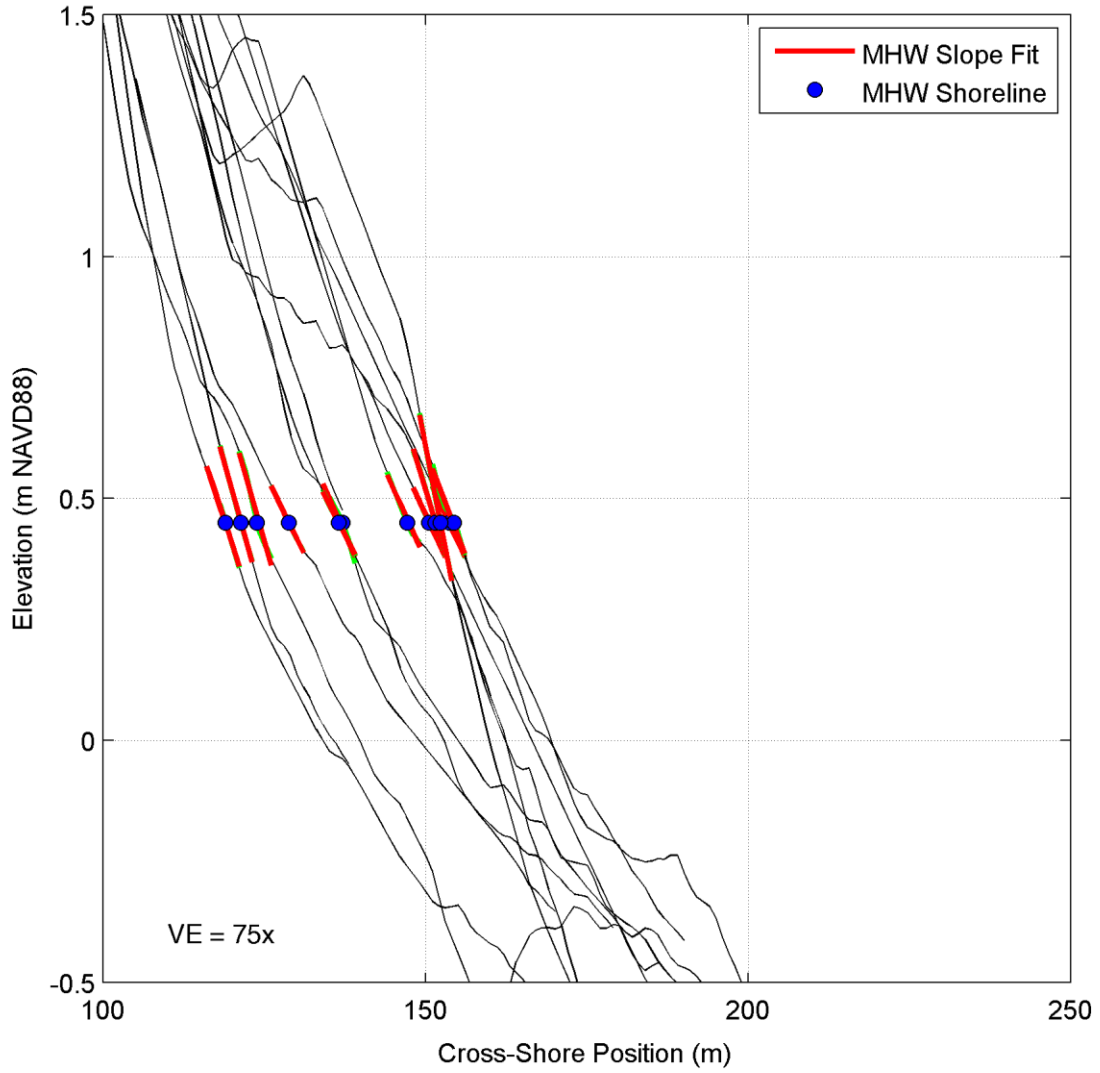
Transect 8



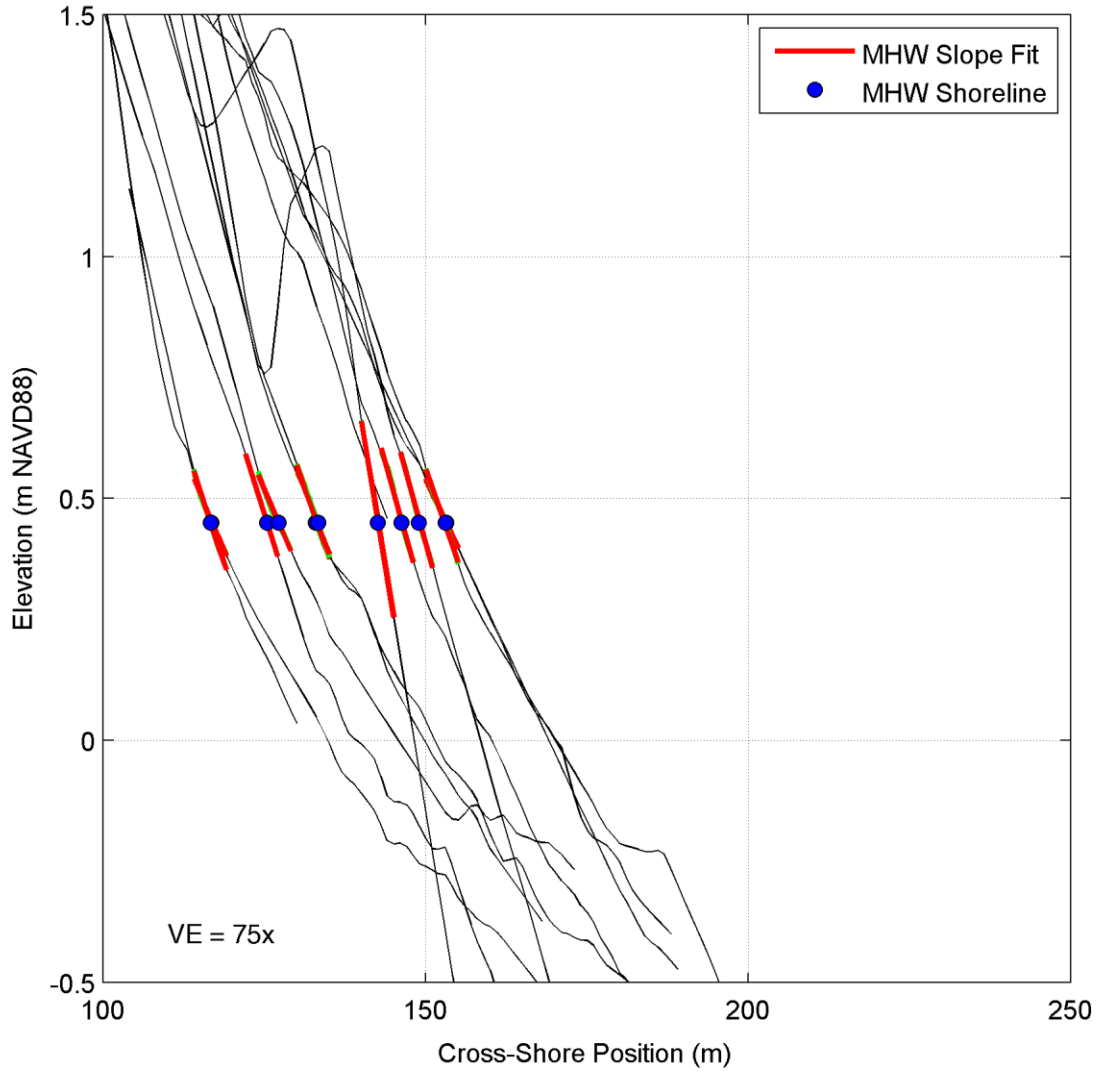
Transect 9



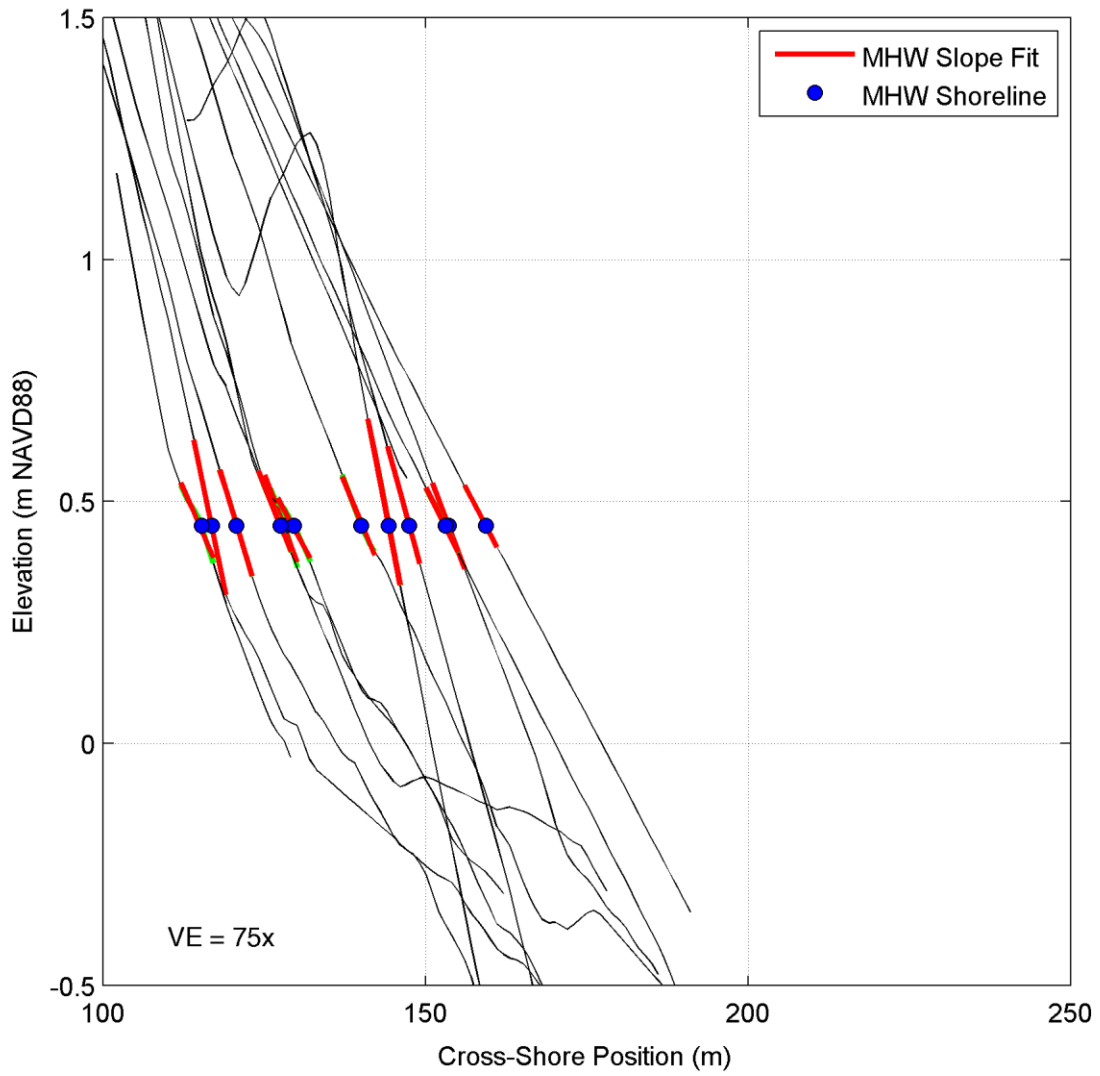
Transect 10



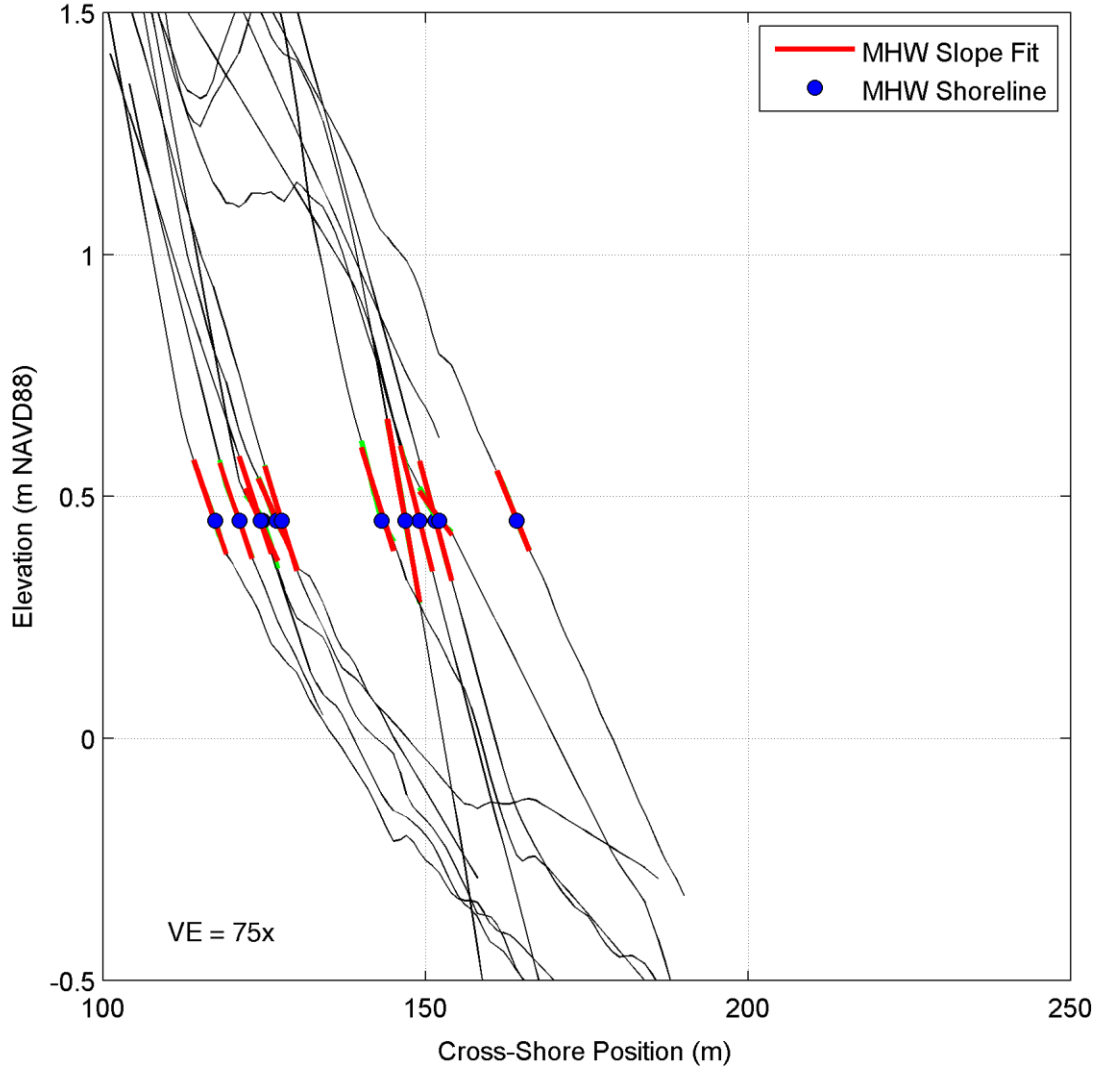
Transect 11



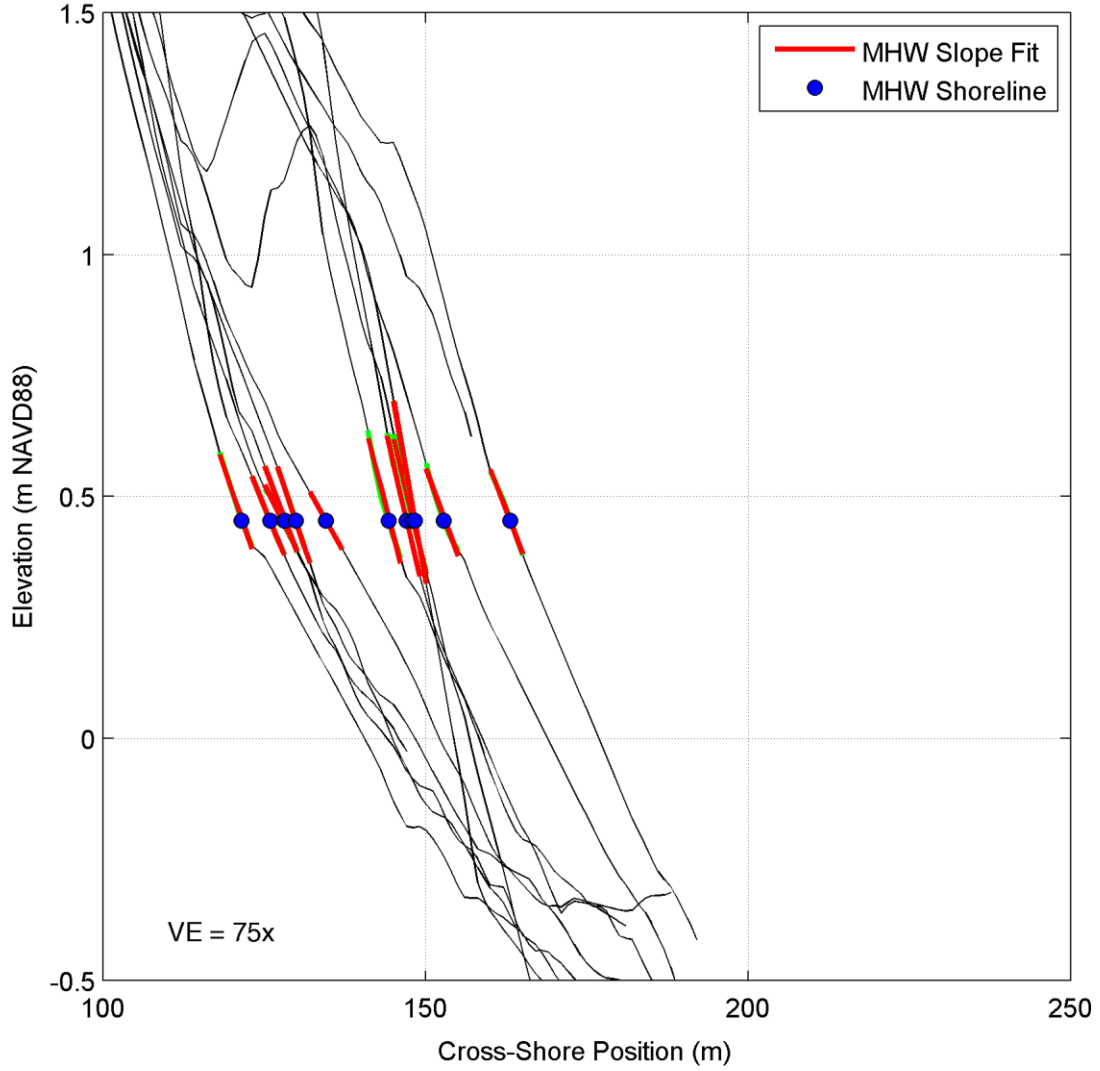
Transect 12

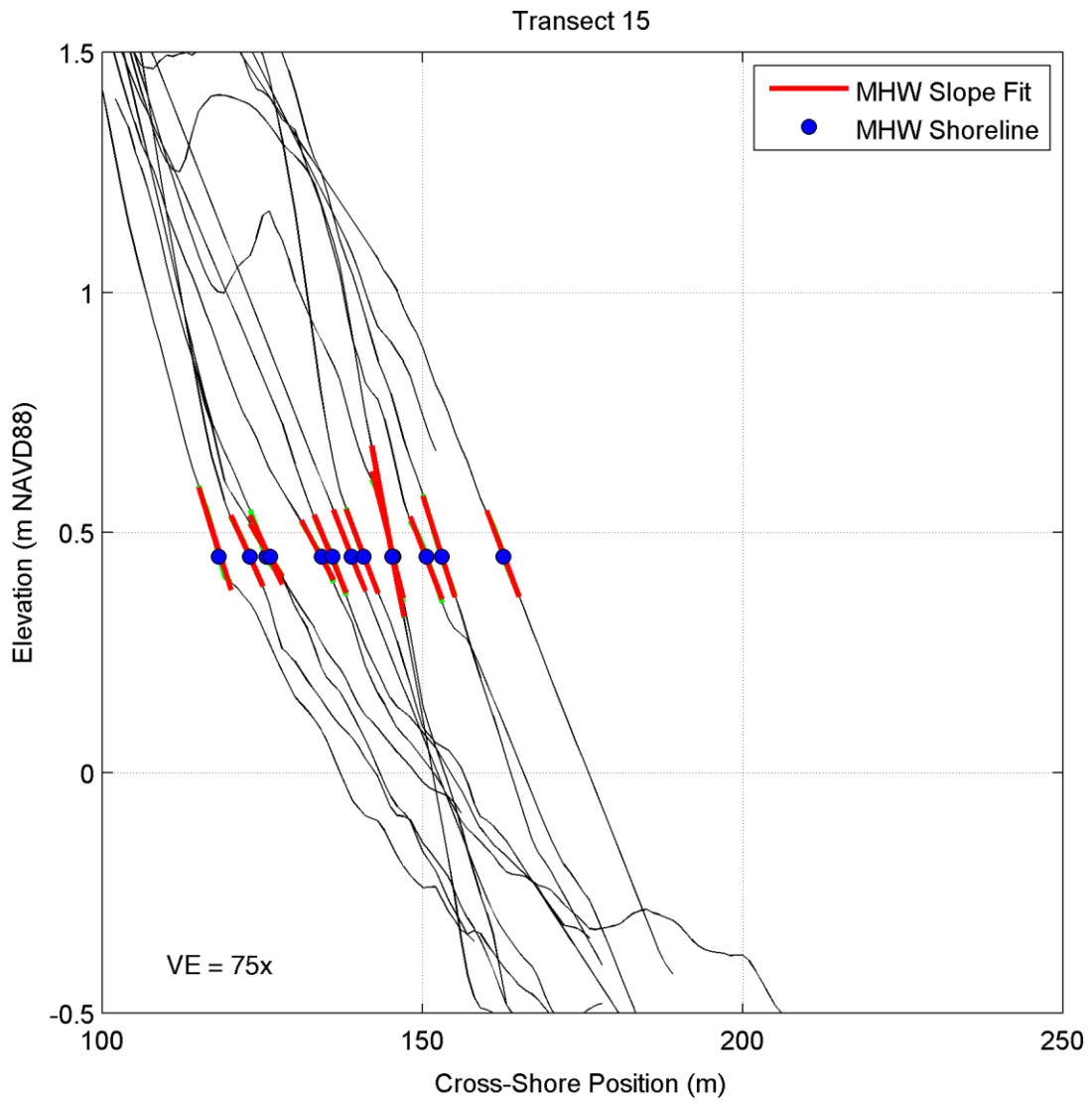


Transect 13

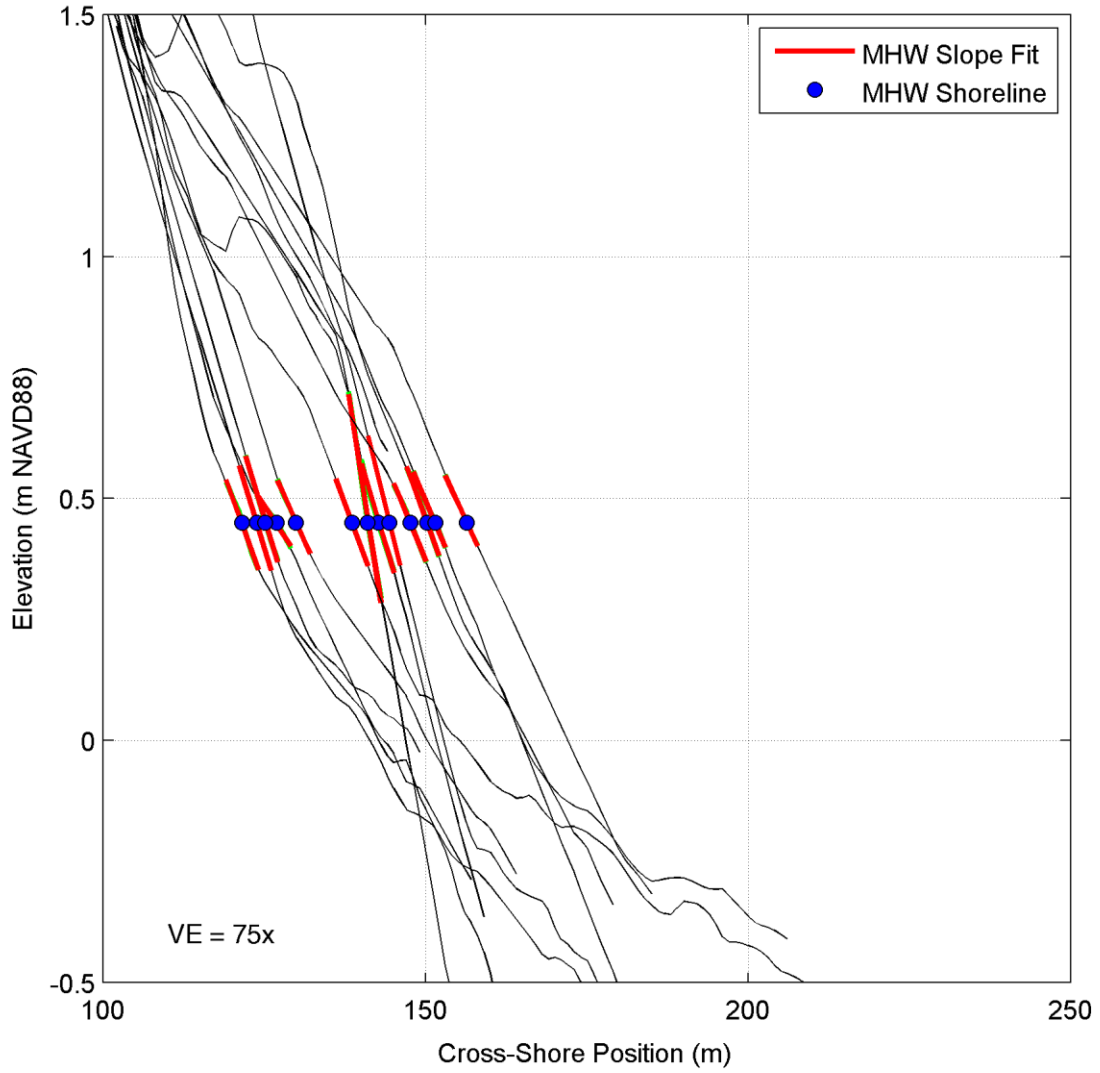


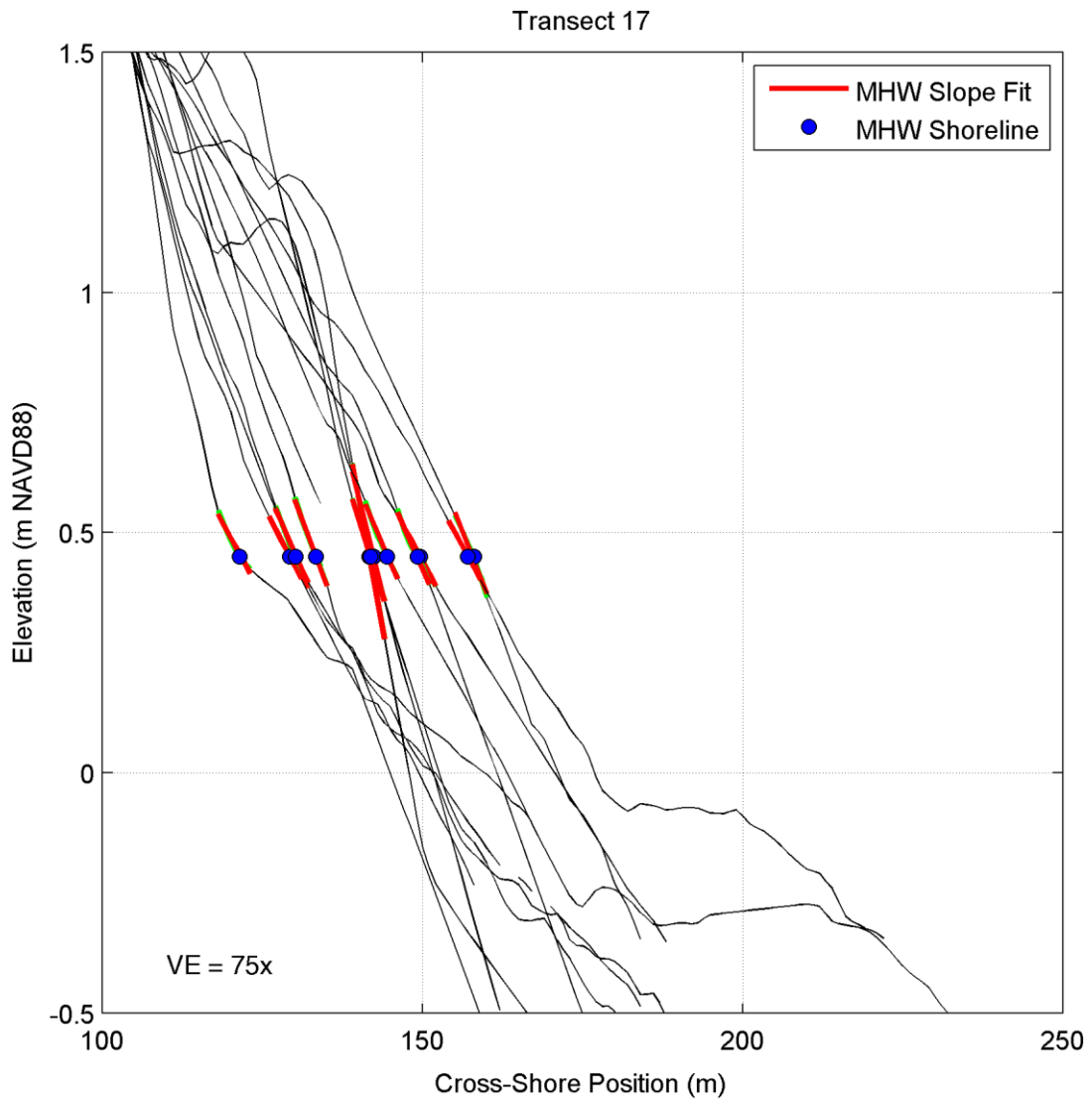
Transect 14



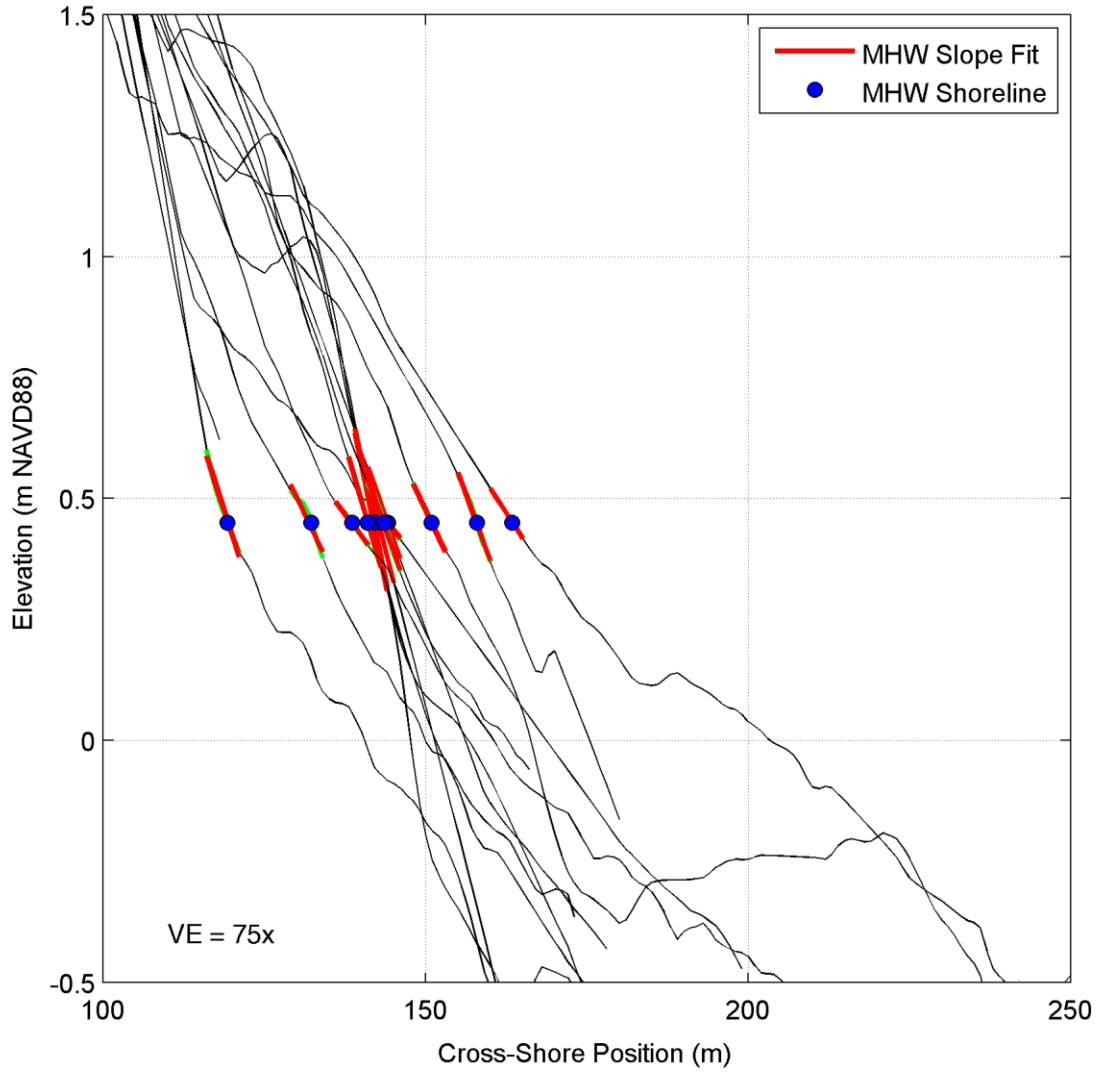


Transect 16

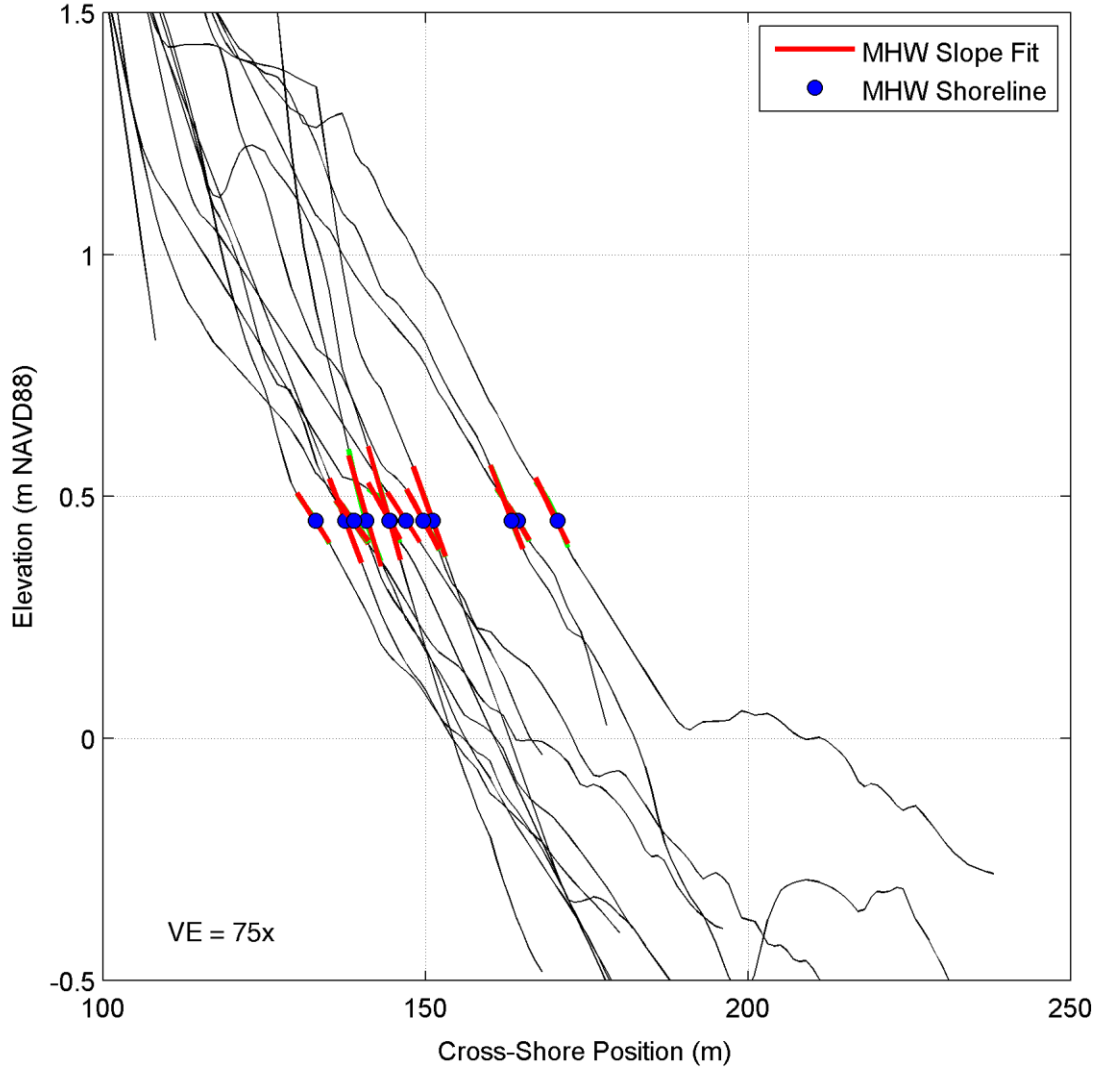




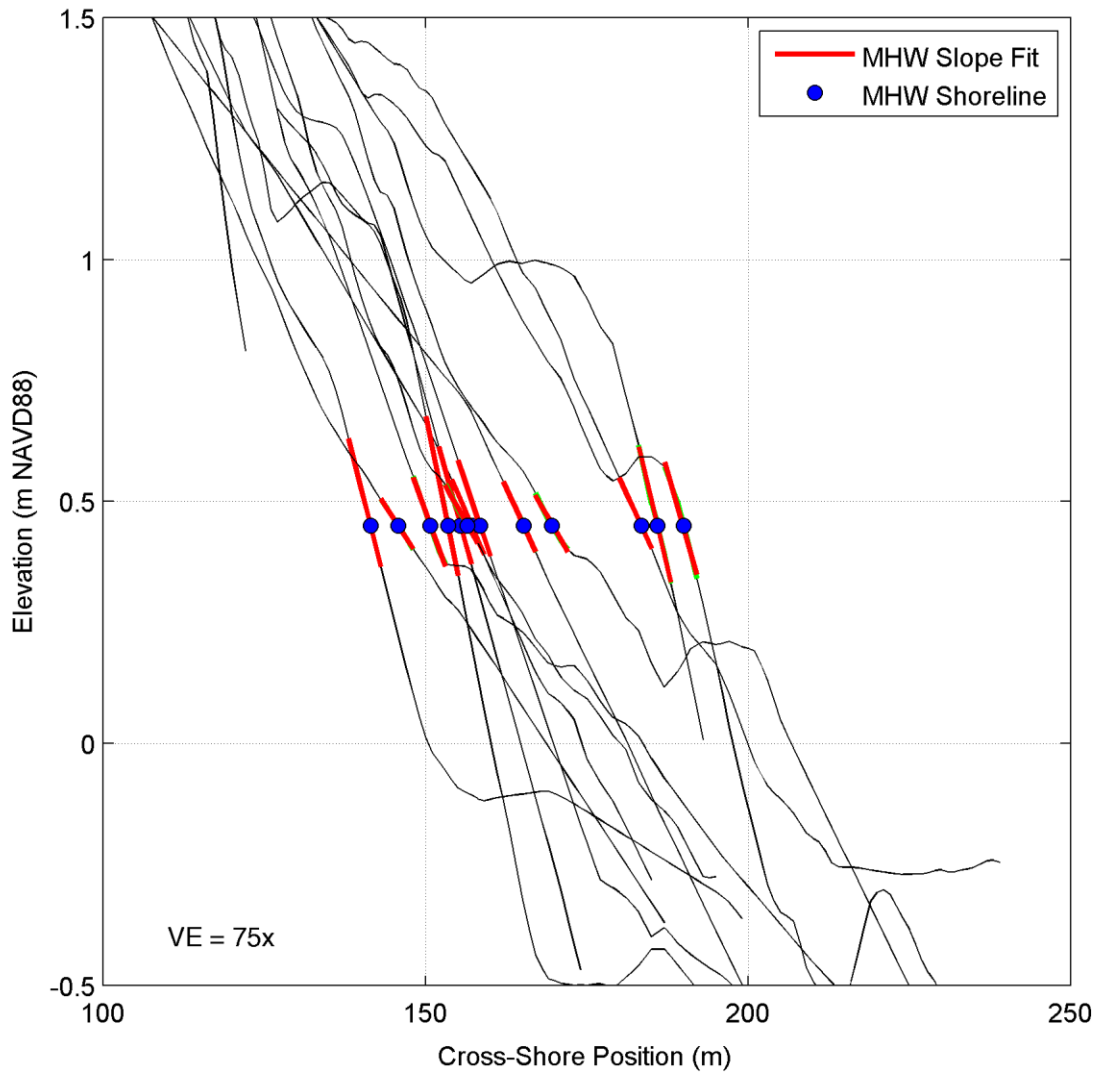
Transect 18

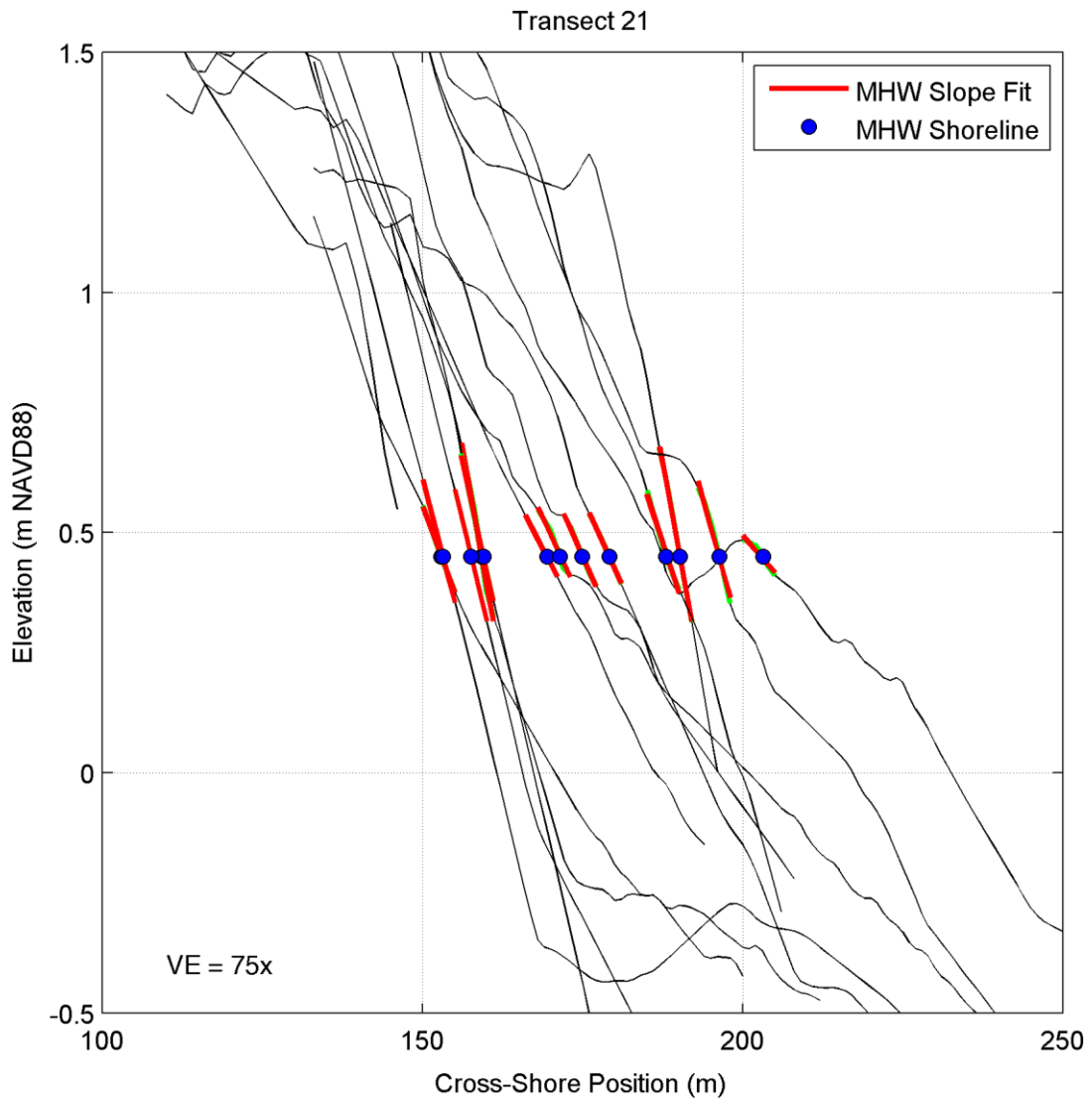


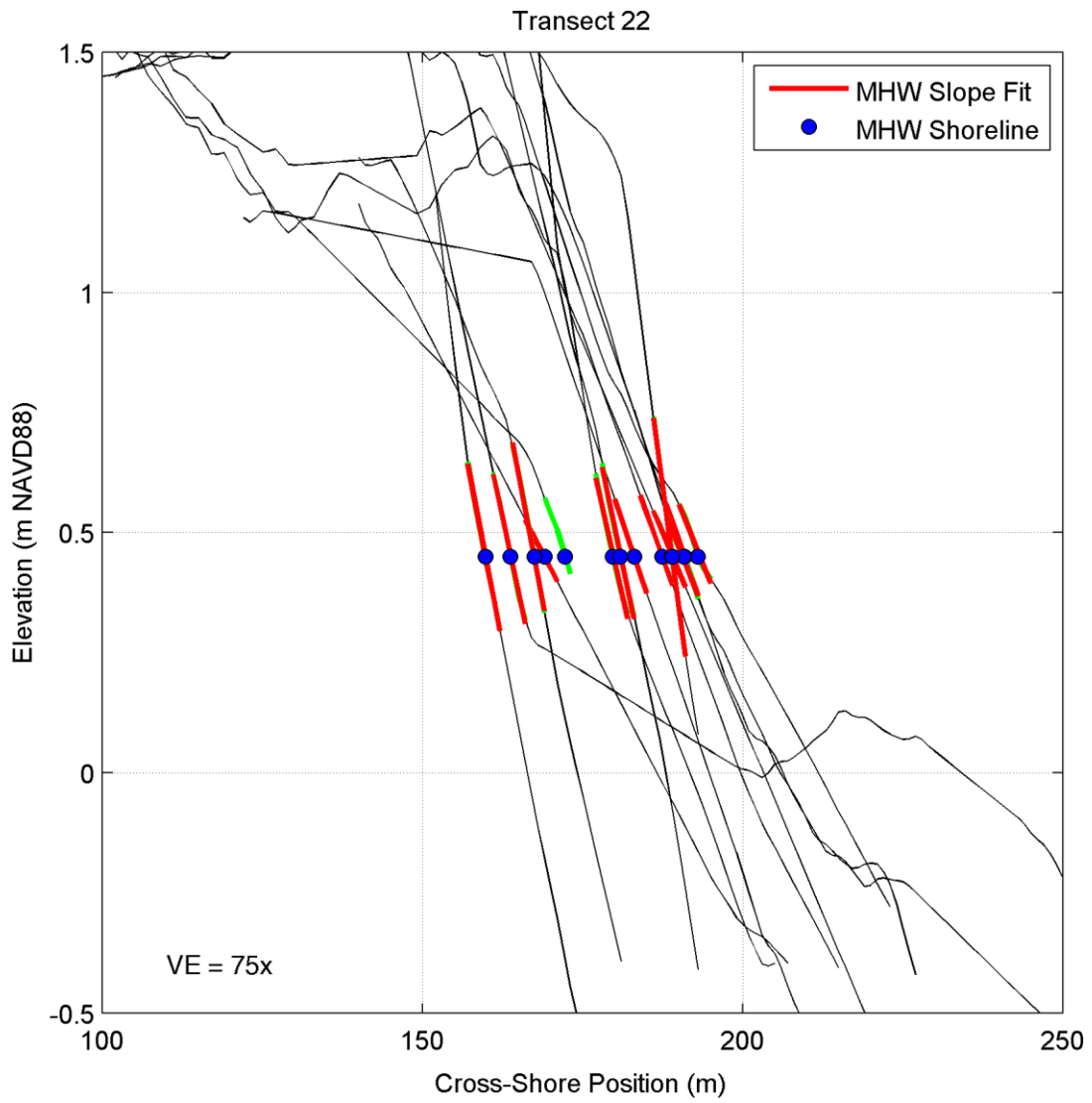
Transect 19

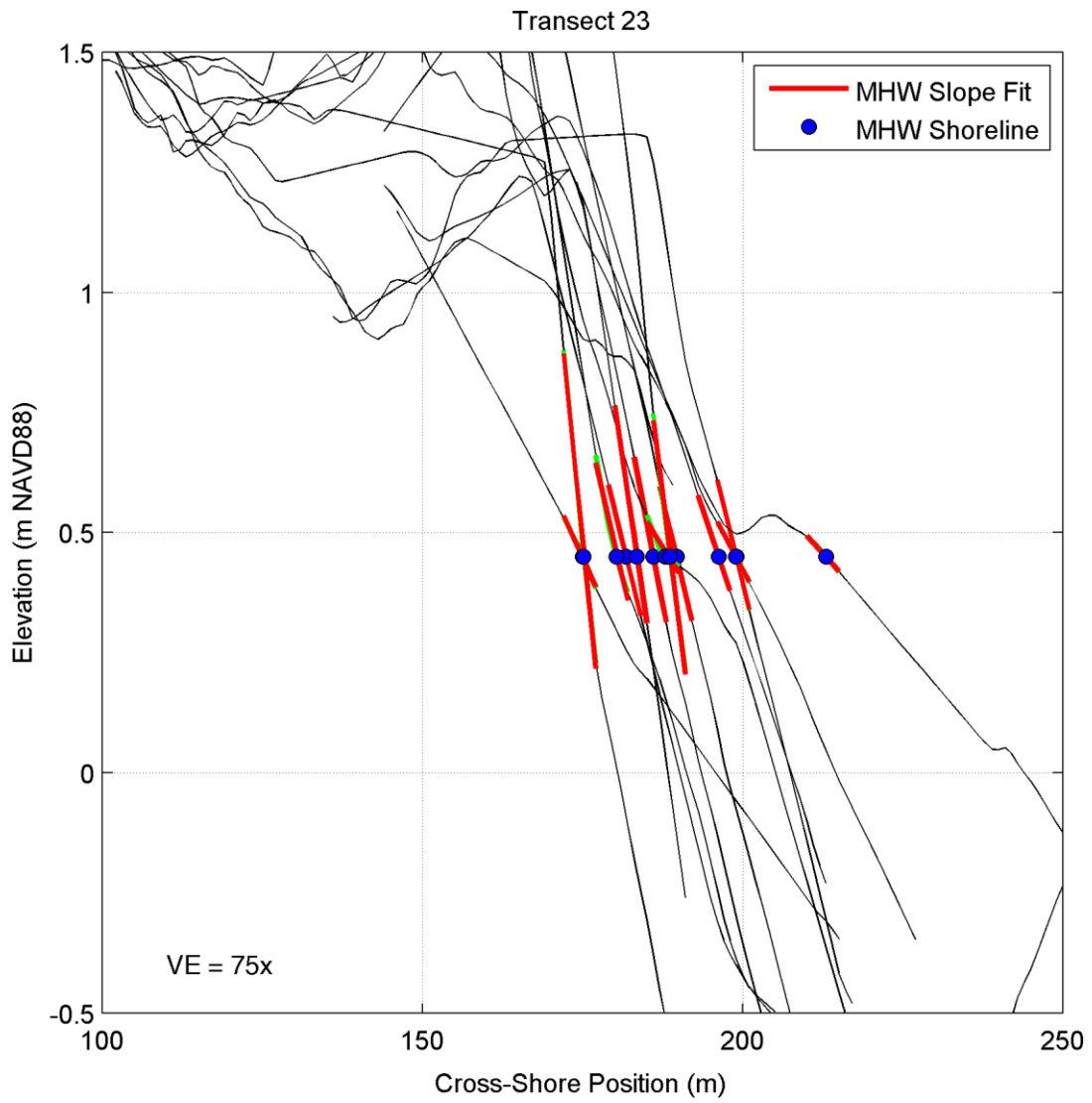


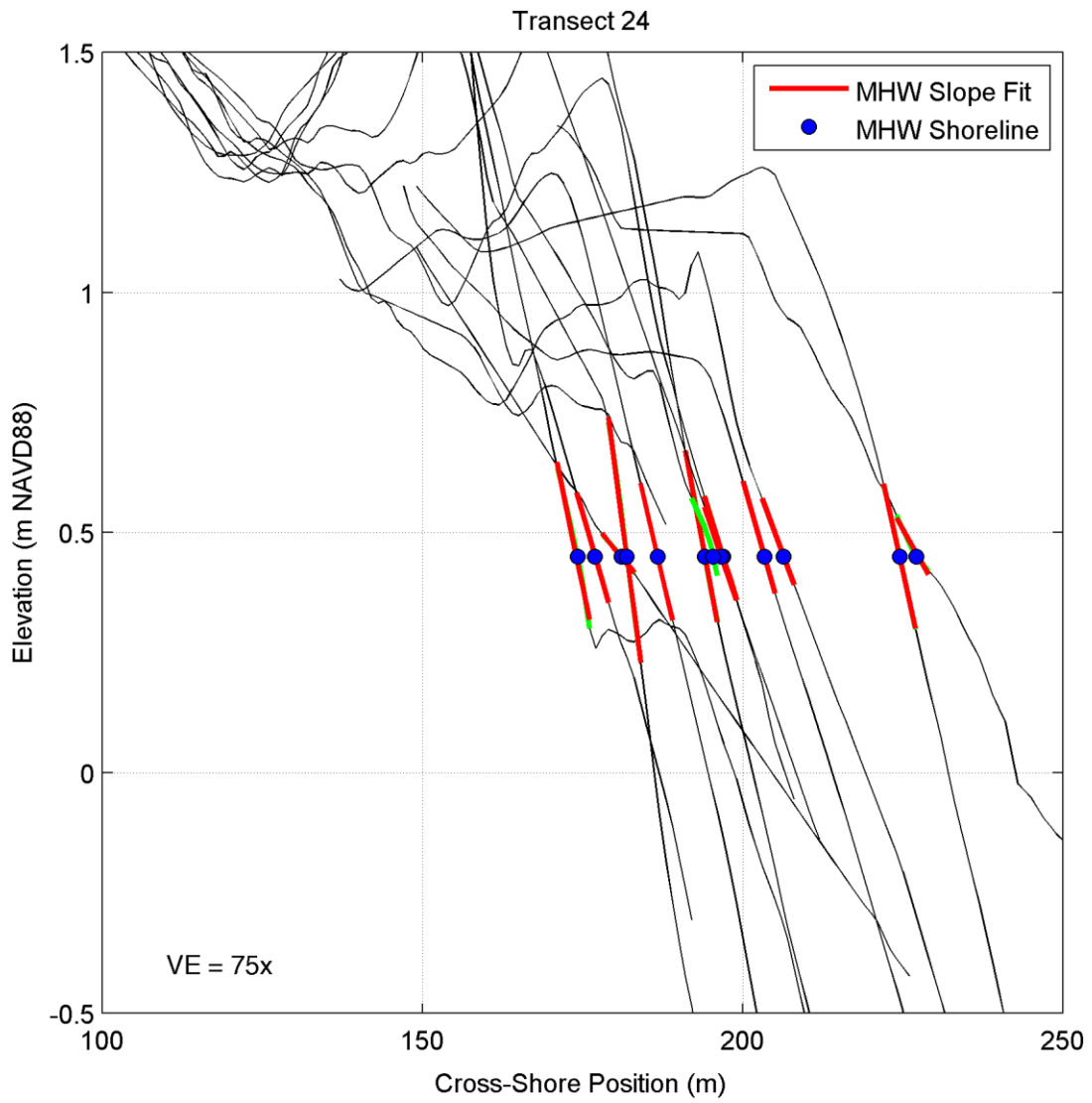
Transect 20

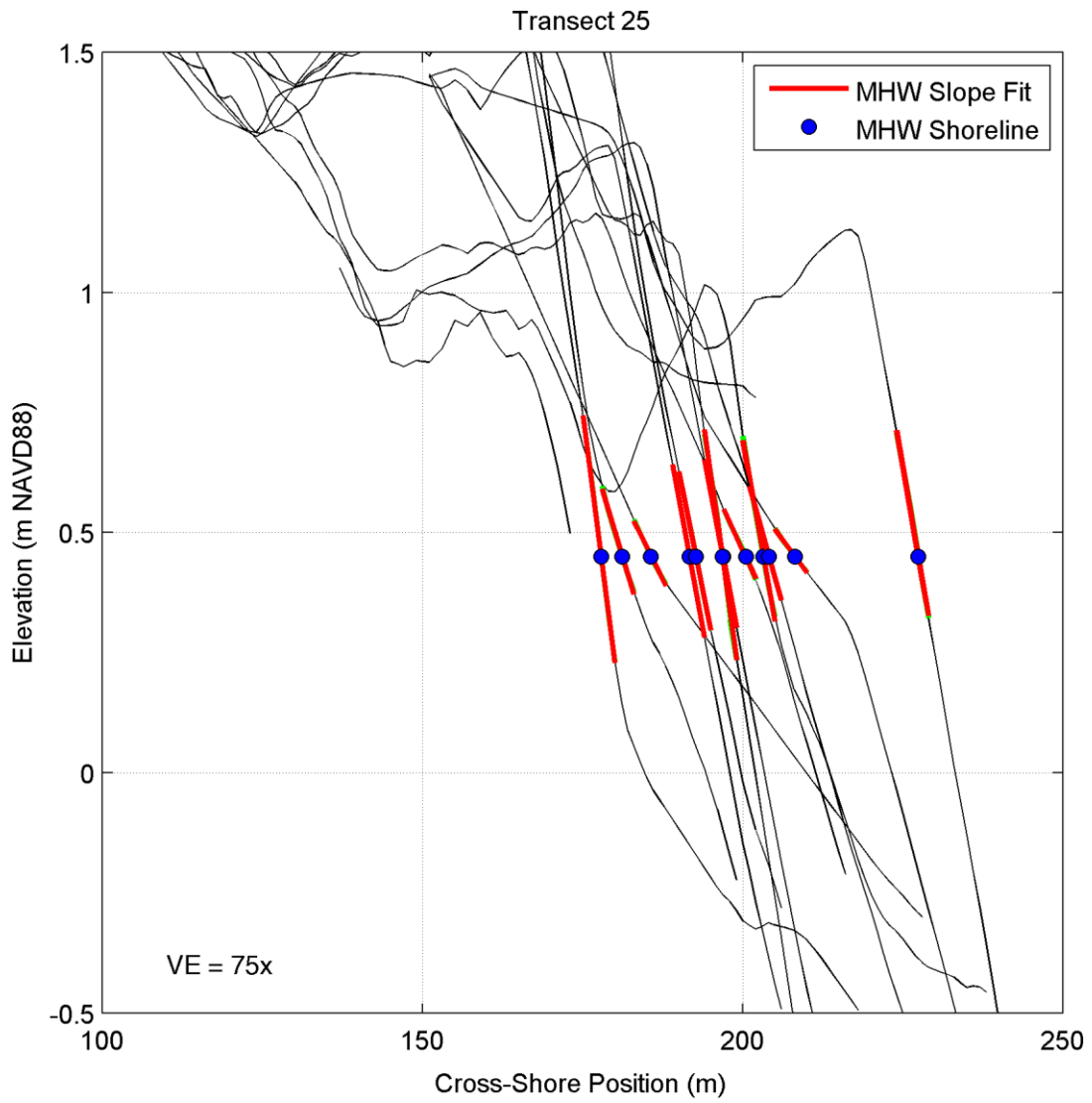


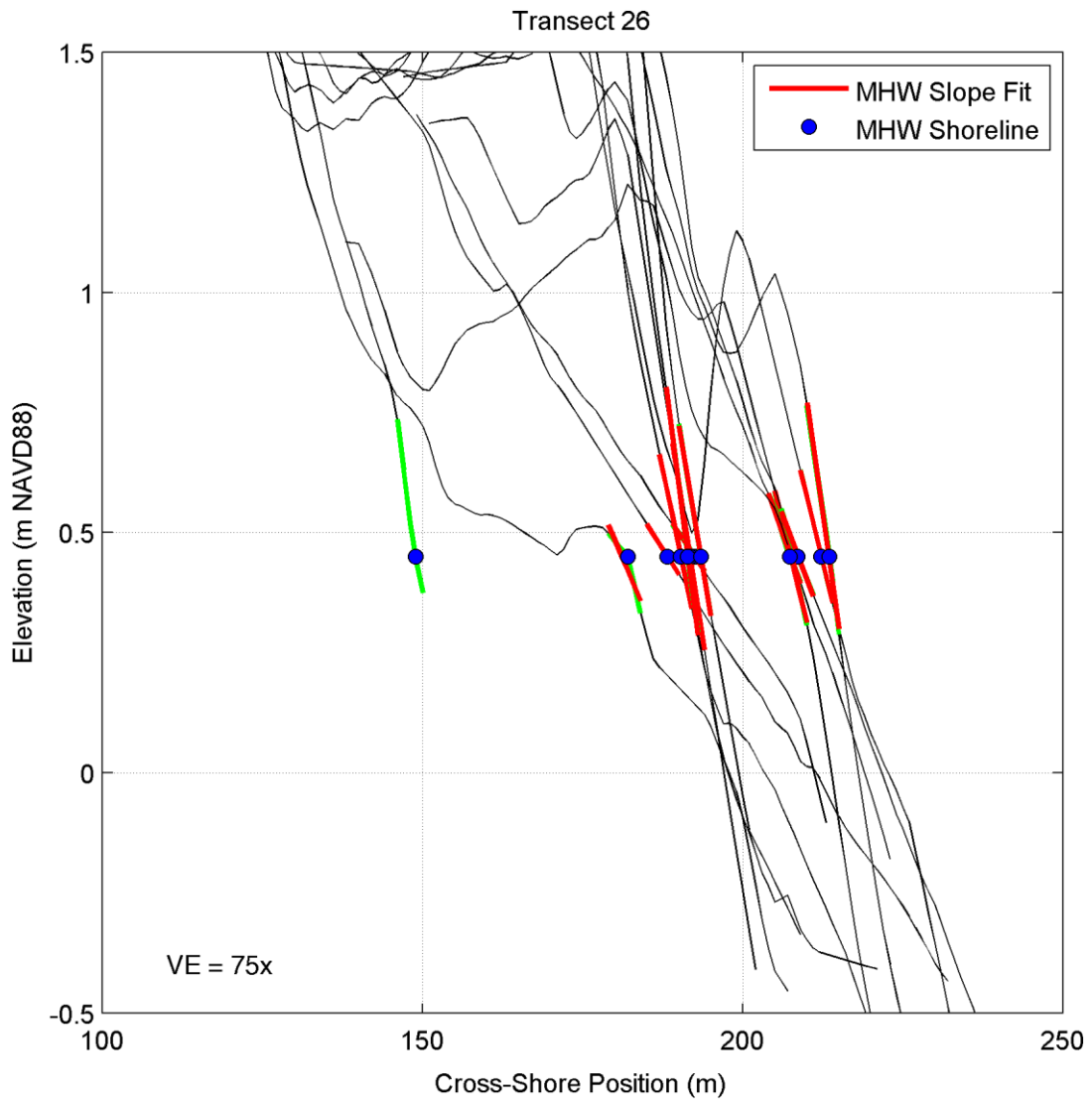


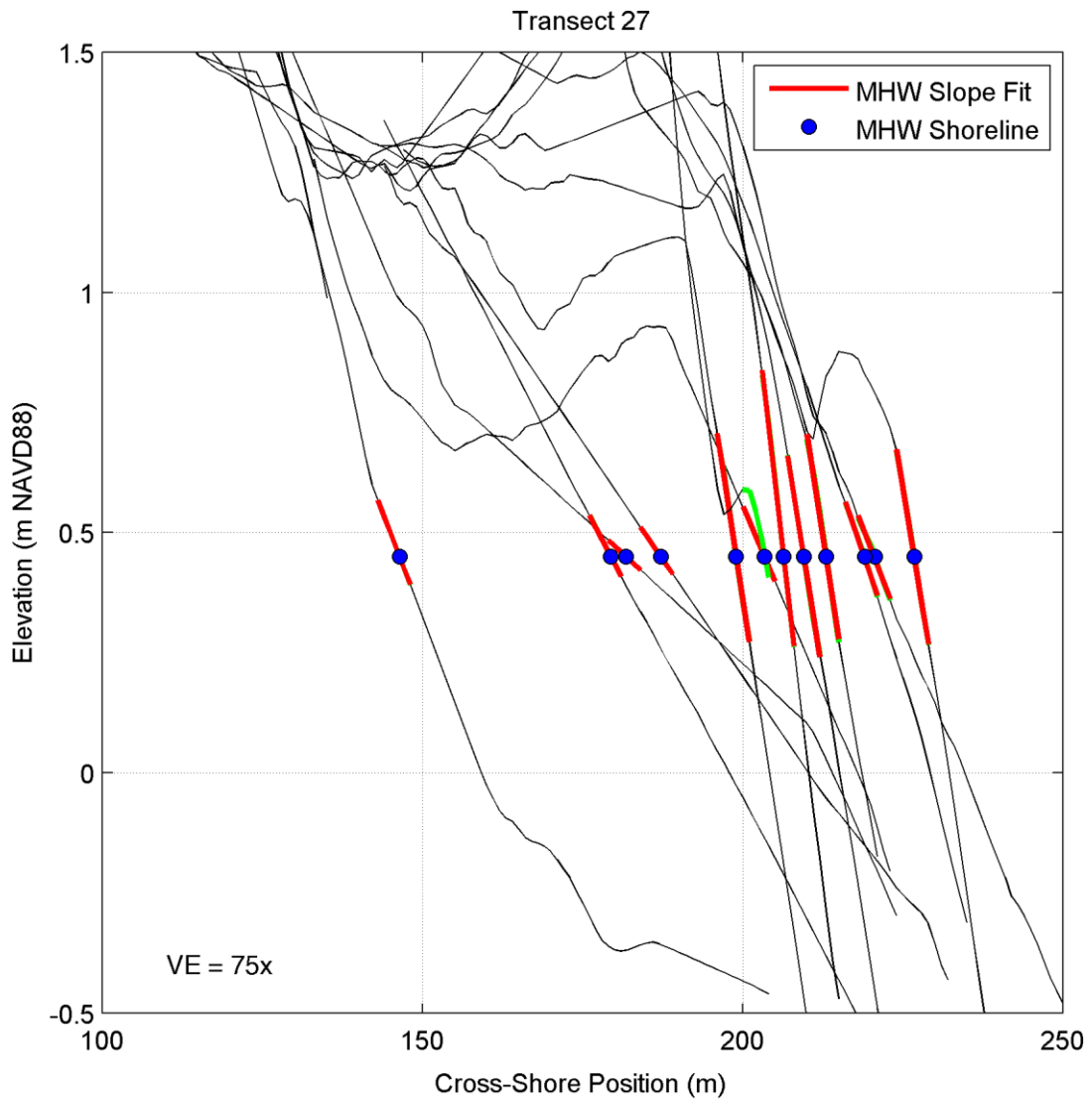


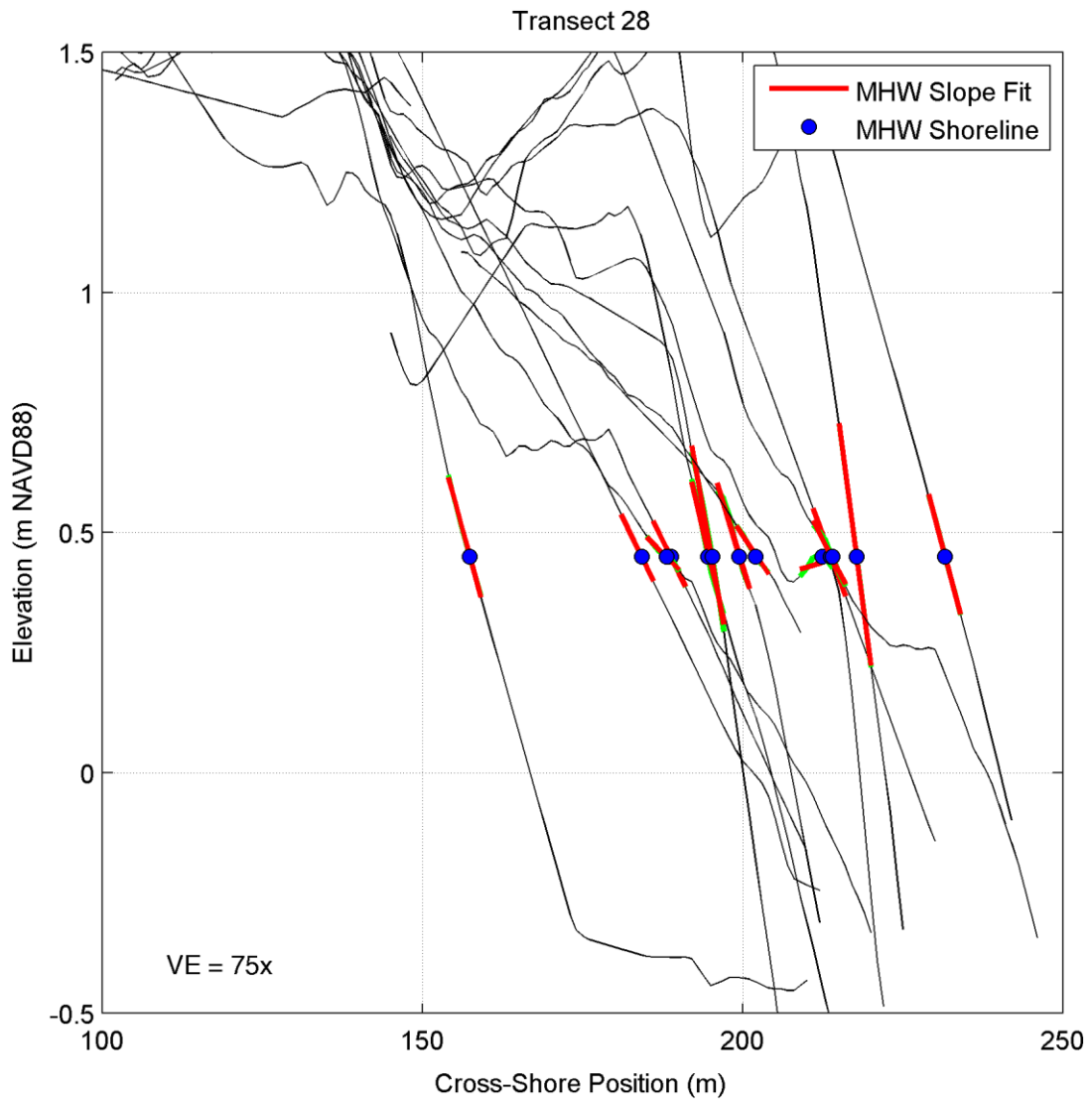


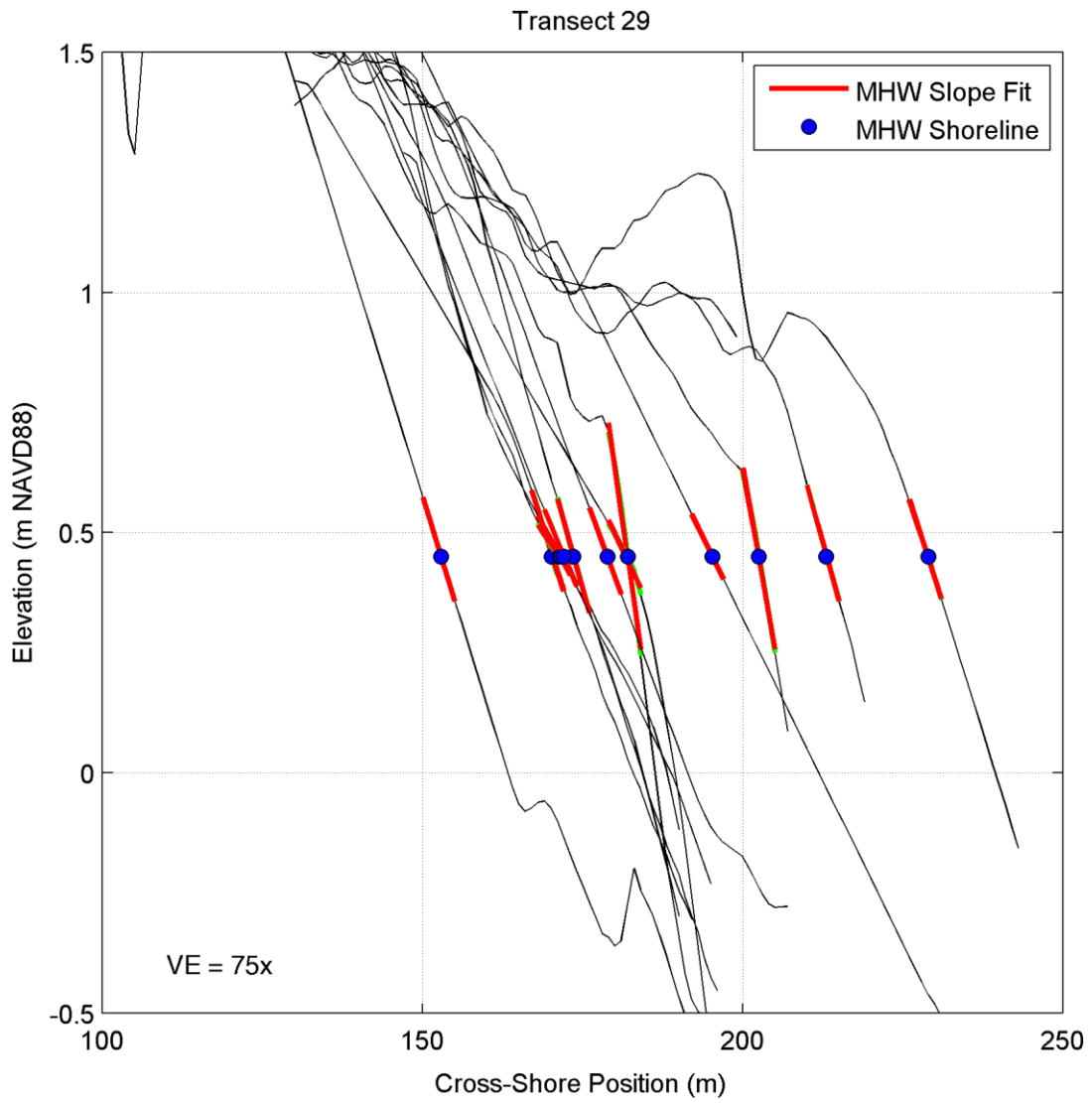


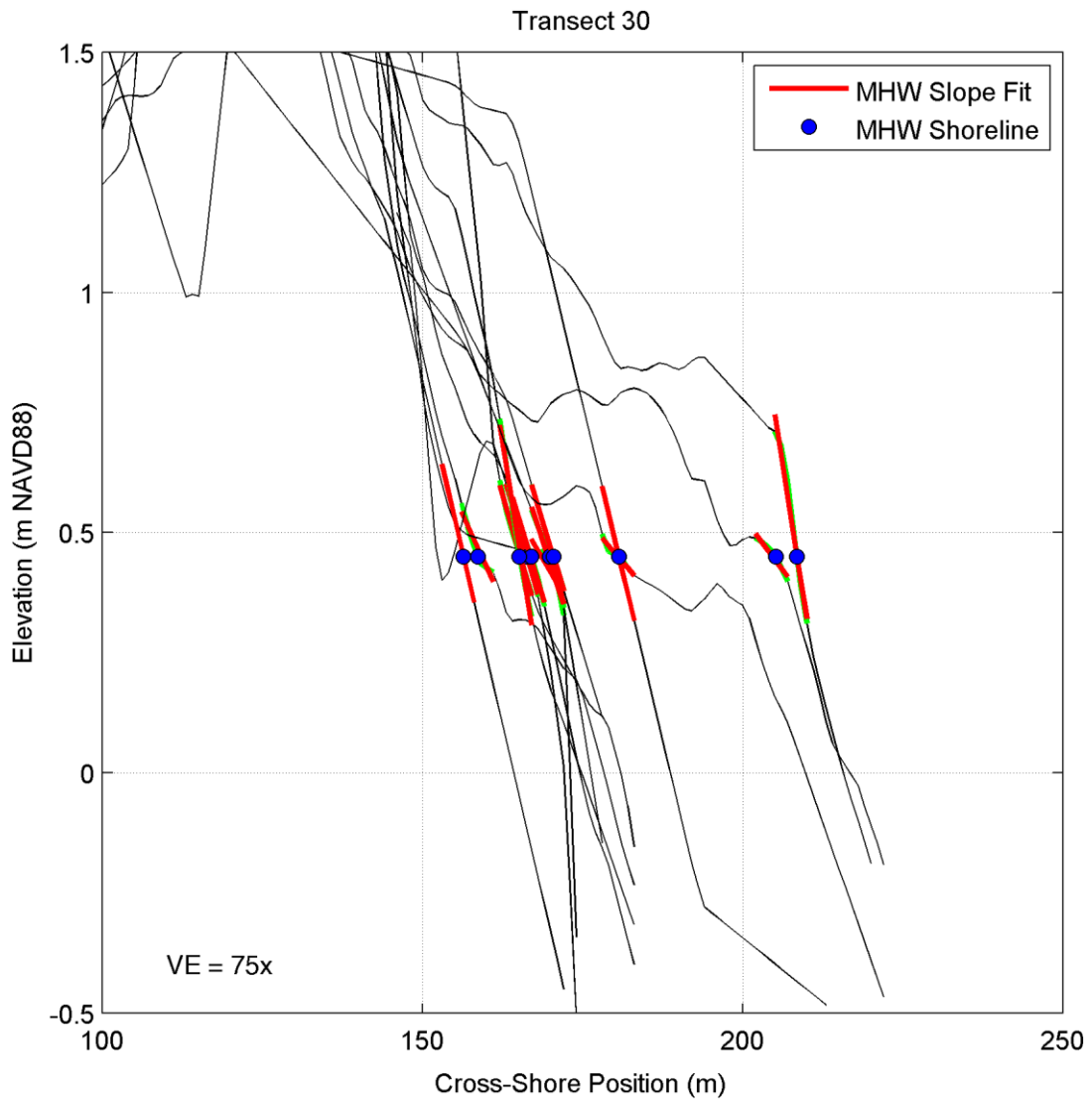




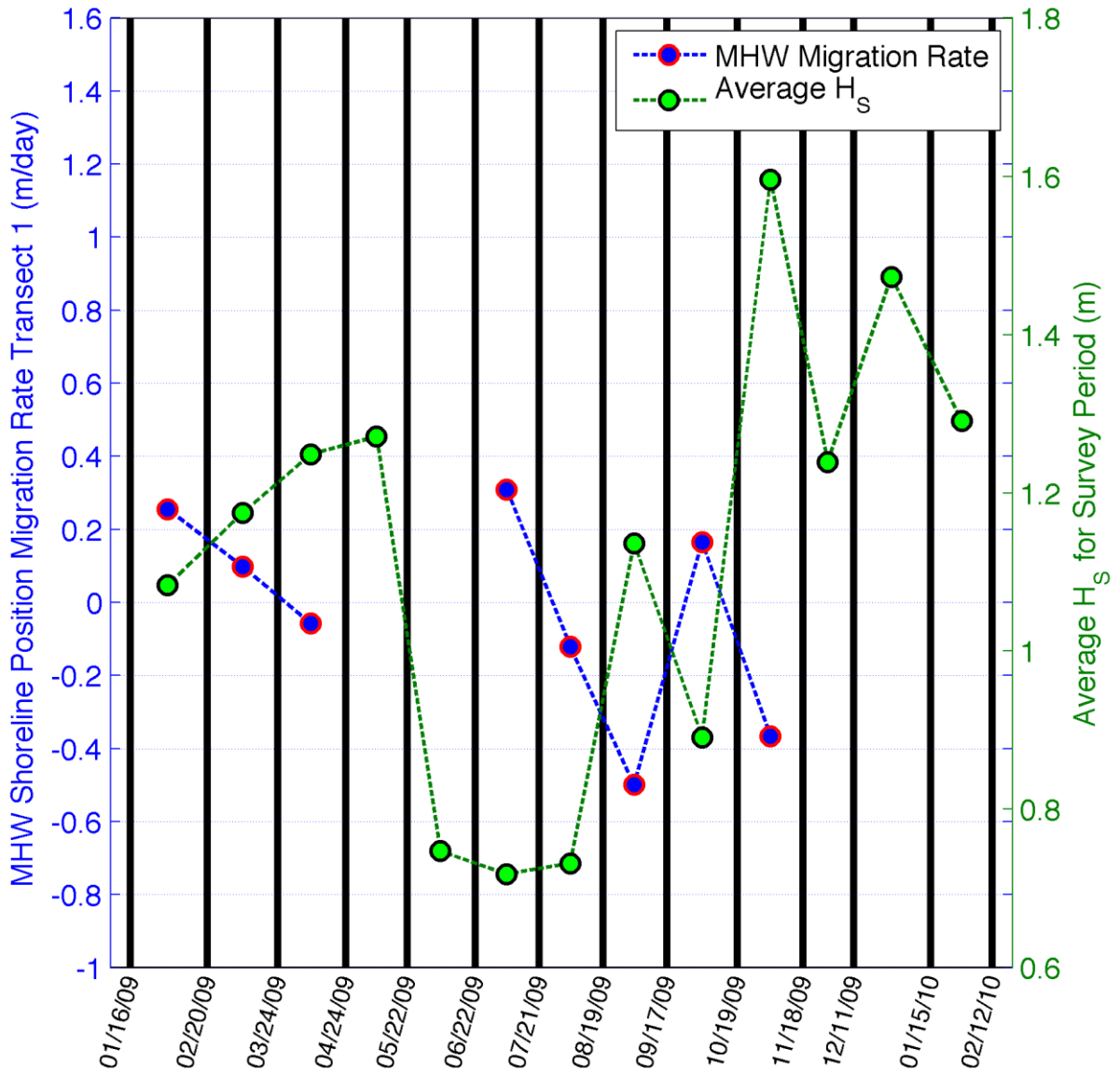




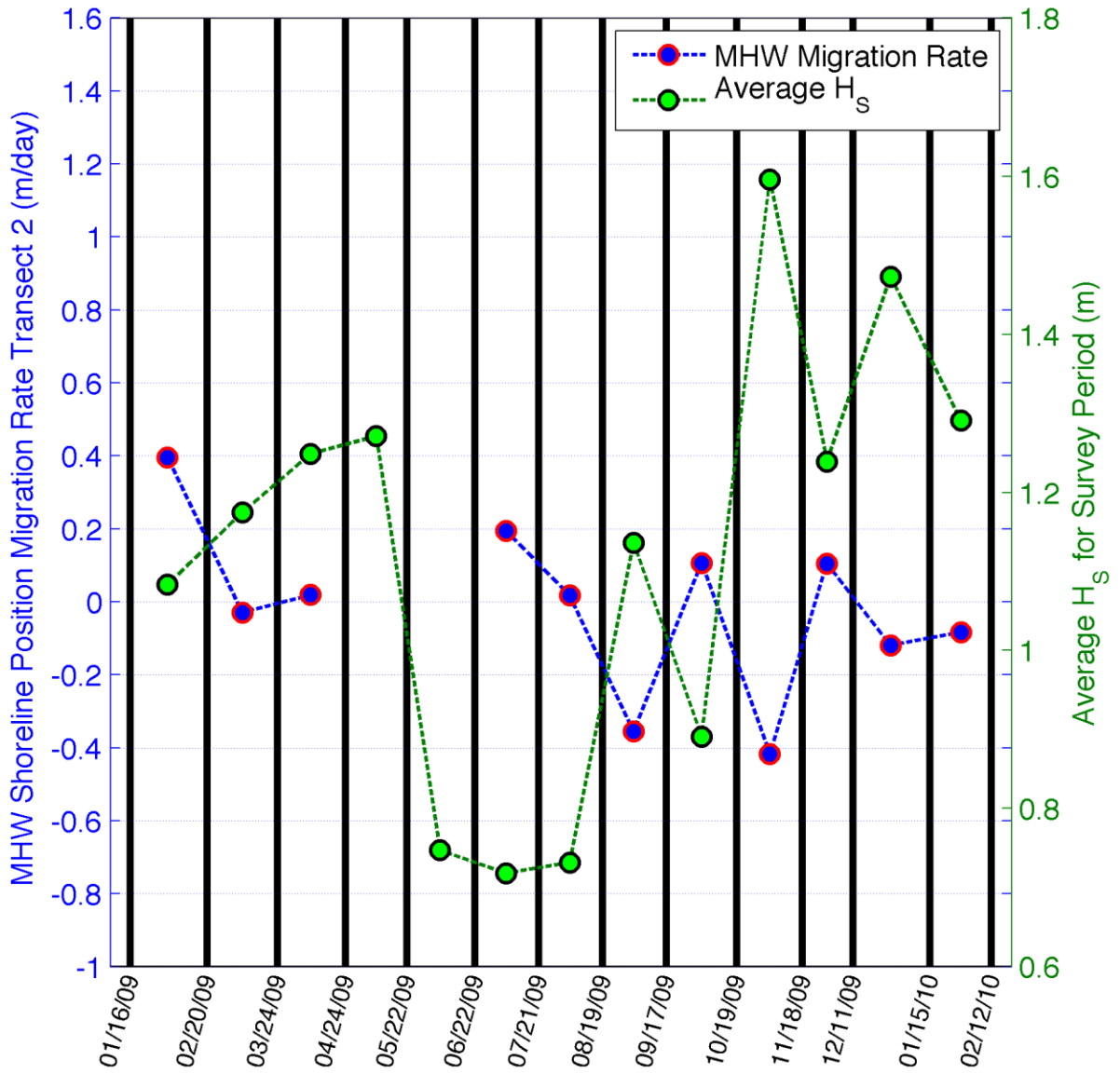




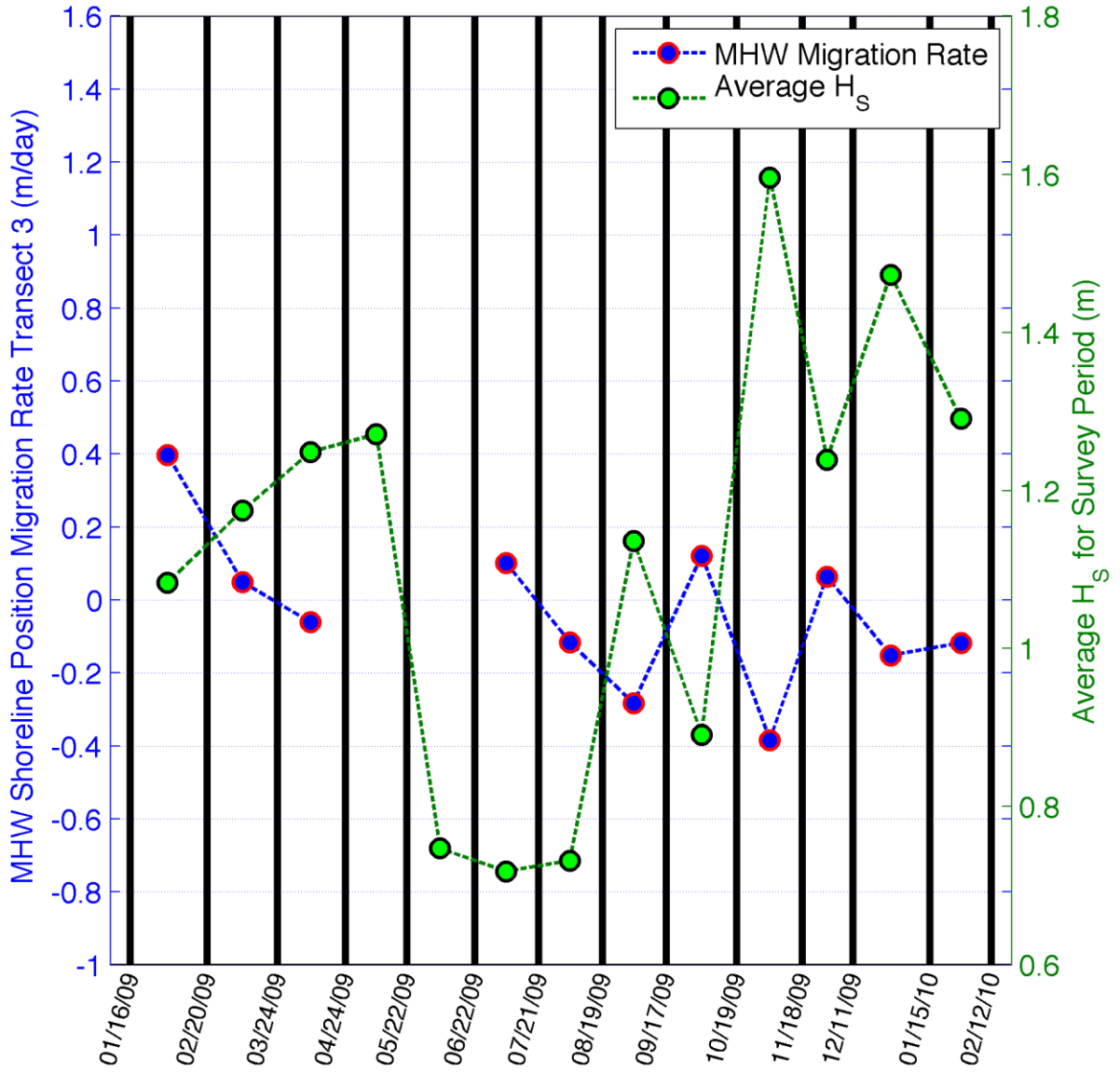
Transect 1



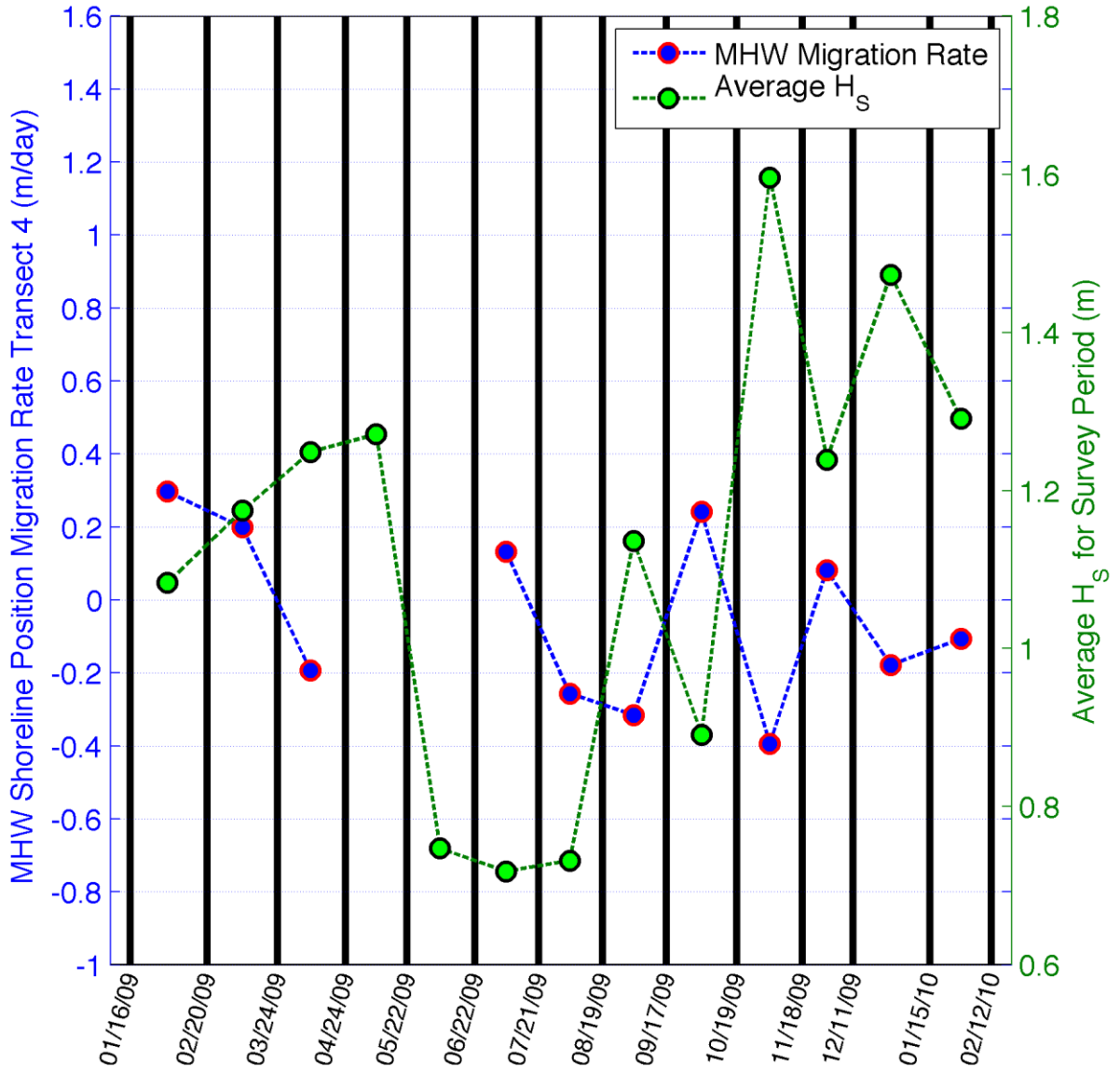
Transect 2



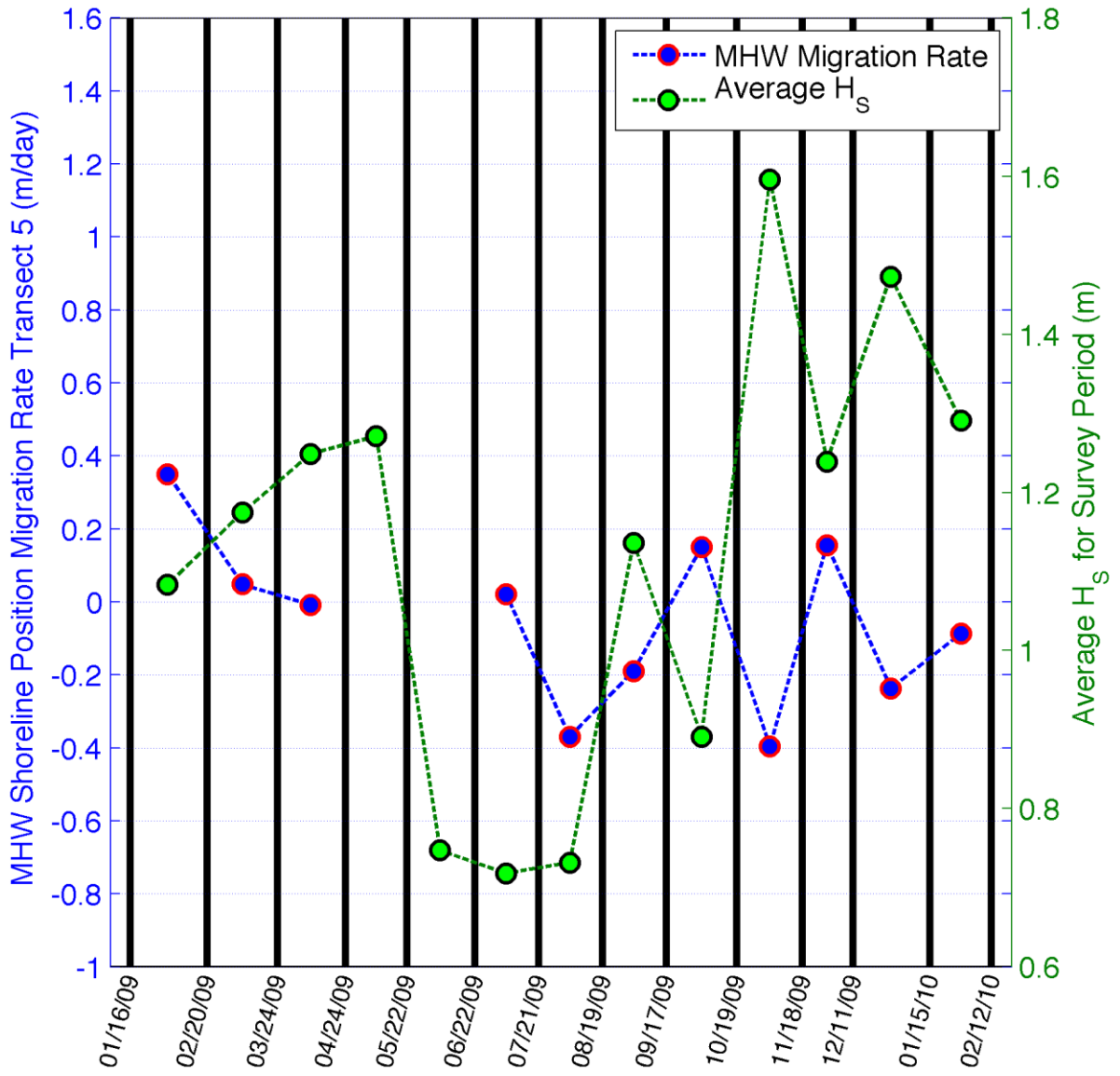
Transect 3



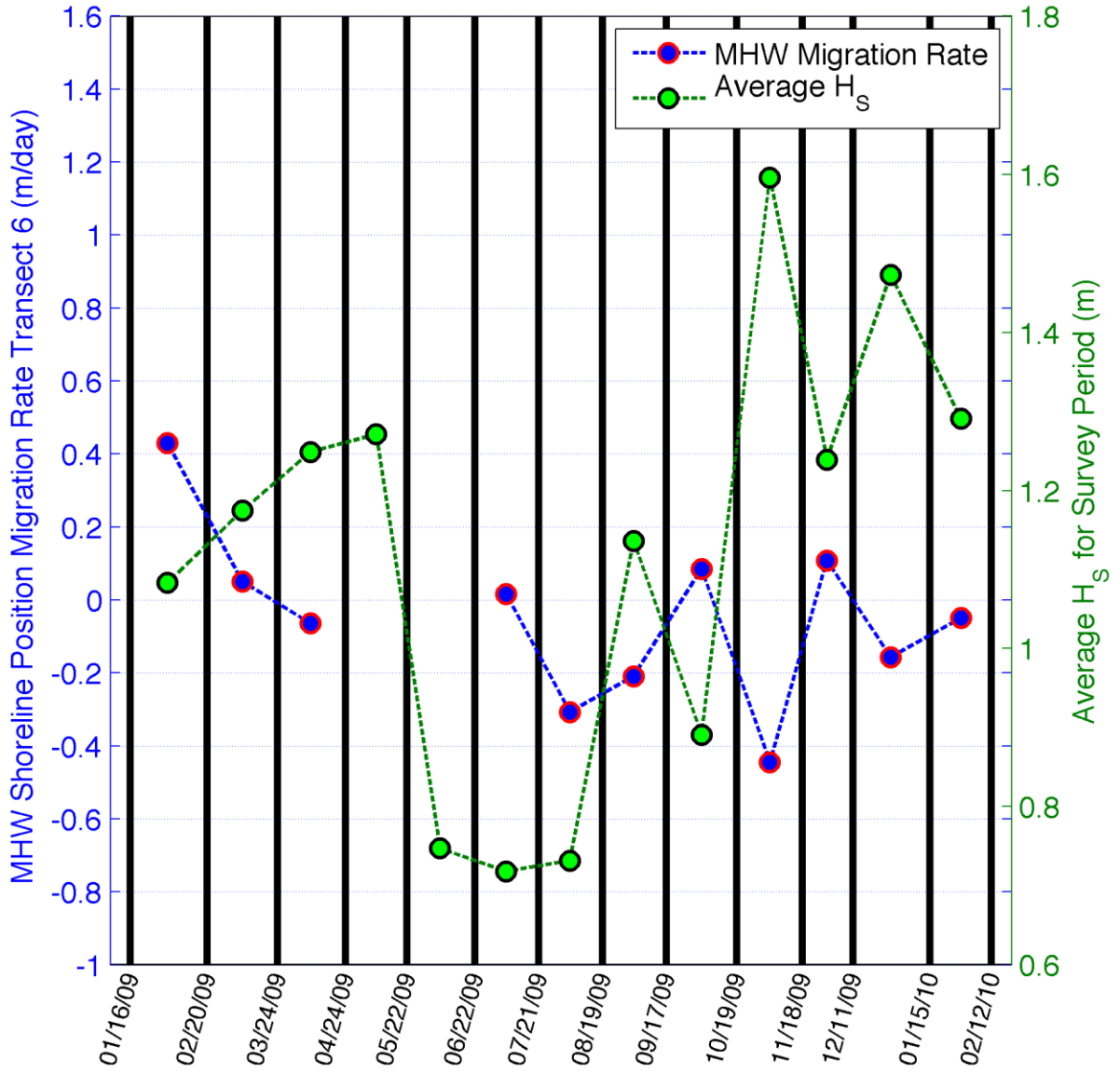
Transect 4



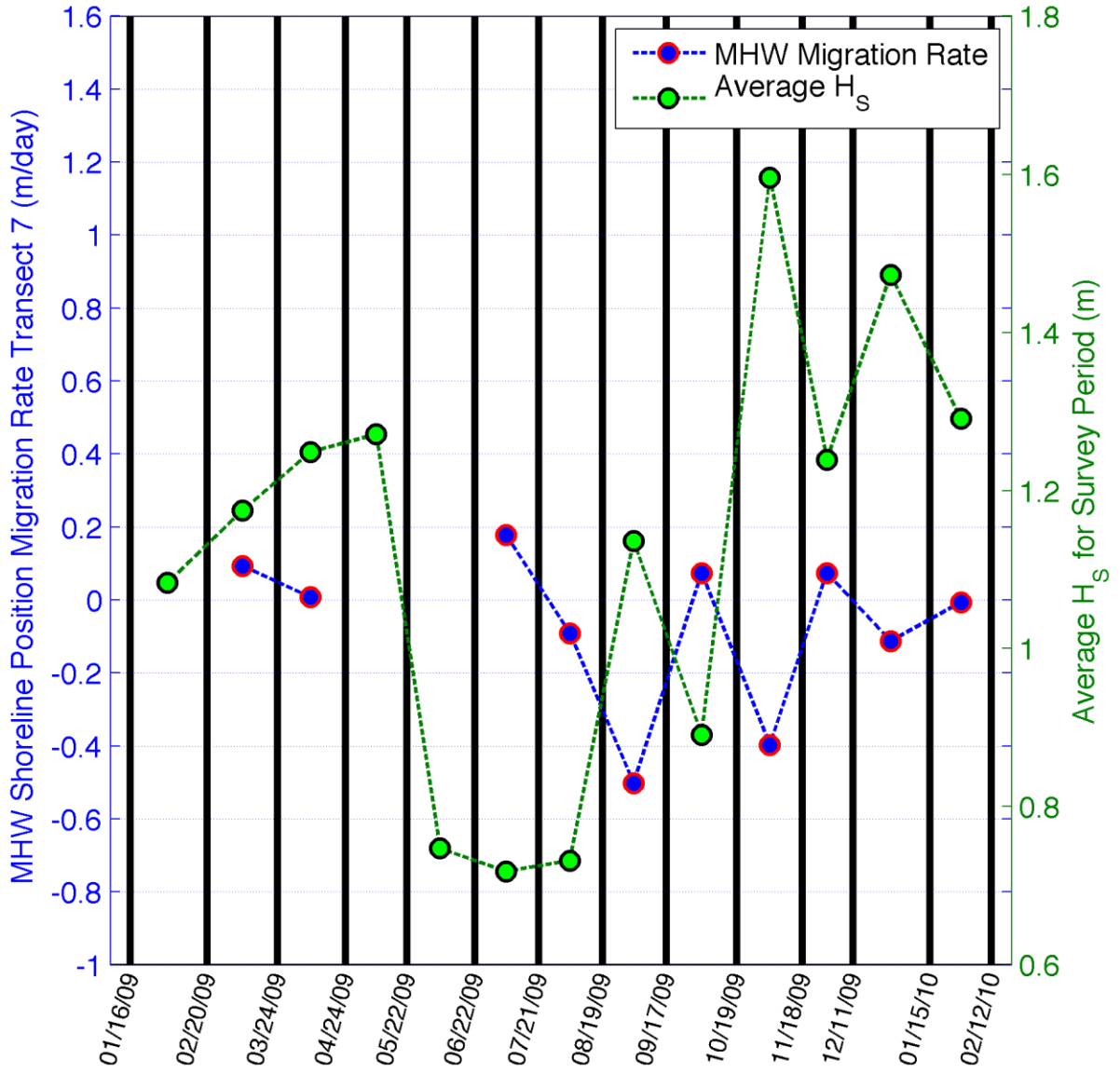
Transect 5



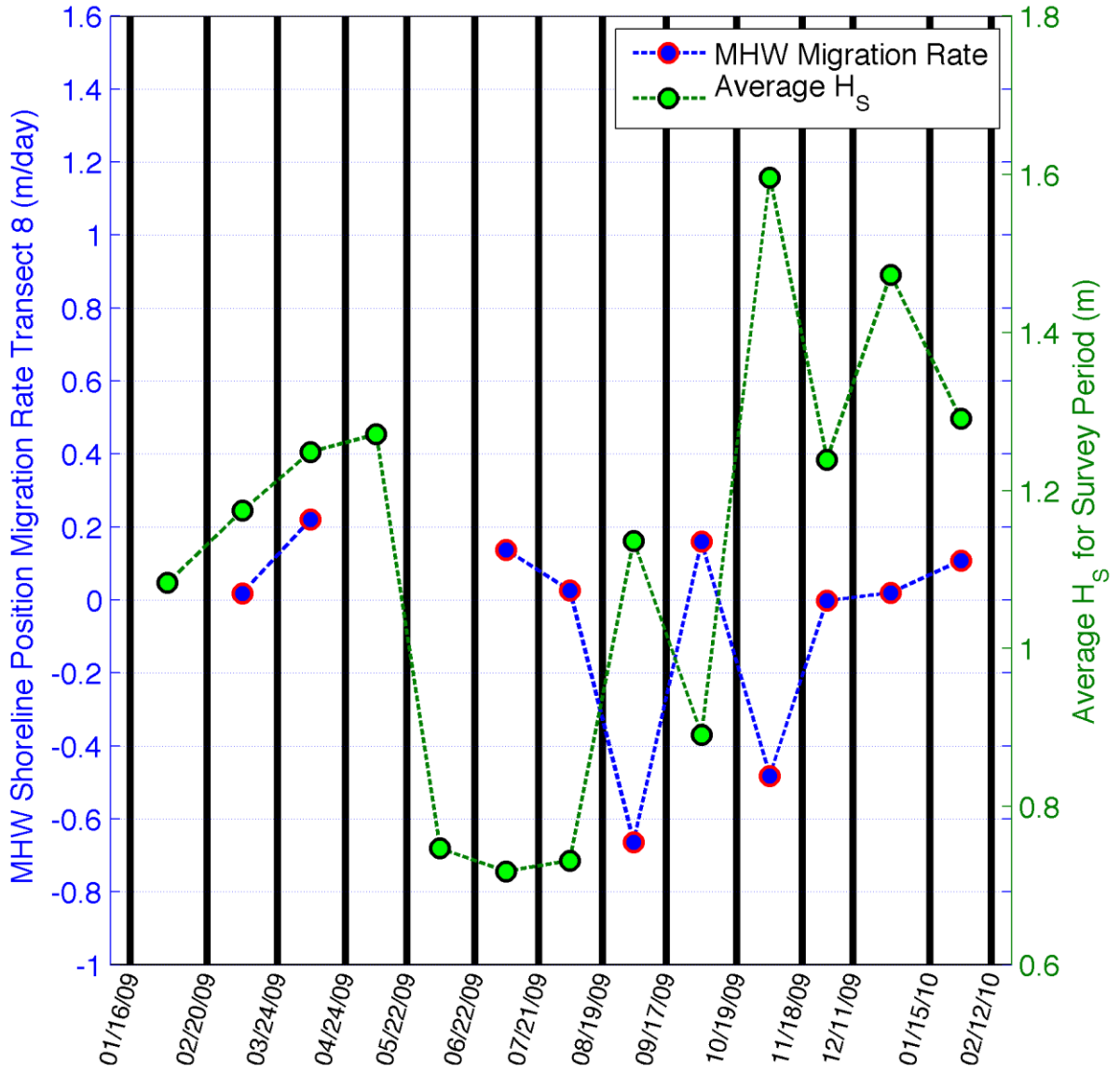
Transect 6



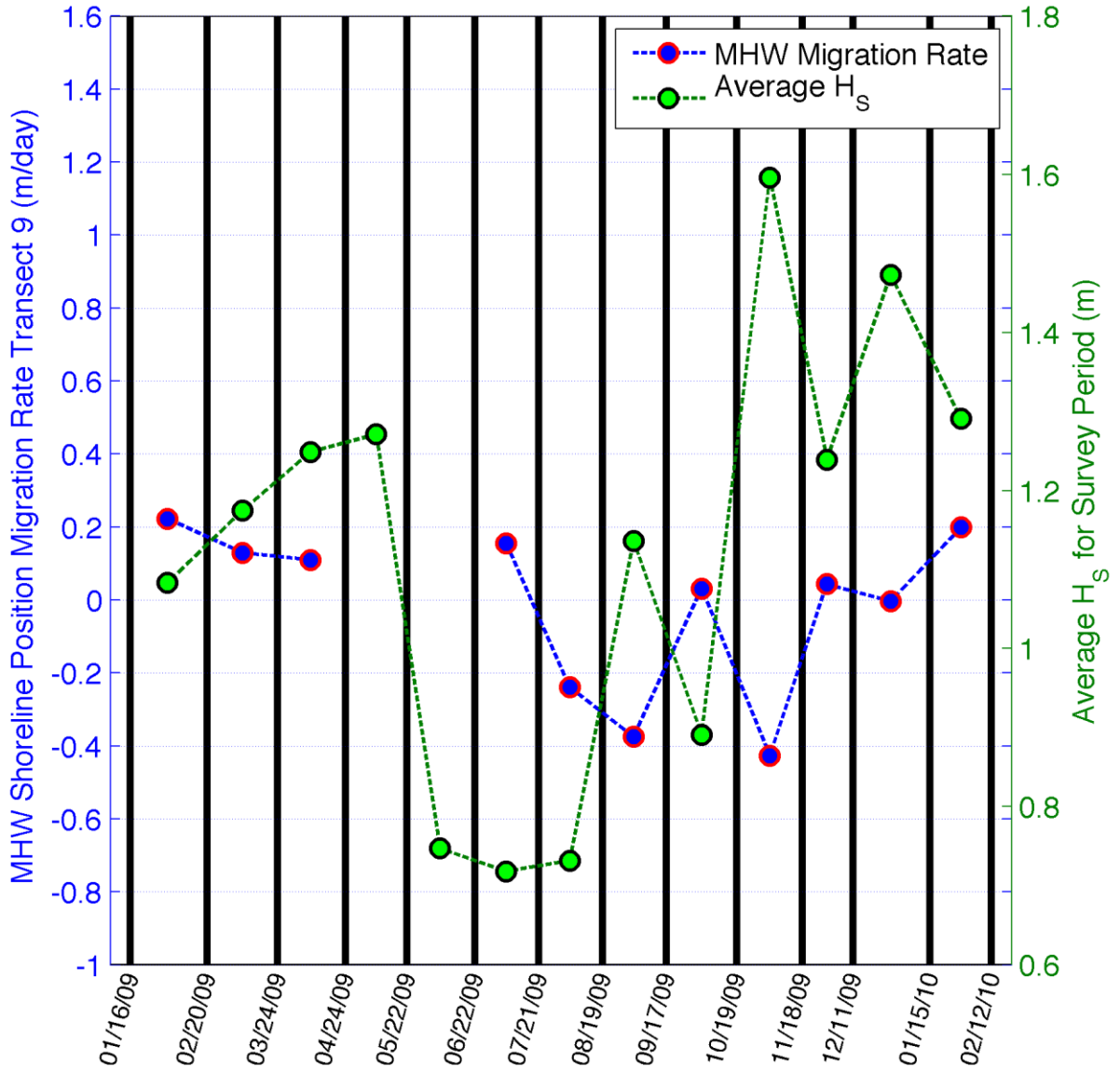
Transect 7



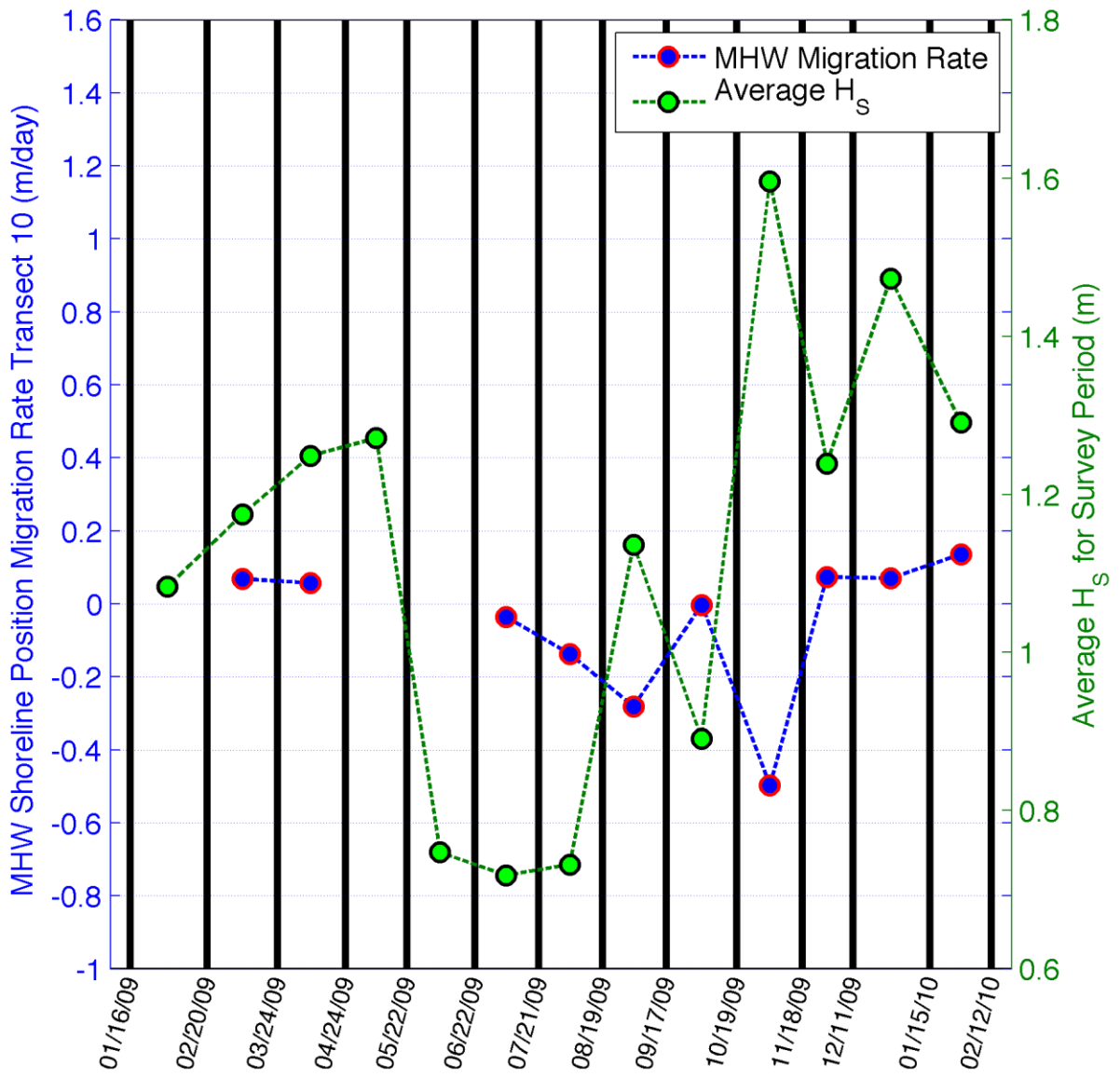
Transect 8



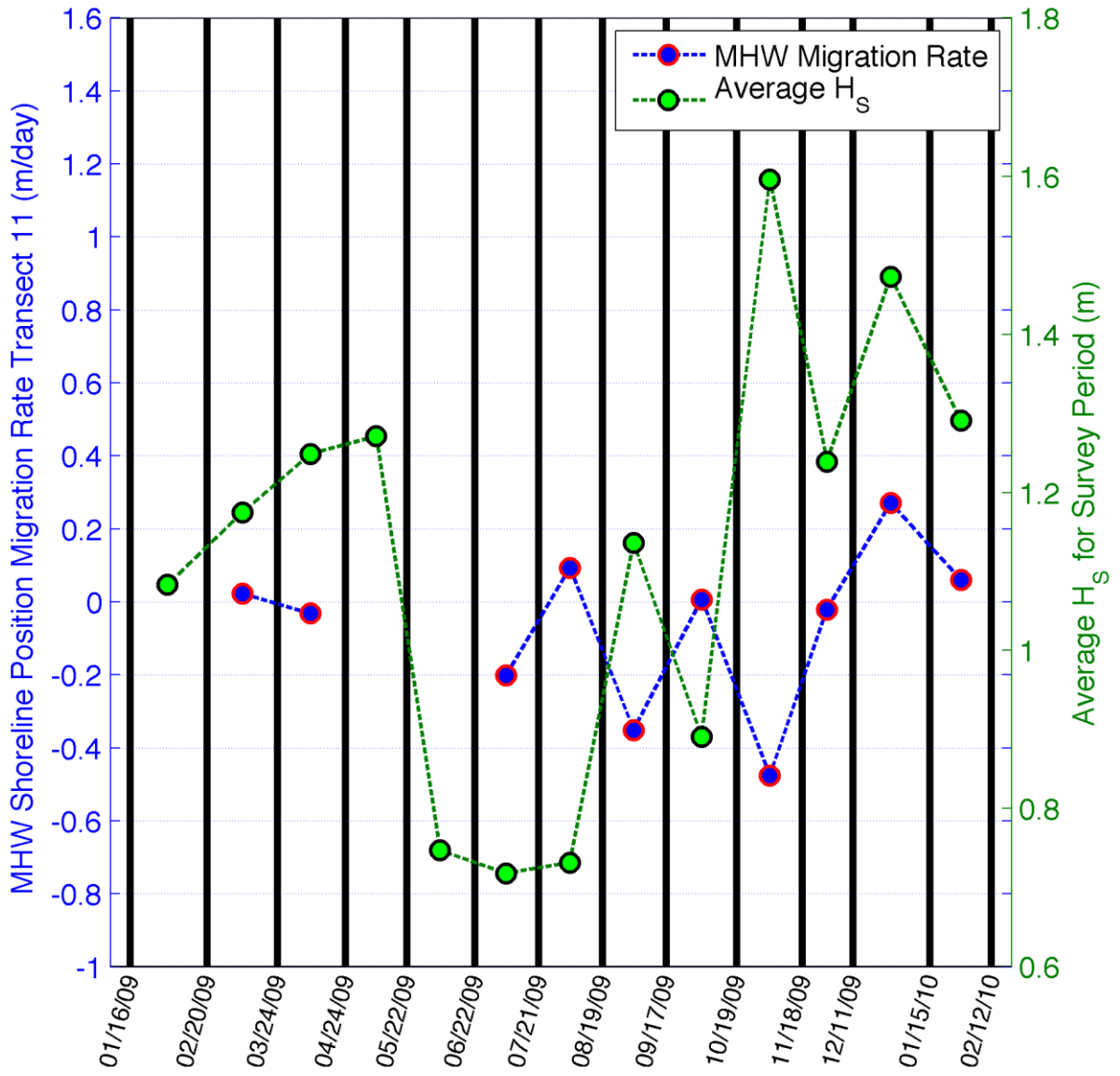
Transect 9



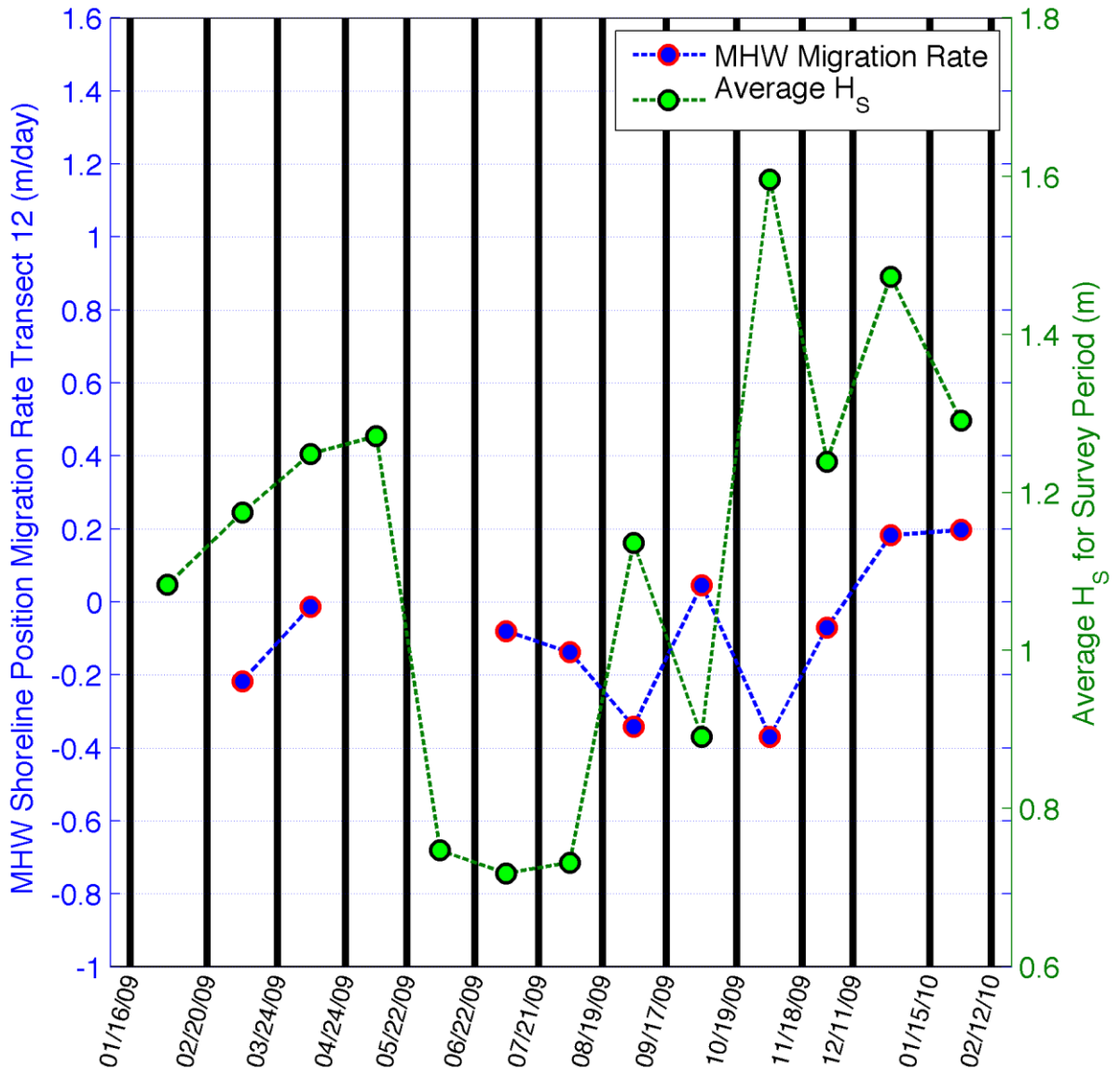
Transect 10



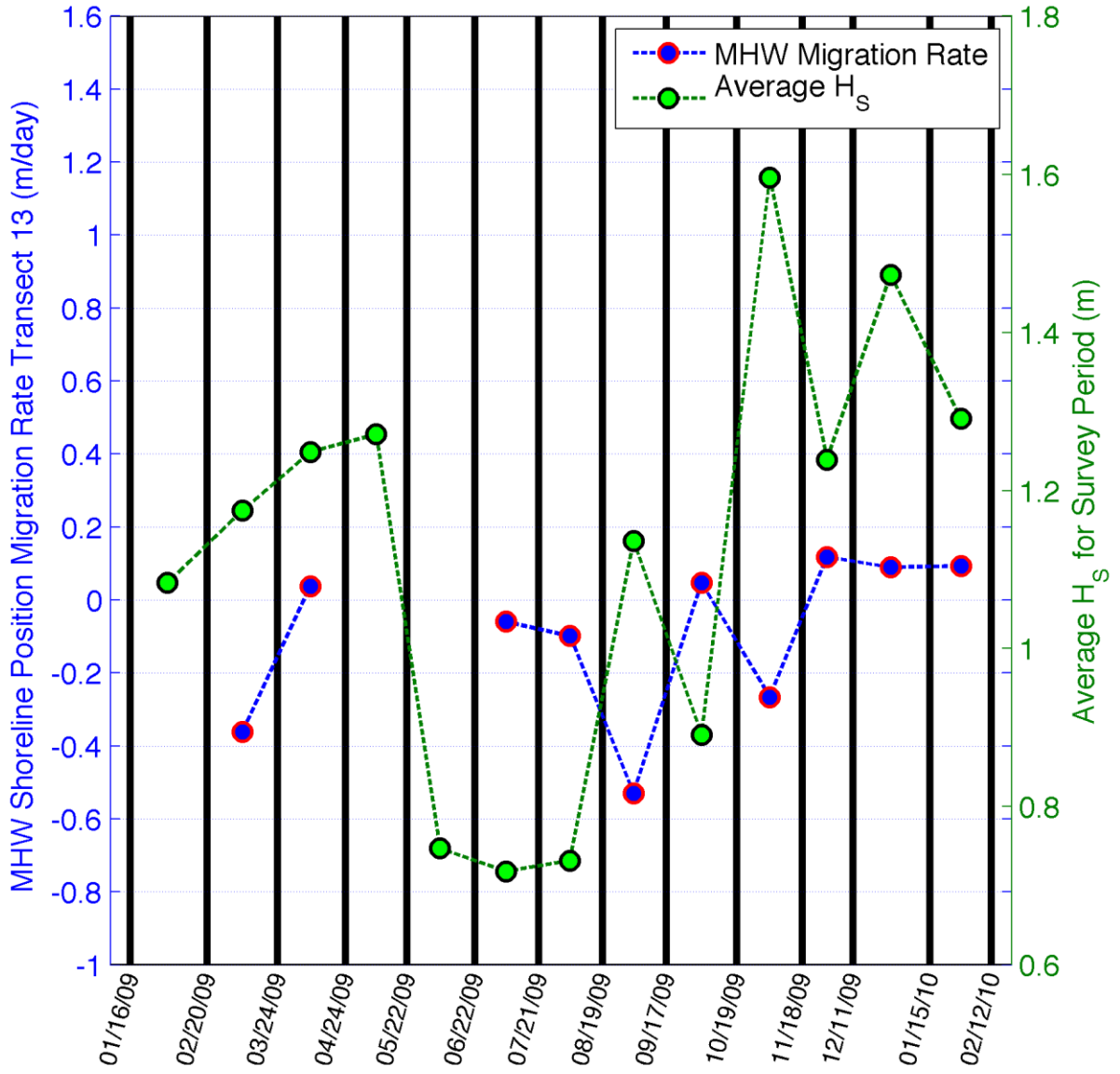
Transect 11



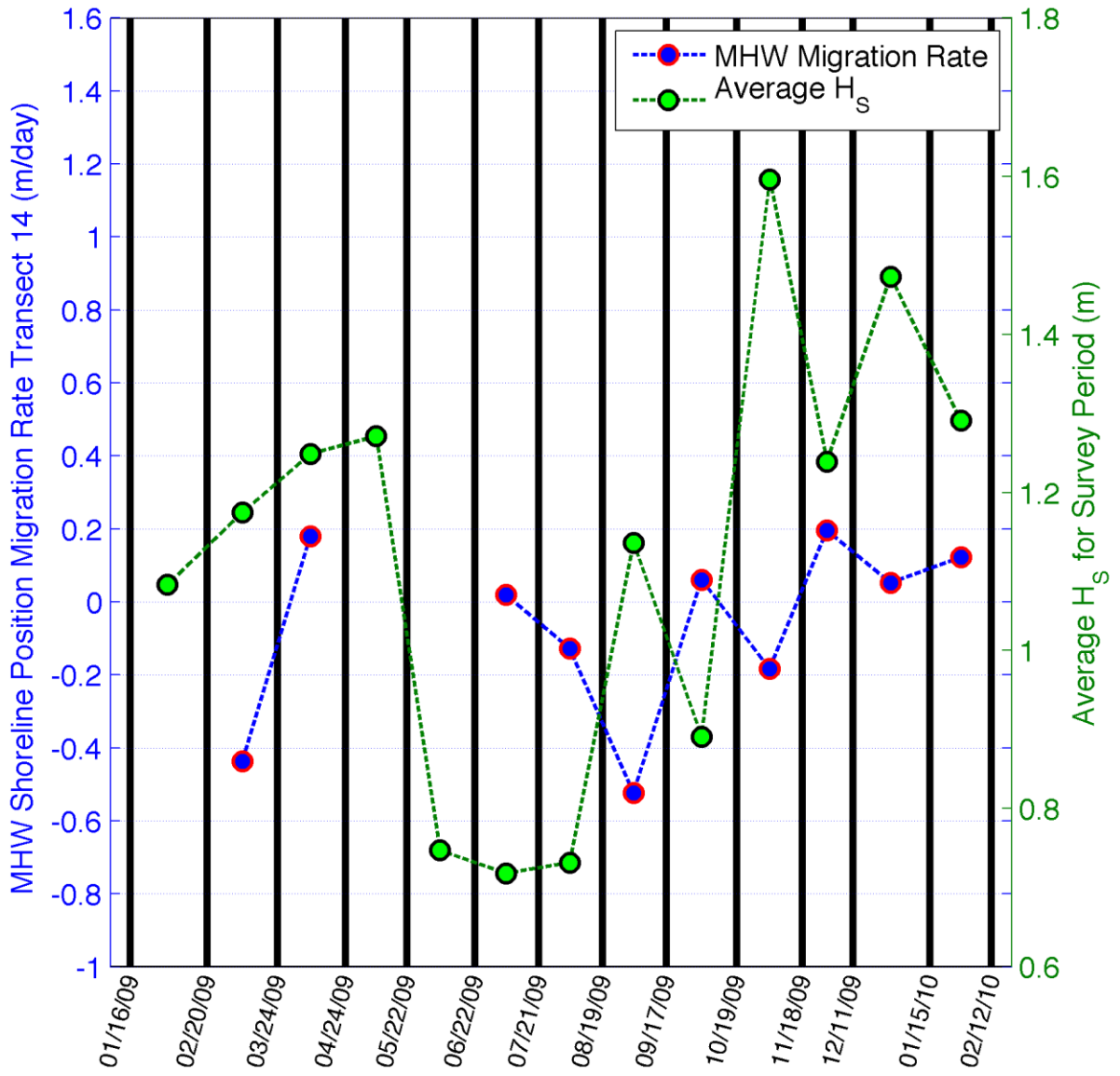
Transect 12



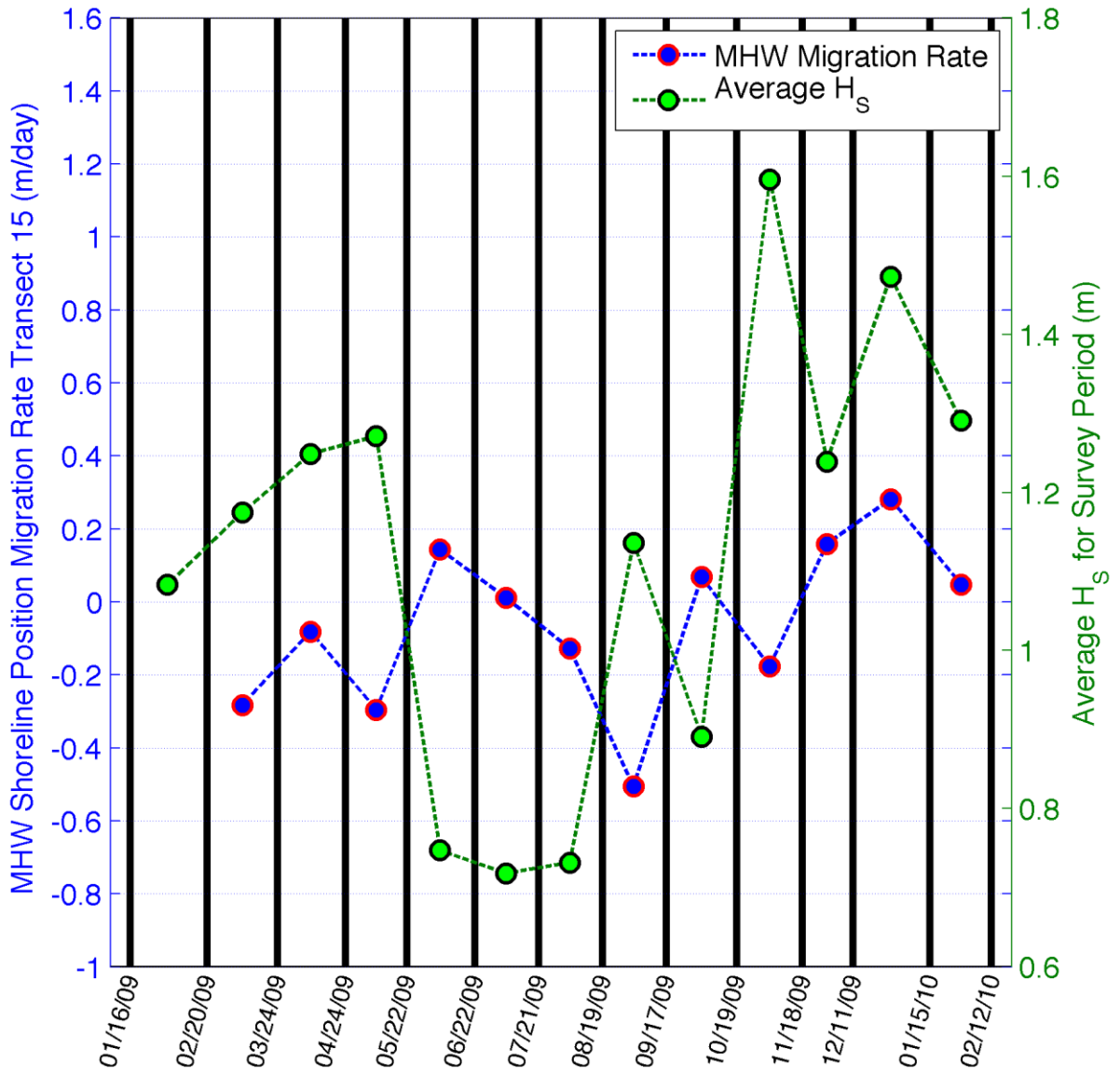
Transect 13



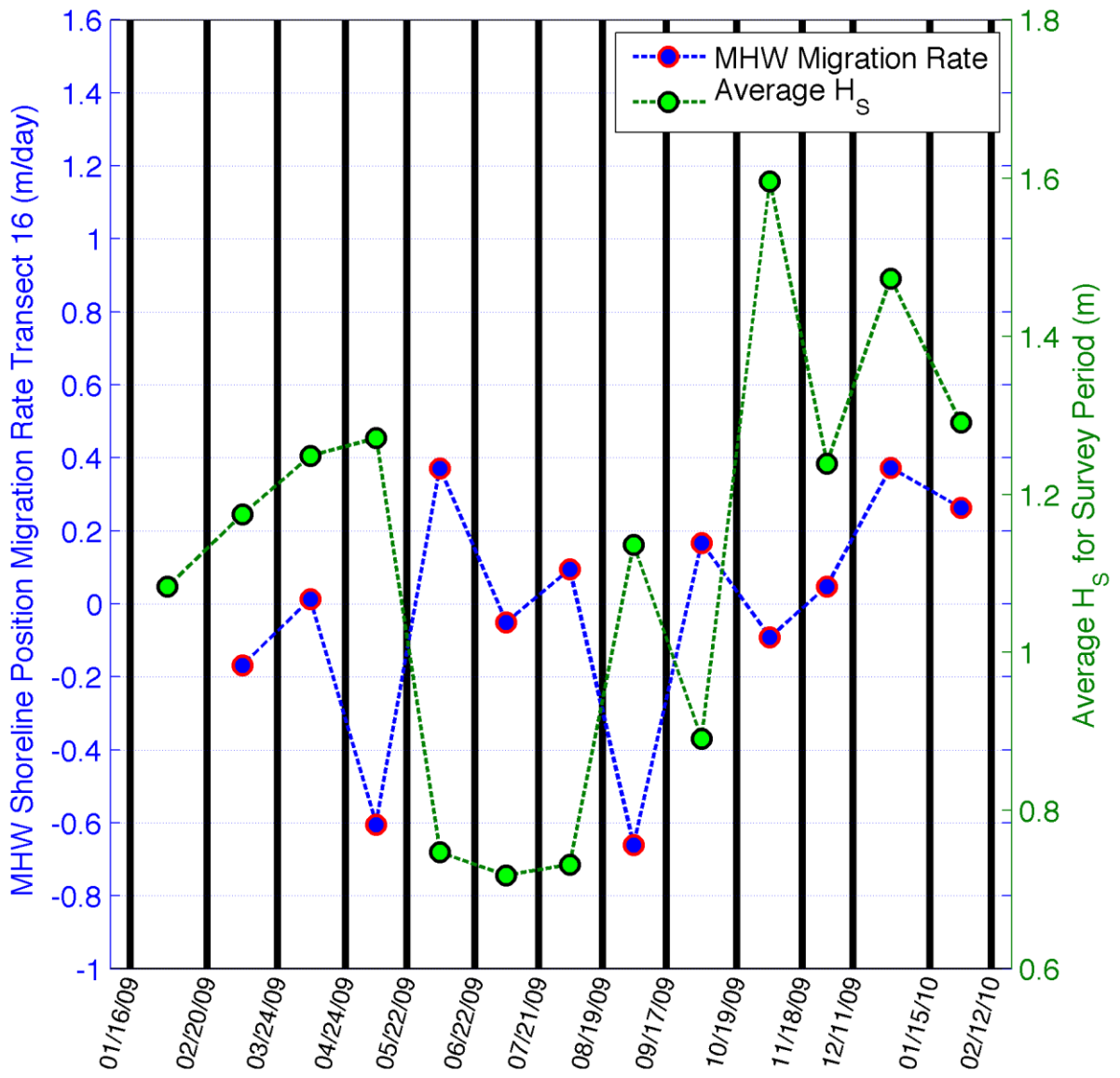
Transect 14



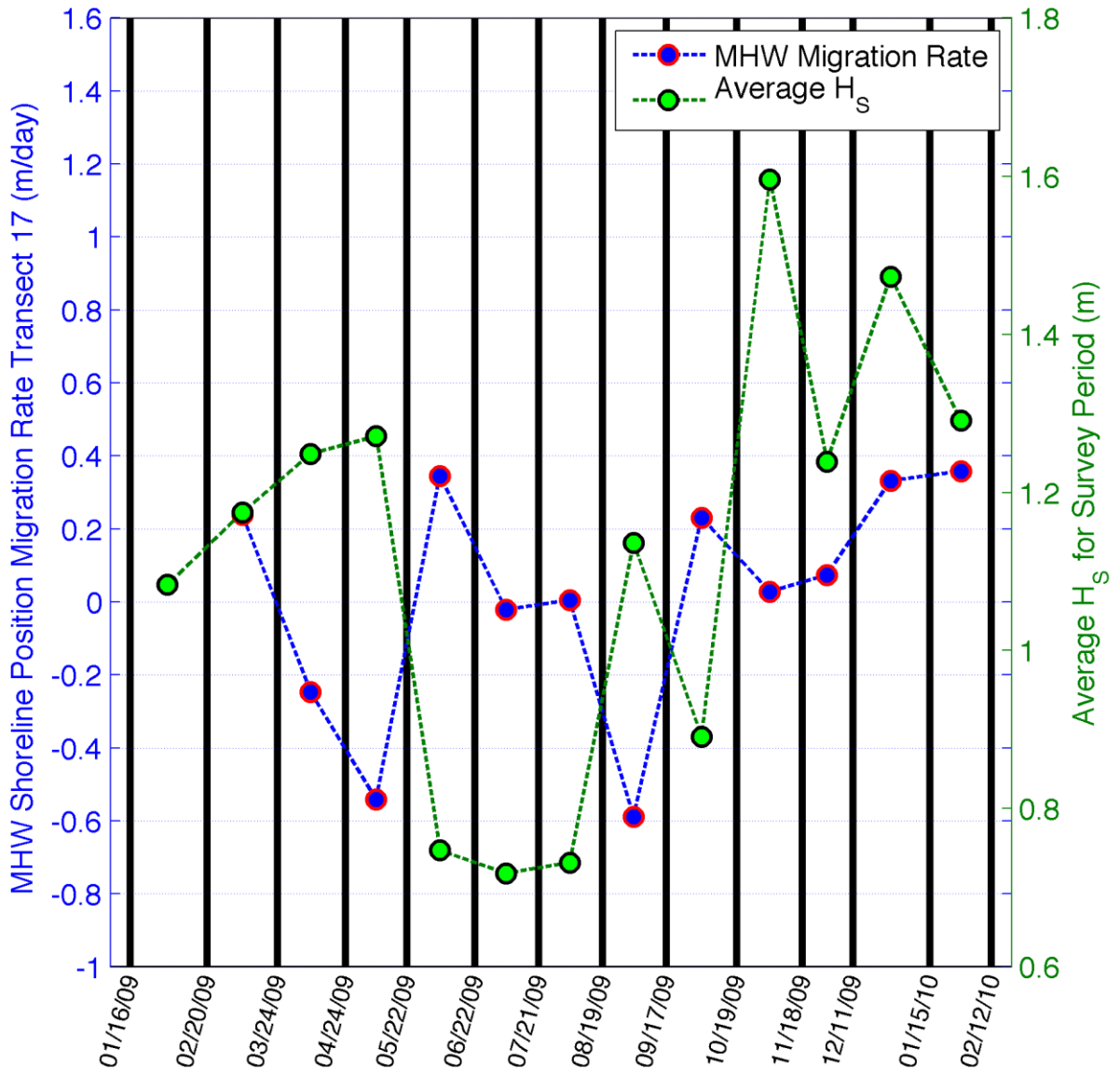
Transect 15



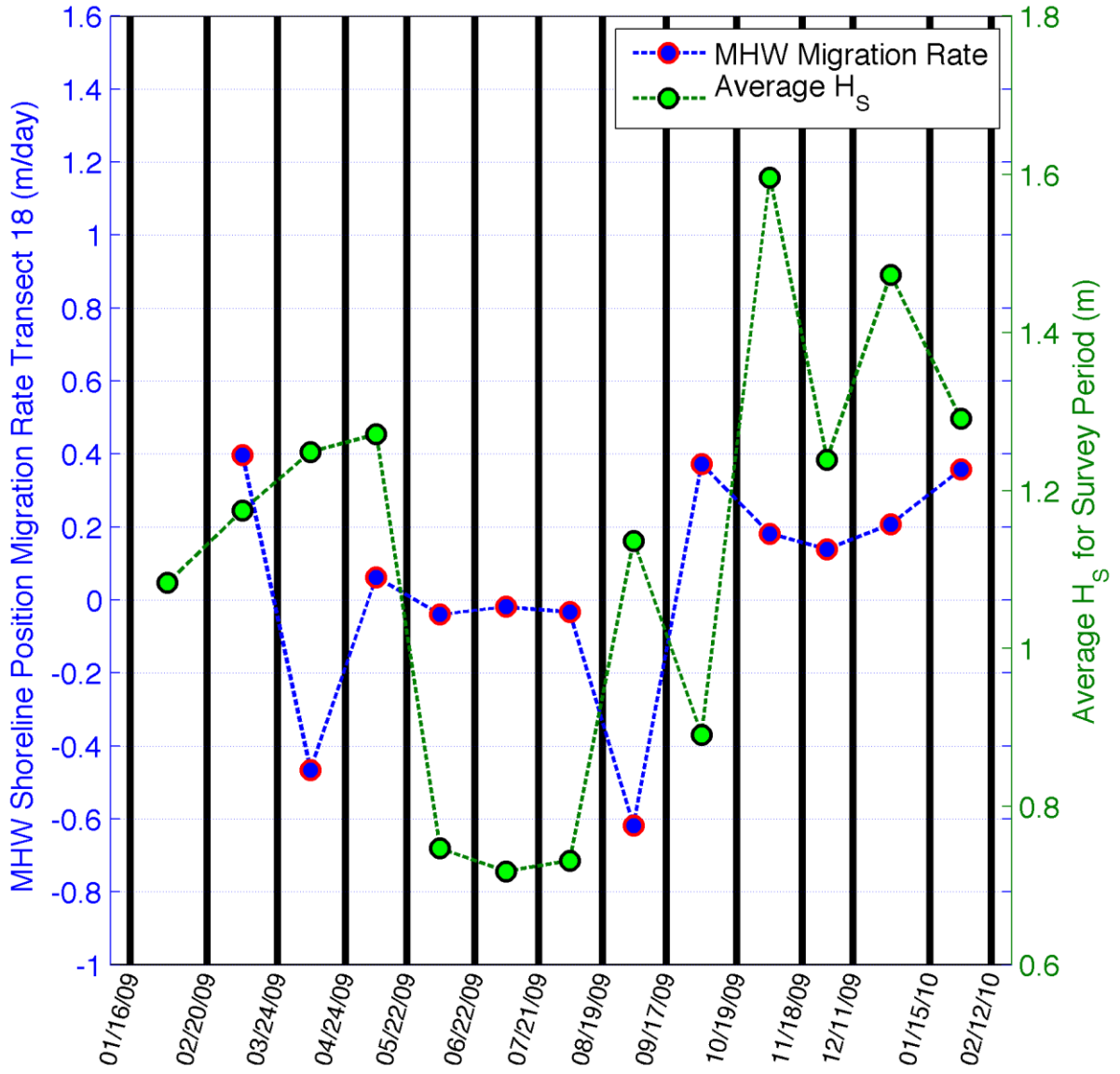
Transect 16



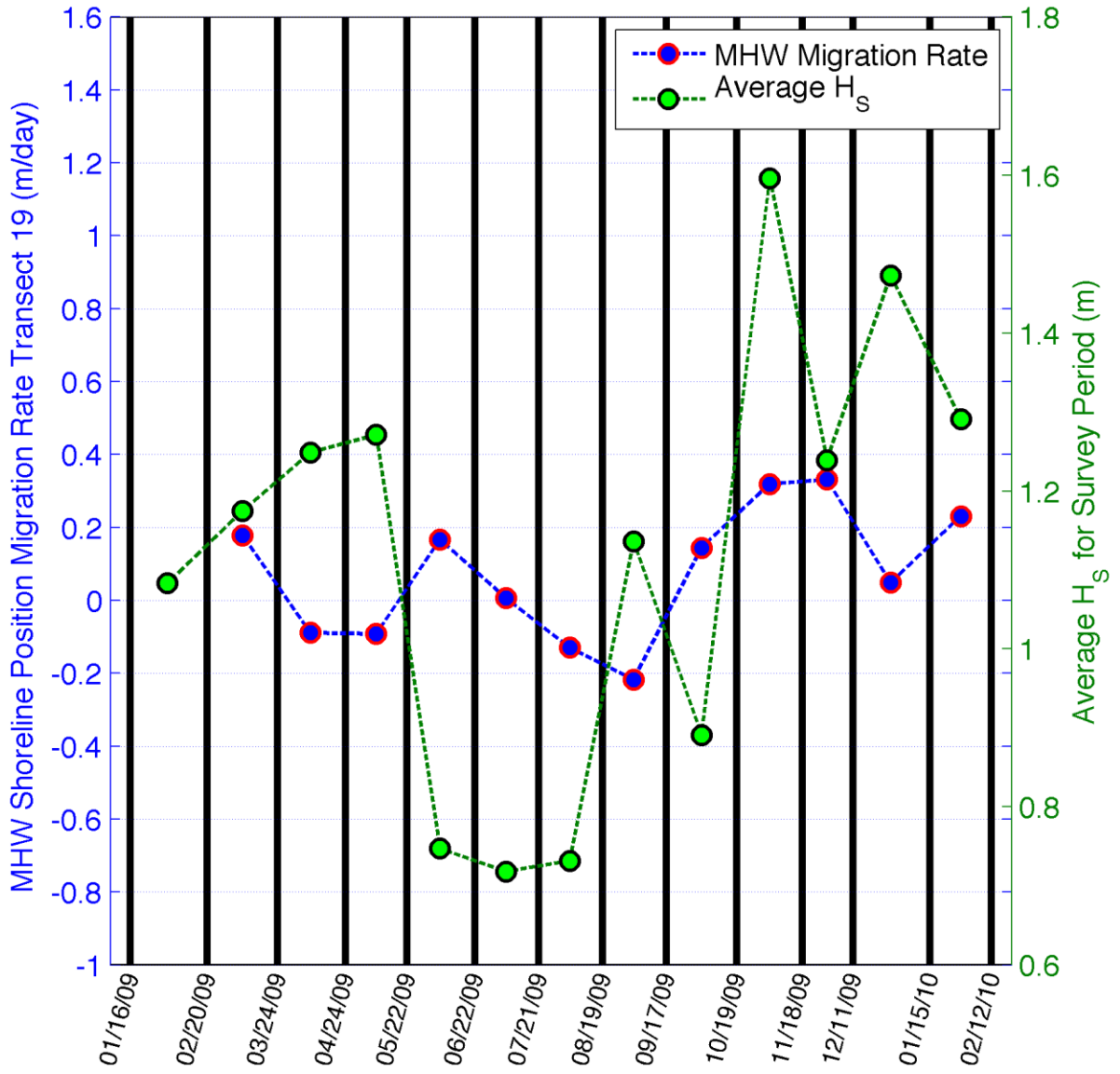
Transect 17



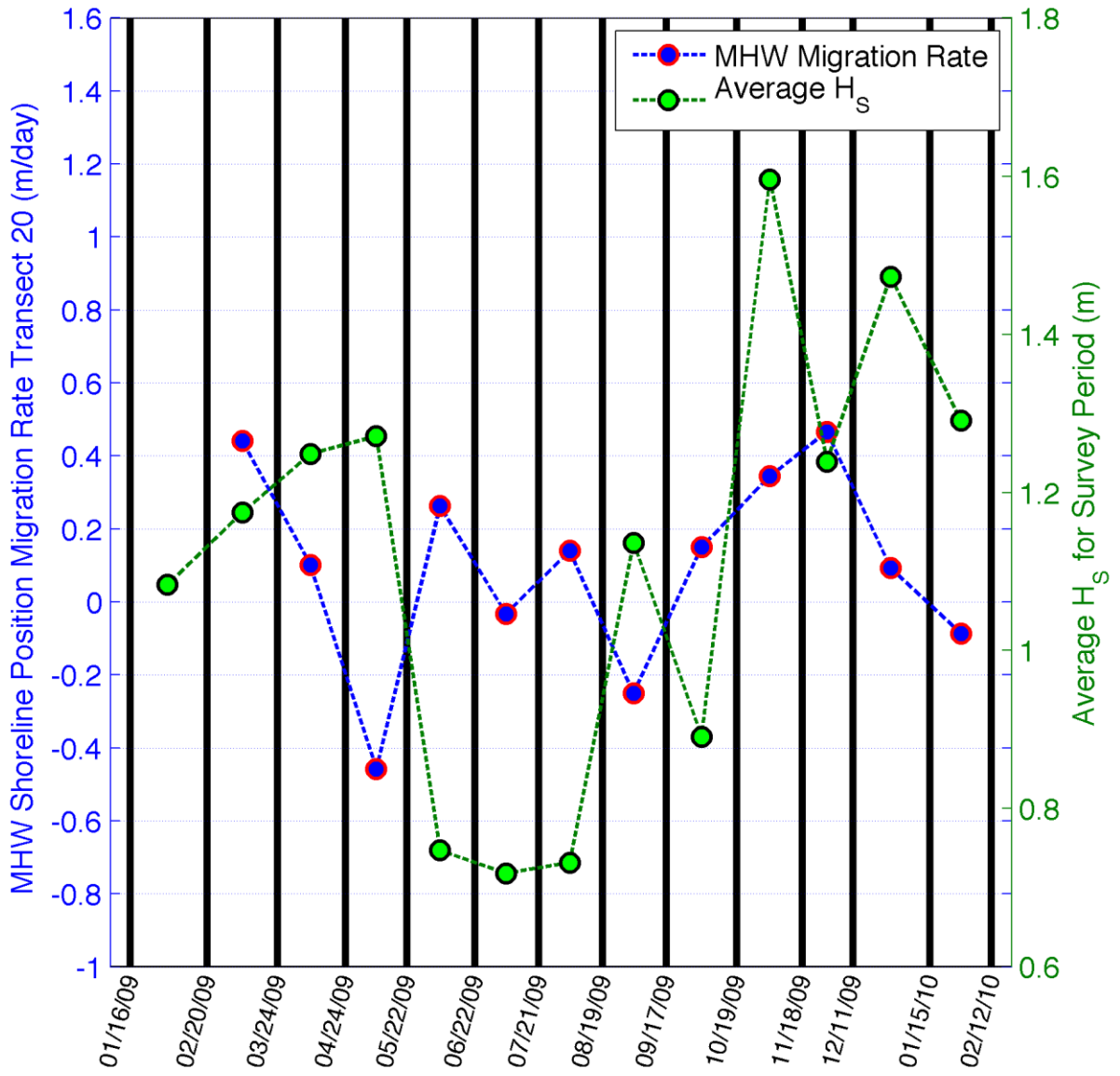
Transect 18



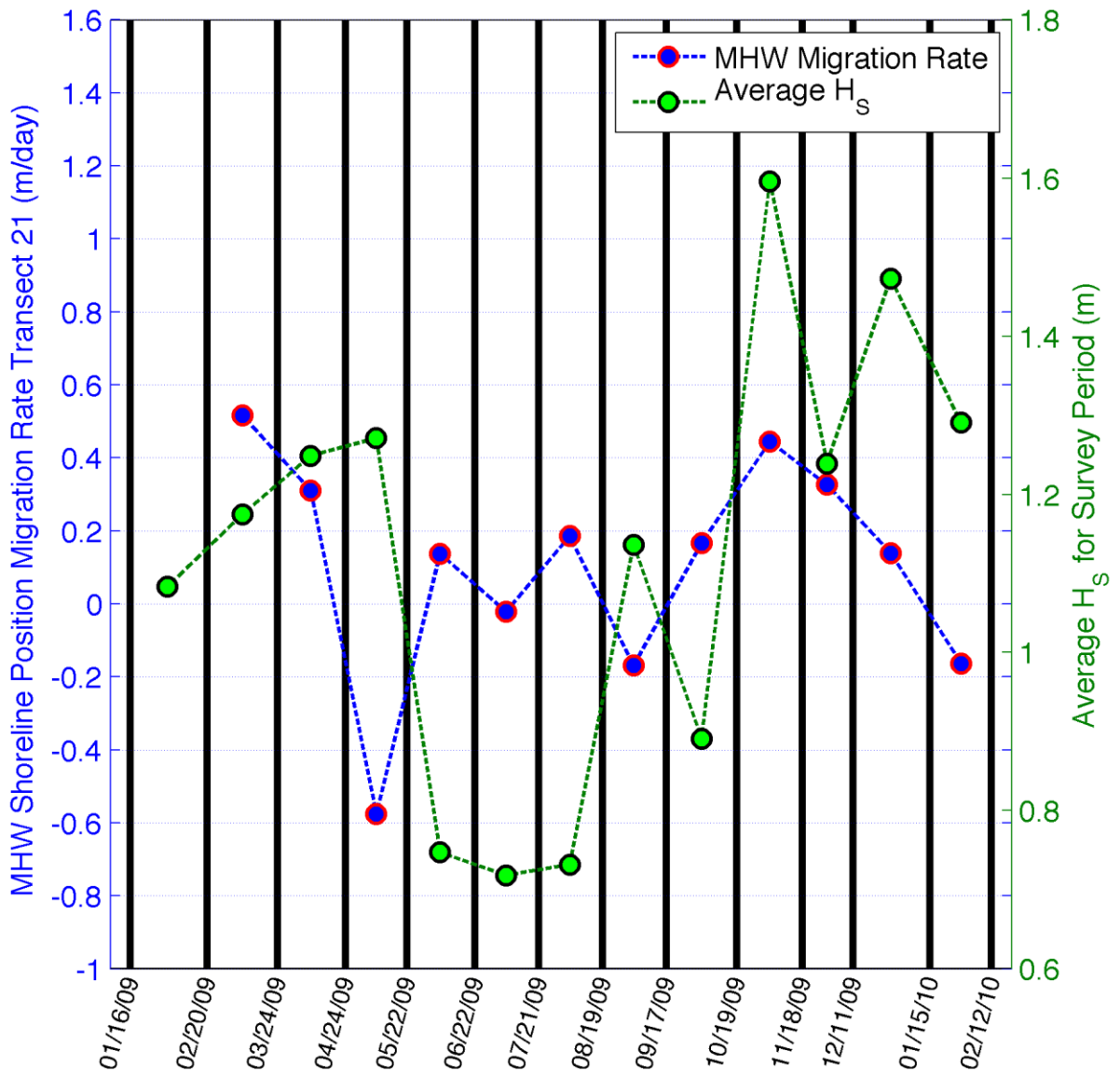
Transect 19



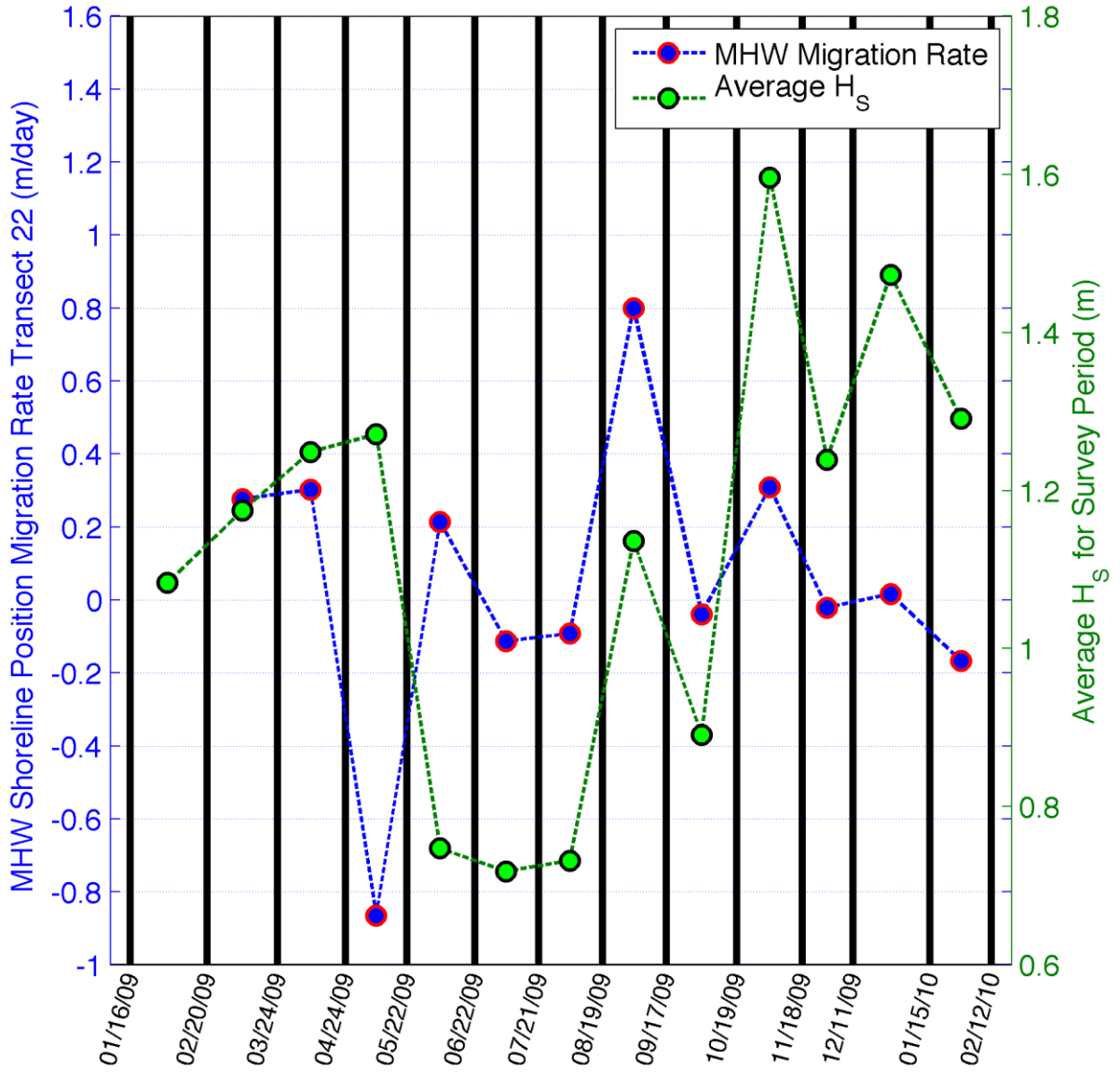
Transect 20



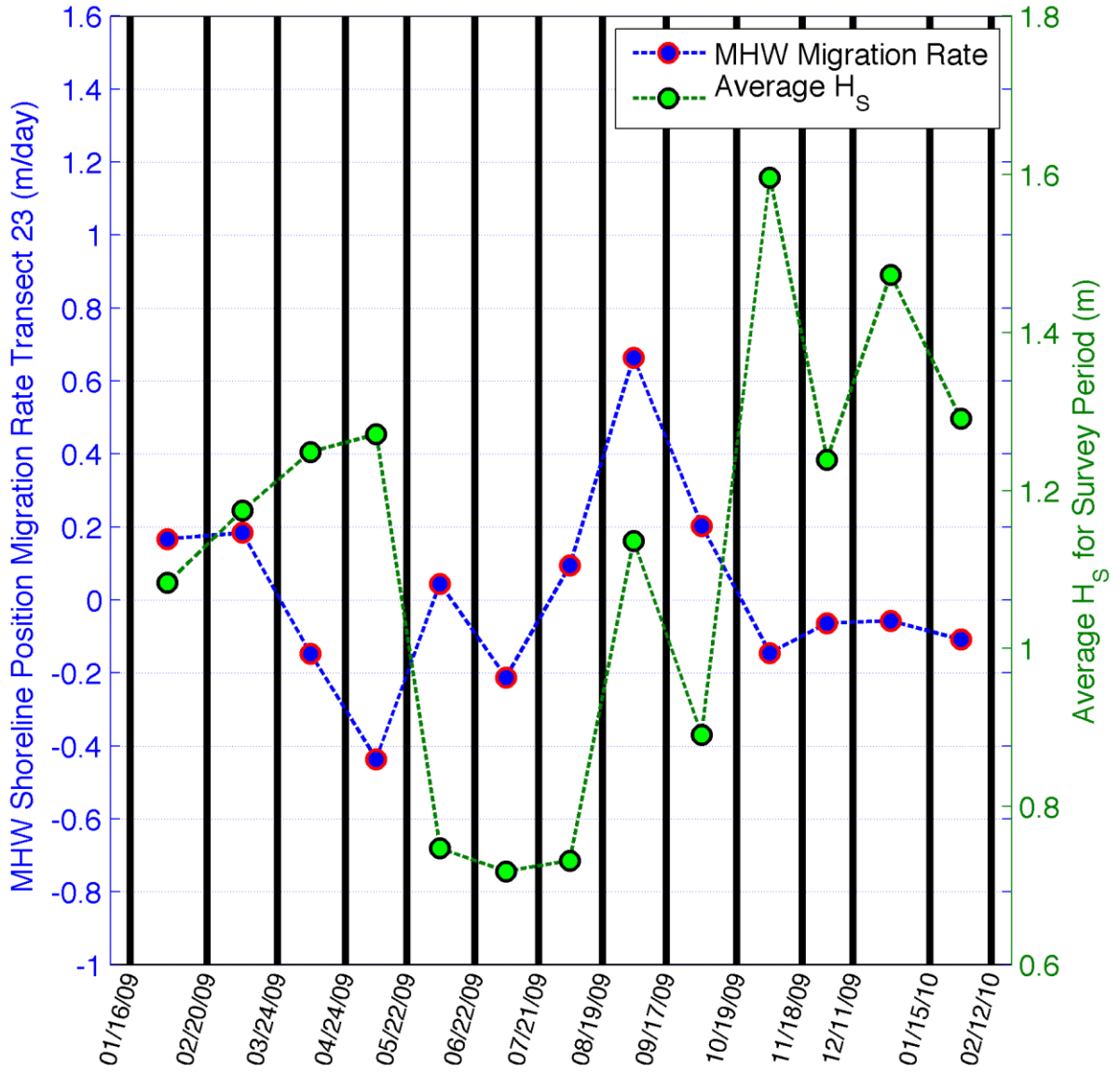
Transect 21



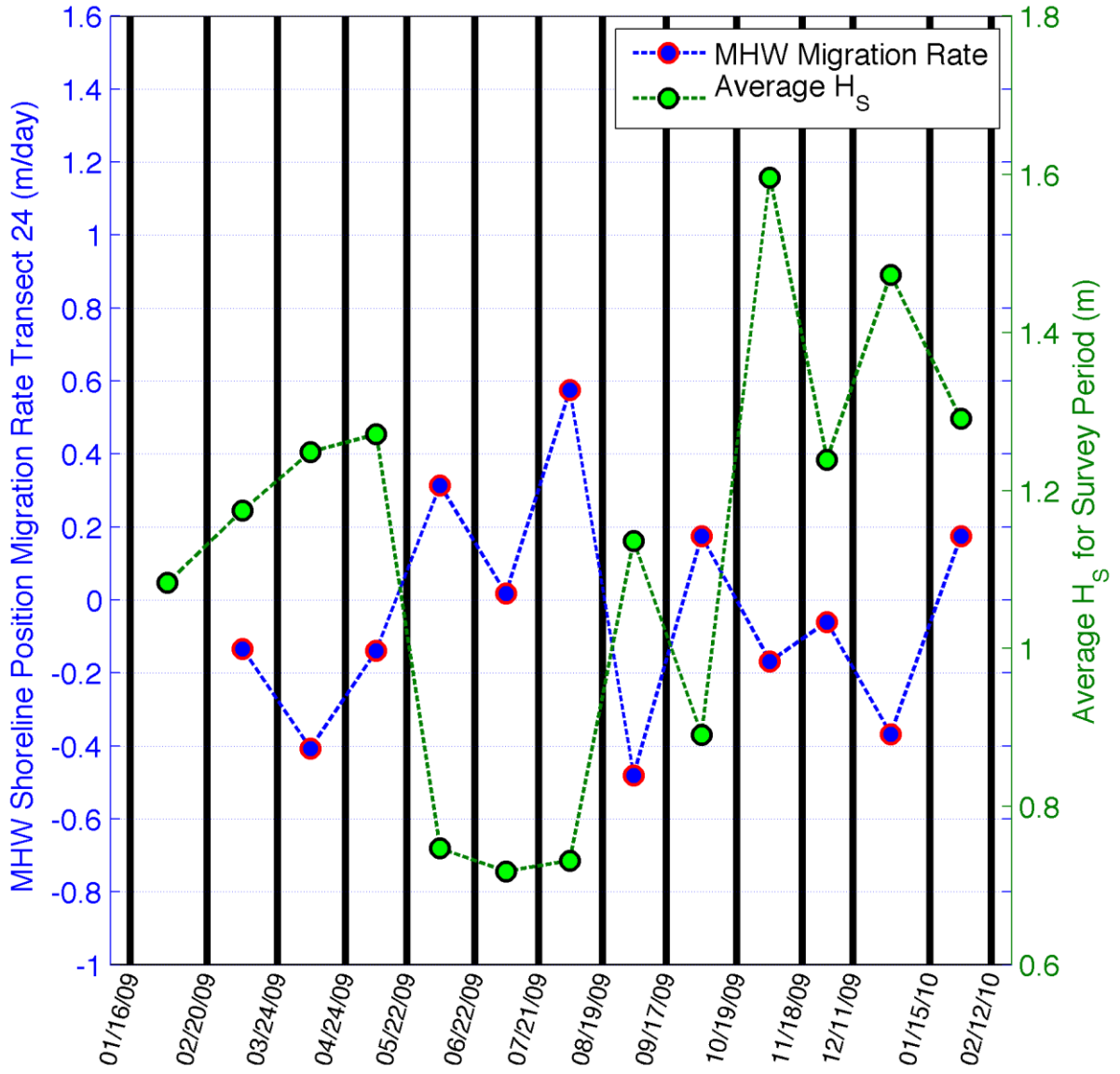
Transect 22



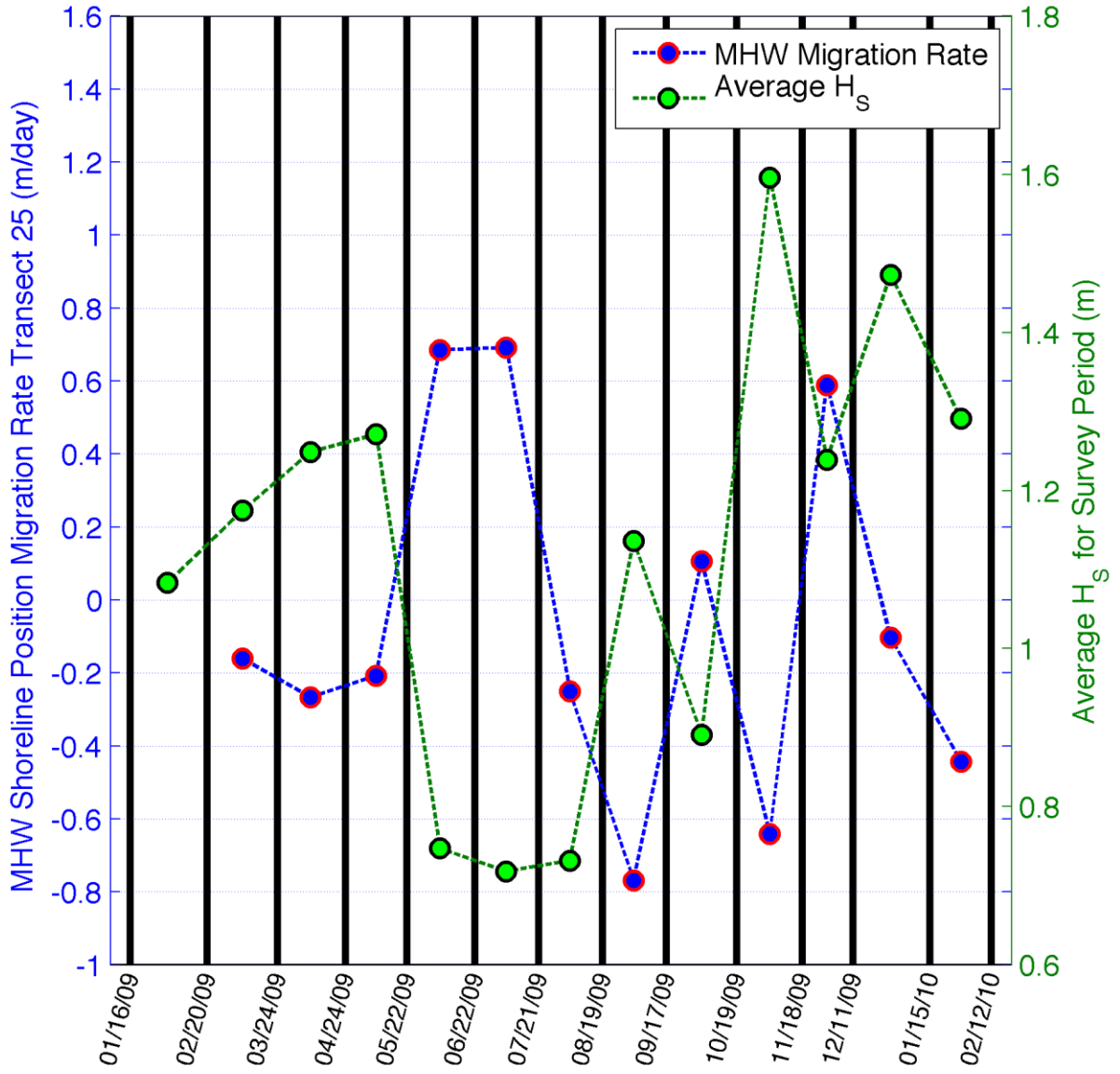
Transect 23



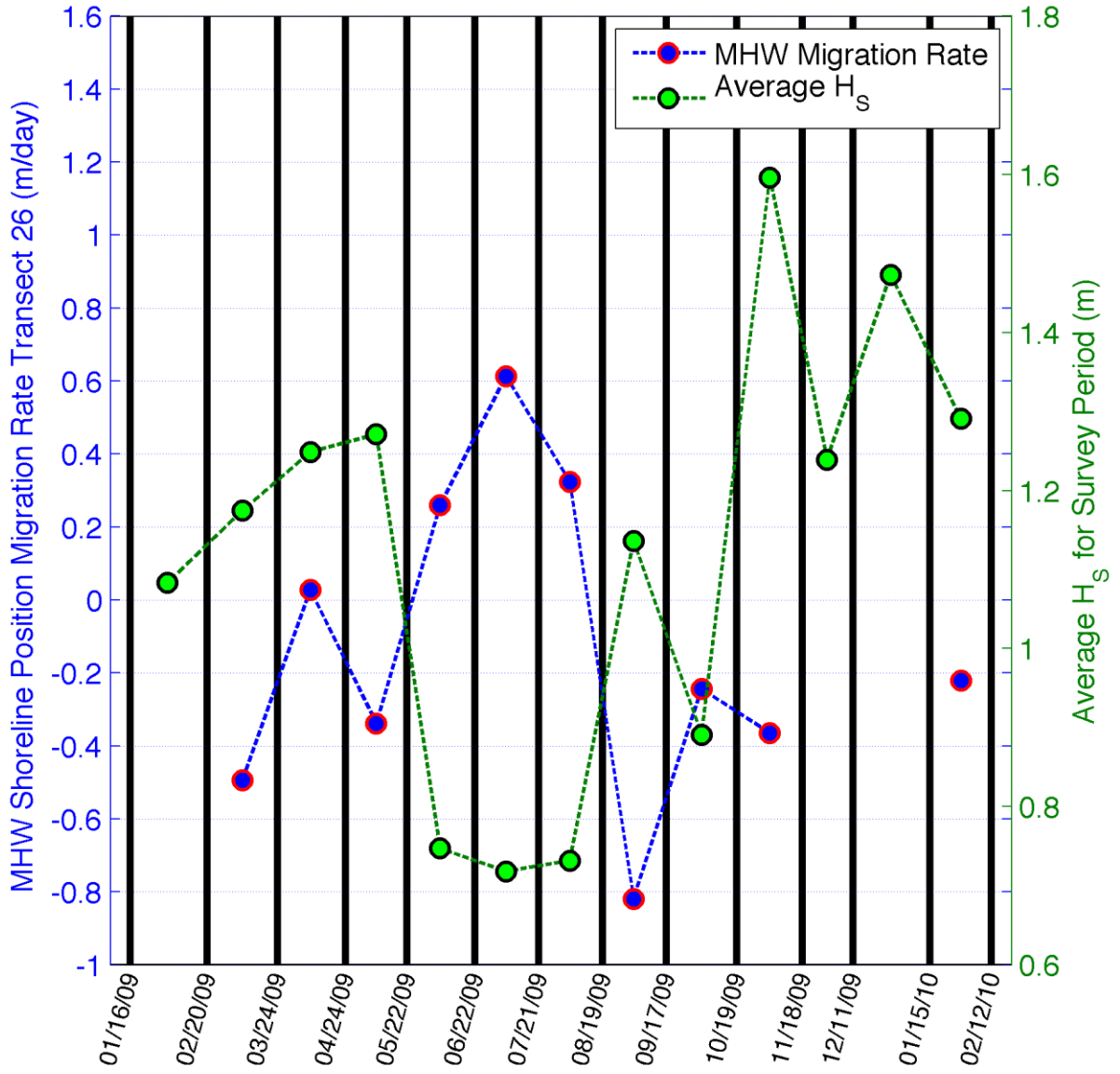
Transect 24



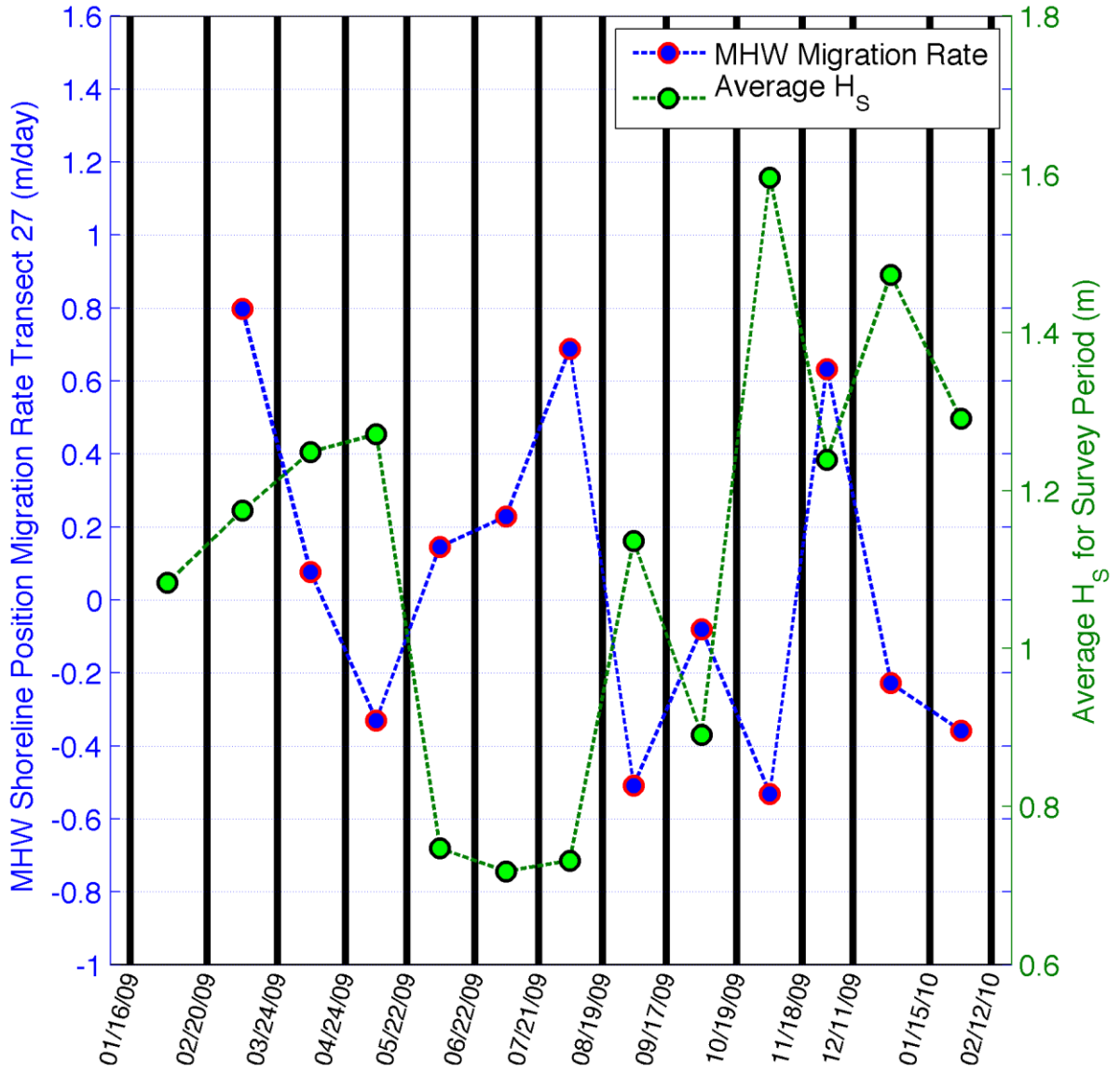
Transect 25



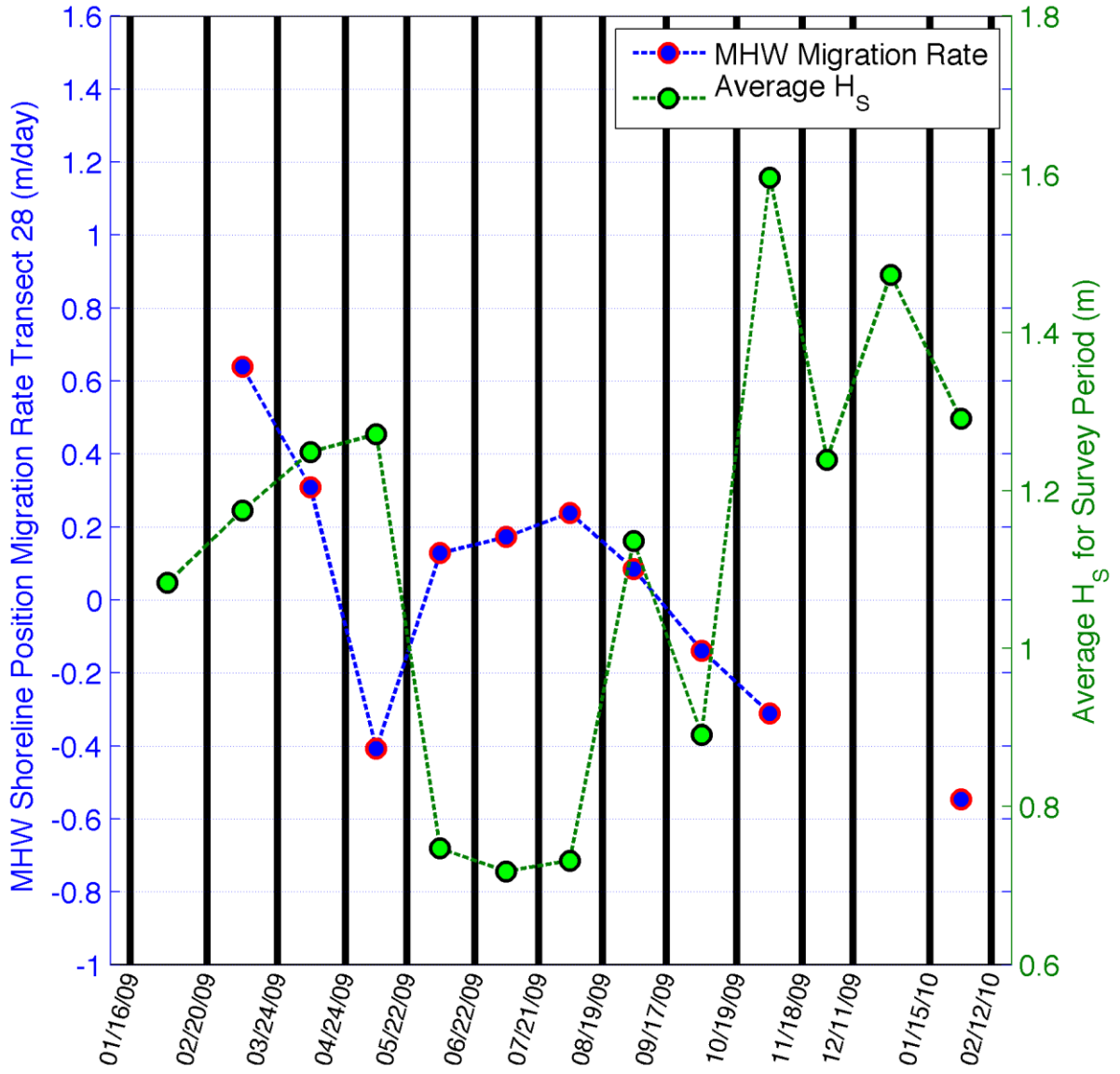
Transect 26



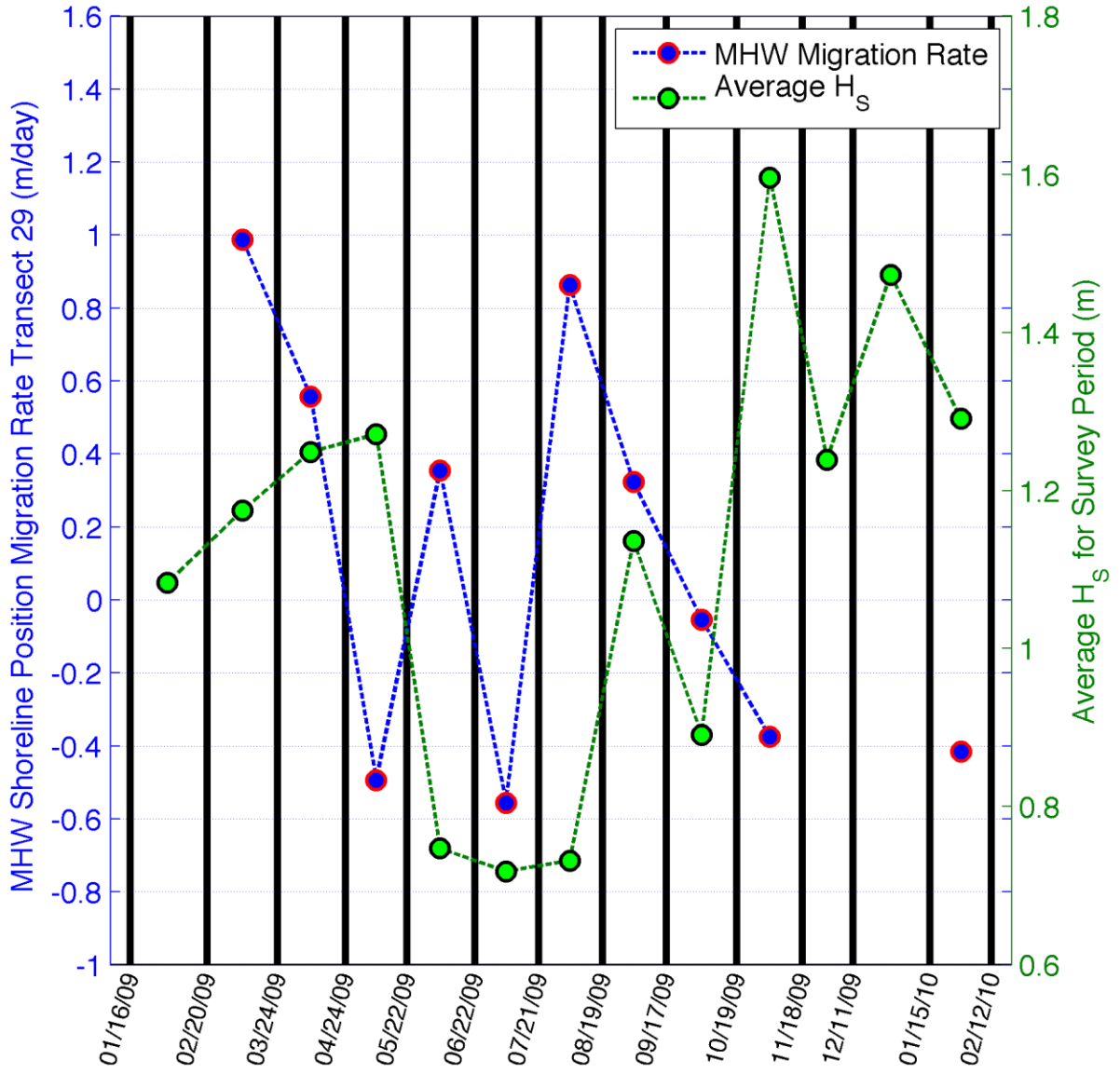
Transect 27



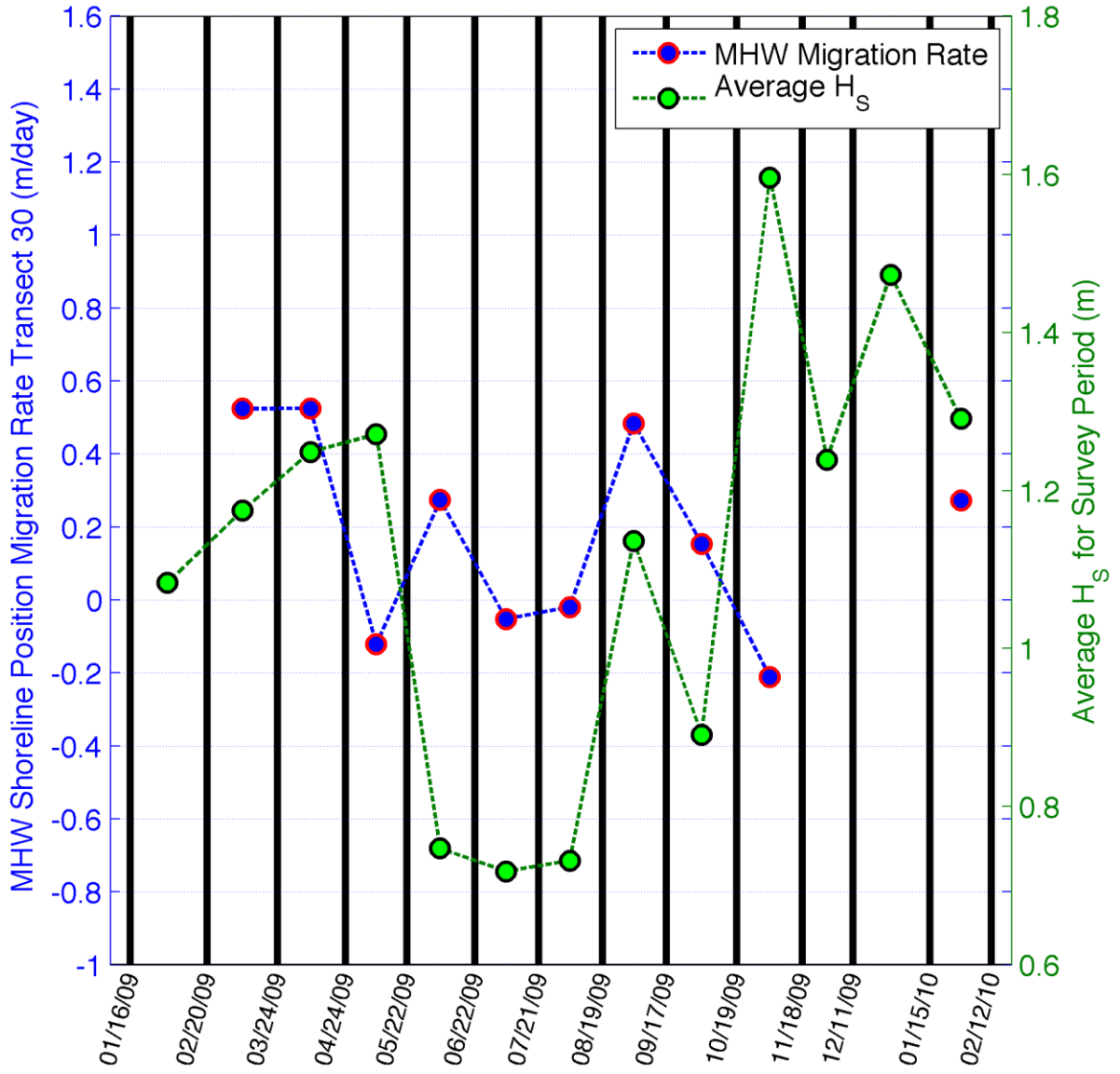
Transect 28



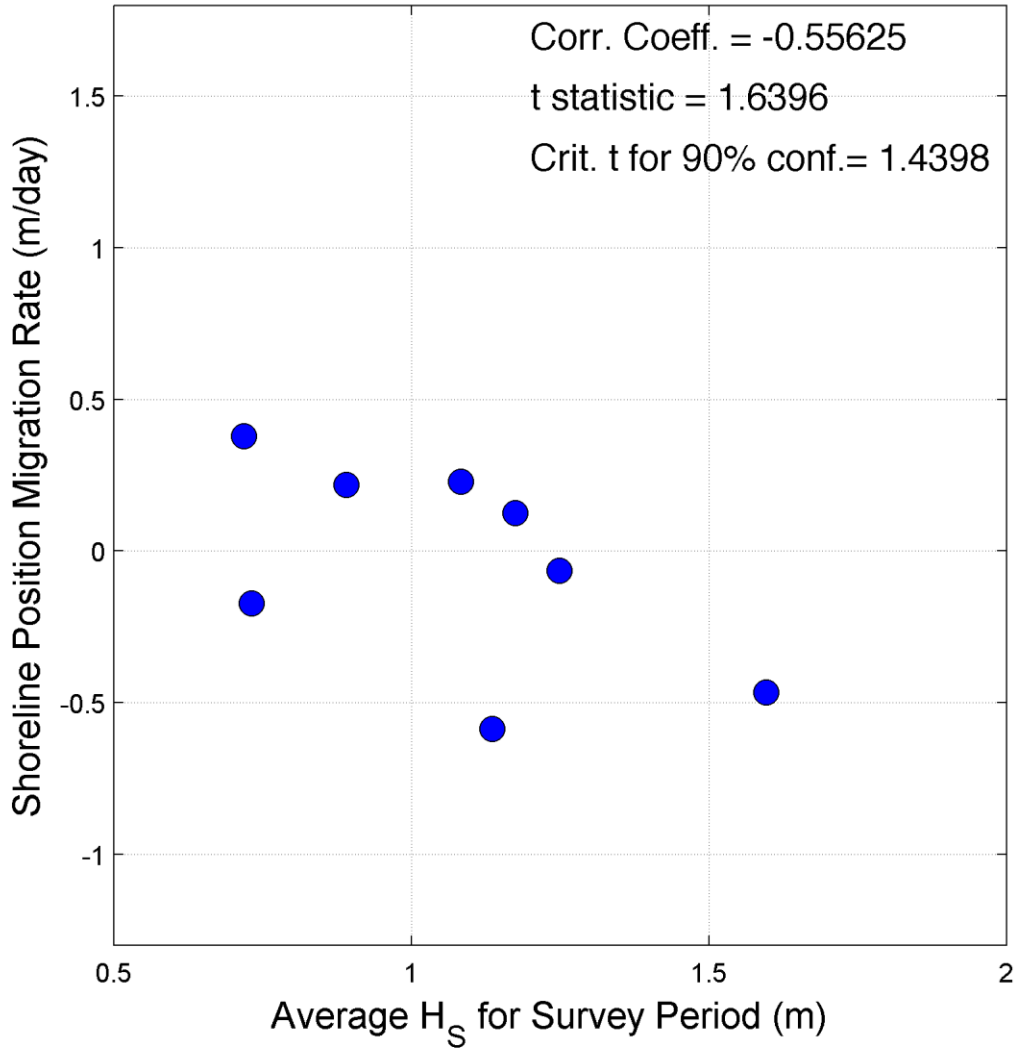
Transect 29



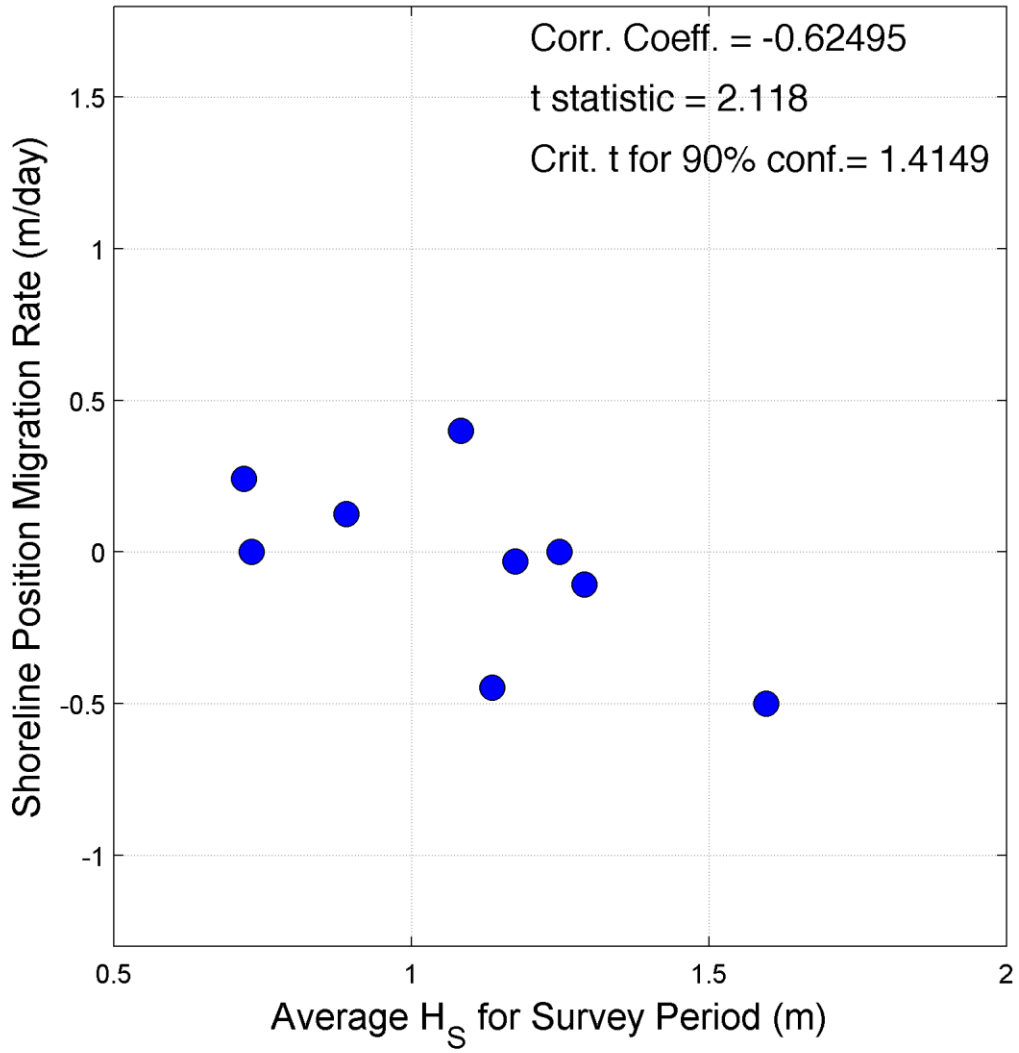
Transect 30



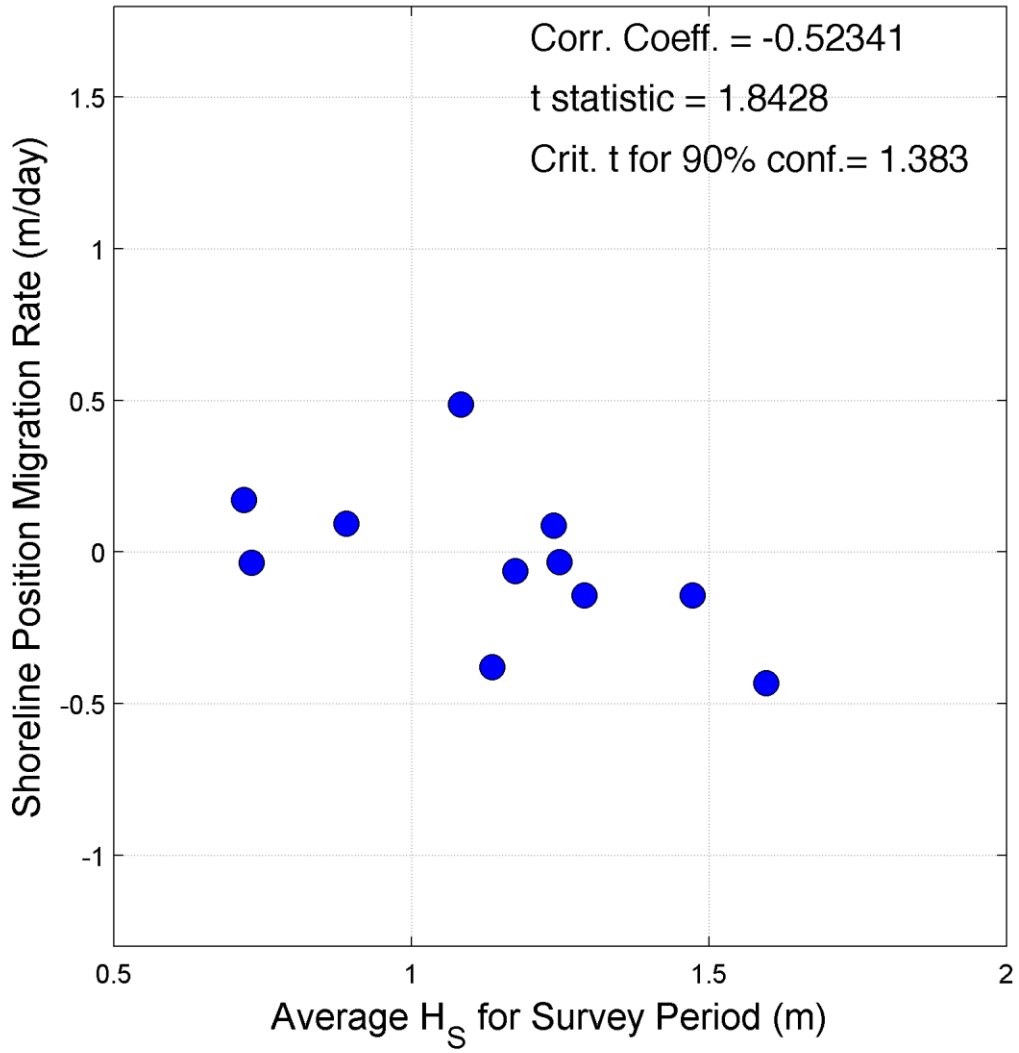
Transect 1



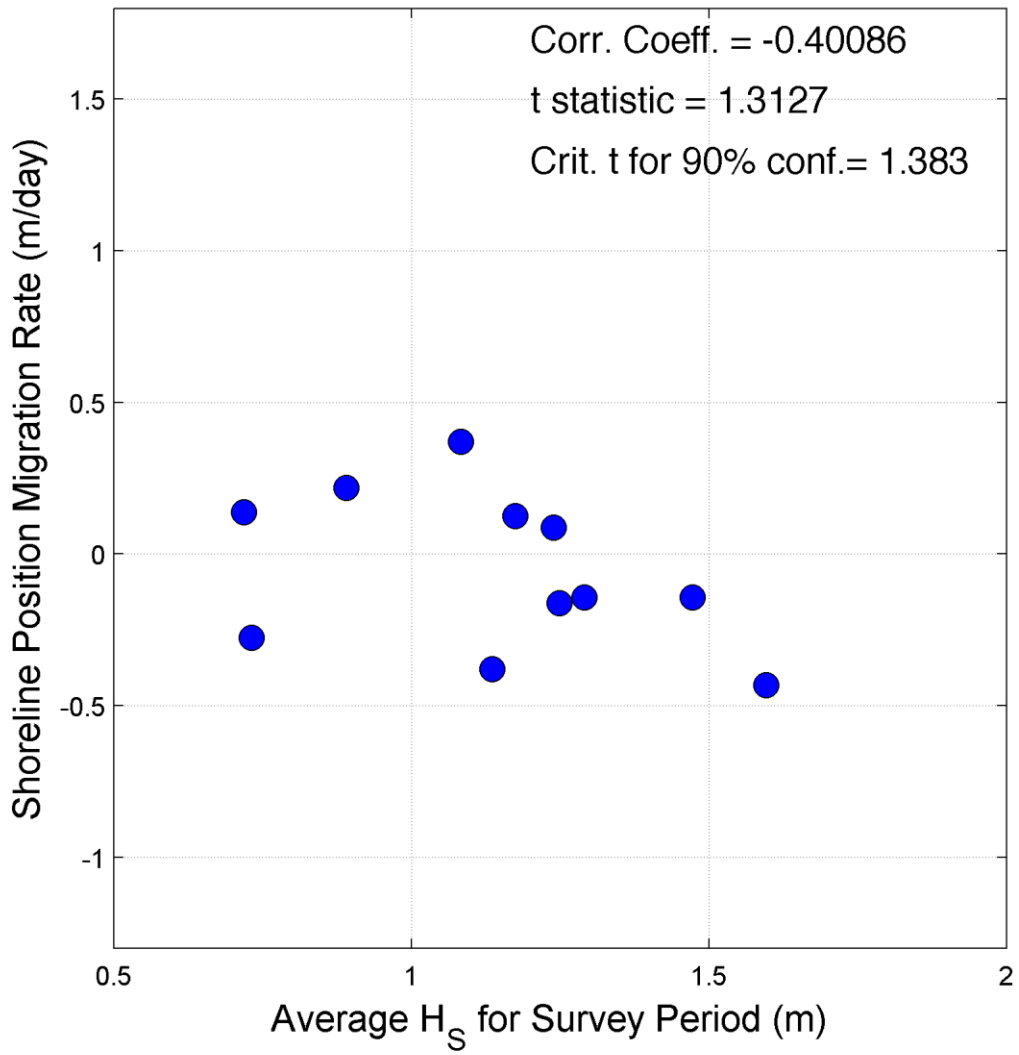
Transect 2



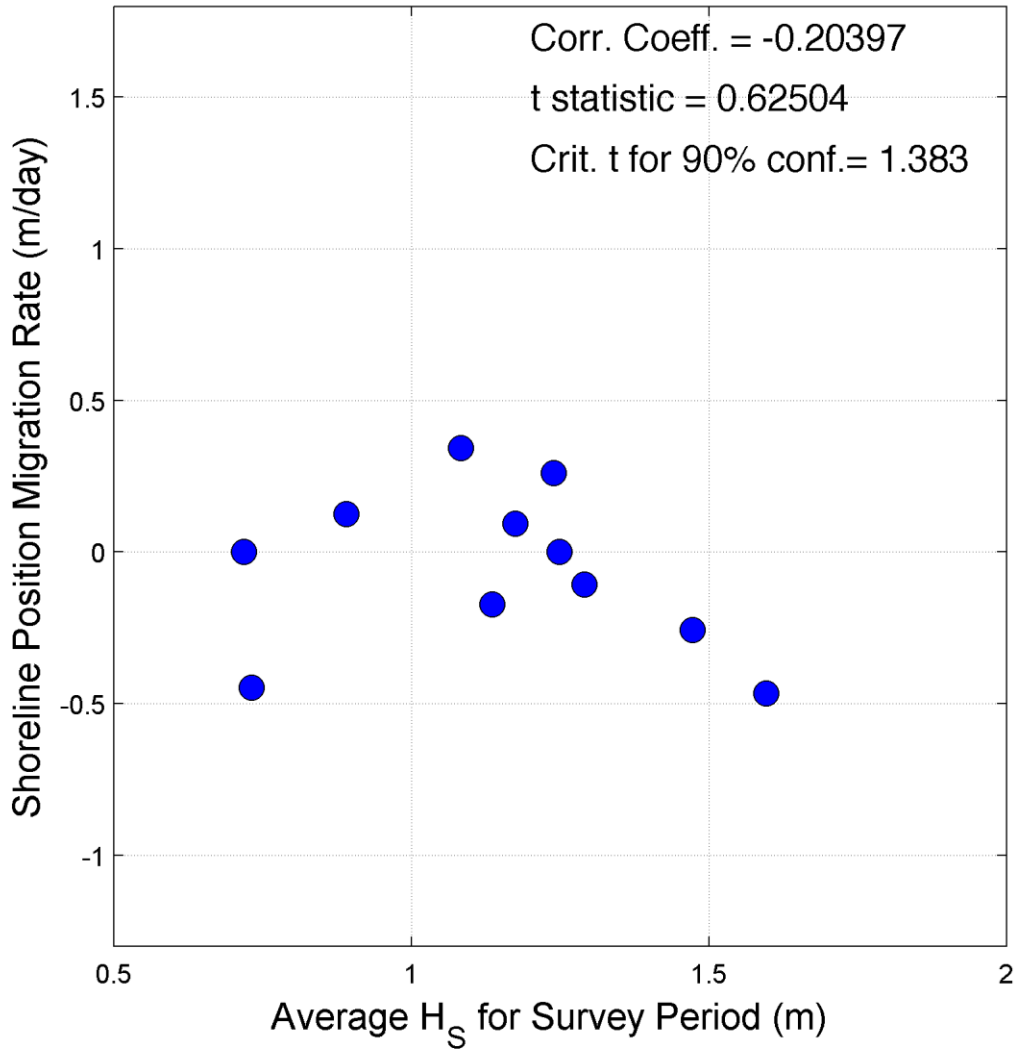
Transect 3



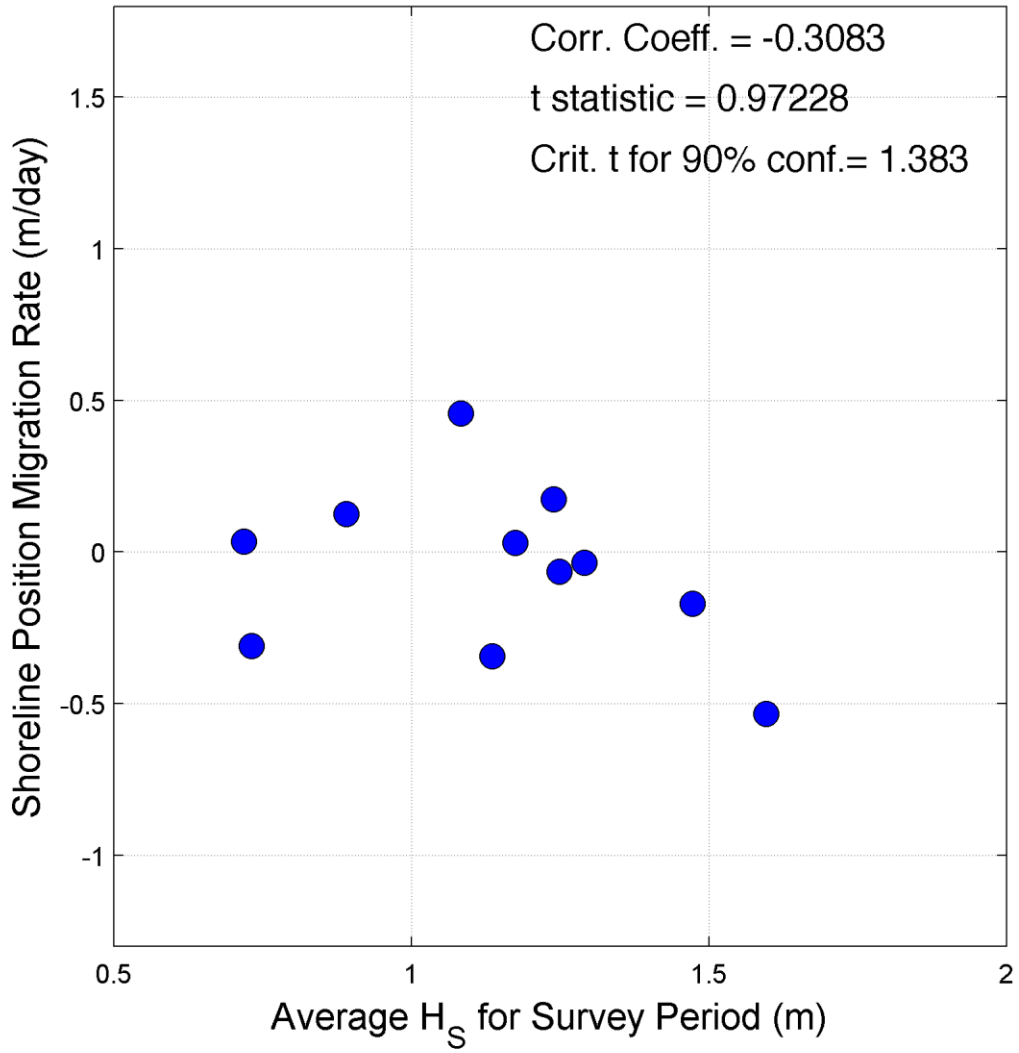
Transect 4



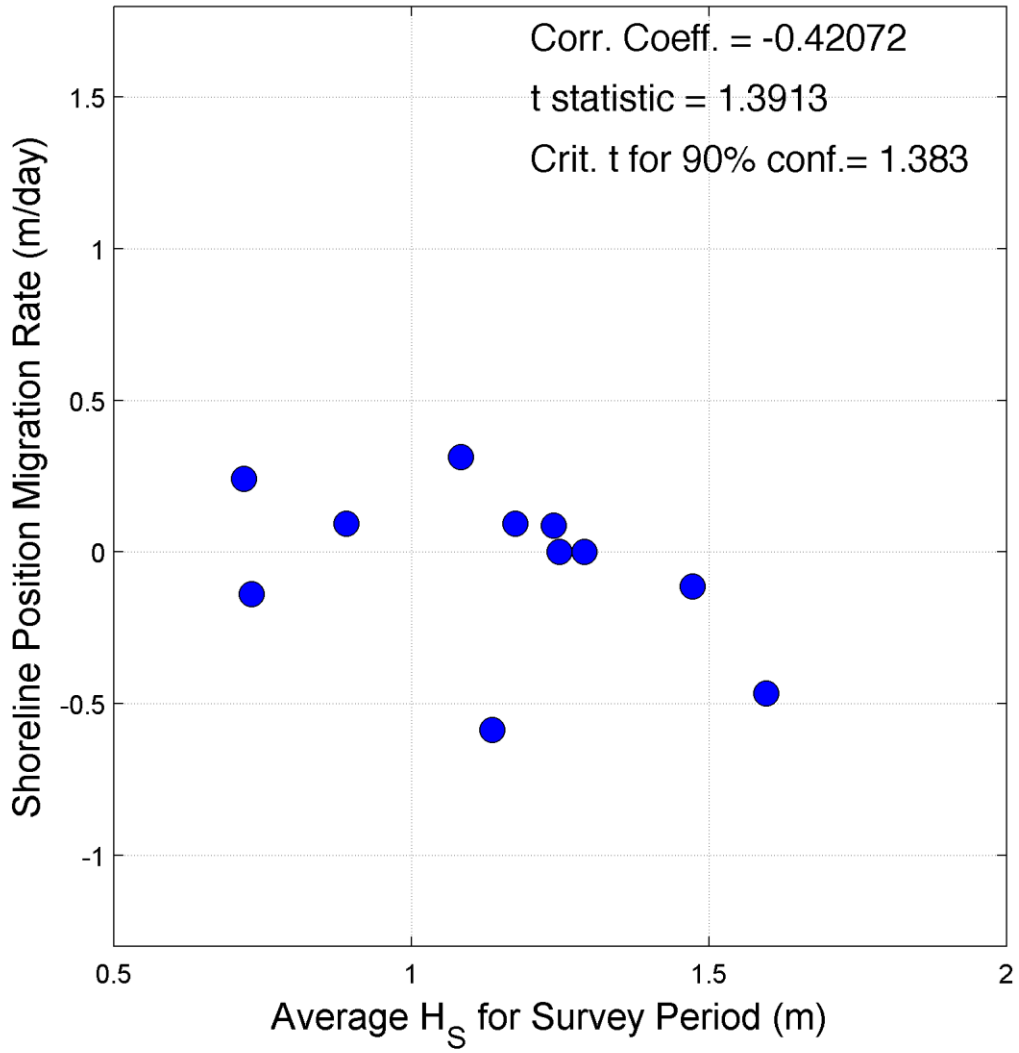
Transect 5



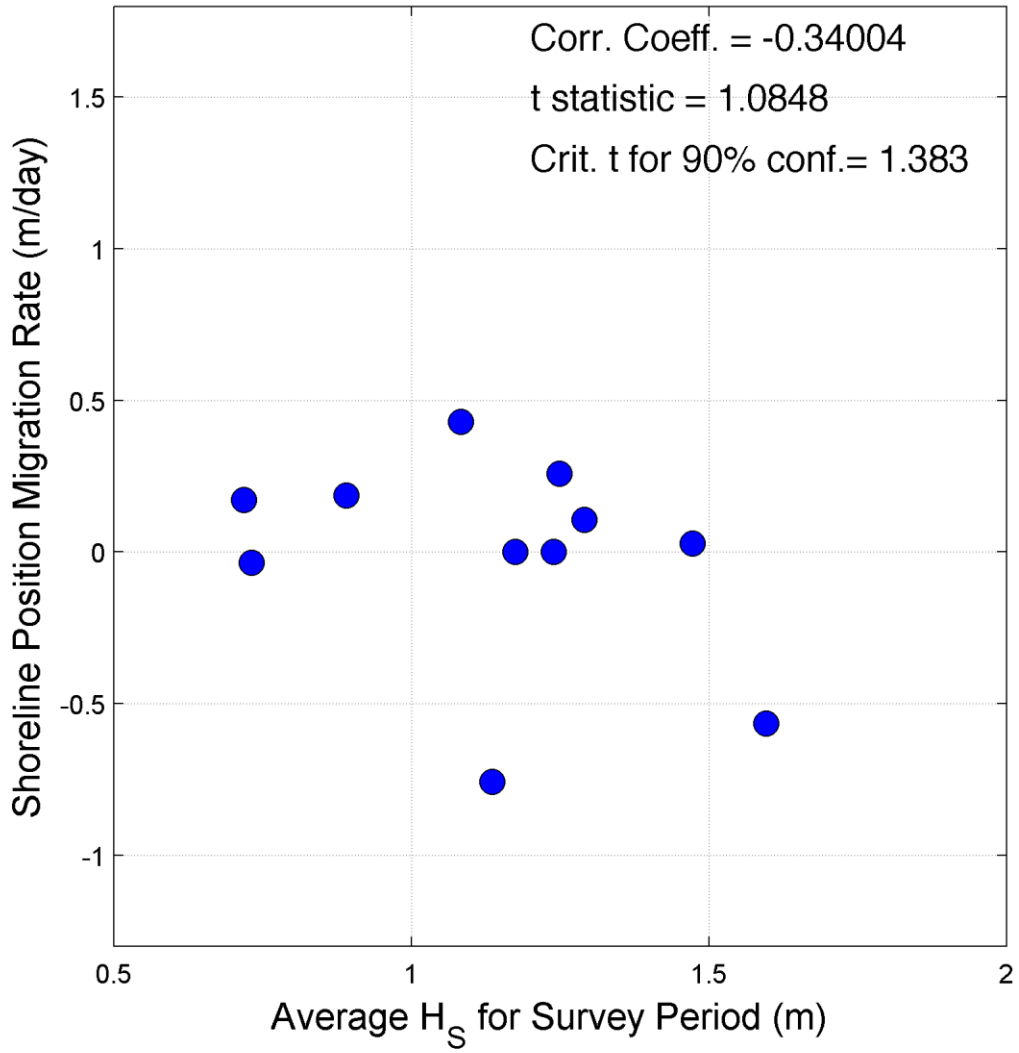
Transect 6



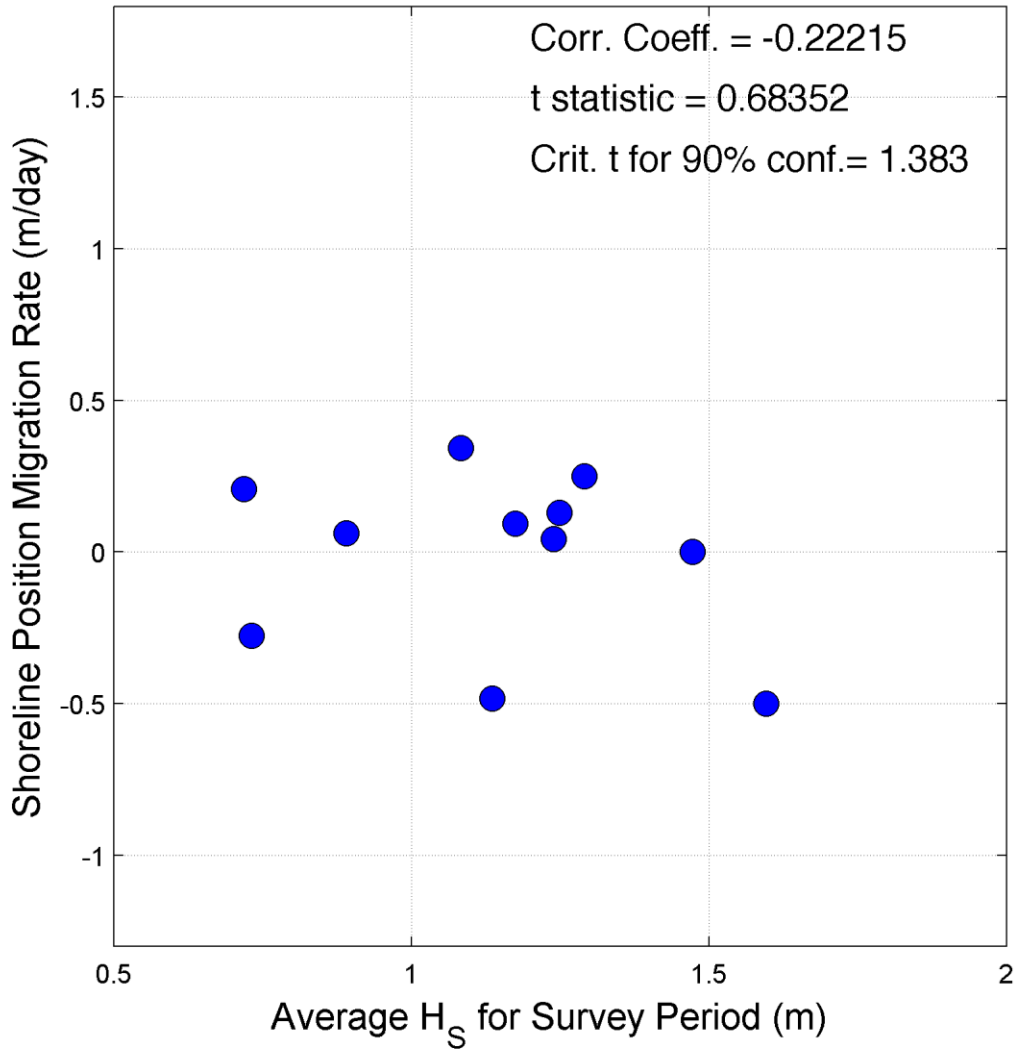
Transect 7



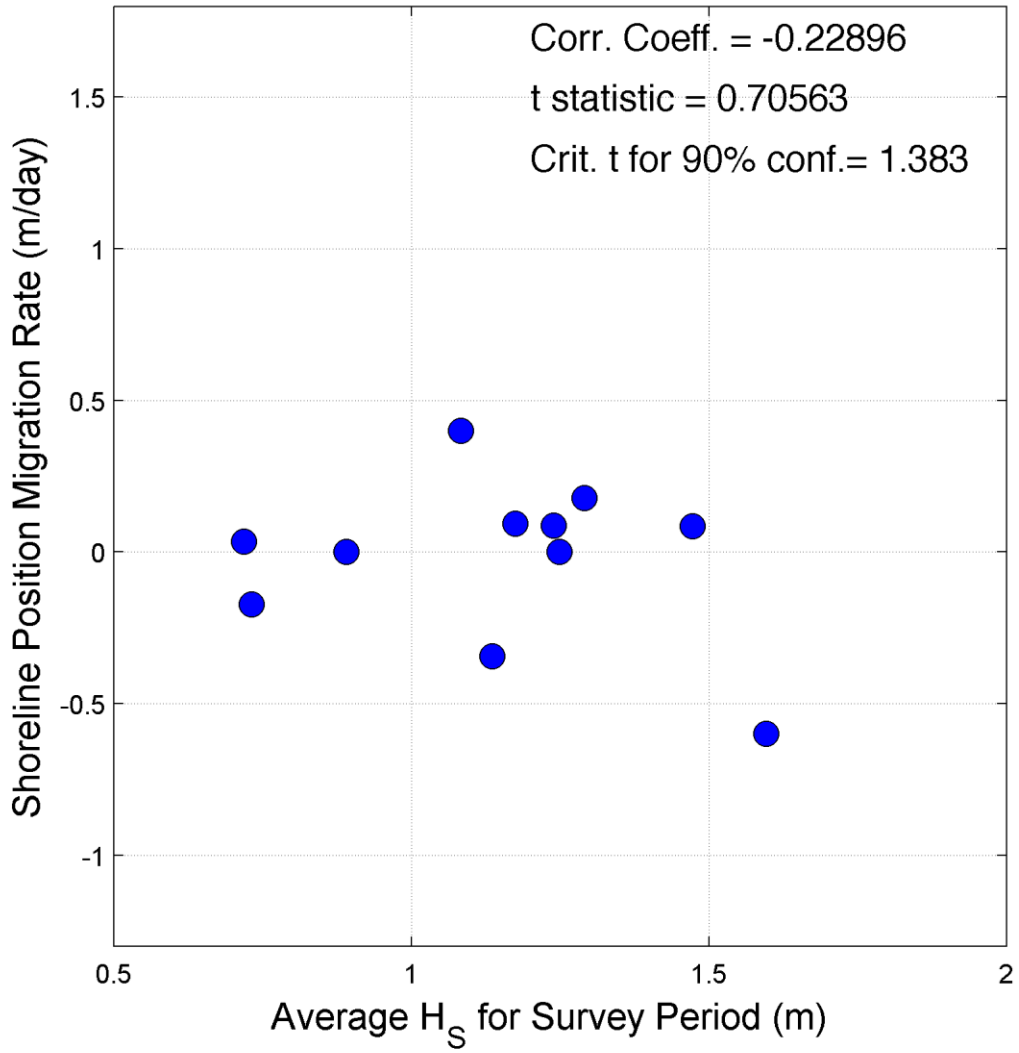
Transect 8



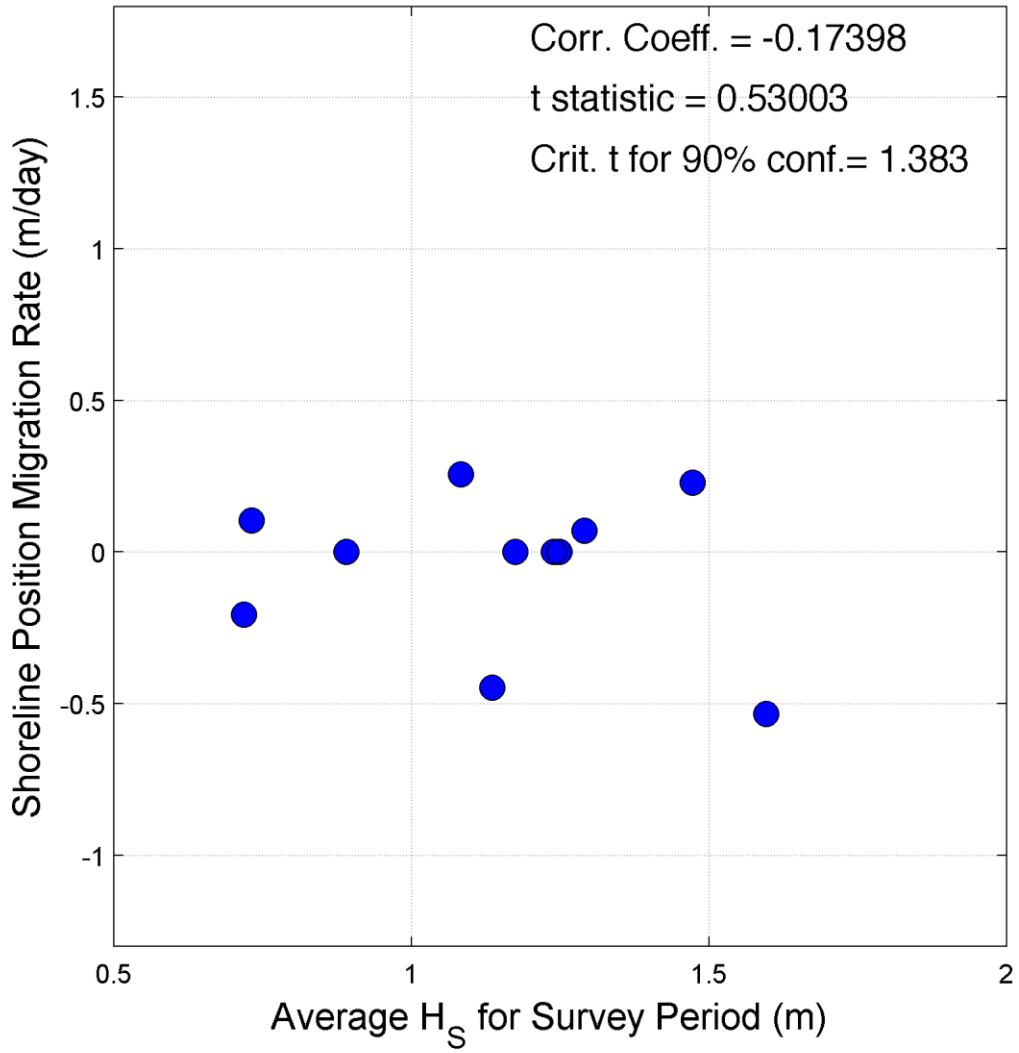
Transect 9



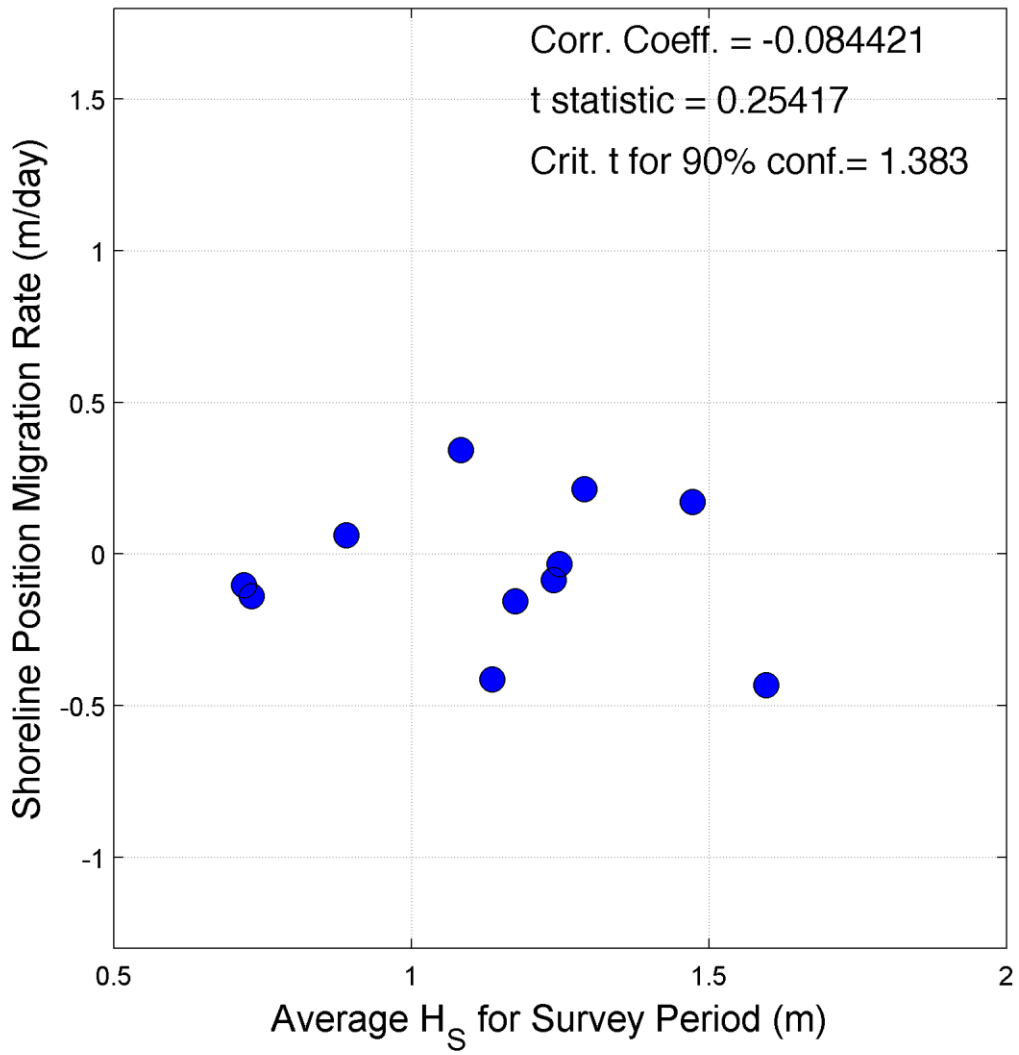
Transect 10



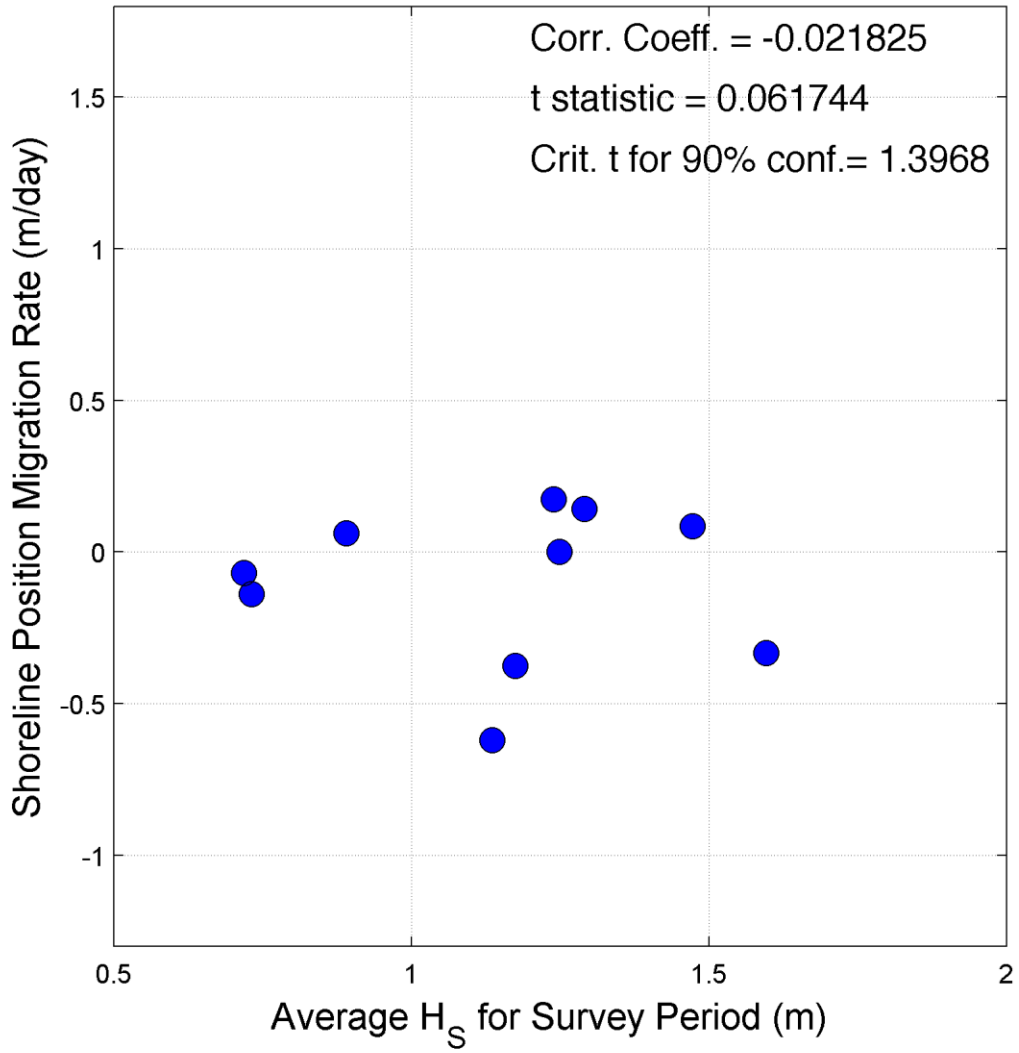
Transect 11



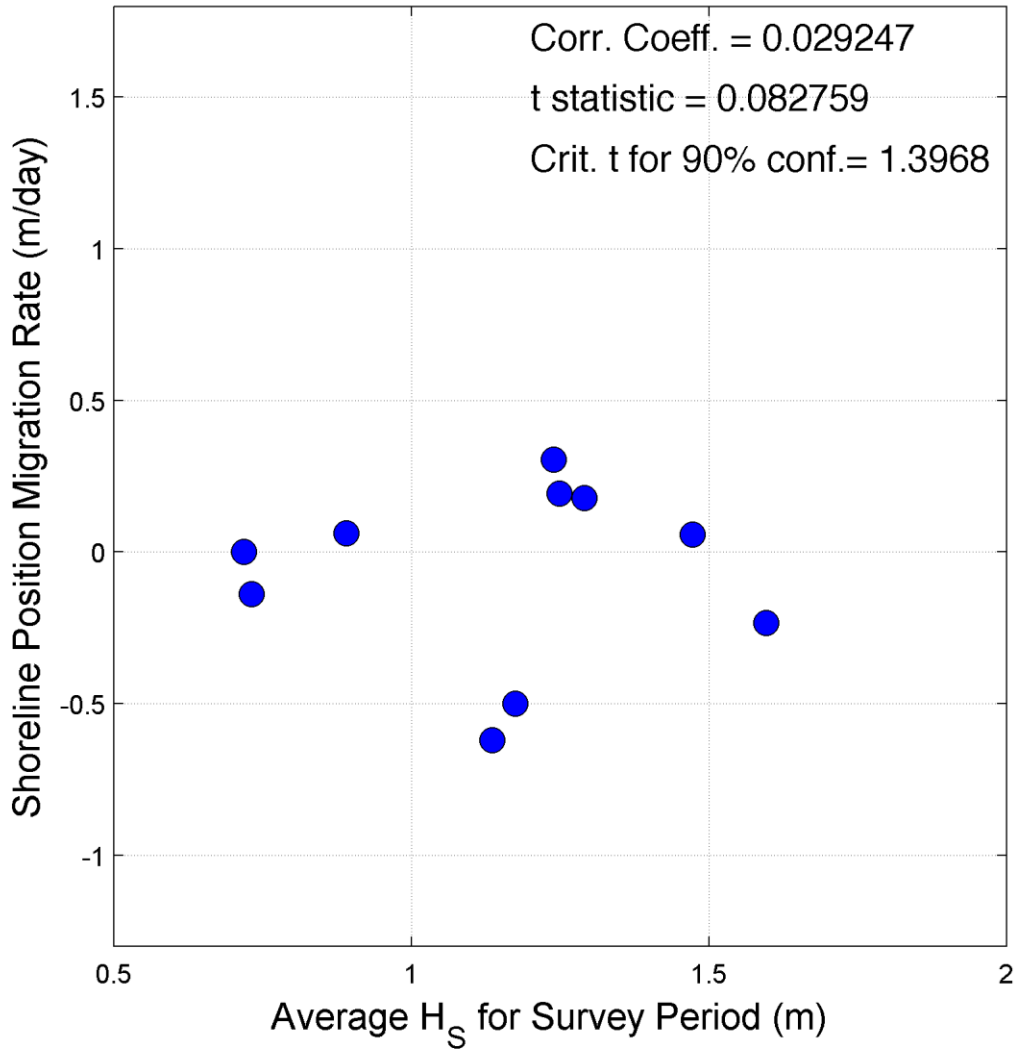
Transect 12



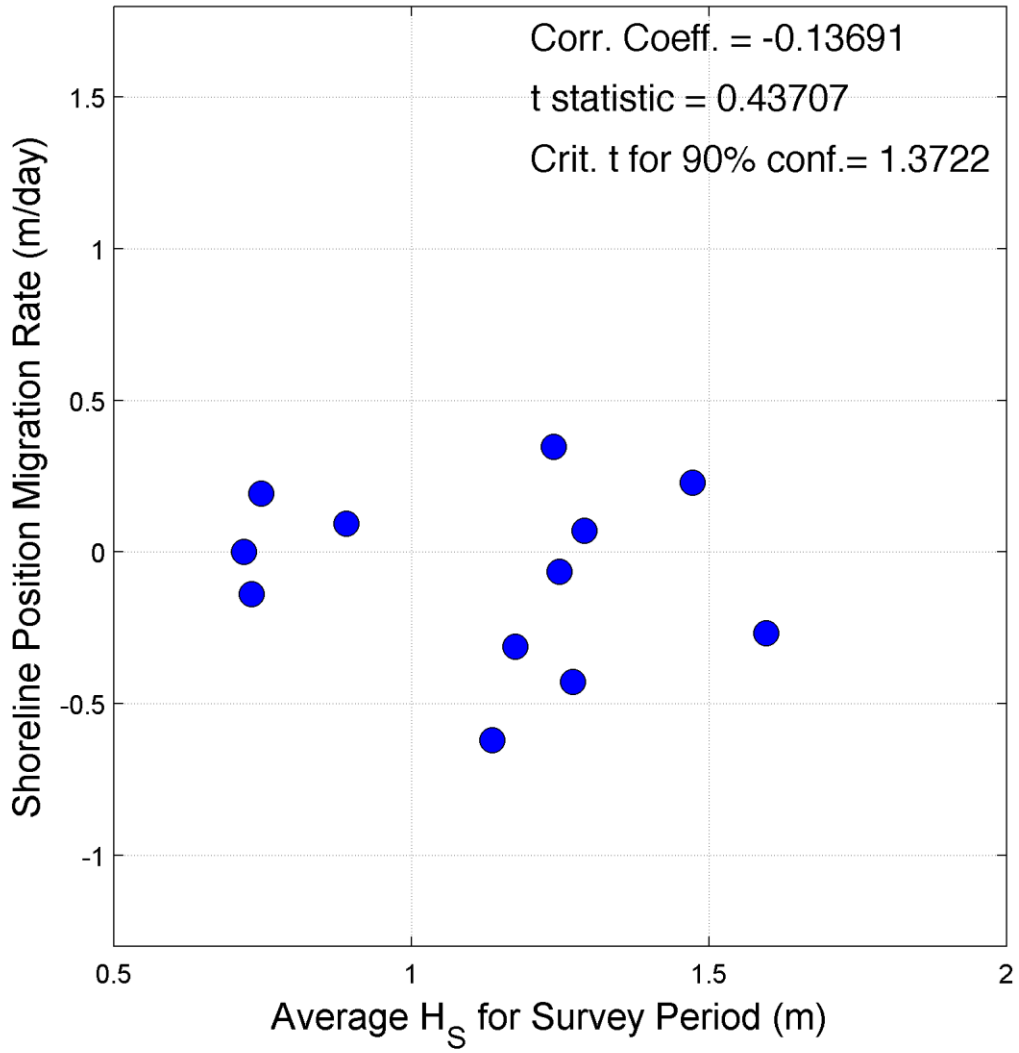
Transect 13



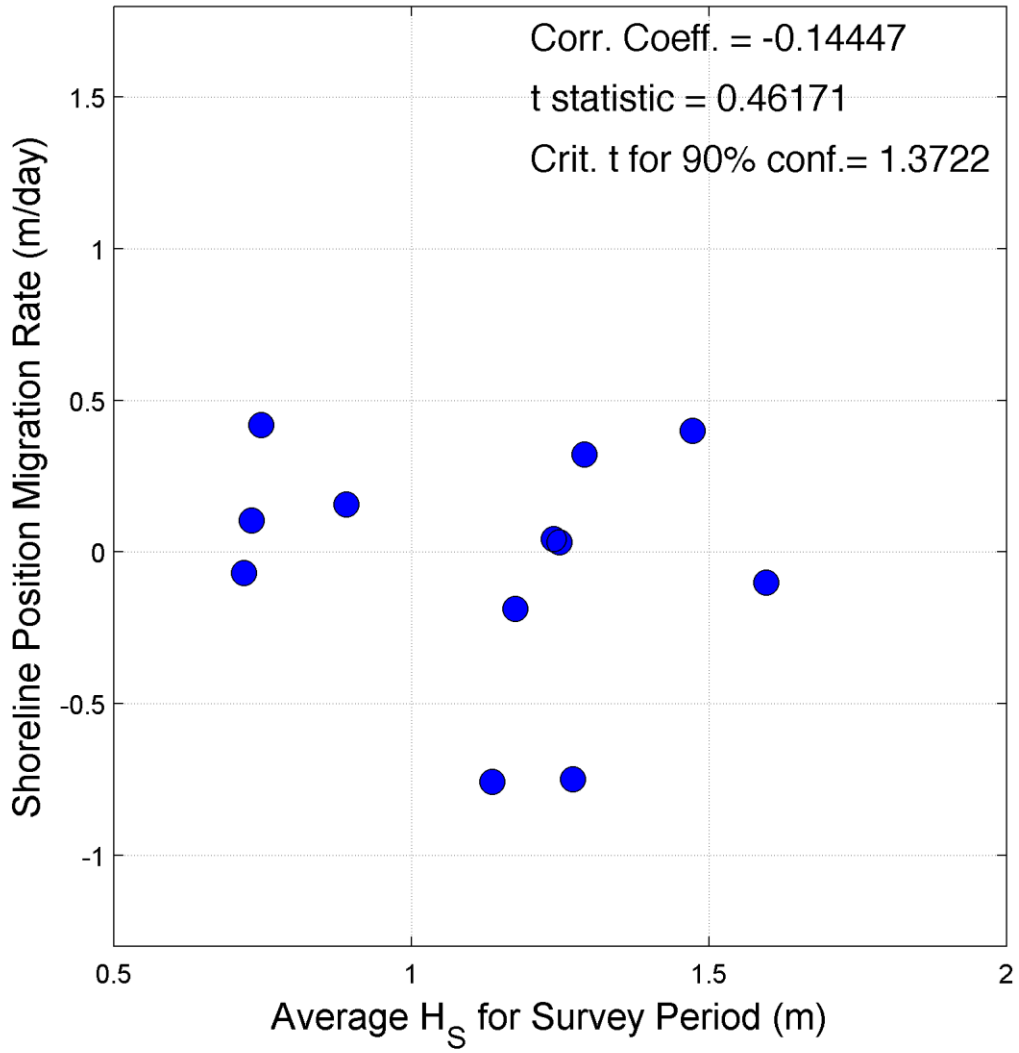
Transect 14



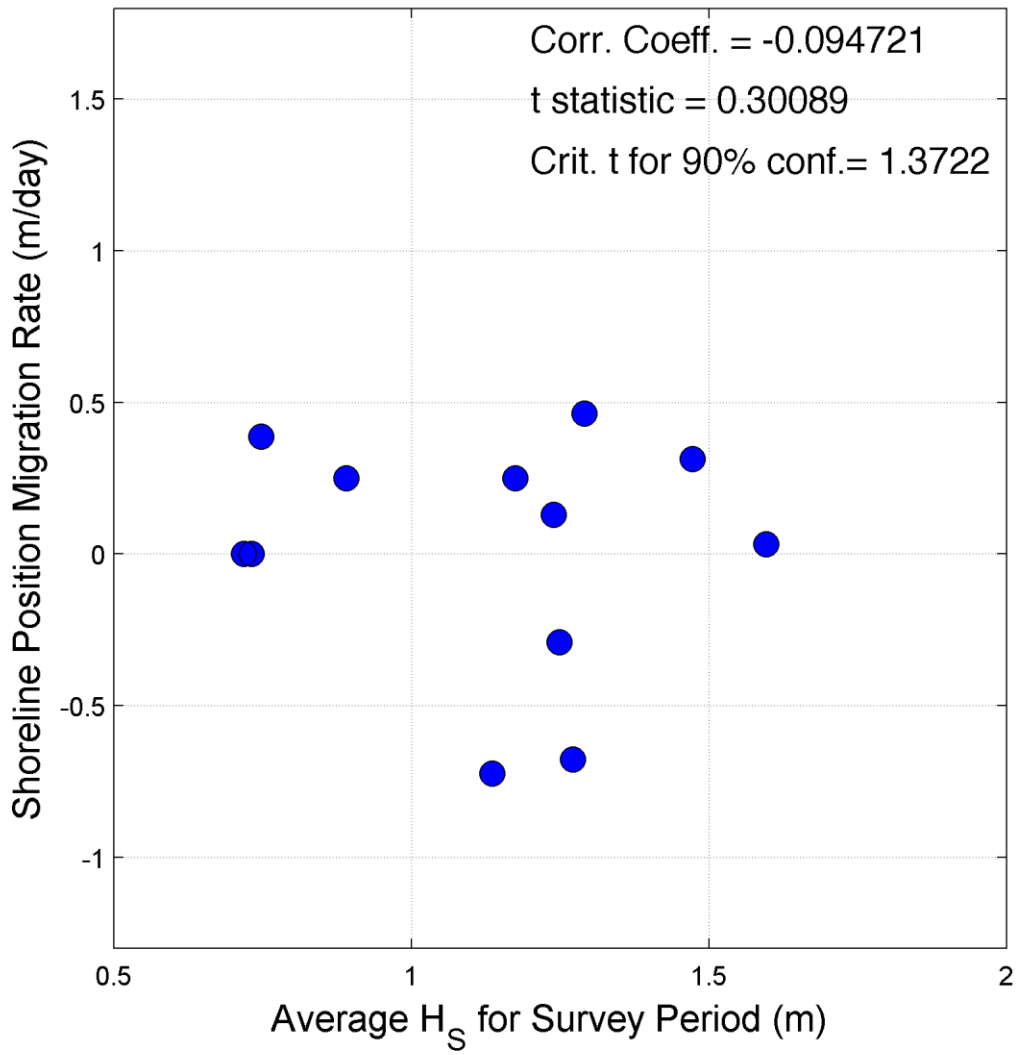
Transect 15



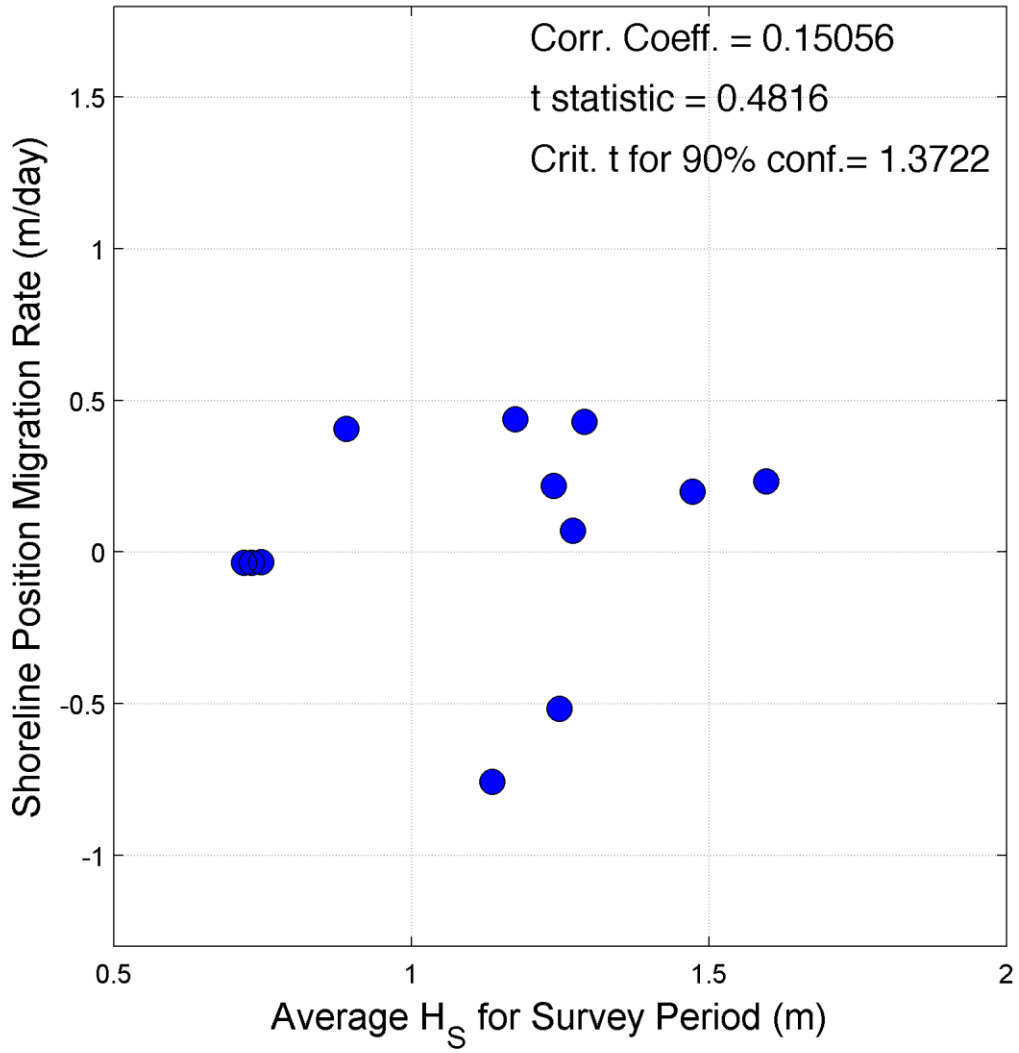
Transect 16



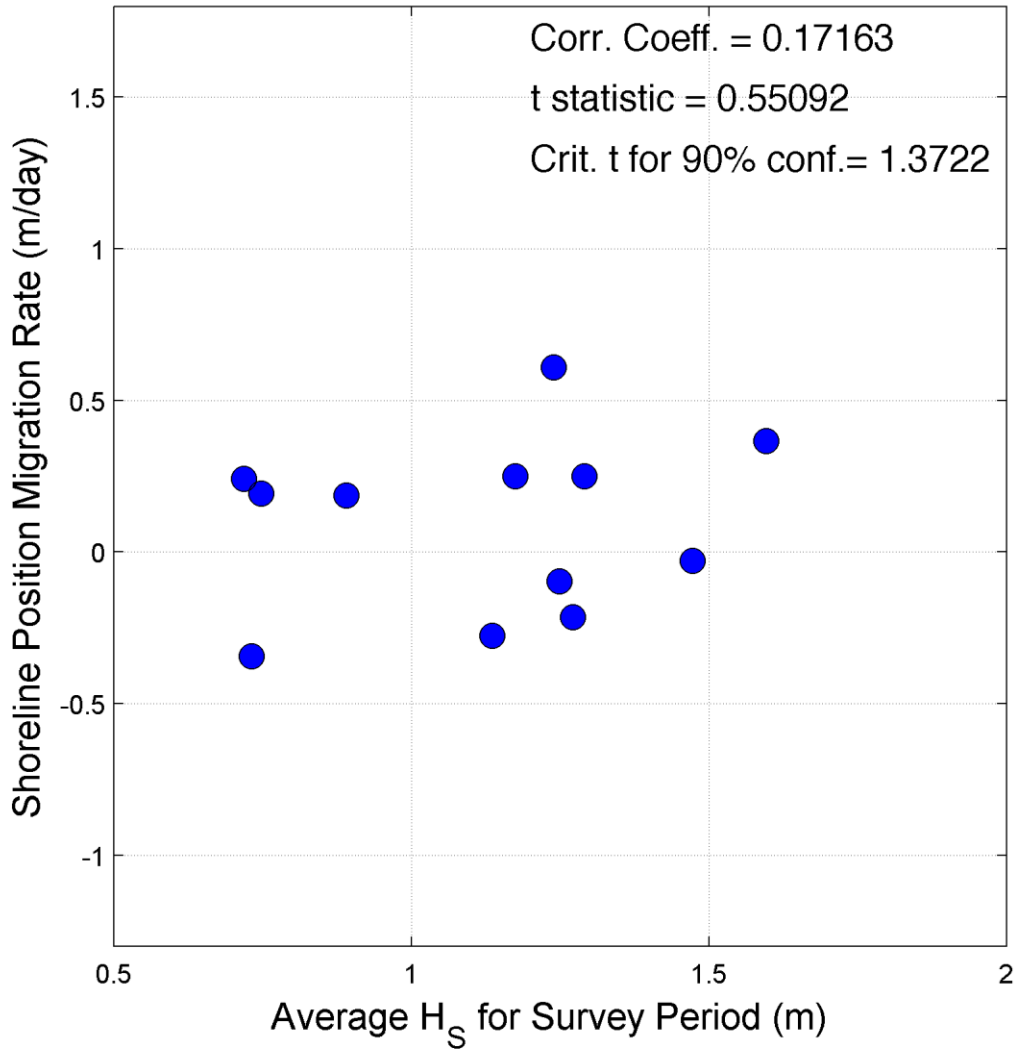
Transect 17



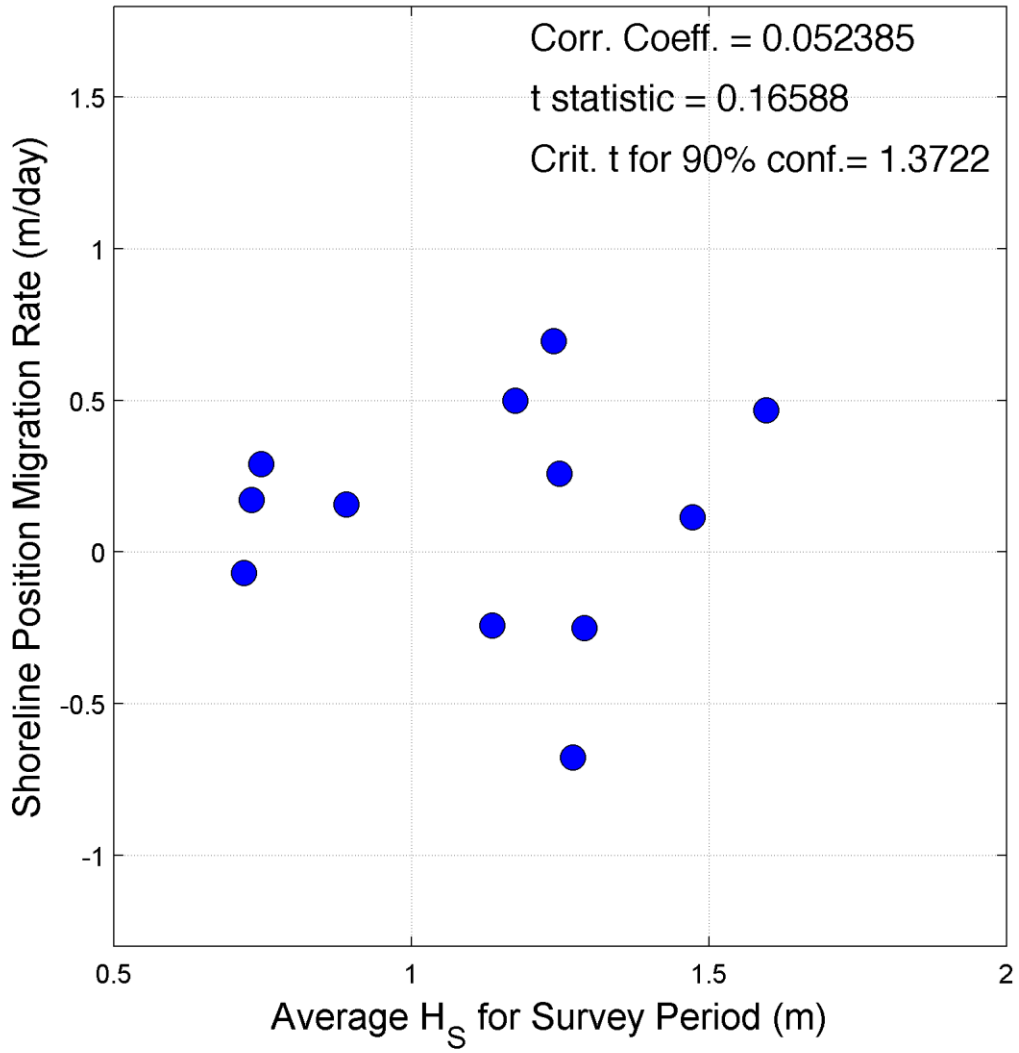
Transect 18



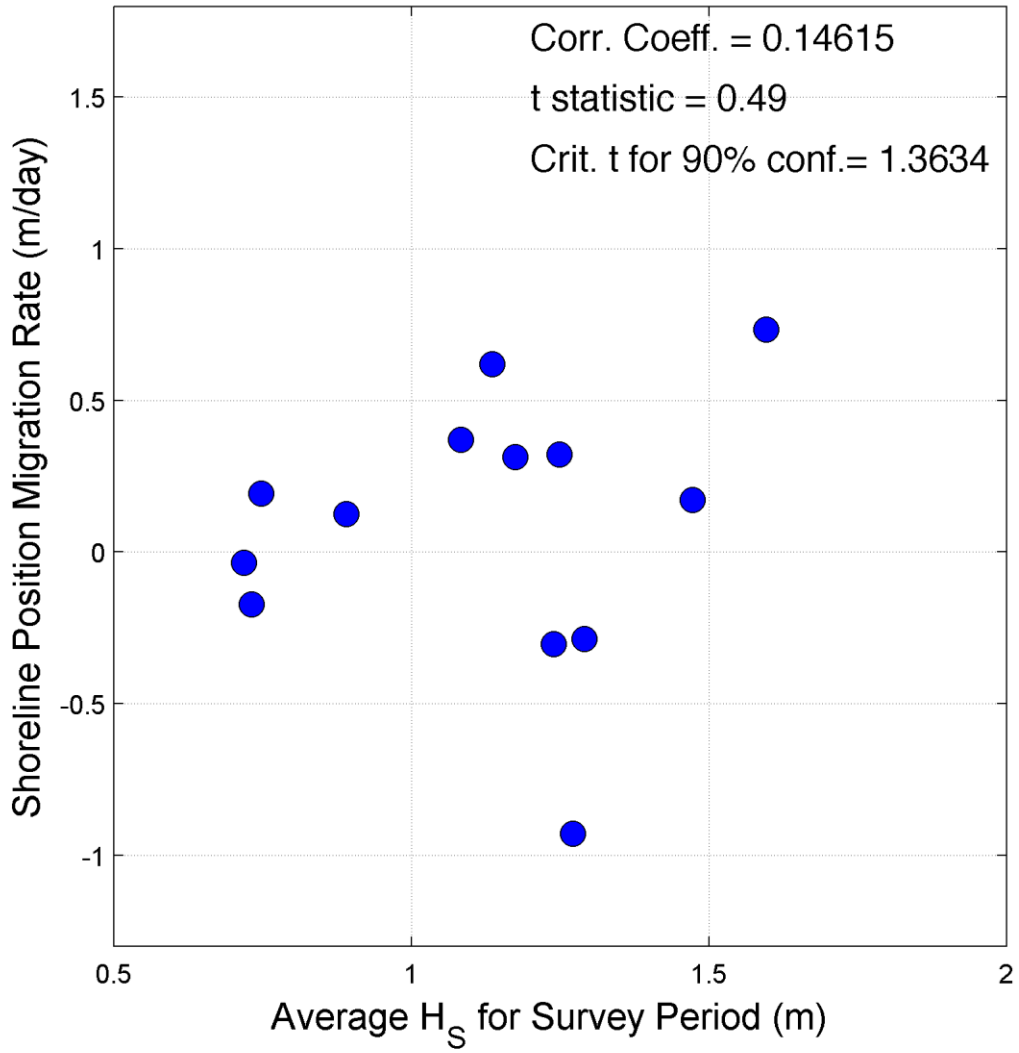
Transect 19



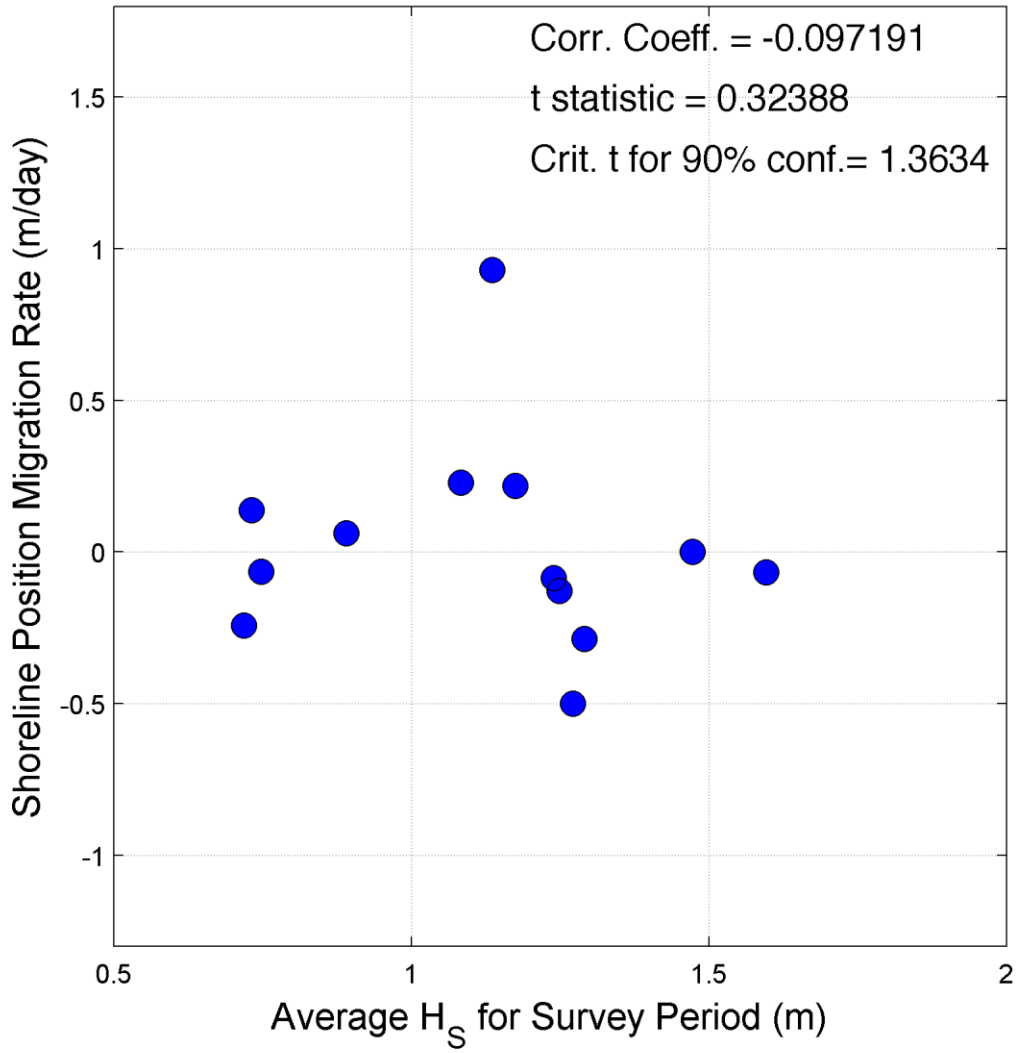
Transect 20



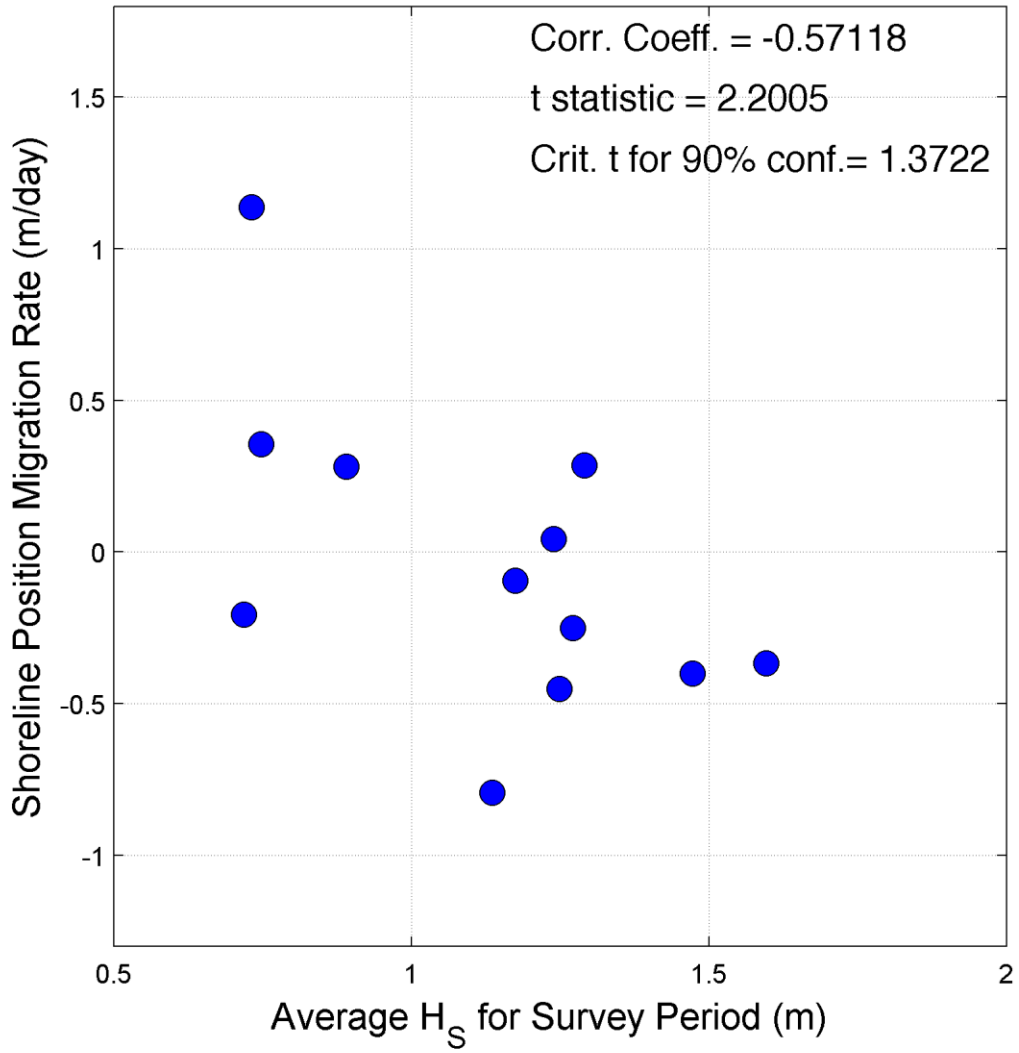
Transect 21



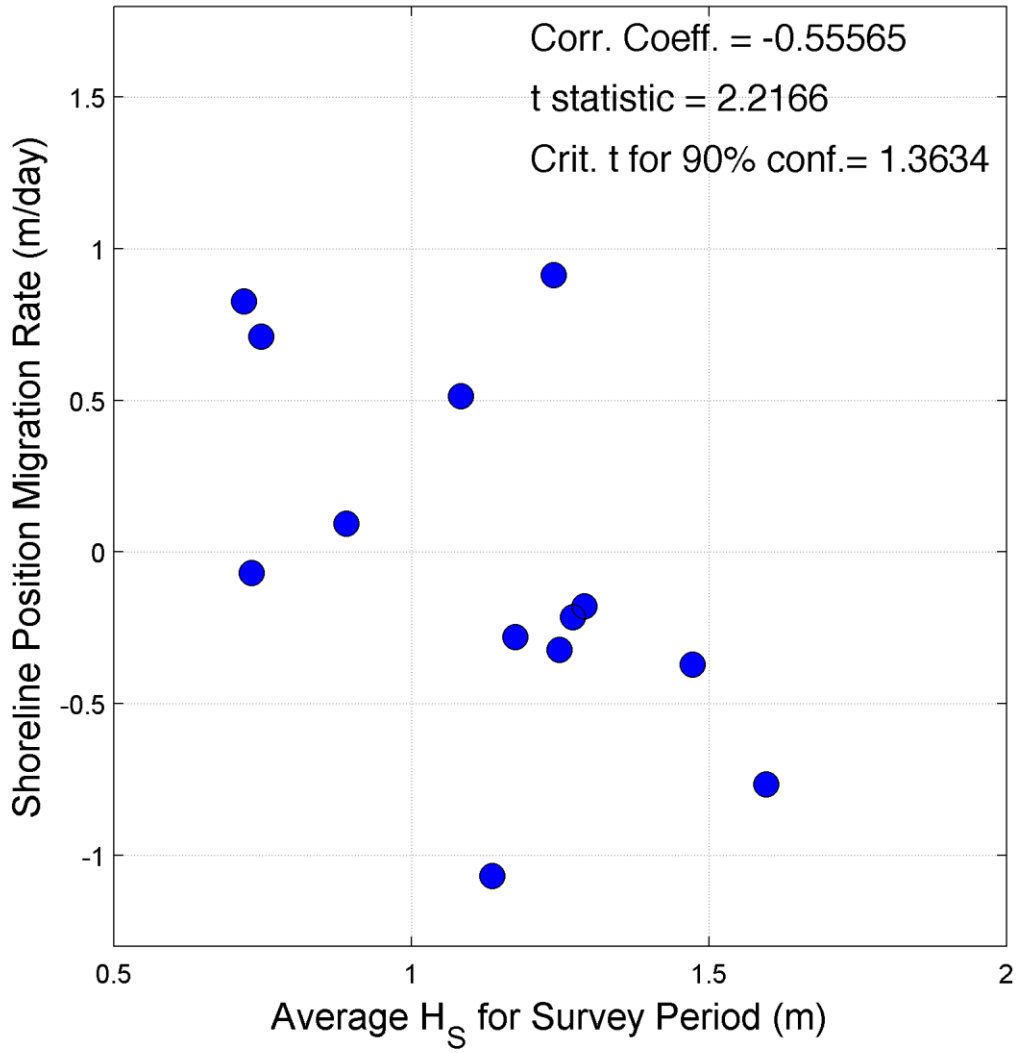
Transect 22



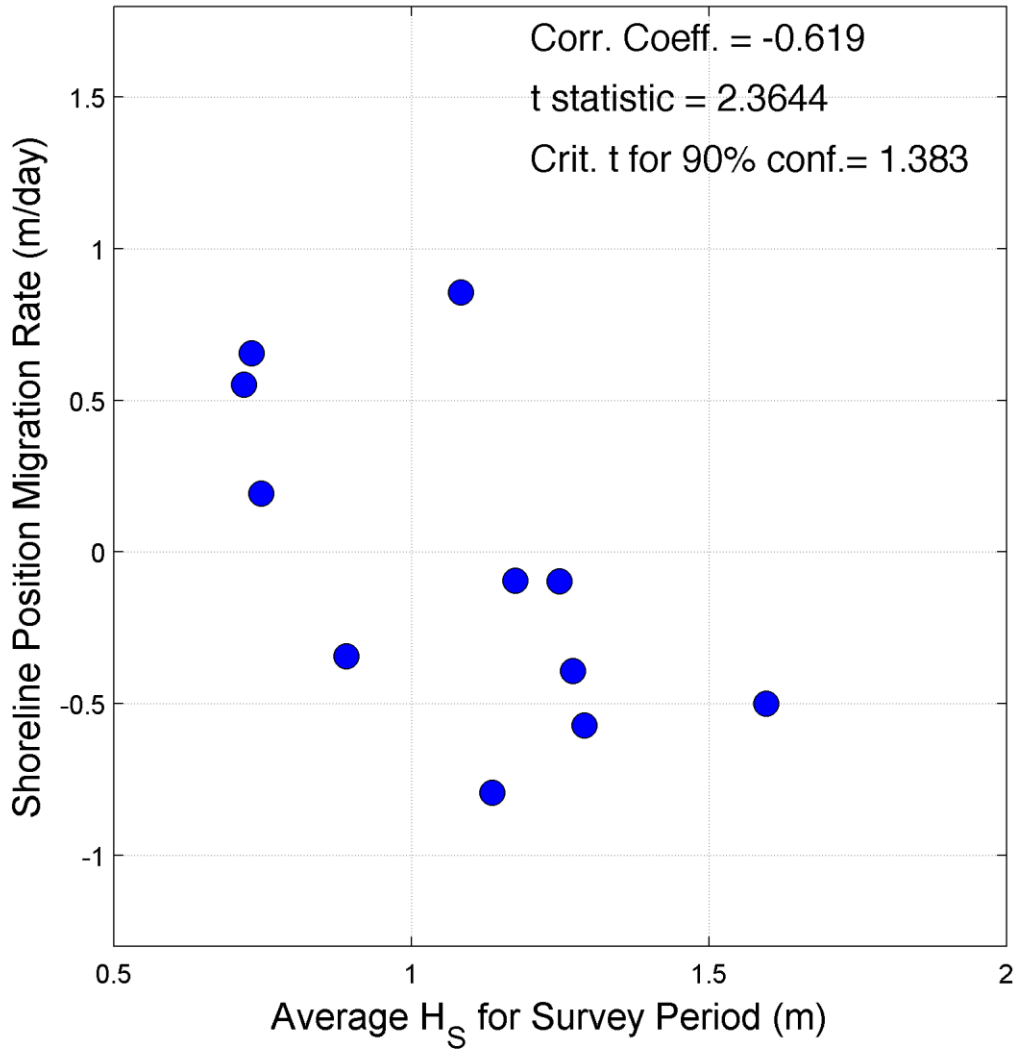
Transect 23



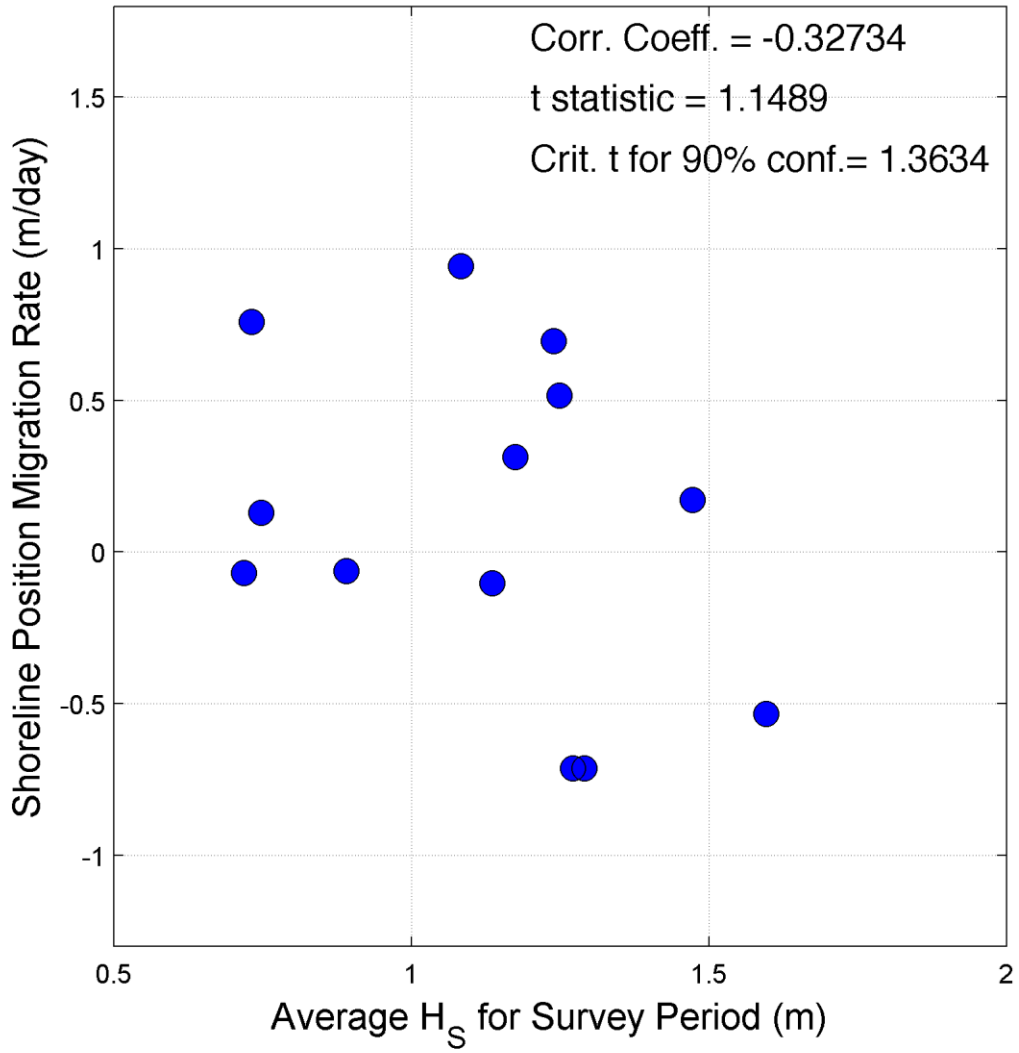
Transect 24



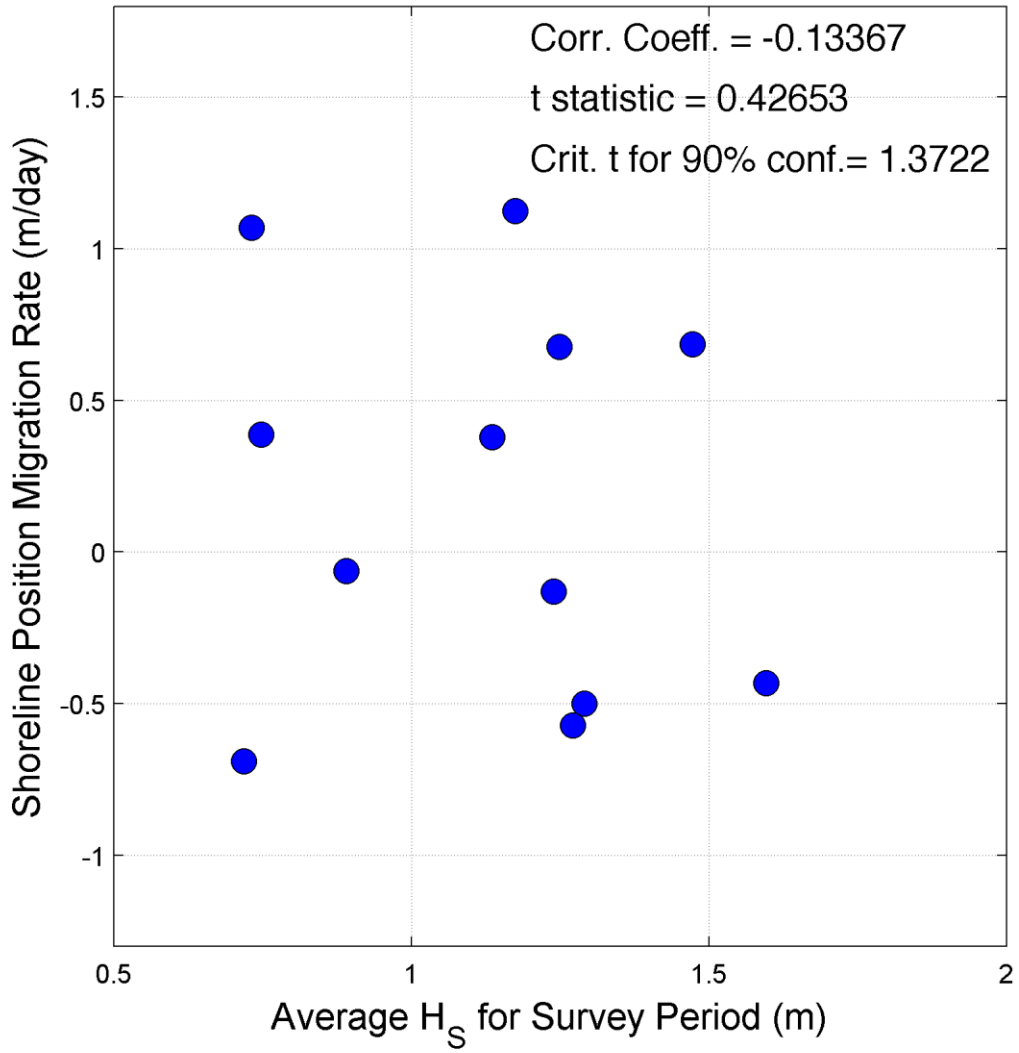
Transect 25



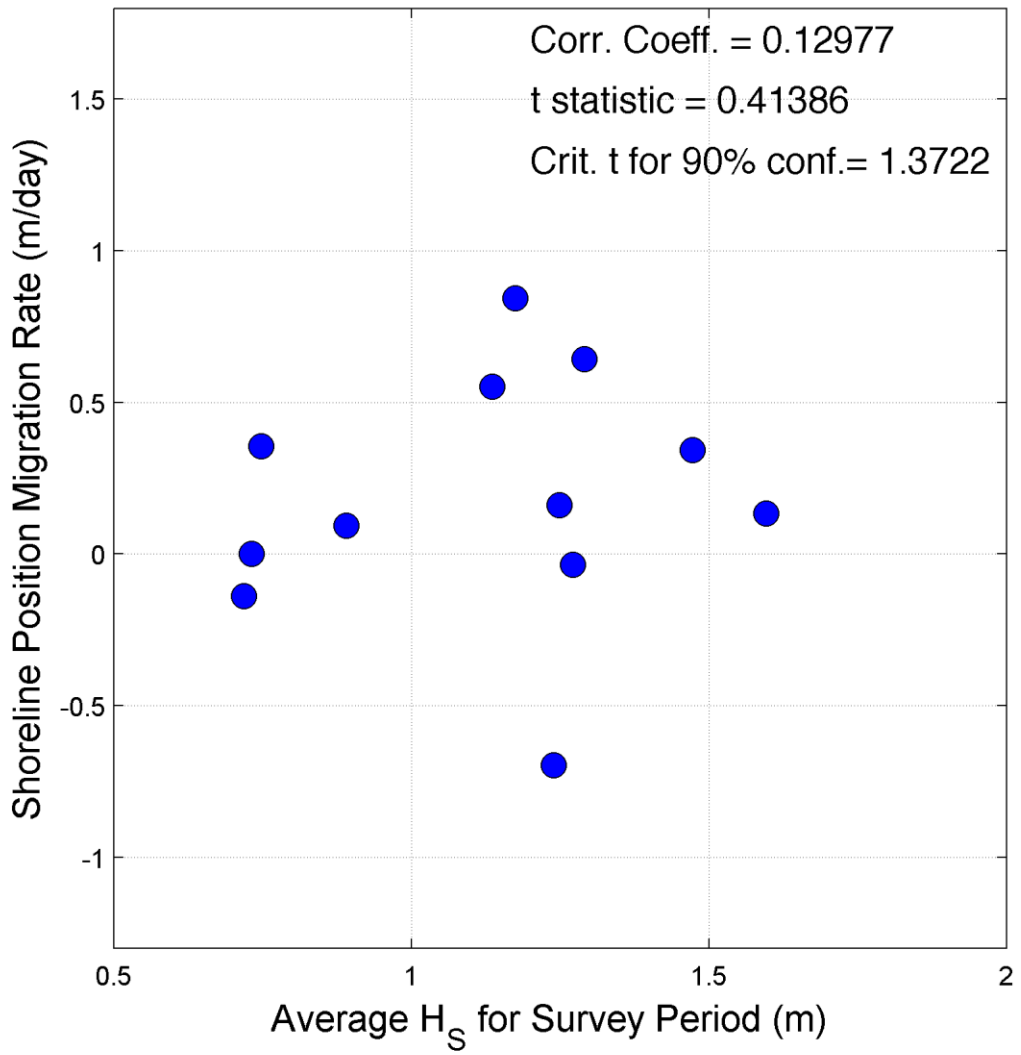
Transect 26



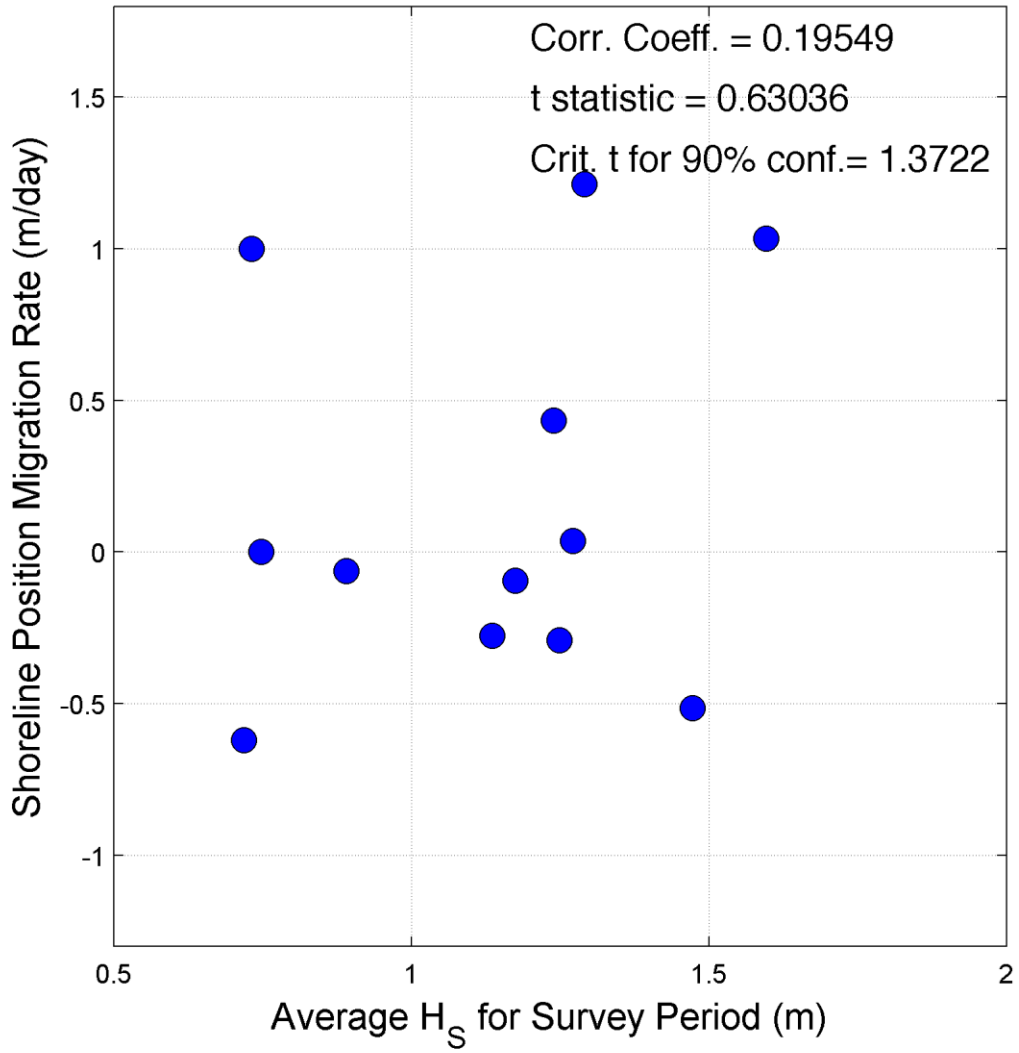
Transect 27



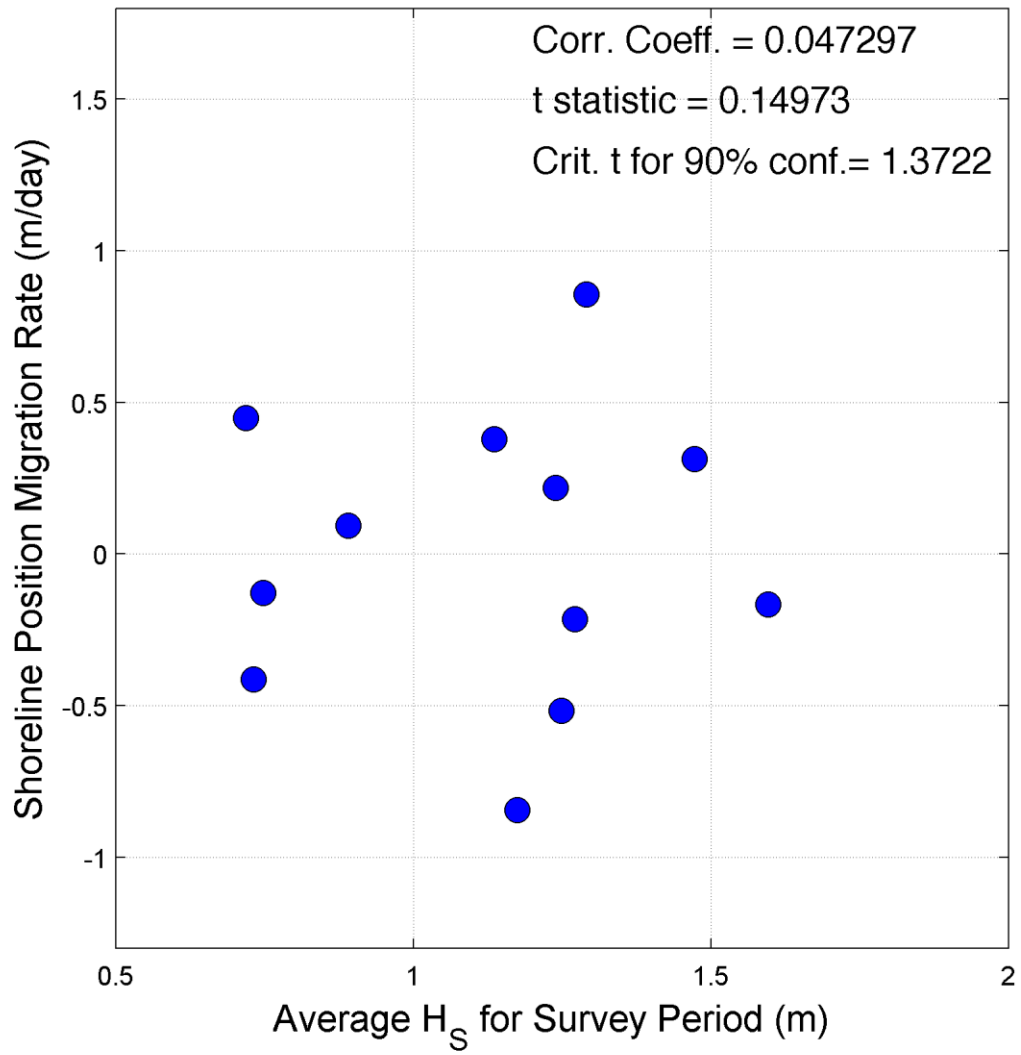
Transect 28



Transect 29



Transect 30



LIST OF REFERENCES

- Ashton, A., A.B. Murray, and O. Arnault (2001), Formation of coastline features by large-scale instabilities induced by high-angle waves, *Nature*, 414, 296-300.
- Aubrey, D.G (1979), Seasonal patterns of onshore/offshore sediment movement, *Journal of Geophysical Research*, 84, 6347-6354.
- Booij, N., R.C. Ris, and L.H. Holthuijsen (1999), A third generation wave model for coastal regions 1. Model description and validation, *Journal of Geophysical Research*, 104, 7649-7666.
- Dean, R.G. (1988), Sediment interaction at modified coastal inlets: processes and policies, in *Hydrodynamics and Sediment Dynamics of Tidal Inlets, Lecture Notes on Coastal and Estuarine Studies*, vol. 29, edited by M.J. Bowman et al., pp. 412-439, Springer-Verlag, New York.
- Dean, R.G. (1991), Equilibrium beach profiles: characteristics and applications, *Journal of Coastal Research*, 7(1), 53-84.
- Dolan, R., B. Hayden, and L. Vincent (1977), Shoreline forms and shoreline dynamics, *Science*, 197, 49-51.
- Dubois, R.N. (1988), Seasonal changes in beach topography and beach volume in Delaware, *Marine Geology*, 81, 79-96.
- Eliot, I.G. and D.J. Clarke (1982), Seasonal and biennial fluctuations in subaerial beach sediment volume on Warilla beach, New South Wales, *Marine Geology*, 48, 89-103.
- Fenster, M. and R. Dolan (1996), Assessing the impact of tidal inlets on adjacent barrier island shorelines, *Journal of Coastal Research*, 12(1), 294-310.
- FitzGerald, D. M. (1996), Geomorphic variability and morphologic and sedimentologic controls on tidal inlets, *Journal of Coastal Research*, 23, 47-71.
- Guza, R.T., and D.L. Inman (1975), Edge waves and beach cusps. *Journal of Geophysical Research*, 80(21), 2997-3012.
- Hayes, M.O. (1980), General morphology and sediment patterns in tidal inlets, *Sedimentary Geology*, 26, 139-156.
- Komar, P.D. and D.L. Inman (1970), Longshore sand transport on beaches. *Journal of Geophysical Research*, 75(30), 5514-5527.

- Kraft, J.C., E.A. Allen, and E.M. Maurmeyer (1978), The geological and paleogeomorphological evolution of a spit system and its associated shoal environments: Cape Henlopen Spit, Delaware, *Journal of Sedimentary Petrology*, 48(1), 211-226.
- Larson, M., Kraus, N.C. (1995), Prediction of cross-shore sediment transport at different spatial and temporal scales, *Marine Geology*, 126, 111-127.
- List, J.H., A.S. Farris, and C. Sullivan (2006), Reversing storm hotspots on sandy beaches: spatial and temporal characteristics, *Marine Geology*, 226(3-4), 261-279.
- Mehta, A.J., and C.P. Jones (1977), Matanzas Inlet glossary of inlets report #5, in *Florida Sea Grant Program, Rep. 21*, pp. 1-79, Coastal and Oceanographic Engineering Laboratory, Gainesville, Florida.
- Masselink, G., and A.D. Short (1993), The effect of tide range on beach morphodynamics and morphology: a conceptual beach model, *Journal of Coastal Research*, 9(3), 785-800.
- National Oceanographic and Atmospheric Association (2011), St. Augustine Beach, FL Station ID: 8720587 Station Information (3/16/2005), Retrieved from: http://tidesandcurrents.noaa.gov/station_info.shtml?stn=8720587%20St.%20Augustine%20Beach,%20FL
- National Oceanographic and Atmospheric Association (2011), Station 41012 (LLNR 845.3) - St. Augustine, FL 40NM ENE of St Augustine, FL. (1/26/2011), Retrieved from: http://www.ndbc.noaa.gov/station_page.php?station=41012
- Quartel, S., A. Kroon, B.G. Ruessink (2008), Seasonal accretion and erosion patterns of a microtidal sandy beach, *Marine Geology*, 250, 19-33.
- Ruggiero, P., P.D. Komar, W.G. McDougal, and R.A. Beach, (1996), Extreme water levels, wave runup and coastal erosion., in *Proceedings of the 25th Coastal Engineering conference*, pp. 2793-2805, American Society of Civil Engineers, Orlando, Florida.
- Ruggiero, P., G. Gelfenbaum, C.R. Sherwood, J. Lacy, and M.C. Buijsman (2003), Linking nearshore processes and morphology measurements to understand large scale coastal change. *In: Proceedings of Coastal Sediments '03*, Clearwater, Florida.
- Ruggiero, P., R.A. Holman, and R.A. Beach (2004), Wave runup on a high-energy dissipative beach, *Journal of Geophysical Research*, 109, C06025, doi:10.1029/2003JC002160.

- Ruggiero, P. and J.H. List, in press, Improving accuracy and statistical reliability of shoreline position and change rate estimates, *Journal of Coastal Research*.
- Ruggiero, P., M.C. Buijsman, G. Kaminsky, and G. Gelfenbaum, in press, Modeling the effect of wave climate and sediment supply variability on large-scale shoreline change, *Marine Geology*.
- Short, A.D. (1979a), Wave power and beach stages: a global model, In: *Proceedings of the 16th International Conference on Coastal Engineering '78*, pp. 1145-1162, Hamburg, Germany.
- Short, A.D., and L.D. Wright (1981), Beach systems of the Sydney region, *Australian Geographer*, 15, 8-16.
- Short, A.D., and P.A. Hesp (1982), Wave, beach, and dune interactions in southeastern Australia, *Marine Geology*, 48, 259-284.
- Stive, M.J.F., S.G.J. Aarninkhof, L. Hamm, H. Hanson, M. Larson, K.M. Winjber, R.J. Nicholls, and M. Capobianco (2002), Variability of shore and shoreline Evolution, *Coastal Engineering*, 47, 211-235.
- Weber, K.M., J.H. List, and K.L.M. Morgan (2005), An operational mean high water datum for determination of shoreline position from topographic lidar data, *U. S. Geological Survey Open File Report 2005-1027*, Retrieved from: <http://pubs.usgs.gov/of/2005/1027/index.html>
- Winant, C.D., D.L. Inman, and C.E. Nordstrom (1975), Description of seasonal beach changes using empirical eigenfunctions. *Journal Geophysical Research*, 80(15), 1979-1986.
- Wright, L.D. (1981), Beach cut in relation to surf zone morphodynamics, In: *Proceedings of the 17th International Conference on Coastal Engineering '80*, pp. 978-996, Sydney, N.S.W.
- Wright, L.D. (1982), Field observations of long-period surf zone oscillations in relation to contrasting beach morphologies. *Australian Journal of Marine and Freshwater Research*, 33, 181-201.
- Wright, L.D., J. Chappell, B.G. Thom, and J. Chappel (1978), Morphodynamic variability of high energy beaches, In: *Proceedings of the 16th Coastal Engineering Conference, American Society of Civil Engineers '78*, pp. 1180-1194, Hamburg, Germany.
- Wright, L.D., J. Chappell, B.G. Thom, M.P. Bradshaw, and P. Cowell (1979), Morphodynamics of reflective and dissipative beach and inshore systems: southeastern Australia, *Marine Geology*, 32, 105-140.

- Wright, L.D., B.G. Thom, and J. Chappell (1979b), Morphodynamic variability of high energy beaches, In: *Proceedings of the 16th International Conference on Coastal Engineering '78*, pp.1180-1194, Hamburg, Germany.
- Wright, L.D., R.T. Guza, and A.D. Short (1982a), Dynamics of a high-energy dissipative surf zone, *Marine Geology*, 45, 41-62.
- Wright, L.D., P. Nielsen, A.D. Short, and M.O. Green (1982b), Morphodynamics of a macrotidal beach, *Marine Geology*, 50, 97-128.
- Wright, L.D., P. Nielsen, A.D. Short, F.C. Coffey, and M.O. Green (1982c), Nearshore and surf zone morphodynamics of a storm wave environments: Eastern Bass Strait, Australia, in *Technical Report no. 82/3, Coastal Studies Unit, University of Sydney*, pp.154, Sydney, N.S.W.
- Wright, L.D. and A.D. Short (1983), Morphodynamics of beaches and surf zones in Australiam, In: KOMAR, P.D. (editor), *Handbook of Coastal Processes and Erosion*, pp. 35-64, Boca Raton: CRC Press.
- Wright, L.D. and A.D. Short (1984), Morphodynamic variability of surf zones and beaches: a synthesis, *Marine Geology*, 56, 93-118.
- Wright, L.D., A.D. Short, and M.O. Green (1985), Short-term changes in the morphodynamic states of beaches and surf zones: an empirical model, *Marine Geology*, 62, 339-364.
- Wright, L.D., A.D. Short, J.D. Boon, S. Kimball III, and J.H. List (1987), The morphodynamic effects of wave groupiness and tide range on a energetic beach, *Marine Geology*, 74, 1-20.

BIOGRAPHICAL SKETCH

Katherine Malone is originally from Annapolis, Maryland. She received a Bachelor of Arts in geological science in 2008 from Mount Holyoke College, South Hadley, MA, and received her Master of Science in geology from the University of Florida in the spring of 2011. Research interests include ocean waves, climate change, and barrier island and inlet morphodynamics.